THE UNIVERSITY
of EDINBURGH

This thesis has been submitted in fulfilment of the requirements for a postgraduate degree (e.g. PhD, MPhil, DClinPsychol) at the University of Edinburgh. Please note the following terms and conditions of use:

This work is protected by copyright and other intellectual property rights, which are retained by the thesis author, unless otherwise stated.
A copy can be downloaded for personal non-commercial research or study, without prior permission or charge.
This thesis cannot be reproduced or quoted extensively from without first obtaining permission in writing from the author.
The content must not be changed in any way or sold commercially in any format or medium without the formal permission of the author.
When referring to this work, full bibliographic details including the author, title, awarding institution and date of the thesis must be given.

Controls on the Structural, Stratigraphic and Climatic Development of the Central North Sea

Rachel J. Jamieson

VOLUME 1

THE UNIVERSITY OF EDINBURGH SCHOOL OF GEOSCIENCES

PhD

2013

PROJECT SPONSORS

BGS via their British University Funding Initiative (BUFI),

The University of Edinburgh's School Scholarship Scheme

and Maersk Oil

SUPERVISORS

Edinburgh University: Professors John. R. Underhill and Dick Kroon

BGS: Professor Michael Stephenson, Dr Robert Knox, Dr Robert Gatliff, Dr Melanie Leng and Dr Jim Riding

Seismic data generously provided by BP, CGG Veritas via Maersk Oil and First Oil. Access to onshore seismic data was made possible by kind permission of the trustees of the UK Onshore Geophysical Library (UKOGL) chaired by Dr Malcolm Butler.

DECLARATION

I have read and understood the University of Edinburgh guidelines on Plagiarism and declare that this written thesis is all my own work except where I indicate otherwise by proper use of quotes and references.

Rachel Jamieson

CONTENTS VOLUME 1

CONTENTS VOLUME 2

CONTROLS ON THE STRUCTURAL, STRATIGRAPHIC AND CLIMATIC DEVELOPMENT OF THE CENTRAL NORTH SEA

CHAPTER 1: INTRODUCTION

INTRODUCTION AND RATIONALE

The North Sea is a marginal, epeirogenic sea lying in an intra-plate setting on the NW European continental shelf in the northern hemisphere at about 54 degrees north. It is a shallow, elongate, saucer-shaped depression that is more than 970 km long and 560 km wide; with an area of around 570,000 km^2 and connected with the Atlantic Ocean both to the north through the Norwegian Sea, and to the south through the Dover Straits and English Channel (Figure 1.1).

However, it has not always had this form nor existed in such a state, the rocks buried beneath the sea-floor indicate a long history of tectonic activity and markedly different environmental conditions from those present today.

The North Sea is an important hydrocarbon province and it is essential to understand how it has evolved into its present form for successful exploration. Additionally, the large amounts of data gathered for use in hydrocarbon exploration provides a unique opportunity to investigate the structural and stratigraphic history of the area which may then provide analogues for understanding tectonic, stratigraphic, sedimentological and climatic responses through time in areas of the world where data is more limited.

Climate is also recognized as playing a vital role in the stratigraphic development of the basin, influencing sedimentary settings and depositional facies. Extreme climate events such as hyperthermals and ice-ages are therefore important to study as these will have the most measurable effect on basin evolution. Additionally, studying hyperthermal events can provide information on the causes and consequences of global warming which is particularly relevant to the present day.

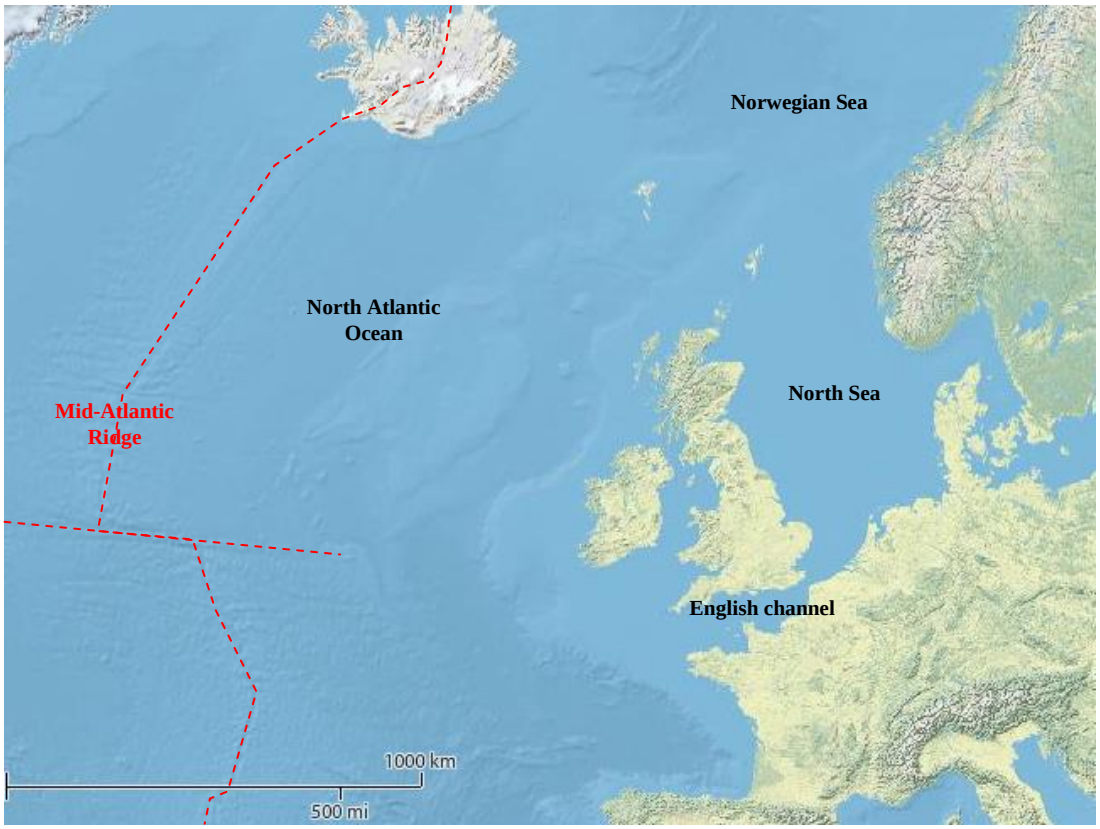

Figure 1.1: Location map of the North Sea showing modern bathymetry and plate tectonic setting.
Image modified from USGS basemap

The accepted understanding of the geology of the Central North Sea is that the current structural configuration arose from a period of rifting during the Jurassic (Underhill 2003). This extension formed a trilete extensional system consisting of three rift arms, the Moray Firth Basin, Viking Graben and Central Graben (Figure 1.2). The underlying structure of the Central North Sea is dominated by the influence of the Central Graben which itself is split into two arms, the Eastern and Western Troughs (Figure 1.3). This dominance highlights one of the central problems in interpreting regional geological histories as the most recent tectonic events tend to overprint and often obscure critical features of older geological events, leading to erroneous and confusing tectonic reconstructions. Additionally, the Jurassic rifting episode created many of the structural traps which today are exploited for hydrocarbons and has therefore been the subject of many of the previous geological studies undertaken within the Central North Sea.

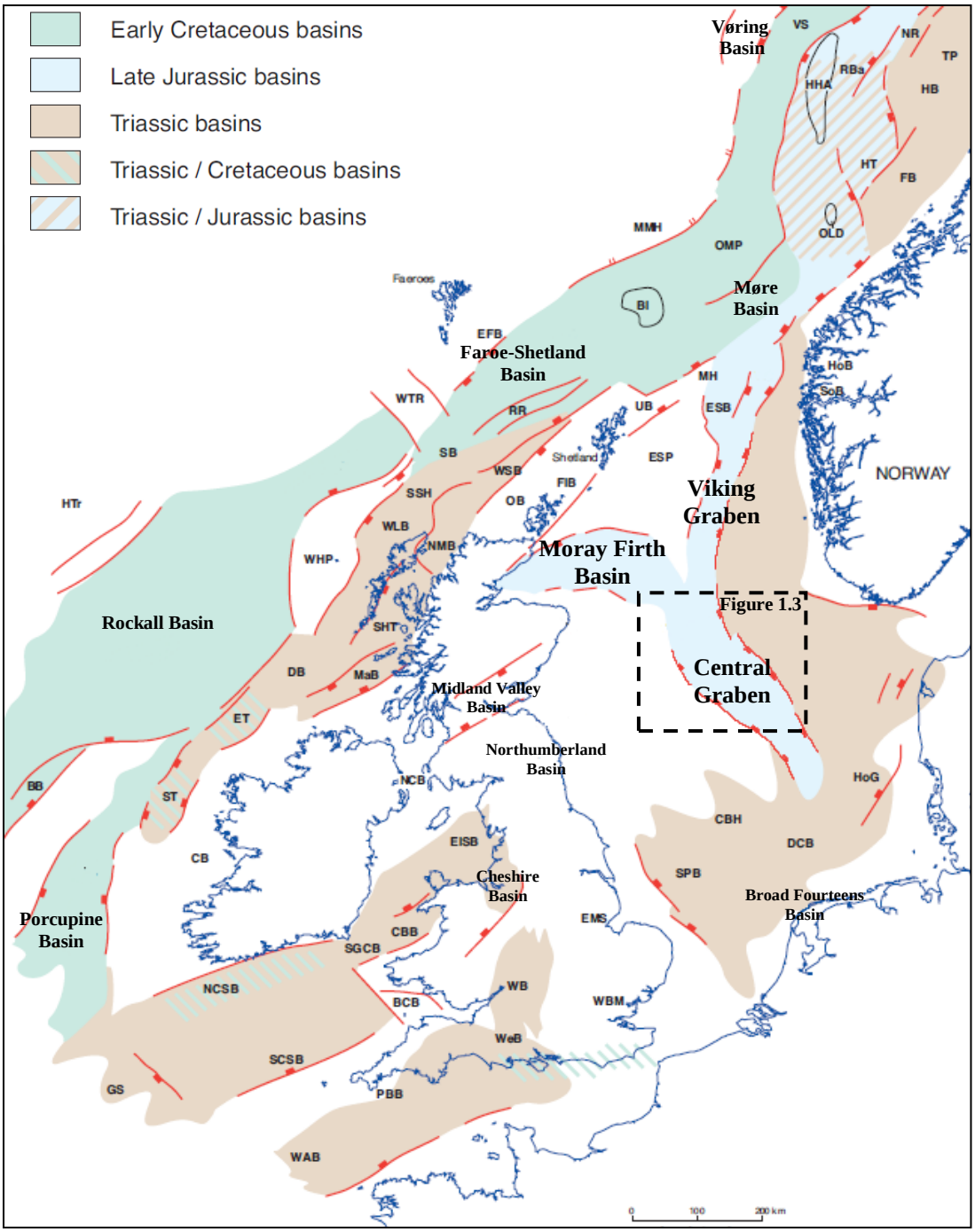

Figure 1.2: Structural elements of the North Sea. The trilete rift system formed in the Late Jurassic can be seen comprising the Moray Firth Basin, Viking Graben and Central Graben.
Major structures mentioned in the text are named.

BB Bean Basin, BCB Bristol Channel, BI Brendan Igneous Complex, CB Clare Basin, CBB Cardigan Bay Basin, CBH Cleaver Bank High, DB Donegal Basin, DCB Dutch Central Basin, EFB East Faroe Basin, EISB East Irish Sea Basin, EMS East Midland Shelf, ESB East Shetland Basin, ET Erris Trough, FB Froan Basin, FIB Fair Isle Basin, GS Goban Spur, HB Helgeland Basin, HoB Hornelen Basin, HHA Helland Hansen Arch, HoG Horn Graben, HT Halten Terrace, Htr Hatton Trough, MaB Malin Basin, MH Magnus High, MMH More Marginal High, NCB North Channel Basin, NCSB North Celtic Sea Basin, NMB North Minches Basin, NR Nordland Ridge, OB Orkney Basin, OLD Ormen Lande Dome, OMP Outer Møre Platform, PBB Plymouth Bay Basin, RBa Rås Basin, RR Rona Ridge, SB Solan Basin, SoB Solund Basin, SCSB South Celtic Sea Basin, SGCB St George's Channel Basin, SHT South Hebrides Trough, SPB Sole Pit Basin, SSH Sula Sgeir High, ST Slyne Trough, TP Trøndelag Platform, UB Unst Basin, VS Vigrid Syncline, WAB Western Approaches Basin, WB Worchester Basin, WBA Wales-Brabant Massif, WeB Wessex Basin, WHP West Hebrides Platform, WLB West Lewis Basin, WSB West Shetland Basin, WTR Wyville-Thomson Ridge

Image modified after (Evans et al. 2003)

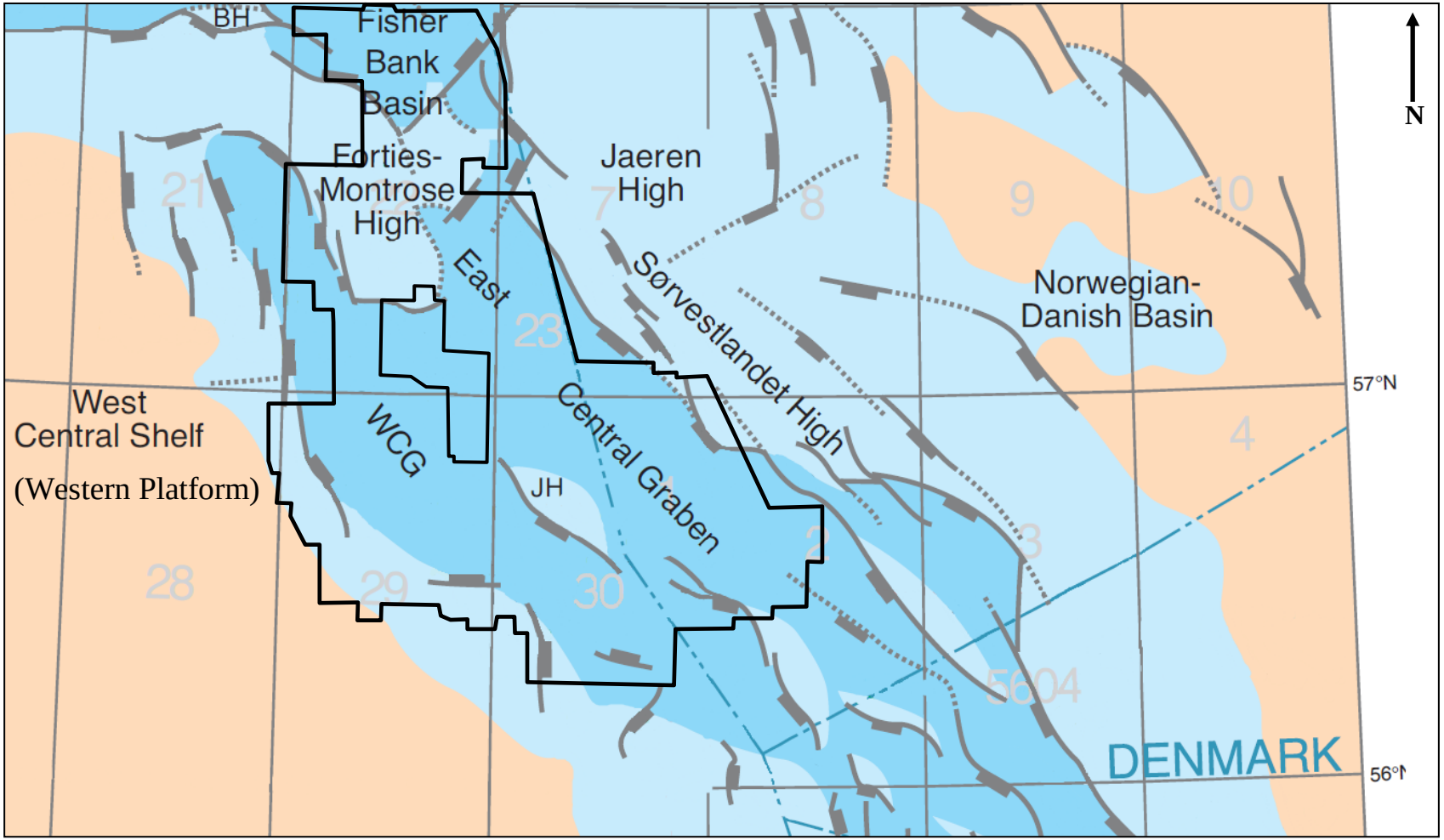

Figure 1.3: Structural elements within the study area of the Central North Sea (black outline). The Central Graben is split into a Western (WCG) and Eastern Trough separated by the median Forties-Montrose and Josephine Highs (JH).
Image modified after (Evans et al. 2003)

Surface and sub-surface mapping in the onshore UK and offshore Southern North Sea demonstrates that the whole area has been affected by episodes of rifting which pre-date the Jurassic event (Coward et al. 1989; Fraser et al. 1990; Chadwick et al. 1991; Chadwick et al. 1995; Underhill 2003; Smith et al. 2005; Brenchley et al. 2006; Pharoah et al. 2011). However, research into pre-Jurassic geology has previously been extremely limited in the Central North Sea due to the great depths to which basement rocks are now buried and by data quality and acquisition. Seismic data, which provides a snapshot of the sub-surface using impedance contrasts between different rock types, was first utilized in the North Sea in the 1960s. Seismic data has transformed our understanding of the subsurface expression of major faults, folds and sedimentary features by elucidating their long history of development and reactivation. Early seismic images were limited by problems in discriminating between reflections of differing amplitude and frequency, by false reflections created by energy bouncing between the subsurface layers before being recorded and by fault aliasing due to the 2D spaced grids that were originally acquired. Since these first images were produced, the size and scale of seismic surveys has increased along with significant concurrent increases in processing techniques and computer power. This has led the seismic industry from laboriously – and therefore rarely – acquiring small 3D surveys in the 1980s to now routinely acquiring large-scale high resolution 3D surveys. However, it is only recently that data quality has improved to the extent that high-quality imaging of the deeply buried Central Graben has been possible.

An additional problem in interpretation of the regional geology of the Central North Sea is one of scale. The primary use of seismic data in the Central North Sea is in

locating and mapping in detail prospective structures which may trap hydrocarbons. This means that the majority of seismic surveys acquired cover a limited area and thus can only provide a snapshot of the structure of the basin. Recent advances in seismic acquisition have led to regional seismic surveys becoming available which allow the full structure of the area to be interpreted but these surveys are rarely available to academics due to the great cost of acquiring them. Well data used to constrain interpretation of seismic datasets, although publically released, is still distributed under a license which is also costly.

Due to these limitations, the interplay of direct tectonic events, far-field stresses and climate has previously been ascertained from a combination of onshore outcrop and sparse 2D and 3D seismic data. Small areas have been studied in detail although attempts to bring these together in a regional interpretation have been undertaken in the past (Glennie 1998; Evans et al. 2003). However, these syntheses were focused on understanding large-scale tectonic (structural) controls on the petroleum prospectivity of the North Sea area and did not emphasized the importance of sedimentary provinces and climatic events in the evolution of the basin. They also did not provide the detailed case studies which have only proved possible to deduce with dense, high-fidelity seismic data and better well-control.

The current study is therefore unique in its use of a high resolution, regional 3D seismic dataset, donated by CGG via Maersk Oil to examine in detail the development, evolution and deformation history of the Central North Sea. Additional 3D and 2D datasets from the Faroe-Shetland Basin and onshore UK were also

studied in order to gain a better understanding of the events which affected its structural evolution but which have been obscured due to overprinting by later deformation. Data from the Southern North Sea was also used to constrain the interpretation. Large amounts of publically released data from wells drilled in and around the Central North Sea was also made available to the study via the Schlumberger operated CDA website. The quality and quantity of the data utilized means that the results of the study provide the first large-scale, consistent evidence for earlier rifting events mapped beneath the Jurassic.

In addition to this, high-resolution imaging of the post-Jurassic section along with access to the records and rock samples from boreholes drilled for hydrocarbon exploration has allowed the effect of extreme climatic events on basin evolution to be investigated on a regional scale. Previous studies into such events have focused on one or two boreholes with little attention paid to the regional geological context. None have previously afforded an opportunity to 'map' the event using seismic data and thus use the interpretation predictively. This study analyses samples from five sections over a period of time known as the Palaeocene-Eocene Thermal Maximum, a hyperthermal event which occurred in the Latest Palaeocene (Zachos et al. 2001). The study also closely examines the regional tectonic events which occurred during the period of extreme climate which has never before been undertaken in studies of the hyperthermal. The results demonstrate that events which could be considered proxies for climatic variations such as sea-level rises can often result from regional tectonic events and indicates that a complete understanding of the geological history

of an area is vital if correct inferences are to be made about the effects of climate on environmental systems

METHODOLOGY, DATA AND THEIR APPLICATION

The aim of the study was to investigate the new insights into the geological history of the Central North Sea which could be gained through application of the latest technology and improved understanding of structural regimes. This demonstrated the importance of large-scale tectonic and climatic events on basin evolution. A case study of the Late Palaeocene during which a significant global climate perturbation occurred, then permitted investigation of the relative importance of short-lived events on sedimentary and biological systems within the basin and how these compared with those found in other areas of the world.

The difference in scale between these two major areas of research means that different types of analysis were undertaken in order to fully investigate them. A standard method of studying large-scale tectonic events is tectonostratigraphy, where periods of deformation are recognised and related to geologic events such as episodes of rifting. Onshore this can be undertaken by surface mapping of stratigraphic units which can then be integrated with other types of geophysical data. Offshore the only method of interpreting buried structures involves the use of seismic data calibrated by hydrocarbon exploration wells drilled into the subsurface. Exploration for hydrocarbons in the North Sea and onshore Britain has had a long and varied history. Initial drilling took place onshore and focused upon surface anticlines with the first exploration well drilled in 1918. Intense exploration continues in the area today and has led to a vast array of data being collected on the

subsurface geology in the form of 2D and 3D seismic volumes and well data. Seismic interpretation was therefore undertaken over a high-resolution 3D megasurvey covering the whole Central North Sea area in order to provide new insights into the geological evolution of the area. Calibration was provided by well data and also by interpretation of onshore 2D seismic data and outcrop data (Figure 1.4).

Other types of data are also publically available through the Schlumberger-operated Common Data Access (CDA) Online Data Store such as industry reports, core data, sedimentological and mineralogical studies and biostratigraphy. These data have been used in the current study in order to give a more detailed view of the impact of globally significant but short-lived events such as the Palaeocene hyperthermal on the Central North Sea. The PETM hyperthermal has been studied in various localities worldwide and these previous investigations informed some of the techniques applied in the North Sea study. Geochemical, mineralogical, sedimentological and biostratigraphic studies were therefore undertaken as described by existing literature (discussed in detail in Chapter 6) in order to assess the impact of this short-lived event on the Central North Sea and compare its effects in this area with those found worldwide (Figure 1.5).

Figure 1.4: WORKFLOW FOR INTERPRETATION OF REGIONAL BASIN EVOLUTION

1.Well inputs and calibration

Well location and Stratigraphy

Well identifier	Surface	X	Y	Z	MD
22/16a-2	Pliocene	389548.00	6360406.00	-948.22	973.22
22/16a-2	Early Pliocene	389548.00	6360406.00	-1017.42	1042.42
22/16a-2	Miocene	389548.00	6360406.00	-1163.72	1188.72
22/16a-2	Mid-Early Miocene	389548.00	6360406.00	-1337.46	1362.46
22/16a-2	Mid-Early Miocene	389548.00	6360406.00	-1593.49	1618.49
22/16a-2	Oligocene	389548.00	6360406.00	-1776.37	1801.37
22/16a-2	Early Oligocene	389548.00	6360406.00	-1977.54	2002.54
22/16a-2	Eocene	389548.00	6360406.00	-2321.96	2346.96
22/16a-2	Tay Sand	389548.00	6360406.00	-2575.00	2600.00
22/16a-2	Balder Formation	389548.00	6360406.00	-2606.95	2631.95
22/16a-2	Sele Formation	389548.00	6360406.00	-2638.04	2663.04
22/16a-2	Forties Formation	389548.00	6360406.00	-2658.76	2683.76
22/16a-2	Andrew/Mey	389548.00	6360406.00	-2770.63	2795.63
22/16a-2	Maureen Formation	389548.00	6360406.00	-2966.31	2991.31
22/16a-2	Ekofisk Formation	389548.00	6360406.00	-3059.58	3084.58
22/16a-2	Tor	389548.00	6360406.00	-3154.67	3179.67
22/16a-2	Hod Formation	389548.00	6360406.00	-3499.00	3524.00
22/16a-2	Flounder	389548.00	6360406.00	-3473.80	3498.80
22/16a-2	Plenus Marl	389548.00	6360406.00	-4041.95	4066.95
22/16a-2	Hidra	389548.00	6360406.00	-4050.79	4075.79
22/16a-2	Cromer Knoll Group	389548.00	6360406.00	-4078.83	4103.83
22/16a-2	Kimmeridge Clay	389548.00	6360406.00	-4139.18	4164.18
22/16a-2	Fulmar	389548.00	6360406.00	-4465.01	4490.01
22/16a-2	Pentland Formation	389548.00	6360406.00	-4561.00	4586.00
22/16a-2	Skagerrak Formatio	389548.00	6360406.00	-4622.59	4647.59
22/16a-2	Base well path	389548.00	6360406.00	-4771.33	4796.33

Wire-line log and core data

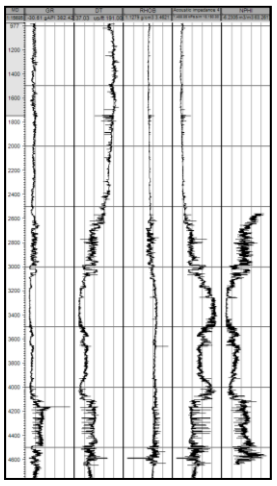

Time/Depth Relationship

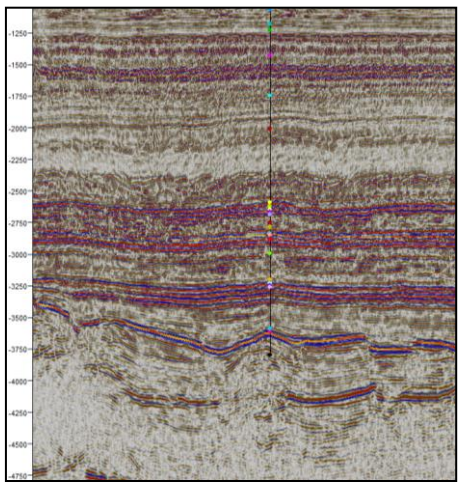

Synthetic seismograms

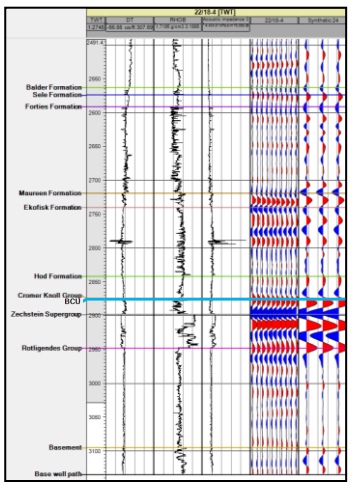

2.Seismic Interpretation

Interpretation of horizons tied to wells

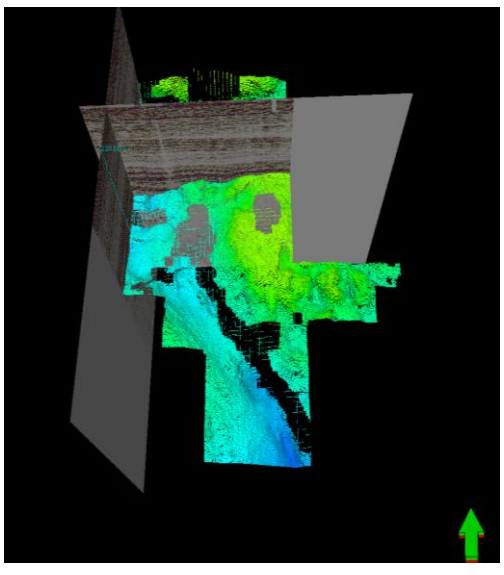

Recognition of periods of deformation bounded by unconformities (tectonostratigraphy)

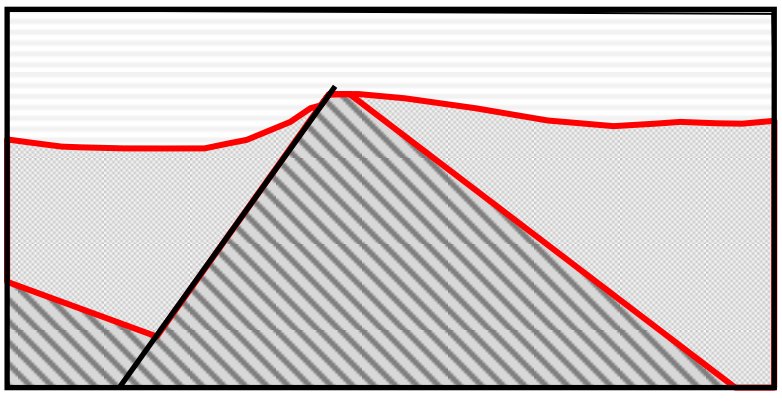

Calibration with onshore analogies

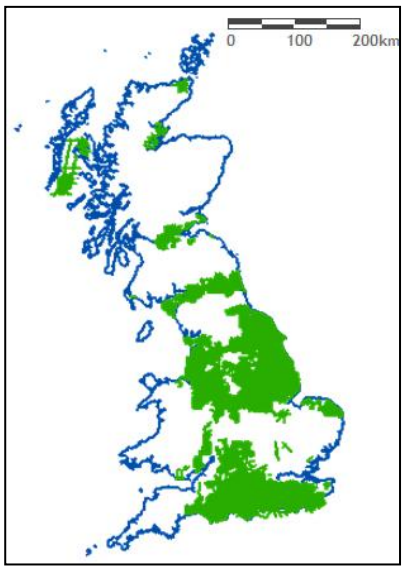

3. Output Maps and interpretation

TWTT Top structure maps

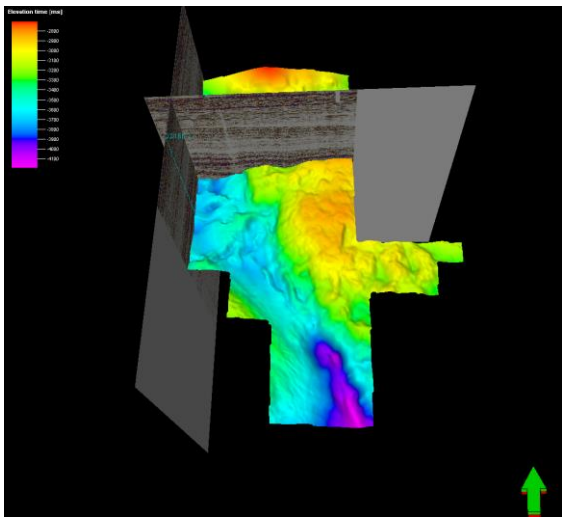

Isochrons between two surfaces

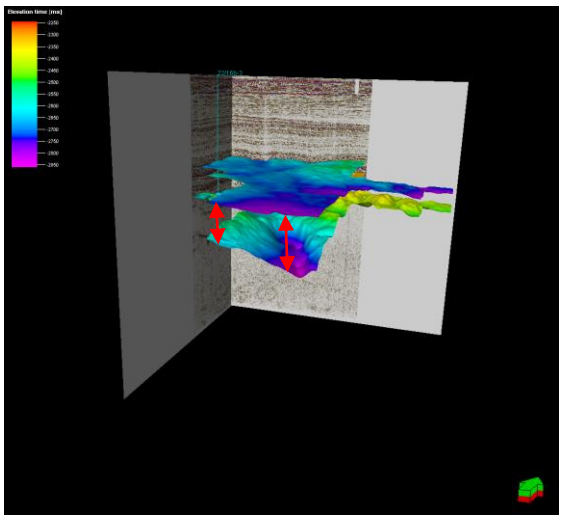

Secondary analysis such as Dip angle, Azimuth and amplitude extractions.

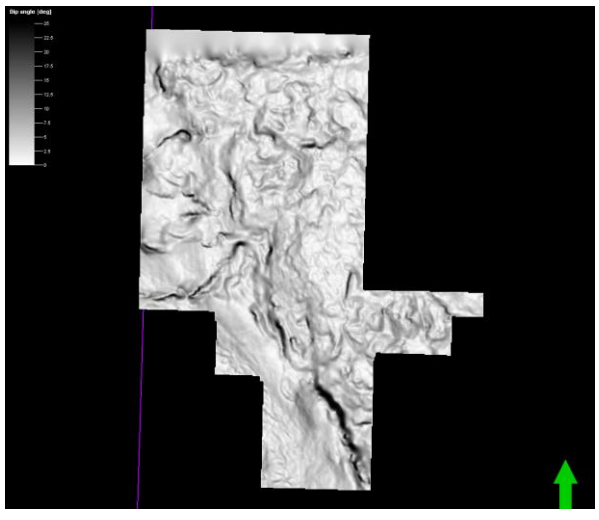

Figure 1.5: <u>WORKFLOW FOR INTERPRETATION OF SHORT-LIVED GLOBAL GEOLOGICAL EVENTS: CASE STUDY THE PETM HYPERTHERMAL</u>

1. Research techniques applied during previous hyperthermal studies

Global changes identified

Negative carbon isotope excursion (Isotopic analysis)

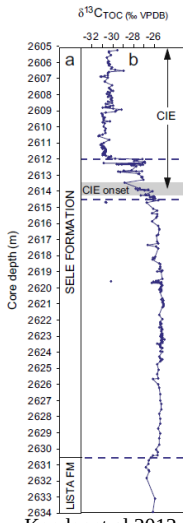

Kender et al 2012

Oceanographic and depositional effects (Clay mineralogy, sedimentation rate)

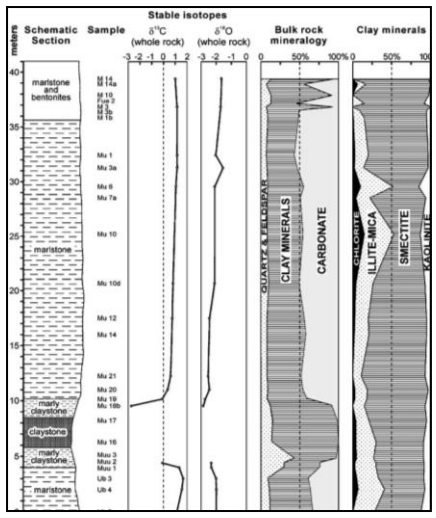

Egger et al 2005

Ecological Effects (Palynology, micropaleontology, palaeontology)

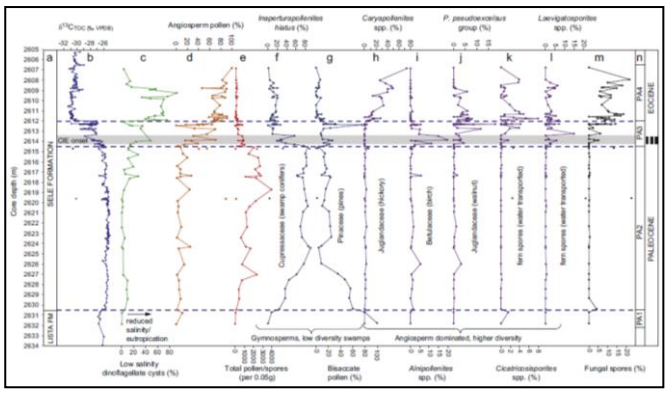

Kender et al 2012

2. Research areas selected for study in the Central North Sea

(i) Effect on Depositional Systems

Recognition of the PETM (Carbon isotopes)

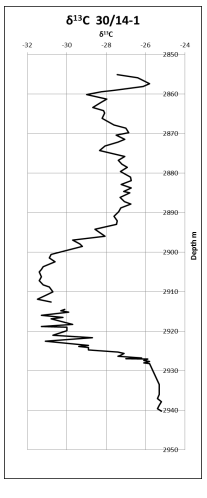

Seismic interpretation (3D mapping of depositional systems)

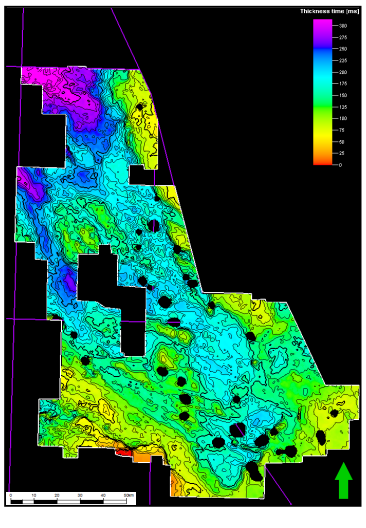

Wireline logs and geochemical reports (Clay Mineralogy)

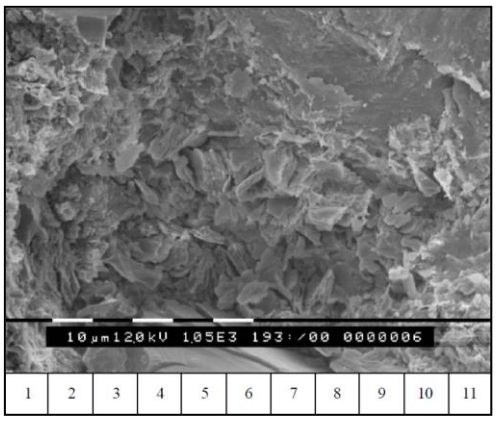

X-Ray Fluorescence (Oceanographic changes and relative timescale)

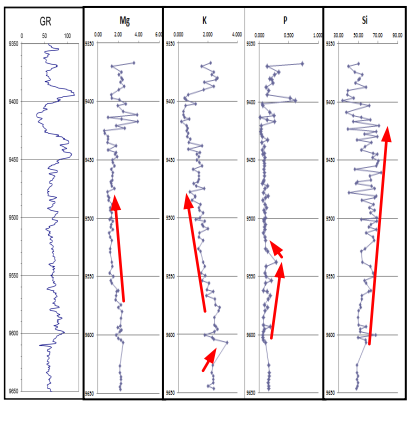

(ii) Effect on Ecological Systems

Biostratigraphy

Palynology

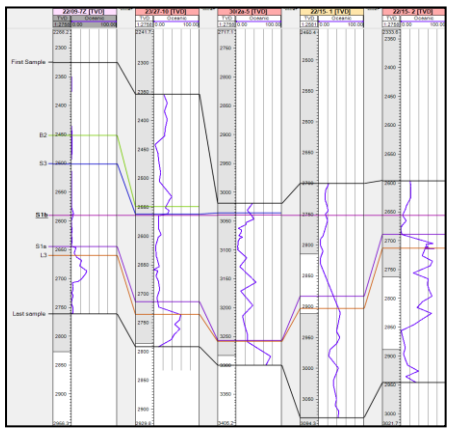

Micropaleontology

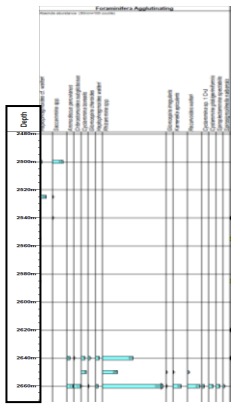

(iii) Evaluation of possible causes of such changes

1.1 SEISMIC DATA

Interpretation of seismic data was undertaken in order to investigate new insights which could be gained into the geological development of the Central North Sea. For the purposes of the study, several offshore 3D and 2D seismic datasets were made available (Figure 1.6). Over the main study area in the Central North Sea, a high-fidelity 3D seismic dataset was made available by BP and CGG via Maersk Oil, covering approximately 17,000km² of the Central North Sea split over 11 grids. (Figure1.7). Further datasets were made available covering 1000km^2 over the West Central Shelf courtesy of First Oil (Figure 1.8) and 75,000 km² in the Faroe-Shetland Basin (Figure 1.9).

In addition to this, 2D seismic lines from the UK onshore were kindly donated by the UK Onshore Geophysical Library (UKOGL) (Figure 1.10).

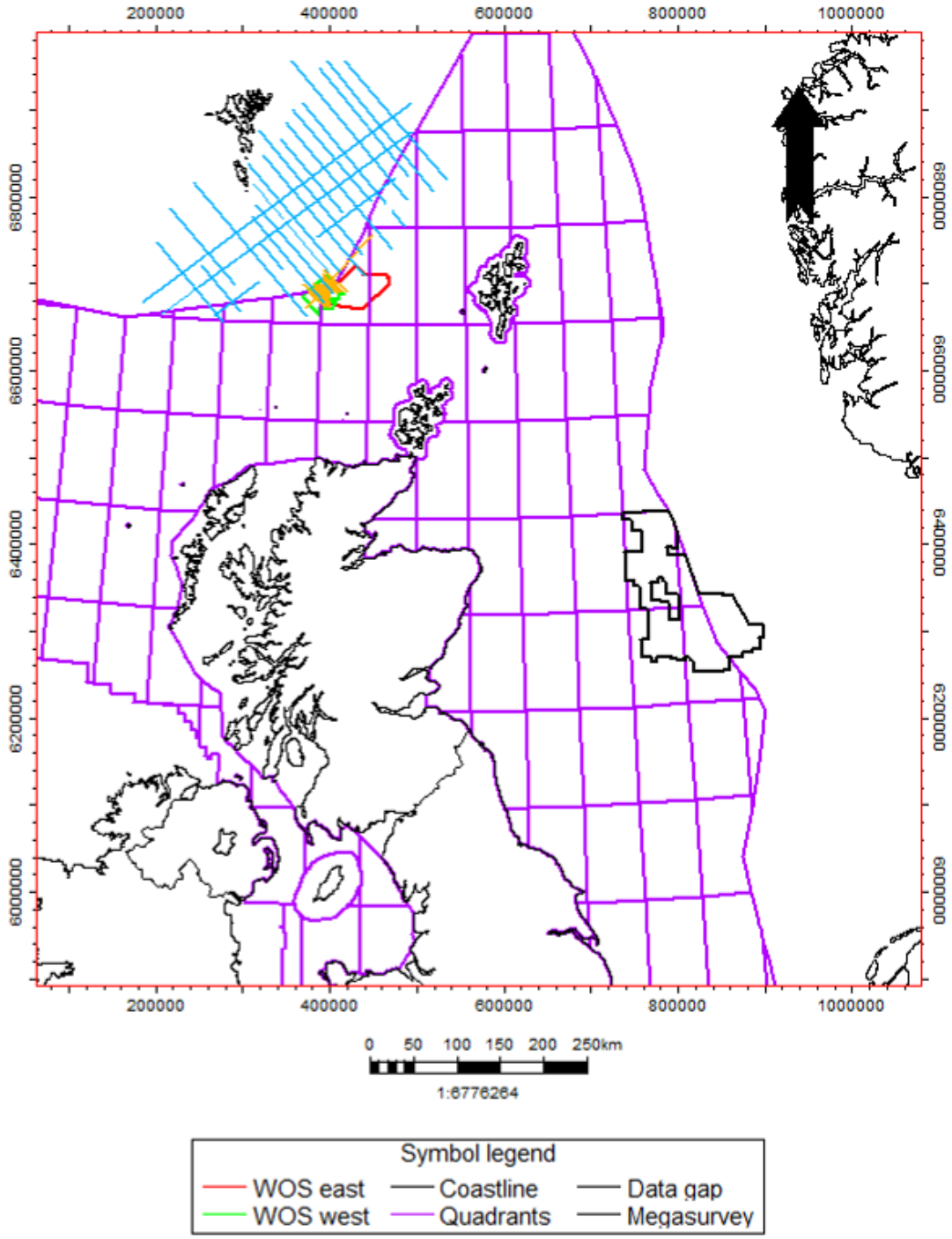

Figure 1.6: offshore 3D and 2D seismic datasets utilised in the study.

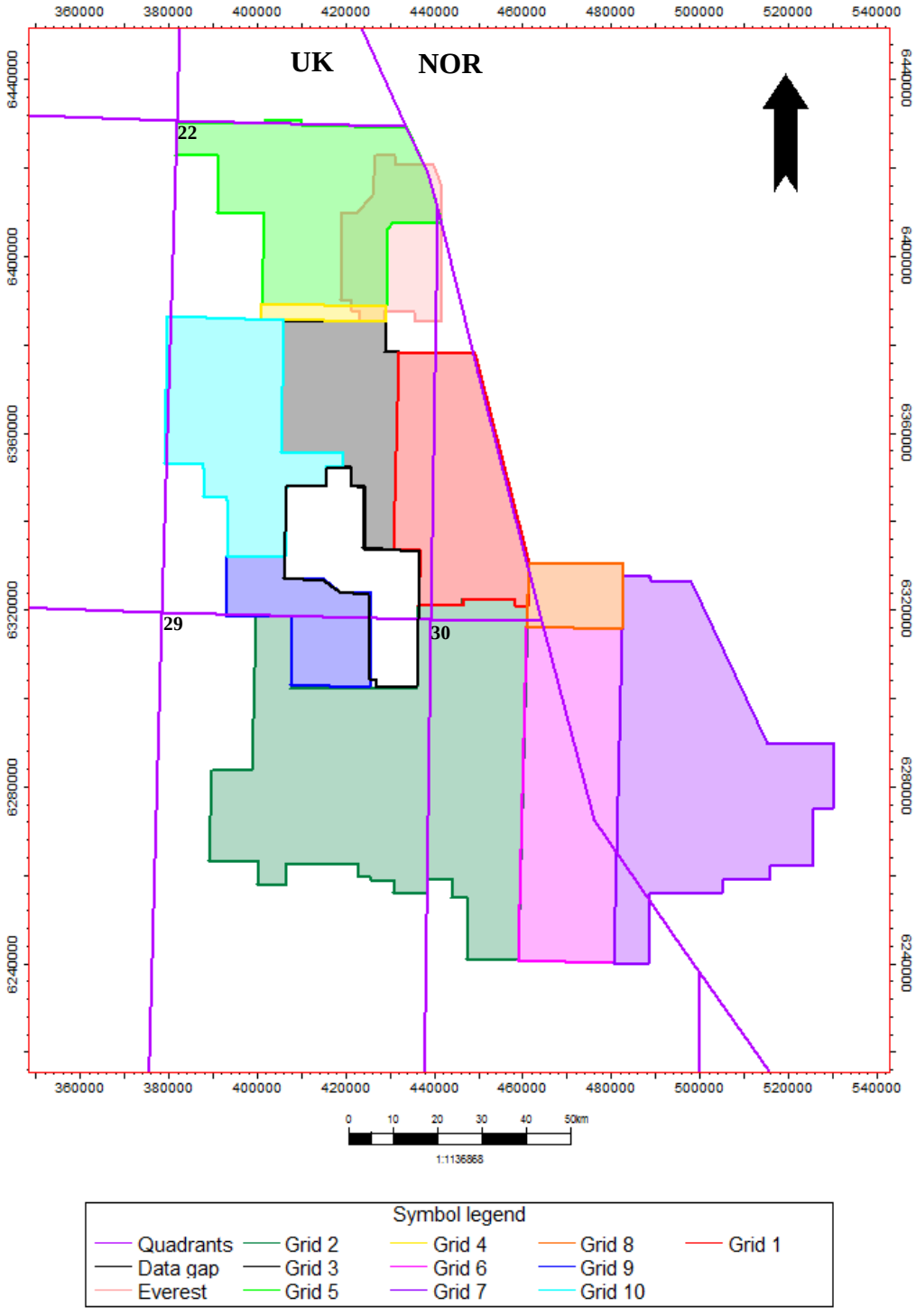

Figure 1.7: Central North Sea 3D survey split over 11 grids.

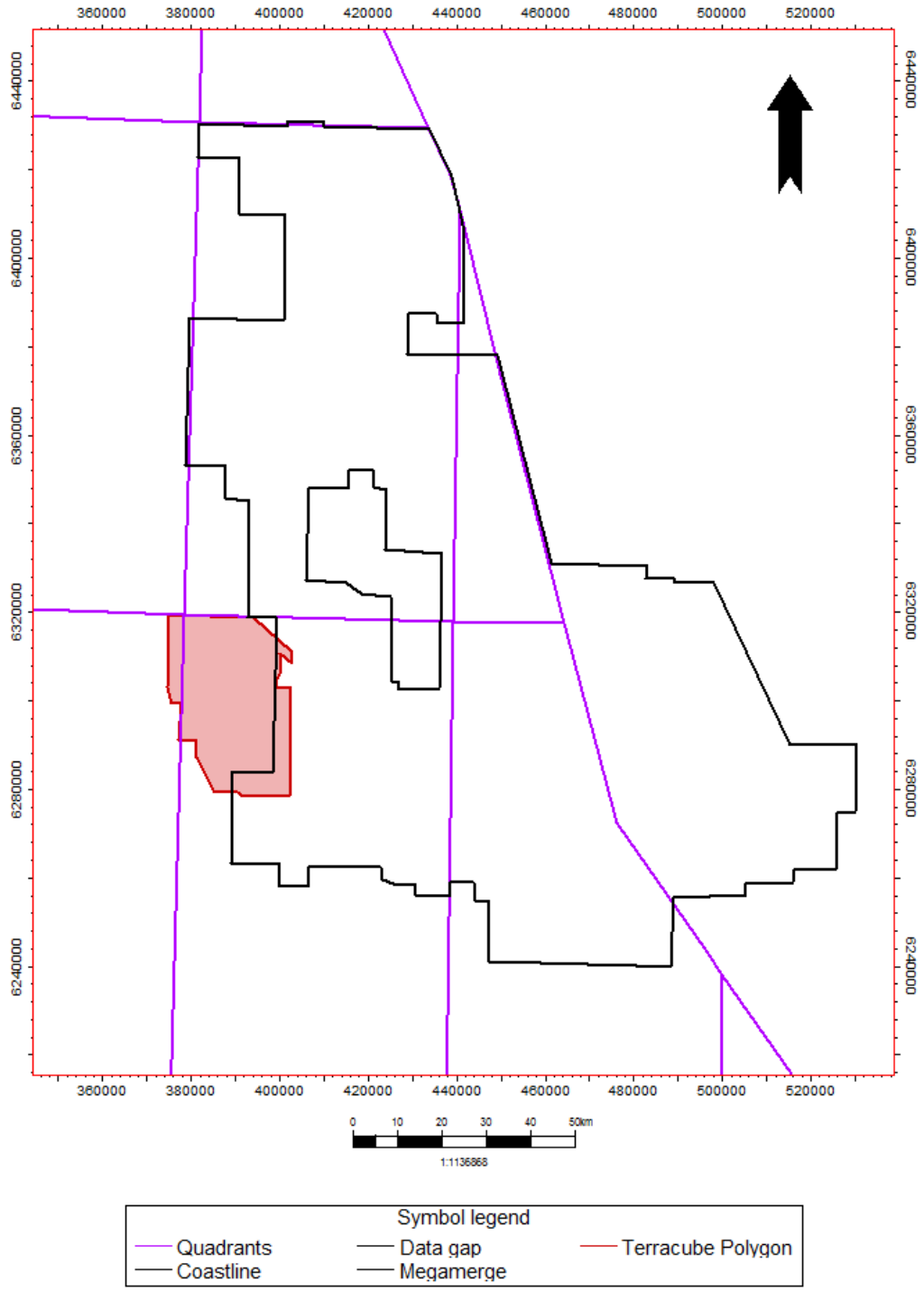

Figure 1.8: First Oil Terracube dataset over the Western Shelf.

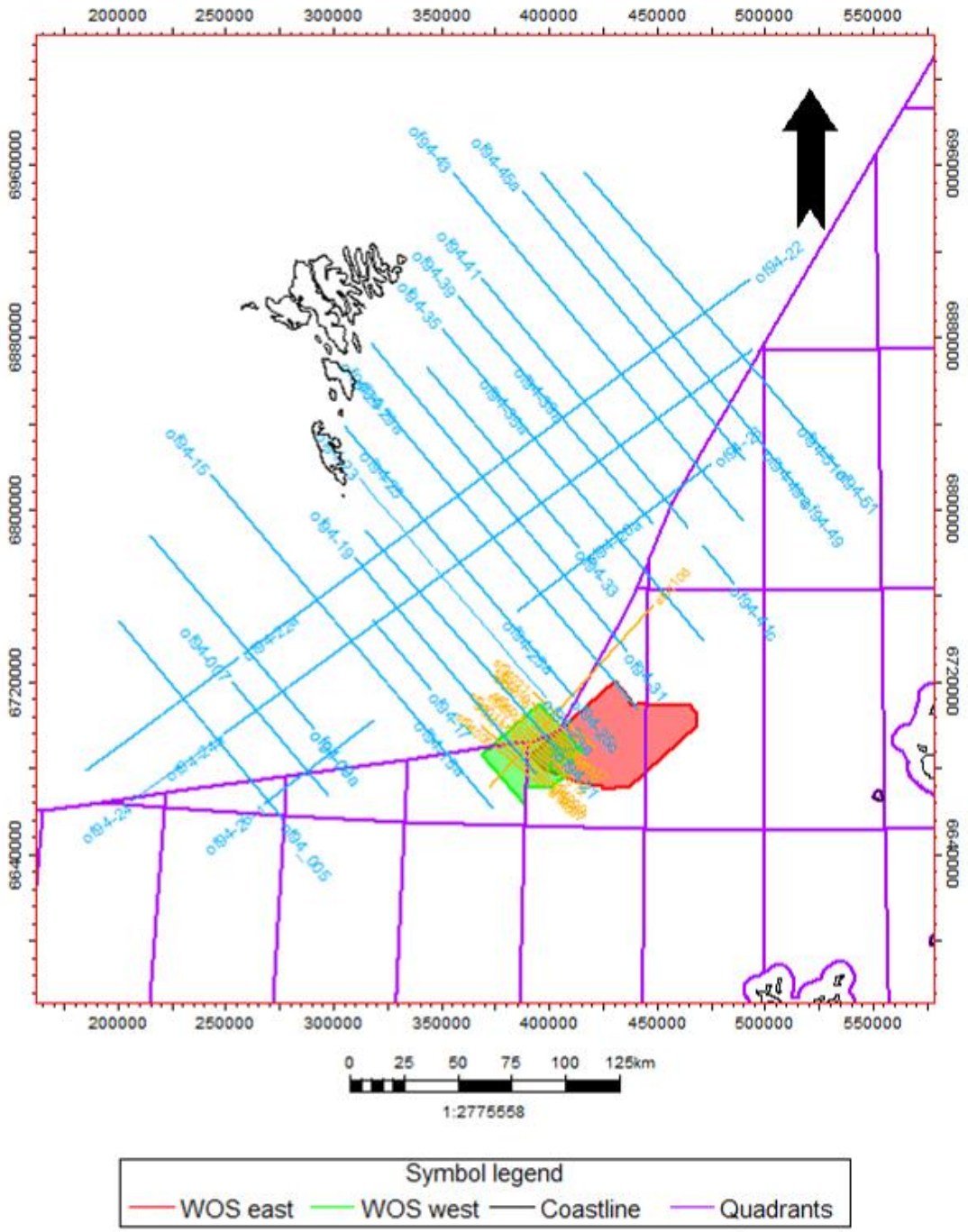

Figure 1.9: 2D and 3D datasets from the Faroe- Shetland Basin.

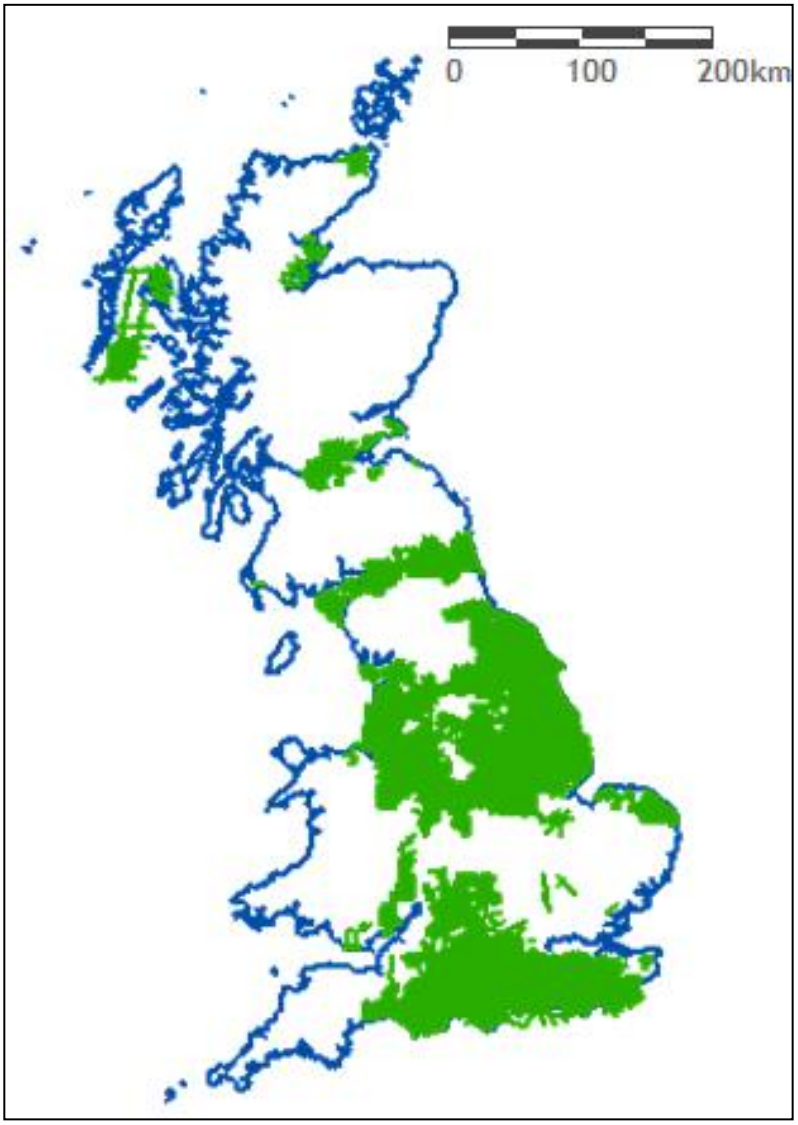

Figure 1.10: 2D seismic data available as printable online images from the UK Online Geophysical Library website or in electronic format.

1.1.1 SEISMIC ACQUISITION AND PROCESSING

Seismic data such as that shown in the example in Figure 1.11 provides a snapshot of the subsurface by imaging contrasts in the properties of rock units of different lithology or chemical composition.

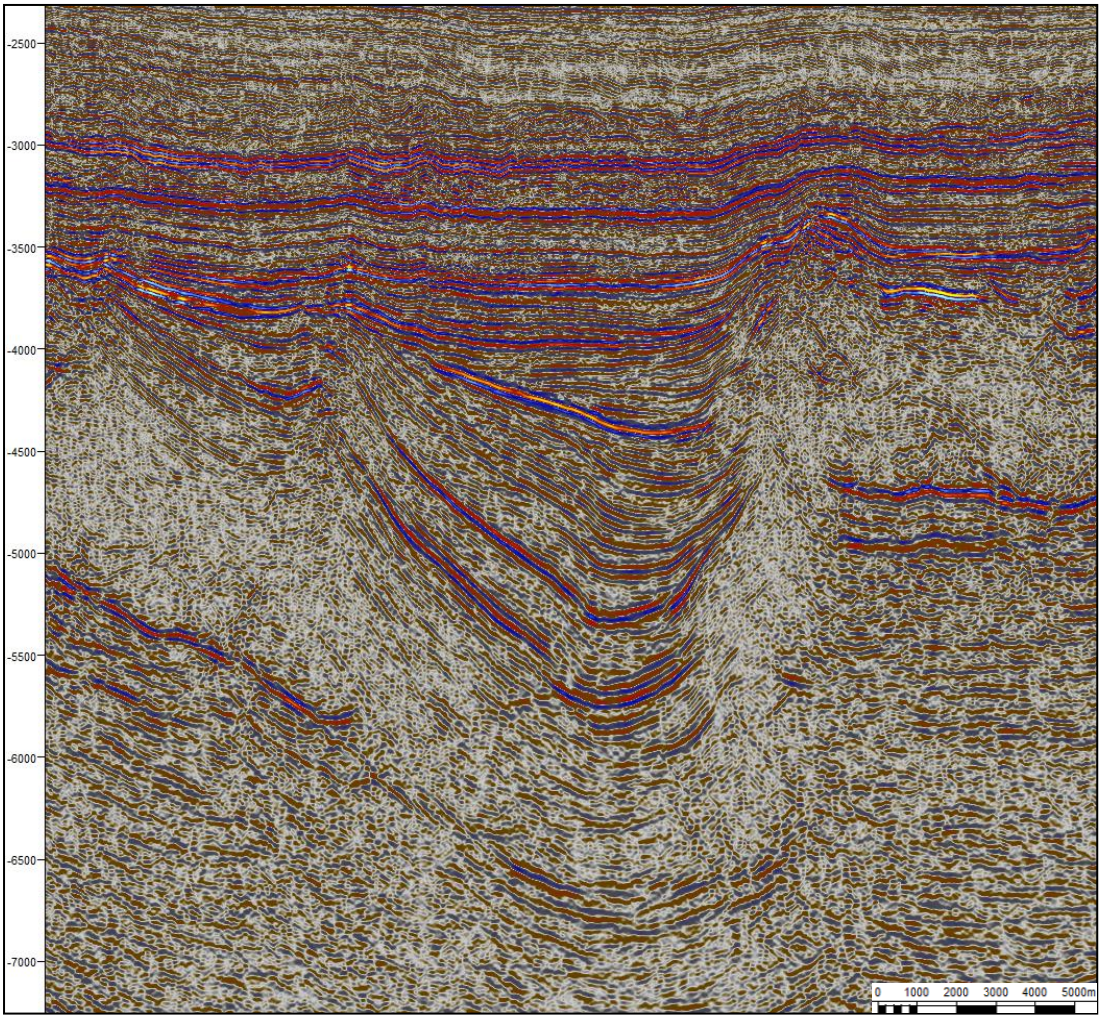

Figure 1.11: A typical seismic line in the dataset.

Seismic data is acquired by transmitting sound waves through the sub-surface from a seismic source, typically an airgun in marine surveys, and recording them as they are reflected back to special receivers. Wave speed is governed by the acoustic impedance of the medium through which it travels and when a wave encounters an interface between two rock types with differing acoustic impedances some of the wave is reflected back and is picked up by the receivers.

An event on a seismic section or within a 3D volume is thus formed by reflection of a wave from the interface between two different geological units, resulting from an acoustic impedance contrast due to a change in rock density, velocity or both. The magnitude of the reflection coefficient indicates the amount of contrast between two lithologies. By drawing a stick or spike of a magnitude equal to the reflection coefficient at the depth of every interface in a sequence, a simplified seismic trace can be generated. Ideally the reflection would form a perfectly sharp spike but the realities of interference and lithological inconsistencies (for an in-depth description of the uncertainties associated in production of the seismic wavelet see (Sheriff et al. 1995) mean that the contrasts are represented by a more gradational wave (Figure 1.12).

The raw waves are replaced by troughs and peaks shaded by appropriate contrasting colours usually dictated by interpreter choice. Typically colours used in Petrel are red for a positive loop and blue for a negative loop or trough and the intensity increases with amplitude. Other software packages such as Kingdom use different colours in their default settings, usually red and black. Other colour combinations can also be

used, black and white is useful for interpretation of poorer quality seismic, salt structures or deep reflectors and is utilised in this study where required.

Each geological interface is represented by a coloured, undulating and often discontinuous ridge across the section and can be interpreted and put into its stratigraphic context in specially designed software packages.

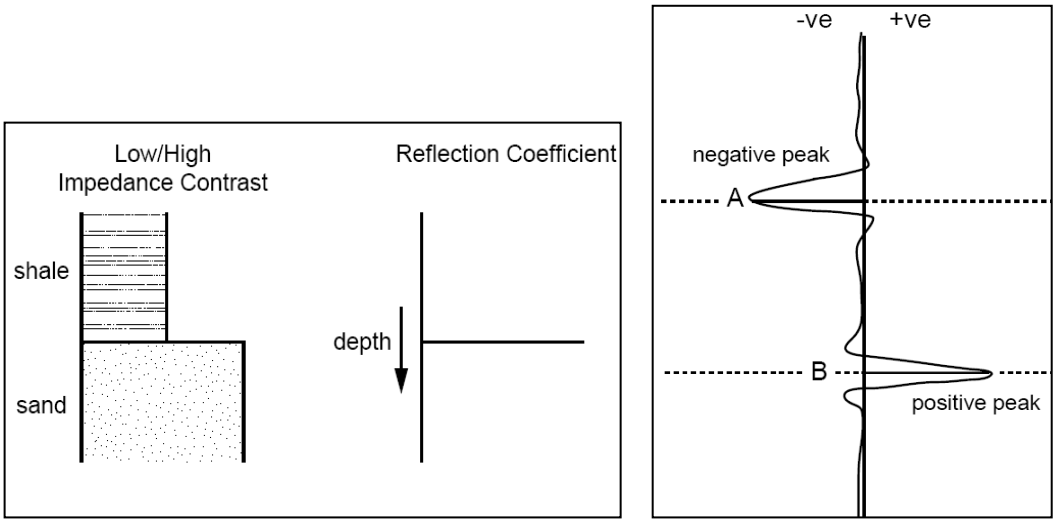

Figure 1.12: Idealised and actual (L-R) shapes of anomalies associated with impedance contrasts in geological materials.
Image after (Rider 1996)

In this study, the 3D seismic data has been interpreted using the interpretation software package Petrel licensed by Schlumberger and the 2D data using the software package Kingdom licensed by SMT , mounted on machines housed in the seismic lab facility located in the Grant Institute at the University of Edinburgh. The software allows mapping of facies which can be assigned to different time periods and depositional regimes, allowing us to build up a picture of the geological evolution of an area.

The vertical axis on a seismic section (Figure 1.13) is in two-way travel time (TWTT) in milliseconds (ms) - that is, the time taken for the waves to travel down from the seismic source to the geological interface and back to the recorder. It is also possible to make a conversion to depth using estimates of velocity (Depth = 0.5* Velocity x TWTT) made during processing along with well-calibration tie points from wire line logs to help give a firmer measure of the thickness and velocity of the rock layers. The seismic interval velocities can be integrated to give a velocity estimate at any depth in the well. Uncertainties can be fairly high when converting time images to depth as there can be unexpected lateral lithological variations (for example, a facies change from shale to limestone), missed compaction trends (due to differential burial), or unidentified high velocity materials (common in the North Sea due to the common presence of salt and volcanics).

The horizontal axis of the section refers to the cross-line direction; this relates to the distance along the direction that the survey has been shot. With 2D seismic sections this is a single line along which the data was acquired (Figure 1.14). In a 3D seismic

volume, the horizontal direction perpendicular to this (out of the plane of the paper) would be referred to as the inline direction (Figure 1.15)

.

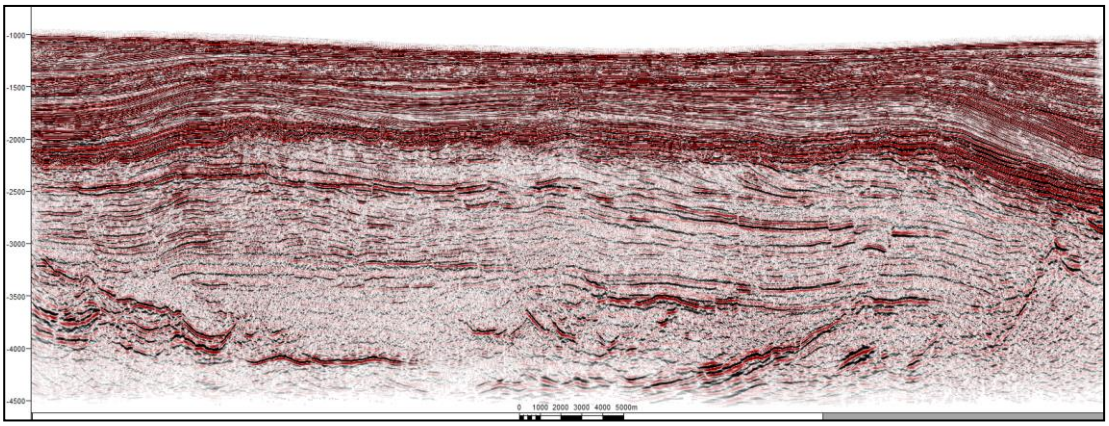

Figure 1.13: An example of a seismic line from a 3D volume showing the TWTT in milliseconds displayed on the vertical axis

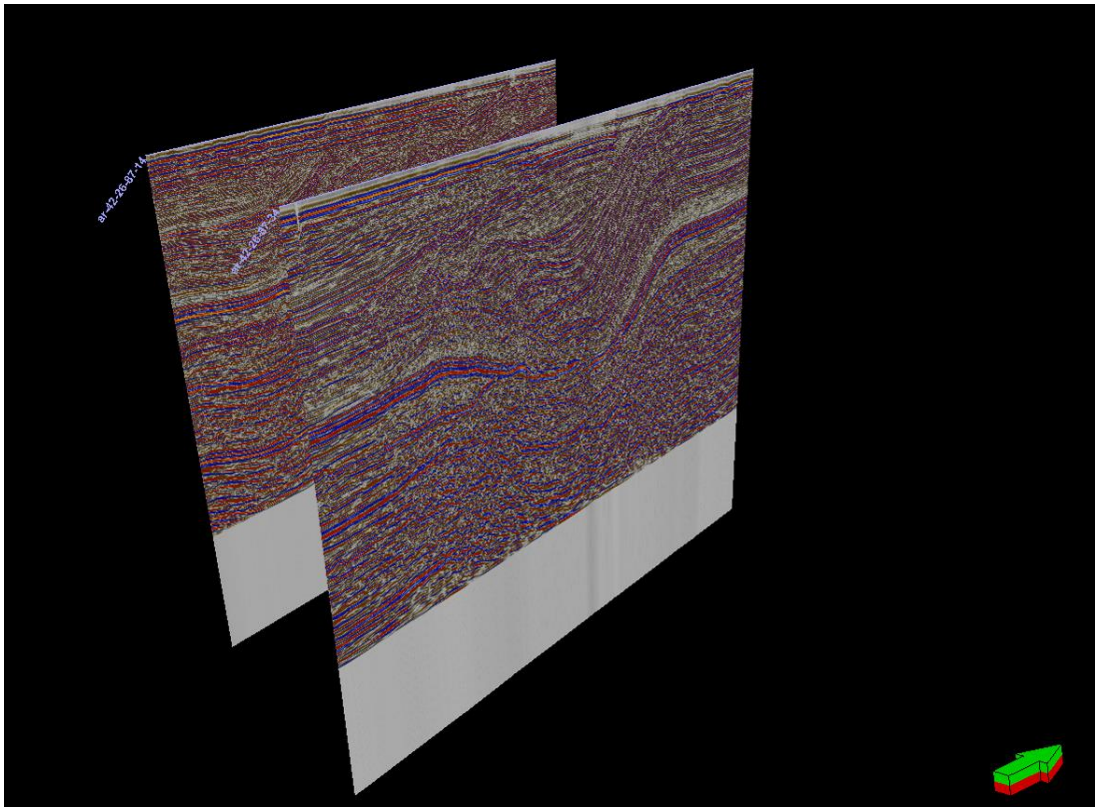

Figure 1.14: An example of two 2D seismic lines.

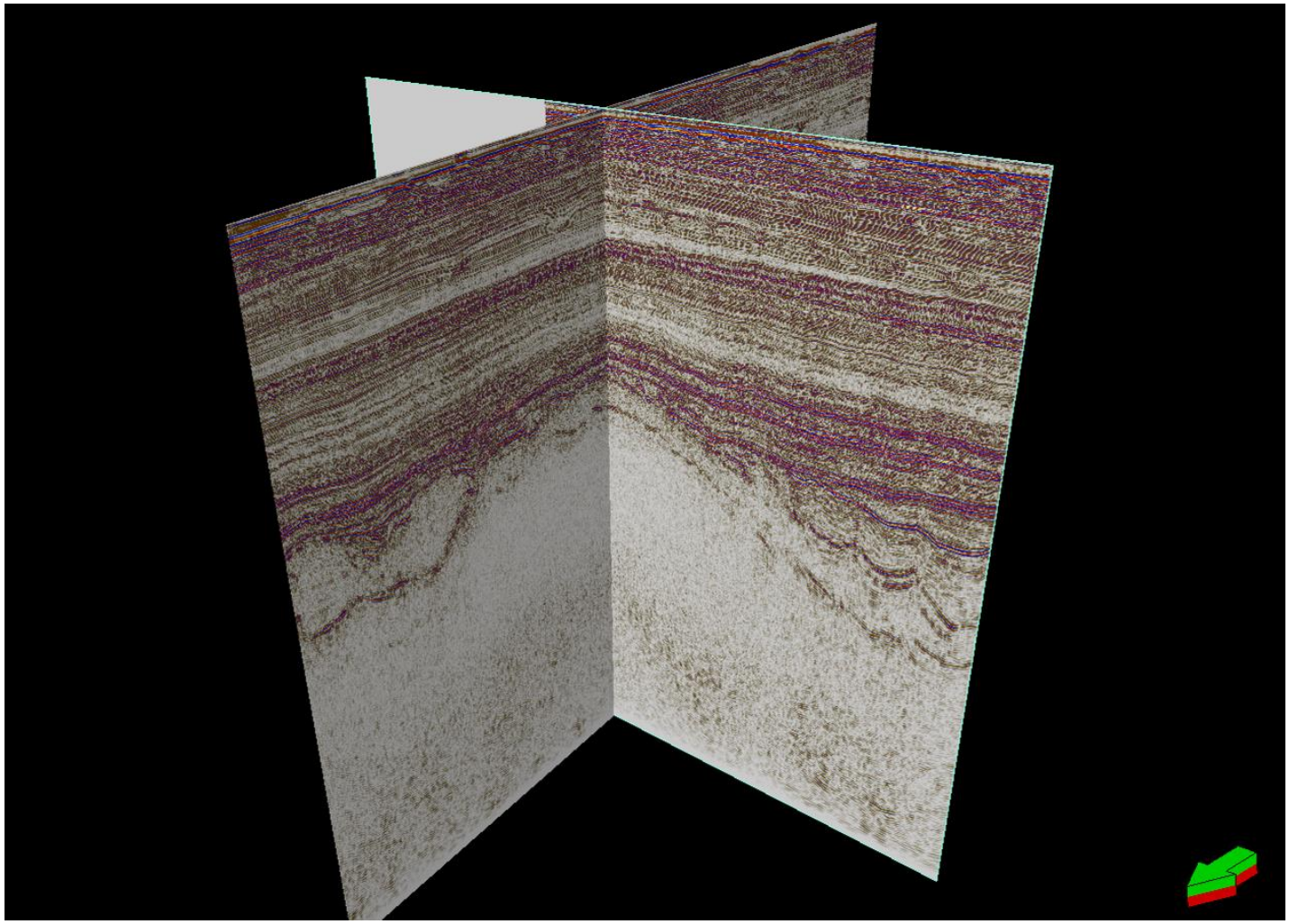

Figure 1.15: An inline and crossline within a 3D seismic volume

Well control can be added to the seismic 3D cube or 2D line to aid interpretation by adding known formation tops to the project which act as marker points allowing the correct surface to be identified.

Well data can also supply higher resolution data such as information on small-scale sedimentary features which seismic data cannot image. The resolution of seismic data is important to consider as it controls the ability to distinguish separate features. Called 'tuning', it defines the minimum distance between two features so that the two can be defined separately rather than as one and thus limits the amount of stratigraphic detail which can be extracted from seismic data.

The generally accepted limit lies at ¼ wavelength (Rayleigh Criterion) due to the fact that in thin beds the top and bottom reflectivity spikes are very close together and as they become thinner, they interfere with one another causing the amplitude of the signal to increase to a maximum at $\lambda/4$ as the interference effects reinforce one another (Figure 1.16) (Badley 1985; Gochioco 1991). Below this bed thickness, the seismic amplitude decreases linearly until eventually beds taper to below the resolvable limit of seismic (Figure 1.17).

There is a practical limitation in generating high frequencies that can penetrate large depths however, as the earth acts as a natural filter removing the higher frequencies more readily than the lower frequencies therefore, the deeper the source of reflections, the lower the frequencies we can receive from those depths and the lower resolution we appear to have (Emery et al. 1996). The importance of this is evident

when we calculate the thickness represented by ¼ wavelengths. With reflector velocity V and wavelet frequency f, the ¼ wavelet is represented by V/4f. Shallow reflectors are characterised by lower velocities and higher wavelengths e.g. 2000m/s, 100Hz so the ¼wavelet thickness is 5m. Very deep reflectors are characterised by higher velocities and lower wavelengths e.g. 5000m/s, 20Hz making the resolvable limit 62.5m.

These are model examples however, and the resolution of any particular seismic volume is unique and must be calculated. For the available seismic volumes the dominant frequencies ranged from 15-40Hz giving a resolution of 10-33m at 1000m where checkshot velocities ranged from 1800-2000m/s. The resolution decreased to 28-75m at 4000m where checkshot velocities were more variable but averaged at 4500m/s.

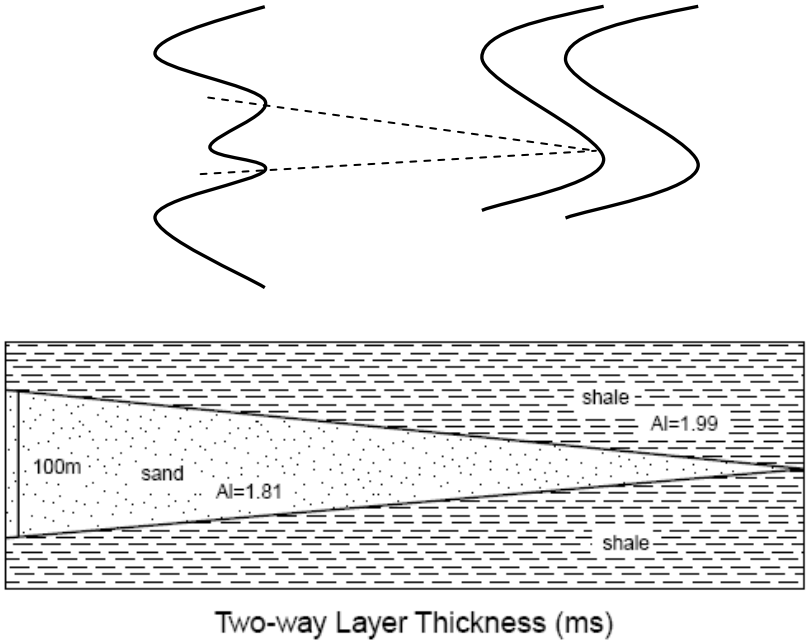

Figure 1.16: Interference of top and base reflectors from a thin bed.
When the bed is thick, the top and base are resolvable but as it thins the top and base reflectors move closer and interfere, with the maximum amplitude occurring when this is constructive at 1/4λ. This is known as 'tuning'.
AI= acoustic impedance
Redrawn from (Badley 1985)

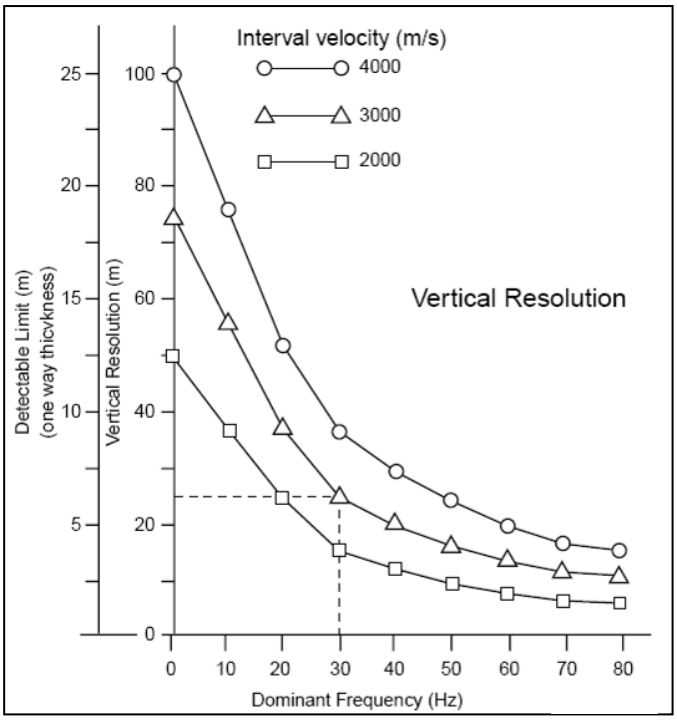

Figure 1.17: Average vertical resolution of seismic data**.**
Note: A bed can be seen on the seismic even though the top and base of the bed are not actually visible. Seismic detection of a bed does not require imaging of the top and base of beds, but simply that the signal rises above the general noise level. It is generally accepted that detection can occur at a limiting thickness of λ/16. Therefore, if the impedance is sufficiently large then detection might be possible for beds ranging from 2 to 10m**.**
Modified after (Heriot-Watt University 2007)

1.1.2 SEISMIC INTERPRETATION

Seismic data can be interpreted by identifying the reflector which corresponds with a particular acoustic impedance contrast, resulting from a change in density, velocity or both. Interpretation of reflectors, calibrated with well data through use of synthetic seismograms and check shots along with biostratigraphic sampling of cores or cuttings permit a robust correlation of horizons through successive seismic lines and geological time periods. Typically interpretation of a 3D seismic grid would begin with calibration of the well data followed by interpretation of the crossline and inline which exactly cut the well path (Figure 1.18). On a 2D grid it would begin with the line closest to the well. Reflectors would then be interpreted from the well and extrapolated to either side of the grid. If several wells exist, arbitrary lines can be created which penetrate all of the well paths and picks can be tied at several points along the section. Once these lines and sections are interpreted any other line intersecting them will be marked in the place where the interpreted horizon is placed creating a further tie point which can again be extrapolated. In this way a horizon can be traced through a seismic survey. Surfaces corresponding to the mapped horizon can be created from the interpretation and isochrons between them can also be generated. These allow the structure of the area to be seen and models of the geological evolution can then be made. Secondary outputs can be created in the form of dip angle maps to look in more detail at fault trends and amplitude extractions which may indicate anomalies due to hydrocarbon or fluid accumulations or lithological variations.

However, simply picking horizons tied to well penetrations does not allow us to understand the structural evolution of an area unless the interpreter is aware of how these fit into the overall basin stratigraphy and structural history. Successful interpretation of a basin involves recognition of the changing geometries of seismic reflection packages caused by deformation events and the correlation of these with data derived from wells. In order to achieve this, a tectono-stratigraphic method was utilized in this study. The basis of the tectono-stratigraphic method relies on the use of integrated geological and geophysical data to define the sedimentary record in terms of depositional sequences linked to major tectonic events. Each depositional sequence identified by this method is essentially a single basin entity, possessing a basin margin, depocentre and internal facies pattern (Hubbard et al. 1985; Hubbard et al. 1985). The boundaries between sequences have no specific lithology and are defined on the basin of unconformities and patterns of reflector terminations. This avoids one of the major problems with the conventional approach to interpretation where the same horizon can have different ages in different areas and similar lithologies of different ages are mistakenly grouped (Figures 1.19 and 1.20).

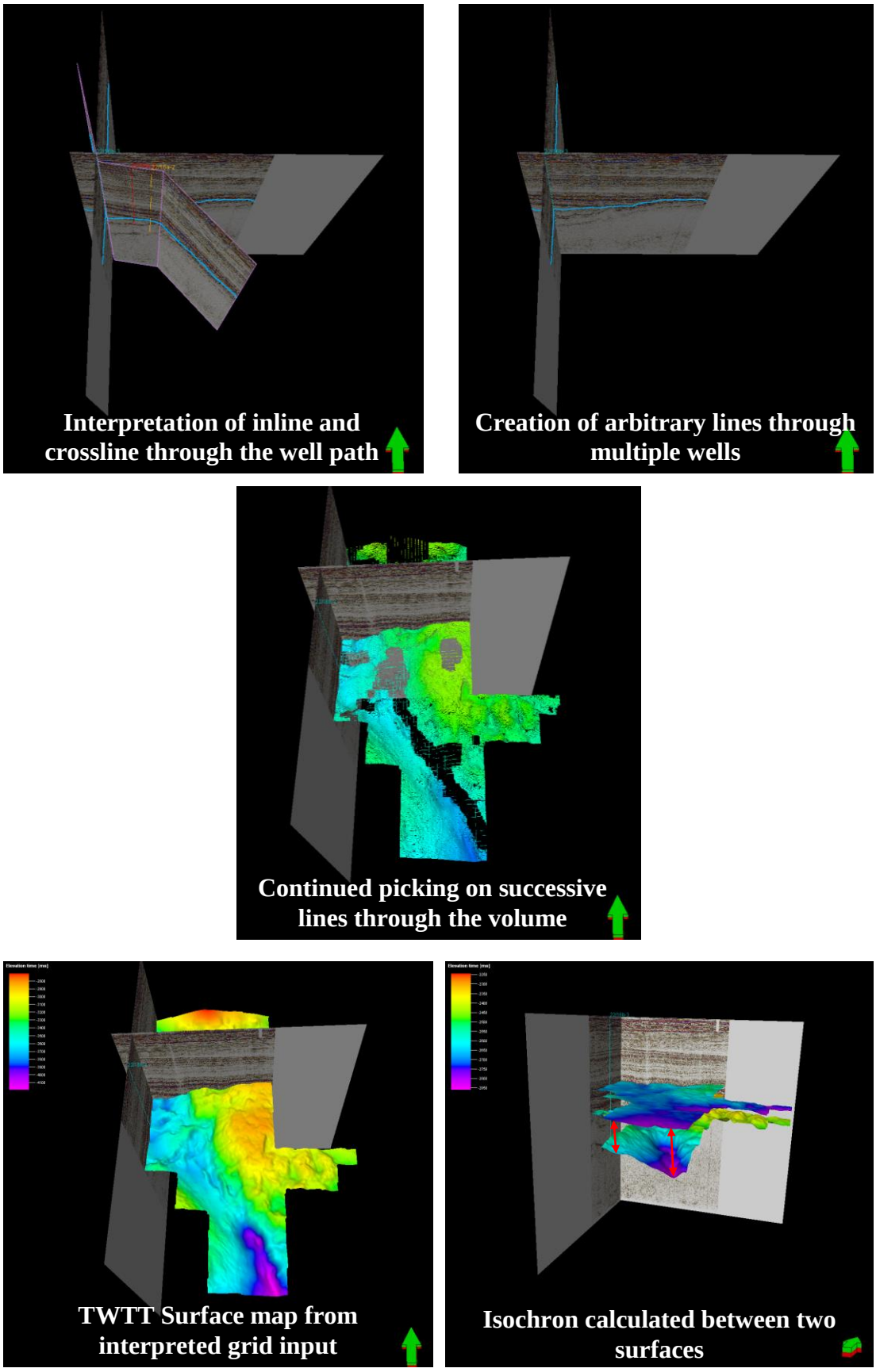

Figure 1.18: Workflow for seismic interpretation.

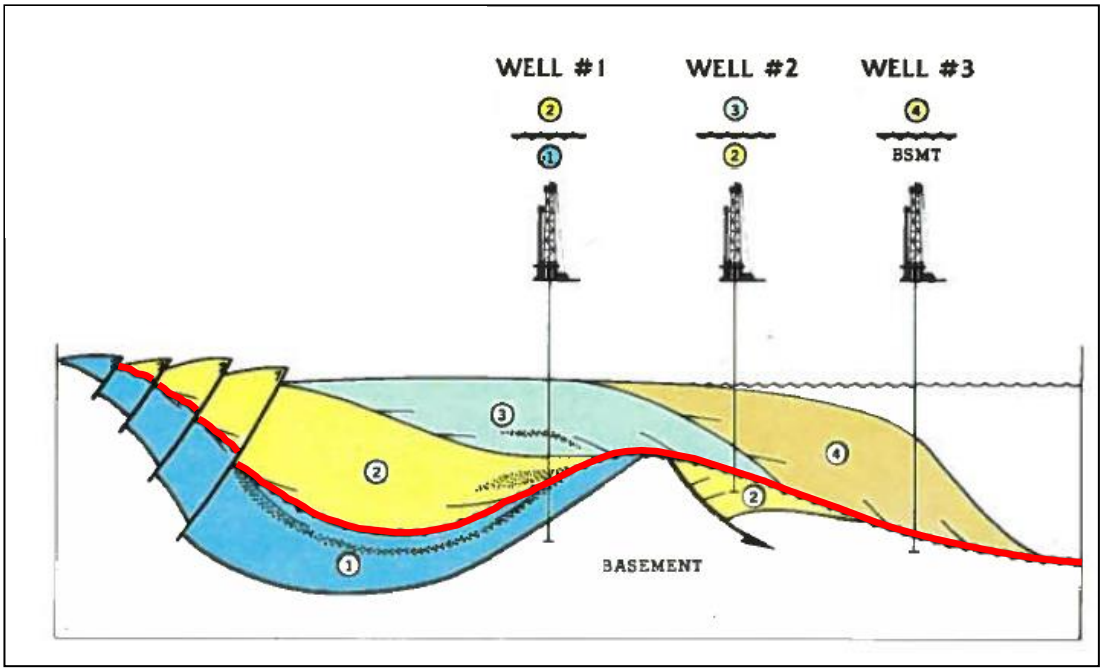

Figure 1.19: Cartoon depicting tectono-stratigraphic sequences defined by characteristic seismic reflector terminations. One of the problems posed by conventional methods of interpretation is illustrated. The same red horizon represents an amalgamation of unconformities and is therefore different ages in each of the wells which penetrate it.
Image modified after (Hubbard et al. 1985)

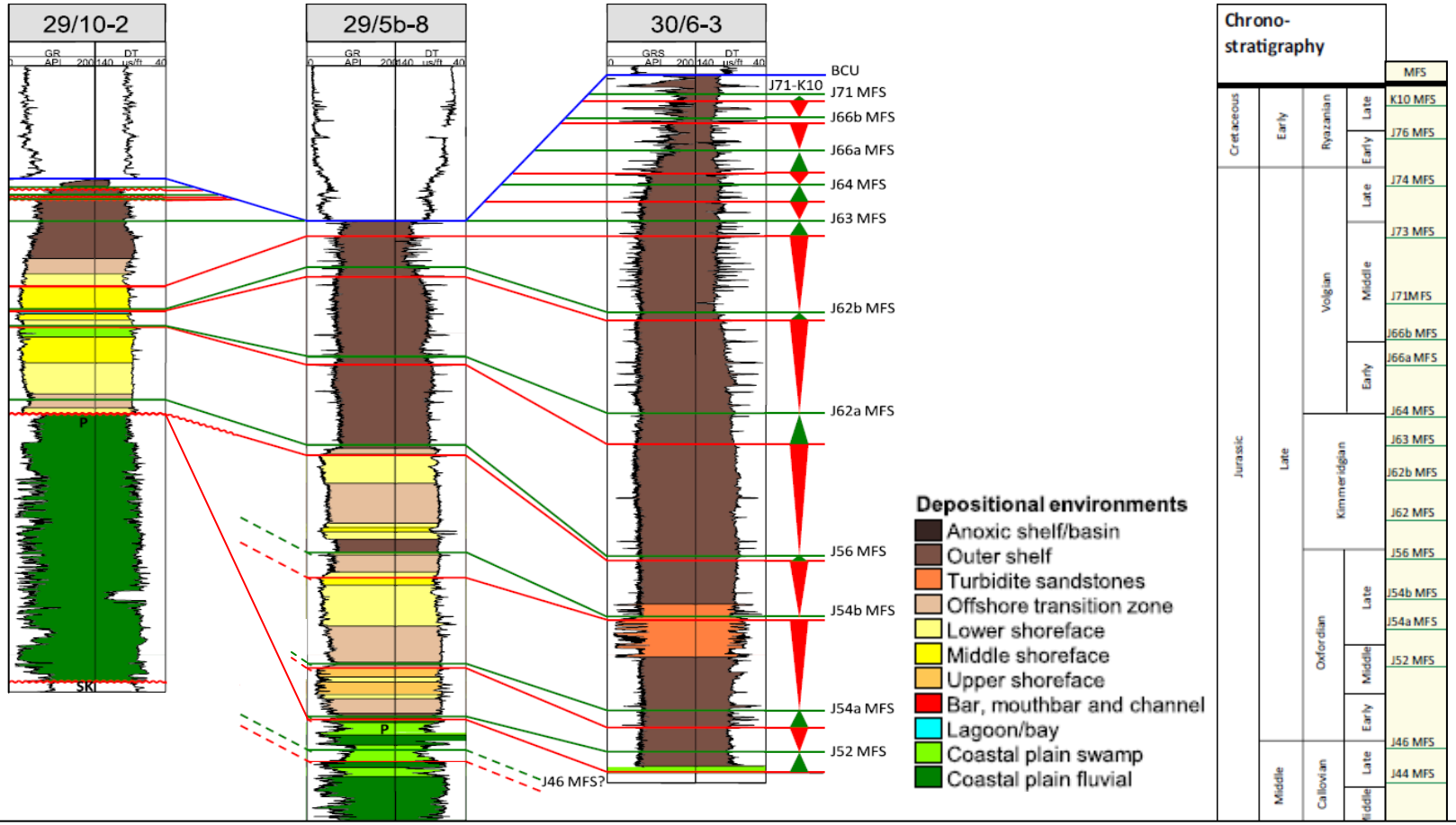

Figure 1.20: A well correlation panel of the Upper Jurassic sequence in Central North Sea sections illustrates another of the problems posed by standard interpretation methods. All of the sand units contained within the Late Jurassic of the Central North Sea are typically known as the 'Fulmar Formation' despite having different ages and depositional environments.

Images after (Sansom 2010)

Depositional sequences can be stacked into groups of related sequences, known as megasequences or sub-divided into sub-sequences (Figure 1.21). Megasequences represent major phases of basin evolution and those which are linked to major deformational episodes are known as Tectono- stratigraphic megasequences.

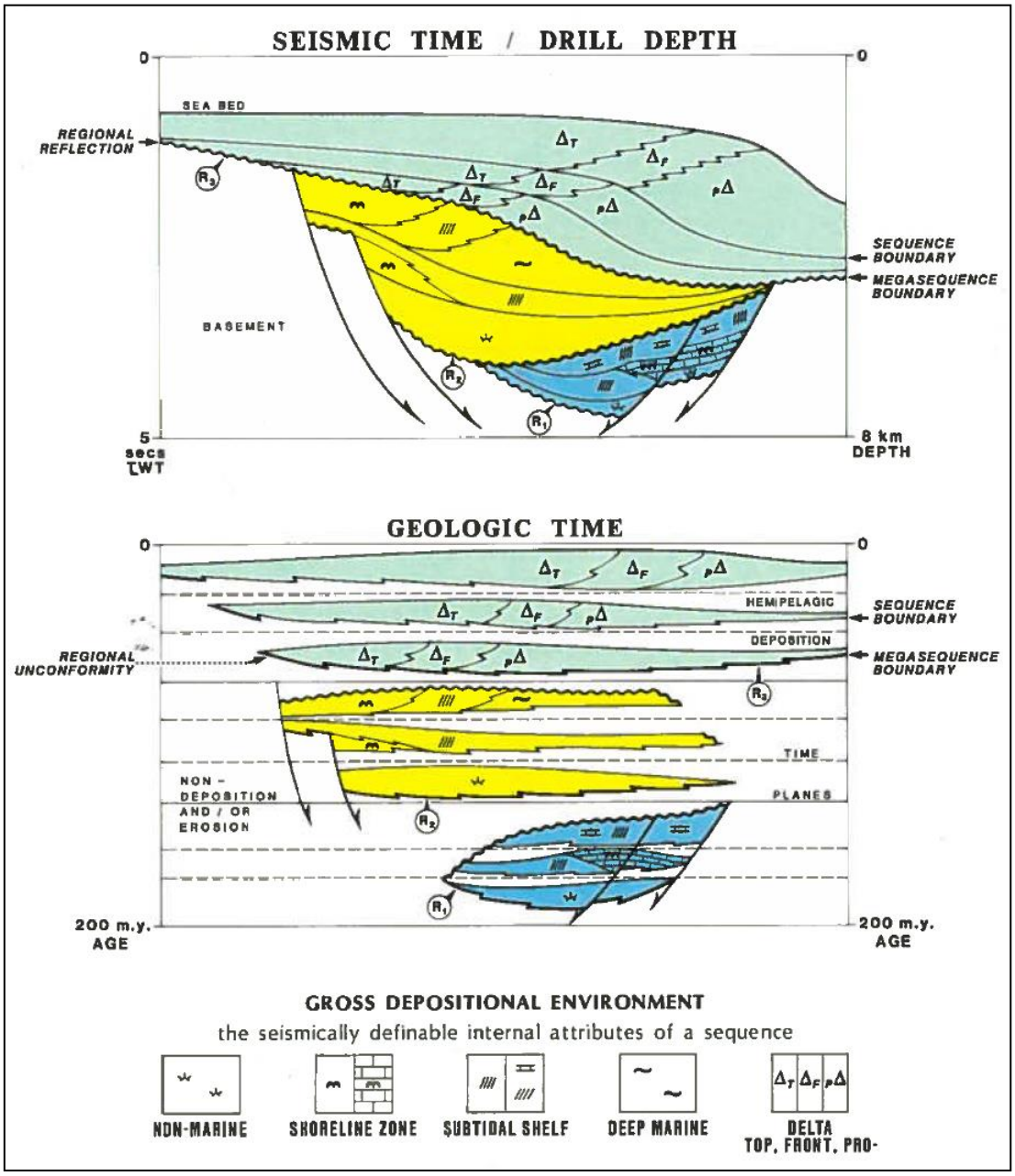

Figure 1.21: Cartoon showing megasequences R1, R2 and R3 and sequences within them defined by their depositional environment. Both seismic and geological time are illustrated.
Image after (Hubbard et al. 1985)

A tectono-stratigraphic megasequence corresponding with an episode of deformation can ideally be split into three main depositional sequences, a pre-rift (also known as a pre-kinematic) sequence deposited prior to deformation, a syn-rift sequence deposited during and a post-rift sequence deposited after deformation has stopped (Morley 1999). The criteria for recognising each of these episodes are,

1. Wedge-shaped reflections that expand towards a fault.
2. Angular unconformities.
3. Onlap of reflectors by those with a lesser dip.

Pre-rift sections may be recognised by their tabular nature but if more than one rift episode is superimposed upon another earlier one this may not be the case. Unconformities between pre and syn-rift sequences may occur on structurally elevated areas but pass into correlative conformities in lower parts of the basin. The main criteria for distinguishing pre from syn-rift sequences is therefore the thickening of the syn-rift package into faults moving during the deformation episode which creates wedge-shaped geometries which are not seen in the pre-rift section. Where syn-rift sections are thin, well data may be the only means of recognition.

The boundary between the syn- and post-rift sequences marks the end of the structural phase when tilted blocks achieve maximum relief. The boundary is usually unconformable with paleotopography onlapped by parallel post-rift sediments (Morley 1999) (Figure 1.22).

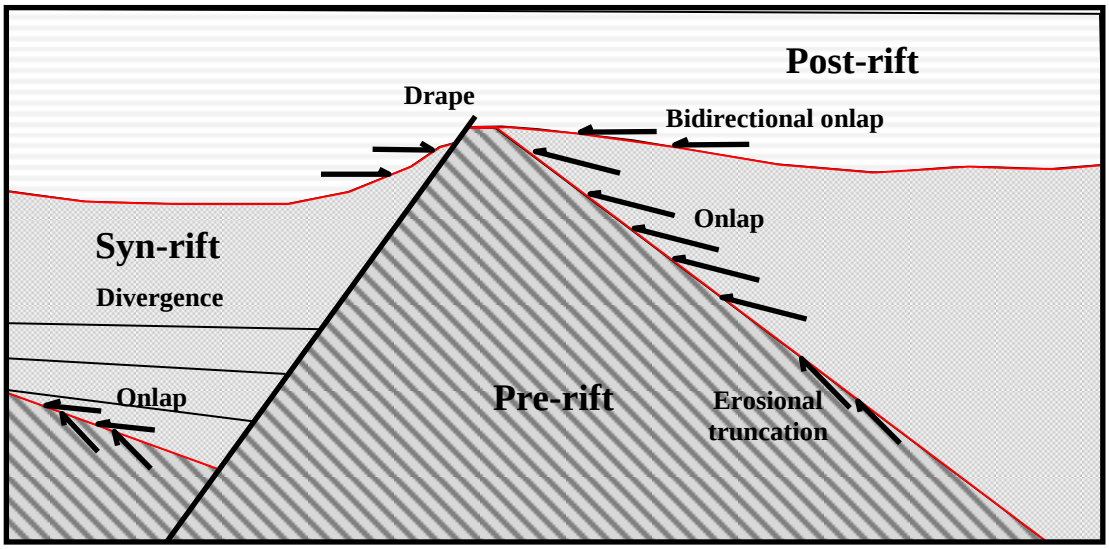

Figure 1.22: Model representation of the geometrical relationships between the 3 ideal sequences generated by a deformation event

The most obvious reflector packages in the Central North Sea which can be identified using these criteria relate to the tectono- stratigraphic megasequence associated with the Jurassic rifting episode which created the failed trilete rift system. The Triassic and beneath is the pre-rift sequence to this deformation event, the base Cretaceous-top Triassic represents the syn-rift and Quaternary-base Cretaceous, the post-rift sequence (Figure 1.23).

However, the Central North Sea has undergone several deformation episodes prior to and post-dating the Jurassic rifting event and in order to investigate these, additional sequences were interpreted. The oldest rocks consistently penetrated by wells in the Central North Sea are Permian in age. Sparse data from rocks older than this can be found and the pre-Permian geological history can be interpreted from preserved

sequences on the rift flanks and intra-basinal highs and correlation with onshore data. However, the oldest tectono-stratigraphic megasequence which can be fully mapped seismically represents a period of intra-continental rifting which occurred during the Triassic. The pre-rift sequence to this is the pre-Triassic succession, the syn-rift is represented by the Lower and Middle Triassic rocks and the post-rift includes all sequences of Upper Triassic age and younger (Figure 1.24). This tectono-stratigraphic megasequence is more difficult to interpret than the later one due to the effect of halokinesis which makes the sequence geometries differ from those expected from rift-related events. The structure of the thesis is split up on the basis of these two mapped tectono-stratigraphic megasequences termed Tectono-stratigraphic megasequence 1 (Triassic) and Tectono-stratigraphic megasequence 2 (Jurassic).

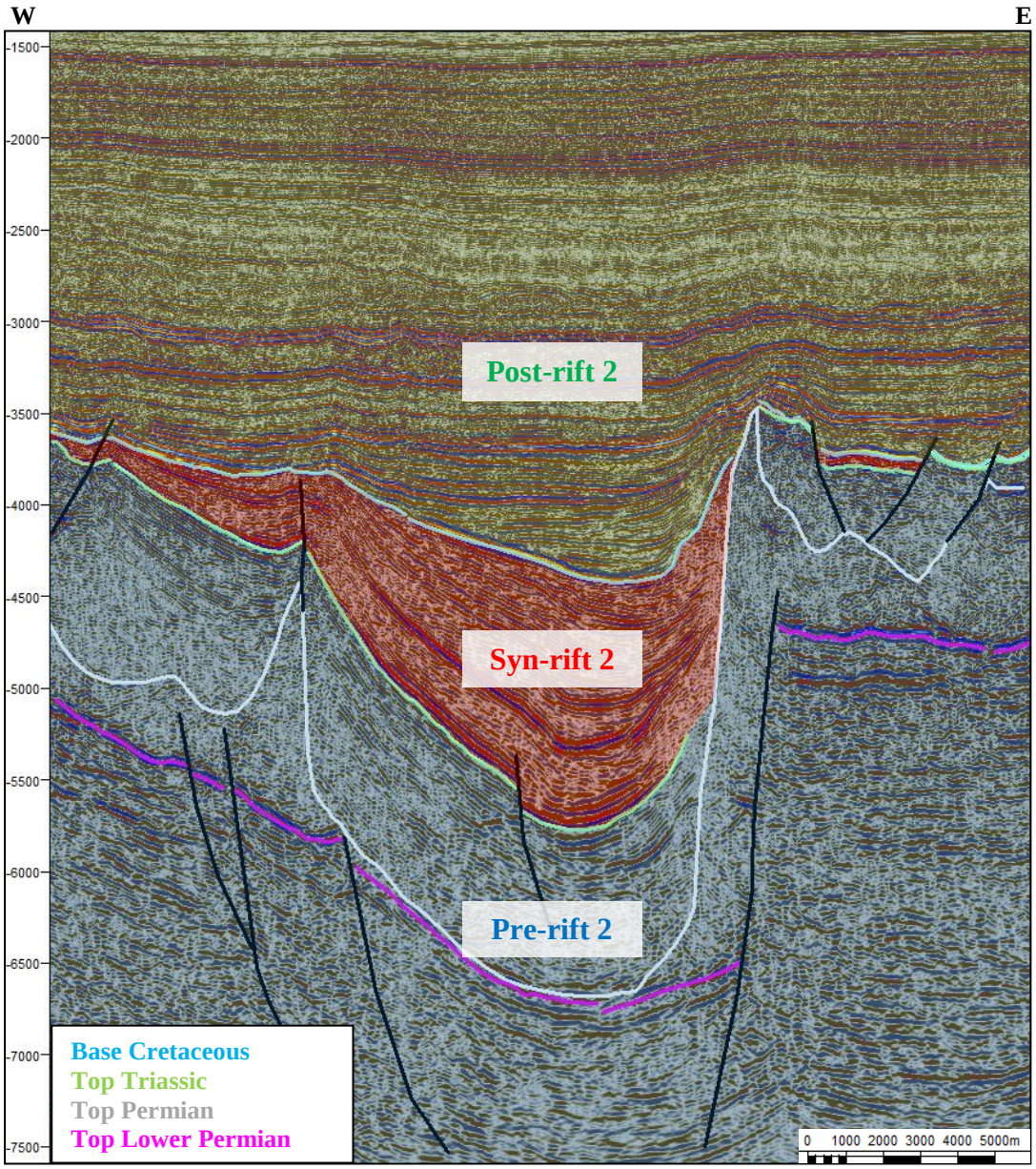

Figure 1.23: **Pre**, **Syn** and **Post**-rift packages of Tectono-stratigraphic megasequence 2 in the Central North Sea generated in response to the Jurassic rifting episode.

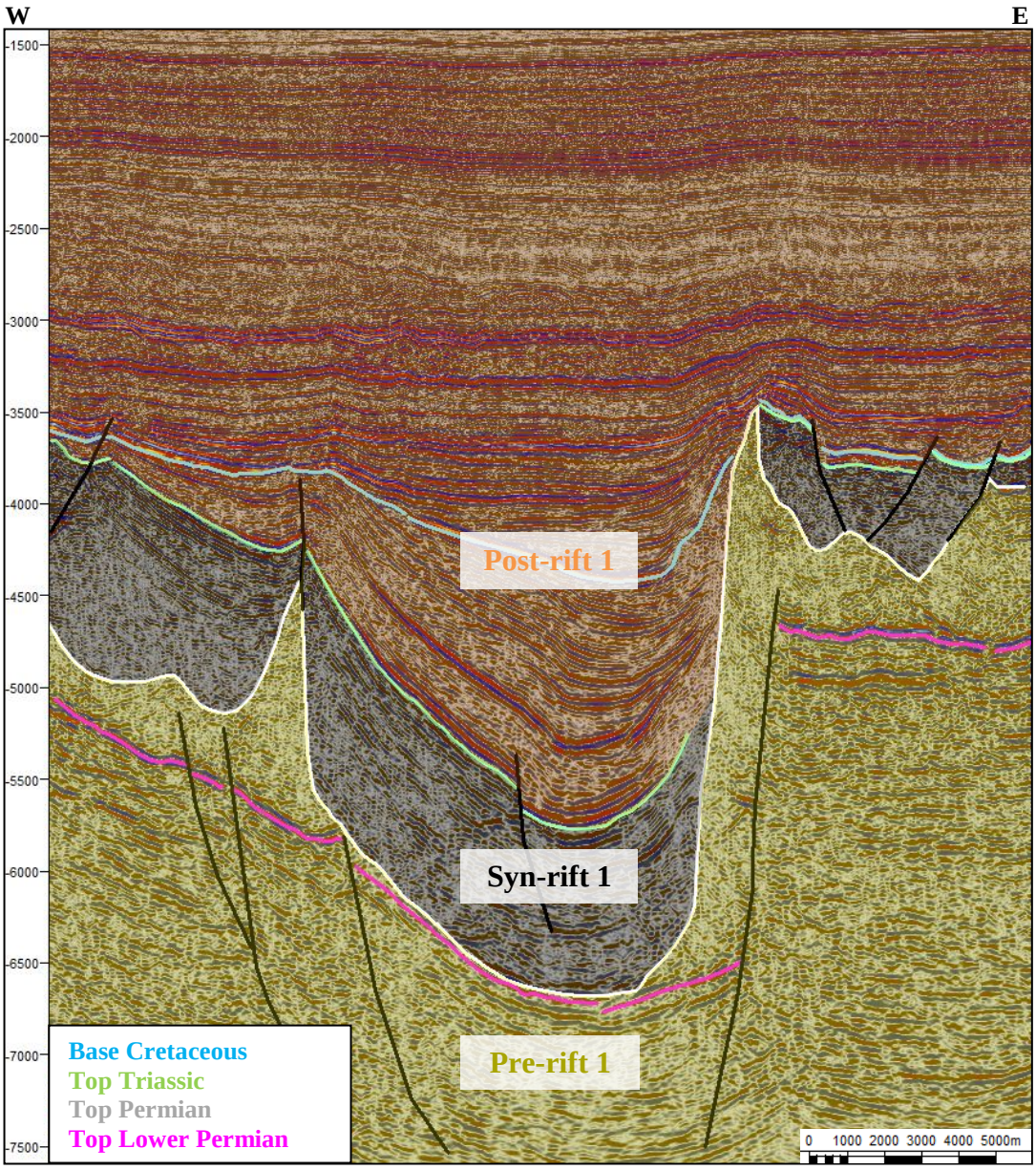

Figure 1.24: **Pre**, **Syn** and **Post**-rift packages of Tectono-stratigraphic megasequence 1 in the Central North Sea generated in response to tectonic events in the Triassic.

1.2 WELL LOG AND CORE DATA

Seismic data provides information on the acoustic impedance contrasts which occur between different rock types. Wells drilled into the subsurface, usually for the purposes of hydrocarbon exploration, provide information on what these rock types are through wire-line logs and core data. Wire-line logs are the result of the continuous recording of a geophysical parameter along a borehole (Rider 1996). They are generally recorded at the end of drilling, when the drilling bit is no longer in the hole.

There are a vast array of geophysical logs which are run including resistivity, density and neutron porosity but the most useful for this study is the Gamma Ray log which is measured in API units, usually on scales of 0-100/150.

Gamma ray logs record the natural radioactivity of the formation. Natural radioactivity occurs in all rocks and comes from three elemental sources- elements of the thorium family, elements of the uranium-radium family and the radioactive isotope of potassium ^{40}K (Adams et al. 1958).

The simple gamma ray log is a composite of all of the radioactive contributions but it can be split to create a spectral gamma log (Figure 1.25). These are useful as the elements have different affinities, and information on lithology and depositional environment can be inferred from the relative contribution of different elements. For

example, potassium can be instructive about the mineralogy of clays since most potassium is contained within illites while kaolinitic clays contain very little. Uranium is the most difficult of the three elements to link to depositional environment but it can be very useful for climatic or stratigraphic studies as its presence in abundance indicates a very unusual environment or a prolonged hiatus (Rider 1996).

Gamma ray logs can also be used for correlation as they are repeatable, not affected by depth and are always run. They can also help to discern the lithology of the rock units in wells they are run in. Lithology data is generated from three data sources, the first of which, data from well cores, is discussed in the section below. The other two sources are from lithological interpretation of the cuttings samples brought to the surface while the well is drilled and wire-line logs. Ideally, all of these data types would be utilized to determine the lithologies encountered in wells but coring is expensive to do and a good lithological interpretation can be based on the remaining two sources of data.

Interpretations of cuttings samples is done first, while the well is drilled and then this is substantiated by analysis of the wire-line log suites (Rider 1996). It is important to do this as certain lithologies such as unconsolidated sands and soluble evaporites are difficult to get to the surface for analysis. Each lithology such as sand or carbonate has its own characteristic gamma ray response, resistivity, density and all of these are measured and used together in a log suite to work out the lithologies encountered.

Gamma ray responses are useful in differentiating between sand (lower radioactivity) and shale (higher radioactivity) and can therefore show gross differences in grain-size.

All wireline logs used in this study are publically available and released through Schlumberger operated CDA datastore (CDA 2009)

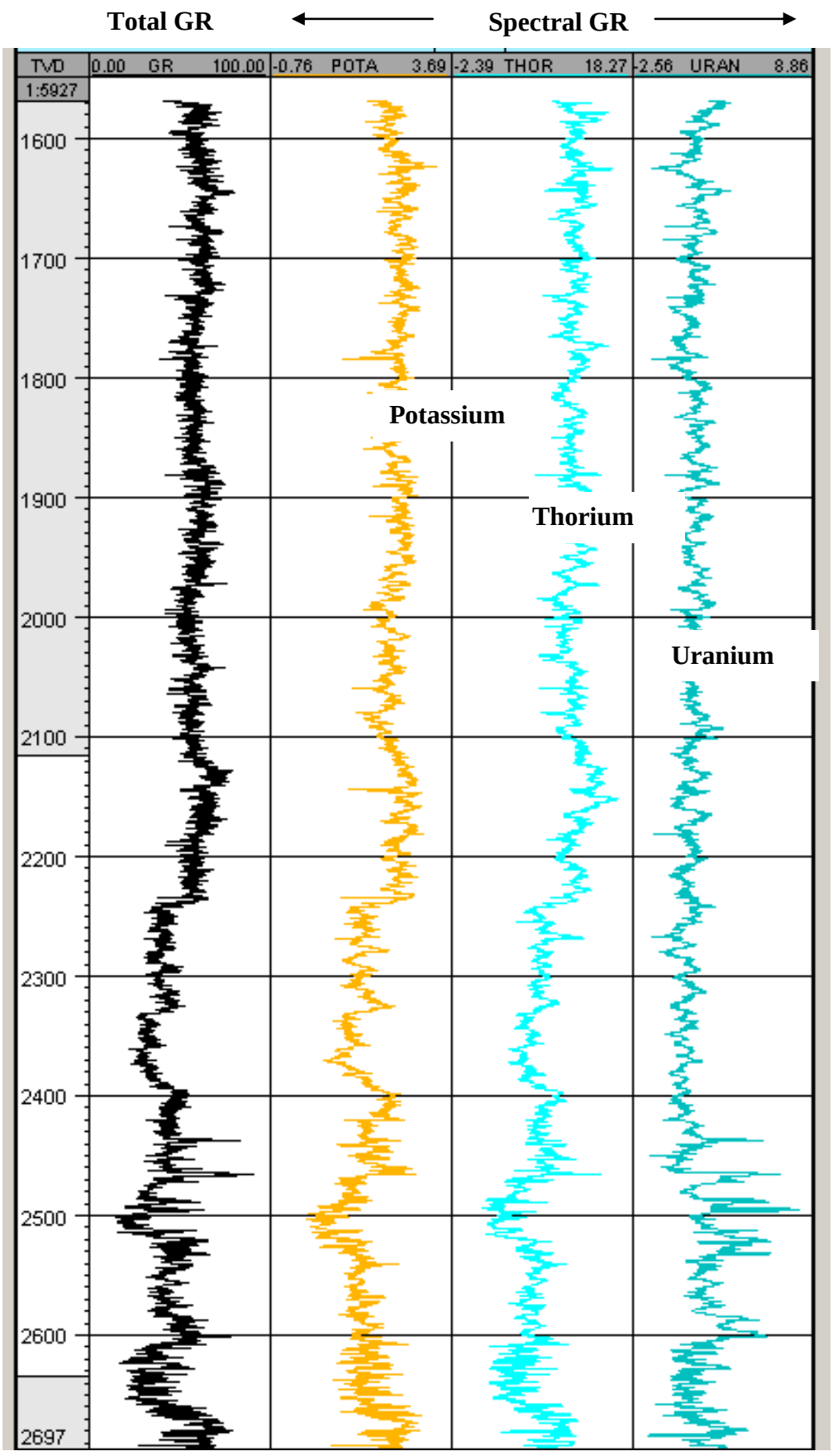

Figure 1.25: Example of a spectral Gamma ray (GR) log split into its 3 components

When wells are drilled for hydrocarbons, material from the sections of interest is often recovered in the form of a vertical slice of rock known as a core (Figure 1.26). Cores are necessary to provide true stratigraphic data to back-up the observations made on wire-line logs. They are also used to test the properties of the potential reservoir rock such as its porosity and permeability. Sometimes more detailed tests are carried out on core material such as mineralogical studies to determine the stratigraphic connectivity of the reservoir where other methods have failed. Such detailed analyses are very useful because they can show variables such as clay mineral types and abundances.

Lithological studies on cores can also be useful. For example, ash layers can be recognised and used as stratigraphic markers, pyrite nodules signifying reducing conditions can be noted as can indications of bioturbation. Disruption in cores can often indicate that some of the section is reworked or slumped and this can be considered when analysing for biostratigraphy or isotopes.

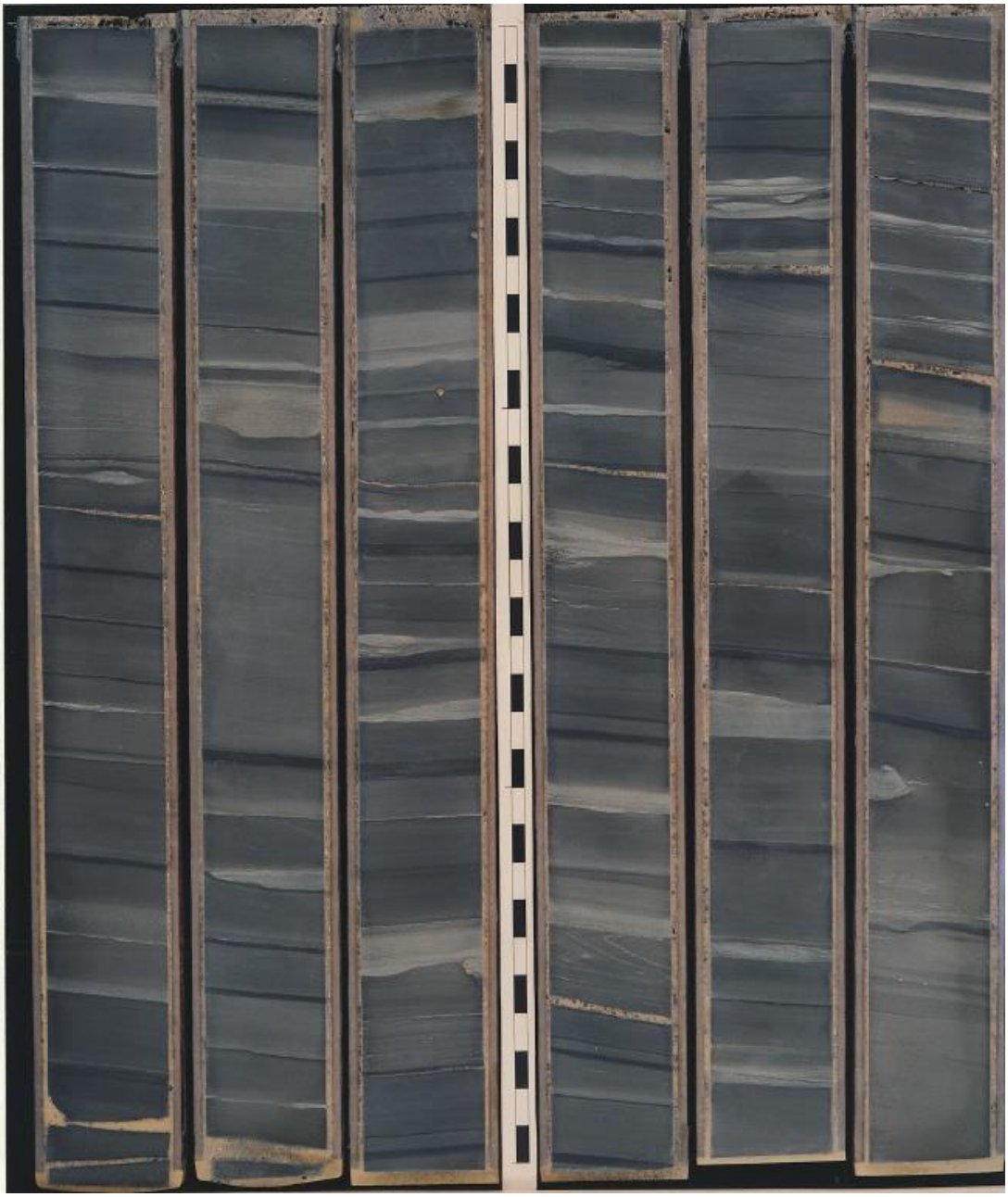

Figure 1.26: An example of core slices from Central North Sea well 30/14-1. Rock samples from these were analysed for isotopes, major elements and biostratigraphy.
Scale bar in inches

1.2.1 INTEGRATION OF WELL AND SEISMIC INFORMATION

Information from wells can be integrated into seismic datasets to provide tie points upon which the geological interpretation is based. Integration of wire-line log curves, check shot surveys, lithological and biostratigraphic data from over 660 wells into the seismic volumes used in the study allowed reflectors corresponding to each stratigraphic marker to be interpreted. These wells were publically released and sourced from the Common Data Access (CDA) data repository operated by Schlumberger (details in Appendix 1).

In order to calibrate the seismic interpretation in this study, well correlation panels were created to identify regional markers. Synthetic seismograms were created from acoustic impedance data calculated from density and sonic logs to allow for greater certainty of the polarity of the horizon considered for interpretation (Figures 1.27-1.35). A stratigraphic chart was also constructed to put them in their stratigraphic context and assess their significance in the tectonic evolution of the basin (Figure 1.36). Regional seismic interpretation of 24 selected horizons allowed the structural history of the Central North Sea basin to be unravelled.

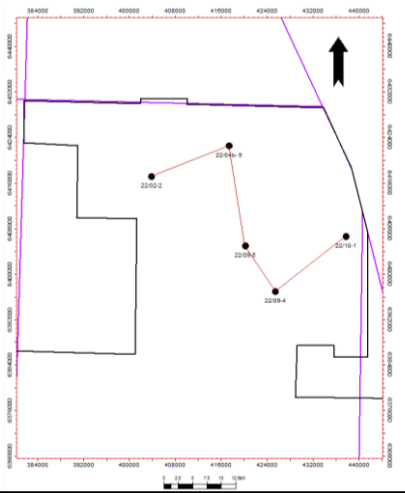

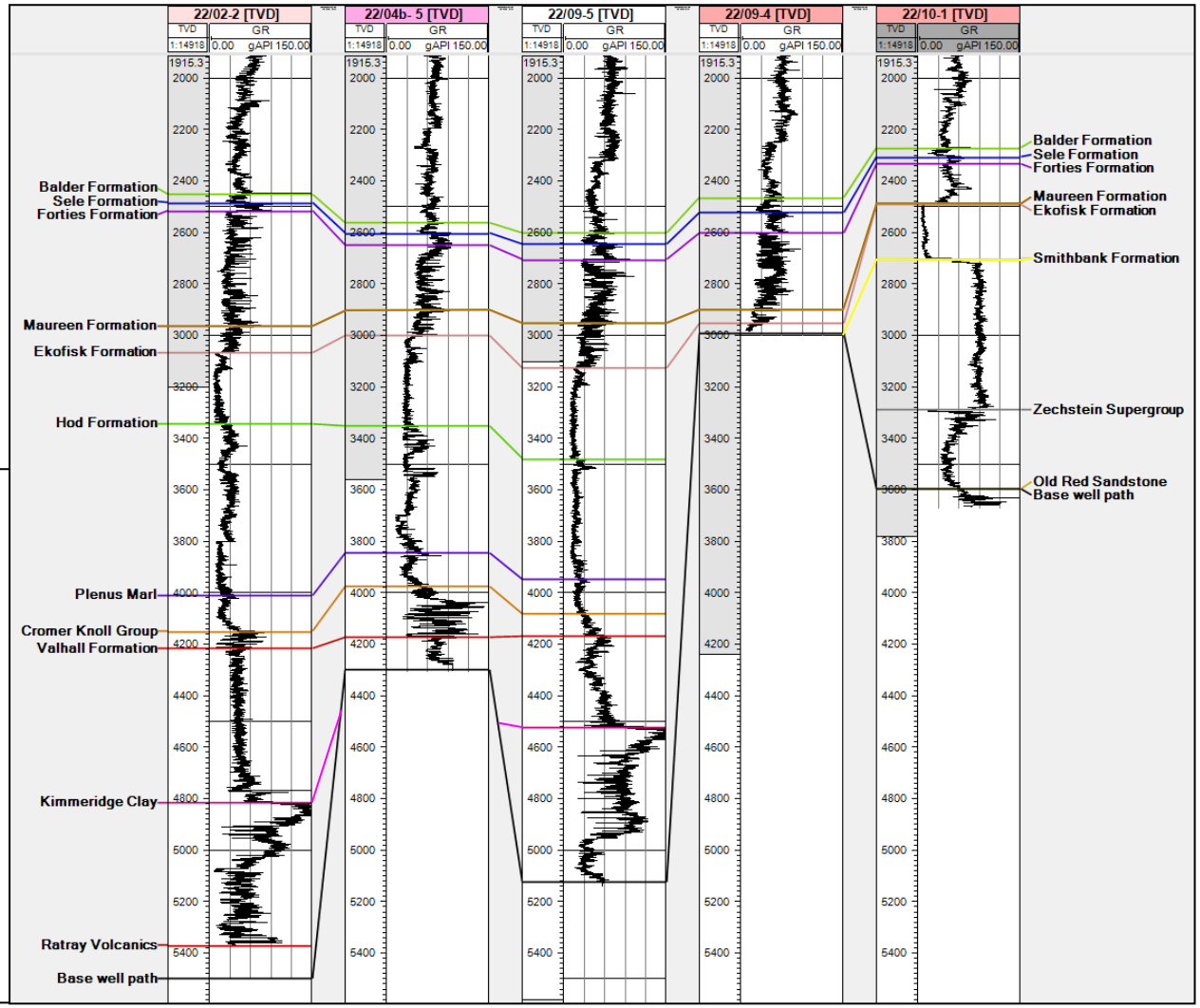

Figure 1.27-1.33: Well sections and synthetic seismograms from the Central North Sea 3D seismic dataset showing major interpreted horizons.

Note that some events are recognised only in selected wells.
The Rattray Volcanics and the Ron Volcanic Member can be considered stratigraphically equivalent as they represent the same phase of Early Jurassic volcanism although from different volcanic centres.
L3 identified in those wells analysed as part of the Palaeocene climatic study.
Top Eocene recognised to constrain timing of post-rift faulting.
The Base Cretaceous Unconformity (BCU) and the top of the Kimmeridge Clay Formation in this area are the same.

Also note the effect of tuning as the Balder Formation thins southwards.

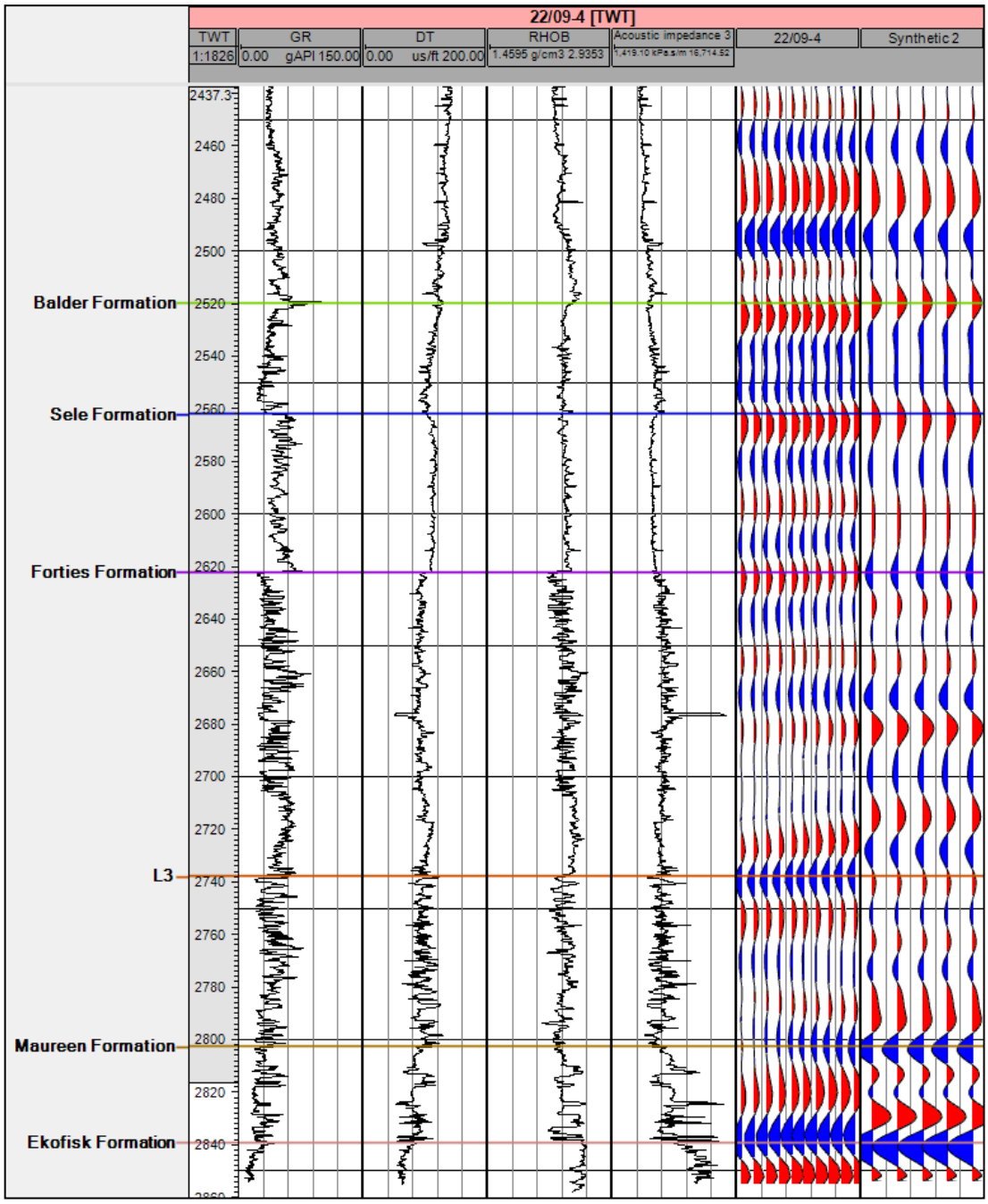

Figure 1.28: A synthetic seismogram created from acoustic impedance contrasts calculated from density and sonic wireline logs from well 22/09-4.
Curves displayed are gamma-ray (GR), sonic (DT), bulk density (RHOB) and calculated acoustic impedance.
The true seismic trace extracted from the well trace is displayed beside the synthetic created for comparison.

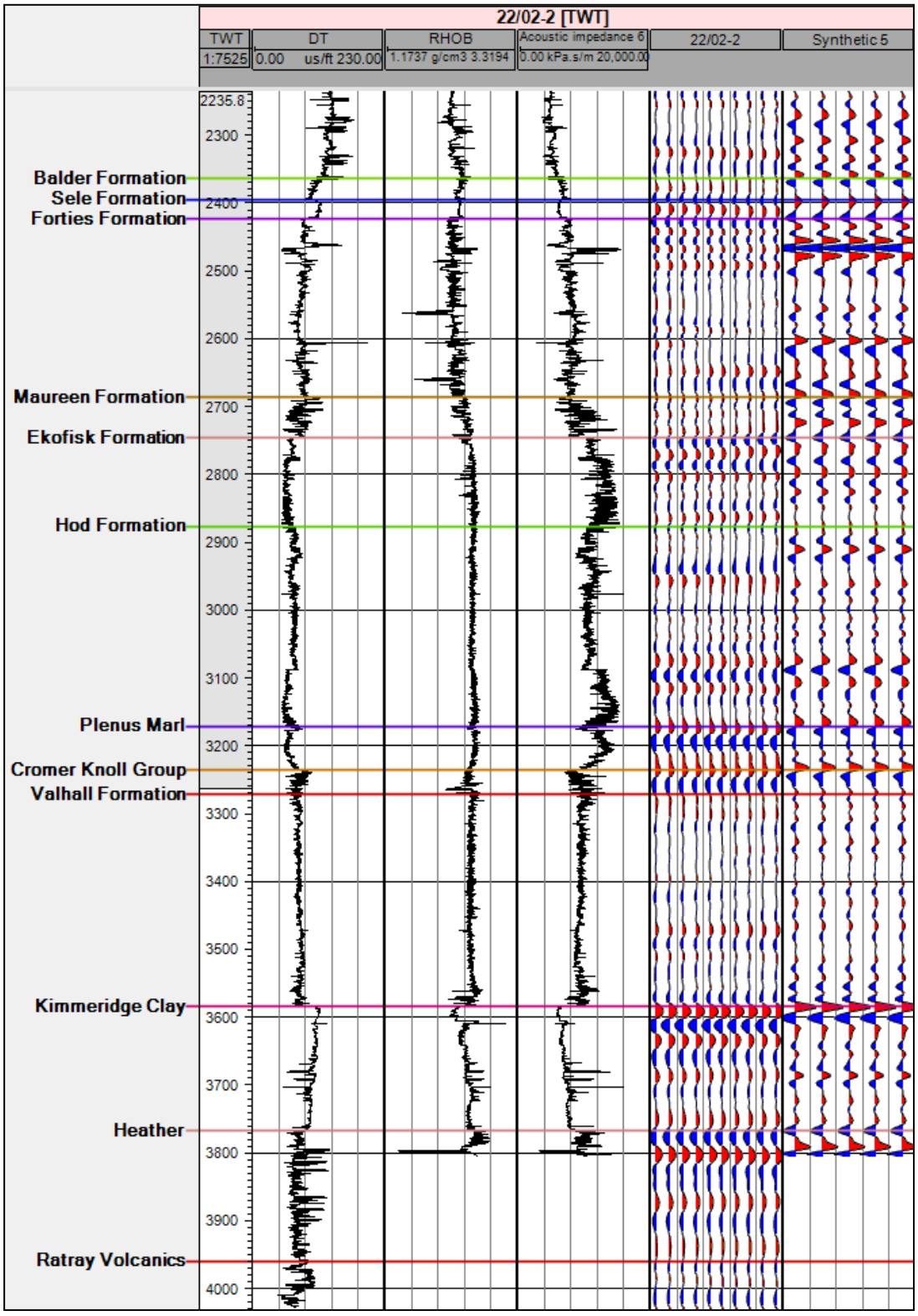

Figure 1.29: A synthetic seismogram from well 22/02-2.

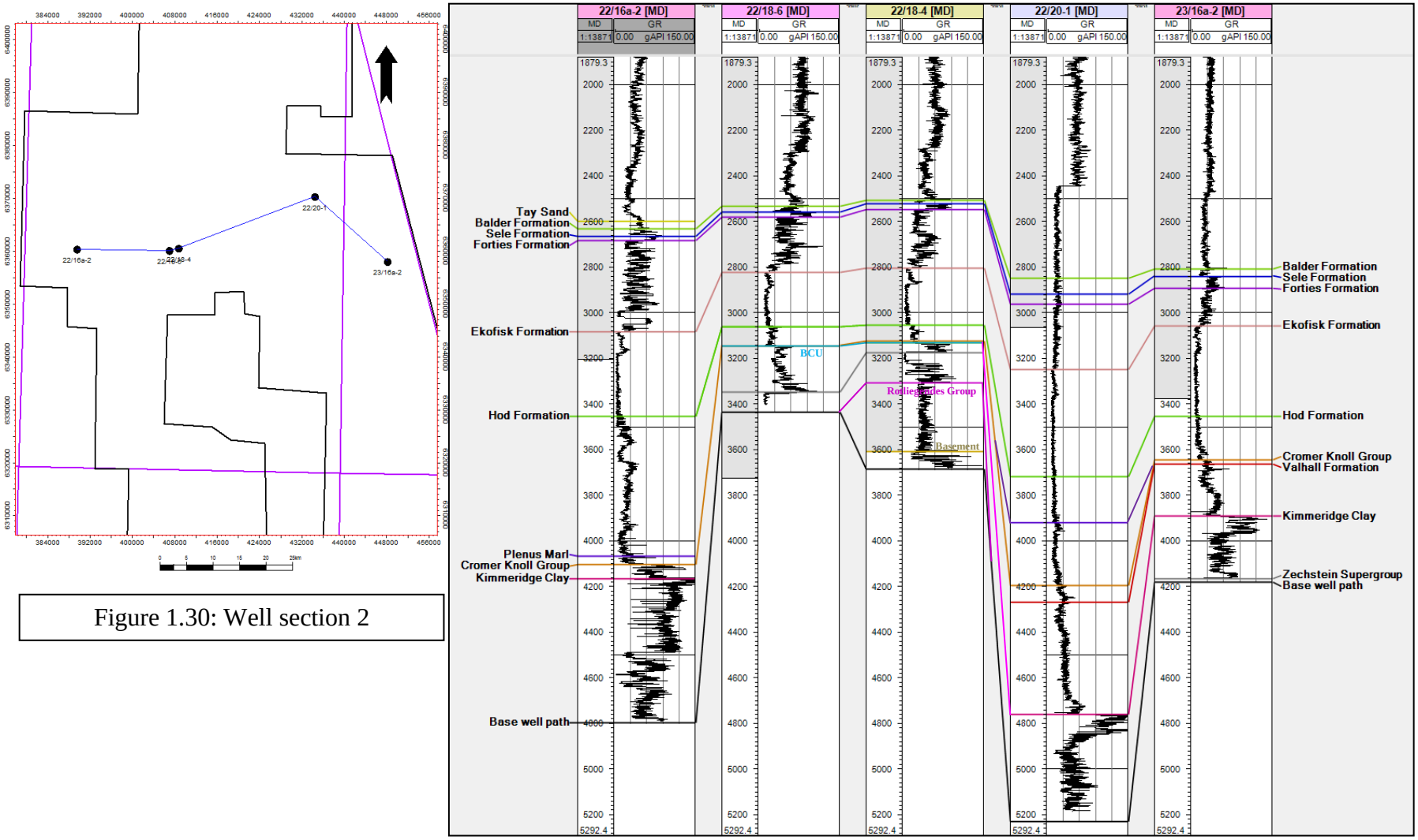

Figure 1.30: Well section 2

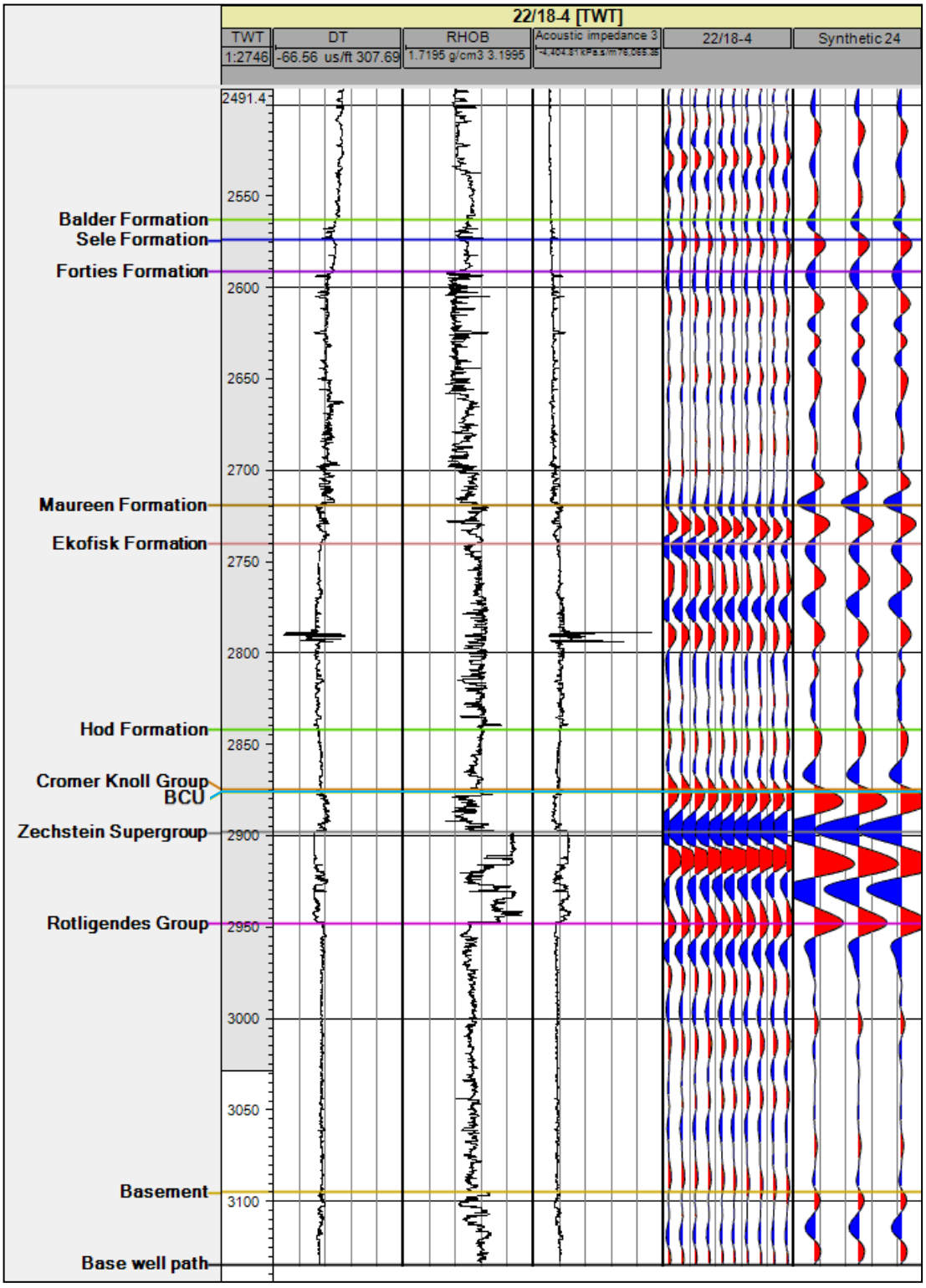

Figure 1.31: Synthetic seismogram from well 22/18-4.

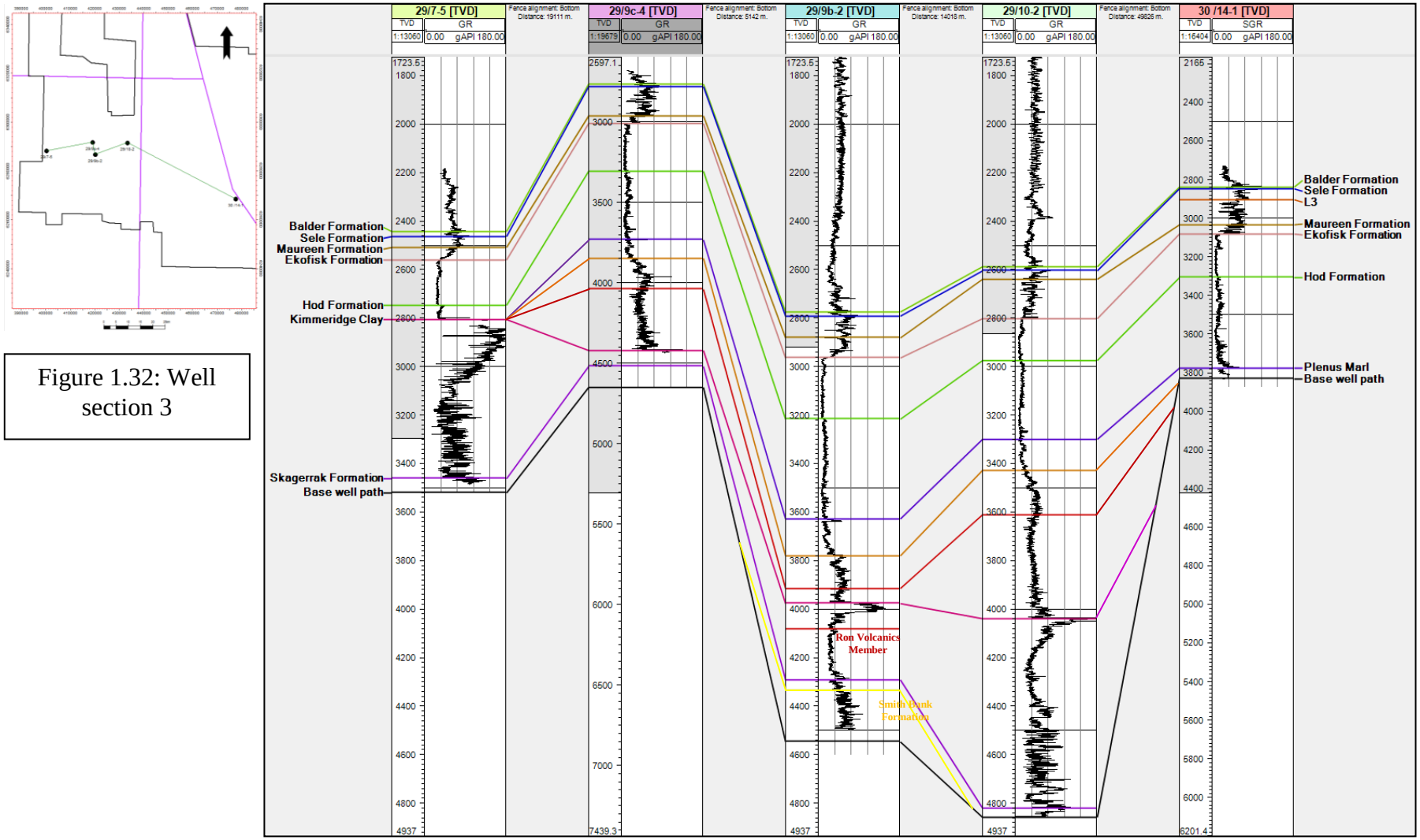

Figure 1.32: Well section 3

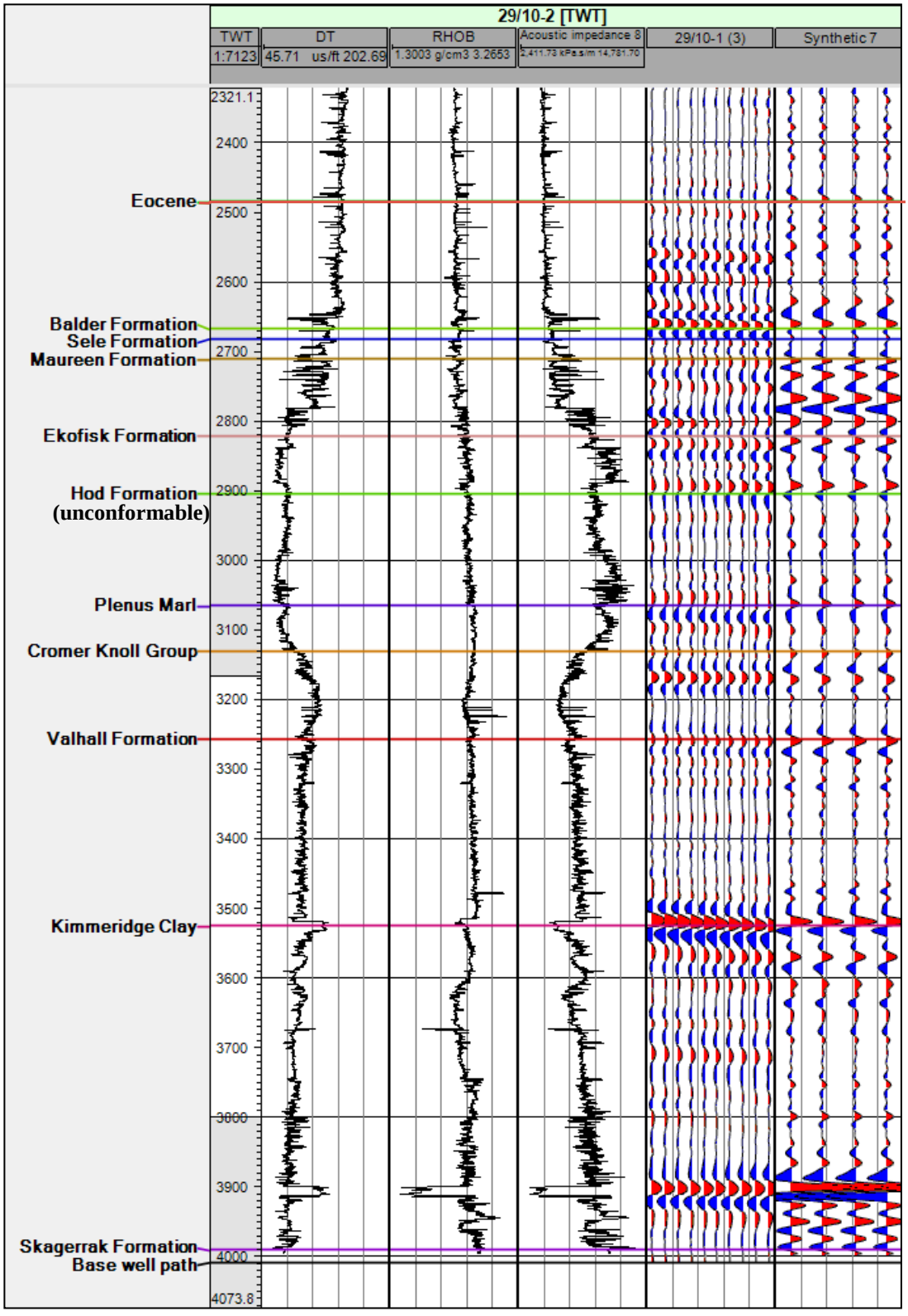

Figure 1.33: Synthetic seismogram from well 29/10-2.

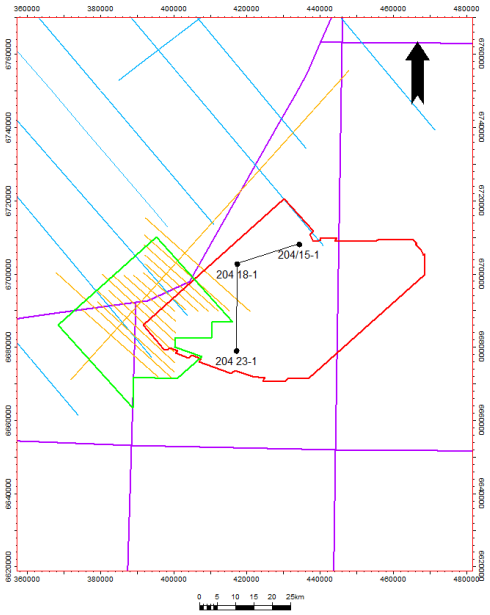

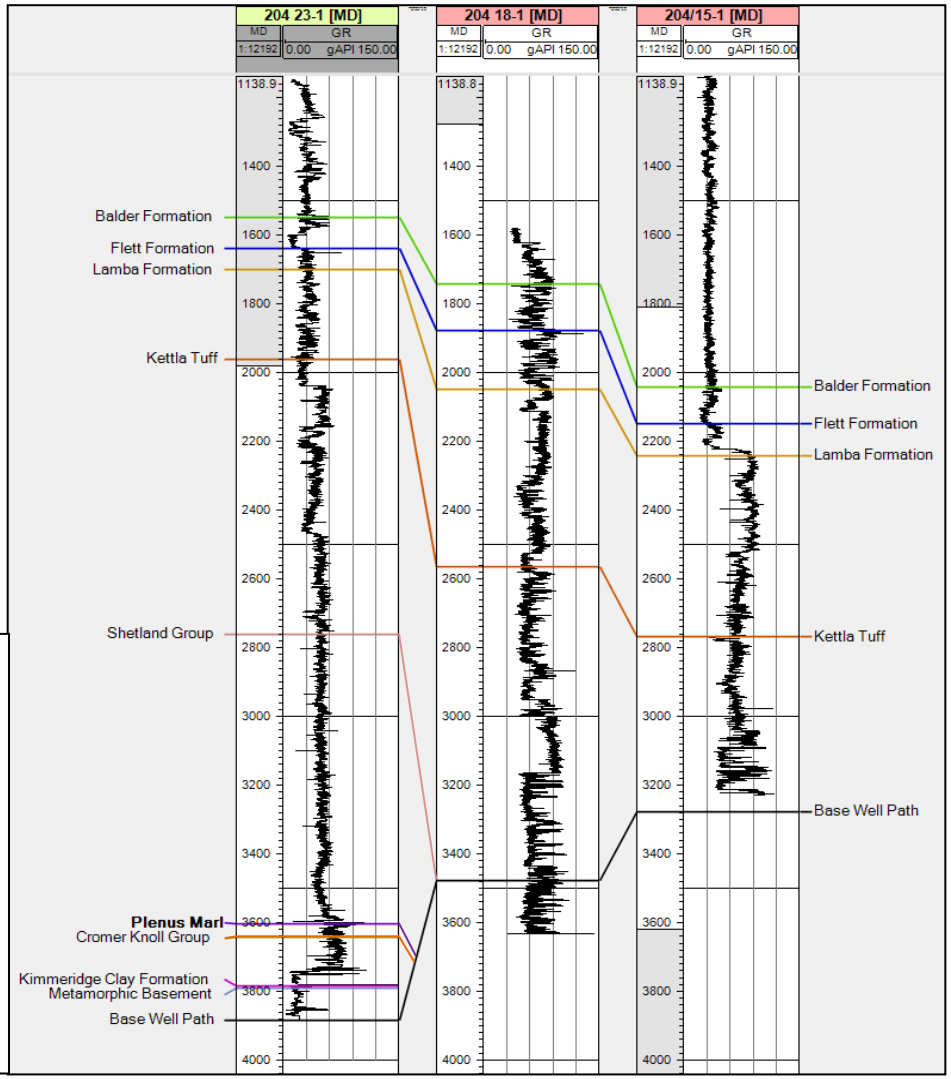

Figure 1.34 and 1.35: Well panel and synthetic seismogram from the West of Shetland dataset.

The Flett Formation is equivalent to the Central North Sea Sele Formation.
The Lamba Formation is stratigraphically equivalent to the base of the Forties Formation.
The chronostratigraphic equivalent of the Kettla Tuff is found within the uninterpreted Mid- Palaeocene section in the Central North Sea.
The Shetland and Chalk Groups are equivalent.

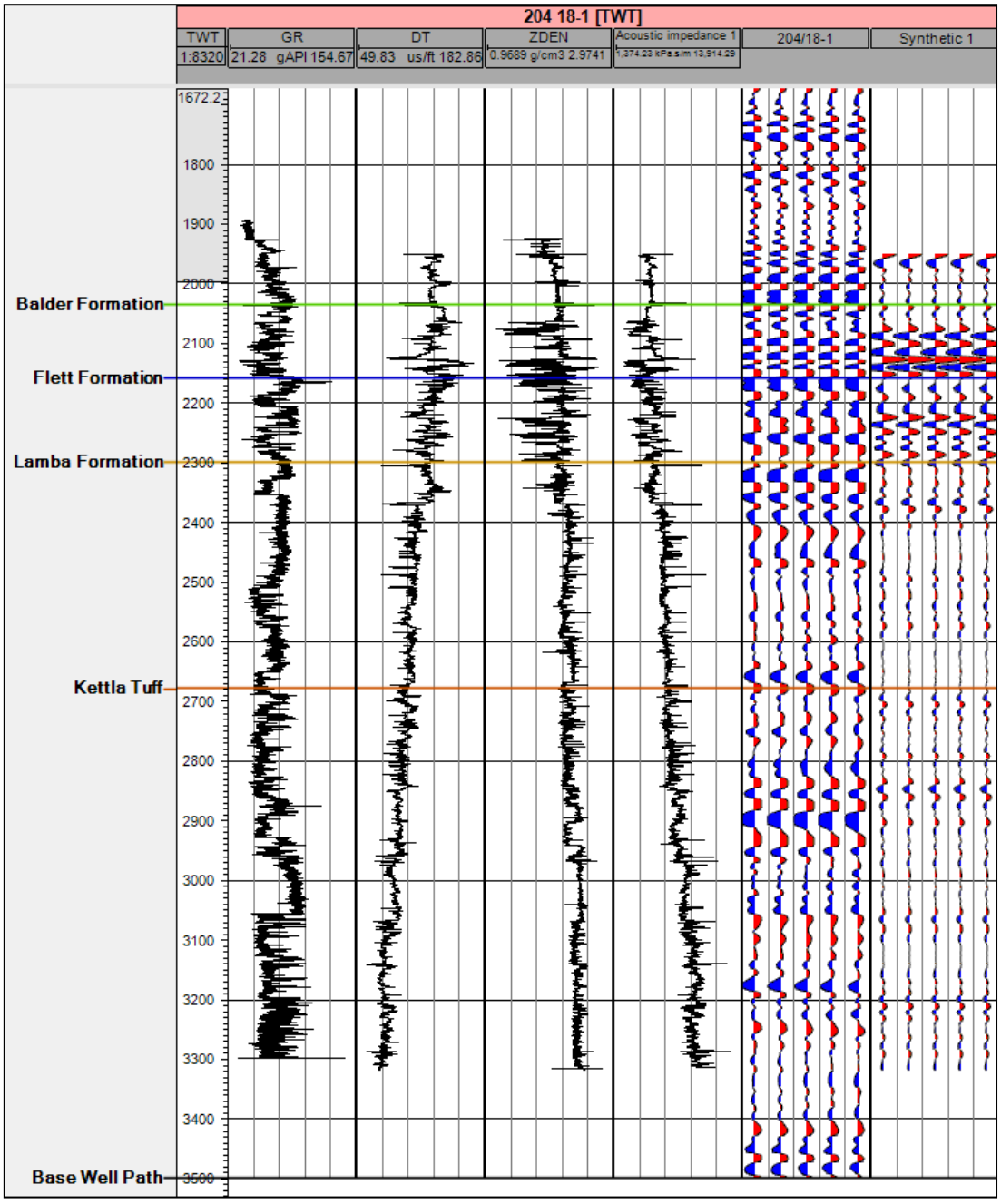

Figure 1.35: Synthetic seismogram from well 204/18-1.

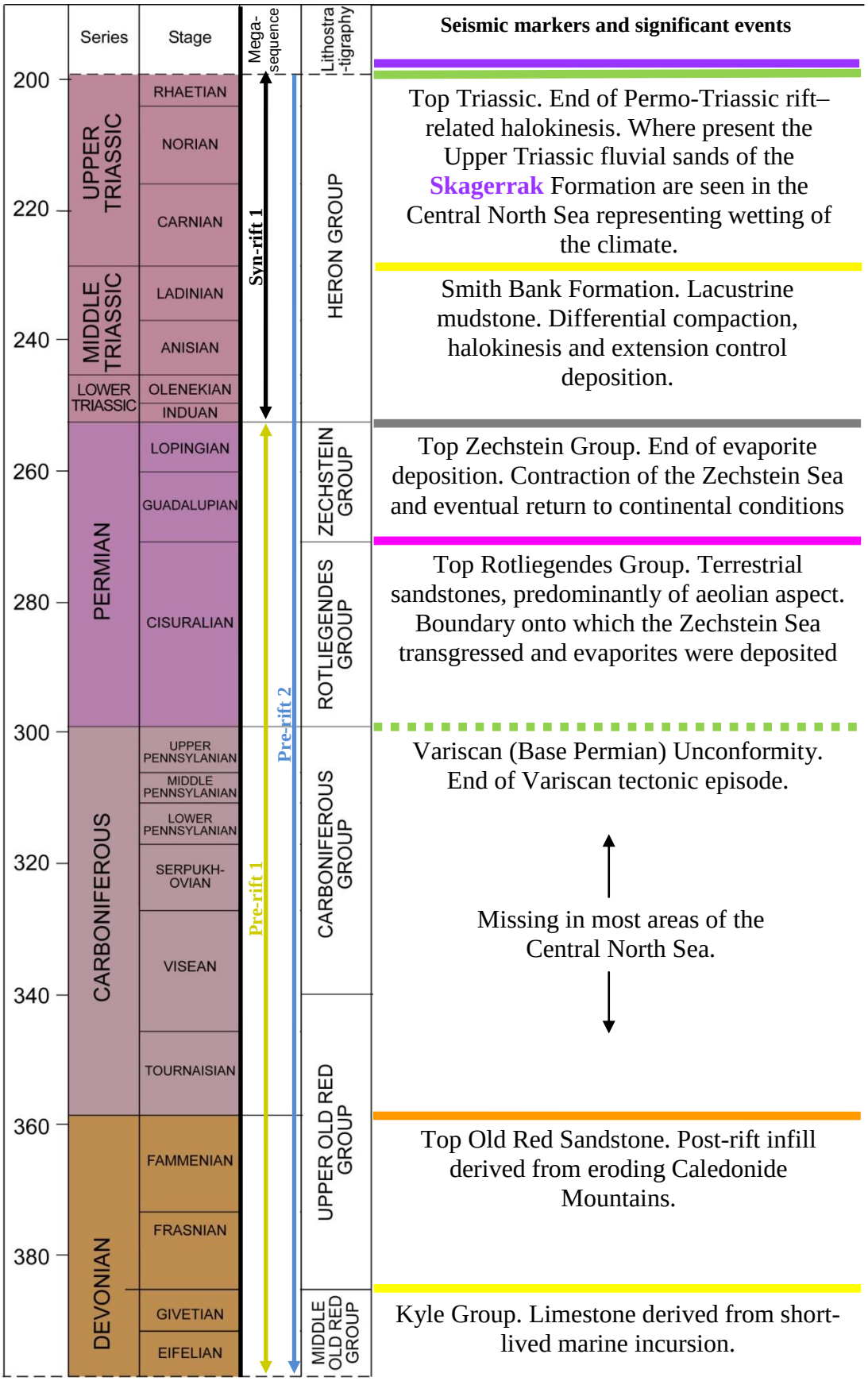
Series
Stage
Mega-sequence
Lithostra-tigraphy
Seismic markers and significant events
200
220
240
260
280
300
320
340
360
380
UPPER TRIASSIC
MIDDLE TRIASSIC
LOWER TRIASSIC
PERMIAN
CARBONIFEROUS
DEVONIAN
RHAETIAN
NORIAN
CARNIAN
LADINIAN
ANISIAN
OLENEKIAN
INDUAN
LOPINGIAN
GUADALUPIAN
CISURALIAN
UPPER PENNSYLANIAN
MIDDLE PENNSYLANIAN
LOWER PENNSYLANIAN
SERPUKH-OVIAN
VISEAN
TOURNAISIAN
FAMMENIAN
FRASNIAN
GIVETIAN
EIFELIAN
Syn-rift 1
Pre-rift 1
Pre-rift 2
HERON GROUP
ZECHSTEIN GROUP
ROTLIEGENDES GROUP
CARBONIFEROUS GROUP
UPPER OLD RED GROUP
MIDDLE OLD RED GROUP
Top Triassic. End of Permo-Triassic rift–related halokinesis. Where present the Upper Triassic fluvial sands of the Skagerrak Formation are seen in the Central North Sea representing wetting of the climate.
Smith Bank Formation. Lacustrine mudstone. Differential compaction, halokinesis and extension control deposition.
Top Zechstein Group. End of evaporite deposition. Contraction of the Zechstein Sea and eventual return to continental conditions
Top Rotliegendes Group. Terrestrial sandstones, predominantly of aeolian aspect. Boundary onto which the Zechstein Sea transgressed and evaporites were deposited
Variscan (Base Permian) Unconformity. End of Variscan tectonic episode.
Missing in most areas of the Central North Sea.
Top Old Red Sandstone. Post-rift infill derived from eroding Caledonide Mountains.
Kyle Group. Limestone derived from short-lived marine incursion.

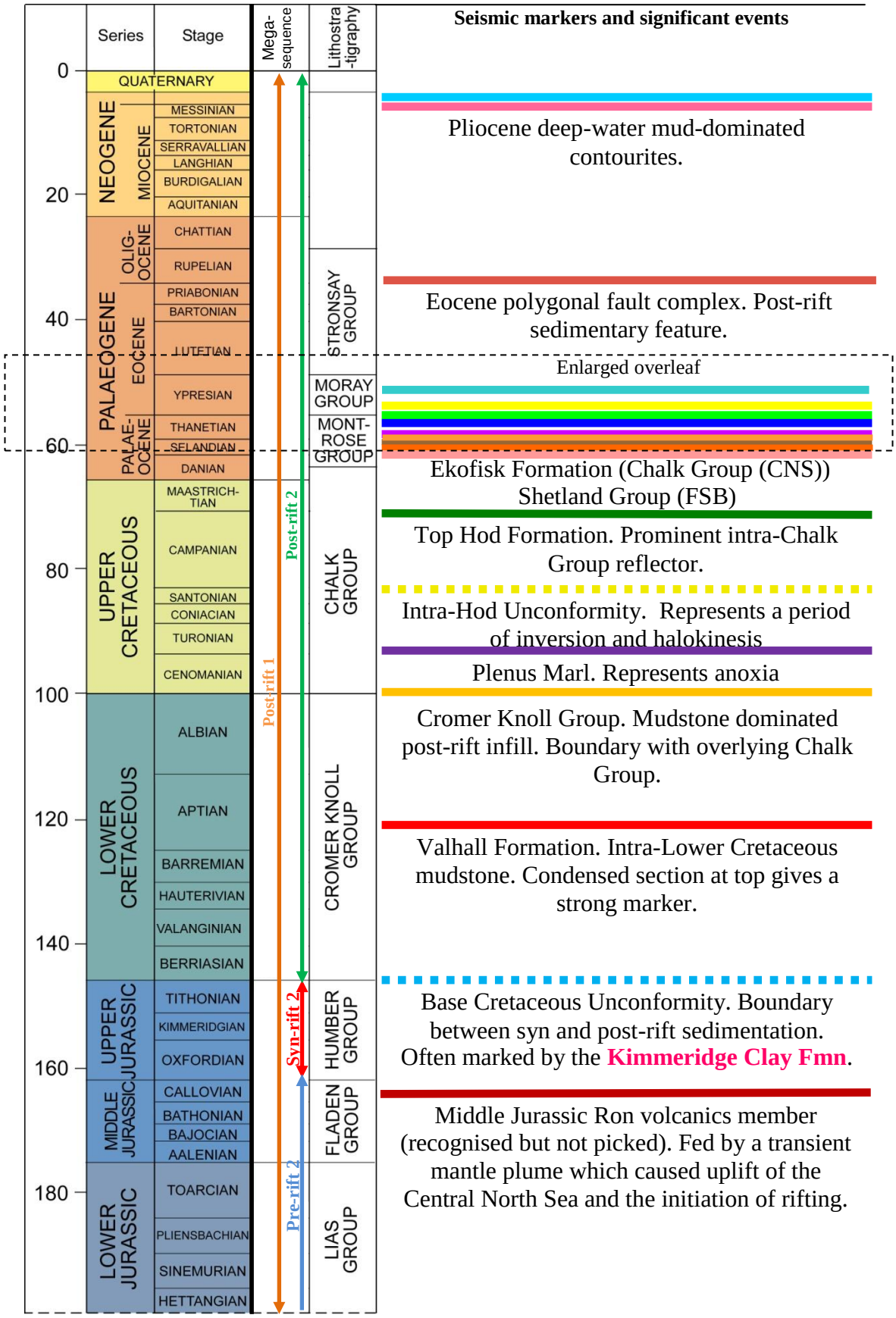
Series
Stage
Mega-sequence
Lithostra-tigraphy
Seismic markers and significant events
0
20
40
60
80
100
120
140
160
180
QUATERNARY
NEOGENE
MIOCENE
MESSINIAN
TORTONIAN
SERRAVALLIAN
LANGHIAN
BURDIGALIAN
AQUITANIAN
PALAEOGENE
OLIG-OCENE
CHATTIAN
RUPELIAN
EOCENE
PRIABONIAN
BARTONIAN
LUTETIAN
YPRESIAN
PALAE-OCENE
THANETIAN
SELANDIAN
DANIAN
UPPER CRETACEOUS
MAASTRICH-TIAN
CAMPANIAN
SANTONIAN
CONIACIAN
TURONIAN
CENOMANIAN
LOWER CRETACEOUS
ALBIAN
APTIAN
BARREMIAN
HAUTERIVIAN
VALANGINIAN
BERRIASIAN
UPPER JURASSIC
TITHONIAN
KIMMERIDGIAN
OXFORDIAN
MIDDLE JURASSIC
CALLOVIAN
BATHONIAN
BAJOCIAN
AALENIAN
LOWER JURASSIC
TOARCIAN
PLIENSBACHIAN
SINEMURIAN
HETTANGIAN
Post-rift 1
Post-rift 2
Syn-rift 2
Pre-rift 2
STRONSAY GROUP
MORAY GROUP
MONT-ROSE GROUP
CHALK GROUP
CROMER KNOLL GROUP
HUMBER GROUP
FLADEN GROUP
LIAS GROUP
Pliocene deep-water mud-dominated contourites.
Eocene polygonal fault complex. Post-rift sedimentary feature.
Enlarged overleaf
Ekofisk Formation (Chalk Group (CNS)) Shetland Group (FSB)
Top Hod Formation. Prominent intra-Chalk Group reflector.
Intra-Hod Unconformity. Represents a period of inversion and halokinesis
Plenus Marl. Represents anoxia
Cromer Knoll Group. Mudstone dominated post-rift infill. Boundary with overlying Chalk Group.
Valhall Formation. Intra-Lower Cretaceous mudstone. Condensed section at top gives a strong marker.
Base Cretaceous Unconformity. Boundary between syn and post-rift sedimentation. Often marked by the Kimmeridge Clay Fmn.
Middle Jurassic Ron volcanics member (recognised but not picked). Fed by a transient mantle plume which caused uplift of the Central North Sea and the initiation of rifting.

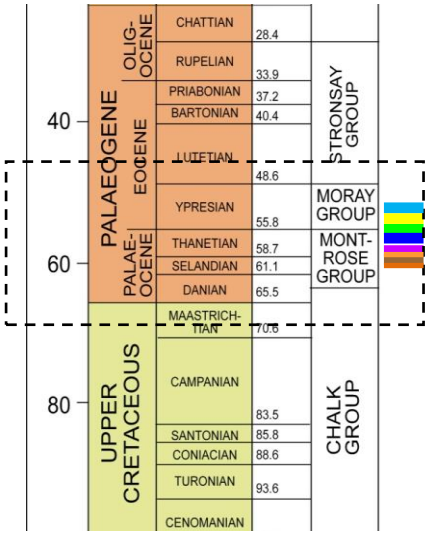

Eocene injectites. Clean sands injected into a mudstone matrix.

Tay Sandstone. Eocene turbidite sand.

Top Balder Formation. Mudstone with variable amounts of ash and tuff exuded from North Atlantic Igneous Province

Top Sele Formation. Grey-black pyritic shales represent anoxia of enclosed basin.

Top Forties Formation (T40/45 boundary in much of Faroe-Shetland Basin (FSB)) Maximum flooding surface. Previously only considered as a stratigraphic boundary where the Forties Sandstone Member was present. Used as a chronostratigraphic marker in this volume due to unconformable nature in the FSB area and condensed section of correlative conformity in the Central North Sea.

Lista Formation (L3). Base of the Forties Formation. Picked only in relation to the Palaeocene hyperthermal event where it represents the onset of warming.

Top Maureen Formation. Variable amounts of clay, sand and chalky debris. Chaotic seismic character

Kettla/Andrew Tuff. Tuff layer produced by North Atlantic Igneous Province volcanic activity. Picked FSB only.

Figure 1.36: Chart showing all seismic reflectors recognised within the dataset.

1.3 ISOTOPIC ANALYSIS

A high resolution study of the Late Palaeocene geological evolution and climate merited usage of a number of further analytical techniques including isotopic analysis. Previous research suggests that a large worldwide negative excursion in the ratio of the two stable isotopes of carbon ^{12}C and ^{13}C is characteristic of the Late Palaeocene hyperthermal and represents a large injection of isotopically light carbon into the ocean-atmosphere system. To investigate whether this excursion is also represented in the North Sea, core data from wells within the Central North Sea was sampled at the BGS Gilmerton Corestore in Edinburgh before its closure and the rock chips were analysed to obtain the ratio of stable isotopes ^{13}C:^{12}C, reported in parts per thousand (per mil, ‰). This is denoted as $\delta^{13}C$.

The definition is $\delta^{13}C$ (in per mil) = 10^3[(Rsample/Rstandard)-1], where Rx = (^{13}C)/(^{12}C) is the ratio of isotopic composition of a sample compared to that of the established standard for marine carbonates (Vienna Pee Dee Belemnite (VPDB)). Non-carbonate samples are compared to a laboratory standard with a known relationship to VPDB.

To obtain measurements of $\delta^{13}C$ rock samples were crushed and ground to form a fine powder and the samples were transferred to the isotope facility. Two separate facilities were used to analyze the samples for all of the sections; the BGS NERC Isotope Laboratory in Keyworth was used to analyze the isotopes from section

30/14-1 and the University of Edinburgh isotope laboratory in Edinburgh was used to analyze samples from sections 22/09-3, 22/10a-T6, 22/06-1 and 30/2a-5.

Samples at the BGS NERC facility underwent a process by which the extraneous hydrocarbons were removed to determine the effect of these on $\delta^{13}C$. The samples were halved and one half treated to remove possible hydrocarbons. The hydrocarbons were removed by allowing the samples to be refluxed for 24 hours in an azeotrophic mixture of dichloromethane and methanol as outlined in (Stephenson et al. 2005). All materials (cellulose Soxhlet thimbles, silica wool, vials) were cleaned with analytical grade organic solvents prior to use and remaining solvents were then removed by evaporation. The dried sediments were then acidified using 5% HCl for 12 hours to remove any calcite (dolomite and siderite are not removed completely by dilute HCl) then filtered and rinsed with de-ionized water. The dried, de-oiled, samples were weighed out to 40mg (i.e. from 1-3%C in the sample) and analyzed for $\delta^{13}C$ by combustion in a Carlo Erba 1500 on-line to a VG TripleTrap and Optima dual-inlet mass spectrometer with $\delta^{13}C$ values calculated to the VPDB scale using a within-run laboratory standard (cellulose, Sigma Chemical product C-6413) calibrated against NBS-19 and NBS-22. Replicate analysis of well-mixed samples indicated a precision of +/- <0.2 ‰.

Samples analyzed at the University of Edinburgh facility did not undergo the de-oiling process and the crushed samples were weighed then acidified to remove carbonates by adding a drop of 5%HCl to the foil capsules (Verardo et al. 1990). Since there was little to no calcite present within the samples, there was no

requirement for extra steps to be taken to avoid sample loss due to effervescence. The samples were placed on a heat plate during addition of the acid and the temperature was gradually increased to ~50°C, allowing the acid to evaporate over the next 6 hours. Possible loss of volatile organic carbon and nitrogen has been found to occur with acidification by the capsule method (Brodie et al. 2011) but other methods have also been associated with losses of volatile and soluble organic matter therefore this method was considered at the time to be the least problematic. However, later analysis on repeat samples using this method found that in certain facies, volatile losses were high and subsequent analyses used the filter method described above. Samples were analyzed using a CE Instruments NA2500 Elemental Analyser which can be interfaced with the Thermo- Electron Delta + Advantage mass spectrometer with dual inlet via dual reference gas injector boxes with additional diluters.

$\delta^{13}C$ values were also calculated to the VPDB scale using an in-house standard. For applications of isotopic data see Chapter 5.

1.4 X-RAY FLUORESCENCE ANALYSIS

Several authors have used major-element data to define orbital cycles over this period (Rohl et al. 2000; Rohl et al. 2007; Westerhold et al. 2008; Charles et al. 2011) in order to estimate the duration of the Late Palaeocene PETM hyperthermal. Other methods of absolute dating such as isotopic analyses have large error bars and are thus not ideal for use over such a geologically short-lived event. Isotope major-element data derived from X-Ray fluorescence analysis (XRF) was therefore performed on samples from the Central North Sea in order to identify orbital cyclicity within the Palaeocene section as part of research into the hyperthermal climate. The elemental data was also used to investigate changes in oceanic chemistry which could be linked to warming over the Late Paleocene interval.

Major-element concentrations were determined after fusion with a lithium borate flux containing La_2O_3 as a heavy absorber, by a method similar to that developed by Norrish and Hutton (Norrish et al. 1969). Rock powder was dried at 110°C overnight then transferred to a desiccator to cool. The samples were then transferred to Pt5%Au crucibles and weighed to precisely 1g before being ignited at 1100°C in a muffle furnace to determine loss on ignition (LOI). Once cool, the residue was mixed with Johnson Matthey Spectroflux 105 to a sample: flux ratio of 1:5 based on the unignited sample mass, and fused, again at 1100C. The crucible was re-weighed after this first fusion and any flux weight loss was made up precisely with extra flux. The samples were then fused for a second time over a Meker burner and the mixture

was agitated several times to ensure proper mixing of flux and sample. The molten mixture was then cast onto a graphite mold and flattened with an aluminum plunger into a thin disk. The casting took place on a hotplate with both mold and plunger maintained at a temperature of 220°C to ensure rapid cooling did not cause the sample to disintegrate.

The fused and pressed samples were analyzed using a Philips PW 2404 automatic X-ray fluorescence spectrometer with a Rh-anode X-ray tube (Fitton et al. 1998).

1.5 PALYNOLOGY

Palynological analysis was used to aid interpretation of Late Palaeocene tectonic and environmental events. It has previously been ascertained that the PETM hyperthermal caused disruption of biological systems and this was investigated in the Central North Sea study area by analyzing palynomorph assemblages for any changes which could be linked to climatic variations. Palynomorphs are organic-walled microfossils between 5 and 500 micrometres in size. For the purposes of most palynological analyses they are split into three groups, dinoflagellates, pollen and spores.

Dinoflagellates are an important unicellular group of phytoplankton consisting of both heterotrophic and autotrophic species which form a significant part of primary planktonic production in both oceans and lakes. The living animals occur as motile cells in surface waters, particularly in neritic settings (Sluijs 2006) and produce preservable organic walled hypnozygotic resting cysts. Some species also produce calcareous and siliceous cysts. These cysts (dinocysts) represent a rich and diverse fossil record from the Mid-Late Triassic to the present (MacRae et al. 1996) and many taxa provide important biostratigraphic markers.

Dinocysts are utilised as palaeo-environmental indicators as extant species are found to be extremely sensitive to changes in surface water conditions such as temperature, salinity and periodic upwelling (Dale 1996; Rochon et al. 1999; Marret et al. 2002;

Sangiogi et al. 2003; Sprangers et al. 2004; Rochon et al. 2008). However, the numbers of extant species decline the further back in time studied and environmental reconstructions rely on morphological and genetic similarity to modern species and combining fossil assemblage distribution with knowledge of probable conditions in specific areas. In addition only about 15% of living taxa are known to produce cysts and several species have been proven to create morphologically different cysts under different ecological conditions (Sluijs 2006). Taxonomy is also problematic as the resting cysts of dissimilar species may be morphologically identical.

In spite of these caveats, fossil dinocyst distribution patterns display similar trends to modern ones allowing the inference that the same niches were inhabited to be made with some degree of confidence. Dinocyst paleoenvironmental reconstructions have been used increasingly as part of multi-disciplinary studies especially in those investigating the Palaeocene and later Eocene hyperthermals (Bujak et al. 1998; Brinkhuis et al. 2003; Sluijs et al. 2005)

Dinocyst diversity has also been linked by several authors to global sea-levels by comparing total diversity of all known species (MacRae et al. 1996) to Haq's sea-level curve (Haq et al. 1987) (Figure 1.37). Despite controversy surrounding the validity of species diversity curves (Alroy 2000; Smith 2007), there appears to be an accepted link between high global sea-levels and high dinocyst abundance.

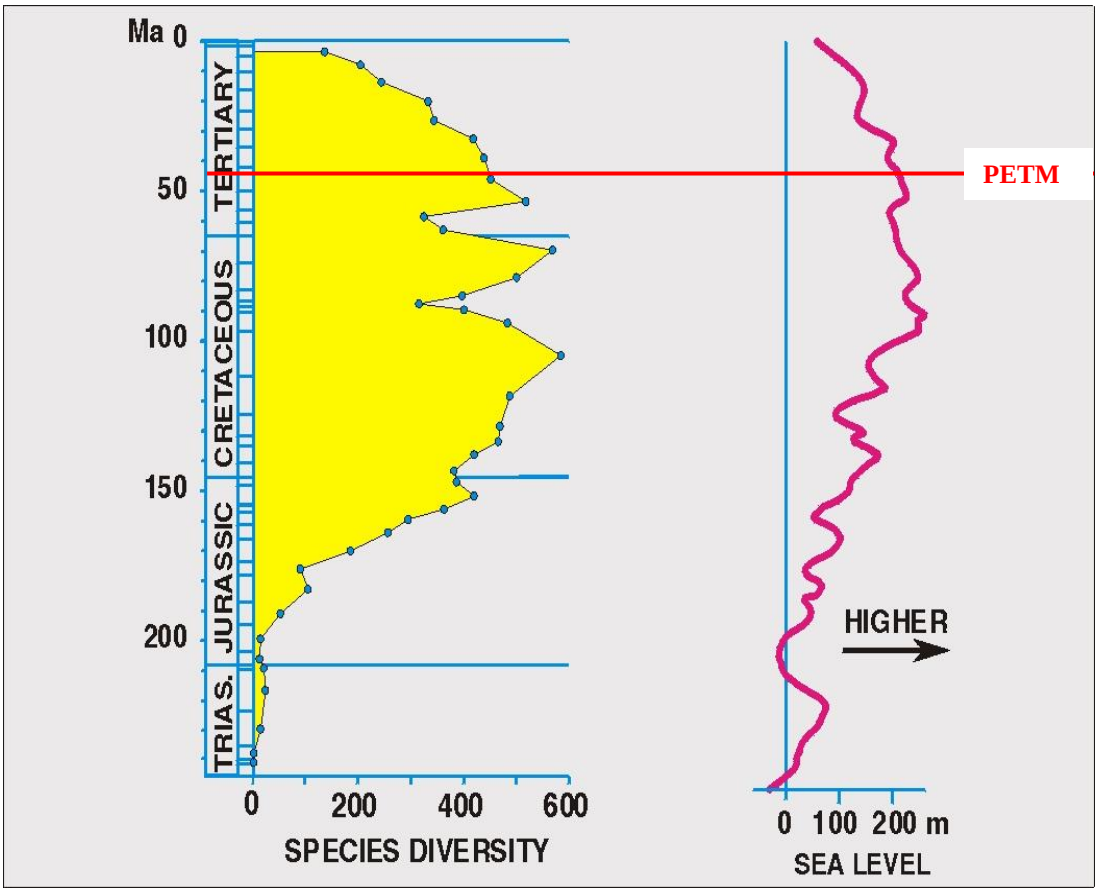

Figure 1.37: Species diversity curve (MacRae et al. 1996) compared to global sea-level curve (Haq et al. 1987; Davison et al. 2000) showing coincidence of high dinoflagellate diversity with high sea-level. Palaeocene hyperthermal noted.

Dinocysts can also inform about nutrient availability and upwelling conditions. Most modern dinoflagellates are marine and photosynthetic but certain groups are holozoic or combine the two characteristics (Bujak et al. 1998). These holozoic dinoflagellates feed on organic detritus or phytoplankton such as diatoms (Jacobson et al. 1986). The different life strategies of these species can be linked to productivity through changes in the ratio of Peridinoid (P) vs. Gonyaulacoid (G) cysts within dinocyst

assemblages. Peridinoid cysts are thought to represent heterotrophic species which rely on phytoplankton and organic debris for food while Gonyaulacoid cysts primarily represent autotrophic species (Devillers et al. 2000; Reichart et al. 2003; Sluijs et al. 2005). It has been argued that some modern Peridinoids are not heterotrophic and that the same is probably true of extinct species (Dale et al. 1994) but the P:G ratio still provides a broad indication of changes in productivity. Dinocysts are also utilised successfully in biostratigraphy, particularly in areas where calcareous microfossils are not preserved or abundant such as the North Sea.

Pollen and spores are analysed along with dinocysts and can also be used as a stratigraphic tool and to gain a better understanding of environmental conditions over a specific period. Some plants such as palms have a distribution determined by climatic conditions and their presence in assemblages can therefore indicate tropical-sub-tropical conditions. Pollen can be divided into two groups, angiosperms (flowering plants) and gymnosperms and palynomorphs in ancient rocks can often be linked to modern plant families allowing insight into the conditions of the paleoenvironment.

1.5.1 PALYNOLOGICAL DATA PREPARATION AND OBSERVATION TECHNIQUES

Palynological samples were acquired by taking rock fragments at regular intervals from rock cores housed in the BGS corestore at Gilmerton. The samples were then processed by breaking them down into <5mm fragments then acidifying with 5% hydrochloric acid to remove calcite (dolomite and siderite will not be dissolved). The samples then underwent chemical disaggregation and were placed in hydrofluoric acid to remove silicates (Wood et al. 1996). Organic residues were oxidised with Schultze's Solution and dilute nitric acid as described by (Stephenson et al. 2005). If mineral matter is present, boiling in hydrochloric acid may be required before oxidation. The sample was removed from the last acid treatment and swirled to separate organic matter from any remaining mineral matter. The acid must be washed out of the sample by either; allowing the acid and sample to settle and decanting off the acid, topping up with distilled water and repeating until the mixture is neutral or by sieving. Sieving involves washing the acid and sample through an acid-resistant sieve gauze with a mesh size of 10μm (Olney 2002). The final sample was mounted onto a slide.

Analysis of samples was undertaken by counting slides to a minimum of 200 specimens then scanning again for rare taxa.

5.2 BIOSTRATIGRAPHIC LOGS AND REPORTS

A database of 66 publicly released biostratigraphic analyses, originally commissioned by hydrocarbon companies was created for use in this study (Figure 1.38). The data can be accessed through the Schlumberger operated CDA datastore along with all other well information used. The most robust of these, containing quantitative data were used to characterise ecological change throughout the North Sea during the PETM (Details in Appendix 2).

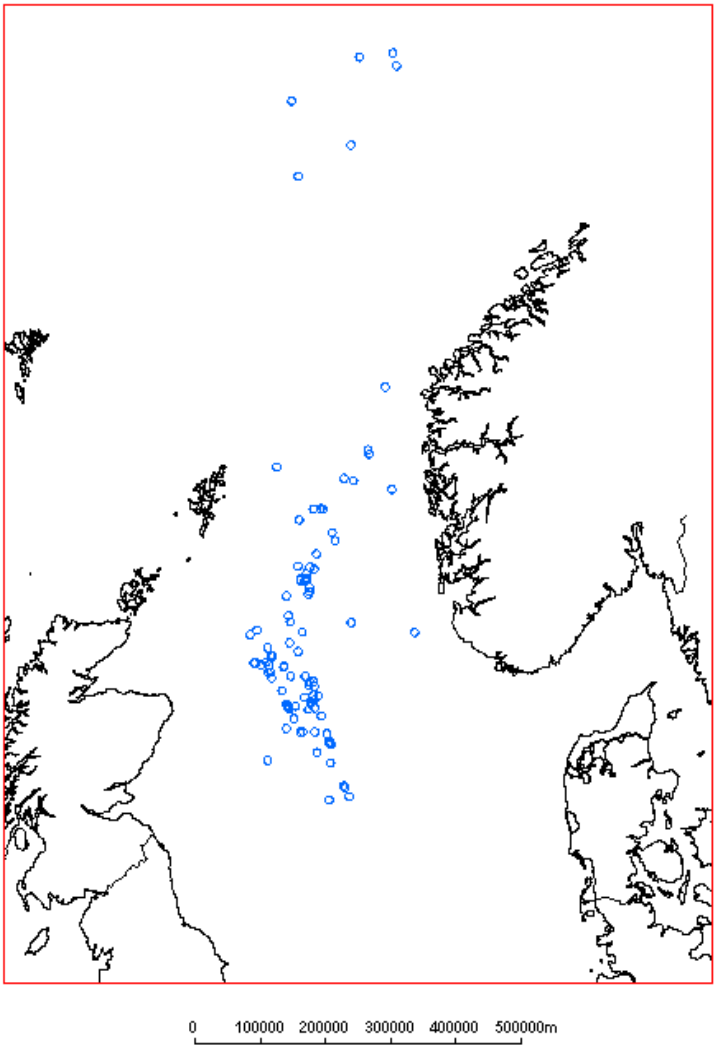

Figure 1.38: Locations of the 66 biostratigraphic analyses compiled.

CHAPTER 2

TECTONO-STRATIGRAPHIC MEGASEQUENCE 1:PRE-RIFT

2.1 INTRODUCTION

Successful interpretation of the evolution of a basin involves recognition of the changing geometries of seismic reflection packages caused by deformation events and the correlation of these with either outcrop or well data. Ideally three main depositional sequences can be identified in any deformation episode, a pre-rift (also known as a pre-kinematic) sequence deposited prior to deformation, a syn-rift sequence deposited during, and a post-rift sequence deposited after deformation has stopped (Morley 1999). These sequences can be grouped together into tectono-stratigraphic megasequences.

In the Central North Sea, a rifting event in the Jurassic provides highly visible examples of each of these depositional sequences and the terms have become synonymous with the Jurassic rift event. However, new, high resolution seismic data provides the opportunity to investigate tectonic events which pre-date this. Within the sequence assigned to the pre-rift section of the Jurassic event is evidence for a period of deformation which occurred in Triassic times. The pre, syn and post-rift sequences developed during these two deformational events are grouped into tectono-stratigraphic megasequence 1 (Triassic) and tectono-stratigraphic megasequence 2 (Jurassic) (Figure 2.1).

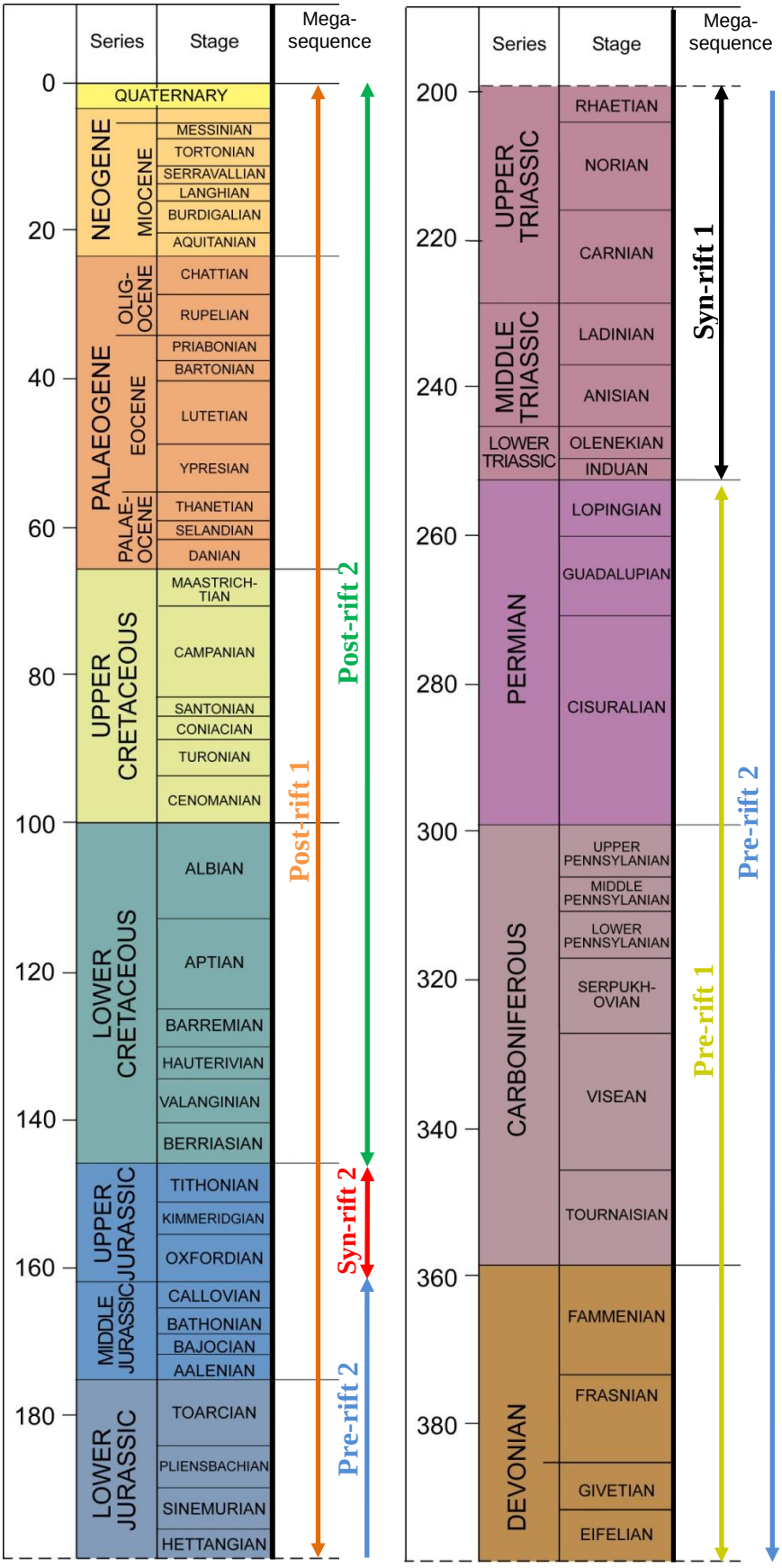

Figure 2.1: Sequences within tectono- stratigraphic megasequences 1 and 2

The pre-rift sequence of tectono-stratigraphic megasequence 1 comprises all of the rocks of Permian age or older. However within this sequence, evidence of much earlier periods of deformation can be found. These are important to understand as underlying structural lines of weakness are often reactivated during later tectonic events. Mapping of areas in the onshore UK provides evidence that the current structural configuration of the Central North Sea was formed in two complete plate cycles followed by the intra-continental rifting episode which is recorded in the Central North Sea by tectono-stratigraphic megasequence 1. The first of these plate cycles commenced with the Grampian and Caledonian orogenies (Figure 2.2) and began as early as the Late Cambrian, continuing into the Early Devonian. In the Central North Sea this episode, known as the Caledonian plate cycle, was important in that it instigated the first of the basement lineaments which subsequently underwent reactivation in later tectonic episodes.

Investigation of Paleozoic events in the Central North Sea is hampered by the influence of the Jurassic rifting episode which caused basement rocks in the areas most affected by extension to be faulted to depths unresolvable to even the most high quality seismic data. Mapping of basement structures is thus limited to the rift flanks and intra-basinal highs. Additionally, less than 100 wells in total in the North Sea as a whole penetrate the pre-Devonian basement (Evans et al. 2003) (Figure 2.3) and only one lies within the area of seismic coverage, well 30/16-5. This well penetrated phyllite and greenschist metamorphosed rocks dated by Ar-Ar to 435 +/- 5 Upper Ordovician (Figure 2.4). A further 3 wells penetrated Devonian basement rocks, 22/10-1, 22/10-2 and 22/18-4.

Investigation of the Caledonian plate cycle was therefore undertaken by seismically mapping the deepest reflectors which could be reliably differentiated and linking these to the well penetrations. Prominent unconformities, seismic character and onshore analogues were also used to constrain the interpretation.

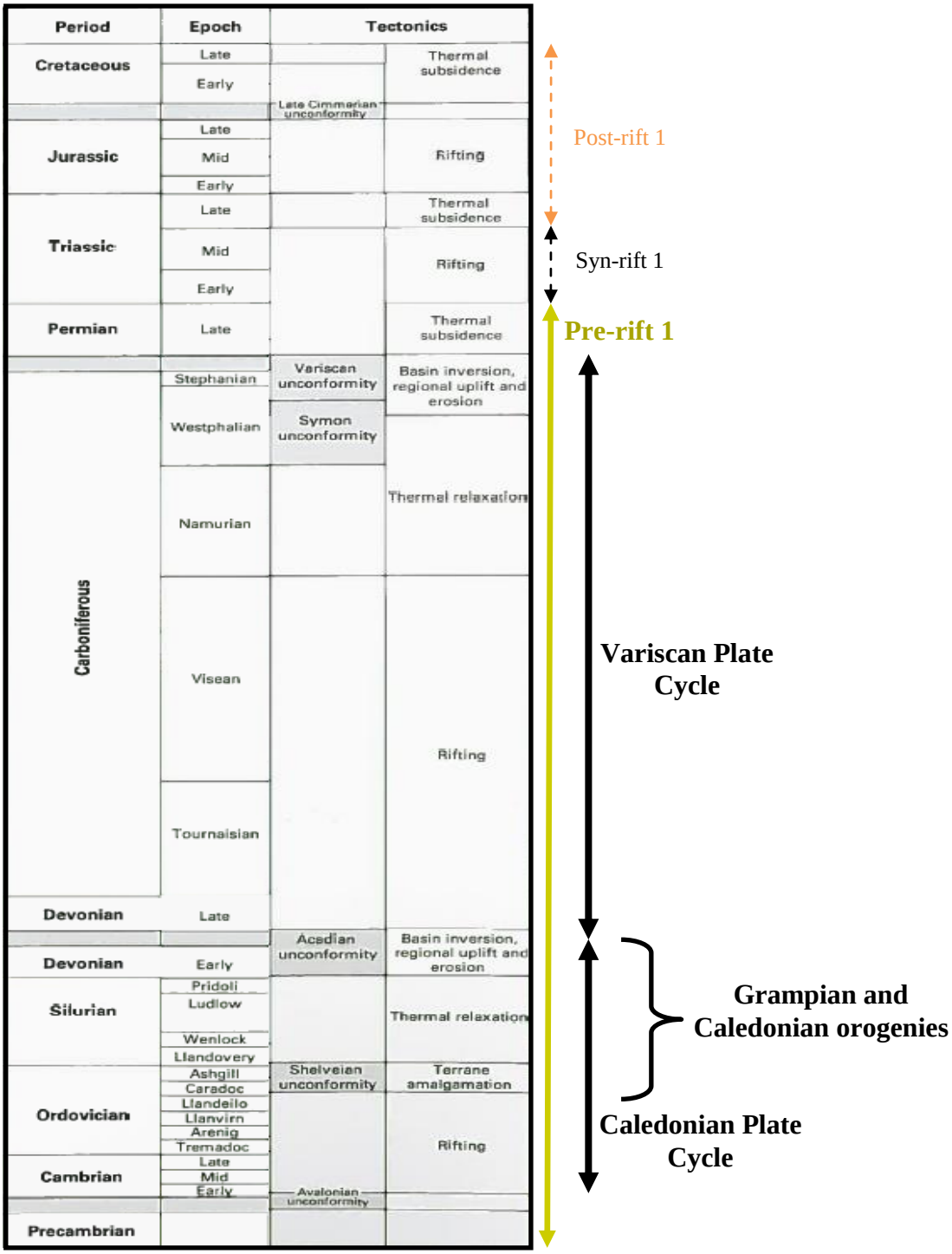

Figure 2.2: Paleozoic and Mesozoic tectonic events highlighting the plate cycles and orogenic events recognised within the pre-rift sequence of tectono-stratigraphic megasequence 1.
Image modified after (Pharoah et al. 2011)

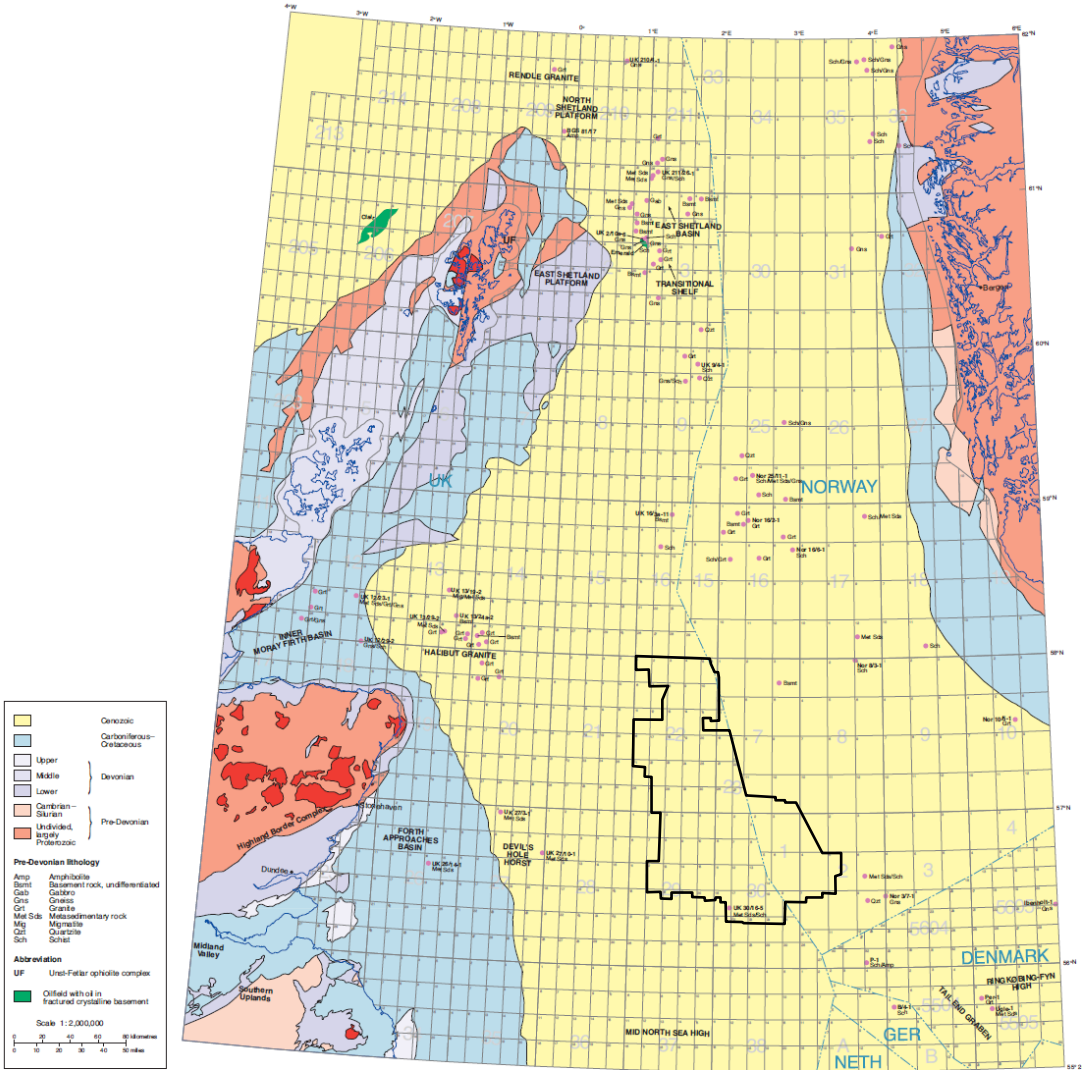

Figure 2.3: Well penetrations of pre-Devonian rocks.
Image after Evans 03

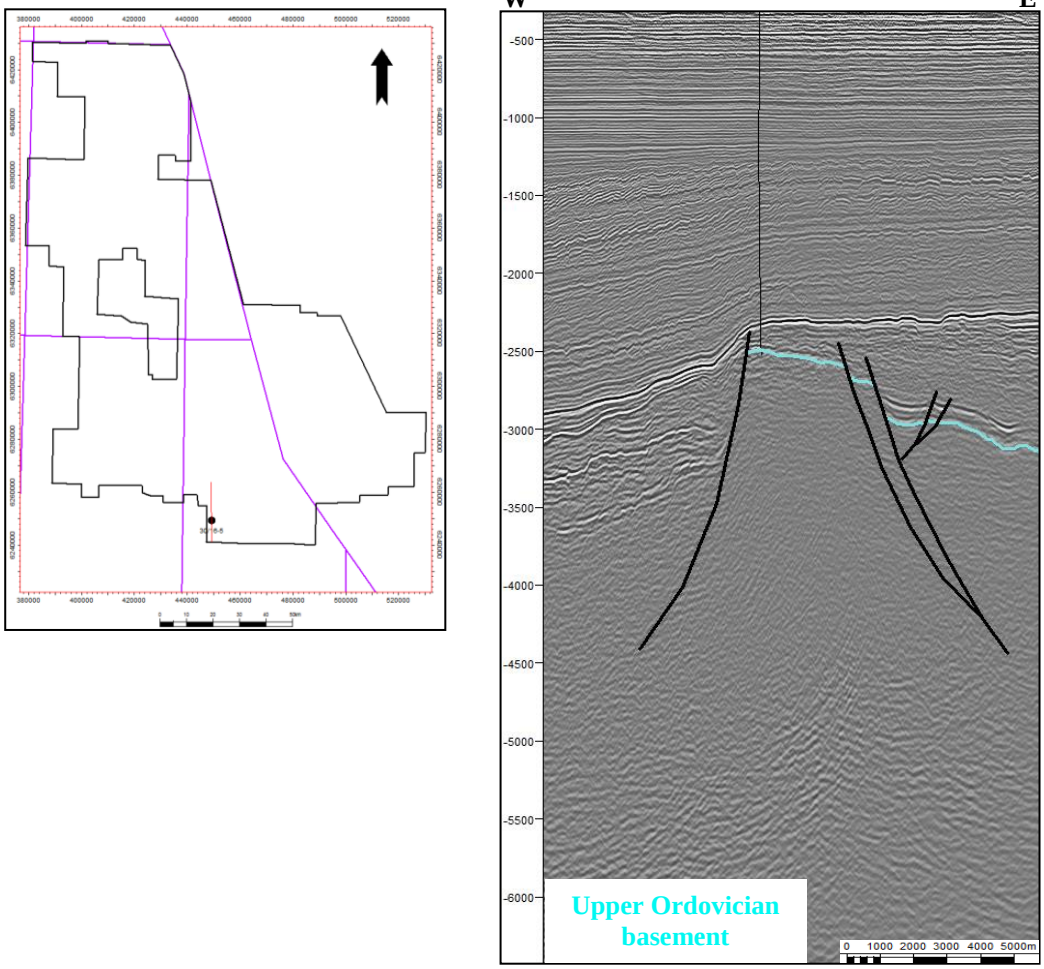

Figure 2.4: W-E seismic line through well 30/16-5 which penetrated Upper Ordovician metamorphics

2.2 THE CALEDONIAN PLATE CYCLE

Devonian and Carboniferous sections can be mapped in the Central North Sea and tied to the sparse well data. Imaging of basement structures on the rift-flanks and intra-basinal highs is good and a deep reflector on the Forties-Montrose High can be mapped over a wide area (Figure 2.5). There are no well penetrations which can provide an exact age date but well 22/18-4 proved a Devonian sequence stratigraphically higher than this marker so it is taken to be Mid-Lower Devonian or older. On the Jaeren High, deep drilling encountered a Devonian sandstone sequence unconformably overlain by Lower Permian Rotliegend sequences (Figure 2.6). Further south, in quadrant 30, well bores prove a Middle Devonian sequence on the Auk Ridge which can be traced around a limited area (Figures 2.7 and 2.8), this may be the same reflector as in the Forties-Montrose High area although this cannot be verified. A major unconformity at the base of the Permian can be mapped on the Auk Ridge and West Central Shelf (Figures 2.9 and 2.10) underlain by Devonian rocks where penetrated by the 30/16-5 well.

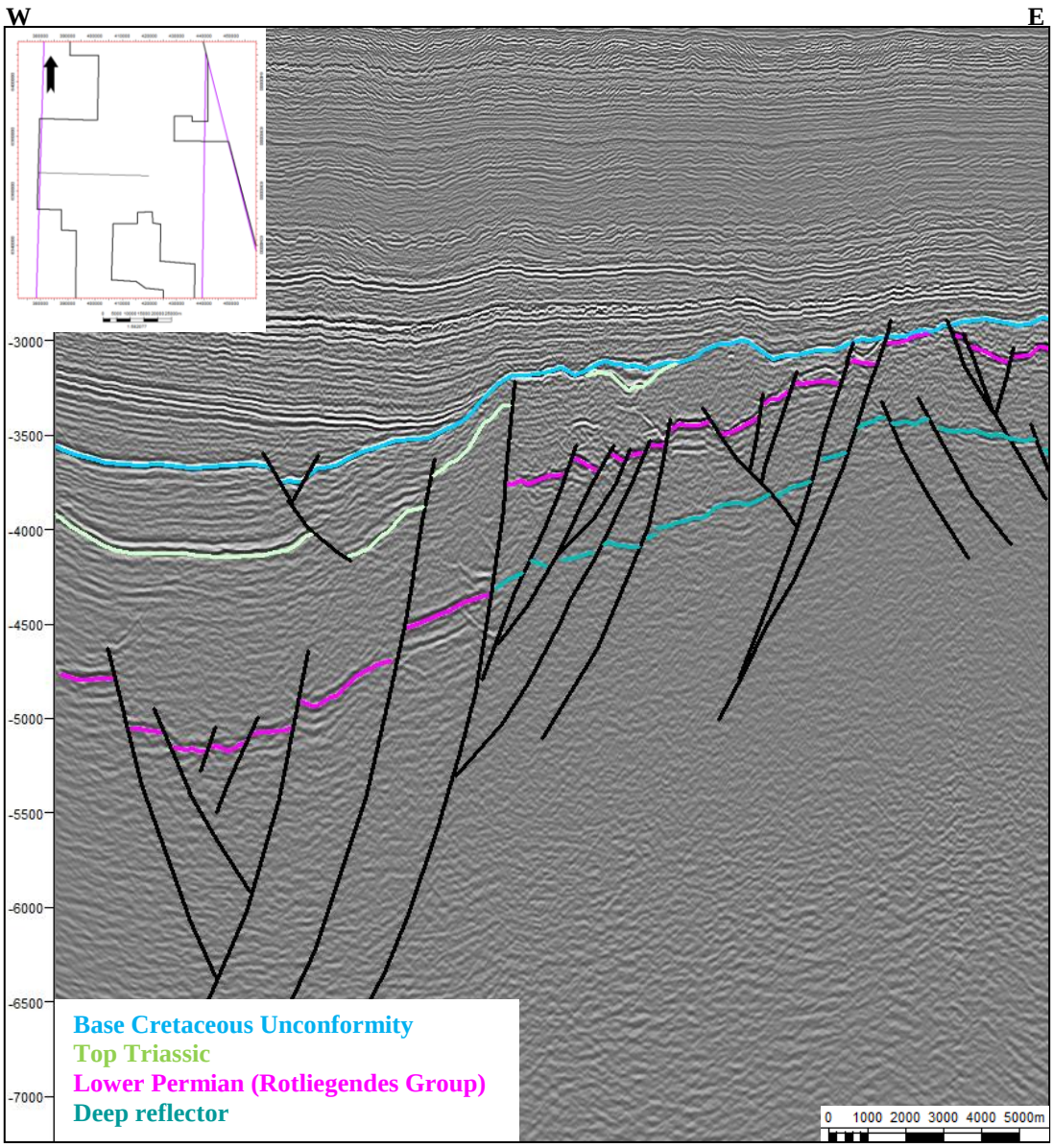

Figure 2.5: W-E seismic line showing deep reflector on the Forties-Montrose High. In the graben it becomes too deep to be interpreted confidently.

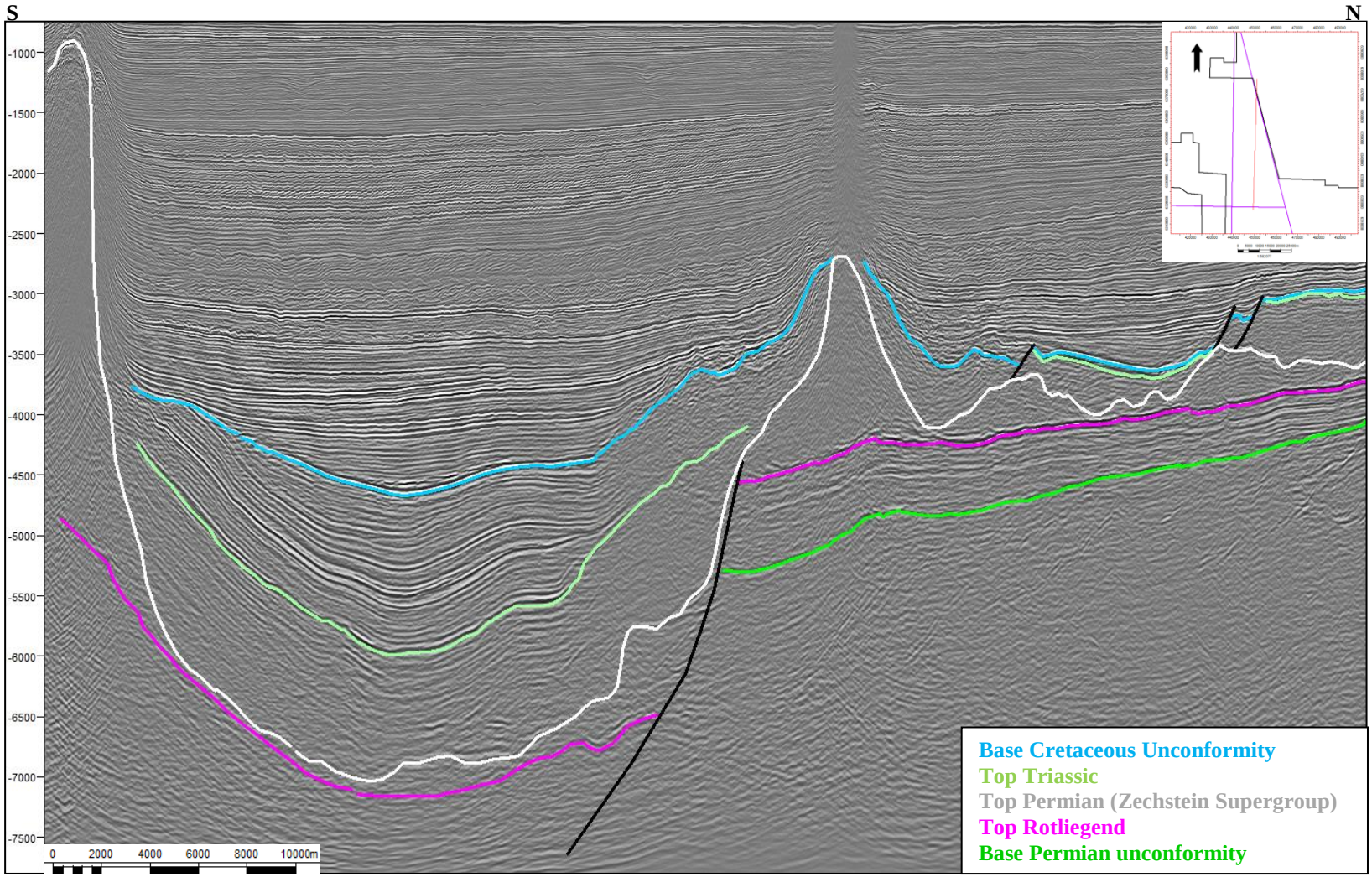

Figure 2.6: S-N seismic line over the Jaeren High showing Base Permian Unconformity.

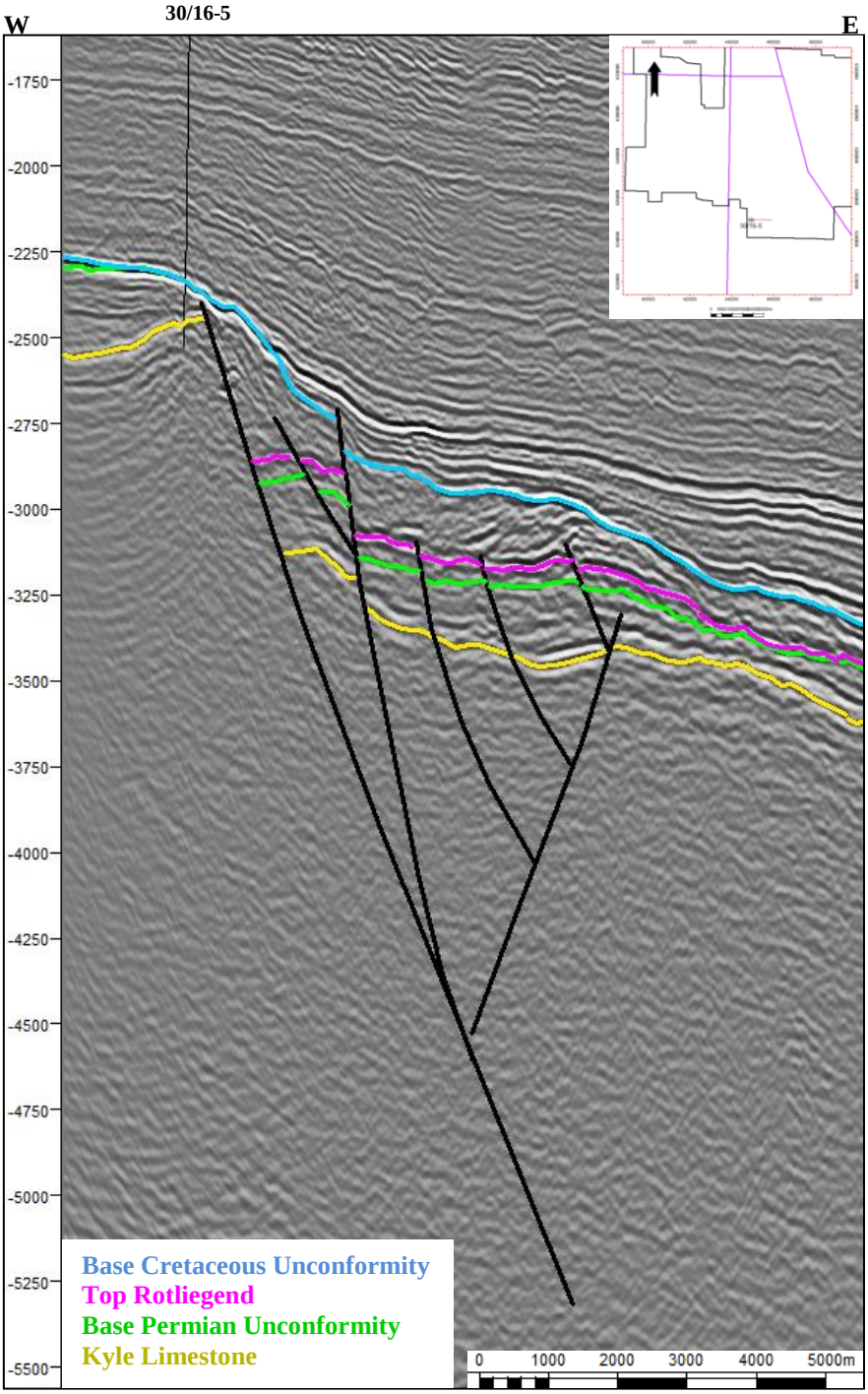

Figure 2.7: W-E seismic line through well 30/16-5 showing Middle Devonian Kyle Limestone. The lack of Jurassic and Cretaceous rocks on the high indicates that this area was elevated through the Mesozoic.

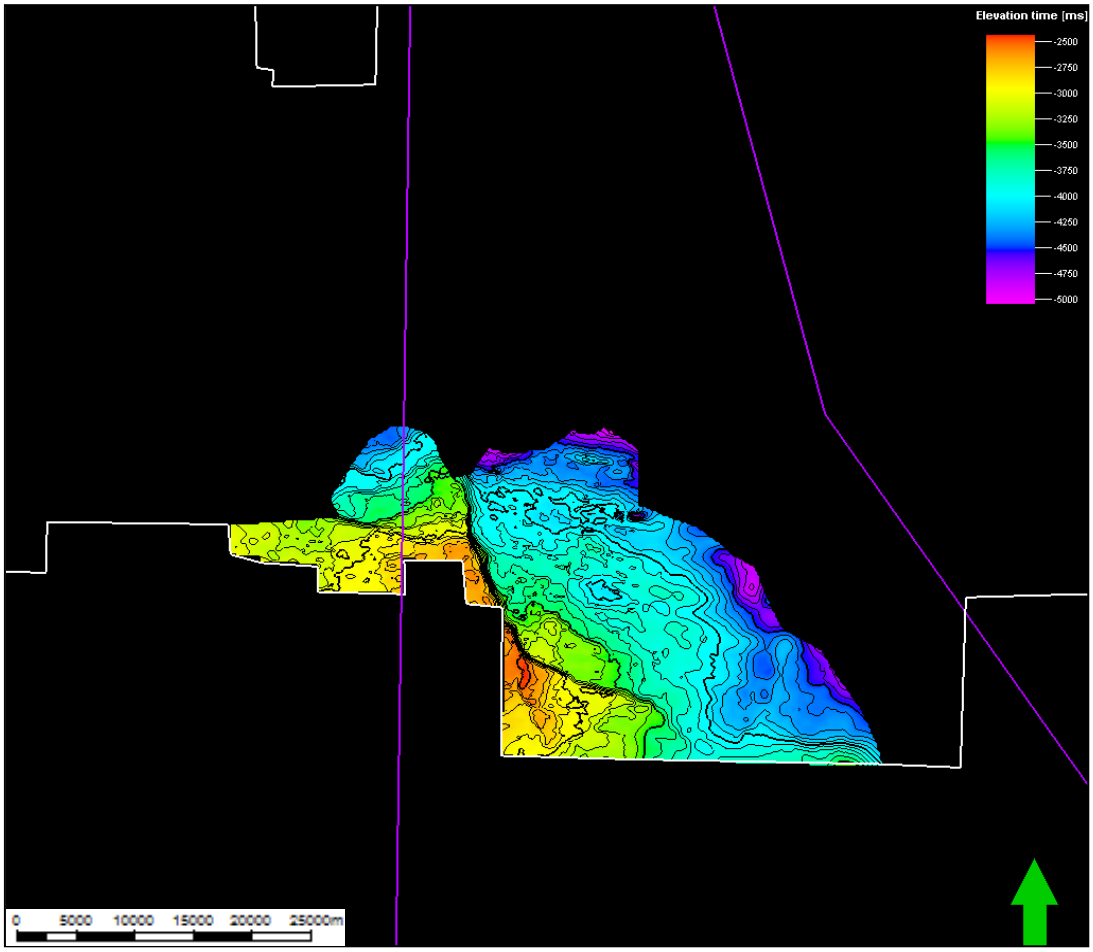

Figure 2.8: Middle Devonian Kyle Limestone TWTT structure map showing mappable extent of Lower Paleozoic rocks.

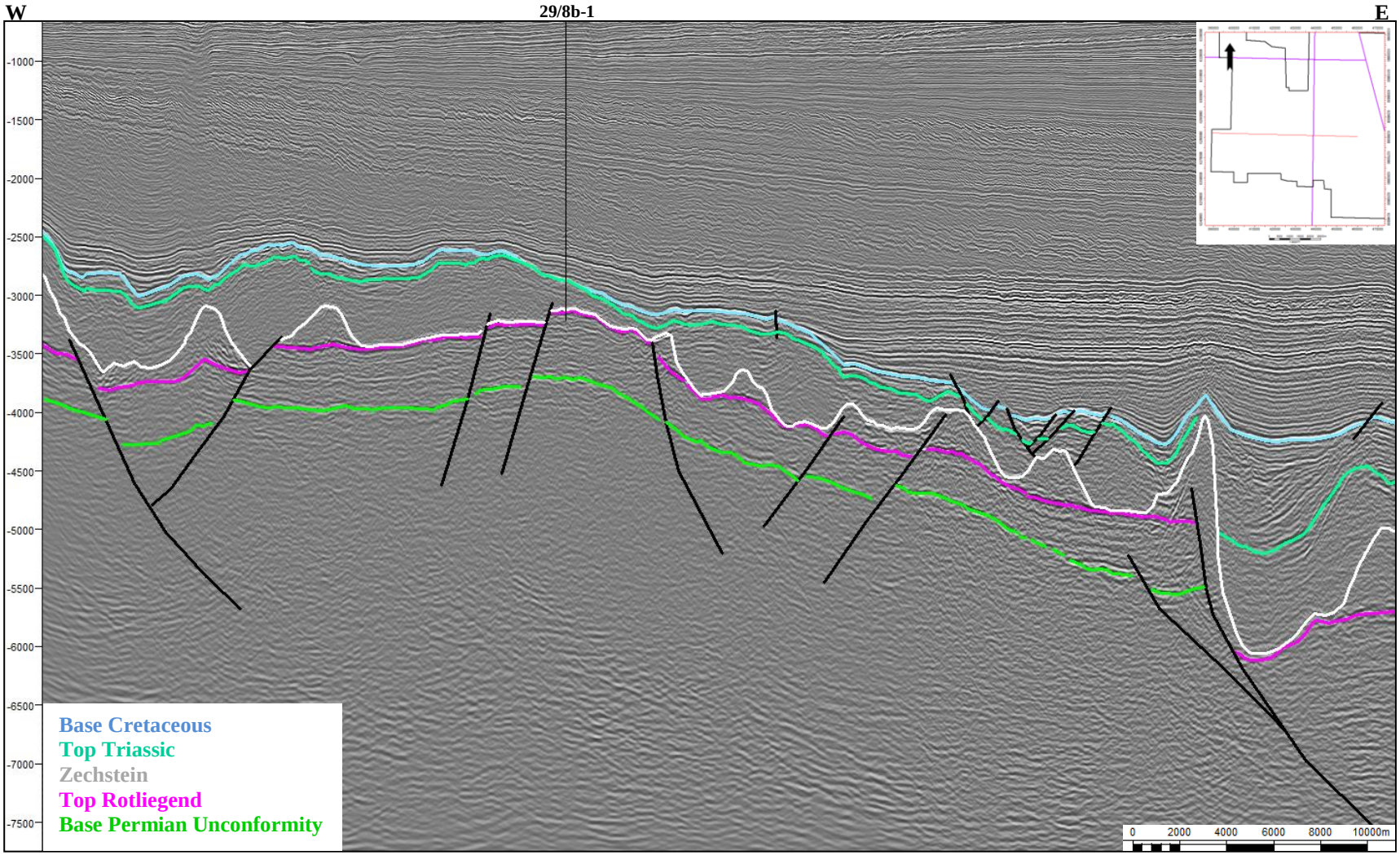

Figure 2.9: W-E seismic section showing the Base Permian Unconformity traced over the Auk Ridge.

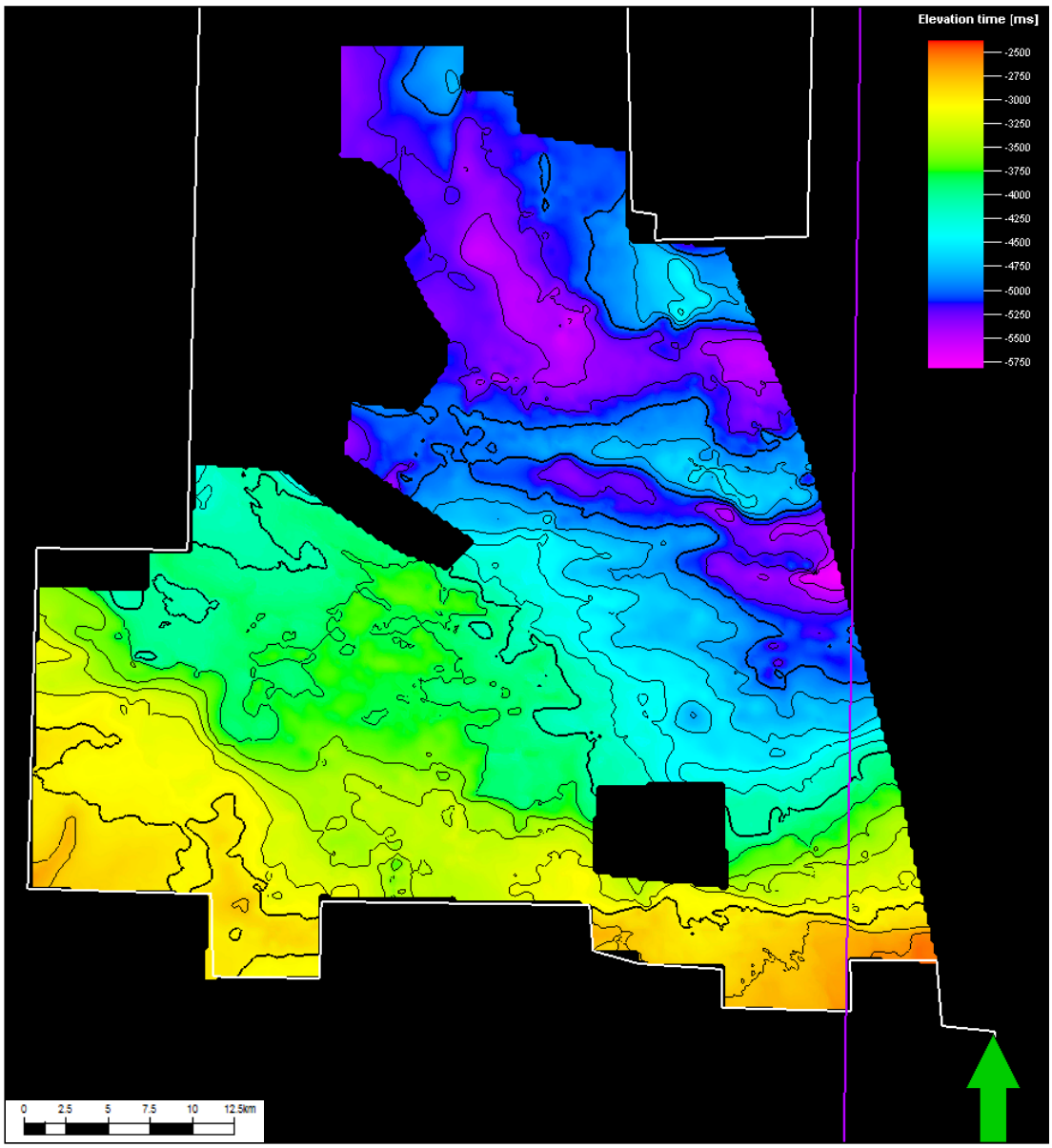

Figure 2.10: TWTT surface map of the Base Permian Unconformity on and around the Auk High.

These small snapshots of the Lower Palaeozoic geology are difficult to interpret on their own, however these sequences are well-imaged on seismic data and at outcrop throughout the onshore UK. Understanding the geological evolution recorded in onshore sections can be extrapolated offshore and put the fragments of data available from the Central North Sea in context.

2.2.1 ONSHORE ANALOGUES AND DISCUSSION

The deep burial of the pre-Permian rocks in the Central North Sea, the lack of well-control and the overprinting by later rift episodes, poses a problem for interpretation of the geological events which occurred during this period. However, these rocks can be easily interpreted onshore at outcrop and on seismic data due to exhumation and the area being outside of the immediate sphere of influence of the most recent episode of rifting which in the Central North Sea, served to bury the Early Paleozoic section beyond the limits of seismic resolution. Use was therefore made of 2D seismic data from the UK Onshore Geophysical Library (UKOGL) (Figure 2.11) together with surface mapping and well information to provide insight into the nature of basin development and deformation that is likely to be buried beneath the Central North Sea. Stratigraphy in the onshore sections differs from the offshore as it includes additional units in the Pre-Devonian section which have not been formally recognised offshore (Figure 2.12).

Paleomagnetic data suggests that during the Early Paleozoic most of the continental landmasses were accreted into a supercontinent Gondwana, which was situated around the South Pole. Around 650-550Ma smaller continents began to separate from this landmass and drift north. One of these detached landmasses Avalonia, together with the Baltica and Laurentian blocks, was to eventually form much of NW Europe including the North Sea area. During the Late Cambrian to Late Silurian, subduction of the Iapetus Ocean and Tournquist Sea between these continental

fragments, led to an eventual continental collision termed the Grampian and Caledonian orogenies (Underhill 2003) (Figure 2.13).

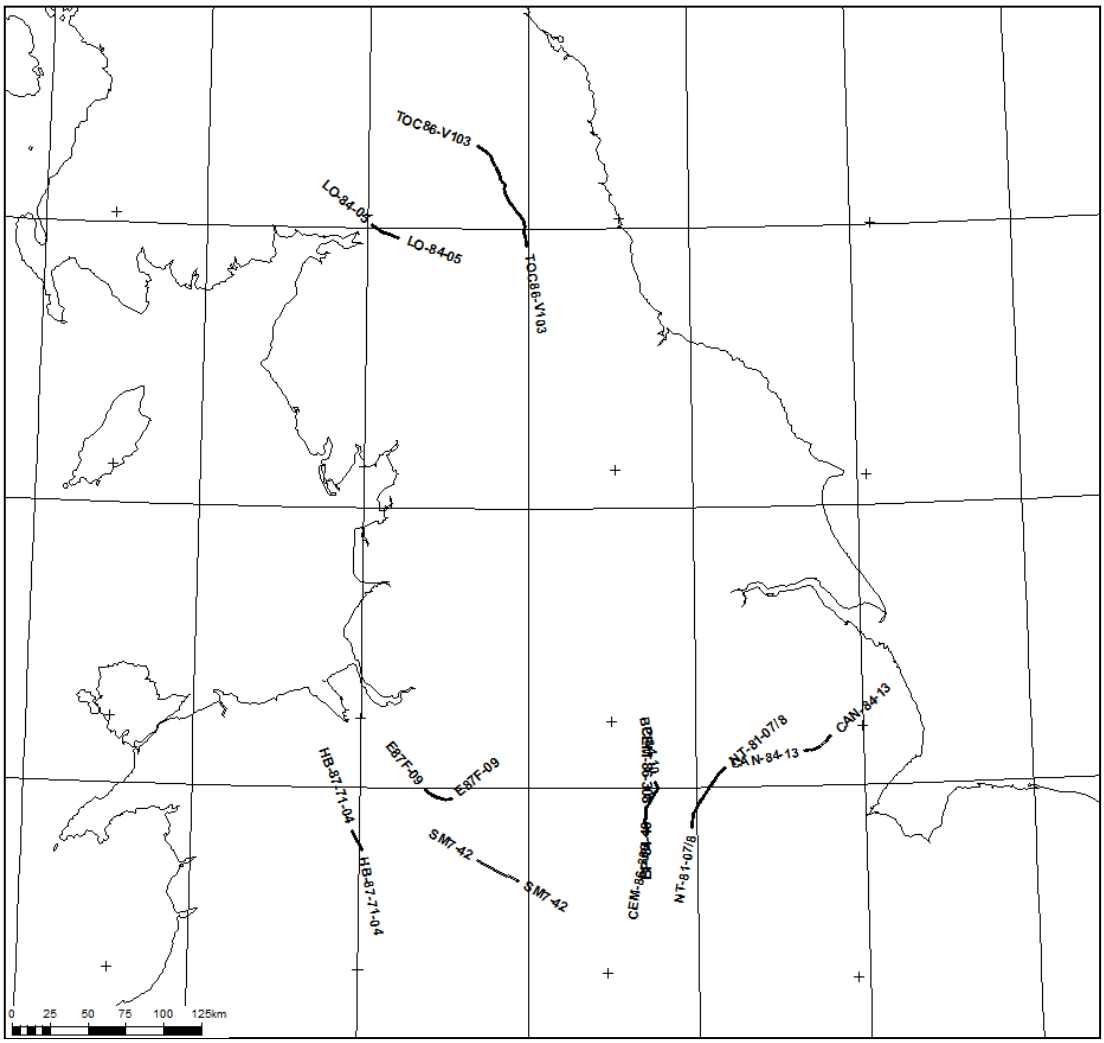

Figure 2.11: 2D onshore seismic lines shown in this volume.
Data courtesy of UKOGL

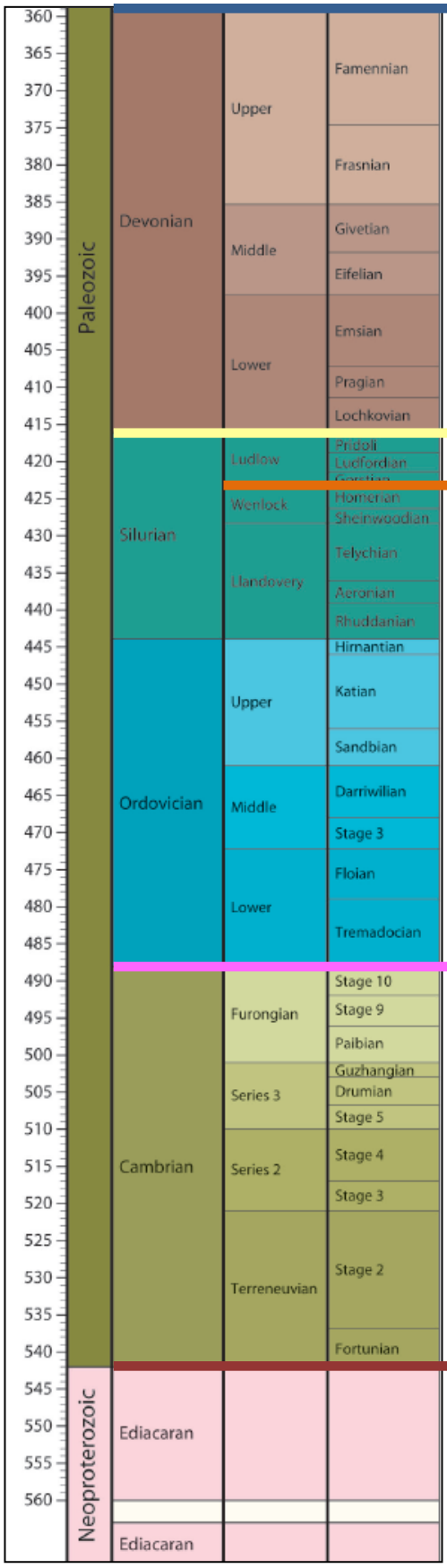

Top Devonian. Old Red Sandstone Group. Represents erosion of Caledonian highlands.

Base Devono-Carboniferous. Often unconformable where Lower Devonian absent. Represents final suturing of Iapetus and start of Devono-Carboniferous extension and infill.

Wenlock Limestone. Intra-Silurian marker, deposited during early Caledonian orogenesis.

Top Cambrian. Preservation is limited and strongly affected by later deformation; little information on original depositional environment in a regional context can be ascertained. Where recognised Cambrian rocks consist of basal quartzite and sandstone with overlying shale and thin limestones.

Top Pre-Cambrian. Schist, gneiss and intrusives.

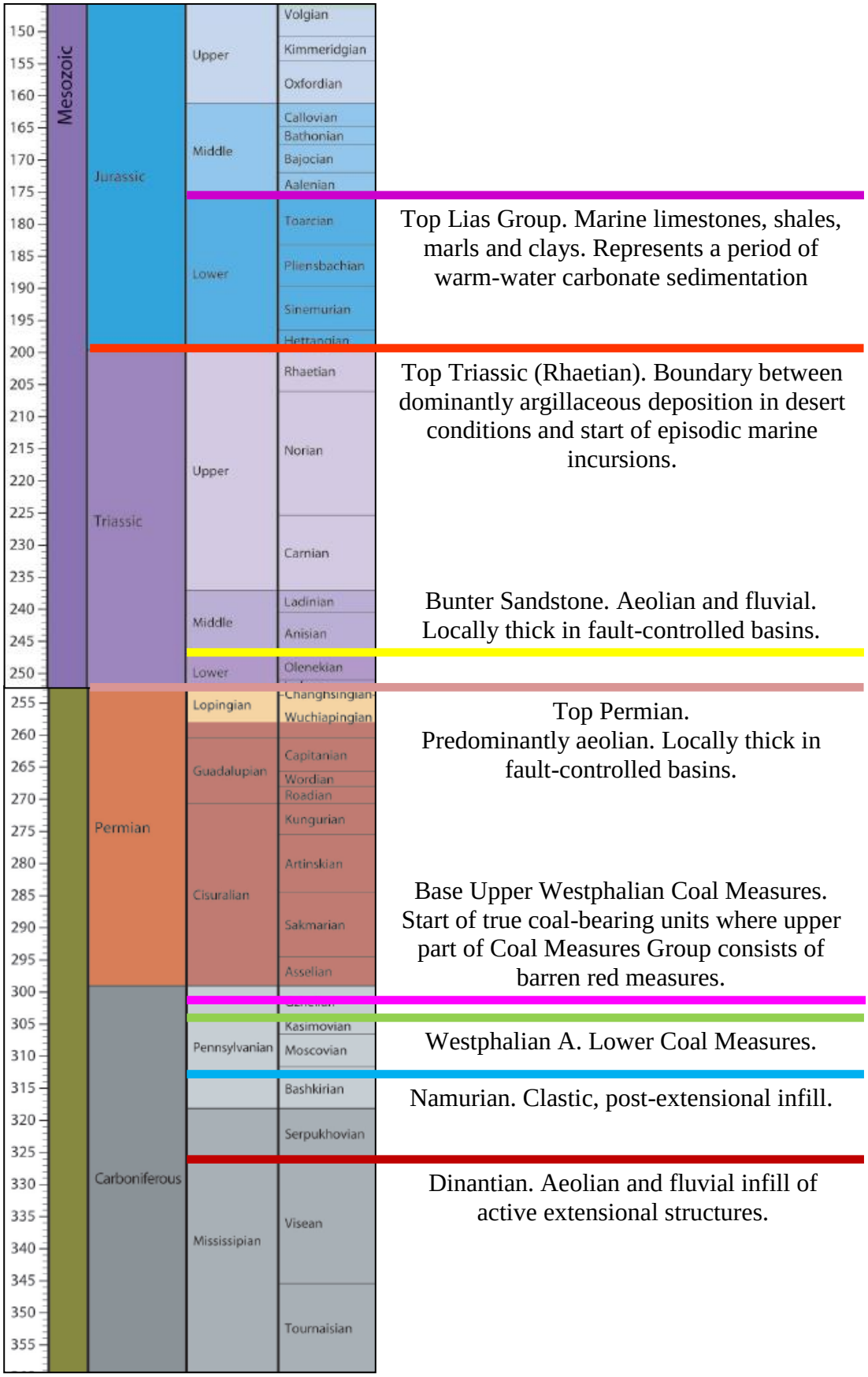

Figure 2.12: Stratigraphic column for the onshore UK sections.

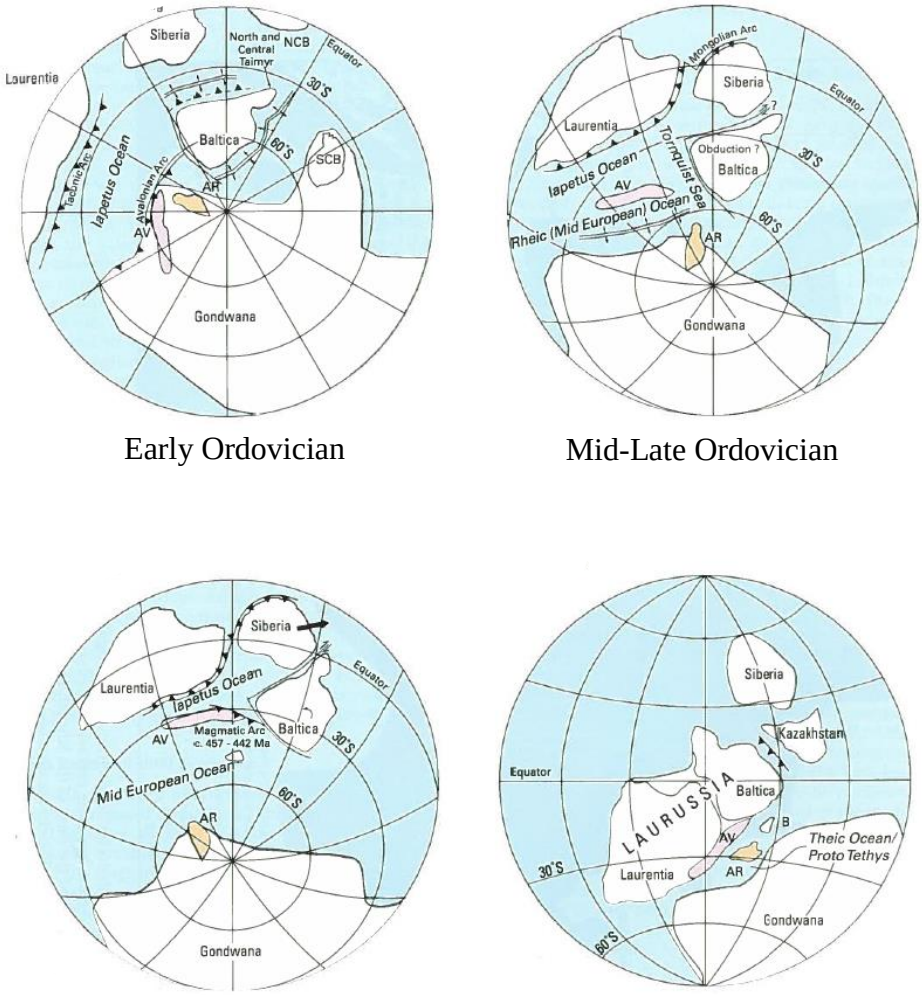

Figure 2.13: Paleogeographic reconstructions to illustrate the accretion events which took place in the Lower Paleozoic.

AR European massifs including Armorica, Iberia and Bohemia, **AV** Avalonia Terrane, B Bohemia Terrane, **NCB** North China Block, **SCB** South China Block

Image after (Pharoah et al. 2011)

The collision is termed the Caledonian orogeny but in fact consisted of several collision events, often localised, which occurred over a period of 200Ma (Pharoah et al. 2011). Onshore field geology has dated a Mid –Late Ordovician collision event which created the Grampian Mountain range in Scotland. Mineralogy suggests that this event was the result of collision between an island arc in the Iapetus Ocean and the edge of the area now known as the Grampian Highlands. The suture zone is marked by the Highland Boundary Fault (Figure 2.14).

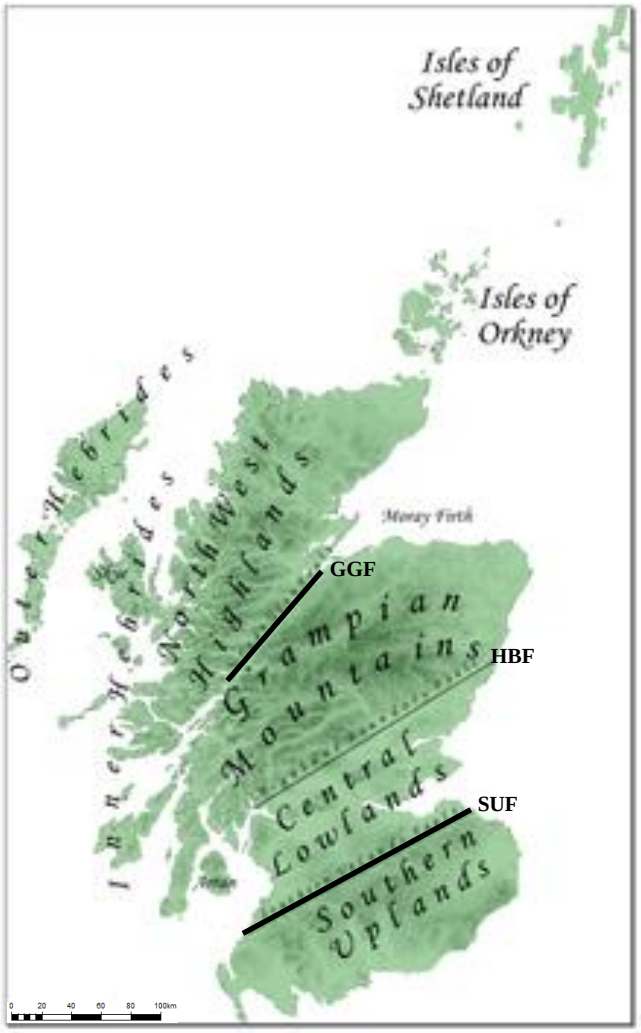

Figure 2.14: Map of Scotland at present highlighting the Lower Paleozoic lineaments.

GGF Great Glen Fault, **HBF** Highland Boundary Fault, **SUF** Southern Uplands Fault

In the Late Ordovician-Early Silurian, Avalonia and Baltica collided to form Balonia, following closure of the Tournquist. The final closure of the Iapetus Ocean resulted in the Acadian deformation phase from Late Silurian to Mid Devonian (Pharoah et al. 2011).

The suture line formed by the eventual loss of the Iapetus Ocean can be traced from the West of Ireland through the Solway Firth to the Northumberland coast (Underhill 2003) (Figure 2.15). The lineament, known as the Iapetus suture, has existed as a major line of weakness since the Devonian and has been reactivated many times under different tectonic regimes. Reactivation in extension during the Carboniferous led to the formation of a deep basin which filled with thick sequences of Carboniferous rocks, making it difficult to image the deep structures on conventional seismic (Figures 2.16 and 2.17). However, long-offset, deep seismic profiles identify a structure dipping 25°N (Chadwick et al. 1991) which could indicate the presence of the Iapetus suture. Its offshore continuation has never been proven but is suggested to bend north and link to the Tournquist suture somewhere offshore Norway (Roberts et al. 1999).

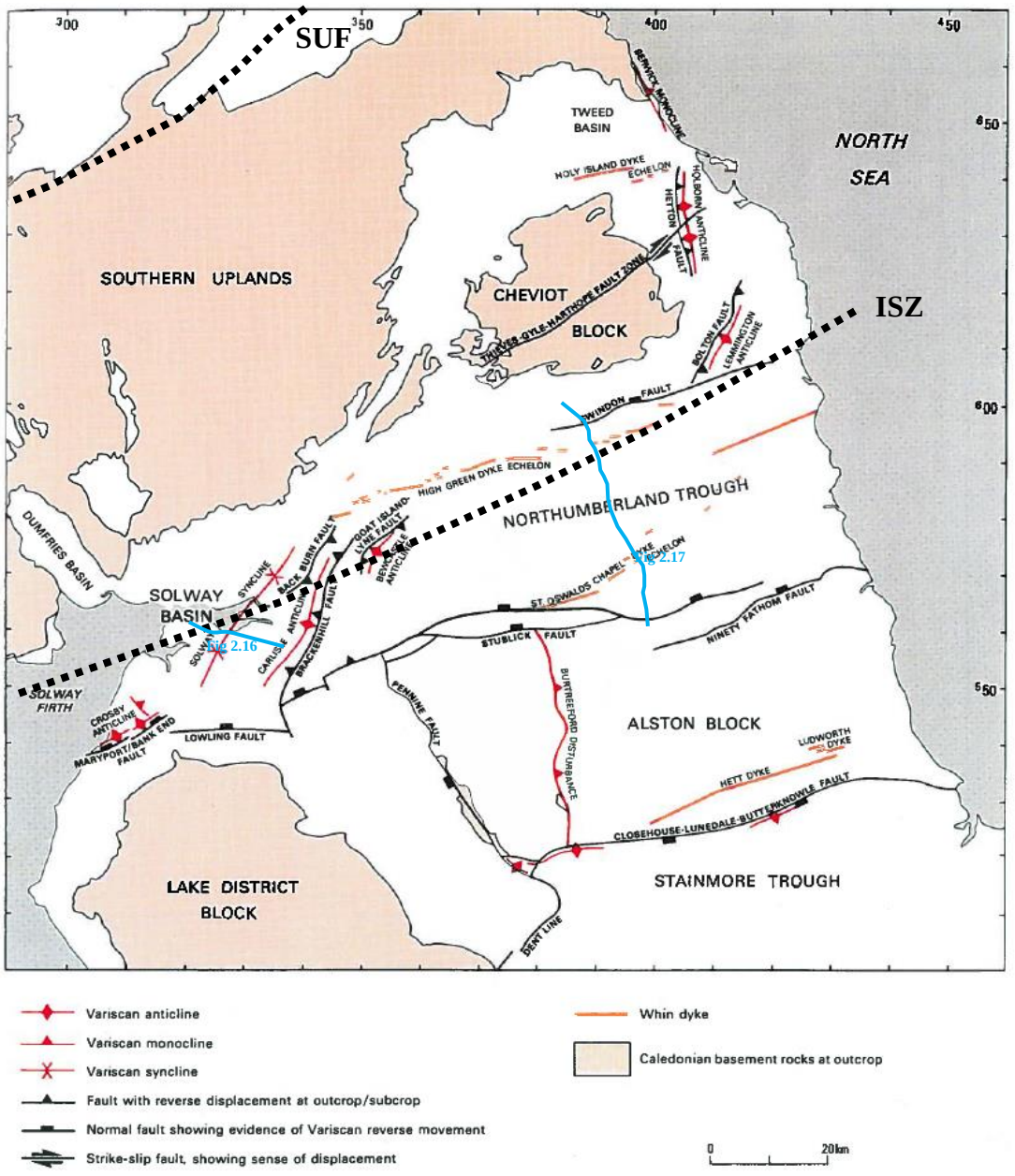

Figure 2.15: Possible geometry of the Iapetus suture zone superimposed on the present day subsurface structure of the area. Note the large Carboniferous Solway and Northumberland Basins and dike intrusions along with later Variscan inversion features which obscure the true trace of the ancient suture. Locations of Figures 2.16 and 2.17 shown.

ISZ Iapetus Suture Zone, **SUF** Southern Uplands Fault
Image modified after (Chadwick et al. 1995)

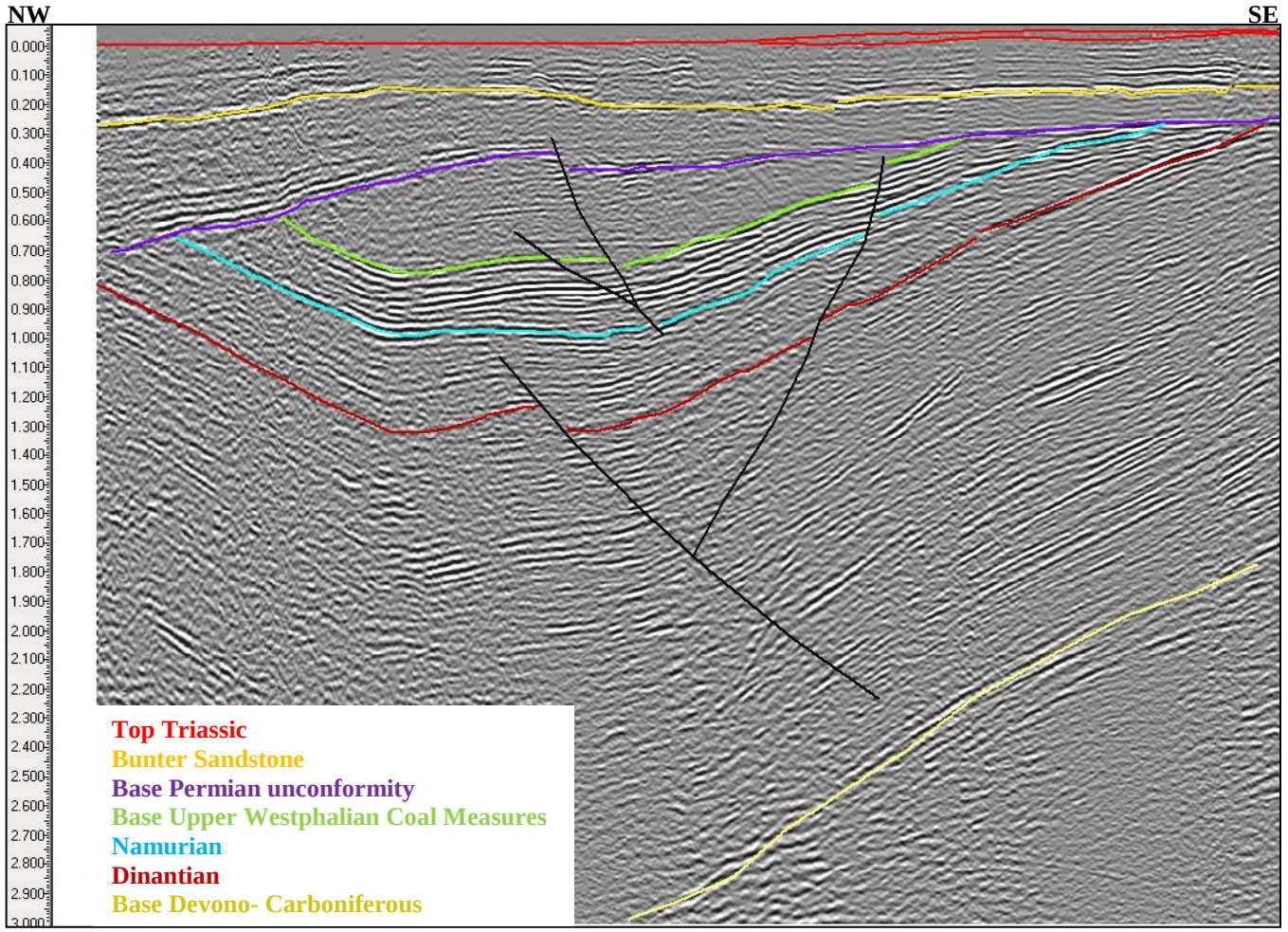

Figure 2.16: NW-SE seismic line across the Solway syncline showing thick Carboniferous sequence obscuring deeper features.
TWTTs in seconds in all onshore sections. UKOGL line LO-85-05. Scale = 12.35km

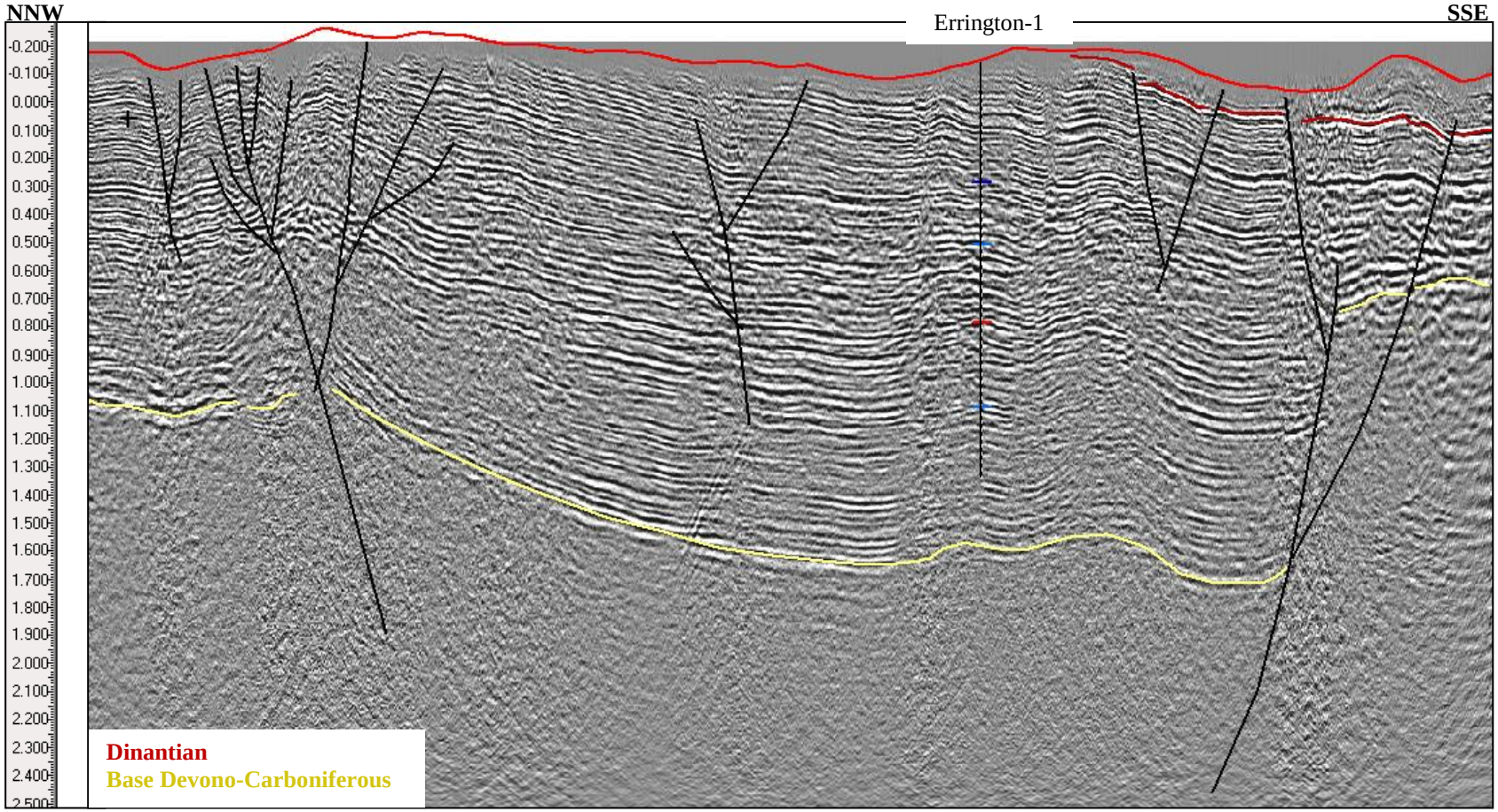

Figure 2.17: NNW-SSE seismic line across the Northumberland Trough showing thick Carboniferous sequence obscuring deeper features

UKOGL line TOC86-V103. Scale =32.2km

The triple junction formed between these continental fragments lies close to the triple junction which was formed almost 300 million years later due to Late Jurassic rifting (Roberts et al. 1999), demonstrating the long-lived nature of basement structural lineaments. In the onshore UK, Lower Paleozoic rocks outcrop extensively in the Welsh Borderlands and the Pennine Basin and additional well penetrations prove its occurrence across the Midlands. Lower Paleozoic rocks range from almost completely undeformed away from the major structural lineaments, (Figure 2.18) to intensely metamorphosed and deformed where they have been caught up in accretionary events.

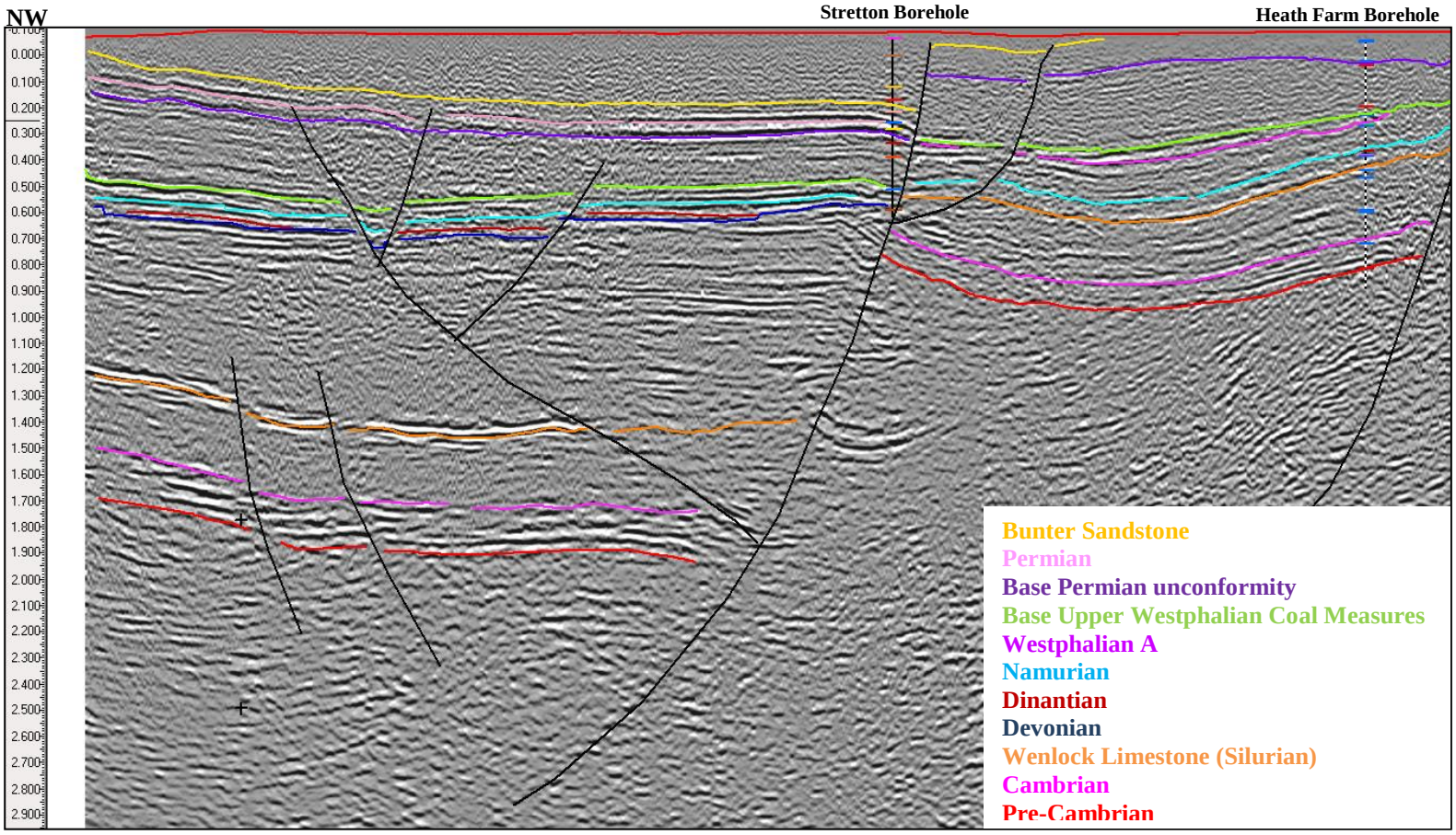

Figure 2.18: NW-SE seismic line showing conformable relatively undeformed Lower Paleozoic rocks in the middle of the Midlands Microcraton.

UKOGL line SM7-42. Scale= 16.1km

A number of granitic plutons were emplaced during Caledonian tectonism which form stable blocks such as the Alston and Askrigg blocks in the UK onshore (Smith et al. 2005)(Figures 2.19 and 2.20) Gravity and magnetic data suggest the existence of such granites offshore also. Seismic data in the Central North Sea also seems to indicate the presence of one of these basement massifs beneath the Auk Ridge in quadrants 29 and 30. The seismic character is transparent with no obvious continuous reflectors which in other areas has been shown to be indicative of igneous or metamorphic rocks (Figure 2.21).

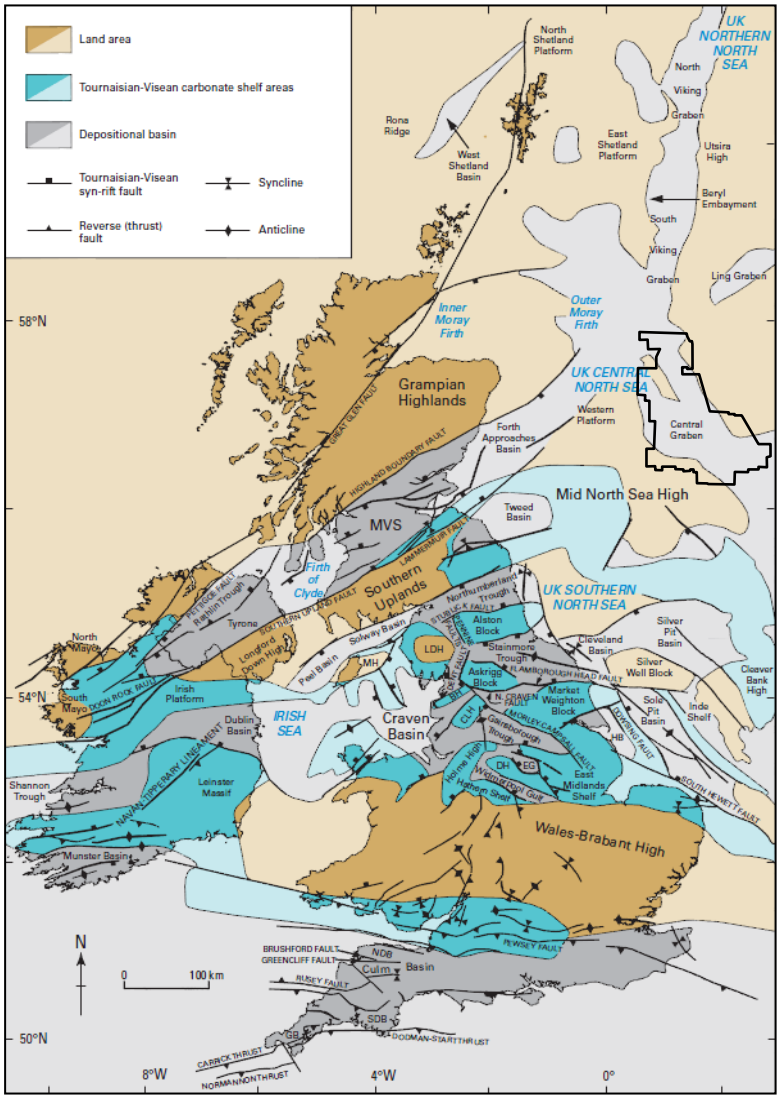

Figure 2.19: Carboniferous basins in the UK with location of dataset noted **BH** Bowland High, **CLH** Central Lancaster High, **DH** Derbyshire High, **EG** Edale Gulf, **GB** Gramscatho Basin, **HB** Humber Basin, **LDH** Lake District High, **MH** Manx High, **NDB** North Devon Basin, **MVS** Midland Valley of Scotland, **SDB** South Devon Basin
Image from (Waters et al. 2007)

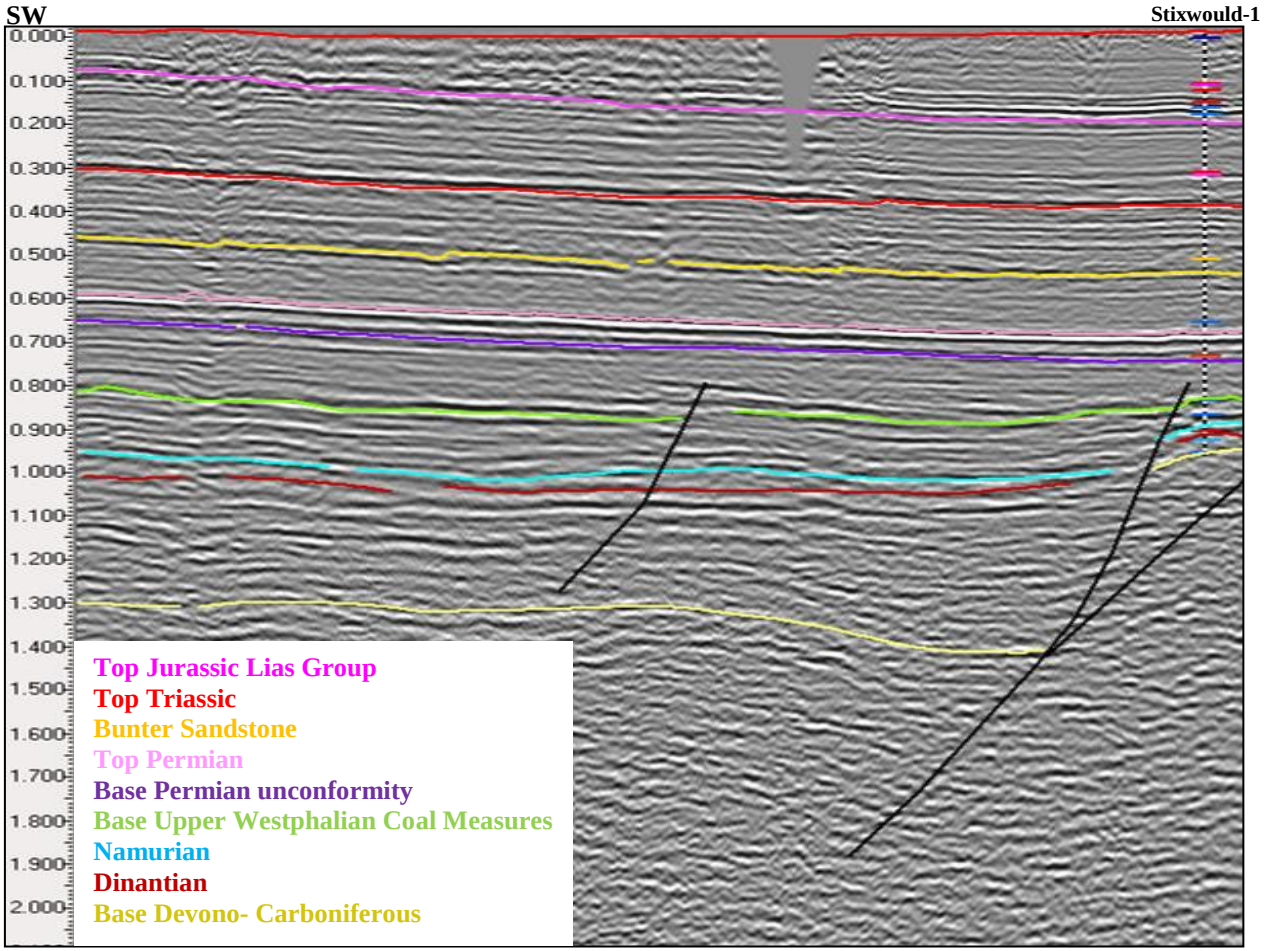

Figure 2.20: SW-NE seismic line over the Stixwould High, considered to be a possible Late Ordovician granite-cored high.
UKOGL line CAN-84-13. Scale= 12.3km

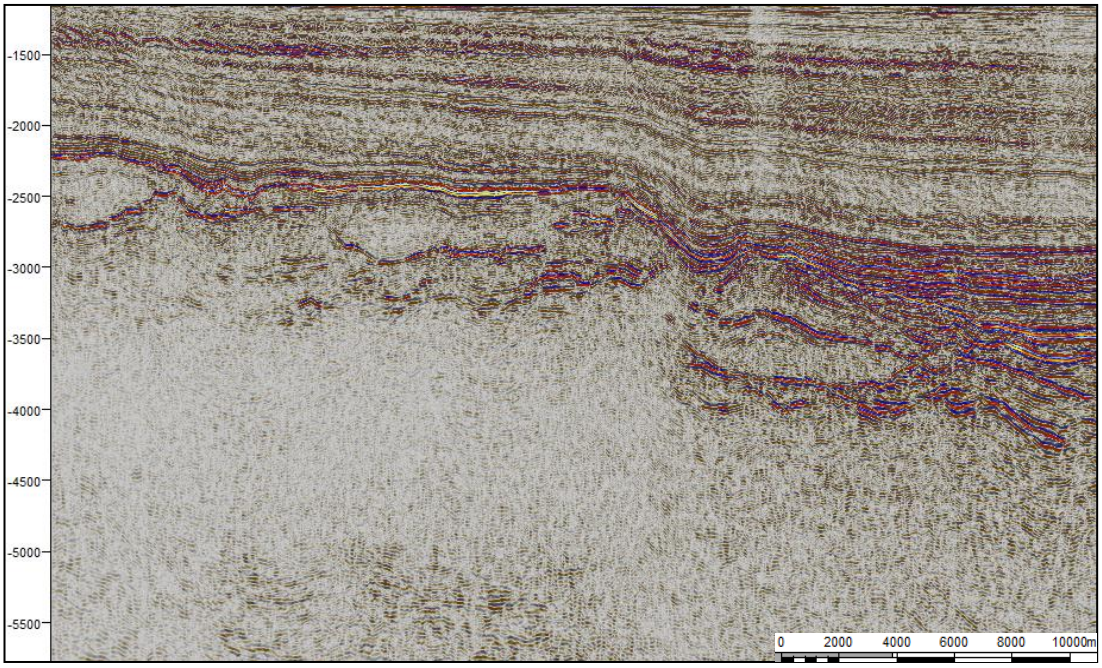

Figure 2.21: Seismically transparent area underlying the Auk Ridge suggests an intrusive mass

After cessation of Caledonian tectonics, intra-montane collapse of the uplifted orogenic belt, along with far field stresses generated by the opening of the Rheic Ocean to the south, led to rifting in the Mid-Late Devonian to Carboniferous (Underhill 2003). Large extensional basins developed, inheriting the basement NE-SW Caledonian trend and the WNW-ESE Tournquist trend (Figure 2.22).

Onshore these basins have been intensively studied and are well-imaged on seismic data and are found to be filled with very thick sequences of Devonian to Carboniferous rocks (Fraser et al. 1990). The Solway and Northumberland Troughs in northern England and the Widmerpool Gulf in the East Midlands contain in excess of 3200m (Chadwick et al. 1995; Pharoah et al. 2011) (Figure 2.23)

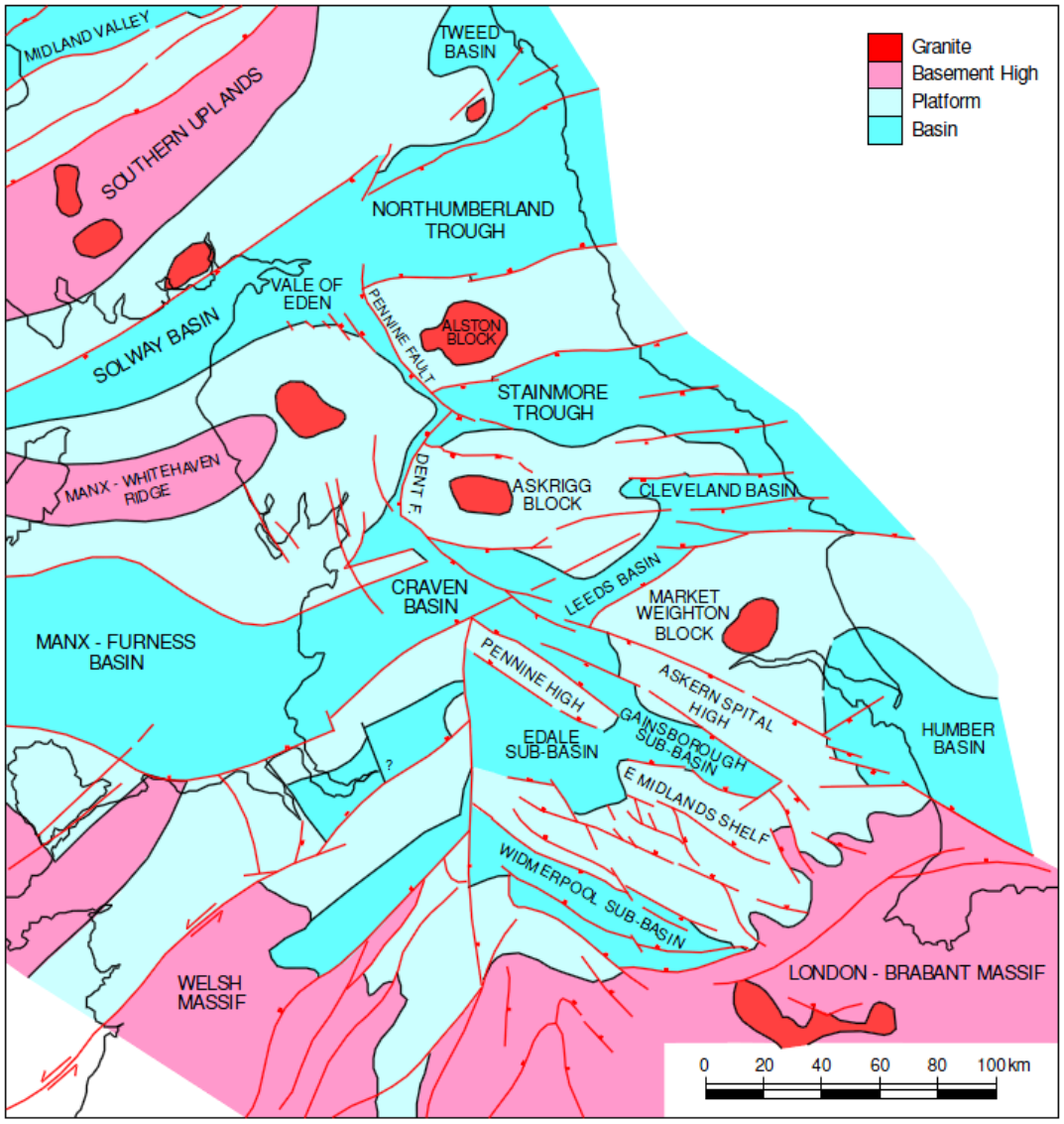

Figure 2.22: Extensional basins inherited the Caledonian and Tournquist trends.
Image from (BGS 2011)

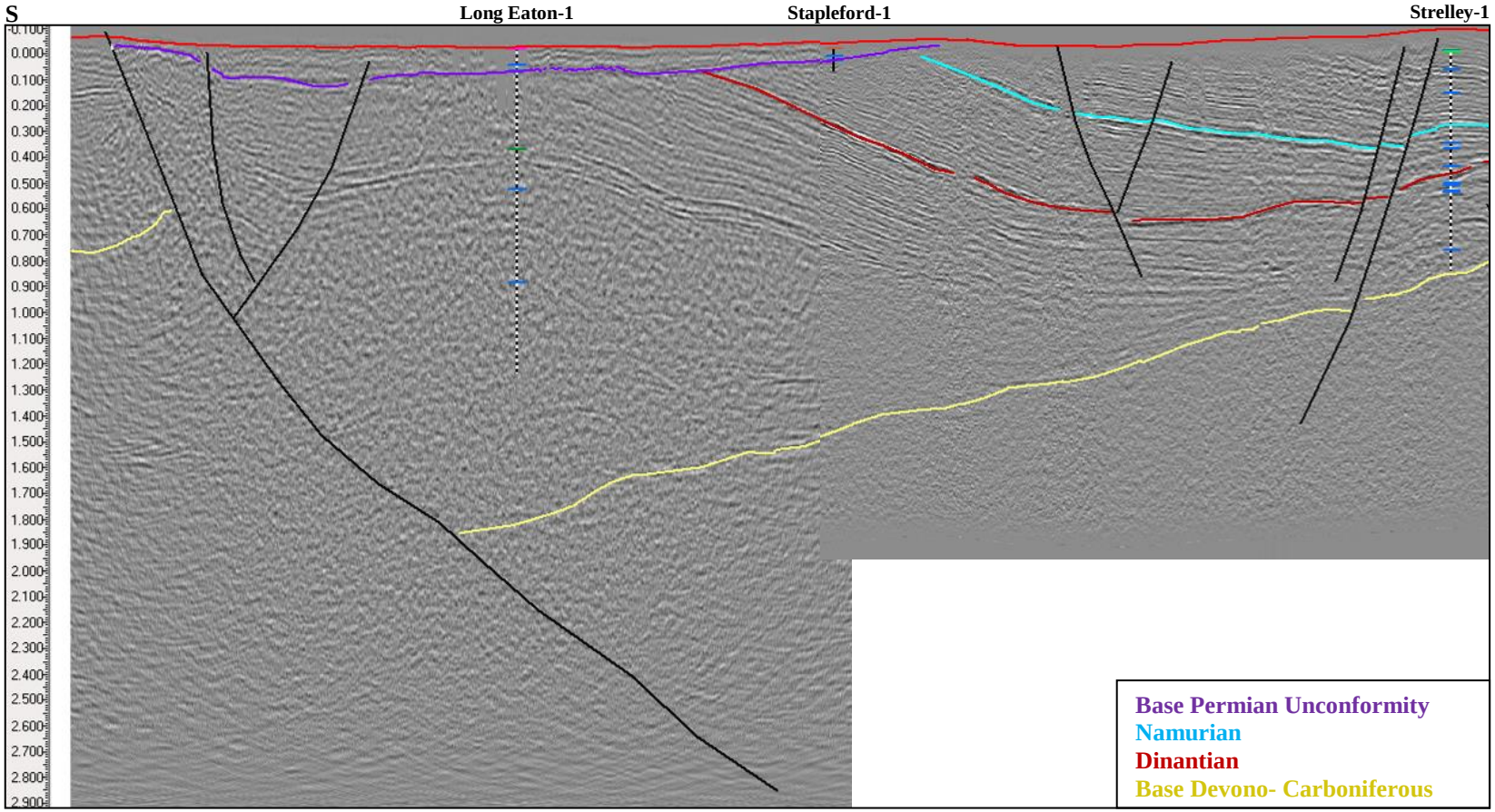

Figure 2.23: S-N composite seismic line across the Widmerpool Gulf showing thick Devono-Carboniferous infill.
UKOGL lines BP-84-10 and CEM-86-308. Scale= 19.6km

Onshore mapping of Devonian sequences coupled with offshore seismic data led to the recognition of major basins in the Faroe-Shetland region, Northern North Sea and onshore and offshore Norway, the largest of these is known as the Orcadian Basin and stretched from the Moray Firth to the Shetland Islands (Coward et al. 1989; Ziegler 1990) (Figure 2.24).

It may be possible to apply this technique to the Central North Sea.

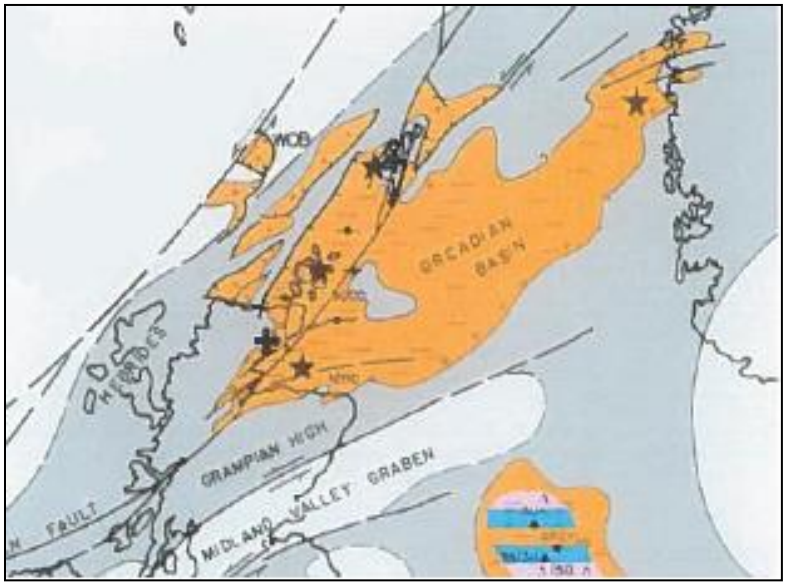

Figure 2.24: Extent of Devonian-age Orcadian Basin.
Image after (Ziegler 1990)

Onshore mapping of the pervasive Caledonian fabric of NE-SW striking lineaments bounding the Midland Valley of Scotland, the Southern Uplands and Solway-Northumberland Basins can be extrapolated offshore. Major faults of this orientation have been mapped from seismic around the Jaeren and Utsira Highs proving that continuation offshore is valid (Figures 2.25 and 2.26).

It may therefore be hypothesised that the Devono-Carboniferous basin trend also extends offshore.

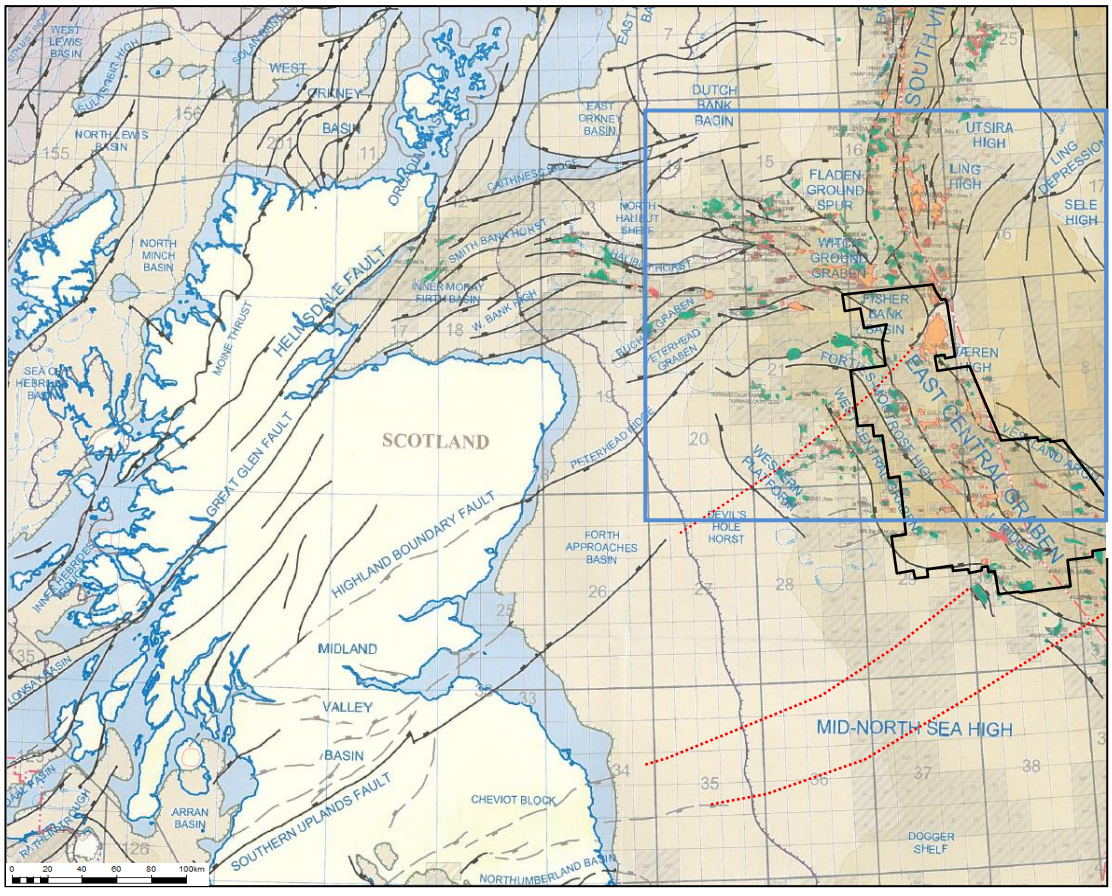

Figure 2.25: Possible continuation of onshore fault trends in the Central North Sea with respect to seismic study area.

Hydrocarbon fields and licence areas are also plotted to show the economic importance of understanding the regional geology. Location of Figure 2.25 outlined in blue

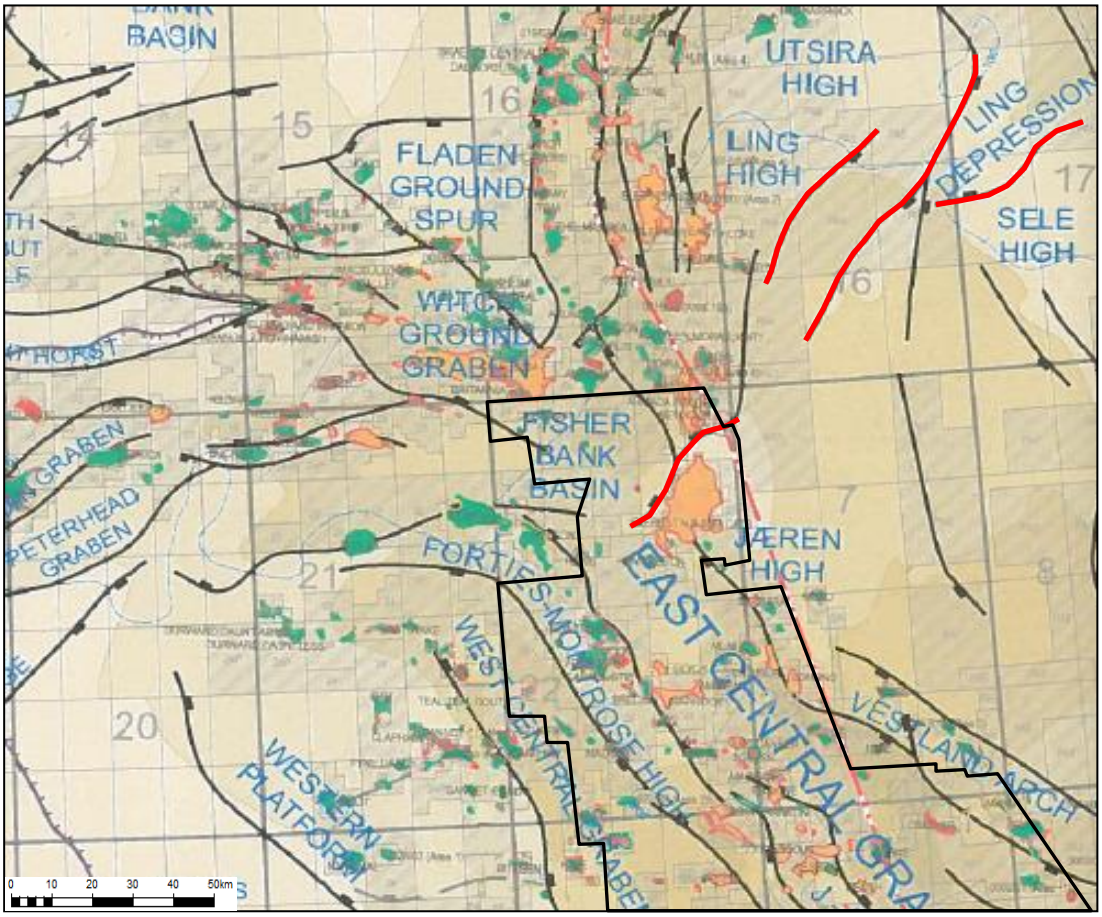

Figure 2.26: Caledonian fault trends of the Utsira, Ling and Jaeren Highs in the Central North Sea.

Mapping of pre-Permian sequences offshore is limited to the structurally higher areas in the Central North Sea. On and around the Auk Ridge in the Central North Sea it is possible to map a Devonian limestone sequence, the Kyle Limestone which represents a short-lived marine transgression in the Mid-Devonian. However, the Auk Ridge is considered to be a granite cored basement high and the Devonian sequence is very thin and therefore not considered representative of the majority of the Central North Sea.

Over the Forties-Montrose High, a Devonian reflector can be mapped and an isochron between this and the top of the Lower Permian Rotliegend shows thickening into lineations of a Caledonian trend (Figure 2.27). It is likely that at least half of this package is Permian in age as proved by the 22/18-4 well but the fault trends suggest that the rest of the section is Devonian in age.

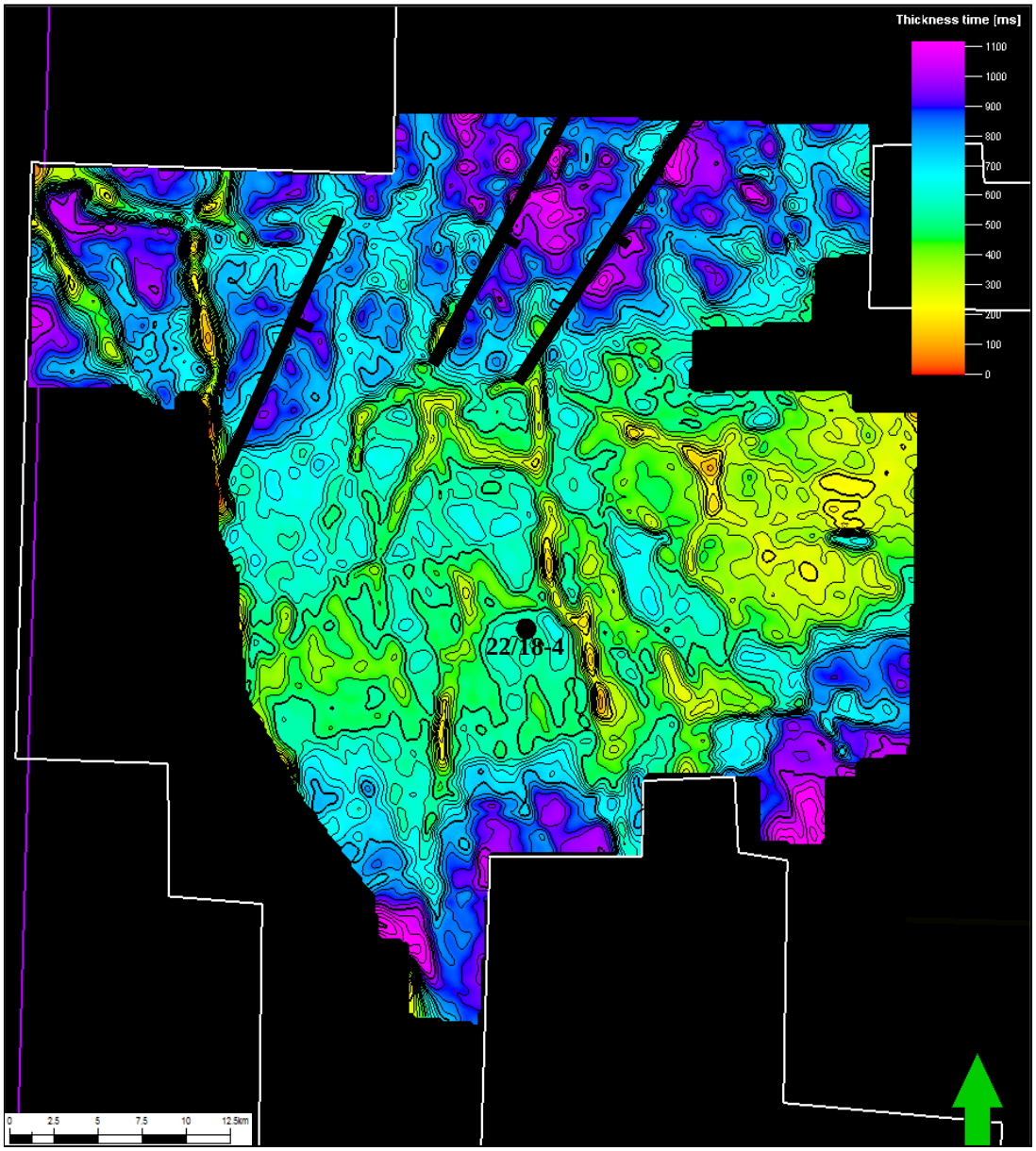

Figure 2.27: Isochron between the undefined basement pick and the Top Lower Permian shows faults following the Iapetus trend.
Note that the apparent thinning over the NW-SE striking lineaments is an artefact caused by the software gridding system.

Evidence of active faulting in the Devonian section in the Central North Sea suggests that basins did form, but the difficulty in separating the Permian and pre-Permian section in this area makes interpretation of their geometry difficult.

On the Jaeren High two wells, 22/10a-1 and 22/10a-2 penetrated a reddened Upper Devonian sandstone sequence beneath unconformably overlying Permian rocks (Figure 2.28). These rocks consist of a terrestrial sequence of sandstones derived from the eroding Caledonian mountain belt under an arid climate (Evans et al. 2003). Such deposits have a characteristic seismic response, forming an acoustically quiet zone due to the lack of sonic or density contrasts within the uniform sand unit (Figure 2.29).

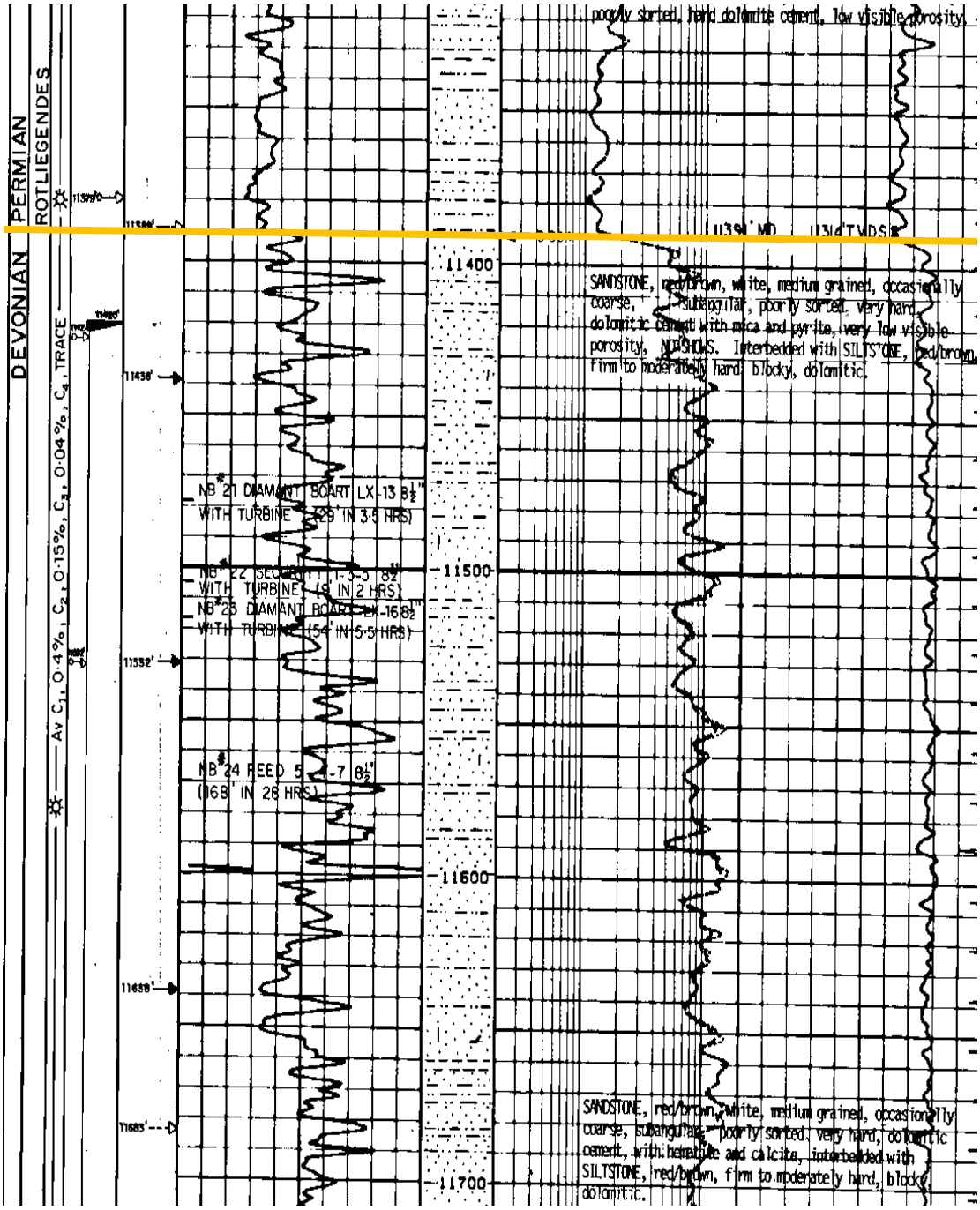

Figure 2.28: Composite log from well 22/10a-2 which penetrated a reddened Devonian sandstone sequence underneath the Base Permian Unconformity. Absence of the Carboniferous sequence suggests that this area was likely to have been a high feature during this period.

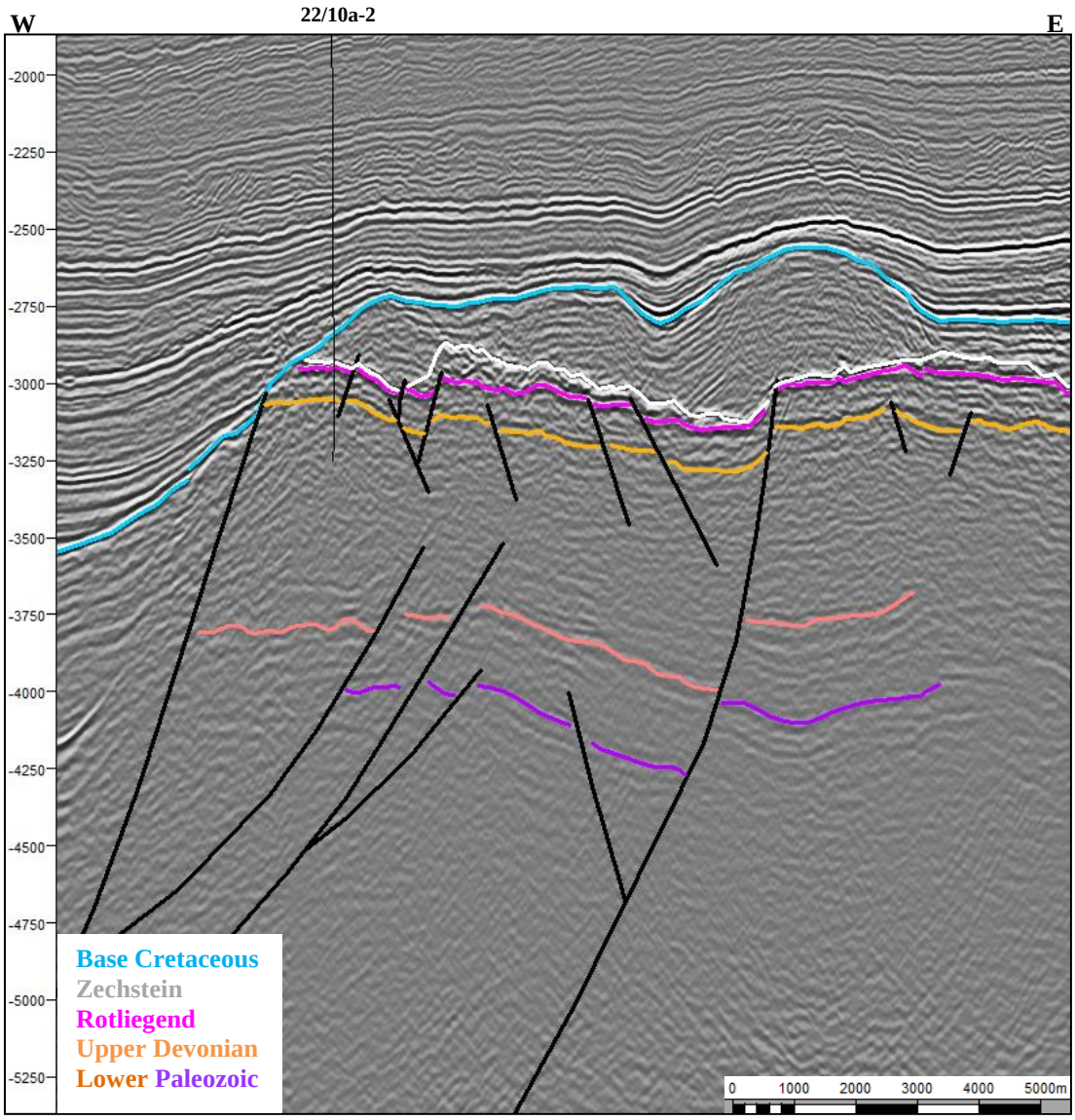

Figure 2.29: Basement sequences on the Jaeren High demonstrating the acoustically quiet response of the Devonian sandstones. Also note the presence of a conformable Lower Paleozoic sequence beneath, thickening to the west across a NW-SE Caledonian-trend fault.

To the south of the Jaeren High, the mappable units beneath the Permian sequence thicken, into a basin or a syncline (Figure 2.30) but it is difficult to determine which due to the section being transected by later faulting. The fault trends in the Forties-Montrose area suggest a basin is likely but analogues in the Midland Valley of Scotland and Solway Firth show significant deformation of the Devonian-Carboniferous section (Figure 2.31) which may extend offshore.

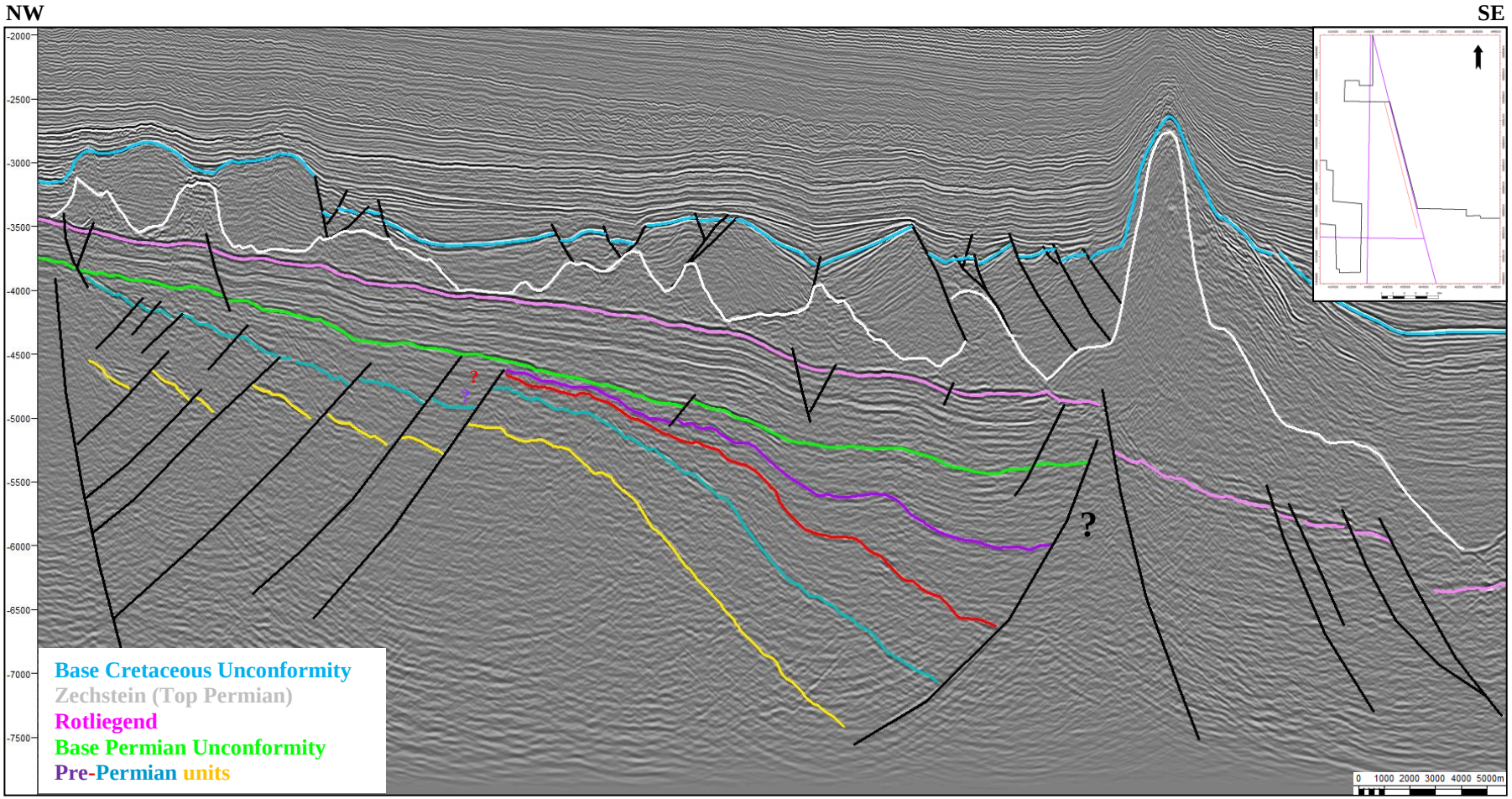

Figure 2.30: N-S seismic section south of the Jaeren High showing thickening of the pre-Permian section into a basin or a syncline.

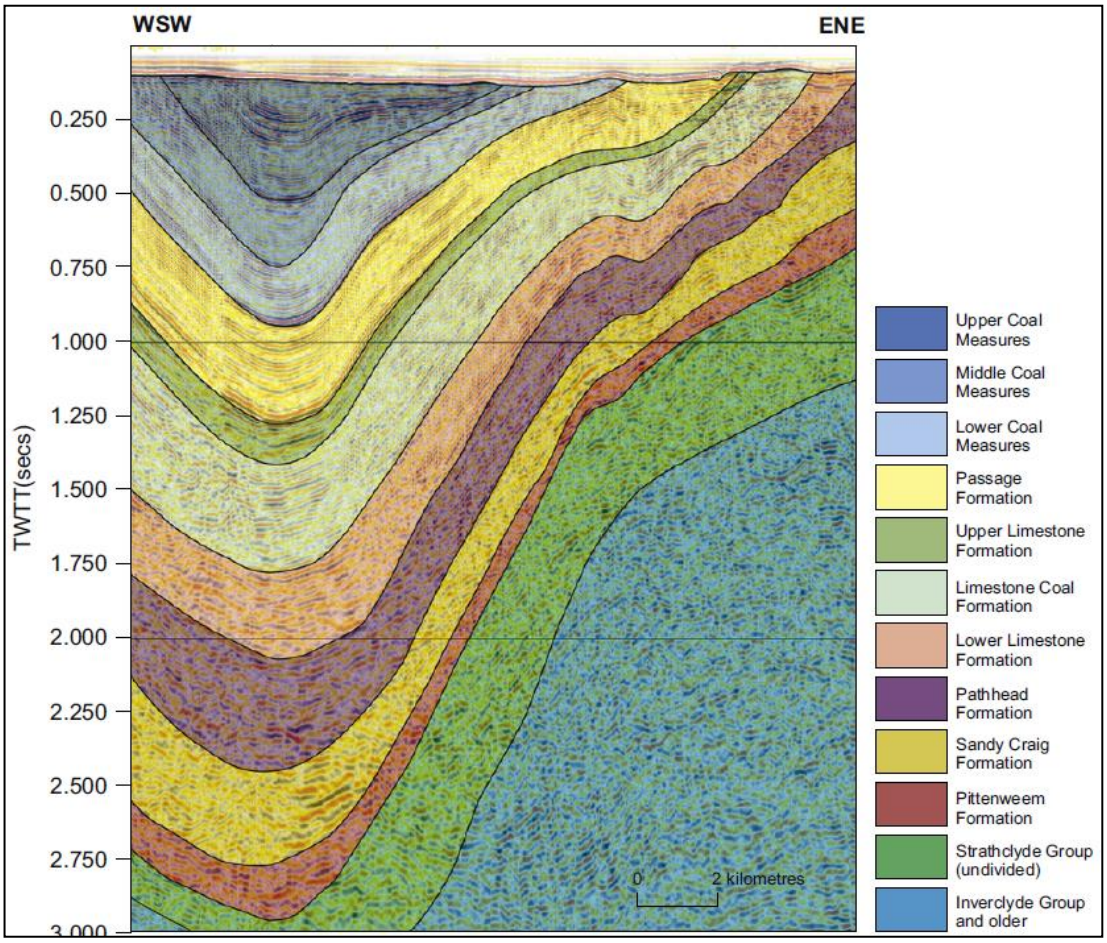

Figure 2.31: An example of highly folded Carboniferous rocks in the Midlothian-Leven syncline in the Midland Valley of Scotland.
Image after (Underhill et al. 2008)

No Carboniferous rocks are noted in well-penetrations throughout the entire study area. Early Carboniferous rocks can be mistaken for Devonian, especially if interpreted on the basis of facies alone but later Carboniferous sequences are more distinct and would have been recognised had they been encountered. During the Early-Mid Carboniferous, the North Sea area had drifted north from its position south of the equator during the Devonian (Figure 2.32) into the equatorial belt. The climate changed from hot and arid to humid (Ziegler 1982) and Carboniferous sedimentation reflects this with increasingly fluvially-derived material (Pharoah et al. 2011).

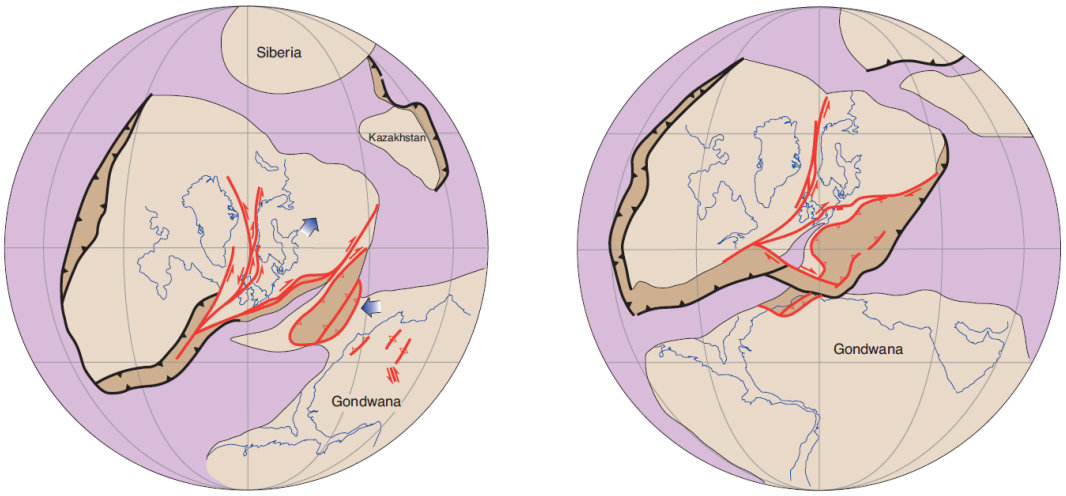

Devonian Early Carboniferous

Figure 2.32: Paleogeographic maps showing the northwards drift of the UK and North Sea area through the Devonian to Carboniferous.
Images after (Evans et al. 2003)

It is possible that Carboniferous strata were deposited in extensional basins but later erosion removed it and would have done so preferentially on the basement highs where most of the pre-Permian information comes from. However, comparison with the Midland Valley of Scotland and Solway Firth, where Devonian and Carboniferous rocks were folded into a series of extensive synclines and anticlines by Late Carboniferous tectonism provides an alternative explanation. Erosion of such a sequence would leave inliers of Carboniferous rocks and this geometry could account for the apparent lack of Carboniferous in the Central North Sea.

Further mapping of the Western and Eastern shelves is the only way to resolve the structural configuration due to better imaging and well control in these areas.

2.2.2 CALEDONIAN PLATE CYCLE SUMMARY

Previous research in onshore areas using both surface and sub-surface mapping techniques has demonstrated that the current structural configuration of north-western Europe was created in two Paleozoic tectonic plate cycles, the Caledonian and Variscan plate cycles. Onshore, Devonian and Carboniferous basins opened after collapse of the Caledonian orogenic belt, following the basement NE-SW Iapetus and NW-SE Tournquist trends. Major granitic intrusives were emplaced during the Carboniferous which today form the cores of stable basement blocks in the onshore section. Evidence for the Caledonian plate cycle is sparse in the Central North Sea due to the paucity of well penetrations of rocks of Lower Paleozoic age and the overprinting of later tectonic events. Older 2D and 3D seismic surveys did not image the deep areas well and little mapping of basement structures was undertaken.

The new high resolution seismic data available for use in this study permitted for the first time, identification of several periods of deformation within the pre-rift sequence of tectono- stratigraphic megasequence 1 which could be correlated to those described and mapped onshore. Previous authors have identified a possible basement block underlying much of quadrant 30 using 2D seismic data (Milton-Worssell et al. 2010). Well penetrations and new 3D seismic interpretation identified strongly metamorphosed Ordovician rocks and a structural high in the region of the Auk Ridge which corroborates this finding. The seismic character of this area and correlation with onshore sections suggests that this may be a granite-cored basement

block emplaced during Caledonian tectonics. The Iapetus trend has been found to be pervasive throughout the Central North Sea with a number of major faults bounding intra-basinal highs of this orientation.

Evidence of syn-depositional faults with Devono-Carboniferous infill is also observed with a particularly large example to the south of the Jaeren High. Devonian strata are confidently identified in the Central North Sea with a number of well penetrations. Carboniferous rocks have not been penetrated in the study area, although difficulty in dating terrestrial sandstone sequences may lead to their misidentification as Devonian. This may be due to the well penetrations encountering pre-Permian rocks being situated on the basement blocks where the potential for erosion of the Carboniferous sequence is much higher.

An alternative explanation is that the Devonian and Carboniferous strata have been folded by Late Carboniferous tectonism into a series of synclines and anticlines as observed in the Midland Valley of Scotland and Solway Firth. It is difficult to determine whether the thickening observed south of the Jaeren High occurs into a fault or a syncline due to later faulting, but erosion of such a geometry would lead to localised inliers of Carboniferous strata which may not be penetrated by the sparse well bores.

2.3 THE VARISCAN PLATE CYCLE

The next plate cycle to affect the UK and Central North Sea area is known as the Variscan plate cycle. It encompasses the development, evolution and destruction of the Rheic Ocean which occurred from the Devonian to Early Permian. The collisional events cumulated in the Hercynian or Variscan Orogeny that was centred upon southern Britain. (Figure 2.33)

Evidence for this tectonic episode can be recognised in the Central North Sea by a major unconformity beneath the top Lower Permian pick which can be correlated to a major period of inversion and erosion recognised onshore (Figure 2.34).

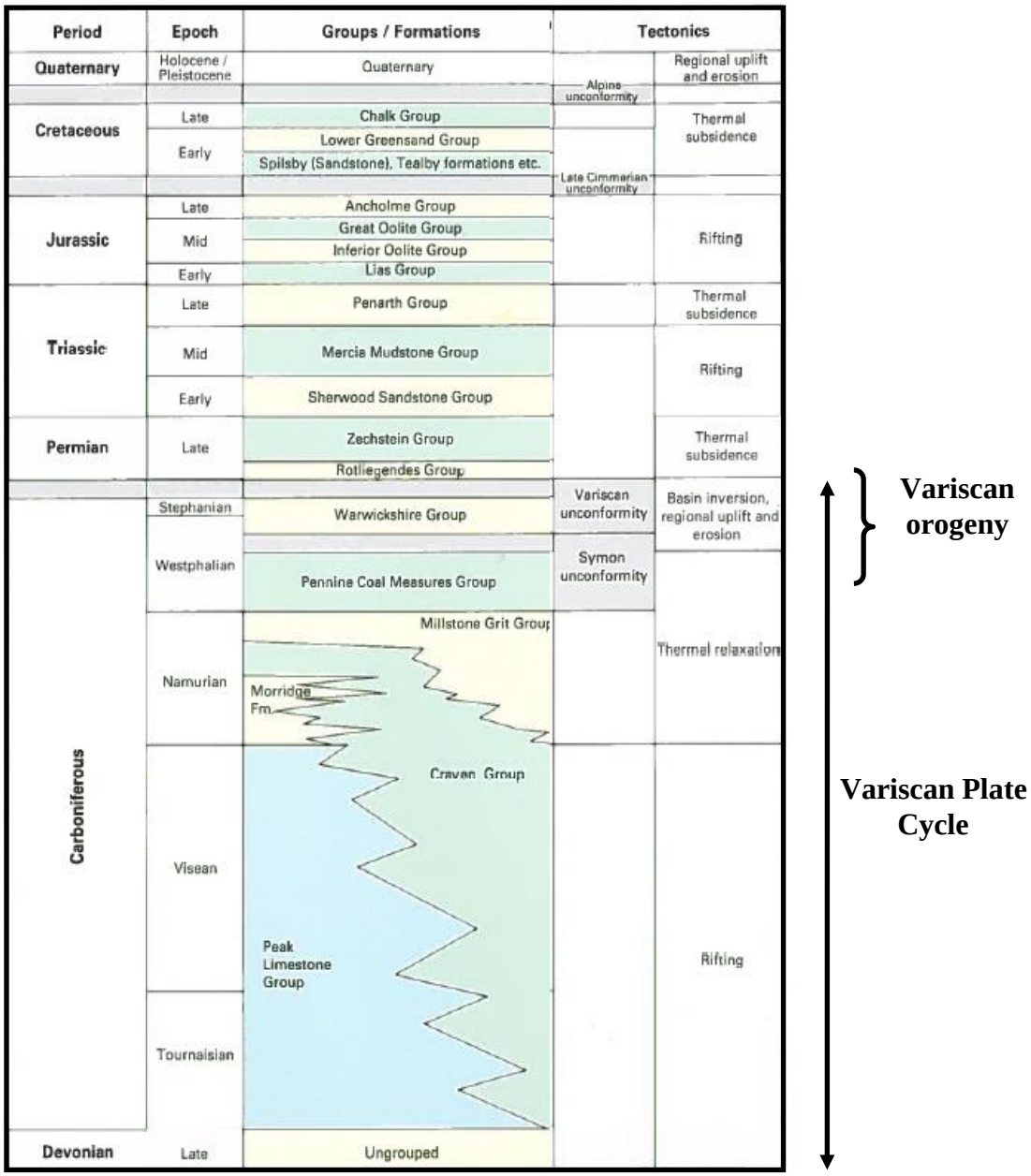

Figure 2.33: Tectonic events affecting the UK and North Sea area with Variscan orogeny indicated.
(Smith et al. 2005)

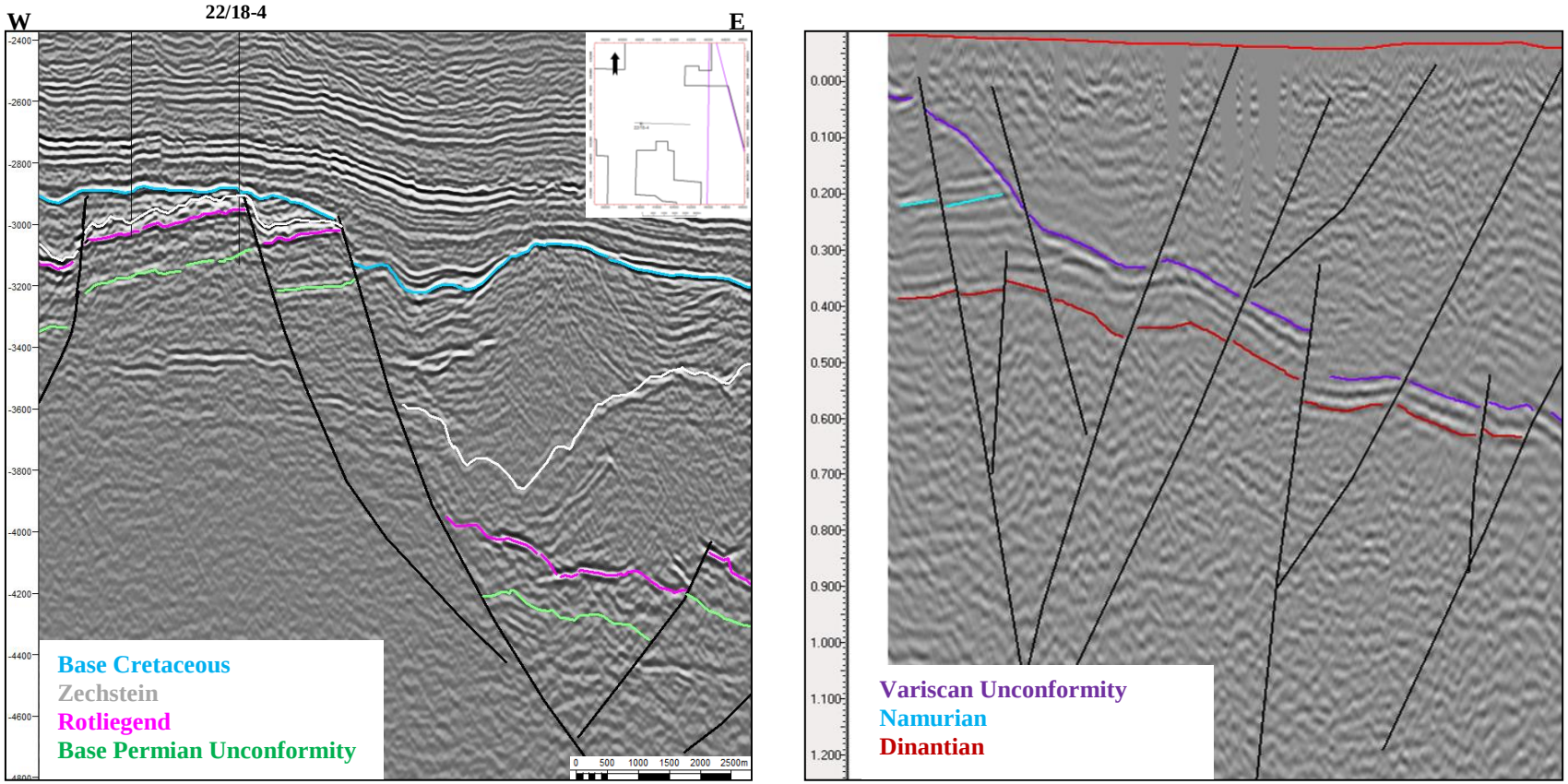

Figure 2.34: A significant unconformity recognised in the North Sea can be correlated with the Variscan Unconformity onshore.
Onshore NW-SE seismic UKOGL line HB-87-71-04 reprocessed. Scale 6.6km

In the Late Carboniferous, a second continental collision took place after subduction of the Rheic Ocean led to convergence of Gondwana and Laurussia (de Jager 2007). The series of events generated by this orogenic episode are collectively termed the Variscan Orogeny (Chadwick et al. 1995). A fold-thrust belt was created with considerable deformation in Northern France, Belgium, and Southern England. The northern limit of the fold-thrust belt generated by encroachment of Gondwana on Laurussia is considered to lie in Southern England (Figure 2.35) with areas north of this on the Variscan foreland less severely deformed.

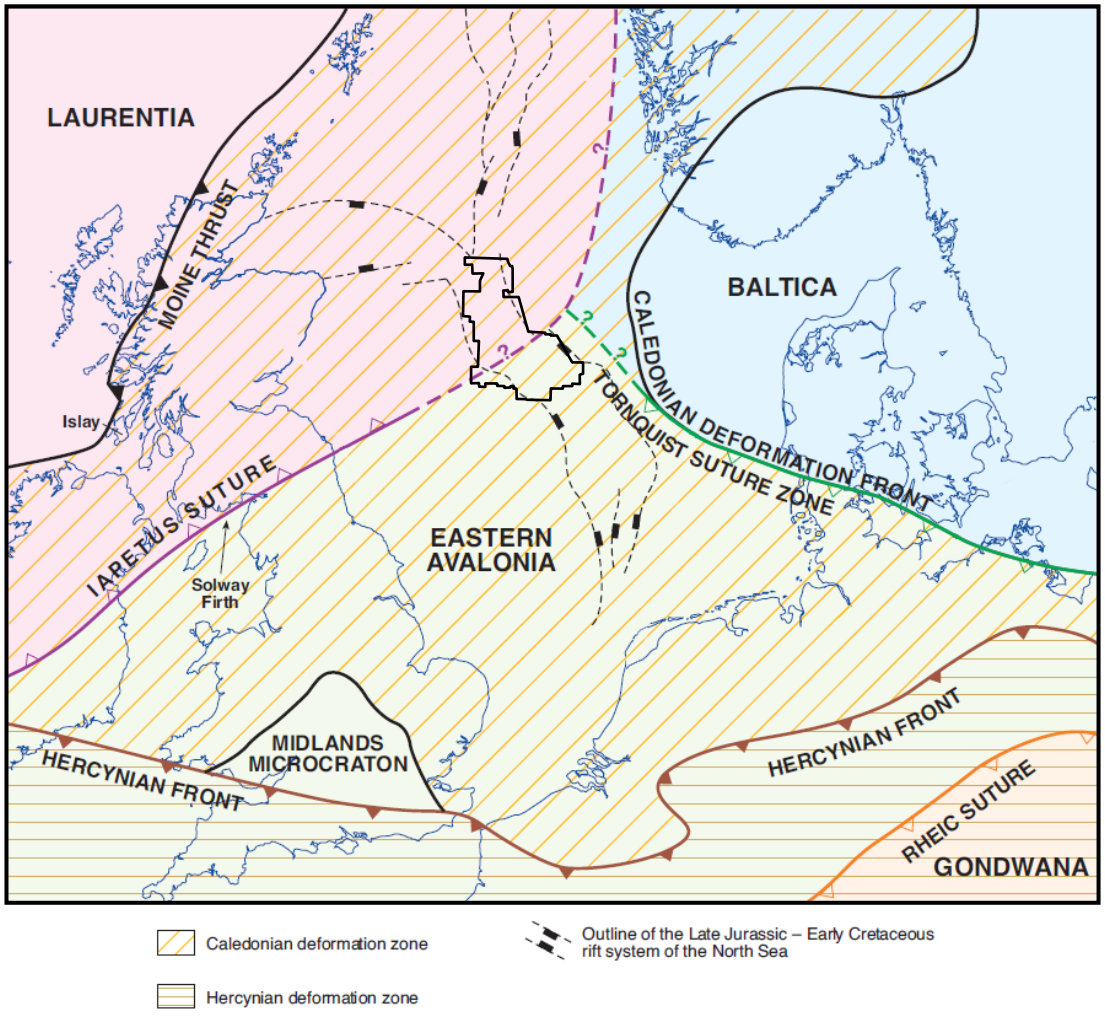

Figure 2.35: Map of the principal accreted terranes which make up the UK and North Sea area showing location of the Variscan (Hercynian) Front. Location of dataset noted.
Image modified after (Evans et al. 2003)

Inversion of the Carboniferous basins was widespread beyond the Variscan front (Corfield et al. 1996) however the offshore record of this is lacking due to the poor preservation of the Carboniferous section. Onshore analogues show reversal on Carboniferous faults creating a variety of structural styles from broad folds to localised reactivation of fault planes. An example of one of these, the Eakring fault, represents Late Carboniferous reactivation of a thrust fault within the Caledonian basement (Wills 1956; Corfield et al. 1996) (Figure 2.36).

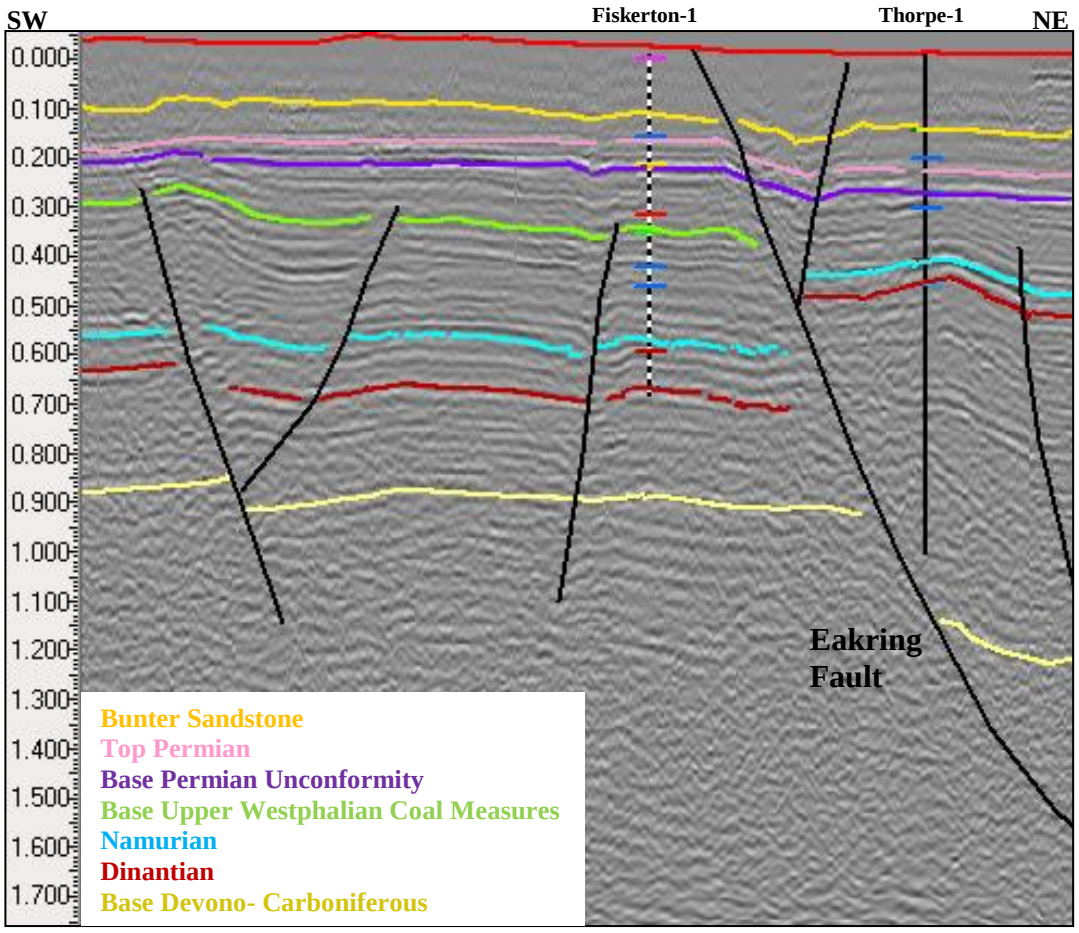

Figure 2.36: SW-NE seismic line showing reactivation of the area surrounding the Eakring Fault system.
UKOGL line NT-81-07/8 Scale= 28km

2.3.1 VARISCAN PLATE CYCLE SUMMARY

At the end of the Carboniferous period continental collision took place after subduction of the Rheic Ocean and thrust sheets and nappes were emplaced over wide areas of France, Belgium and southern England. Further north, ahead of the Varsican front in foreland areas, deformation was less intense but still led to the inversion of many of the Carboniferous basins, as far north as the Inner Moray Firth.

Offshore the evidence for Carboniferous inversion is lacking due to lack of preservation, although the Devono-Carboniferous thickening described in the previous section to the south of the Jaeren High may represent a syncline creted during Varsiscan compression. In general however, the entire Variscan plate cycle is represented in the Central North Sea by the major erosive event at the Carboniferous/Permian boundary which marked its end.

2.4 INTRA-CONTINENTAL RIFTING

2.4.1 EARLY PERMIAN

A widespread unconformity recognised in the Central North Sea following Variscan tectonics is known as the Base Permian Unconformity (BPU). The BPU is actually the amalgamation of several unconformities into one mega unconformity but none of these separate events can be distinguished (Geluk 2007). Isochrons of the Lower Permian sequence show predominantly SW-NE and W-E striking fault sets (Figure 2.37).

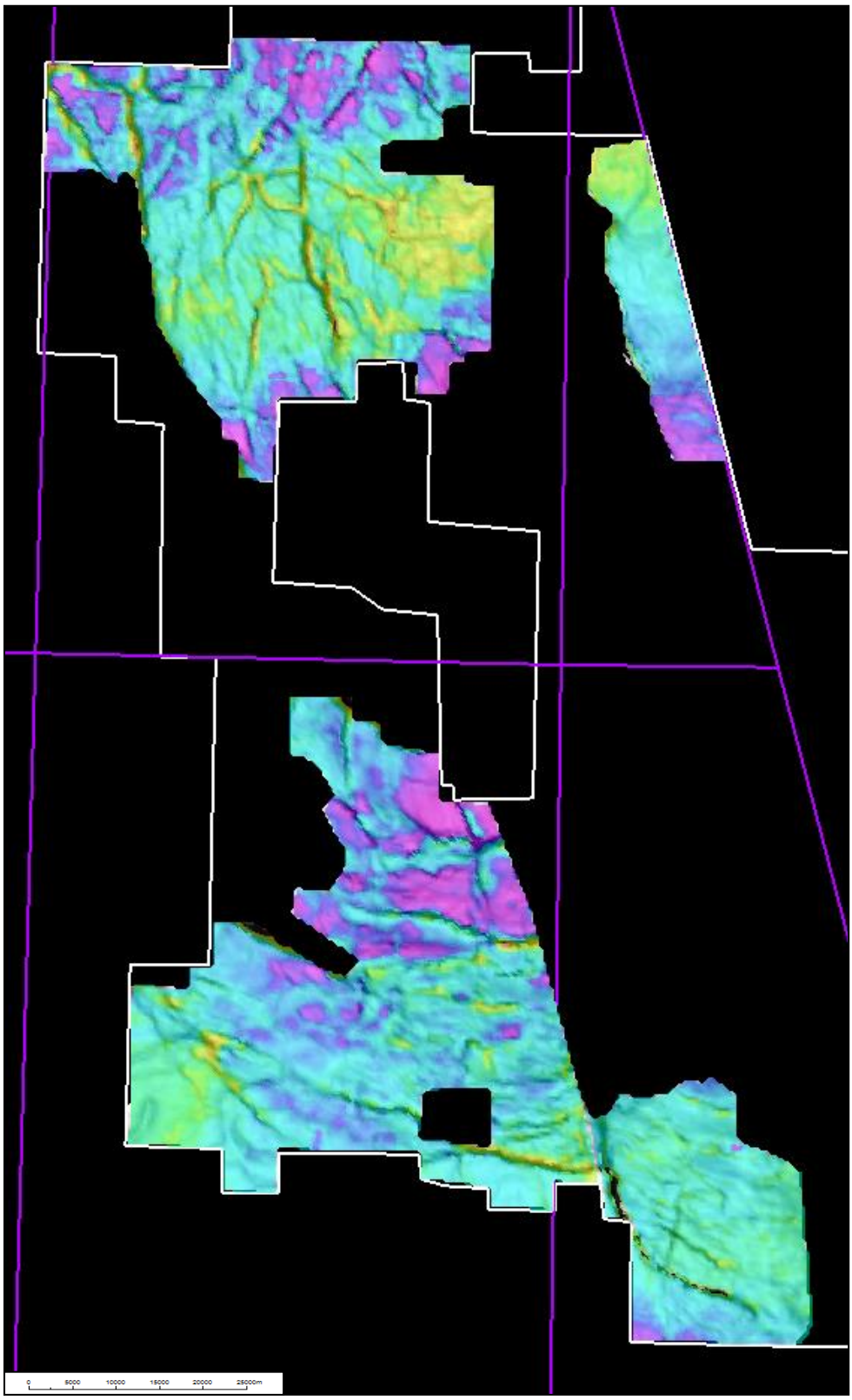

Figure 2.37: Isochron of the Lower Permian sequence superimposed on a dip angle map to enhance the fault trends. Most faults strike sub-W-E and SW-NE. Note however that over the area around the Forties Montrose High the 'Lower Permian' isochron includes some Upper Devonian.

As before, the thinning observed over the faults is a feature caused by gridding within the software package and is not a true trend.

This fault trend is related to the formation of two large east-west striking basins in the Early Permian, the North and South Permian Basins (Figure 2.38)

These basins were created due to intra-montane collapse of the Variscan Mountains almost directly after orogenesis leading to subsidence of intra-montane and peripheral collapse basins (Ziegler 1990; Underhill 2003). Basin development also occurred in Norway, East Greenland and Northern Britain (Dore et al. 1999). This period of intra-continental rifting is often included in the subsequent Triassic rifting event (tectono-stratigraphic mengasequence 1) with both Permian and Triassic rocks ascribed to the syn-rift sequence. This is due to the Permian faults being reactivated under extensional stress in the Triassic making it difficult to separate the two events. In this study such faults are referred to as Permo-Triassic indicating their involvement during both deformation events.

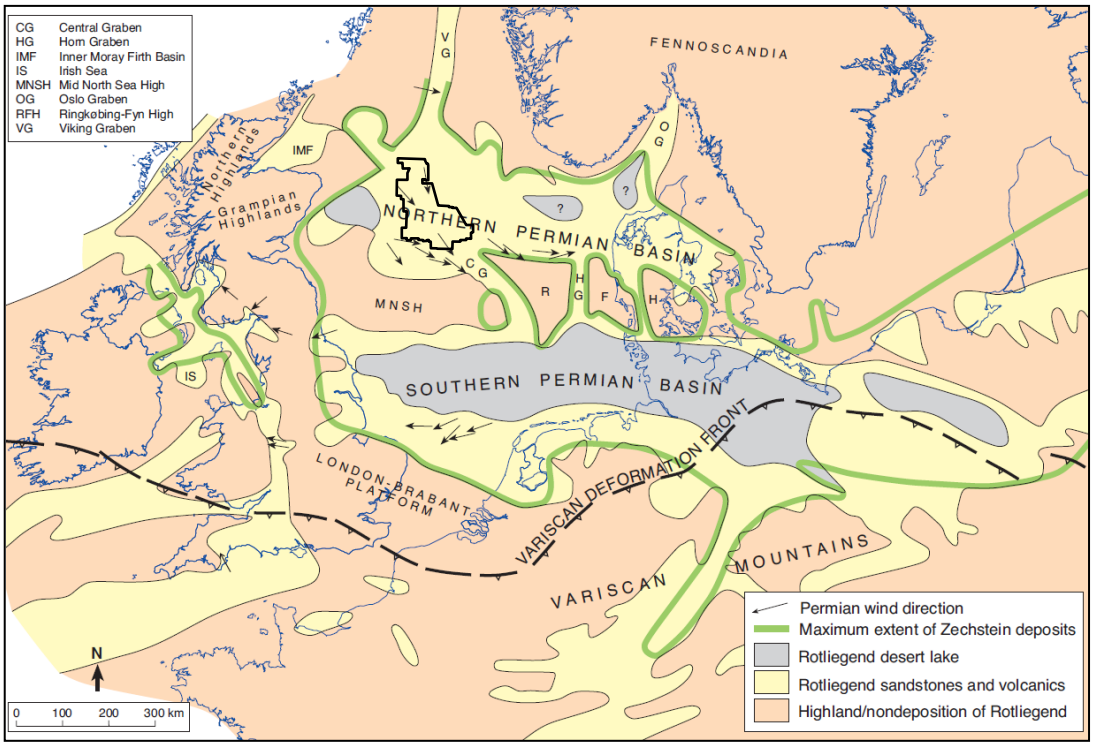

Figure 2.38: Maximum extent of the Permian basins in north-west Europe with respect to study area.
Image after (Evans et al. 2003)

The climate had also become more arid by the Permian, reflecting the continental conditions and continued northward drift from the equatorial regions to the same latitude as that occupied by the Sahara Desert today (Figure 2.39). The Variscan Mountains also blocked the trade winds and led to even drier conditions than would be expected (Glennie 1998). Climatic conditions exerted an important control over stratigraphic development throughout the Permian and Triassic.

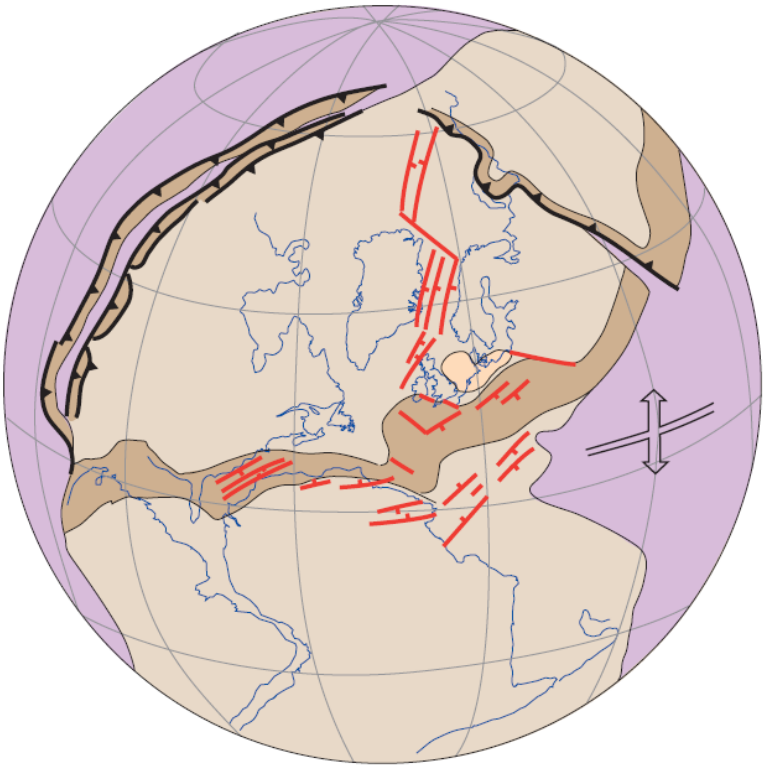

Figure 2.39: Early Permian paleogeography showing that the UK and North Sea area drifted northwards through the Carboniferous. Brown shading represents the remnants of the eroding Variscan Mountain Belt.
Image after (Evans et al. 2003)

Erosional products, derived from the Variscan orogen, were shed into the developing basins creating the vast thicknesses of aeolian and fluvial sandstones seen today beneath the Central and Southern North Sea. In the Central North Sea study area, centred over the North Permian Basin, the top of the Lower Permian Rotliegend Group can be mapped throughout the study area (Figures 2.40-2.42).

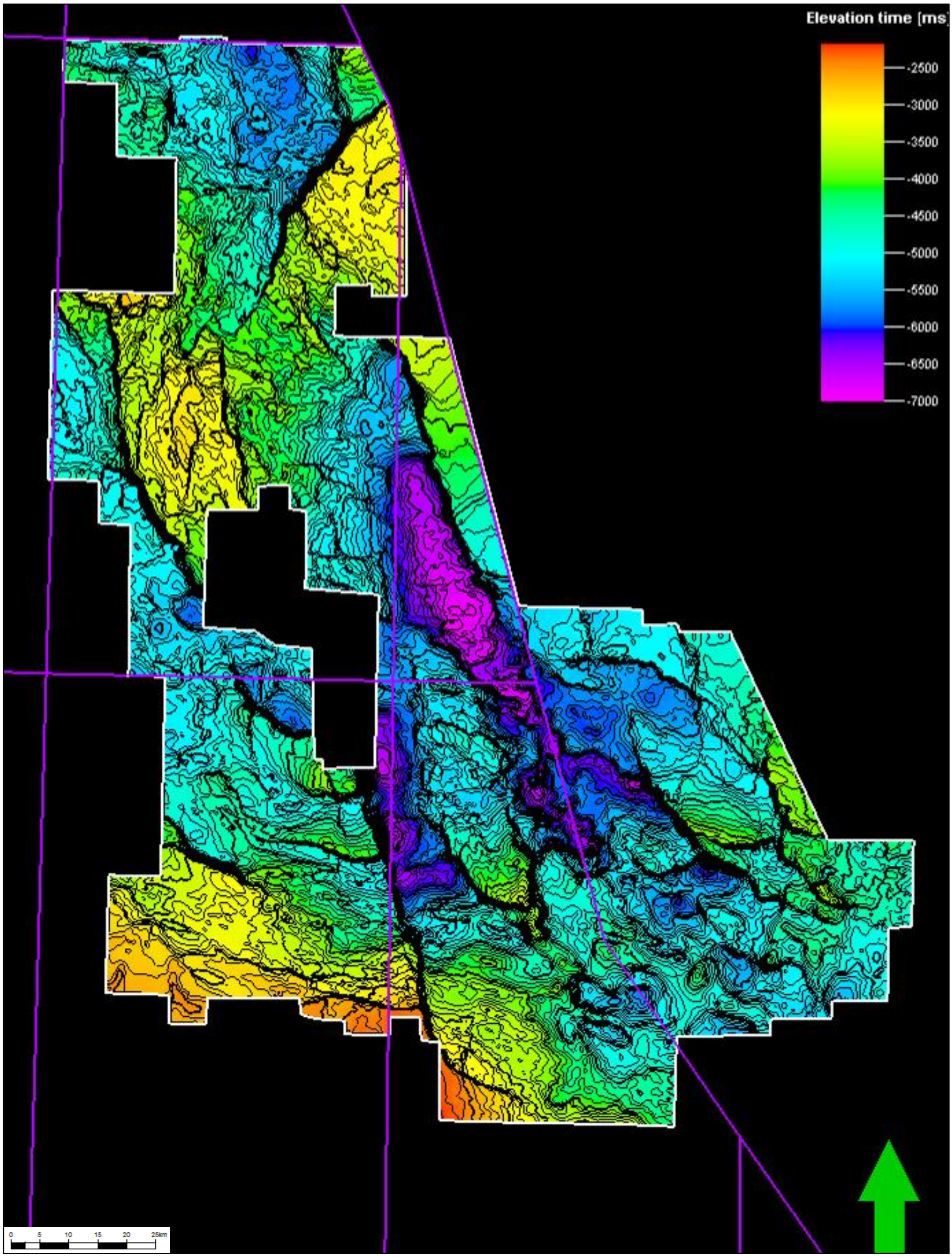

Figure 2.40: Rotliegend TWTT structure map. Note the cross-cutting fault trends seen throughout the dataset.

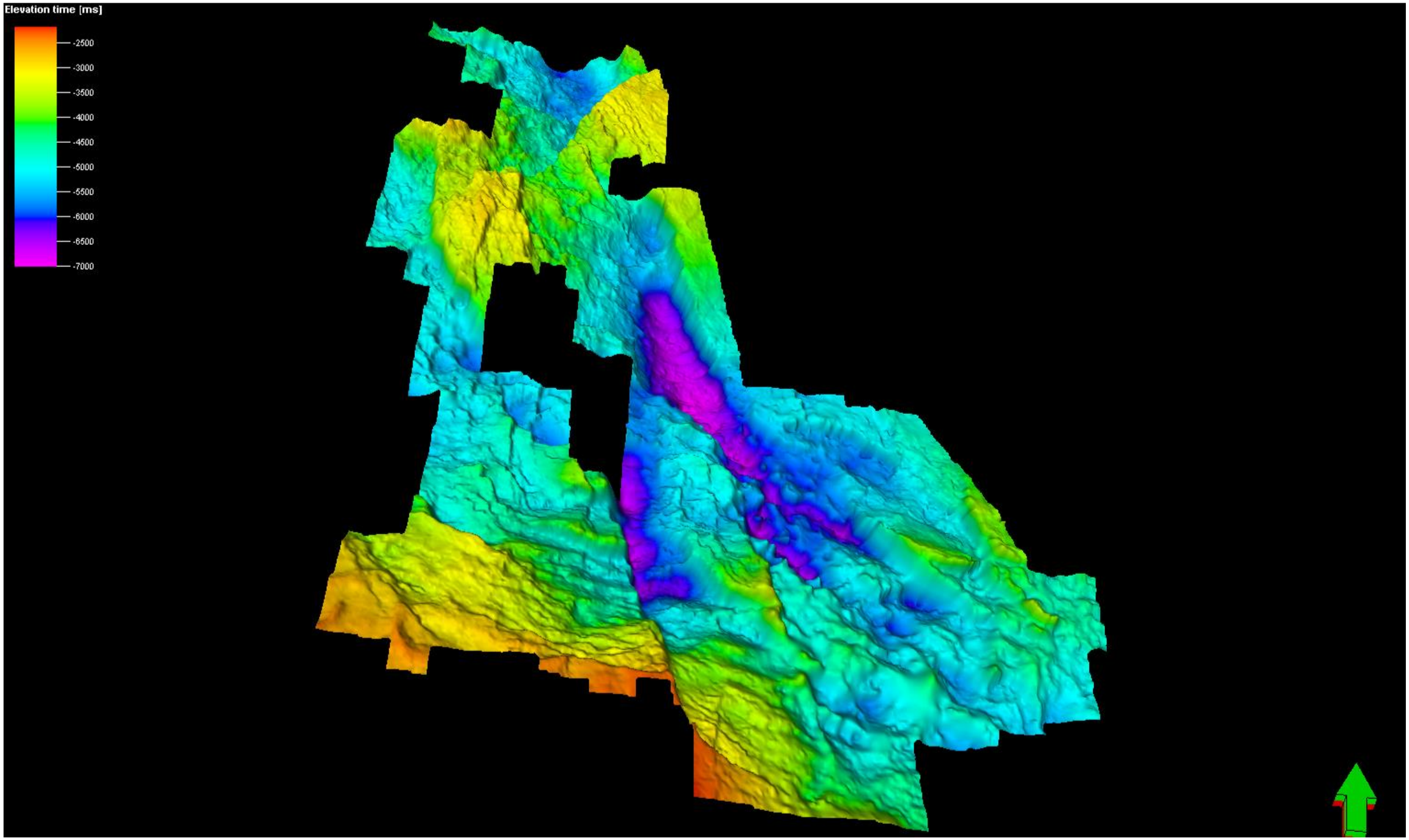

Figure 2.41: 3D image of the TWTT Rotliegend structure map.

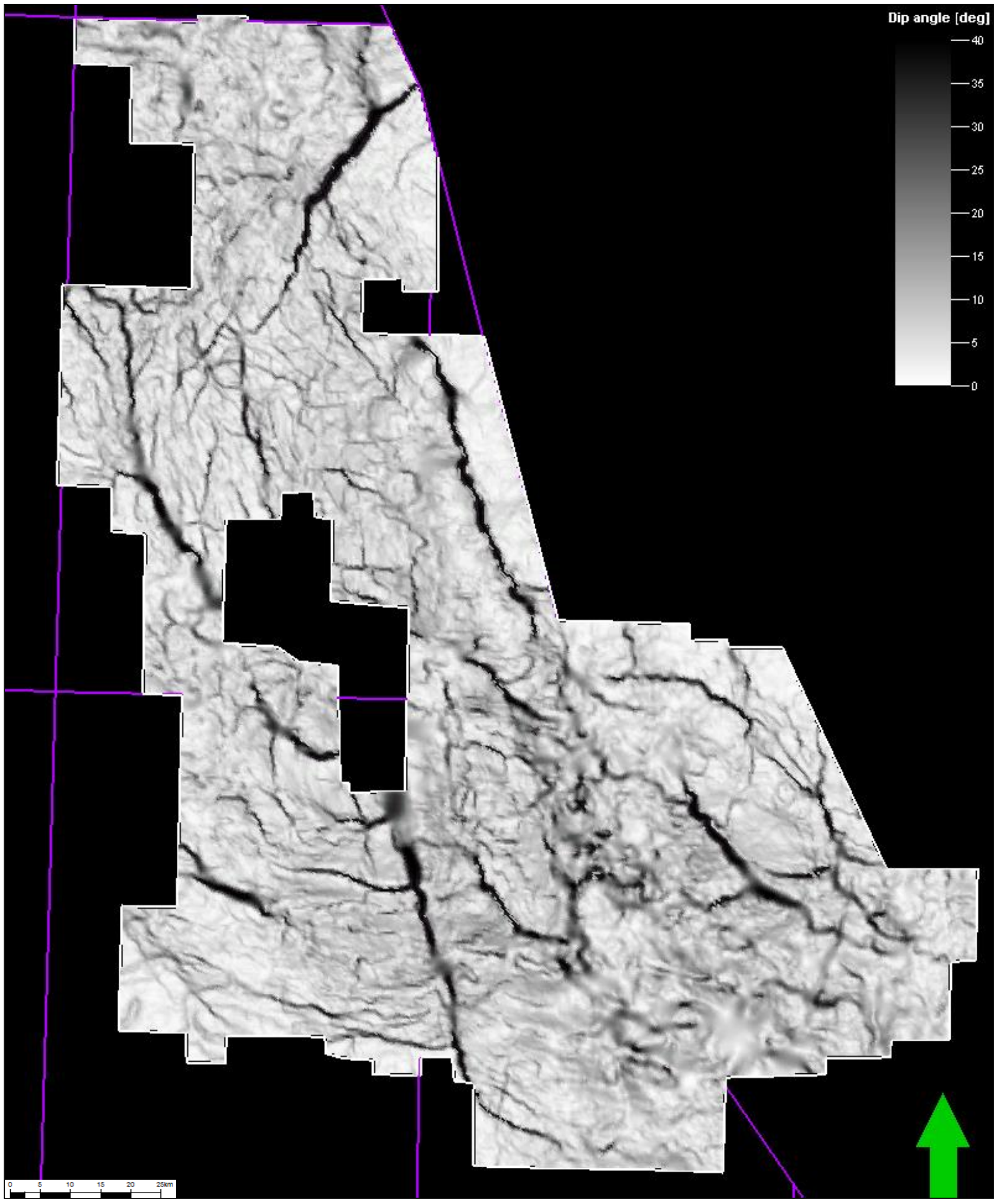

Figure 2.42: A dip angle map of the Rotliegend structure clearly brings out the three major fault trends in the Central North Sea, the NE-SW Caledonian trend, W-E Permo-Triassic faults and the dominant NW-SE rift arms.

Dip Angle is the steepest angle between the surface and the horizontal plane. The value is 0 horizontal, 90 vertical, measured in degrees.

An isochron between the top Rotliegend and the basement pick on the Forties Montrse High demonstrates the existence of a significant Permian structural high, striking WSW-ENE across to the south of the Jaeren High which cross-cuts the Caldedonian trend of the Jaeren High Fault. This feature is itself cut through by later rifting and its continuation is only recognised by considering the cross-cutting nature of successive tectonic episodes (Figure 2.43). It is also evident on magnetic anomaly maps as a sub-east-west striking ridge (Figure 2.44).

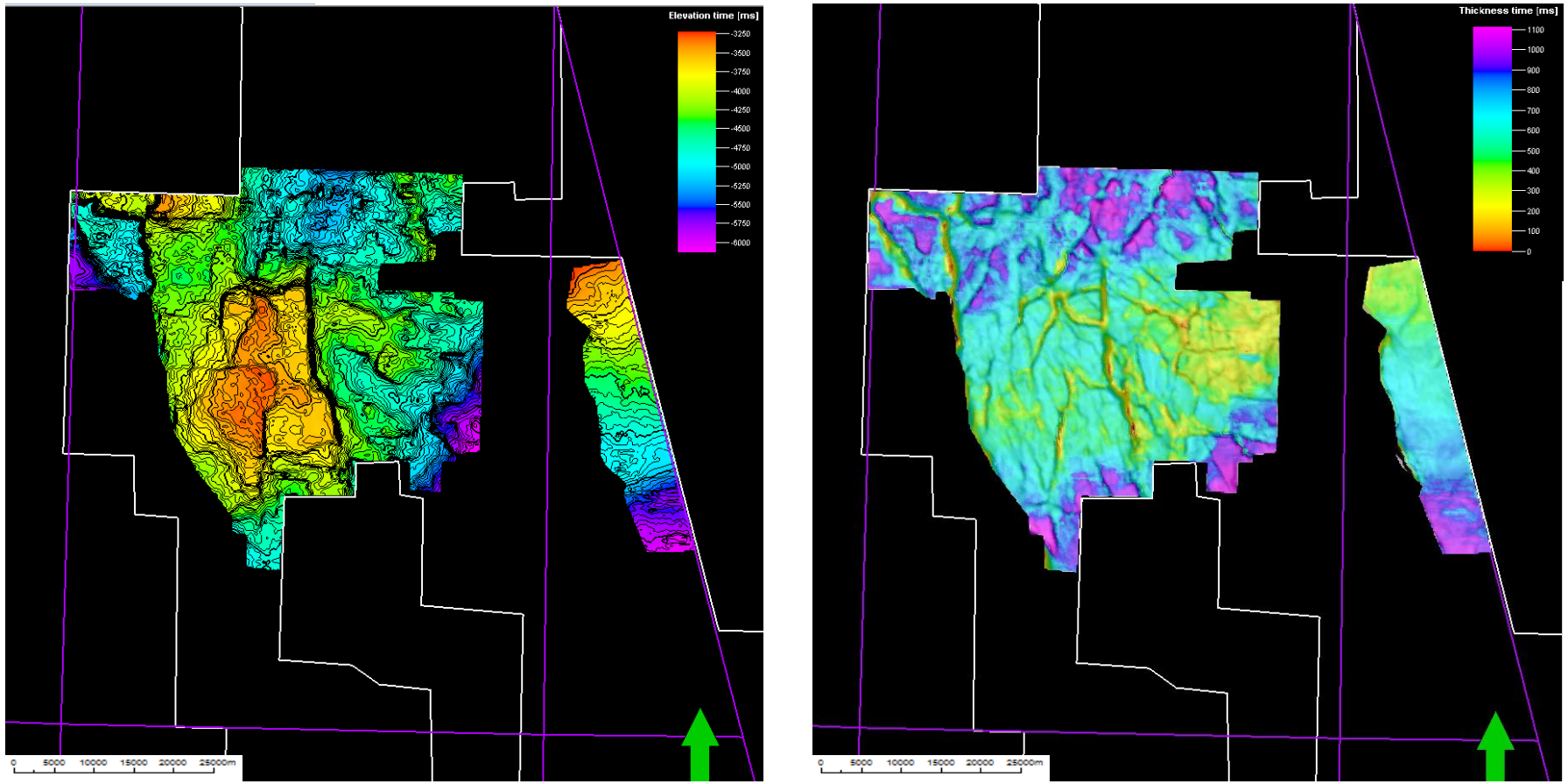

Figure 2.43: A structure map of the basement pick (L) compared with an isochron of the Lower Permian and upper Devonian interval (R). On the structure map, the pre-Permian high is cross-cut by later faults and the true geometry can only be observed on the isochron.

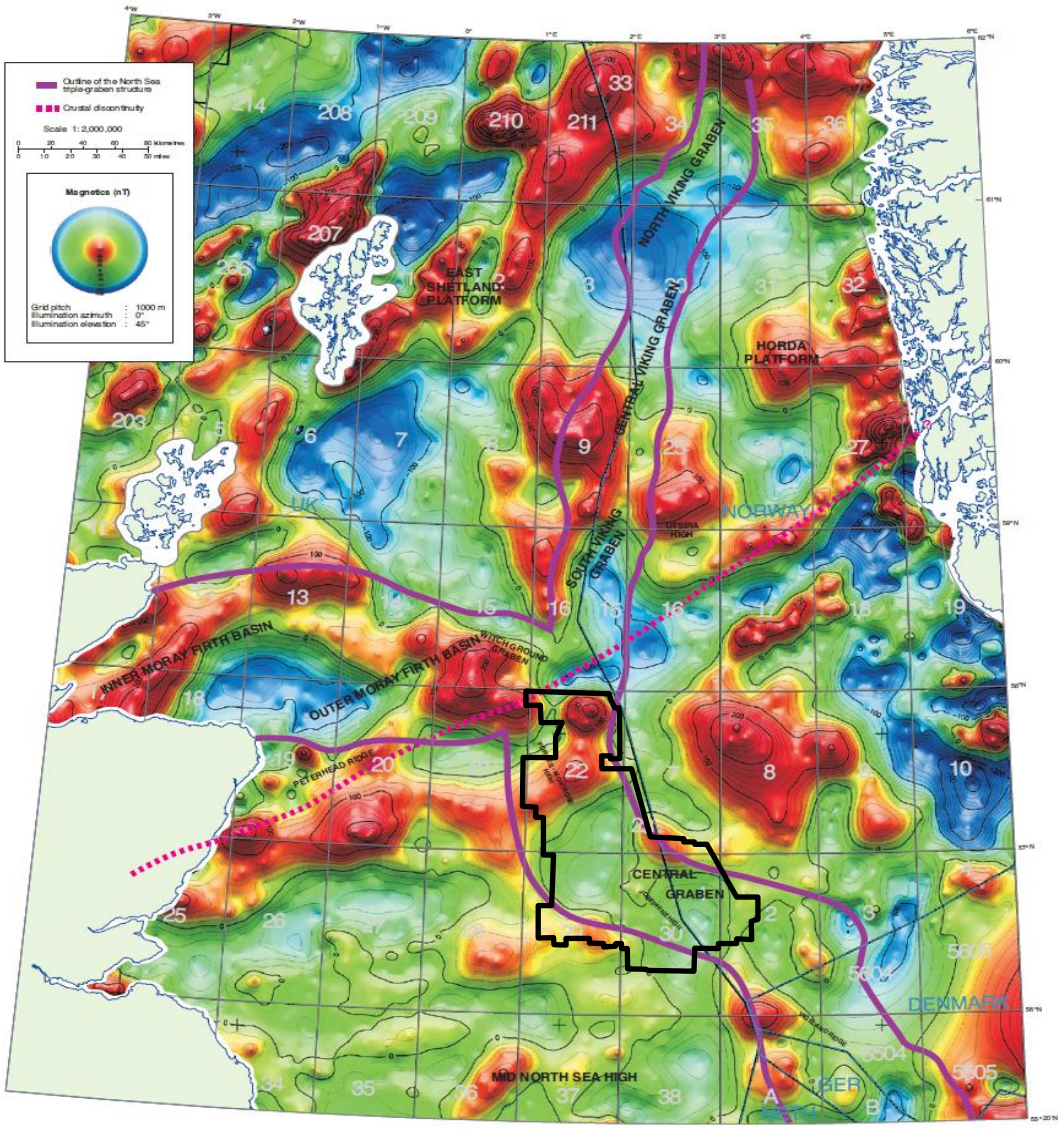

Figure 2.44: Magnetic anomaly map showing the pre-Jurassic Forties-Montrose Ridge cutting through the study area.
Image modified after (Evans et al. 2003)

The WSW-ENE strike of the faults that cross the Forties-Montrose Ridge as it should now be known, is unusual as faults further south which are regarded as following a North Permian Basin trend, are oriented WNW-ESE (Figure 2.45) . Identification of this fault trend as well on the Forties Montrose Ridge suggests two separate stress regimes at different times. The second trend could be an Upper Permain or Triassic trend but it is difficult to determine due to the nature of the Upper Permian facies and the effect of this in controlling deposition of the Triassic.

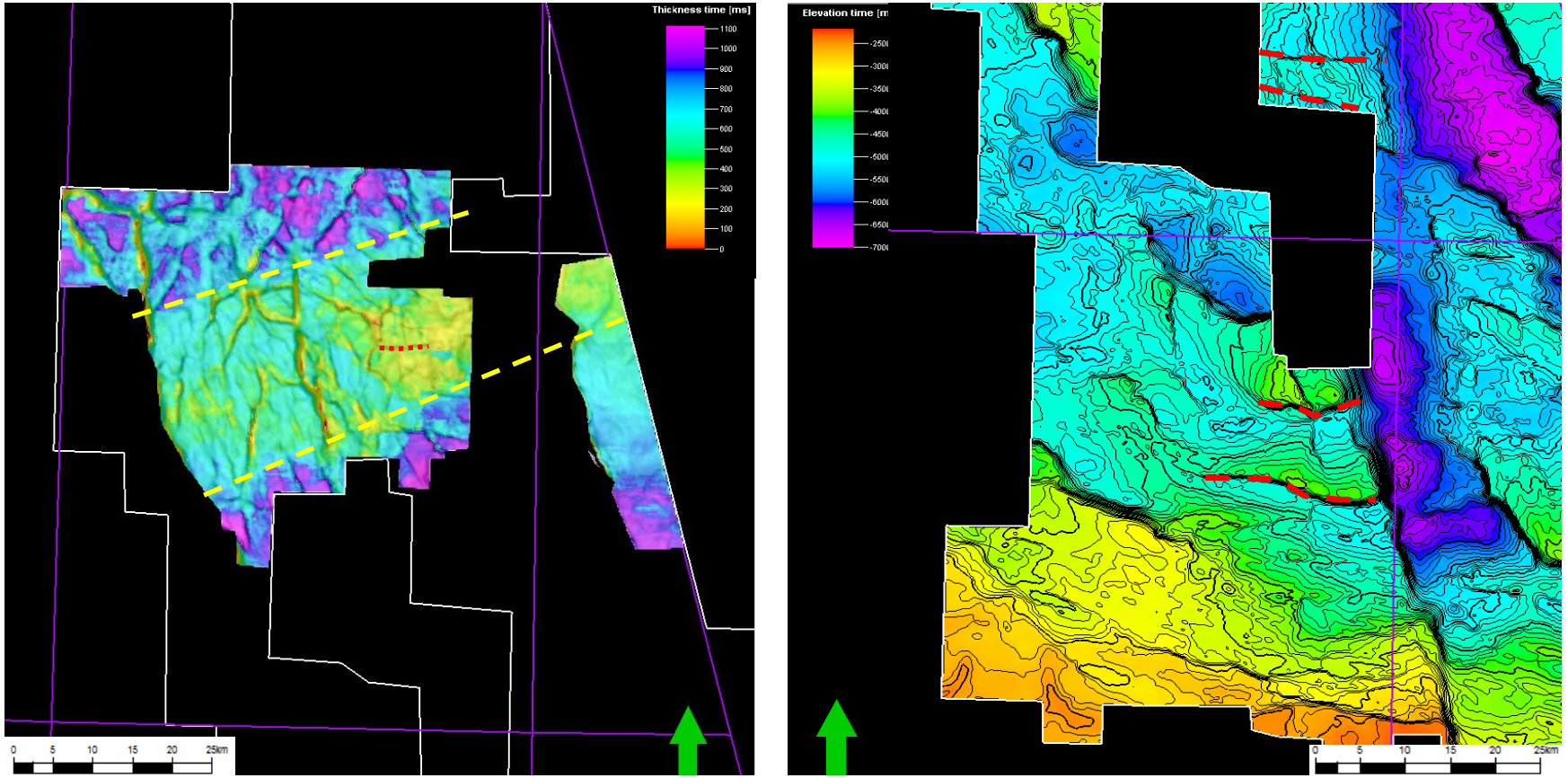

Figure 2.45: Differences in Permo-Triassic fault orientations between the Forties-Montrose Ridge bounding faults which strike WSW-ENE and other faults identified in the area as being of the same age which are W-E oriented. A possible example of a W-E fault is seen on the Forties-Montrose Ridge suggesting the trends are different ages.

An alternative explanation for the anomolous trend of the Forties-Montrose Ridge is that it represents the offshore continuation of the Iapetus suture and is underlain by highly deformed and intruded Lower Paleozoic rock. This would account for the strong magnetic anomaly and the transparent seismic character of the structure (Figure 2.46). A transparent seismic character is often an idicator of intrusive or metamorphic rocks at depth.

A Lower Permian isochron on the Auk Ridge also identifies a different geological history for this structure as it is evident that parts of what is currently known as the 'Auk Ridge' were not structurally elevated in the Permian (Figure 2.47)

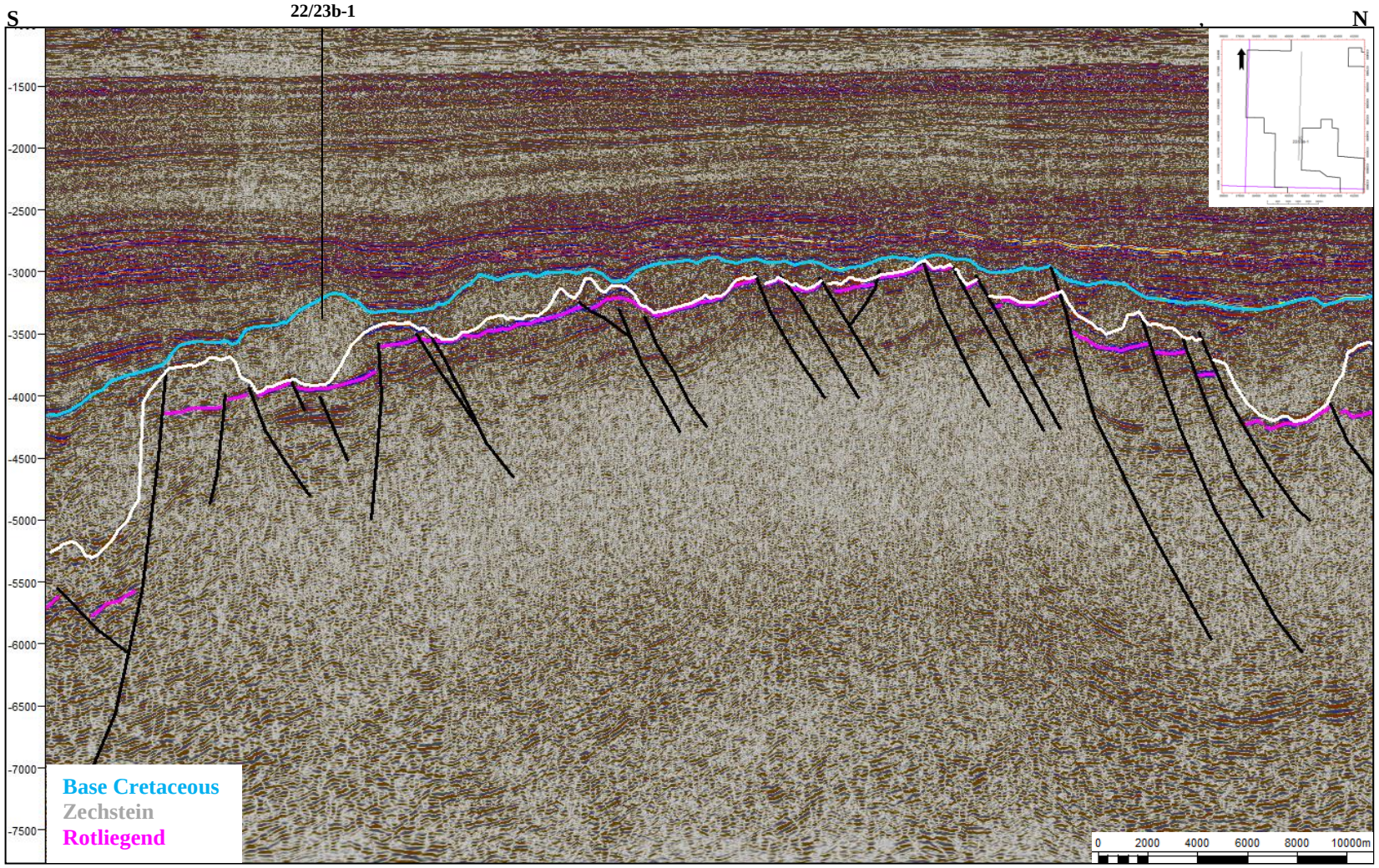

Figure 2.46: Deep seismic profile across the Forties-Montrose Ridge showing transparent character possible representing highly metamorphosed and intruded Lower Paleozoic rocks caught up in the Iapetus suture zone.

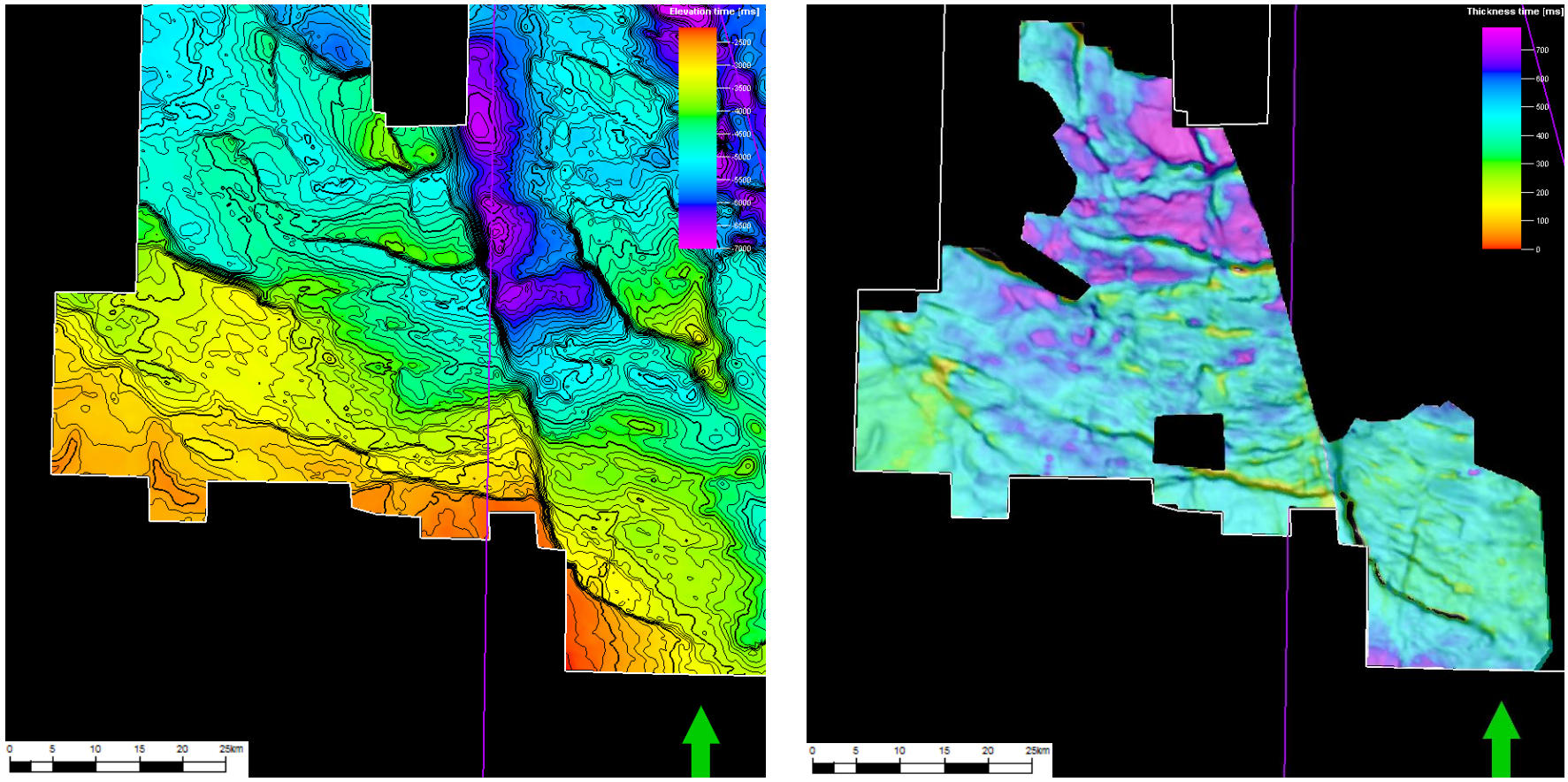

Figure 2.47: A TWTT Lower Permian structure map shows a pervasive high area over the south of the dataset but an isochron of the interval reveals that some of this area was not elevated in the Early Permian.

2.4.2 LATE PERMIAN

In the Central North Sea, the Upper Permian is represented by a variably thick sequence of evaporites ascribed to the Zechstein Supergroup. This was deposited due to catastrophic flooding of the underfilled Permian Basins from the Barents Sea (Ziegler 1990) . The hot climate sigmnificantly impacted the development of this sea, known as the Zechstein Sea, through high levels of evaporation. Periods of marine regression allowed the shallow basin to evaporate leaving thick layers of evaporites which were then flooded over to begin the cycle again. In total, six sedimentary Zechstein cycles are recognised (Underhill 2003). Zechstein evaporites significantly affected the structural styles seen in the basin.

Salt mobility occurs as a response to the anomalous physical properties of the mineral halite (NaCl) relative to other lithologies. It is typified by low strength, high thermal conductivity, high solubility, low density and low porosity (Jackson et al. 1986). Calculating the mechanical responses of various lithologies to force, namely that of the overlying rocks, is a complex process relying on knowledge of its rheology (how it flows) which is dependent on the thermal structure, fluid content, thickness of compositional layers and various boundary conditions. In general terms however, we can think of most rocks as having a linear increase in strength with depth (Jackson et al. 1994) (Figure 2.48) .

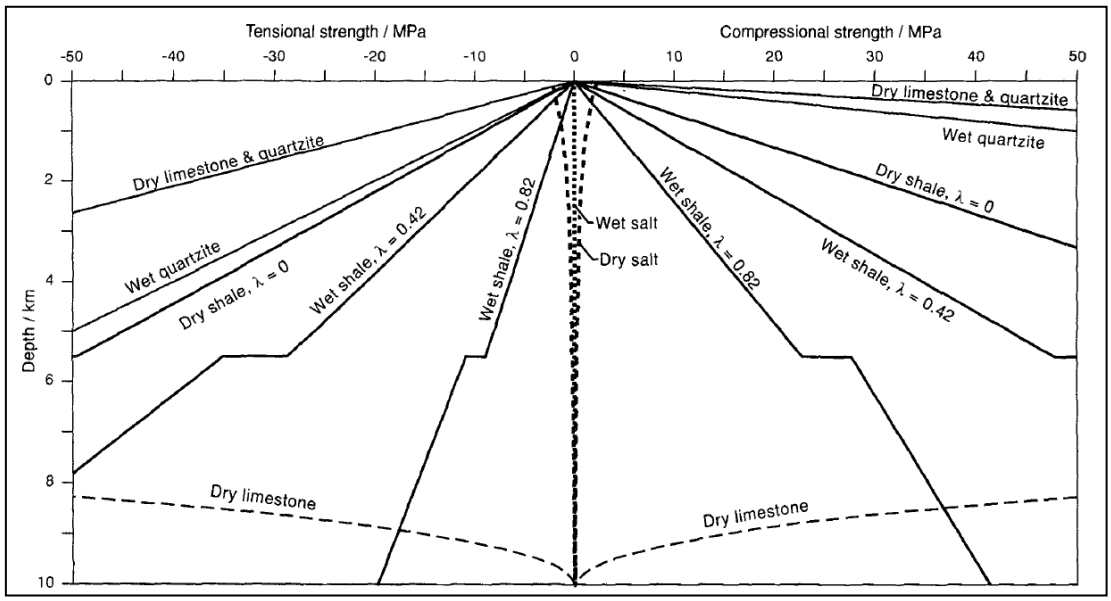

Figure 2.48: Comparison of creep and frictional strengths of wet and dry salt with equivalent strengths of wet and dry sedimentary rocks.
λ= pore pressure coefficient, the ratio of pore pressure to lithostatic pressure. For dry rocks this is 0, rising as the rock becomes more hydrostatically pressured.
Image after (Jackson et al. 1994)

From this diagram we can see that both wet and dry salt have a small amount of strength at the surface which decreases to almost 0 with depth. Under typical geological stress salt deforms as a near Newtonian fluid. On the surface and at shallow depths therefore, salt has some strength and importantly has a density greater than most clastic sediments (although lower than that of carbonates) (Banbury 2006). Upon burial sediments compact to greater densities but salt develops a polycrystalline microstructure of low permeability during accumulation and remains almost incompressible throughout subsequent burial (Jackson et al. 1986) (Figure 2.49)

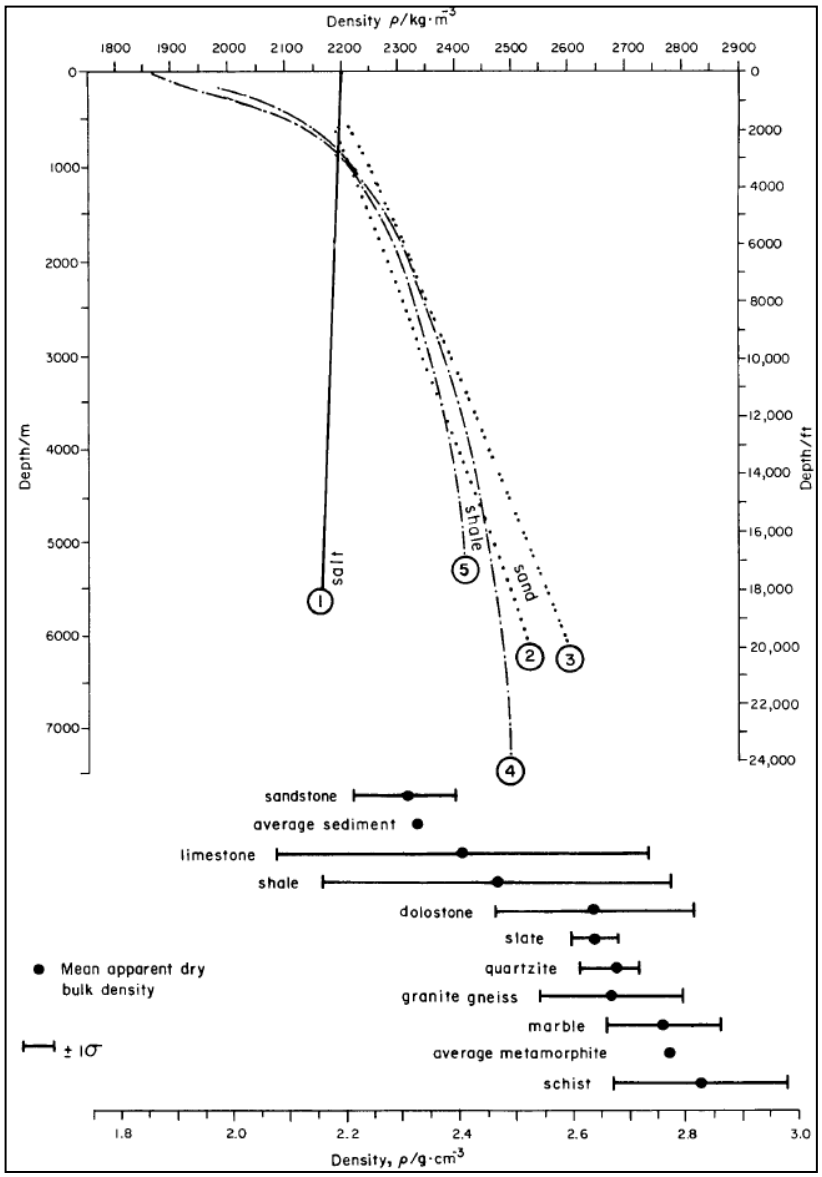

Figure 2.49: Relationship between bulk density and depth of salt compared to other terrigenous sediments.
Image after (Jackson et al. 1986)

Due to this low density and negligible field strength, salt can flow in the solid state driven by gravity alone. Tabular salt may rise beneath an arched but concordant overburden forming a salt pillow or anticline, if movement continues this salt may pierce the overburden (usually beneath a pre-existing weakness such as a major fault) and become a diaper or salt wall (Jackson et al. 1994).

In the Central North Sea, Zechstein evaporites have been affected by later tectonic movements leading to salt mobility (halokinesis) due to its ability to flow under stress. In the areas most affected by later rifting, it is not possible to image the evaporites at all. Salt is difficult to image on seismic due to the loss of seismic energy witin it. Halite, the main consitituent of the Zechstein of the Central North Sea away from the intra-basinal highs, is most problematic and is nearly transparent to seismic energy. It is also very mobile and any trace of layering within it becomes quickly homogeneous over time (Bishop 1996). Salt can be identified by its lack of reflectivity (Figure 2.50) but identification of this is hampered in the Central North Sea by the equally unreflective nature of the Lower Triassic sequence which lies directly on top (Figure 2.51).

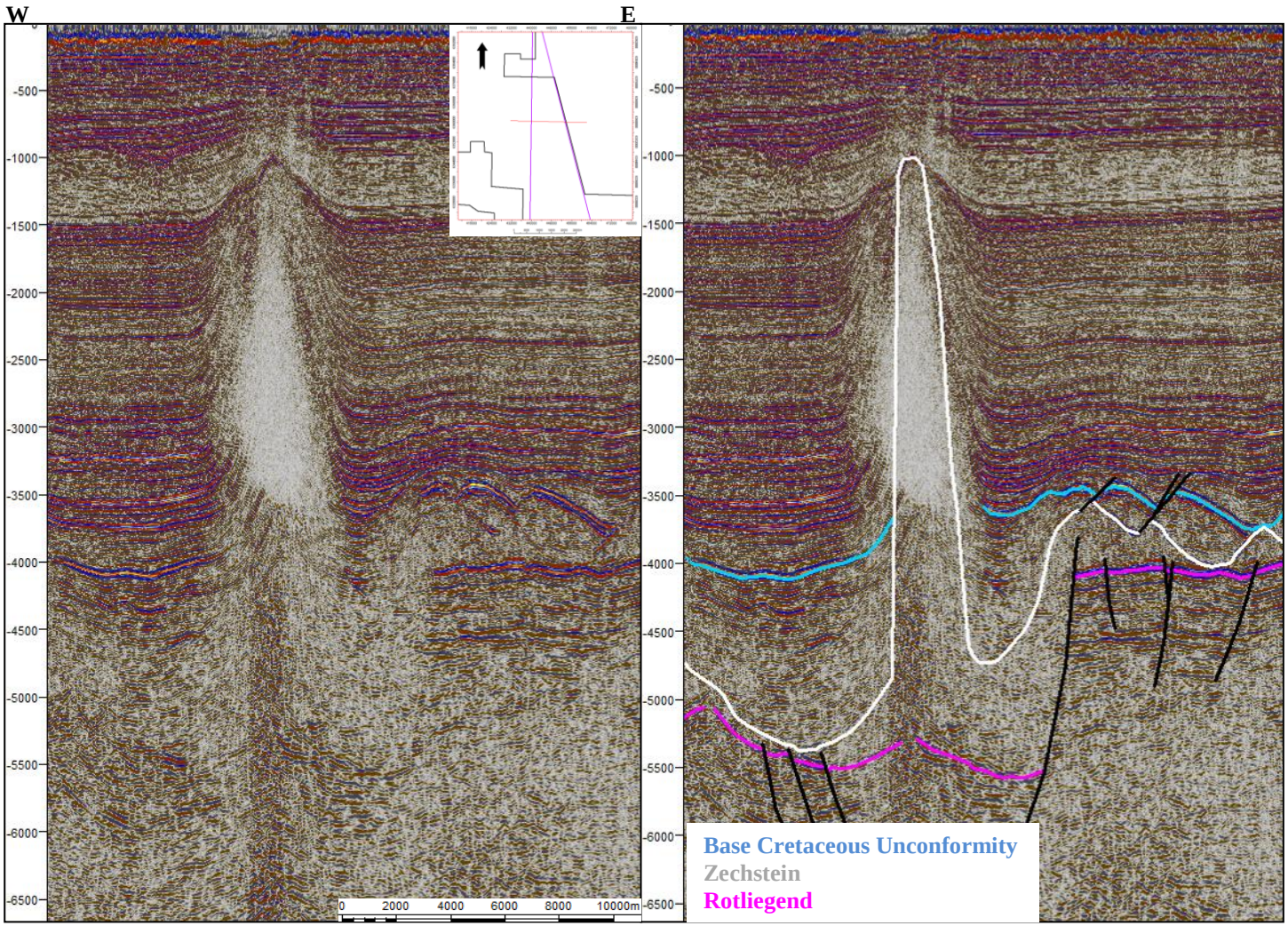

Figure 2.50: An example of the transparent and sometimes chaotic appearance of salt on seismic.

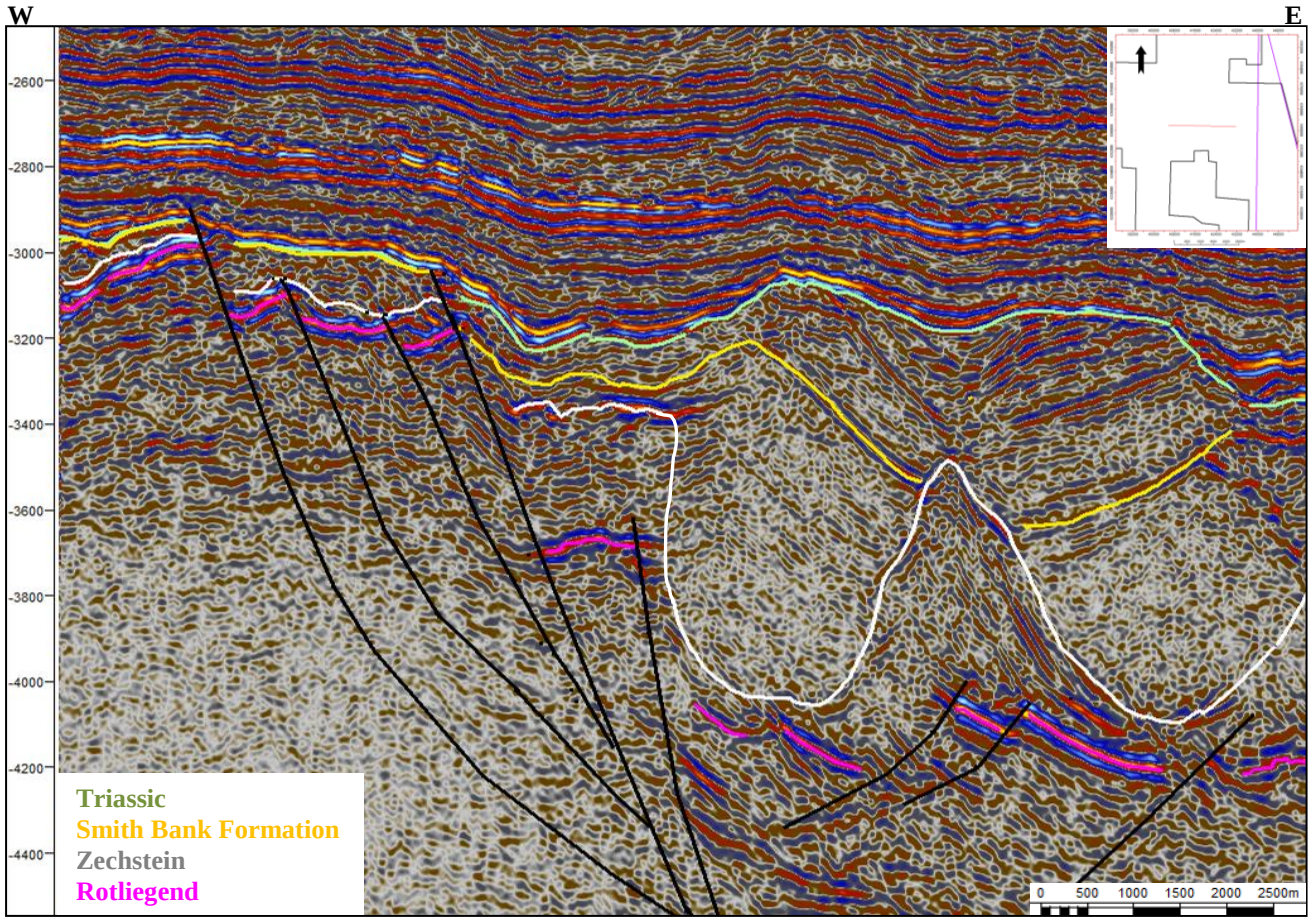

Figure 2.51: W-E seismic line showing the chaotic and transparent character typical of salt surrounded by the equally transparent Triassic Smith Bank Formation. The lack of reflectivity here results from the uniformity of the facies in the Smith Bank Formation.

The Zechstein sequence has been highly modified by later halokinesis but the original halite-dominated deposits probably infilled and smoothed the bathymetry created by the underlying Rotliegend in the basin. The sequence thickens into the centre of the North Permian Basin in the south-east of the study area. On the intra-basinal highs and basin margins the Zechstein contains anhydrite, dolomite and limestones. Deposition of such a carbonate-rich succession on the Forties-Montrose Ridge provides evidence that this area remained structurally high throughout the Permian (Figure 2.52). Halokinesis began in the Triassic when the Zechstein Sea withdrew and terrestrial sedimentation of the Triassic sequences began.

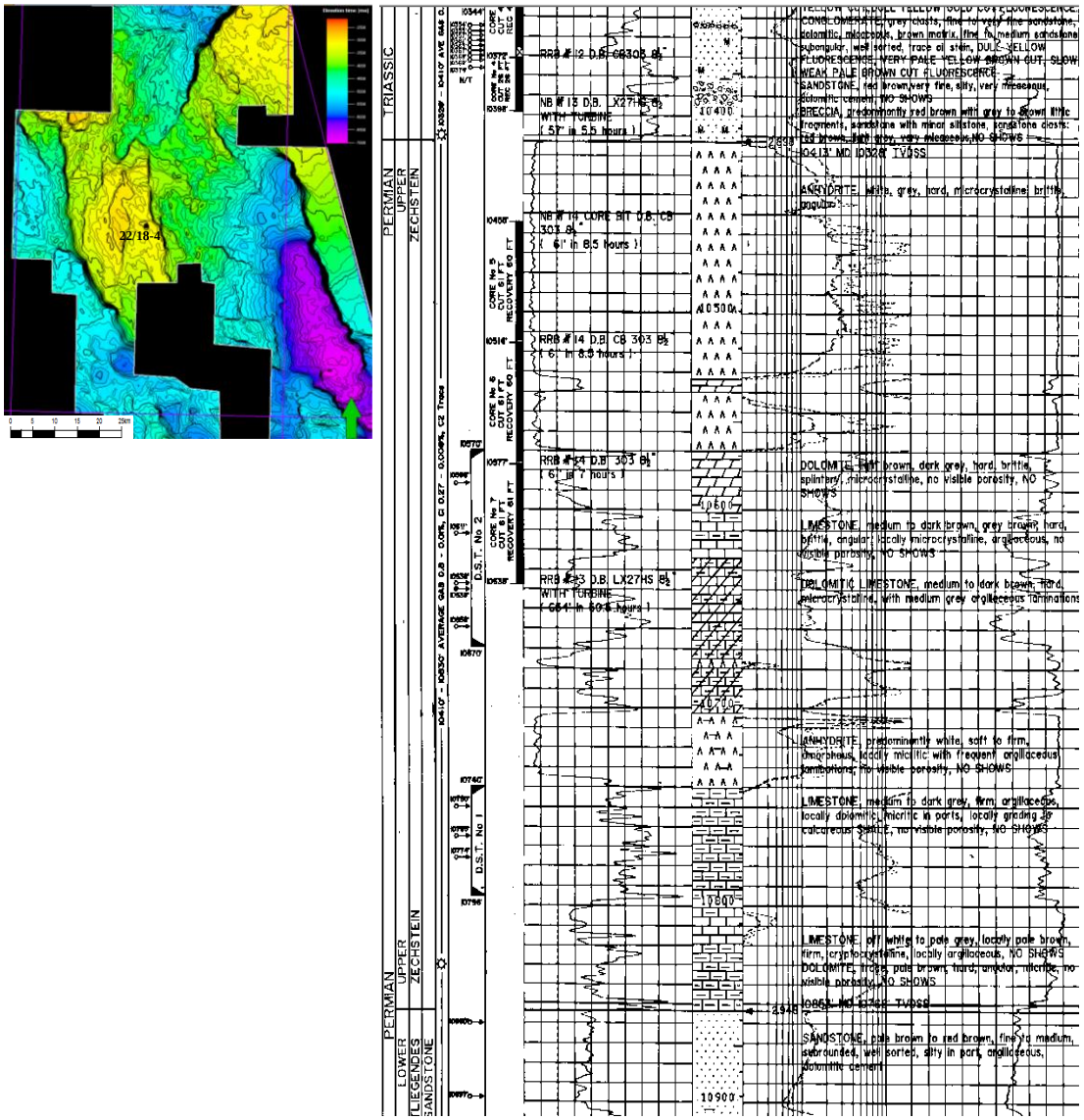

Figure 2.52: Composite log for well 22/18-4 on the Forties-Montrose High (location on Rotliegend TWTT structure map shown). The Zechstein section consists of Anhydrite, Dolomite and Limestone indicating that this area was either on the Zechstein basin margins or structurally high during evaporite deposition.

2.4.3 INTRA-CONTINENTAL RIFTING SUMMARY

Following Variscan inversion, a long period of erosion occurred creating the widespread unconformity identified all over north-west Europe known as the Base Permian Unconformity (BPU). W-E fault trends resulted from the creation of two large intra-continental basins during the Early Permian, the North and South Permian Basins. Late Permian evaporite deposistion occurred due to the cyclical flooding and desiccation of the Zechstein Sea within these basins.

In the Central North Sea the BPU is also identified and can now be mapped over a significant area. The new seismic data permitted identification of a Permian-age ridge extending WSW-ENE from the current Forties Montrose High to an area south of the Jaeren High . Cross-cutting by later faults meant that it has never been recognised before and was previously considered to be oriented NW-SE.. Transection of underlying fault trends can have important implications for the structural interpretation of an area as these basement faults may reactivate during the next peiod of extension or compression.Two Permo-Triassic fault sets oriented WSW-ENE and WNW-ESE to W-E were identified suggesting a shifting of the stress orientation between the Early Permian and Triassic.

The evaporites laid down in the Late Permian have had an important effect on the structural evolution of the areas covered by the North and South Permian basins due

to the ability of salt to flow under pressure differences and to act as a decollement surface for later faulting.

CHAPTER 3: TECTONO-STRATIGRAPHIC MEGASEQUENCE 1: SYN- AND POST-RIFT EVOLUTION

3.1 TRIASSIC RIFTING

A marine regression and return to continental climate marked the start of the Triassic (Ziegler 1990). The climate was semi-arid with sedimentation largely controlled by local and regional tetonics, base-level changes and humidity changes due to continental drift (Glennie 1998). The Lower-Mid Triassic Smith Bank Formation consists of fine red clastic mudstones and siltstones laid down in a widespread lacustrine/floodplain environment (Hodgson et al. 1992). Increasingly extensive drainage systems developed in the Upper Triassic which brought Skaggerak Formation fluvial sands in to the area.

Crustal extension in the Arctic-North Atlantic and Central Atlantic rift systems initiated in the Early Triassic (Ziegler 1990). These tectonic stresses led to rifting in the Northern North Sea, particularly in the East Shetland Basin (Figure 3.1) where Triassic thickening packages can be demonstrated pre-dating the formation of the Jurassic rift arms (Figure 3.2) (Underhill et al. 2003). In some areas these can be observed despite having been cut by later faults suggesting that these were major lineaments (Figure 3.3). Onshore, large Permo-Triassic basins are also preserved and lack of transecting Jurassic faults make these easier to observe (Figure 3.4).

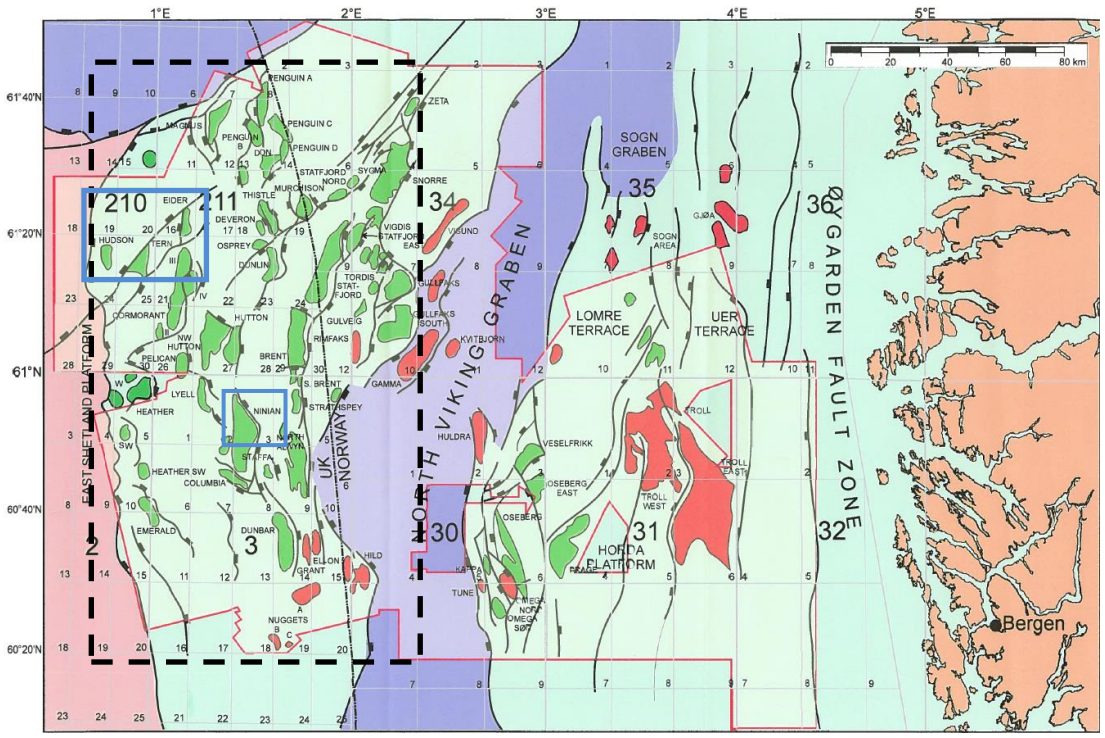

Figure 3.1: Location map of the East Shetland Basin (dashed box). Hydrocarbon fields are named and those noted in Figures 3.2 and 3.3 are boxed in blue. The extent of 3D seismic data used to constrain interpretation of Triassic extensional faulting is also shown outlined in red.
Image after (Underhill et al. 2003)

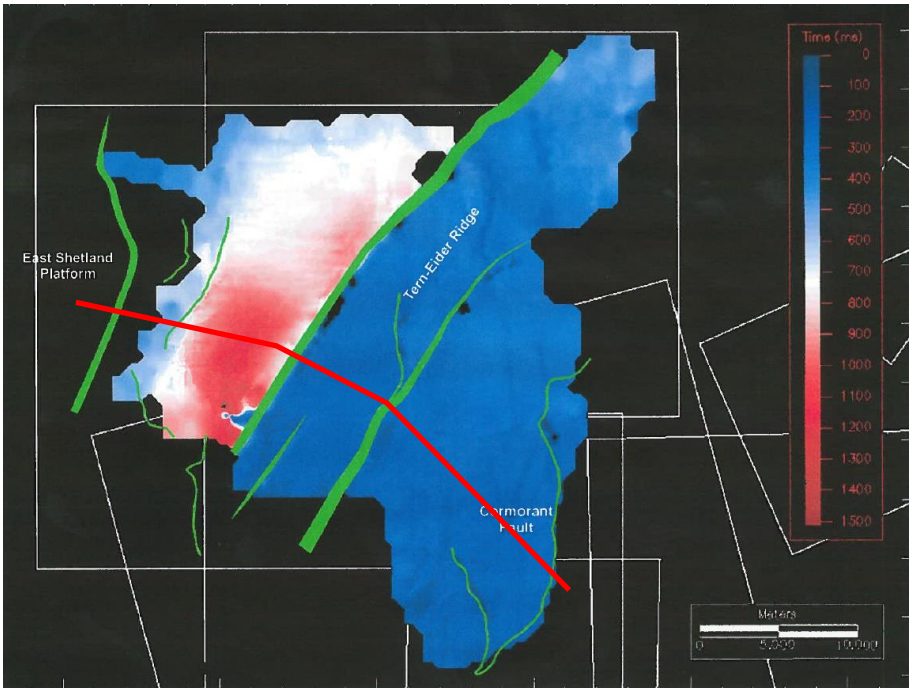

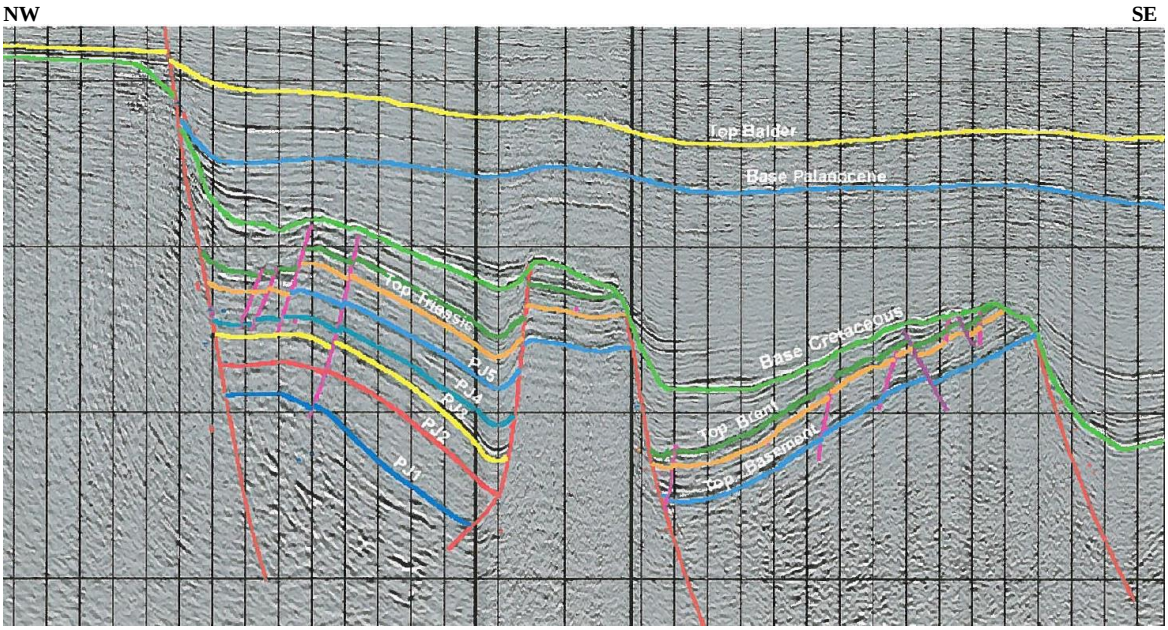

Figure 3.2: Isochron and seismic section of the Triassic interval showing a syn-rift thickening package against the Tern-Eider Ridge.
Image after (Underhill et al. 2003)

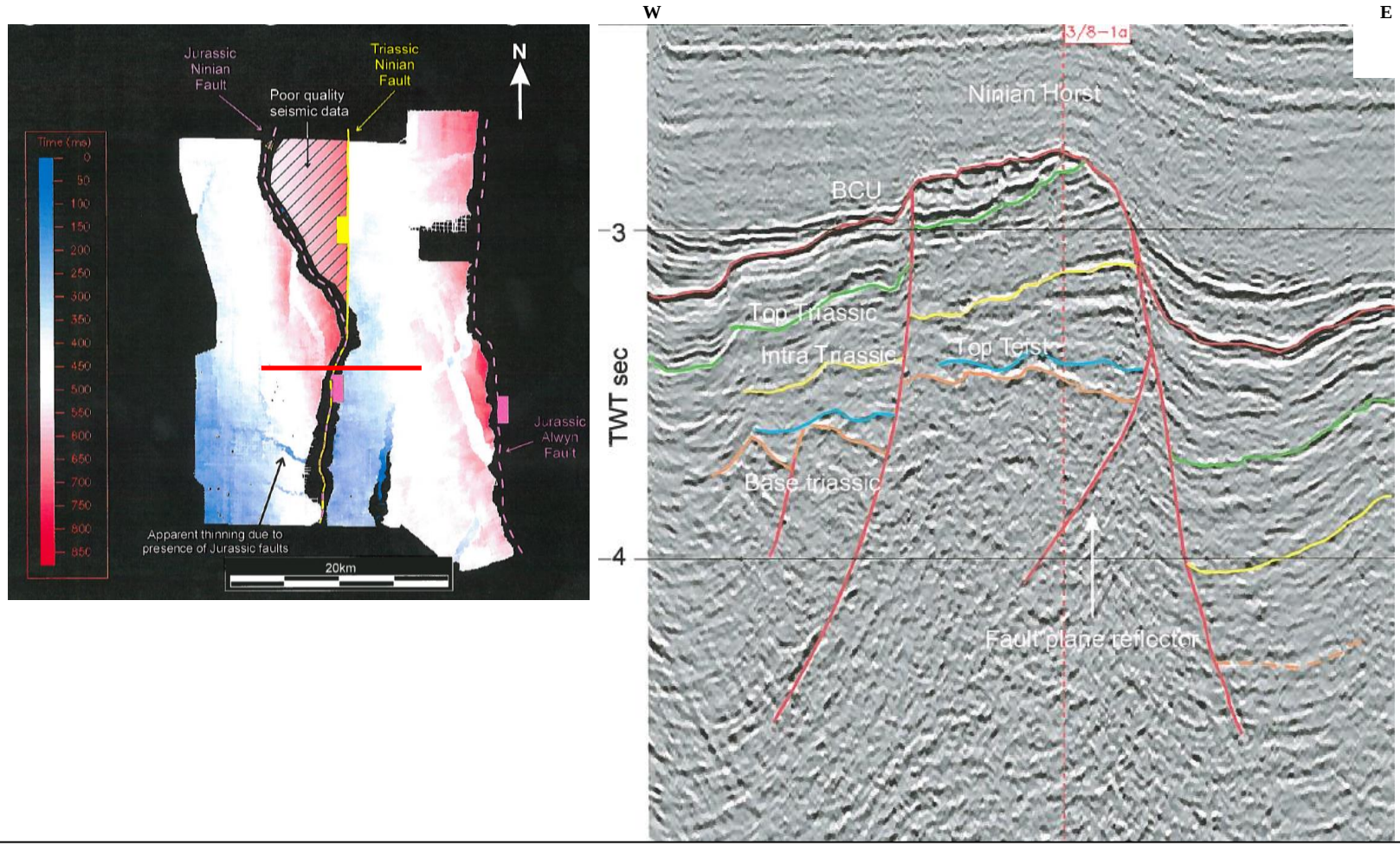

Figure 3.3: An isochron of the Triassic interval and seismic section over the Ninian area showing thickening into a transected Triassic fault.

Image after (Underhill et al. 2003)

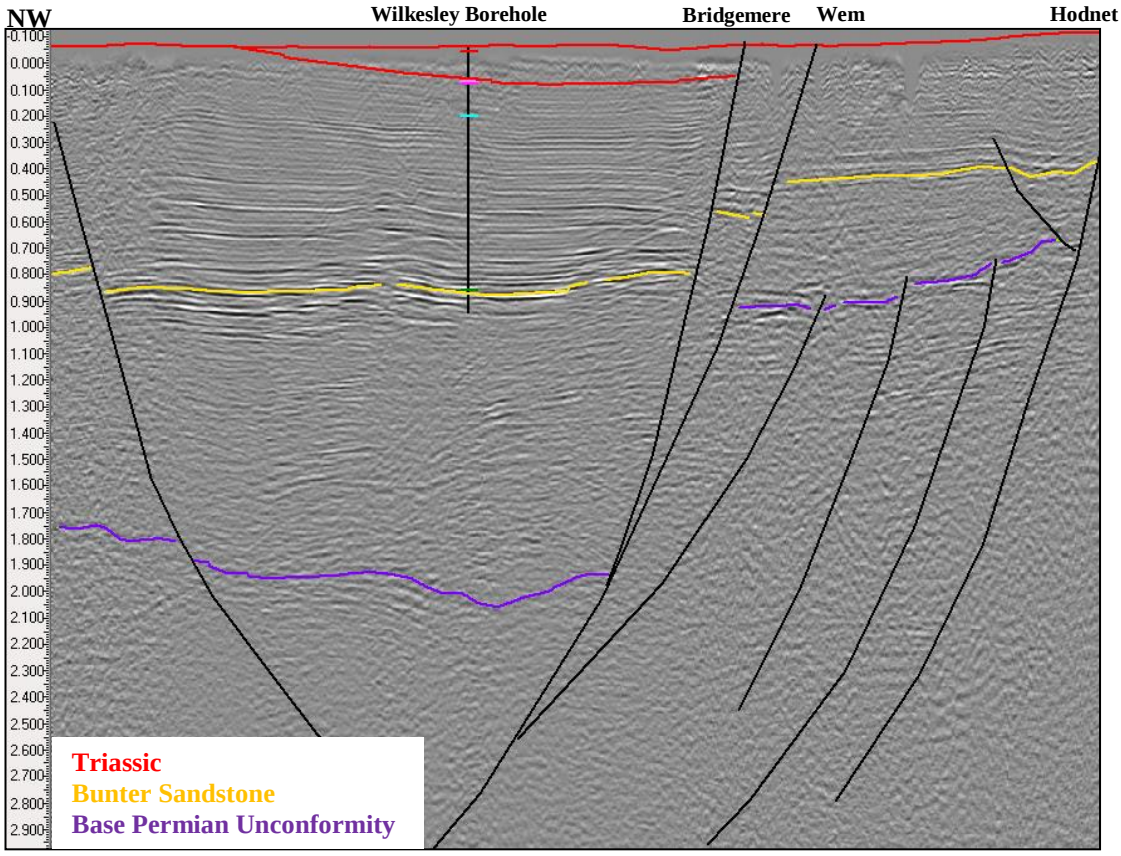

Figure 3.4: NW-SE seismic line across the Cheshire Basin showing syn-depositional growth of the Permo-Triassic section into the Wem and Bridgemere Faults.

UKOGL seismic line E87F-09 Scale= 11.7km

3.1.1 SYN-RIFT 1

In the Central North Sea there is debate about the occurrence of extensional tectonics in the Triassic as there appears to be no clearly defined syn and post-rift packages as predicted by the standard rift model. On the Forties-Montrose, Jaeren and Auk Highs where the Triassic section is well-imaged it has a distinctive morphology of thick rounded deposits separated by areas of Zechstein salt (Figures 3.5-3.7) with none of the characteristic thickening patterns typically associated with extensional domains. Additionally, W-E striking extensional faults which are of the correct orientation to have been active under the Triassic stress field, show thickening of the Permian section and could be ascribed to intra-basinal faulting during this time.

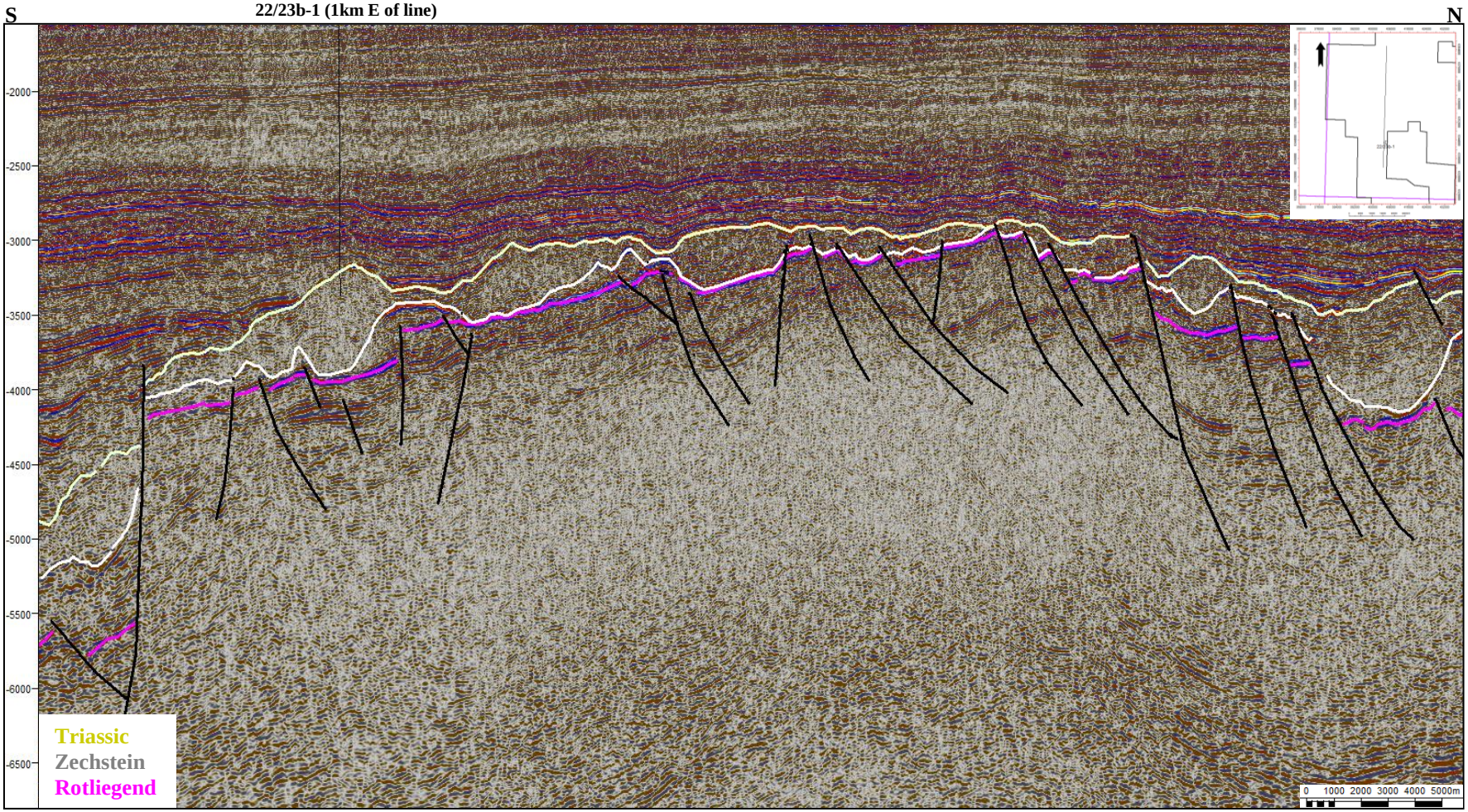

Figure 3.5: N-S seismic line over the Forties-Montrose High showing the morphology of the Zechstein and Triassic units. The Triassic is preserved as elongate 'pods' between Zechstein salt walls. The Triassic section here consists mainly of Smith Bank Formation mudstones.

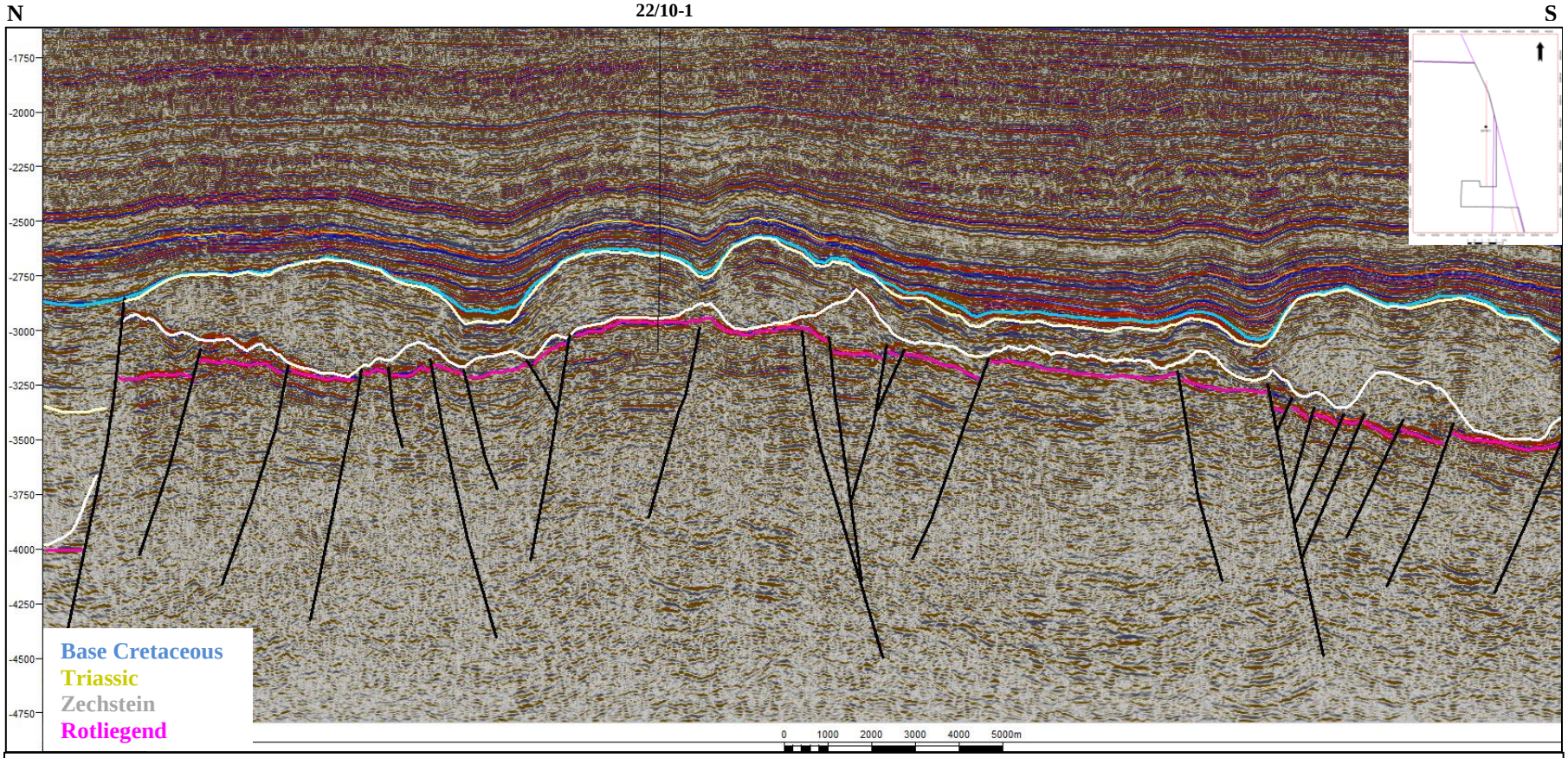

Figure 3.6: N-S seismic section over the Jaeren High showing the Triassic Smith Bank pod geometry. Within the inter-pods thin Upper Jurassic Kimmeridge Clay source rock is deposited.

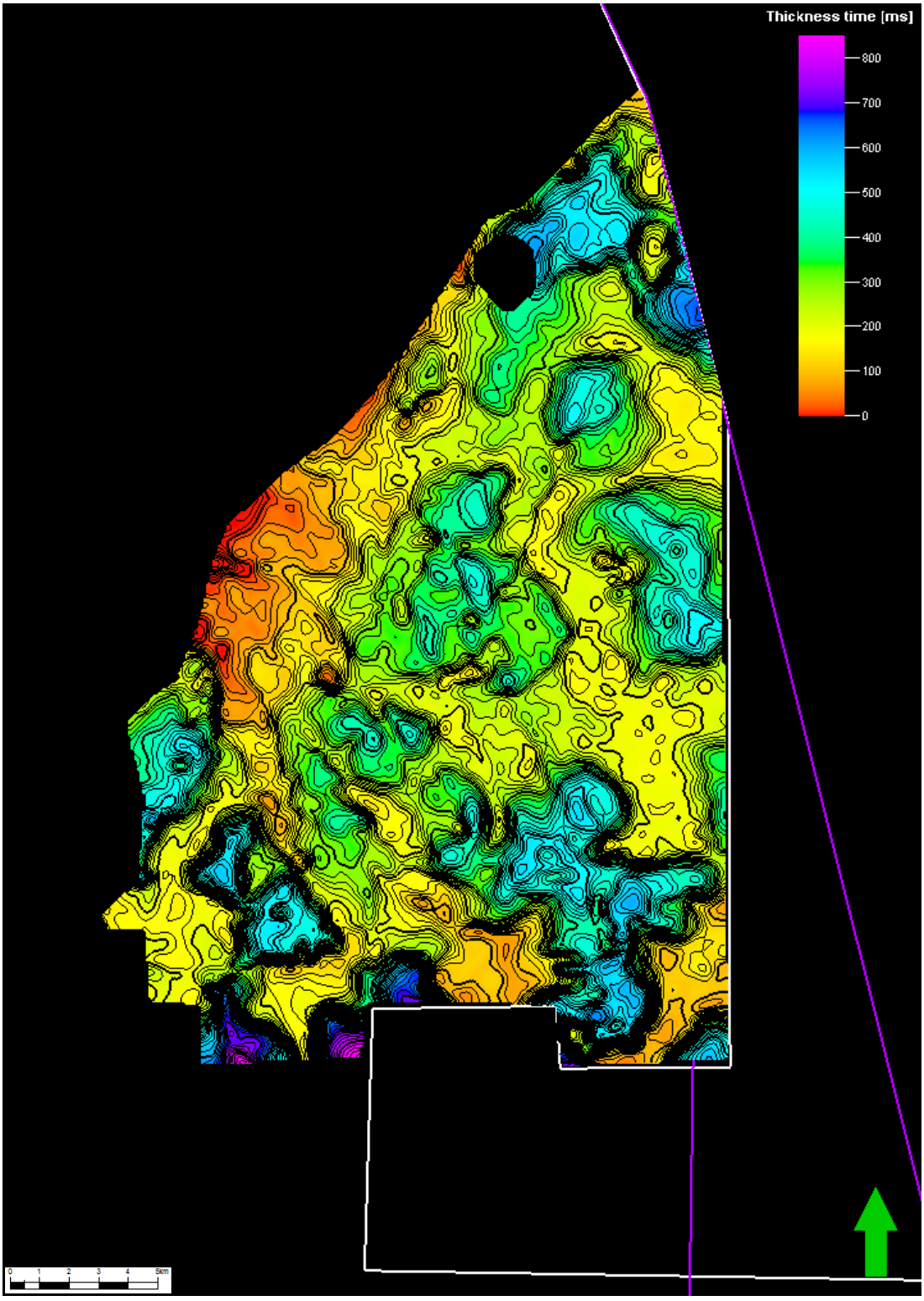

Figure 3.7: An isochron of the Triassic sequence on the Jaeren High demonstrating the presence of thick pods. The Jurassic infill of the inter-pod areas may be a migration route for oil generated in deeper source areas to get onto the shelf and into reservoirs such as those which are exploited along the Ula-Gyda trend in the Norwegian Central North Sea.

However, the presence of a mobile evaporite layer modifies the regional response to extensional tectonics by taking up some of the strain and modifying depositional patterns (Richardson et al. 2005). The unusual geometries seen in the Triassic section are also noted in evaporite provinces in Oman (Heward 1990) and Utah (Matthews et al. 2007) and result from withdrawal of mobile salt from underneath developing depocentres. Extensional faulting led to slight variations in deposition of Lower Triassic Smith Bank mudstones and differential loading in these areas was enough to cause the underlying salt to flow creating 'pods' of Triassic infill surrounded by salt 'walls' (Hodgson et al. 1992; Erratt 1993; Stewart et al. 1999) (Figure 3.8).

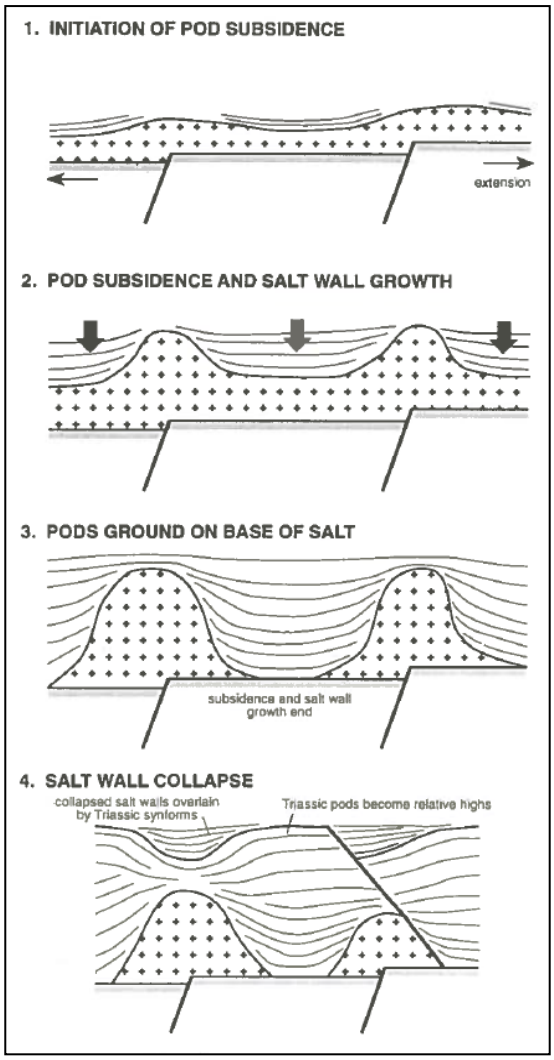

Figure 3.8: Depositional model for Triassic sediments in the Central North Sea.
Image after (Hodgson et al. 1992)

On the Auk Ridge, imaging of the Triassic sequence is good due to the shallow depth and lack of a significant Cretaceous Chalk Group overburden. Here it is possible to see the complex relationship between Triassic deposition and salt movements with numerous unconformities developed as the salt walls either side grew (Figure 3.9).

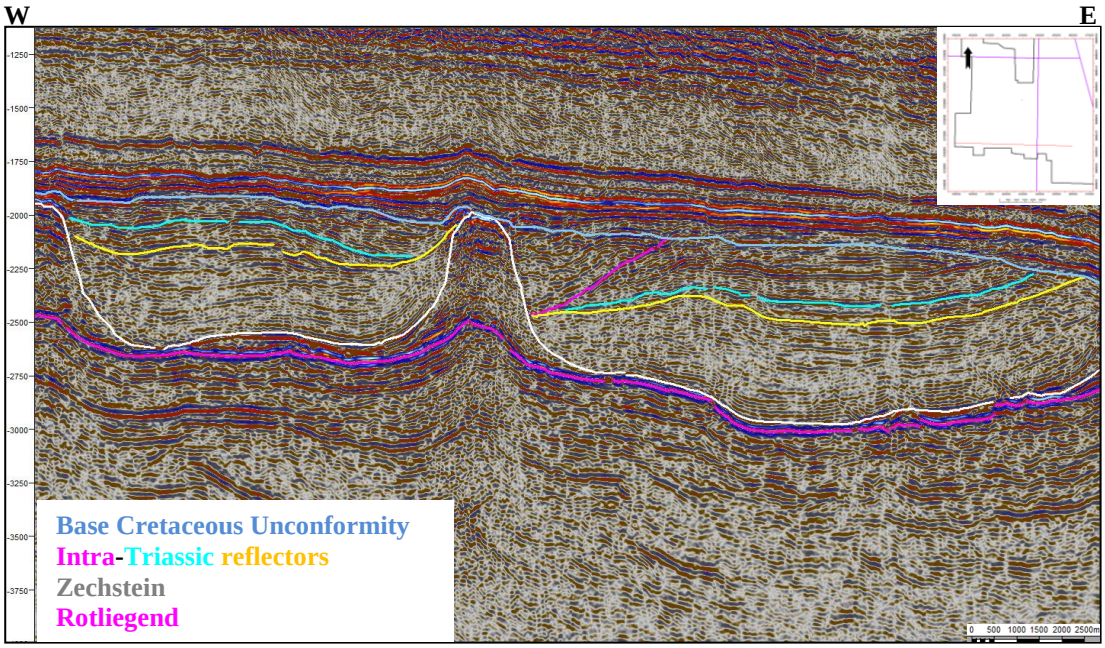

Figure X 3.9: A W-E section over the Auk Ridge demonstrating unconformities formed at the sides of salt walls due to differential loading.

.

In this model the Triassic Smith Bank Formation which forms the majority of the pods is the Triassic syn-rift section and the extension is taken up by the basement Rotliegend faults due to their favourable orientation with respect to the Triassic stress-field.

However, it could be suggested that differential subsidence caused by slight variations in initial thickness of Smith Bank deposits, possibly in lakes, could have produced the pod geometry without invoking regional extension. This is a possible mechanism for Triassic sedimentation but does not fully explain the presence of diapirs or their presence above W-E striking basement faults.

Diapirs occur when the density contrast between salt and the overburden are such that the salt rises to the surface (Figure 3.10) However, special conditions are required to initiate diapirs as piercement is more difficult than just getting salt to flow due to the overburden strength usually being greater than the pressure difference (Jackson et al. 1994). Regional extension has been linked to diapirism (Davison et al. 2000) and although many of the diapirs in the Central North Sea are thought to have initiated during later periods of tectonic activity, some occurred during the Triassic. Additionally, many diapirs are situated where basement faults are cross-cut by later extensional faults (Figures 3.11 and 3.12) suggesting a significant basement control on the position of the initial salt-walls.

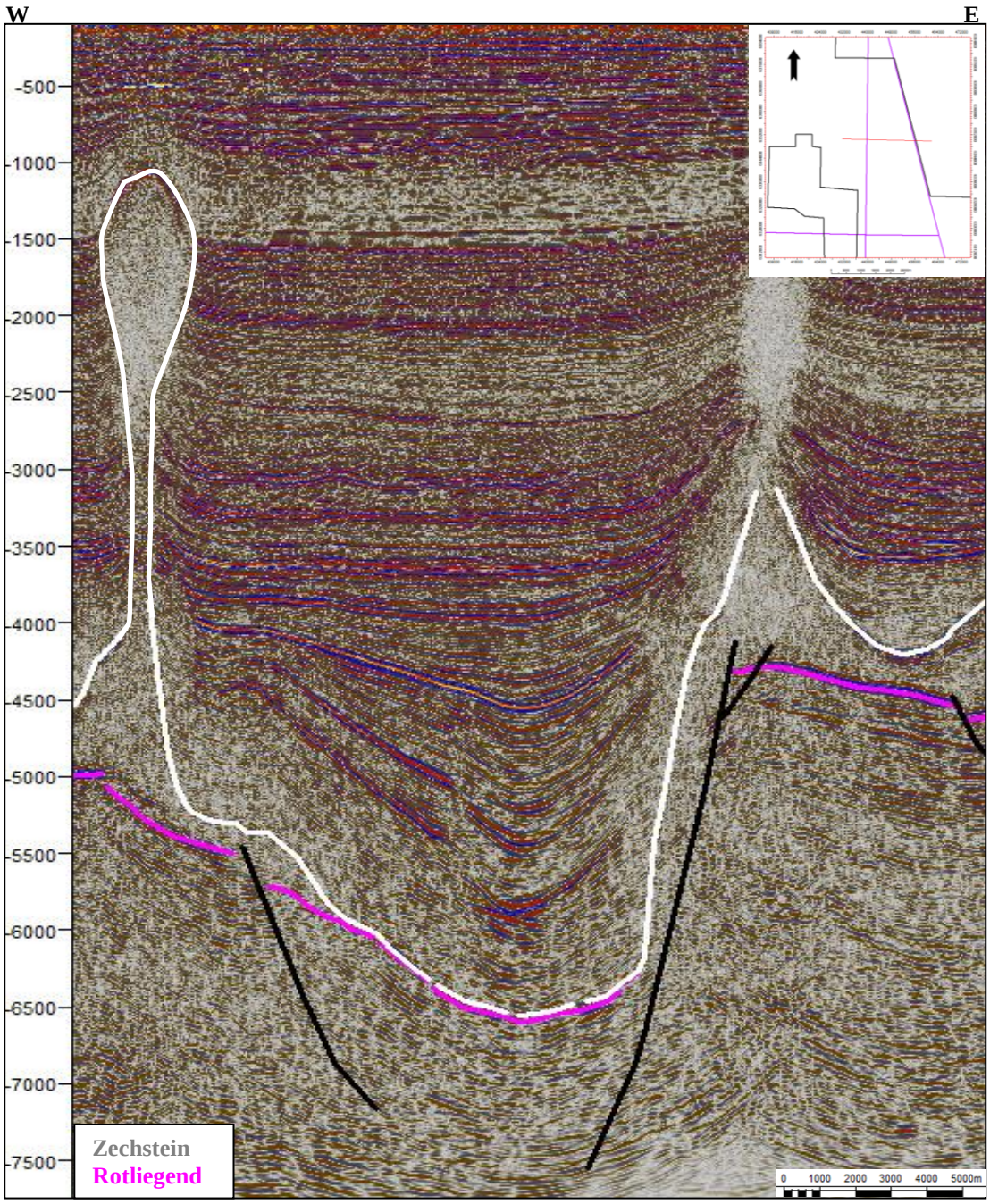

Figure 3.10: W-E seismic line across the Central North Sea dataset showing salt diapirs.

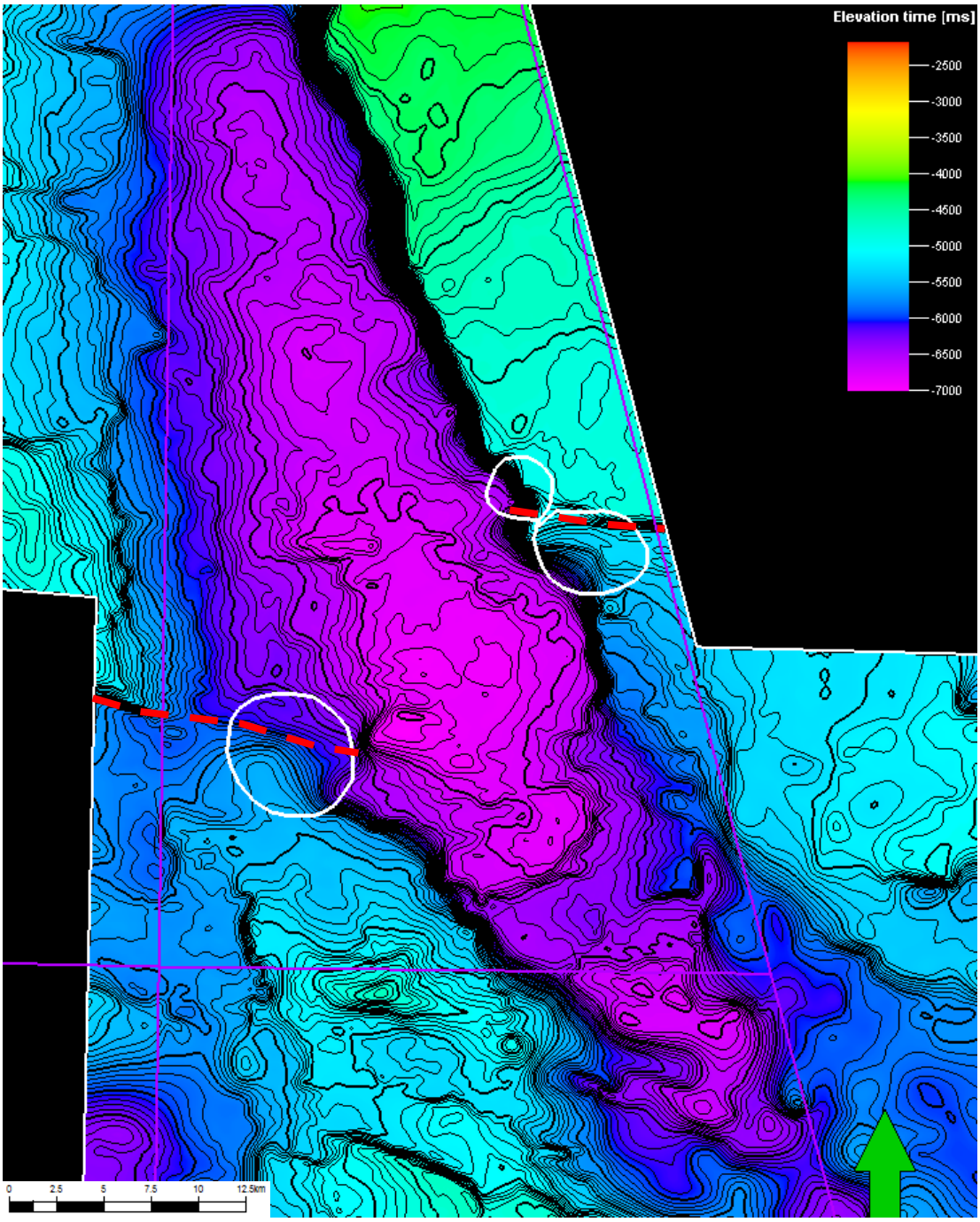

Figure 3.11: TWTT structure map of the Rotliegend with diapirs indicated. Diapirs lie over junctions between sub-W-E Permo-Triassic faults and the NW-SE Jurassic rift arms.

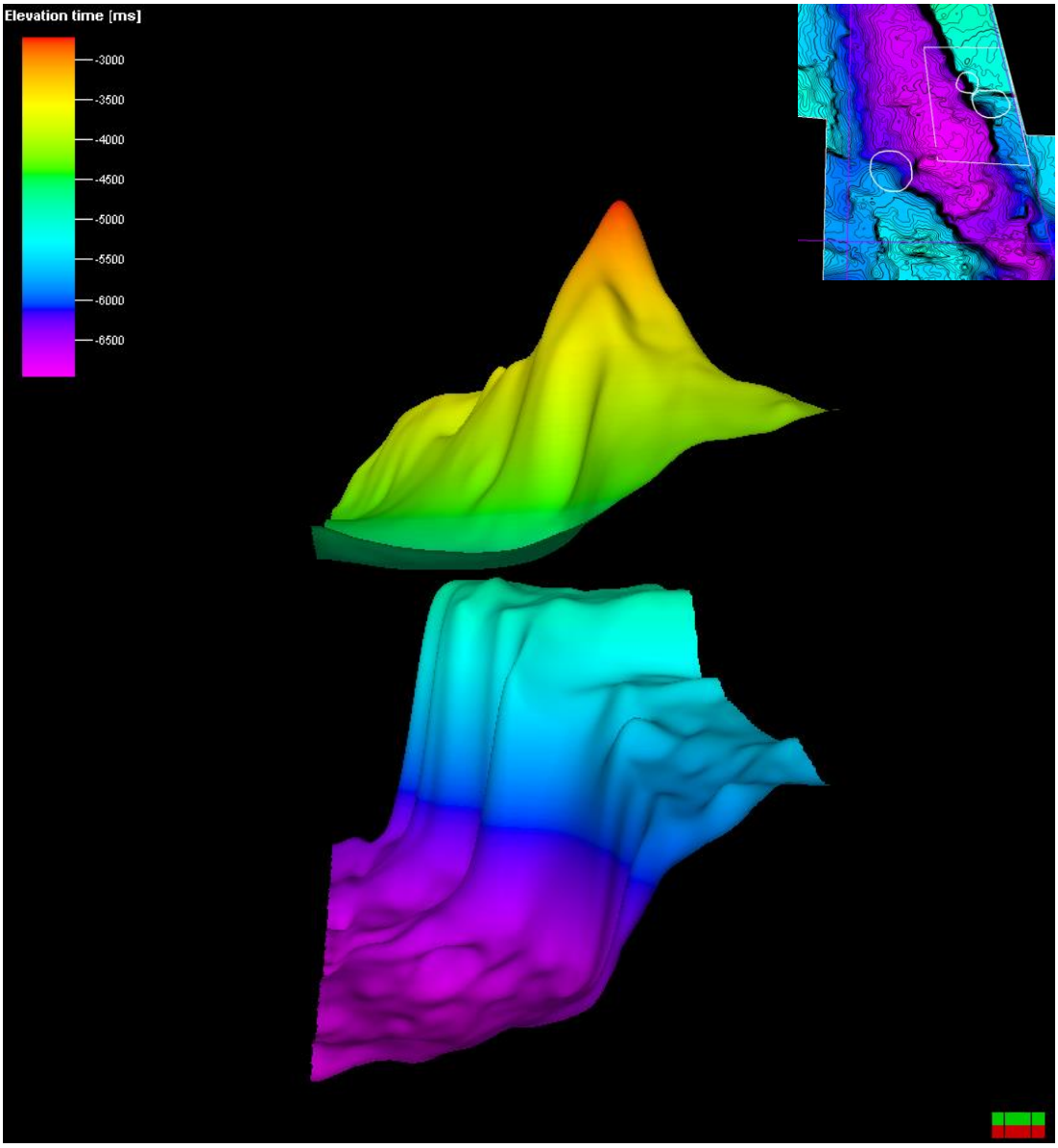

Figure 3.12: 3D image of the TWTT Rotliegend and Base Cretaceous structure maps showing the salt thick over the fault junctions.
View from the south. Location with respect to Figure 3.11 noted.

3.1.2 POST-RIFT 1

The evidence from analysis of fault tends suggests that the Smith Bank Formation comprises the syn-rift section of the Triassic rift cycle. The post-rift should therefore be easily identified by an unconformity or as a change from pod geometries to parallel-bedded infill. Triassic rifting in northern areas ceased by the Late Triassic so the post-rift section may be represented by the Upper Triassic Skagerrak Formation. However, erosion and later salt movements have all modified the preservation of the Triassic so it is unclear in some areas what the relationship is between the Skagerrak and Smith Bank Formations. Placing all of the data collected from Triassic well-penetrations over a structure map of the Permian shows no observable trend except that on the basement highs there is a predominance of the Smith Bank Formation which is entirely consistent with a simple model of higher erosion rates over areas of elevation and tells us little about the original deposition (Figure 3.13).

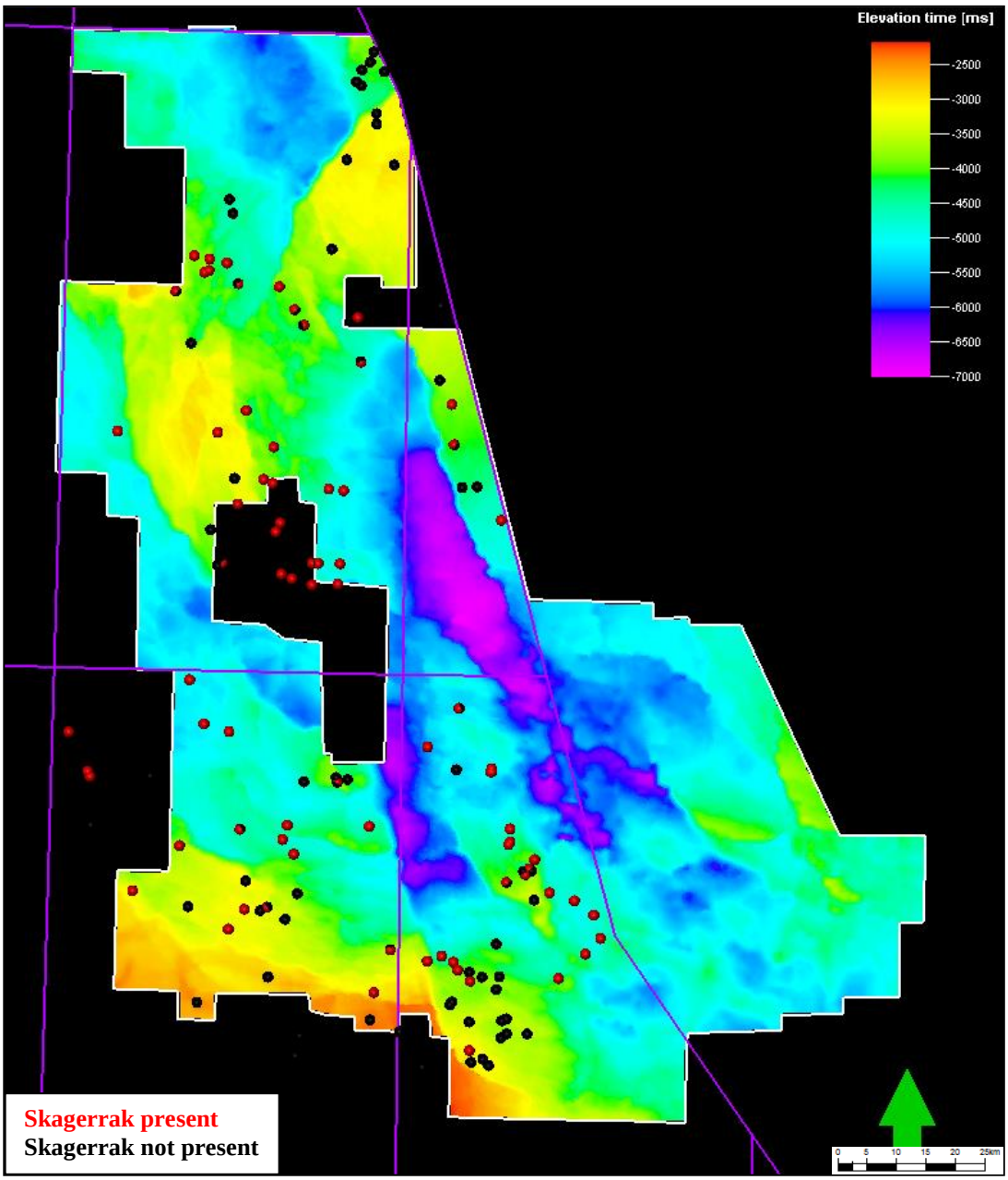

Figure 3.13: Wells in the Central North Sea study area with Skagerrak Formation present and not present/eroded.

Note that the interpretations of these formations made at the time of drilling have not been re--interpreted thus assignment of units to the Skagerrak Formation cannot be guaranteed to be accurate by present standards.

In order to assess whether the Skagerrak Formation represents a continuation of the syn-rift infill or represents the post-rift sequence of tectono-stratigraphic megasequence 1, three study areas were examined in detail. One of these was situated on the Forties-Montrose basement high, one in the deep Eastern Trough in quadrant 23 and one in an area identified on structure maps as having Permo-Triassic age W-E striking faults (Figure 3.14)

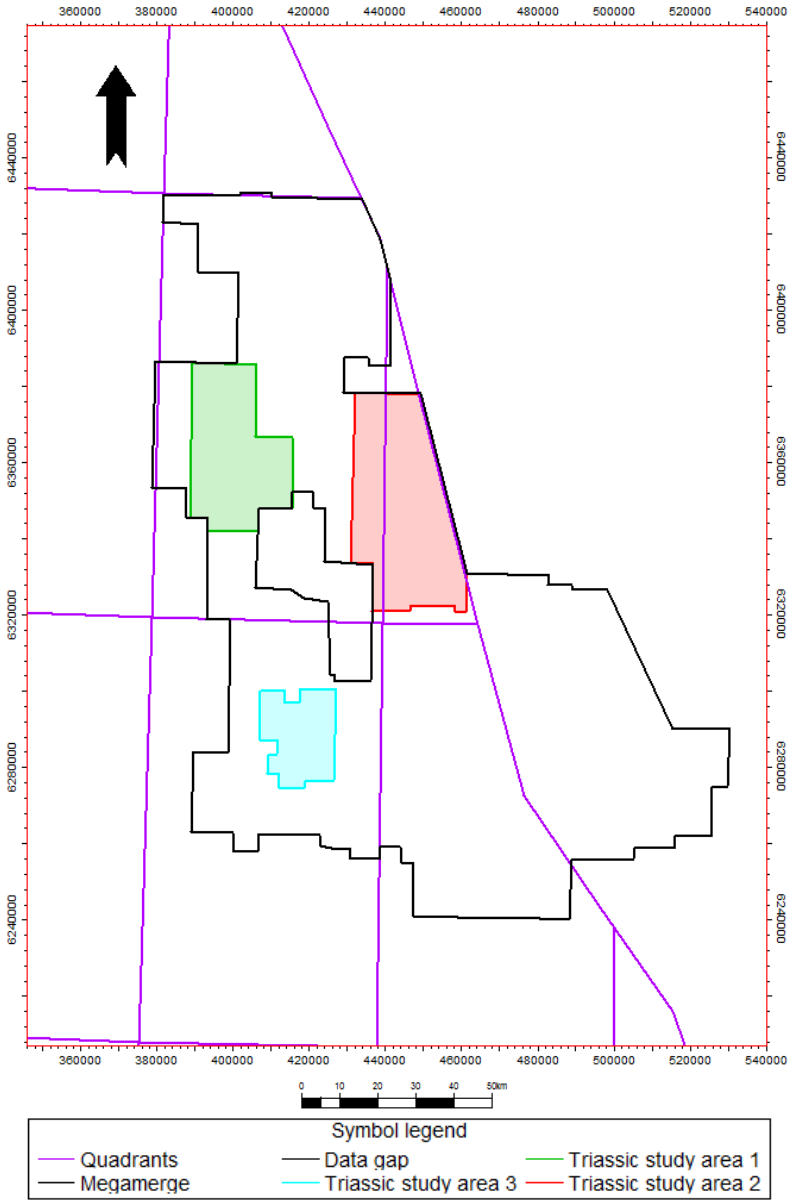

Figure 3.14: Location map of Triassic case study areas.

In study area 1 over the Forties-Montrose High, the Smith Bank pods are clearly imaged (Figure 3.15) but the entire Triassic section has been severely affected by erosion. In some places the Cretaceous rests directly on the Lower Triassic so most of the information about Triassic thickening trends may be unrepresentative. In order to study the area in detail, seismic interpretation of the Triassic and Zechstein was undertaken and an isochron of the Triassic unit created (Figures 3.16-3.19)

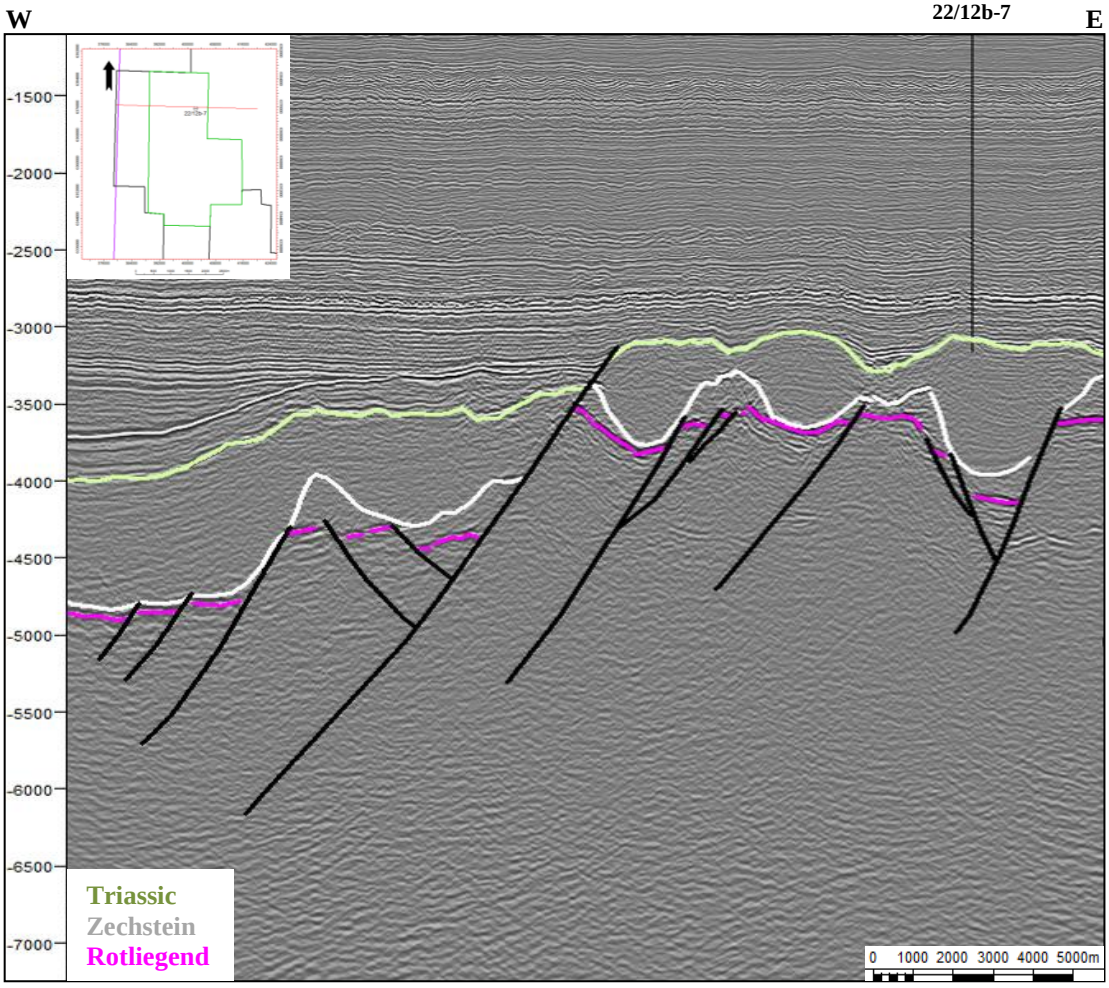

Figure 3.15: W-E seismic line across study area 1 showing the Triassic pod and Zechstein salt wall geometry.

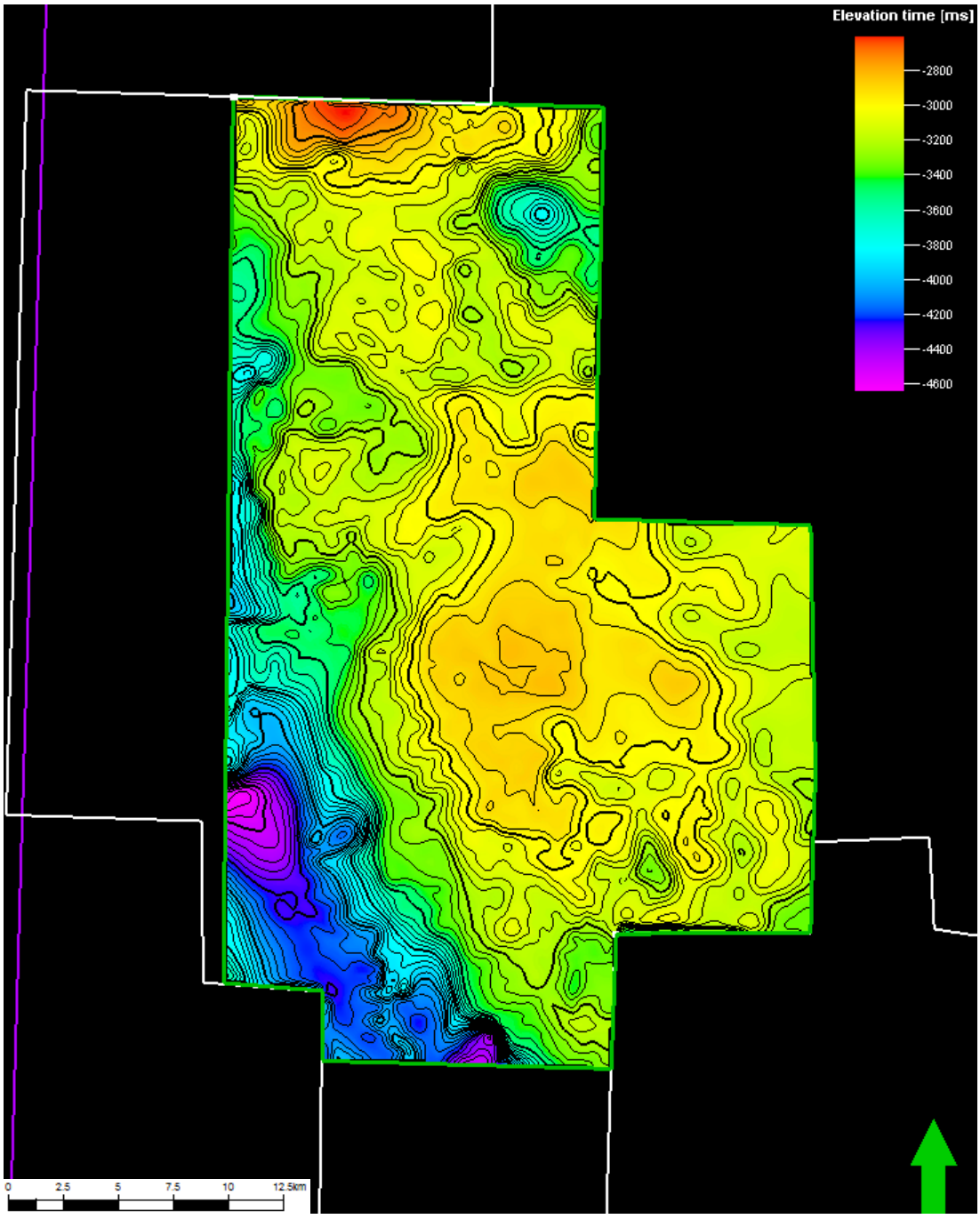

Figure 3.16: TWTT structure map of the Triassic section

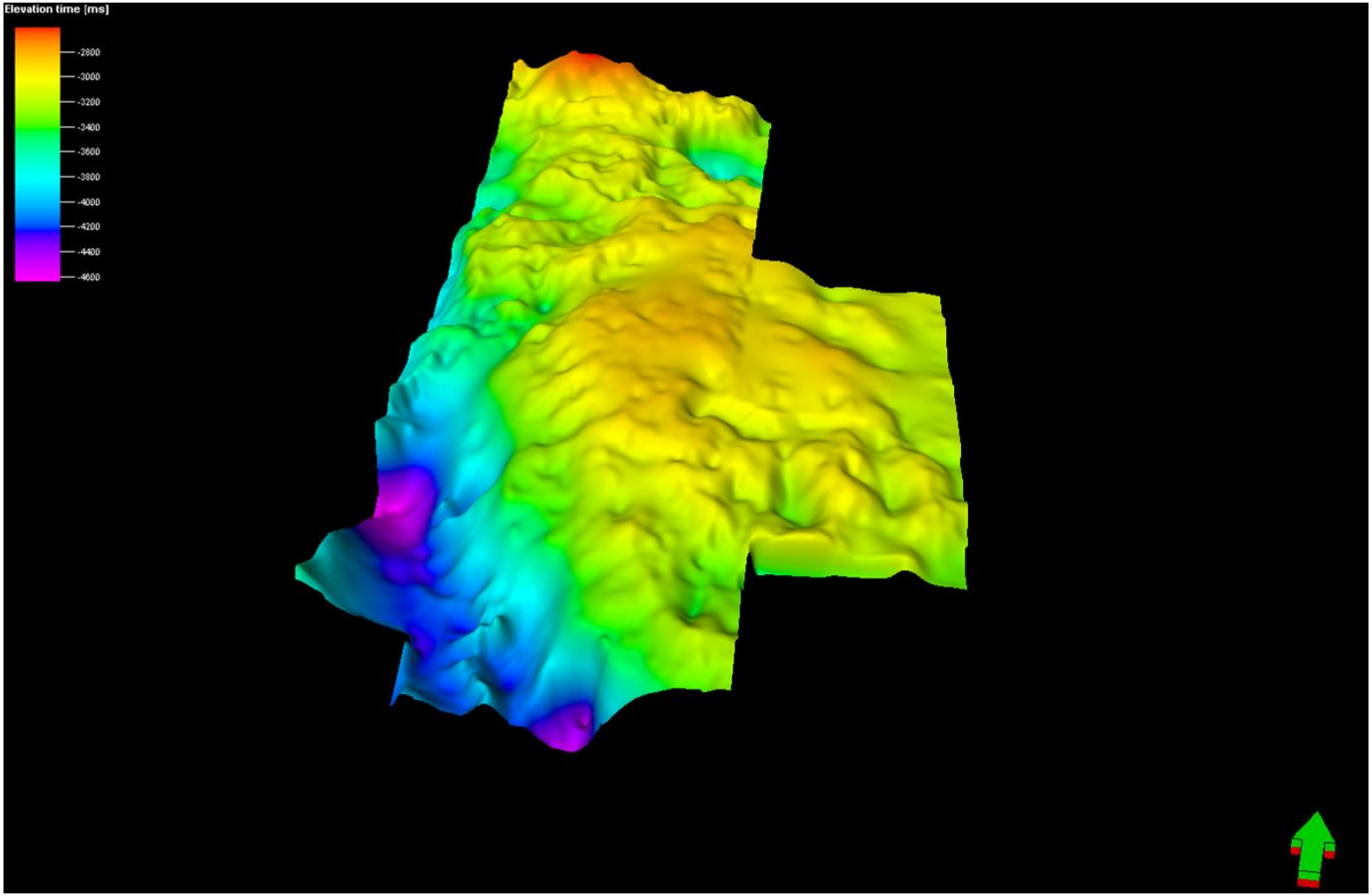

Figure 3.17: 3D image of the Triassic structure map. The variable relief can be clearly seen due to the pod morphology and collapse of salt structures.

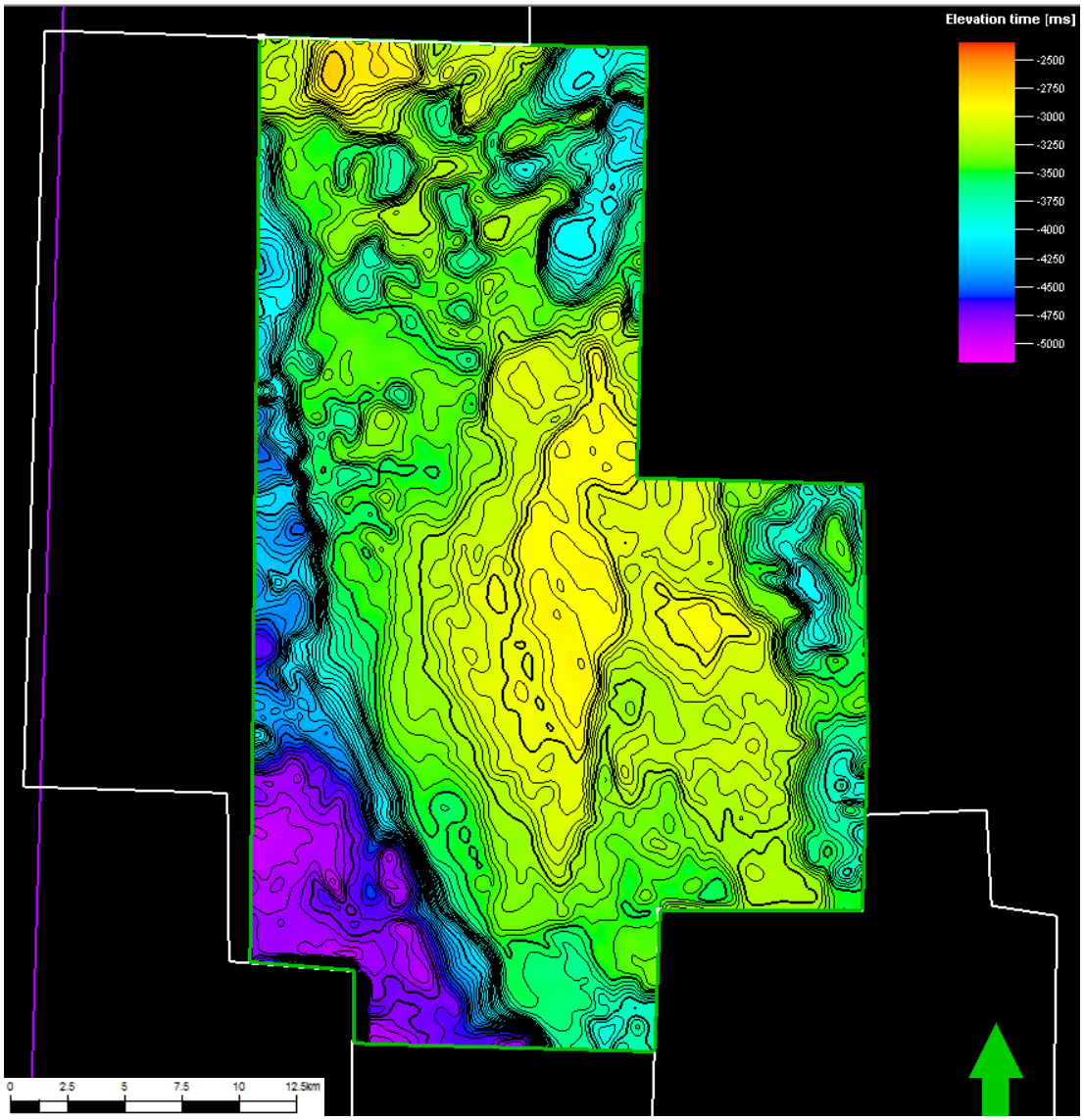

Figure 3.18: TWTT structure map of the Zechstein sequence. The areas of salt withdrawal can be clearly seen as elongate depressions.

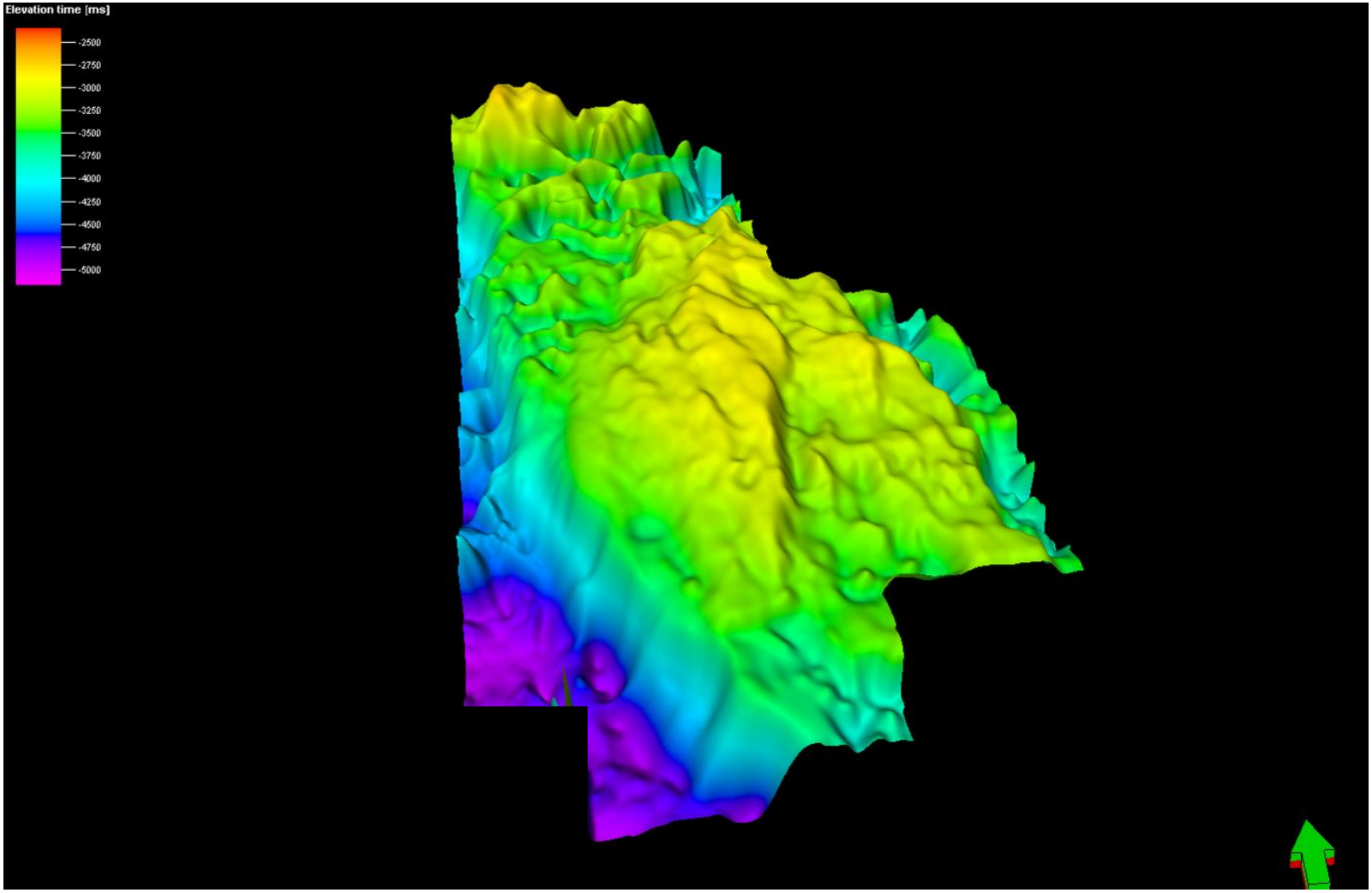

Figure 3.19: 3D image of the Zechstein structure map. The highly variable relief of the salt can be clearly seen.

Despite its position on a basement high, some of the wells in the area contain a Skagerrak sequence and in order to test the depositional models for this unit seismic sections across each of the wells containing Triassic rocks were examined (Figures 3.20-3.22).

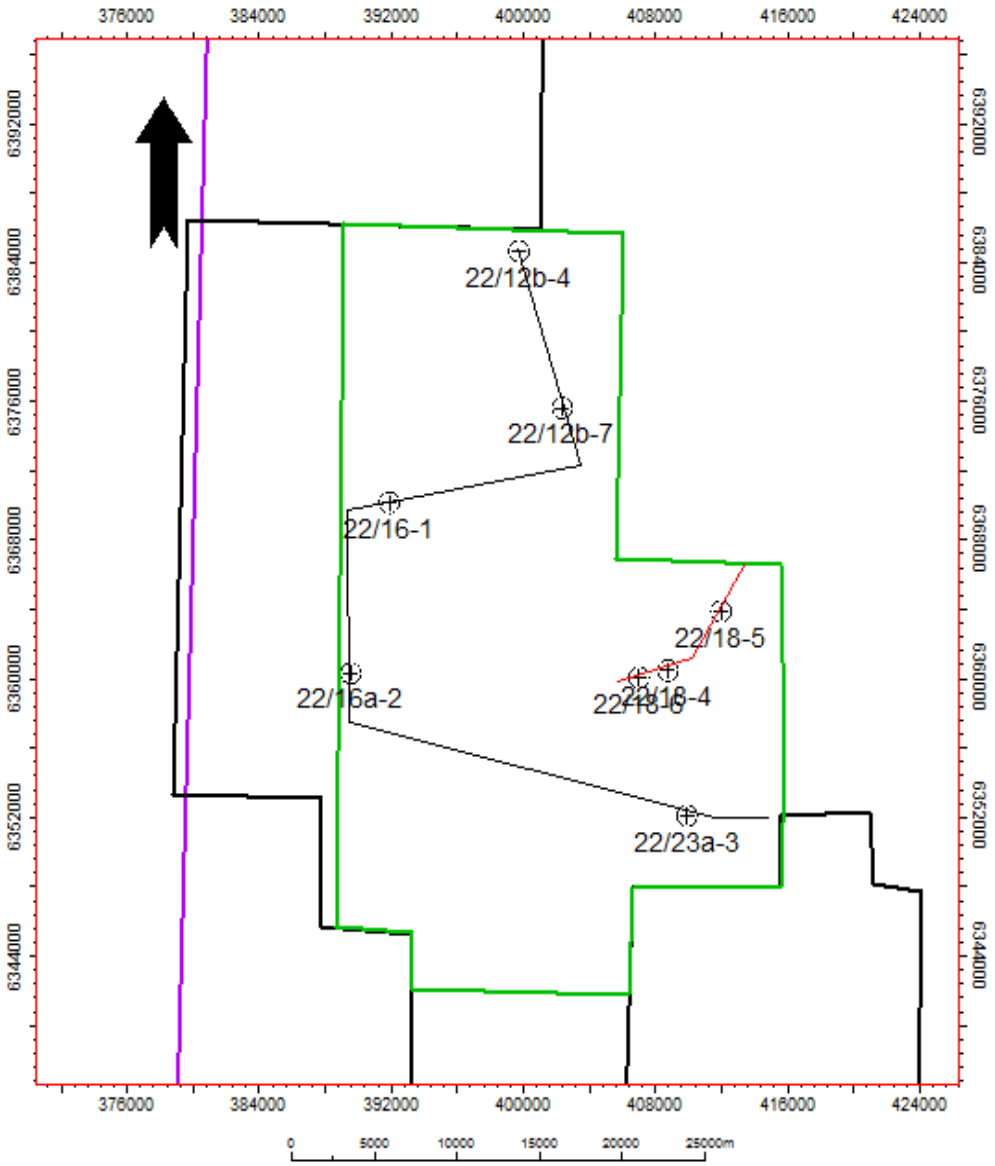

Figure 3.20: Map indicating wells which penetrate the Triassic within the study area and the locations of the composite seismic lines.

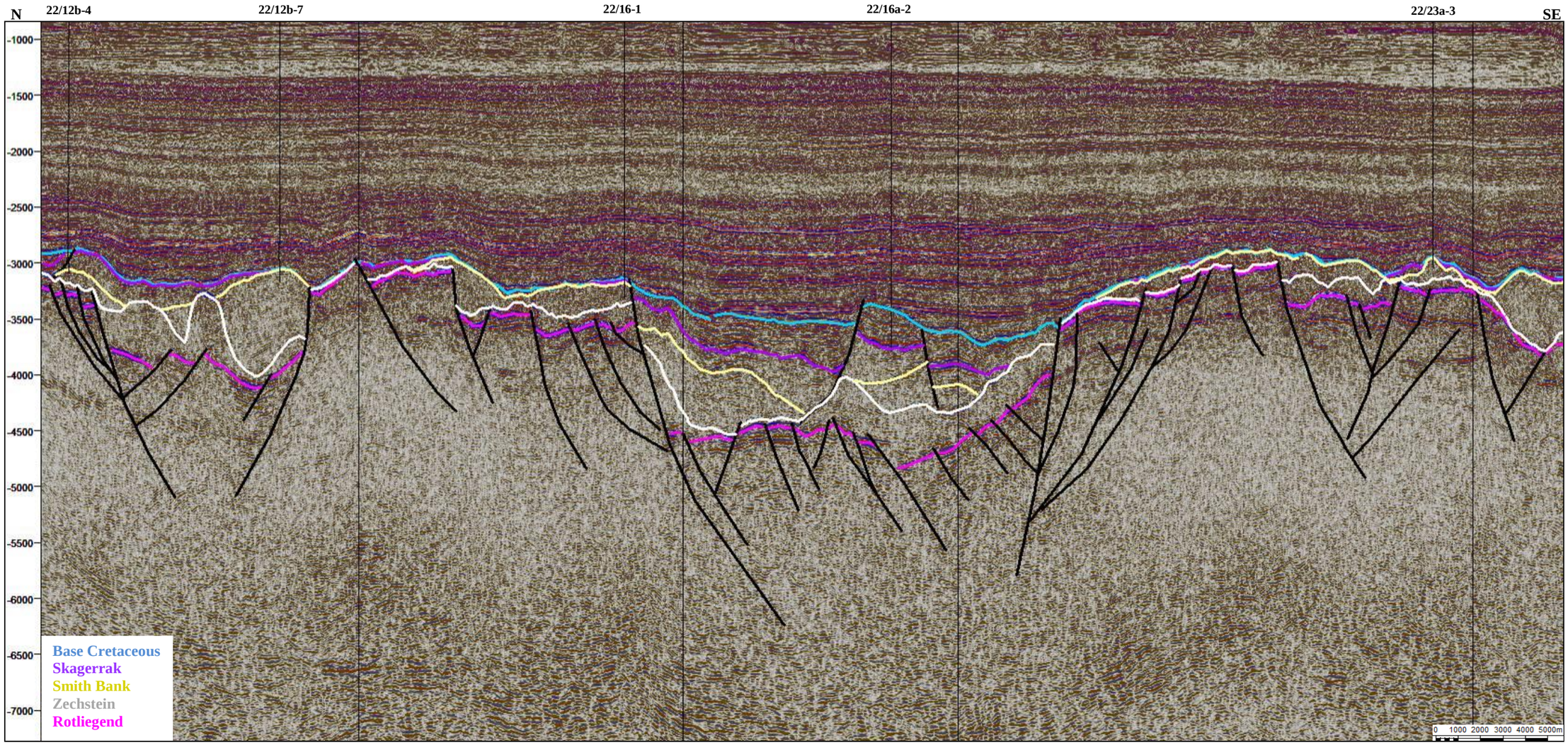

Figure 3.21: Composite seismic 1 line through wells in the study area which penetrated Triassic rocks.

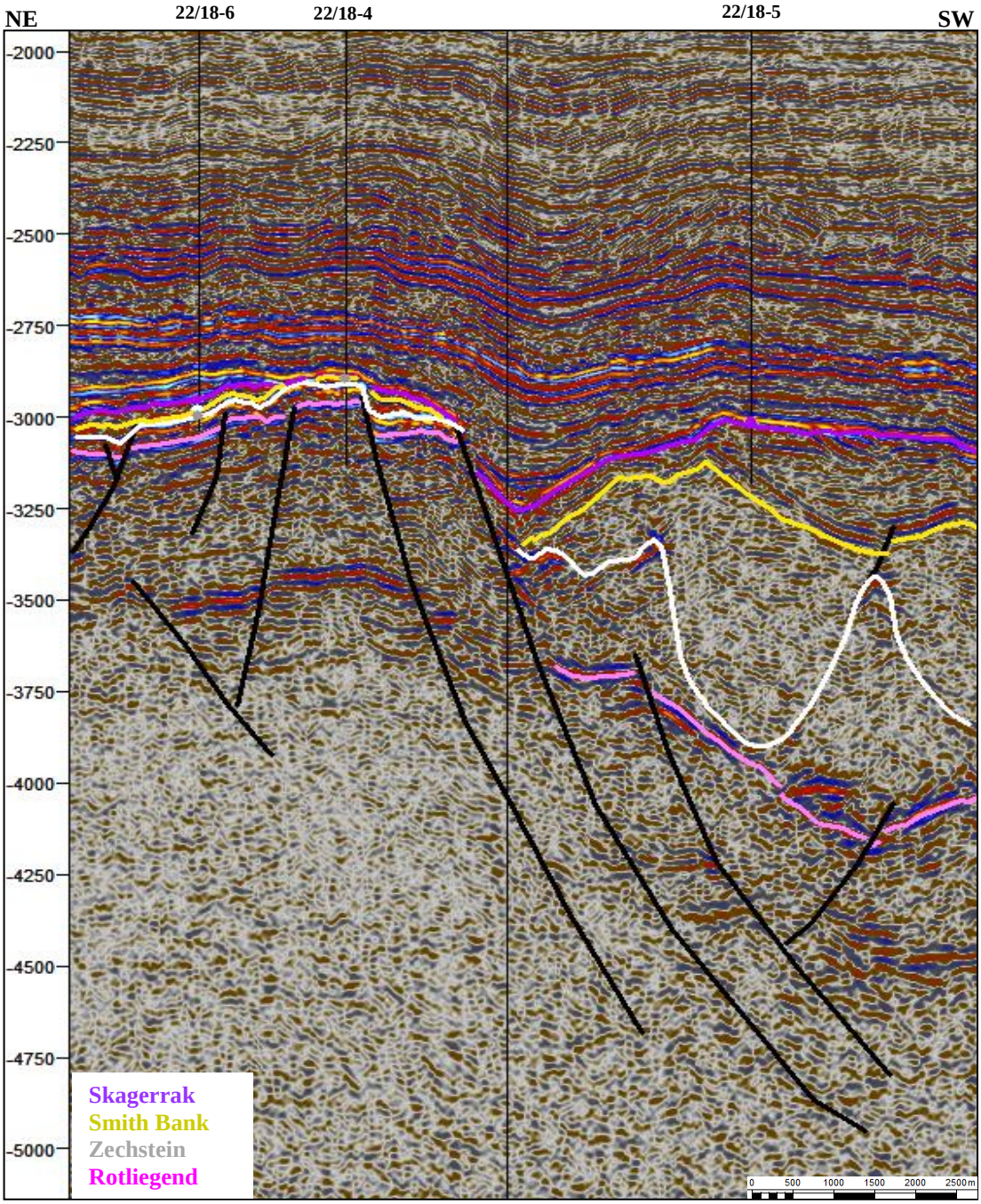

Figure 3.22: Composite seismic line 2 through wells in the study area which penetrated Triassic rocks.

The sections demonstrate that in the highest areas, erosion has removed most of the evidence of the relationship between the Smith Bank and Skagerrak deposition. However, where Skagerrak is preserved in section 1 which runs down the axis of the Forties-Montrose High, there appears to be a corellation between its occurrence and the Zechstein salt walls and it has an opposing thickening trend to the underlying Smith Bank Formation. This suggests that accommodation space for Late Triassic deposition was created by dissolution of the salt walls or that it was preserved due to later salt dissolution, perhaps during the Early Jurassic.

In section 2 which runs from the high into the basin, there is no such correlation and the Skagerrak is deposited conformably on top of the Smith Bank pod and thins over the salt walls. In this area then, salt withdrawal was still underway and creating accommodation space throughout the Late Triassic.

The second study area is situated over the East Central Graben (Figure 3.23. A composite seismic line (Figure 3.24) was created through wells which penetrated the Triassic section in order to invstigate the structures seen.

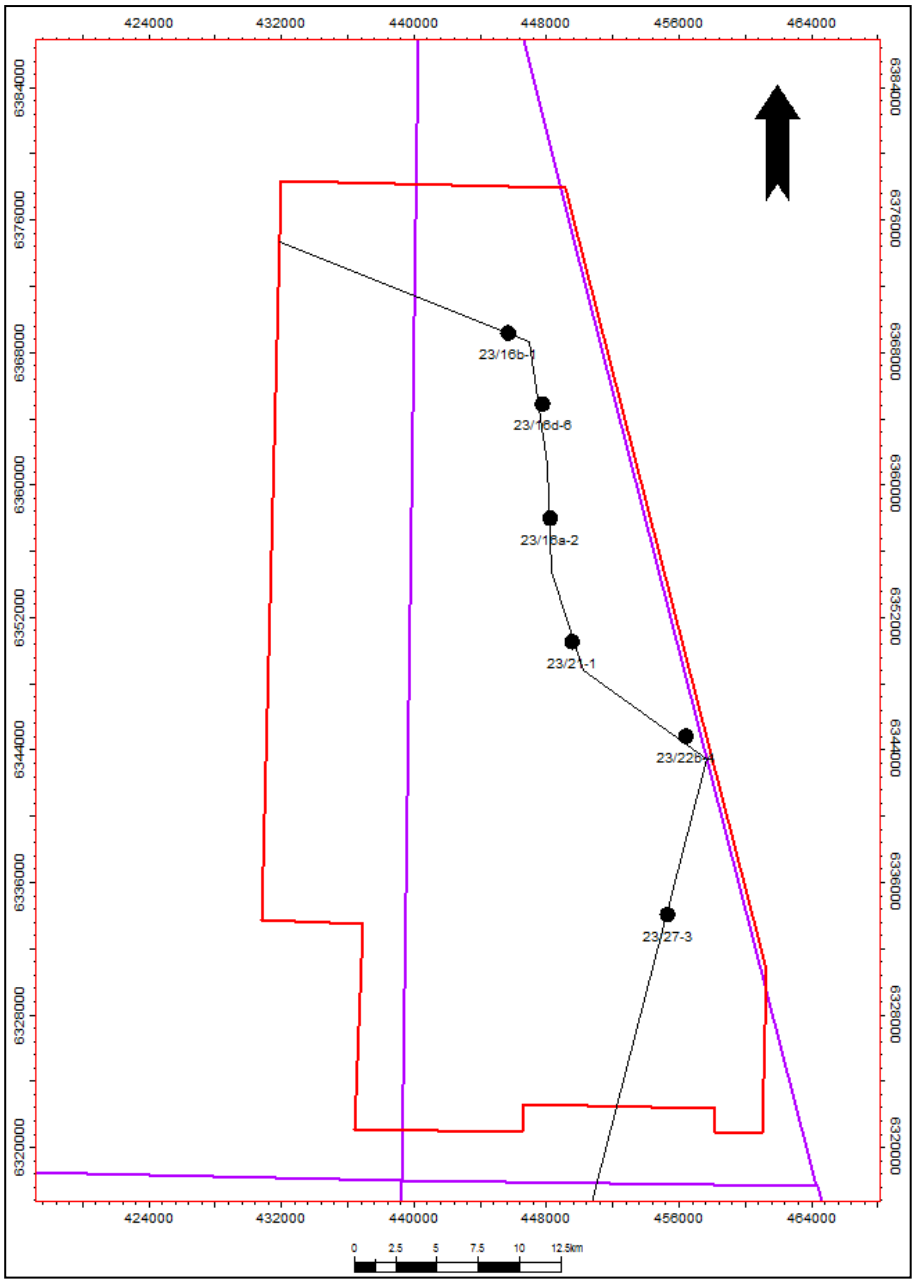

Figure 3.23: Location of composite seismic line through wells penetrating Triassic rocks.

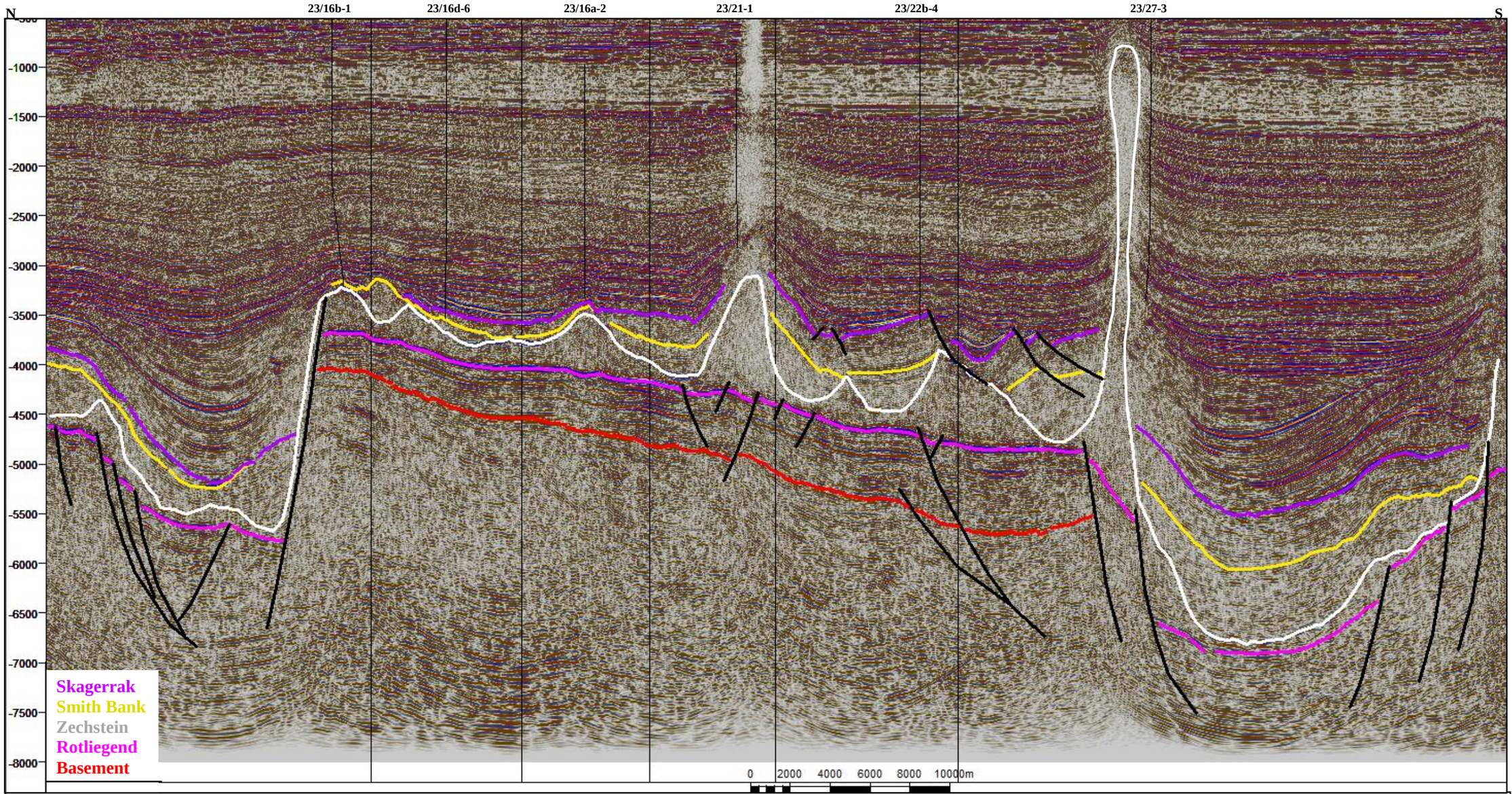

Figure 3.24: Composite seismic section through wells in study area 2 which penetrate Triassic rocks.

In this area both the Skagerrak and Smith Bank Formations form the pod geometry suggesting again, that Zechstein withdrawal controlled the deposition of the entire Triassic sequence. Faulting of the basement sequence occurs beneath the majority of the salt-walls providing further evidence that extension played an important role in their development. A Triassic isochron created between the top Triassic marker and Zechstein shows thickening in the graben area due to erosion on the flanks. Superimposed on this are a number of W-E striking ridges (Figure 3.25) which correspond with the emplacement of diapirs and are likely to indicate the positions of Zechstein salt walls overlying precursor faults.

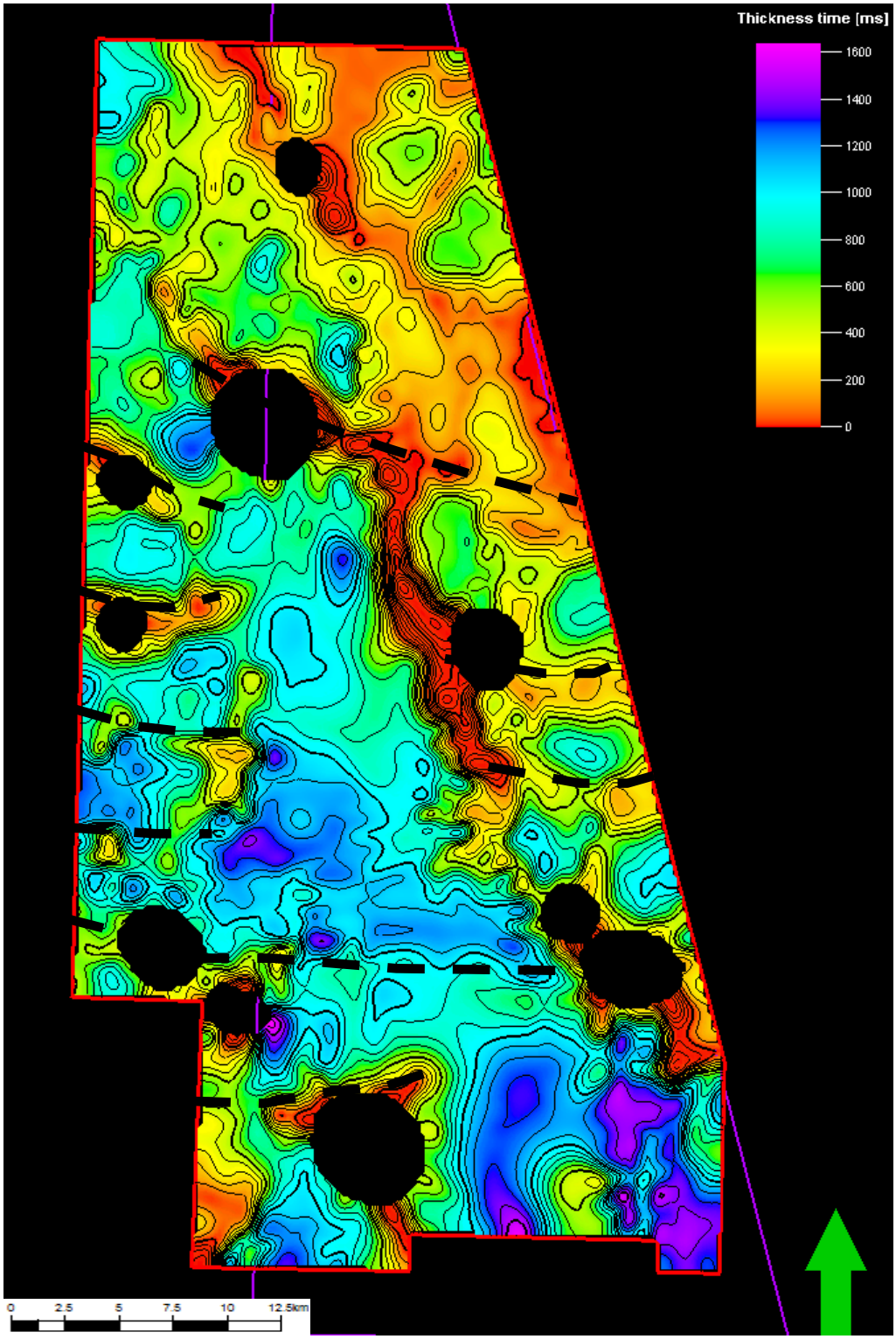

Figure 3.25: A Triassic isochron across study area 2. Extreme thinning over NW-SE striking lineaments can be seen corresponding with salt intrusions up the graben-bounding faults. Other lineations running sub-E-W can also be observed and these correspond with diapir locations and salt walls.

The third study area is centred around some of the most evident W-E sriking structural lineaments observed on the Rotliegend TWTT structure map (Figure 3.26 and 3.27) as these would be most likely to show the effects of extension and a complete syn and post-rift succession. Seismic mapping of the Triassic and Zechstein sequences shows that these W-E striking lineaments clearly controlled the Zechstein salt wall positions.

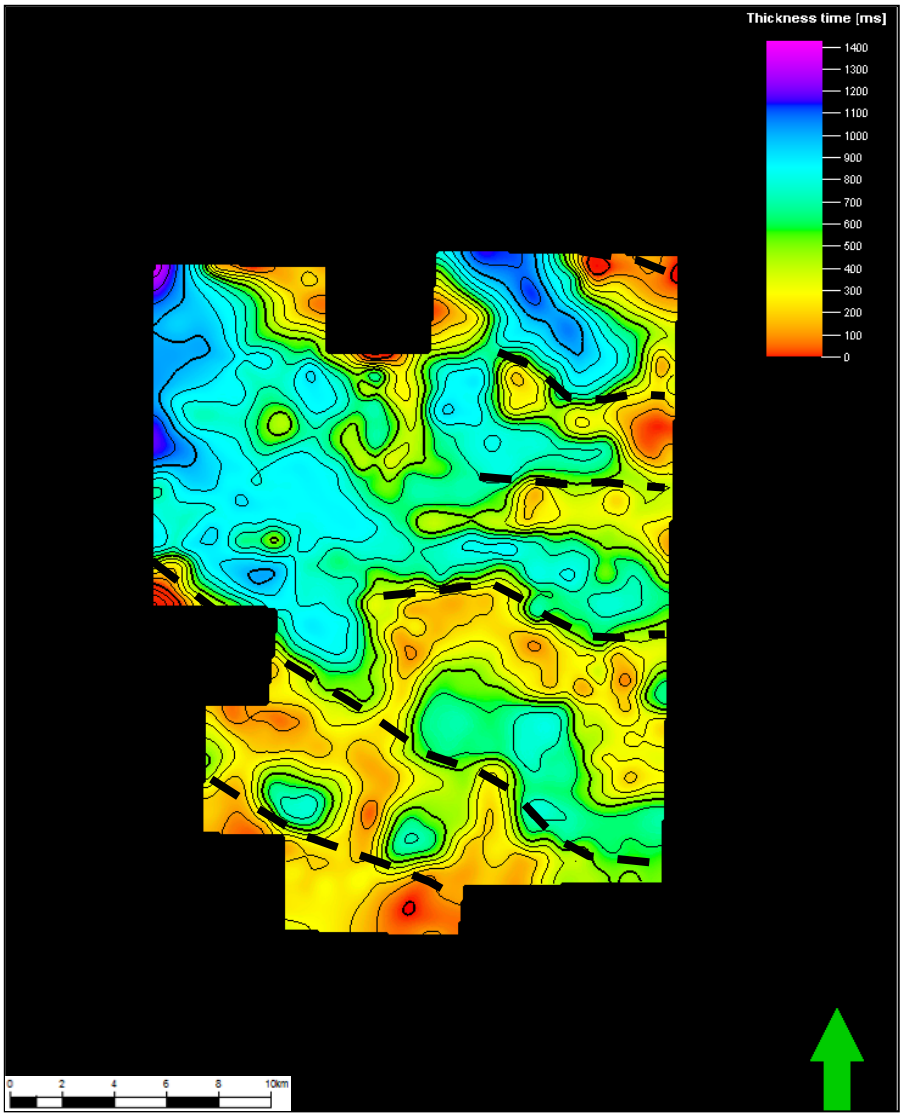

Figure 3.26: An isochron of the Triassic sequence with thinning evident over W-E striking salt walls overlying faults. The edge of the Auk Ridge can also be observed with clearly circular thicks representing the pods also observed on the Forties-Montrose High.

A composite seismic line show was created through selected wells to investigate the structural configuration of the Triassic sequence (Figures 3.27 and 3.28)

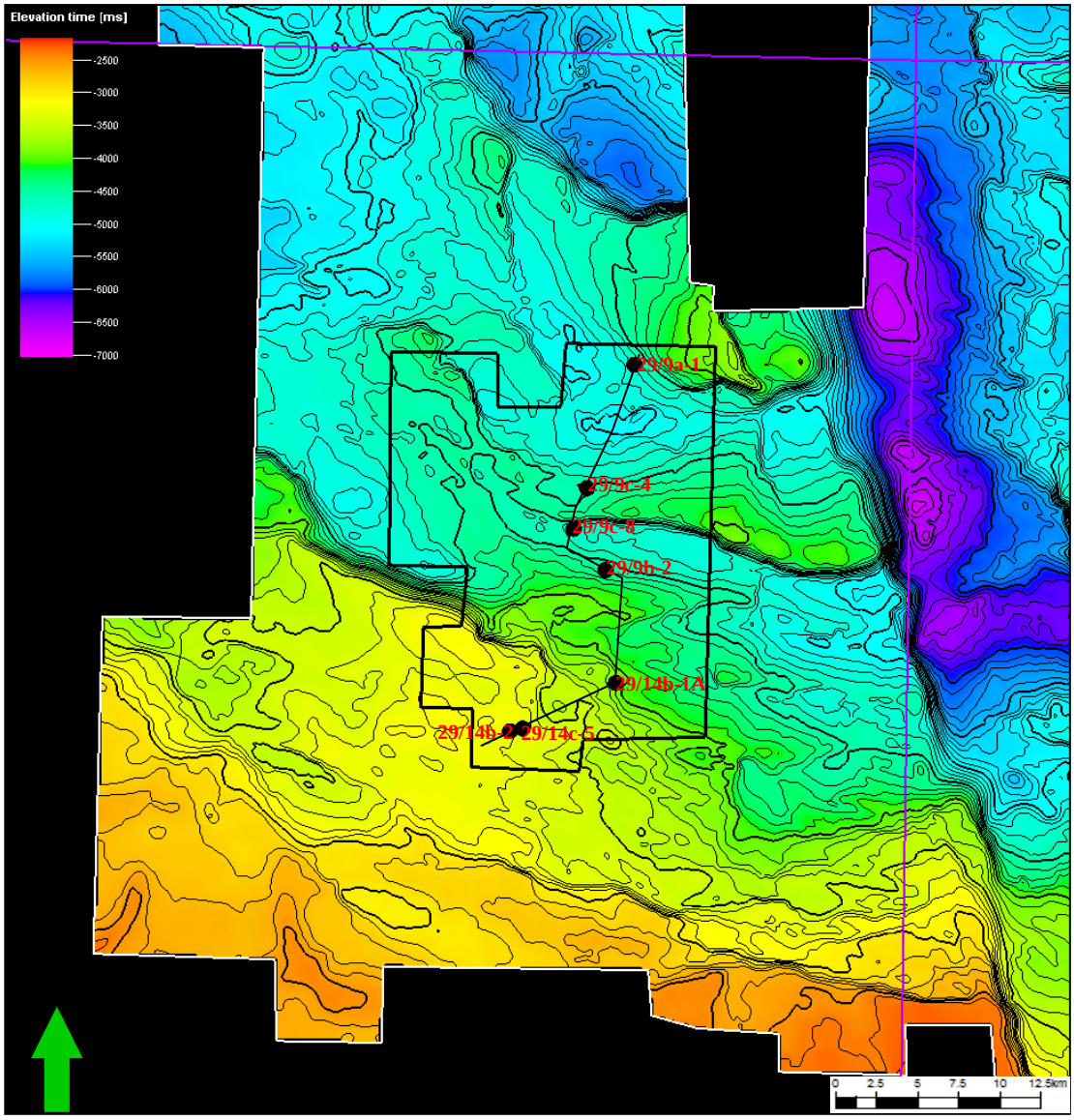

Figure 3.27: Location map of study area 3 showing composite seismic line with respect the W-E striking faults seen on the Rotliegend TWTT map. Note that the area is slightly west of the main throw of the faults as Zechstein salt intrudes where they are juxtaposed with the rift arm causing imaging to be poor.

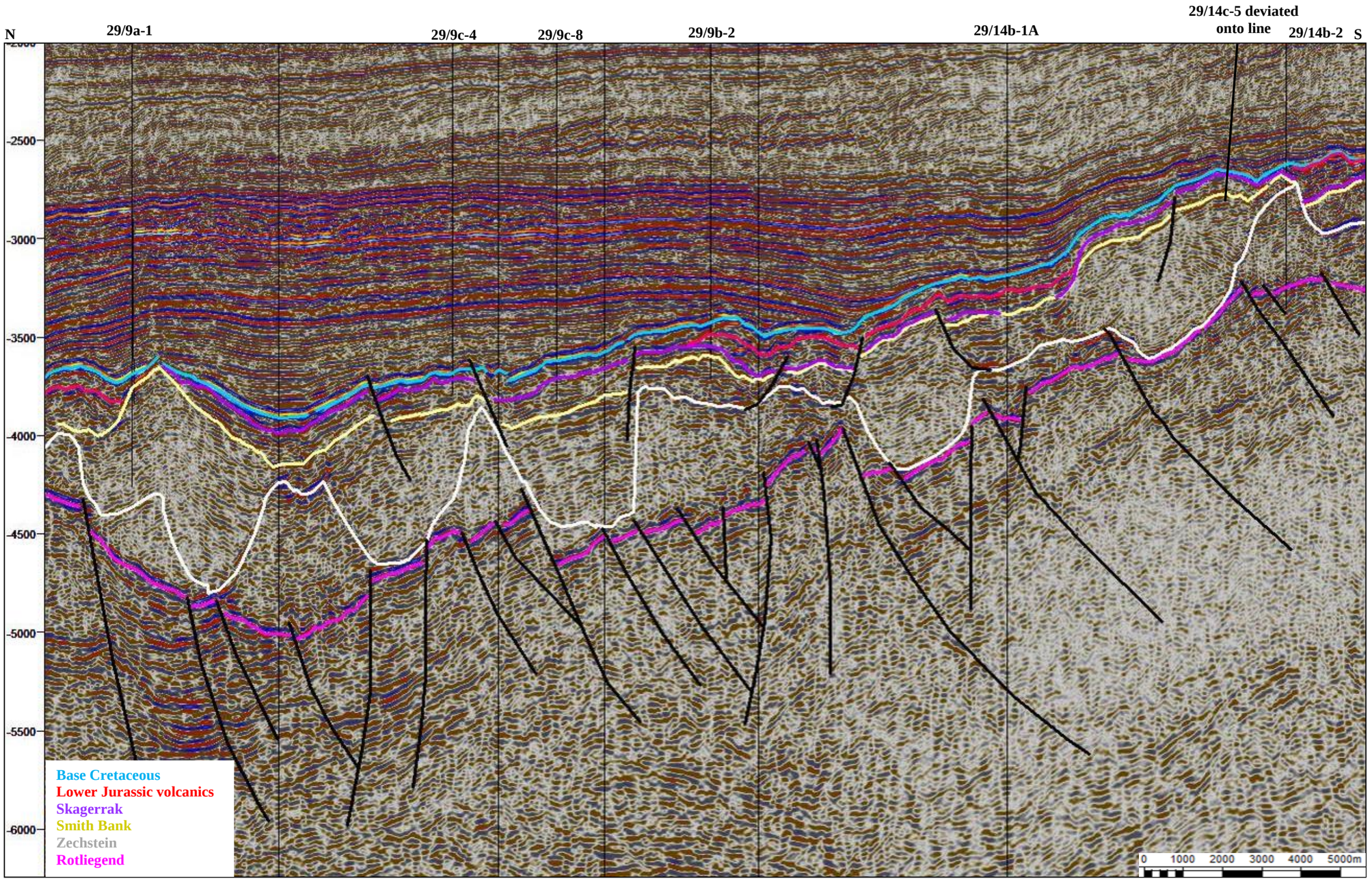

Figure 3.28: Composite seismic line through study area 3 linking wells which penetrate Triassic rocks.

In this area, the Skagerrak section is again seen to be conformable on the Smith Bank. To the north, slight thickening over a salt wall is observed but the main sequences which appears to be linked to dissolution of the Zechstein salt walls are the Mid Jurassic Ron Volcanics Member and Fulmar Formation which represent the pre and syn-rift sections of the Jurassic tectono-stratigraphic megasequence.

Evaluation of these three study areas demonstrates the effect of Zechstein salt on Triassic deposition and preservation. In all of the study areas, Smith Bank deposition was controlled by extension-driven salt withdrawal and differential subsidence over the hanging walls of Permian basement faults but Skagerrak deposition is not as simple. In some cases Skagerrak sands are found overlying thin Smith Bank shales indicating that they have infilled accommodation space left by a collapsed salt wall. However, in other areas the Skagerrak Formation lies conformably on the Smith Bank as part of a pod with thinning on the salt walls either side suggesting that salt-withdrawal from underneath created the space for sedimentation. None of the areas studied showed evidence that deposition of the Skagerrak Formation occurred in a typical post-rift environment. The fact that true rifting had ceased by the Late Triassic suggests that salt tectonics, once activated, continued to exert an influence over depositional trends even without continued extensional stress. This highlights an important complication of interpreting tectono-stratigraphic megasequences in areas of active salt tectonics. The effect of continued and often diachronous halokinetic activity during and post-dating rifiting means that there is no stratigraphic break or unconformity separating the syn and post-rift sequences of tectono-stratigraphic megasequence 1. The domianant control on the deposition of the Skagerrak

Formation was the creation of accommodation space by salt-withdrawl. In some areas it appears that withdrawal of the Zechstein from beneath the Smith Bank depocentre ceased and the wall began to collapse prior to Skagerrak deposition. This is generally due to all of the salt having evacuated from beneath the depocentre (known as grounding) and is particulary prominent on the basement highs where the Zechstein was originally thinnest.

The presence of Jurassic sequences overlying the areas between the Triassic pods also demonstes the preservational potentail of halokinesis as collapse of the salt walls protected these areas from erosion during subsequent uplift.

3.1.3 TECTONO-STRATIGRAPHIC MEGASEQUENCE 1: SYN- AND POST-RIFT SUMMARY

Previous research suggests that far-field extensional stresses caused rifting during the Triassic. The occurrence of extensional tectonics in the Northern North Sea and onshore UK is easily demonstrated by mapping clearly defined syn-rift thickening wedges. However, the evidence for extension and syn-rift deposition in the Central North Sea is complicated by the presence of the underlying Zechstein Supergroup evaporites and problems with imaging deeper targets. Previous authors have considered the unusual geometry of the Triassic section; where the mobile Zechstein sequence has flowed into salt walls flanking Triassic depocentres, to have resulted from halokinesis driven by either differential compaction or extensional forces or a combination of the two. However, the relative influence of these drivers regionally has never been shown and the Triassic deposits, particularly the Late Triassic Skagerrak Formation, have never before been placed into a tectono-stratigraphic framework.

Mapping of the new high-resolution seismic data over the basement highs where the Triassic section is best imaged and in three case study areas has shown that salt walls and diapirs occur over Permo-Tiassic faults indicating that extension was the main driver for halokinesis. Extension in evaporite provinces in other areas such as Oman has also been shown to produce a similar geometry. These findings for the first time demonstrate the importance of underlying linaments in controlling Zechstein

mobility which is ofen difficult to image and model at depths. It is also demonstrated that diapirs occur where Permo-Triassic faults are transected by later Jurassic faulting.

The mapping also permits characterisation of the Triassic sequence into tectono-sequences. The Early-Mid Triassic Smith Bank Formation, despite its unusual geometry, represents the halokinetically modified syn-rift sequence of the Triassic rift episode. The post-rift succession should be recognised in the Late Triassic section but mapping proved different relationships between the Late Triassic Skagerrak and Early-Mid Triassic Smithbank Formations in different areas. The Skagerak Formation is therefore placed in the post-rift section of tectonomegasequence 1 but continued and often diachronous halokinesis during deposition means that it does not conform to the standard post-rift model and should be considered as representing a post-rift, syn-halokinetic stage.

CHAPTER 4

TECTONO-STRATIGRAPHIC MEGASEQUENCE 2: SYN-RIFT EVOLUTION

4.1 JURASSIC RIFTING

The Triassic syn-rift succession is directly overlain by another syn-rift sequence of Jurassic age. During the Early to Middle Jurassic a trilete rift system developed in the North Sea due to the emplacement of a transient mantle plume which caused thermal uplift, erosion and net extension as it deflated (Underhill et al. 1993) (Figures 4.1 and 4.2). Failure of this rift to lead to true sea-floor spreading left large basinal areas which were transgressed and finally flooded in the Late Jurassic.

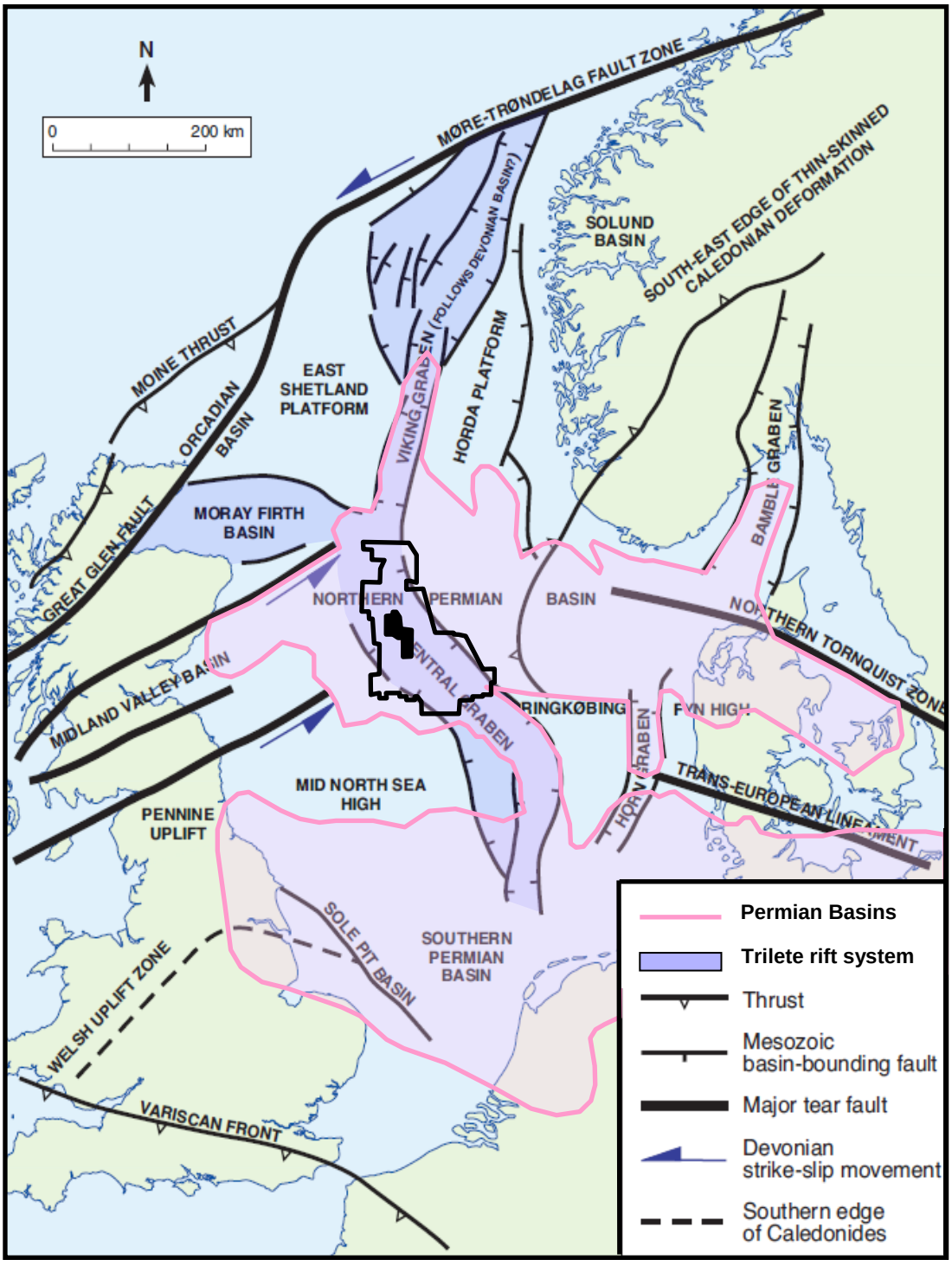

Figure 4.1: Location map showing the Jurassic trilete rift superimposed on the older structural features.
Outline of Central Graben dataset shown.
Modified after (Evans et al. 2003)

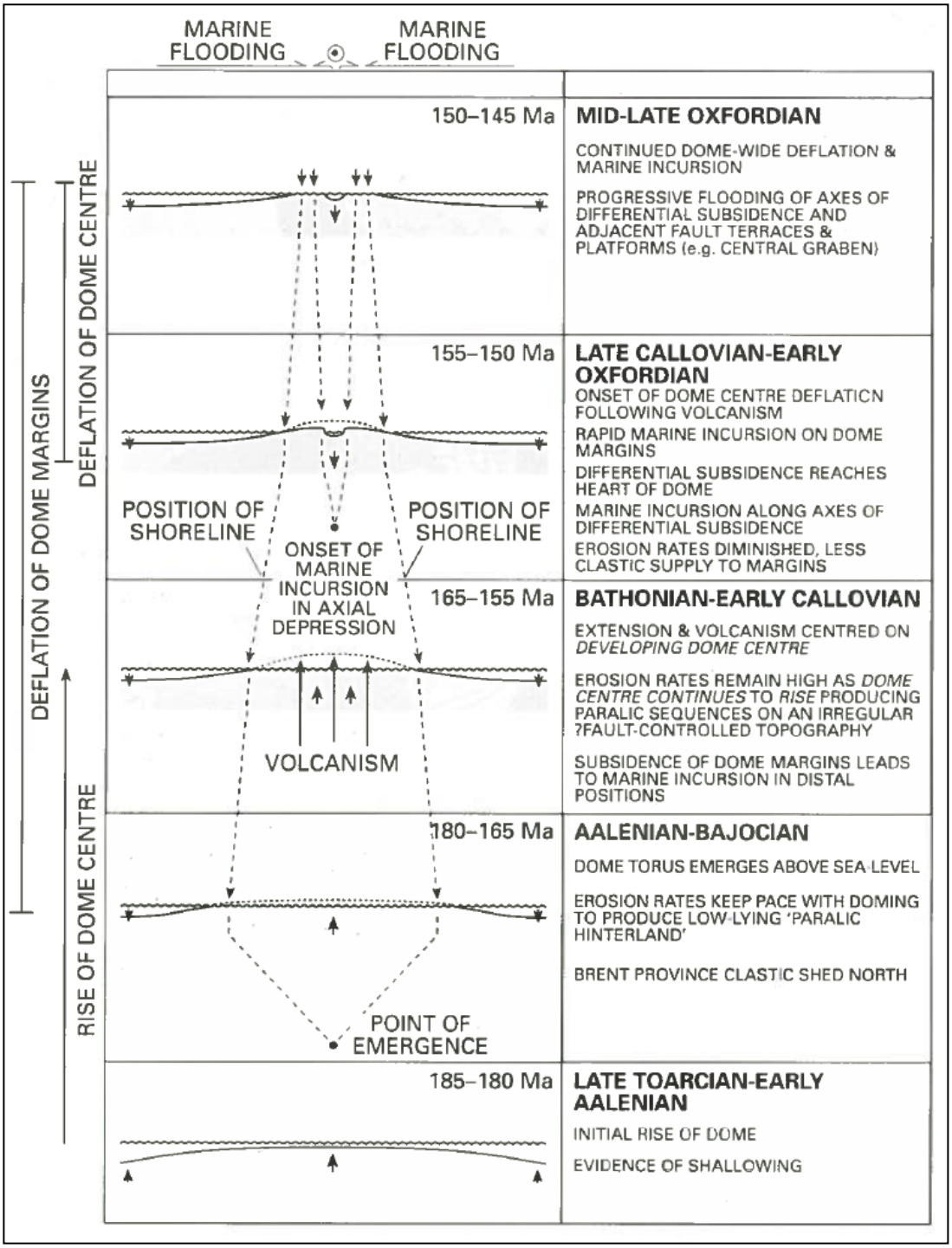

Figure 4.2: Diagrammatic representation of the development of the North Sea Dome.

Image after (Underhill et al. 1993)

The Jurassic structure of the Central North Sea is dominated by the Central Graben which is divided into two NNW-SSE striking depocentres, the Western and Eastern Troughs, separated by a similarly oriented Forties-Montrose High. Addition of an extra dataset provided by First Oil aided interpretation of the full structure of the Central Graben (Figures 4.3 and 4.4).

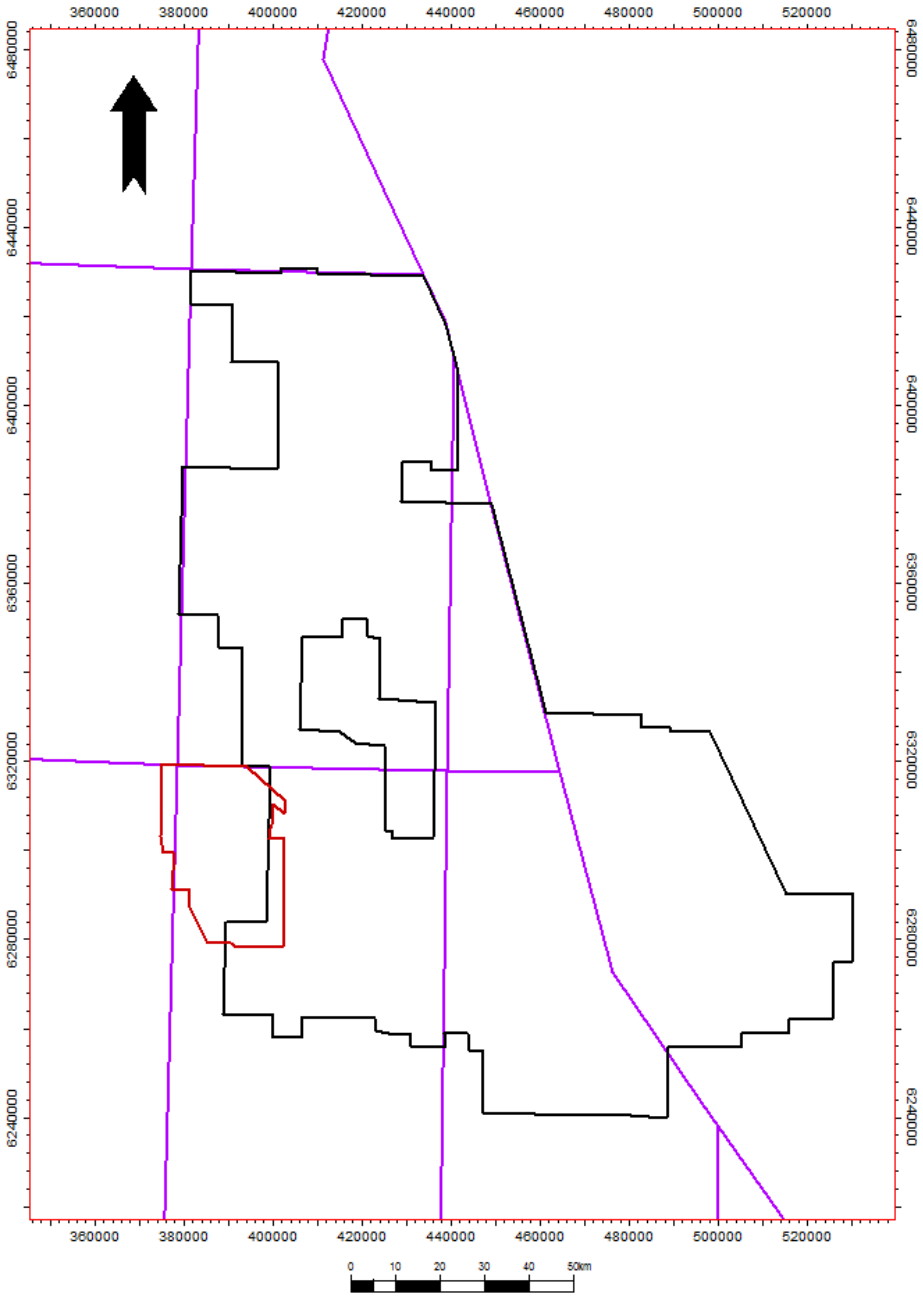

Figure 4.3: Location of First Oil additional dataset with respect to Central Graben main dataset.

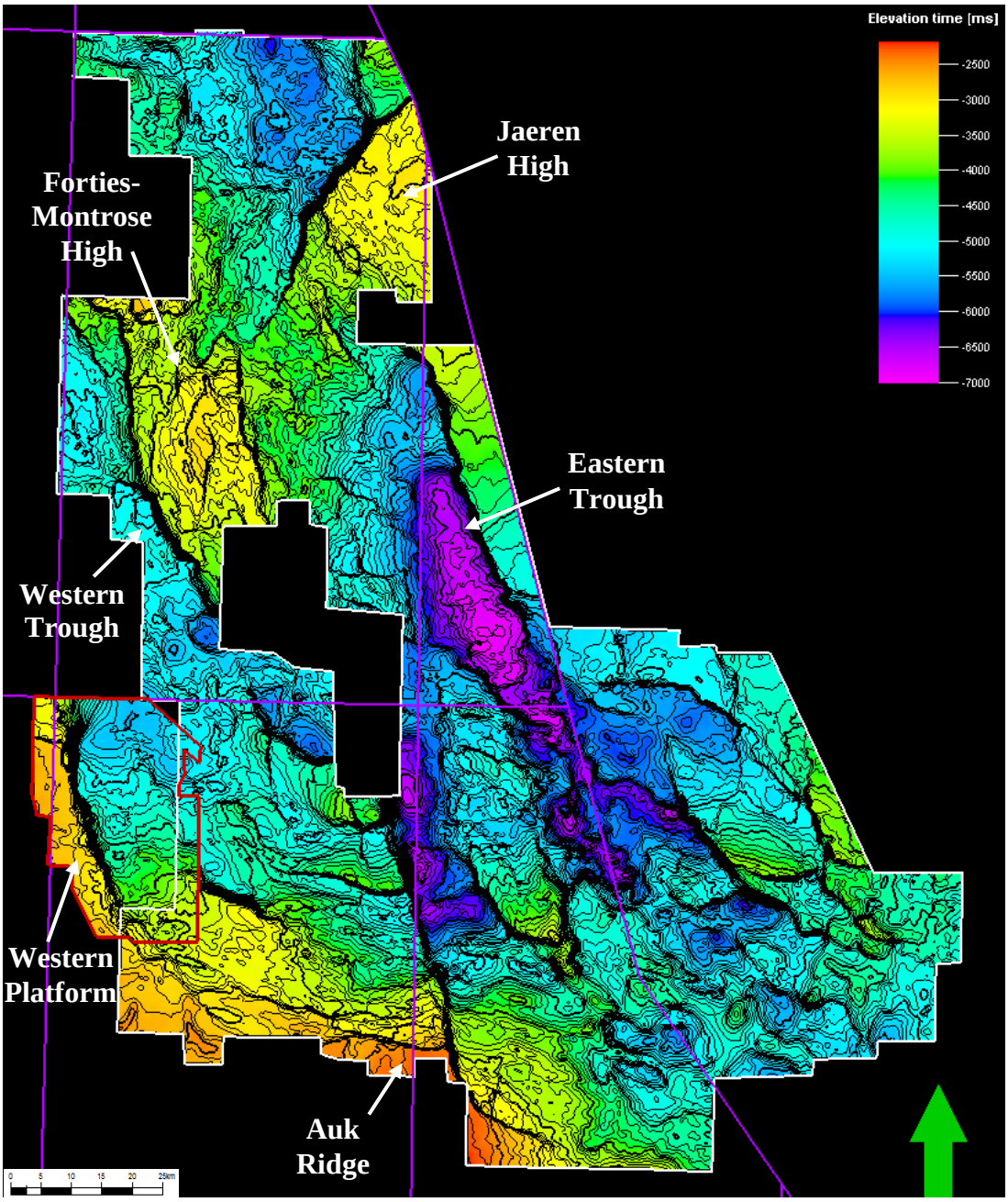

Figure 4.4: Rotliegend TWTT structure map highlighting the major structural features within the Central North Sea dataset.

Detailed mapping of the Mid-Late Jurassic syn-rift packages has not been included in this study but analysis on this sequence has been undertaken by many previous authors (Jeremiah et al. 1999; Sansom 2010). Instead the focus is on the interaction of the Jurassic rift arms with the pre-existing fault geometries.

A total syn-rift isochron created from mapping of the base Cretaceous and top Triassic can be seen in Figure 4.5, highlighting the thickening packages into the major graben-bounding faults and variable thickness on the rift flanks where later erosion has taken place.

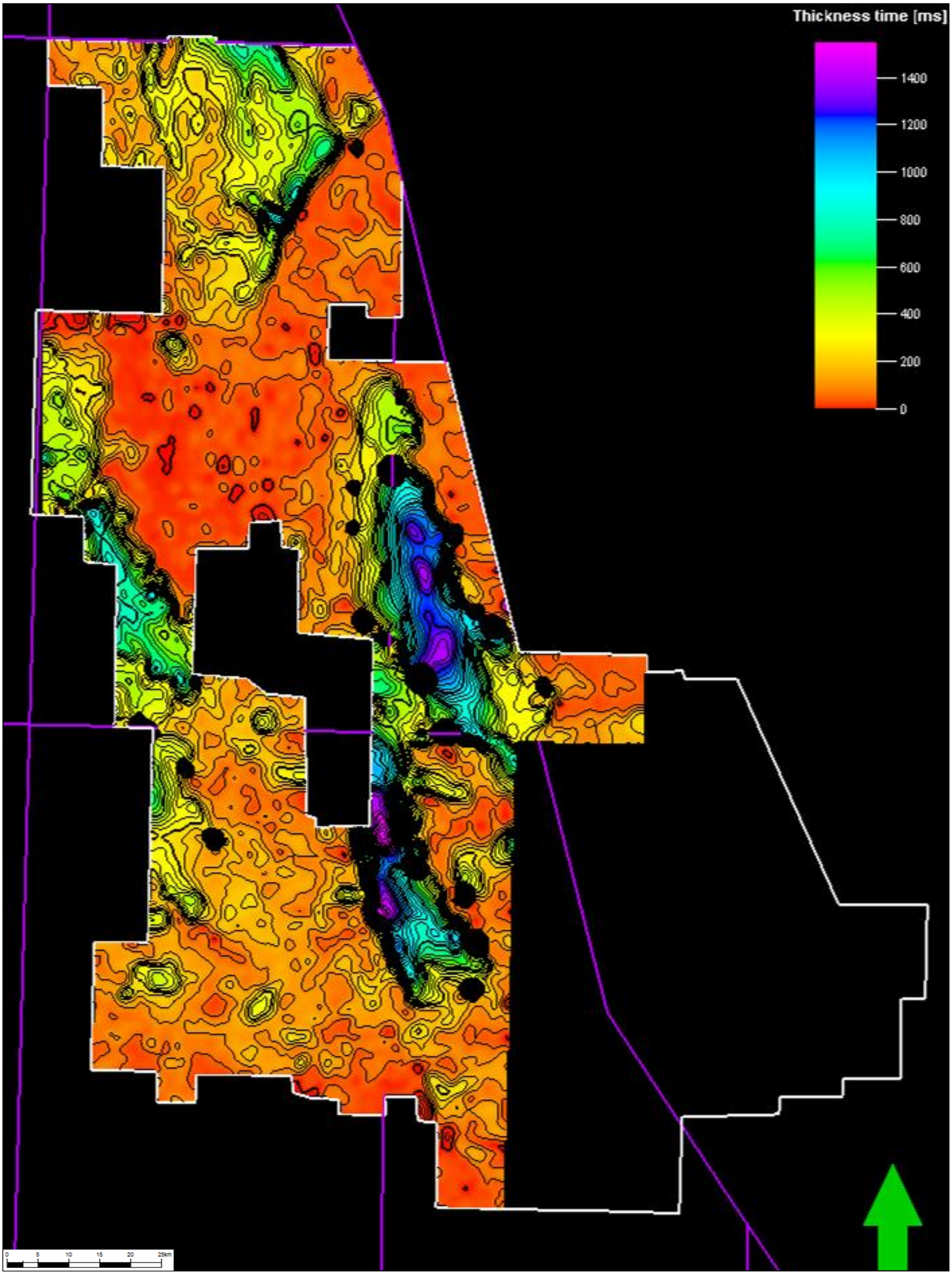

Figure 4.5: An isochron of the Jurassic syn-rift section showing thickening into the rift arms.
Note that the Jurassic pick does not extend into grids 6 and 7 or the extra FirstOil dataset. See suggestions for further work on page X

4.1.1 THE INFLUENCE OF TECTONO-STRATIGRAPHIC MEGASEQUENCE 1 ON THE JURASSIC RIFT SYSTEM

The structural and stratigraphic development of the Jurassic sequences in the Central North Sea is complicated by the presence of the Zechstein evaporites. Propagation of the rift arms induced flow from under the developing grabens initiating diapirism and renewed salt tectonics. However, it was established in the previous chapter that diapirs tend to be initiated where the Jurassic rift arms transect Zechstein salt walls overlying Permo-Triassic faults and these faults also seem to have been important in the propagation of the Jurassic rift arms.

An isochron of the Jurassic interval in the Eastern Trough demonstrates the existence of several separate depocentres suggesting that the rift arm was previously made up of segments which then joined to act as a single fault. The W-E striking Permo-Triassic lineaments can be shown to occur between the separate depocentres suggesting that these may have acted as barriers to the development of the separate faults and then as possible soft-linkage zones when the Jurassic faults joined (Figure 4.6). Much of the evidence for this early fault linkage stage is obscured by later hard-linkage but is preserved in an area in quadrants 29 and 30 where this later stage has not occurred and the W-E striking basement faults are prominent (Figure 4.7).

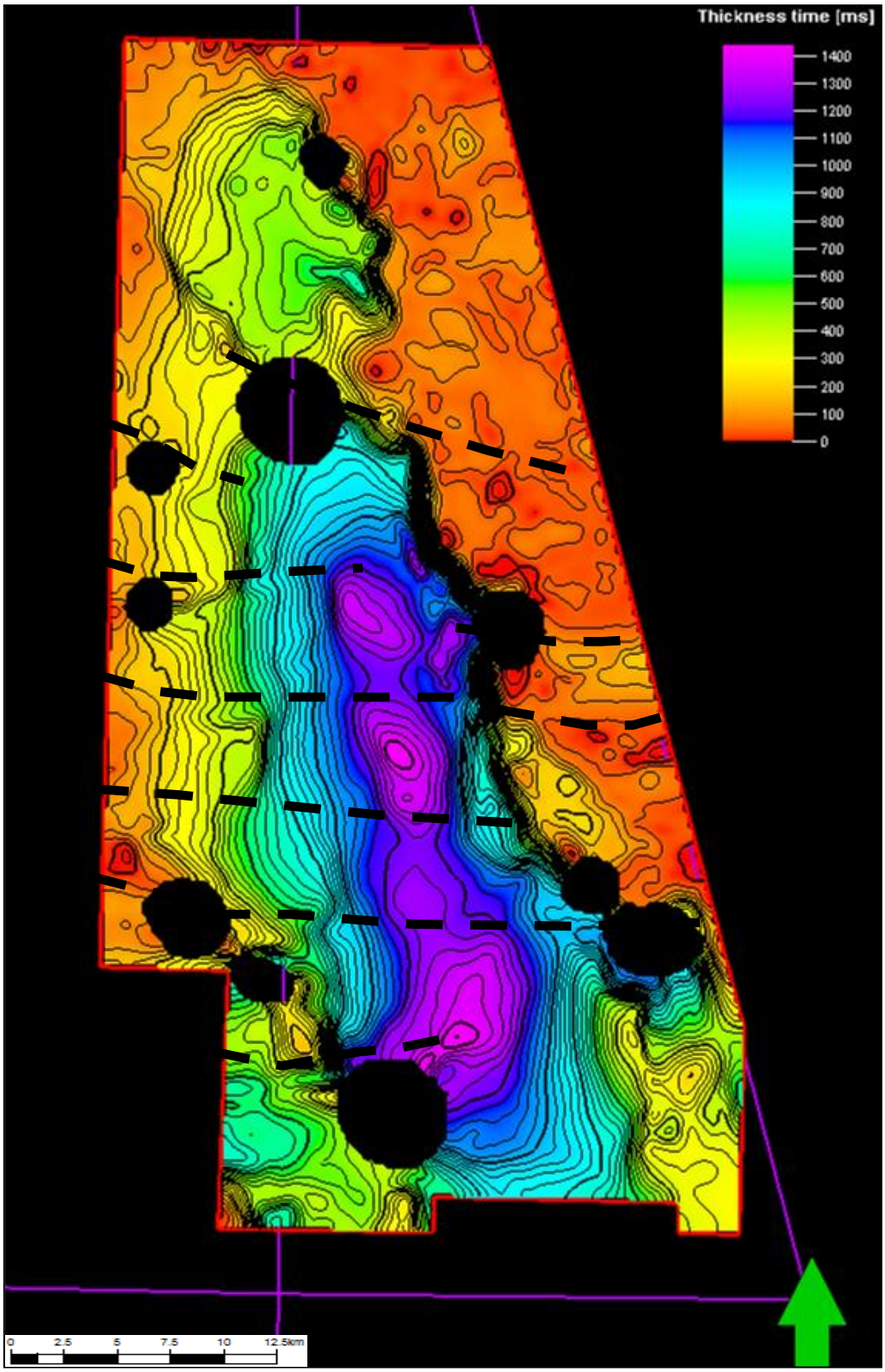

Figure 4.6: An isochron of the Jurassic interval showing syn-rift thickening into the rift arms. There is a possible W-E trend which can be observed suggesting that Permo-Triassic faulting and salt movements in the vicinity of these faults may have played a role in Jurassic fault development.

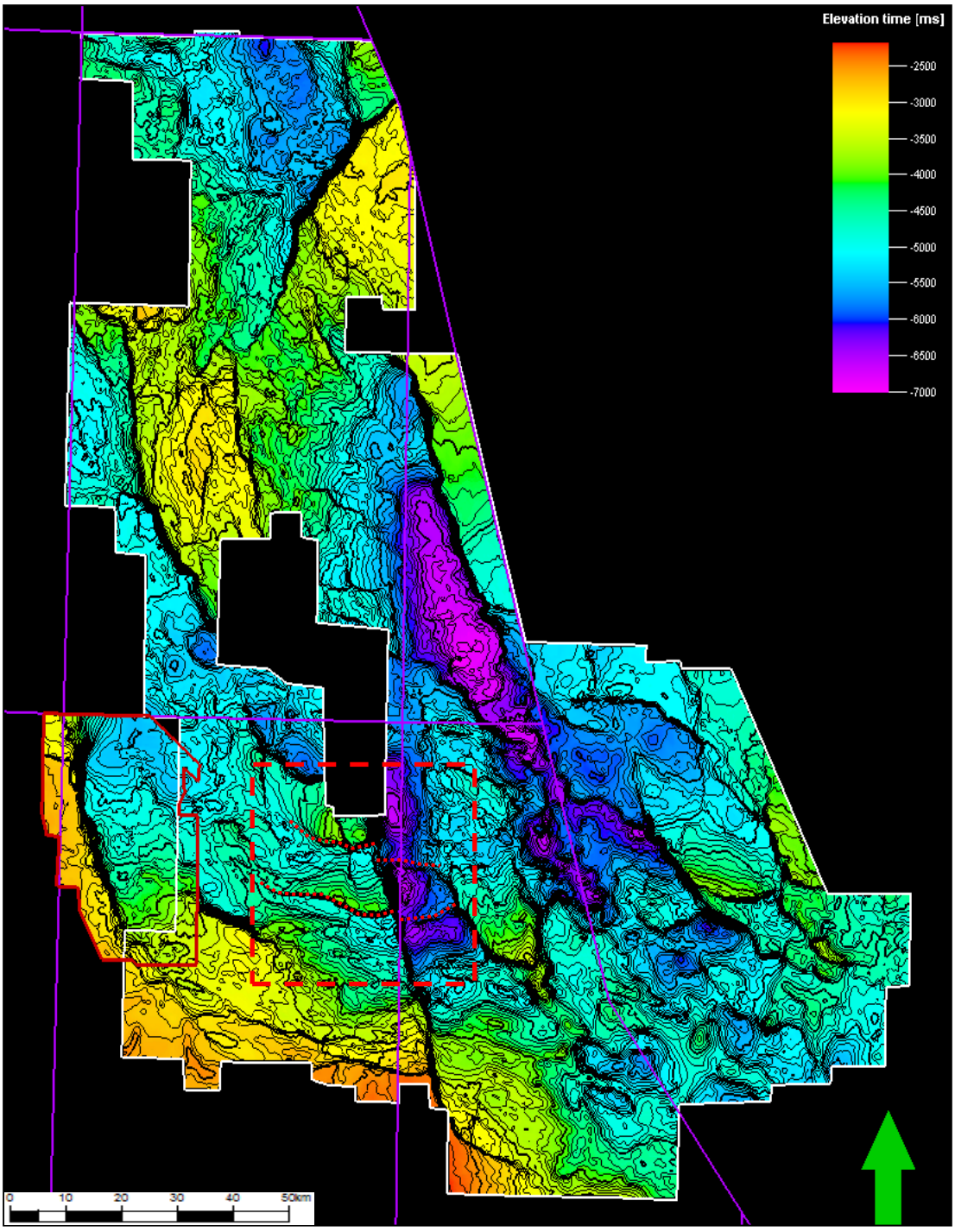

Figure 4.7: Rotliegend structure map highlighting the prominent W-E faults which have been cross-cut and laterally offset by the Jurassic rift arm.

Faults such as these, perpendicular to the main structural trend can act to take up the strain from the through-going master fault. The most common cause of oblique fault trends in extensional systems is the development of a relay ramp or zone which is formed during fault growth to facilitate the linkage of successive fault segments.

Propagation and linkage of fault segments is the process by which most of the major Jurassic rift-related faults formed. Relay ramps (Figure 4.8) are areas between two normal fault segments with identical dip which accommodate the displacement, representing soft-linkage of the segments (Larsen 1988; Trudgill et al. 1994; Cartwright et al. 1995). Eventual breaching of these, hard-links the two fault segments which then act as one, providing the stress regime continues. Faulting within relay zones is therefore perpendicular to the dominant trend and may reactivate underlying structural lineaments with the same trend.

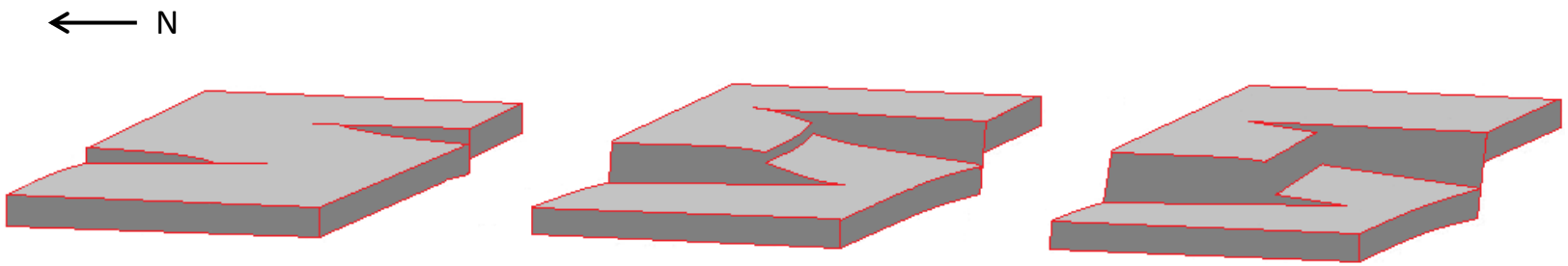

A relay zone forms between two faults with identical dip to accommodate the displacement.

As the faults propagate, the stress in the relay zone increases and faulting occurs.

The relay zone finally breaches and the two segments now move as a single irregular fault.

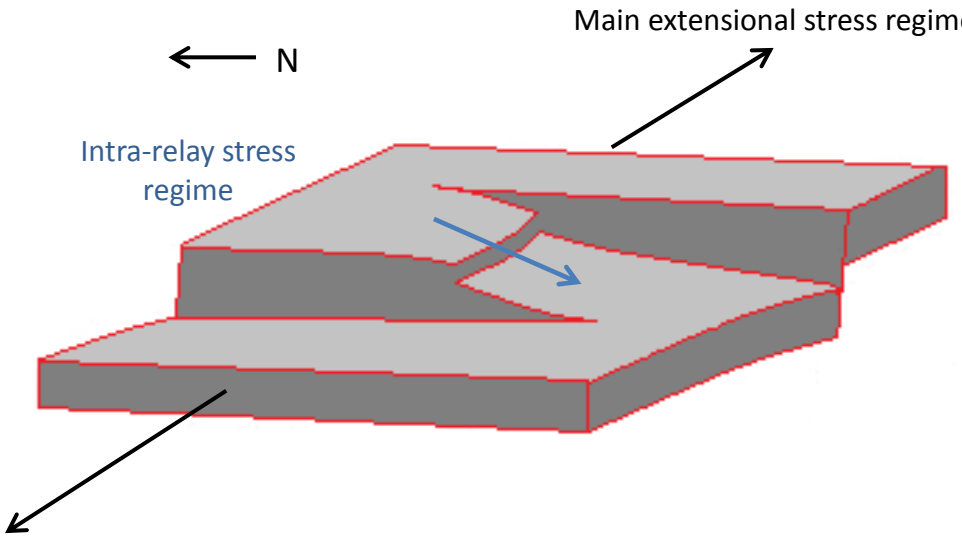

Figure 4.8: Block diagrams illustrating the development of a relay ramp.

A Rotliegend TWTT structure map and dip angle map over the area (Figures 4.9-4.11) clearly highlight all of the major lineations showing the Jurassic NE-SW striking graben-bounding faults and the W-E striking Permo-Triassic ones in a structural configuration indicative of a relay ramp.

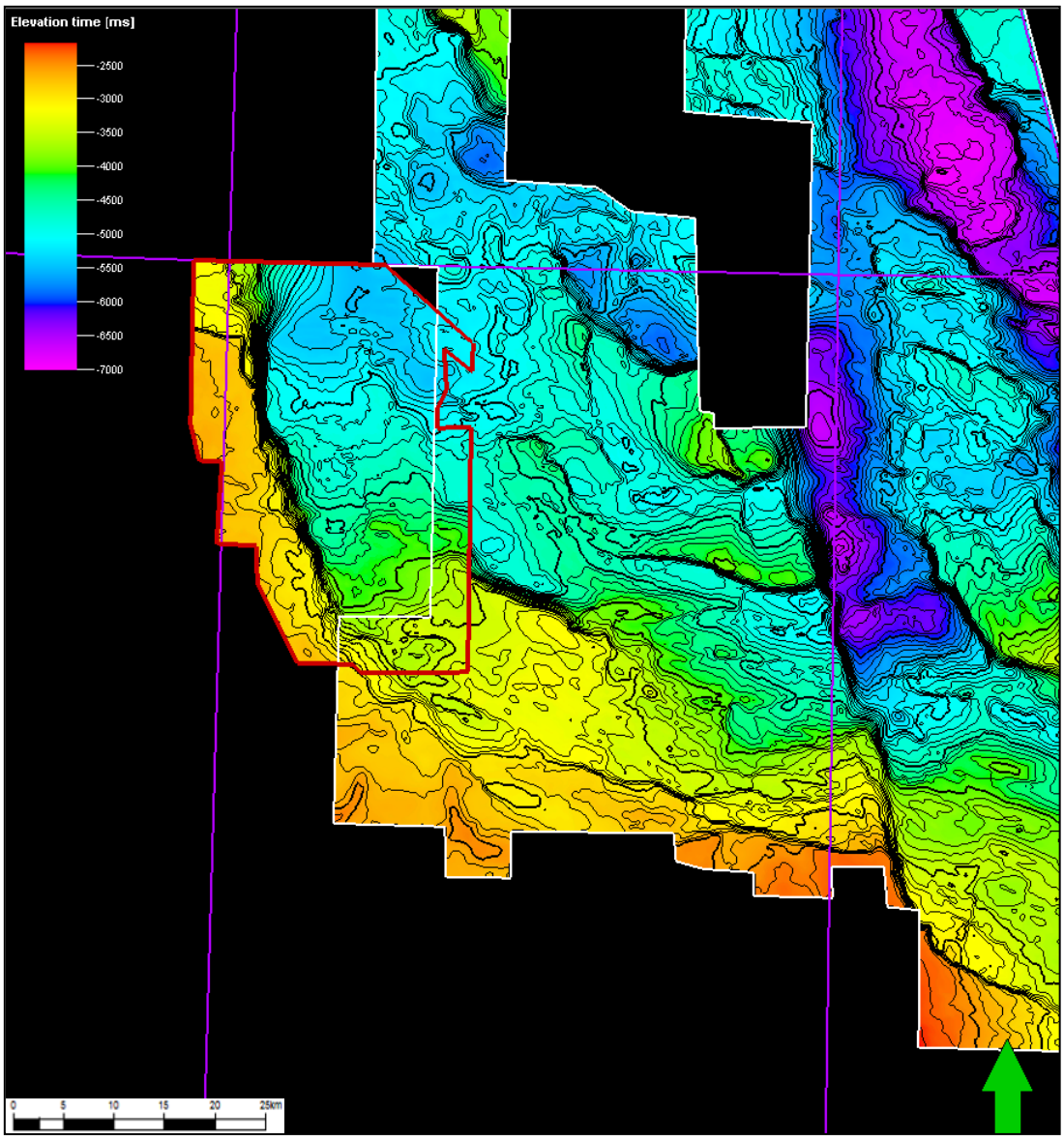

Figure 4.9: Top Rotliegend TWTT structure map with extra interpreted dataset added showing the two NW-SE Jurassic master faults and the apparent W-E striking relay ramp between them

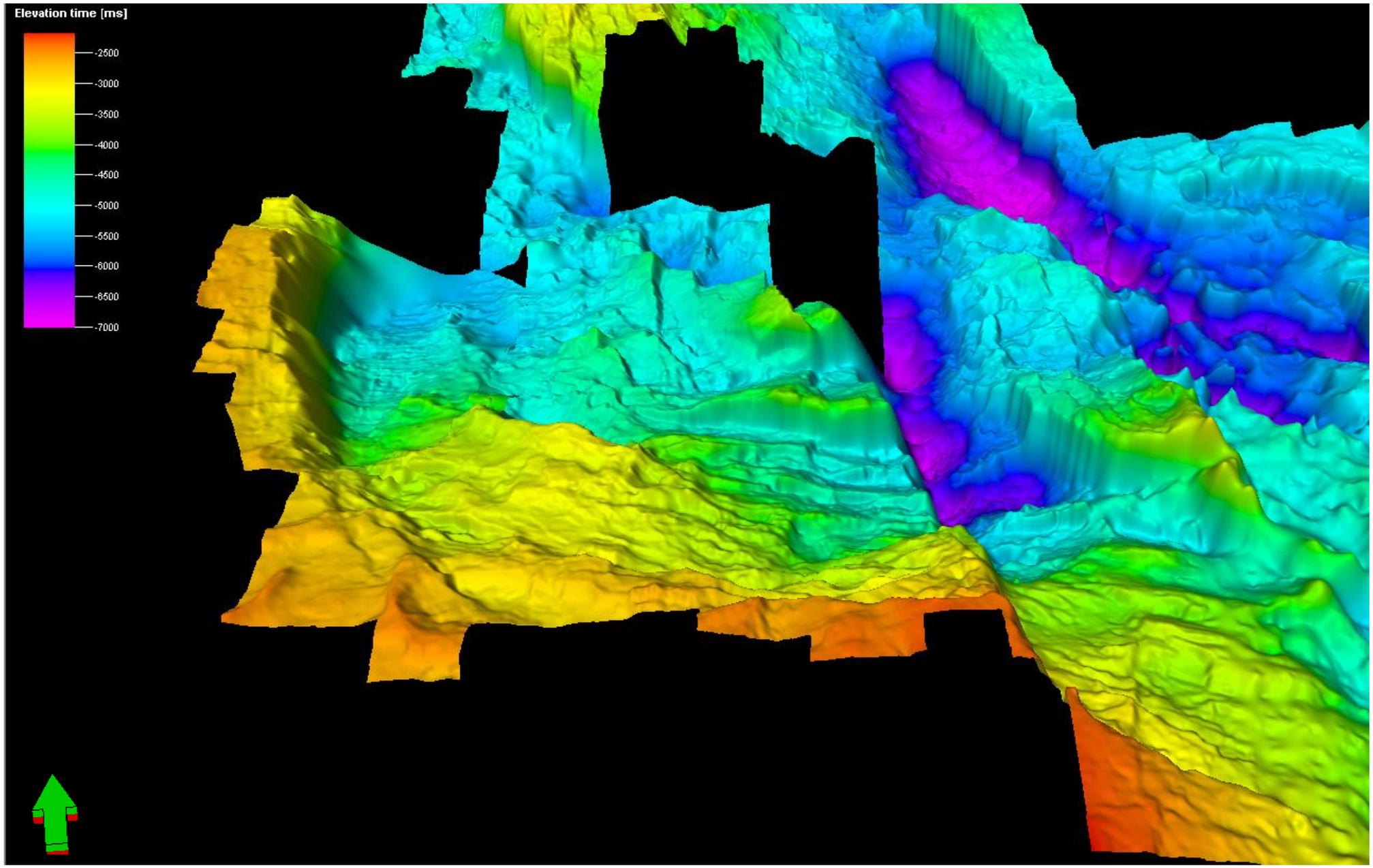

Figure 4.10: A 3D view up the potential relay ramp in the Central North Sea.

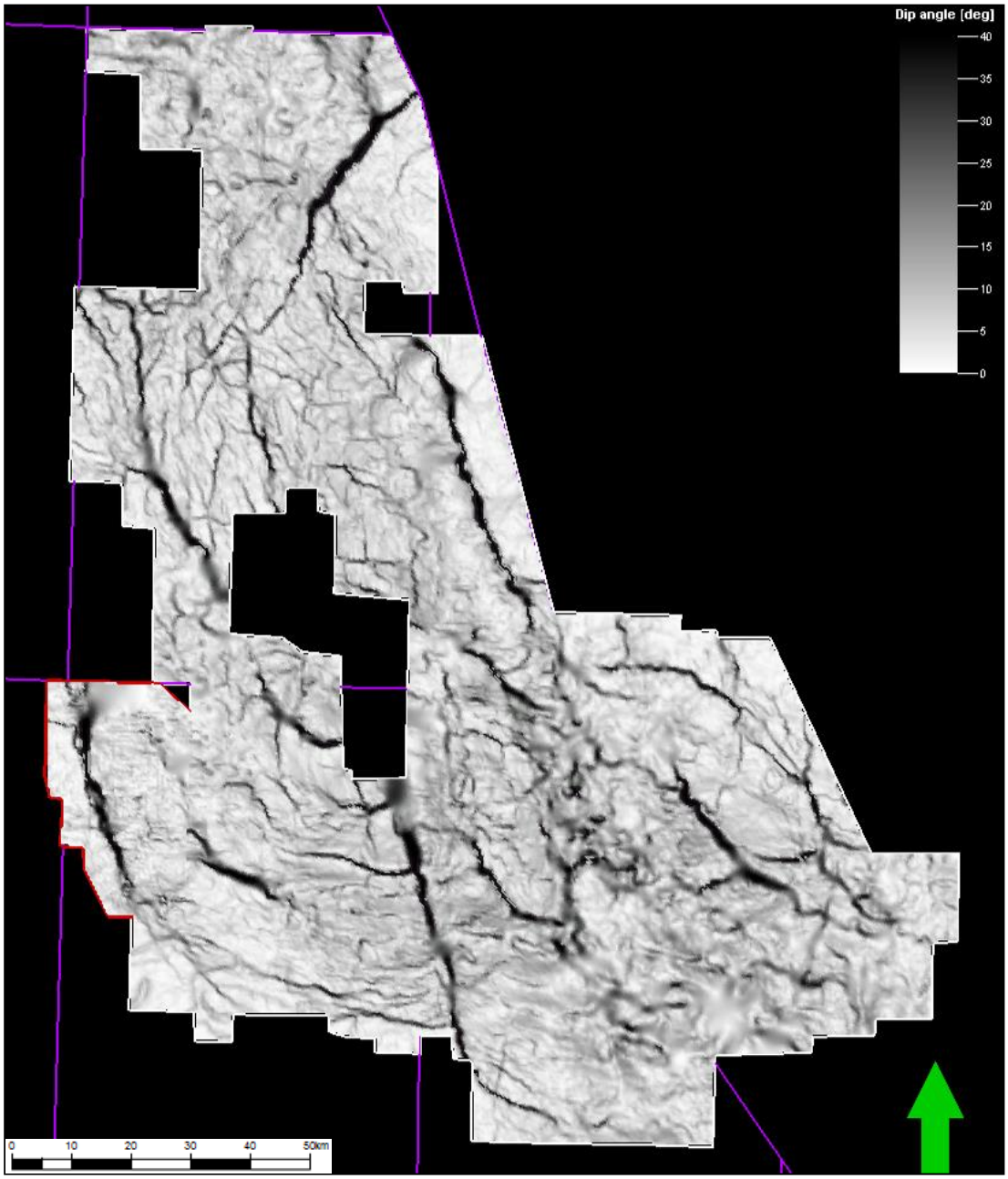

Figure 4.11: A dip angle map of the Rotliegend highlighting the prominent W-E faults between the two major Jurassic ones.

Seismic data is required to ground-truth this interpretation and two well-calibrated W-E striking seismic sections through the two major Jurassic faults were created along with a N-S section through the Permo-Triassic faults (Figures 4.12-4.15).

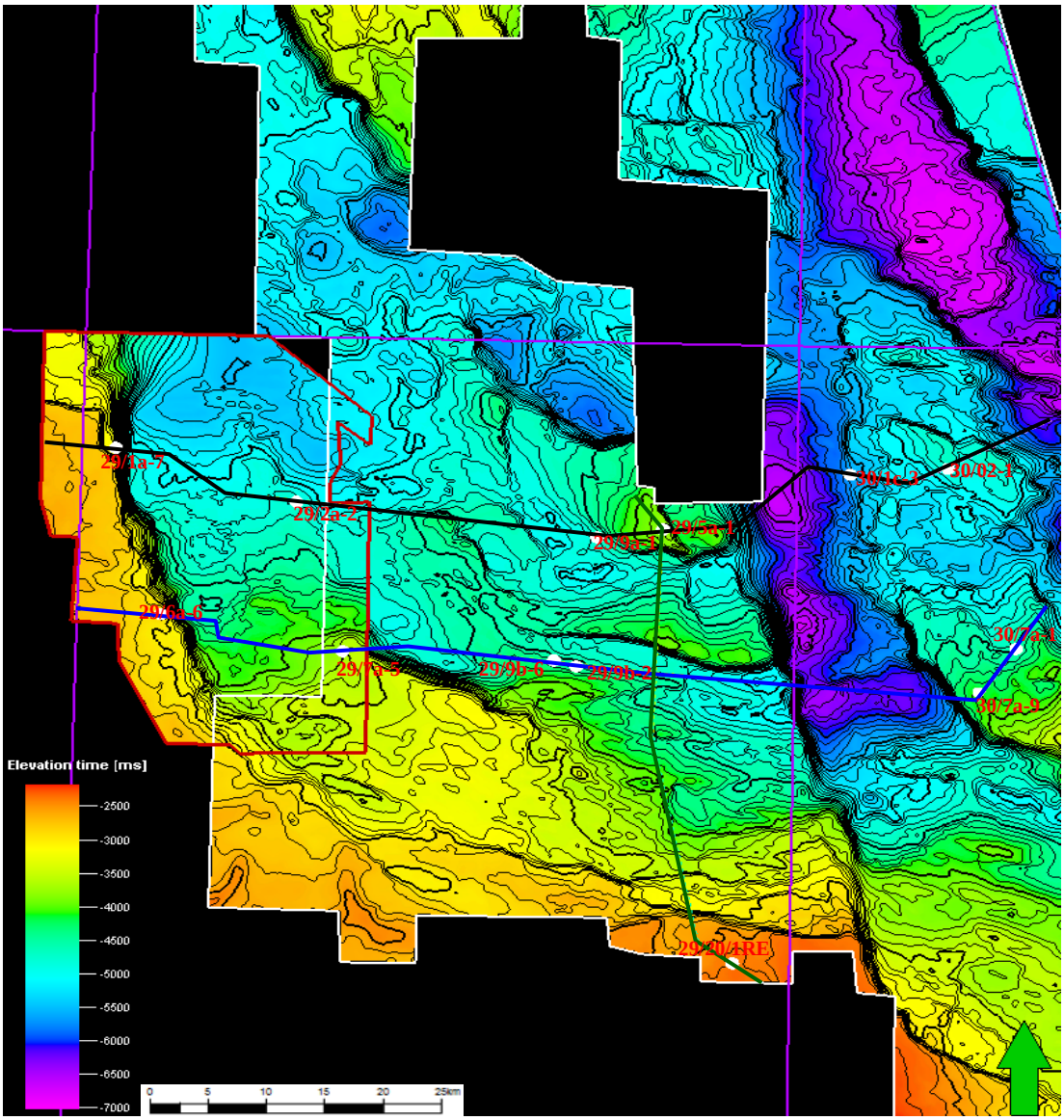

Figure 4.12: Location map of the composite seismic lines with respect to the structural configuration of the area.

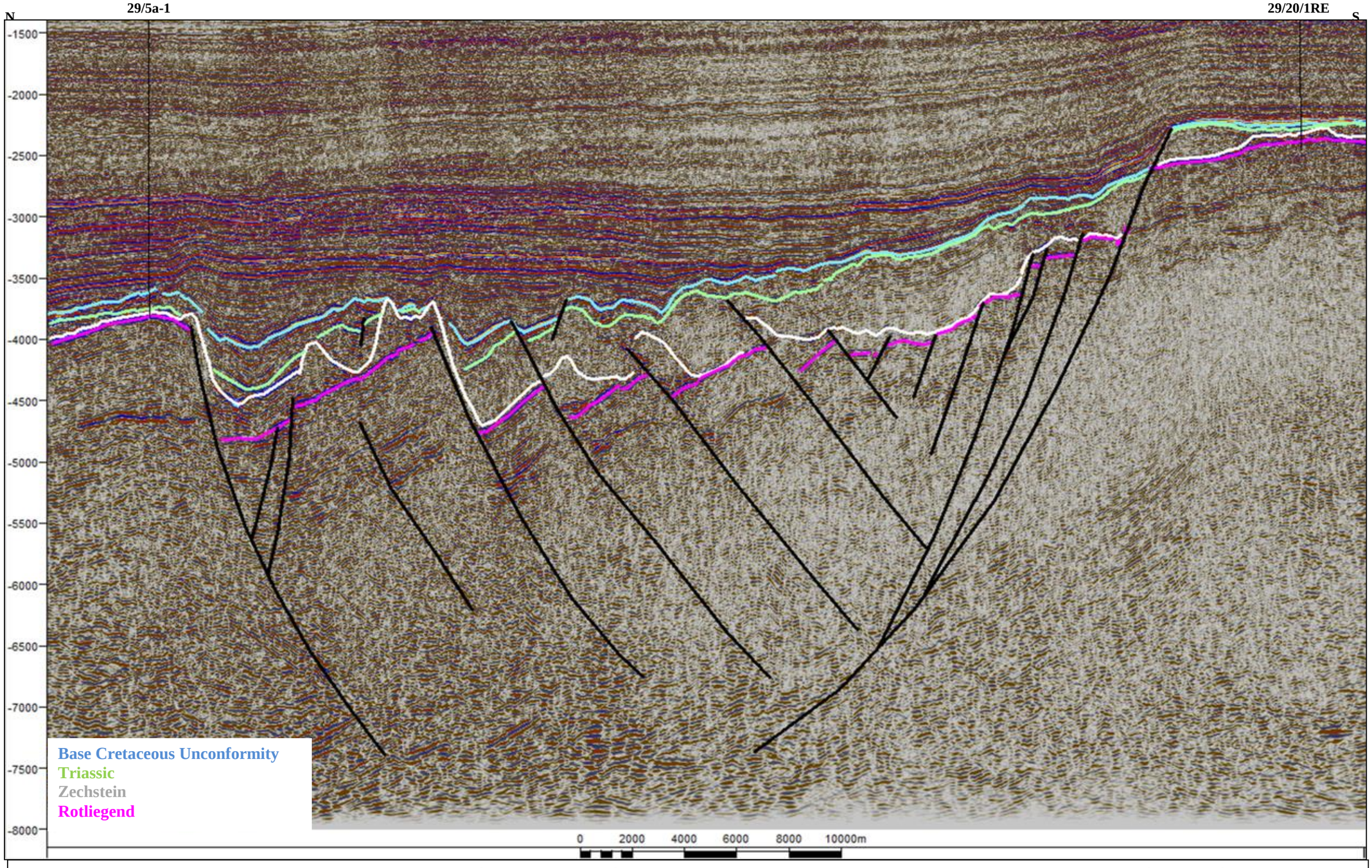

Figure 4.13: N-S composite seismic section across the W-E striking faults. Thickening of the Triassic section is observed into the hanging-walls along with thickening of the syn-rift section suggesting that these faults remained active or were reactivated during Jurassic rifting.

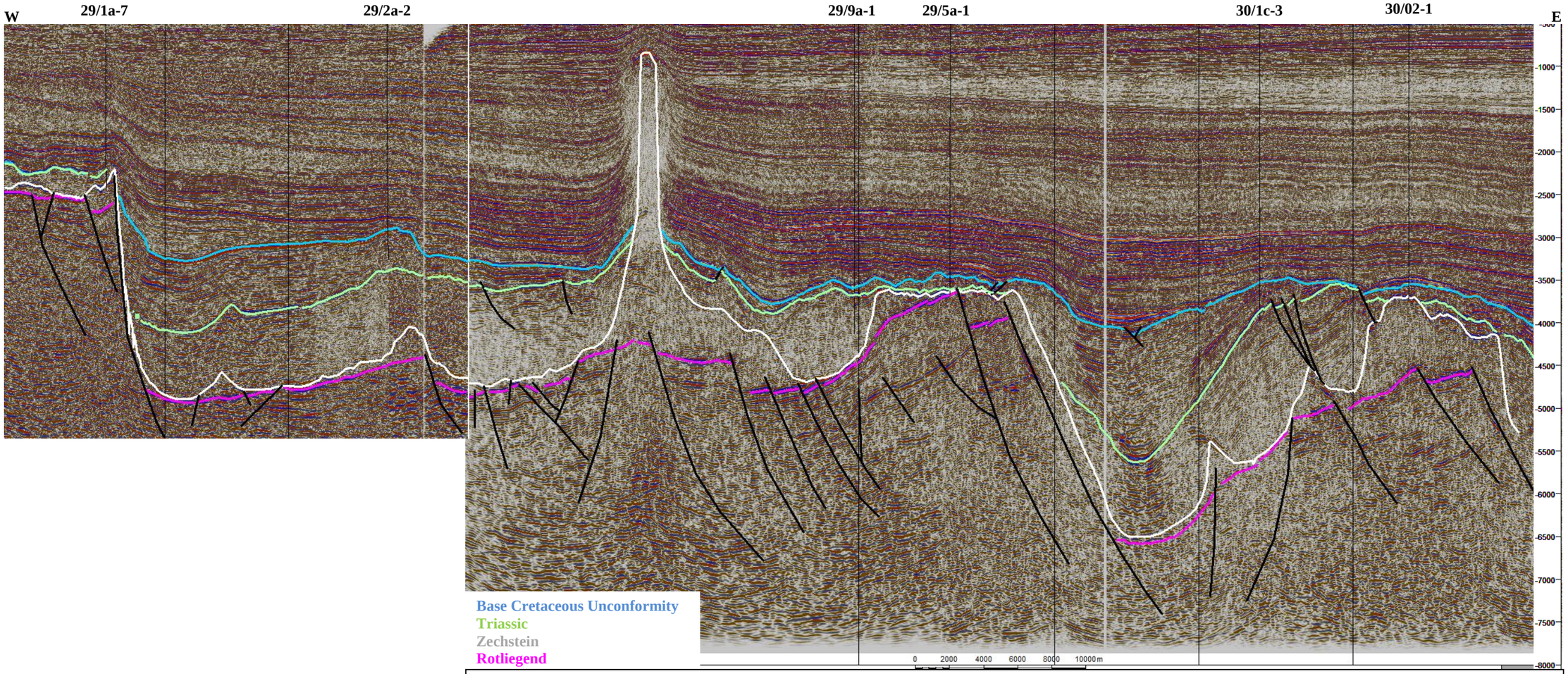

Figure 4.14: W-E composite seismic line across the two Jurassic master faults showing the syn-rift thickening into them.

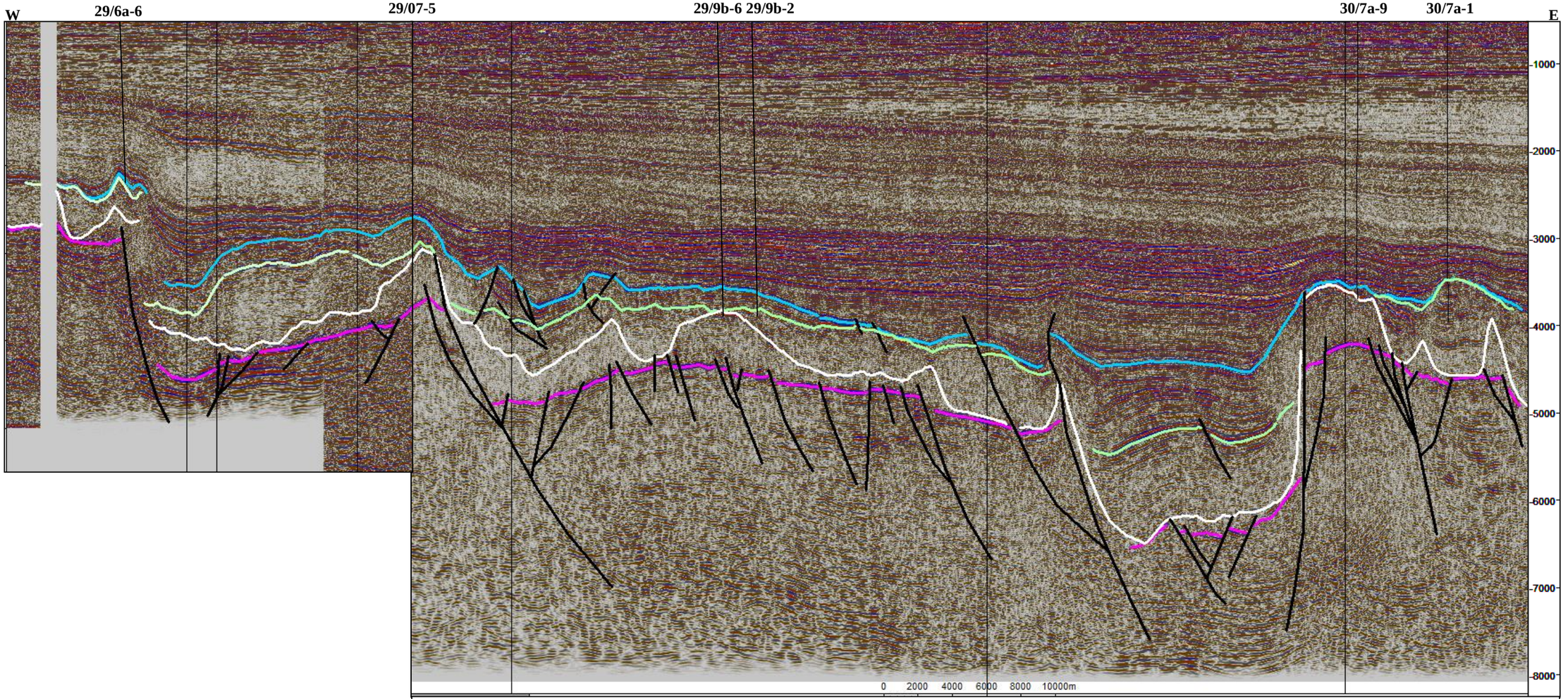

Figure 4.15: W-E composite seismic line across the study area. Note the apparent thrust over the West Central Shelf caused by Zechstein salt being squeezed over the fault and taking the overburden with it.

The W-E sections show the syn-rift thickening into each of the Jurassic faults while the N-S section demonstrates a component of Jurassic thickening into the Permo-Triassic faults. This geometry indicates that the Permo-Triassic faults were also active during Jurassic syn-rift deposition in a relay ramp configuration.

Most of the relay zones formed during the Early Jurassic were breached, and there may be a specific reason that this one was preserved. Thick volcanic deposits of the Ron volcanics member in the area (Figure 4.16) suggest the presence of a large volcanic centre between the major propagating fault segments (Richards et al. 1993; Smith et al. 1993). Uplift of the centre itself or simply the presence of a large mass of hard intrusive and extrusive volcanics could have prevented the relay ramp from being breached before the rift failed and the extensional stress abated.

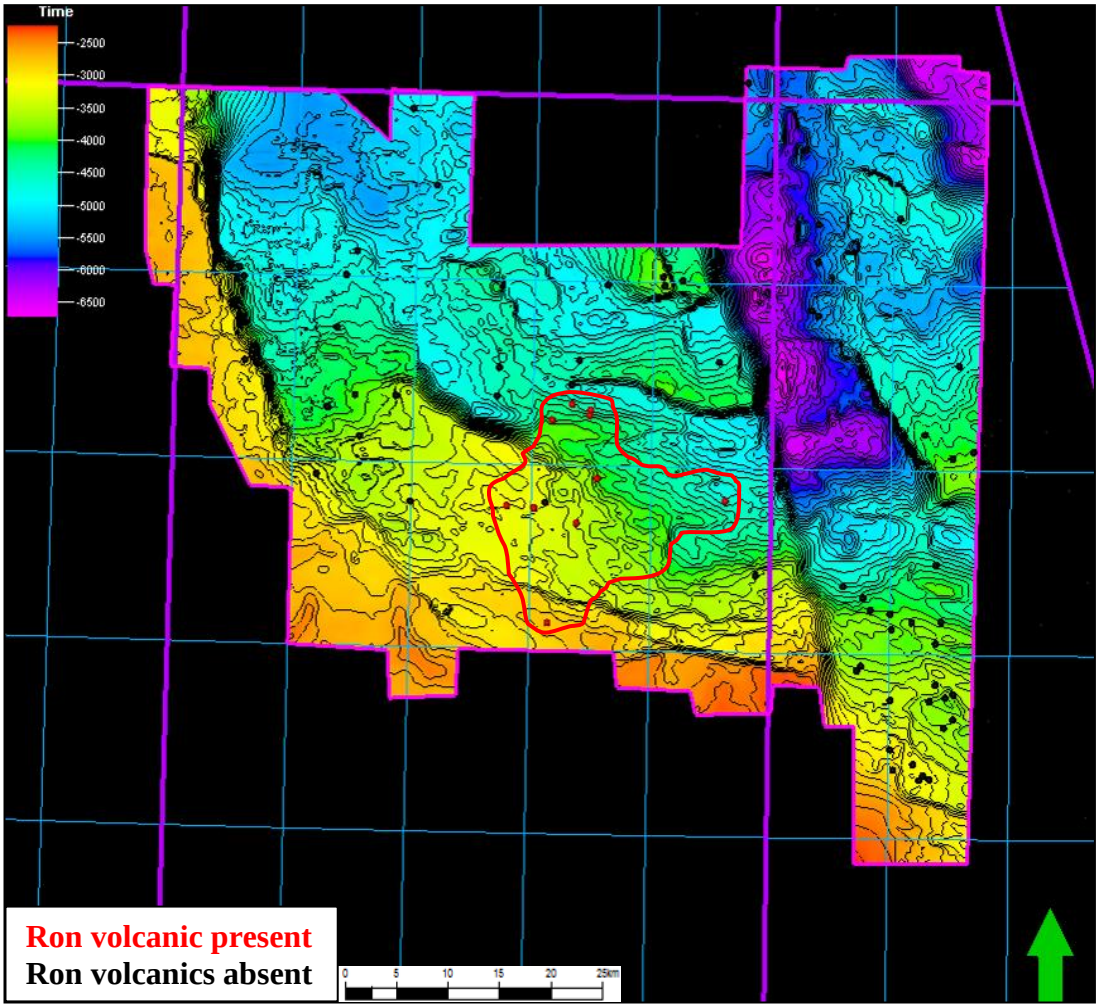

Figure 4.16: A TWTT map of the Rotliegend with colour-coded wells indicating penetrations of the Ron volcanics (encircled in red). The presence of this volcanic centre in the middle of the relay zone may have prevented hard-linkage of the Jurassic fault segments, preserving the relay structure. Note that faults curve around or truncate against the area of volcanics.

4.1.2 FAULT CONTROLS ON JURASSIC DEPOSITIONAL ENVIRONMENTS

The formation and preservation of this relay ramp has important implications for deposition of the syn-rift Jurassic section. With the deflation of the Jurassic dome and/or a eustatic rise in sea level (Rattey et al. 1993), a transgression occurred throughout the Upper Jurassic, gradually flooding the rift and finally the entire North Sea Basin (Ziegler 1990; Underhill et al. 1993; Sansom 2010). Careful analysis of previous studies of Upper Jurassic sequence stratigraphy and biostratigraphy from core data and wire-line logs (Figure 4.17) shows that the transgression gradually moved across faults and around basement highs leading to changes in the depositional environment of different areas (Figure 4.18). The transgression moved down the relay ramp, gradually filling the hanging walls of the Permo-Triassic reactivated faults and spilling over to the footwalls. This is particularly important for hydrocarbon prospectivity as it charts the development of the shoreface environments in which deposition of the highly prospective Fulmar Formation reservoir sandstone occurred. It also explains the existence of very late Jurassic sands on and around the Jaeren High as it was the last area to be drowned.

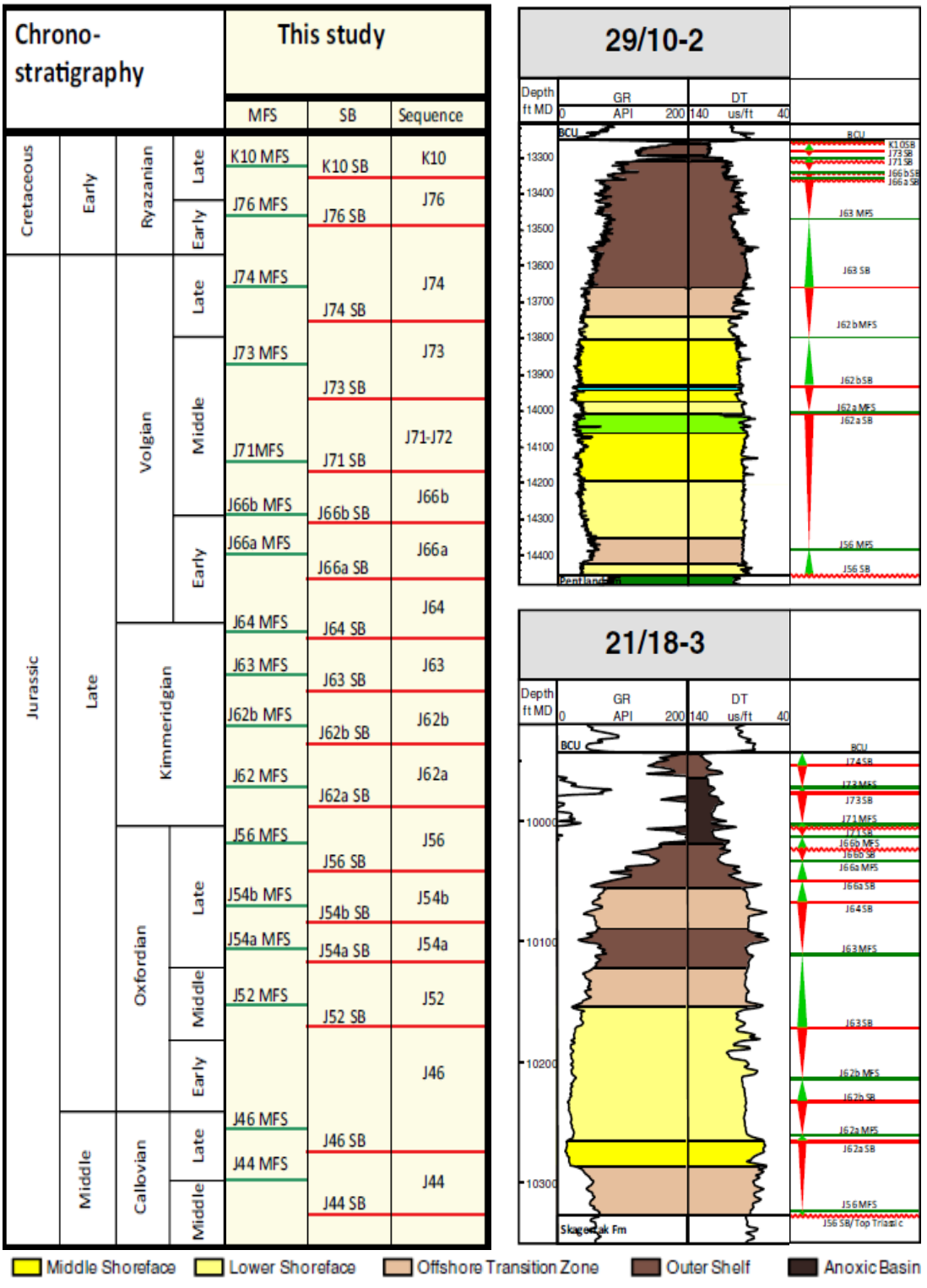

Figure 4.17: Example of previous studies of Upper Jurassic sequence stratigraphy used the interpretation.
Images after (Sansom 2010)

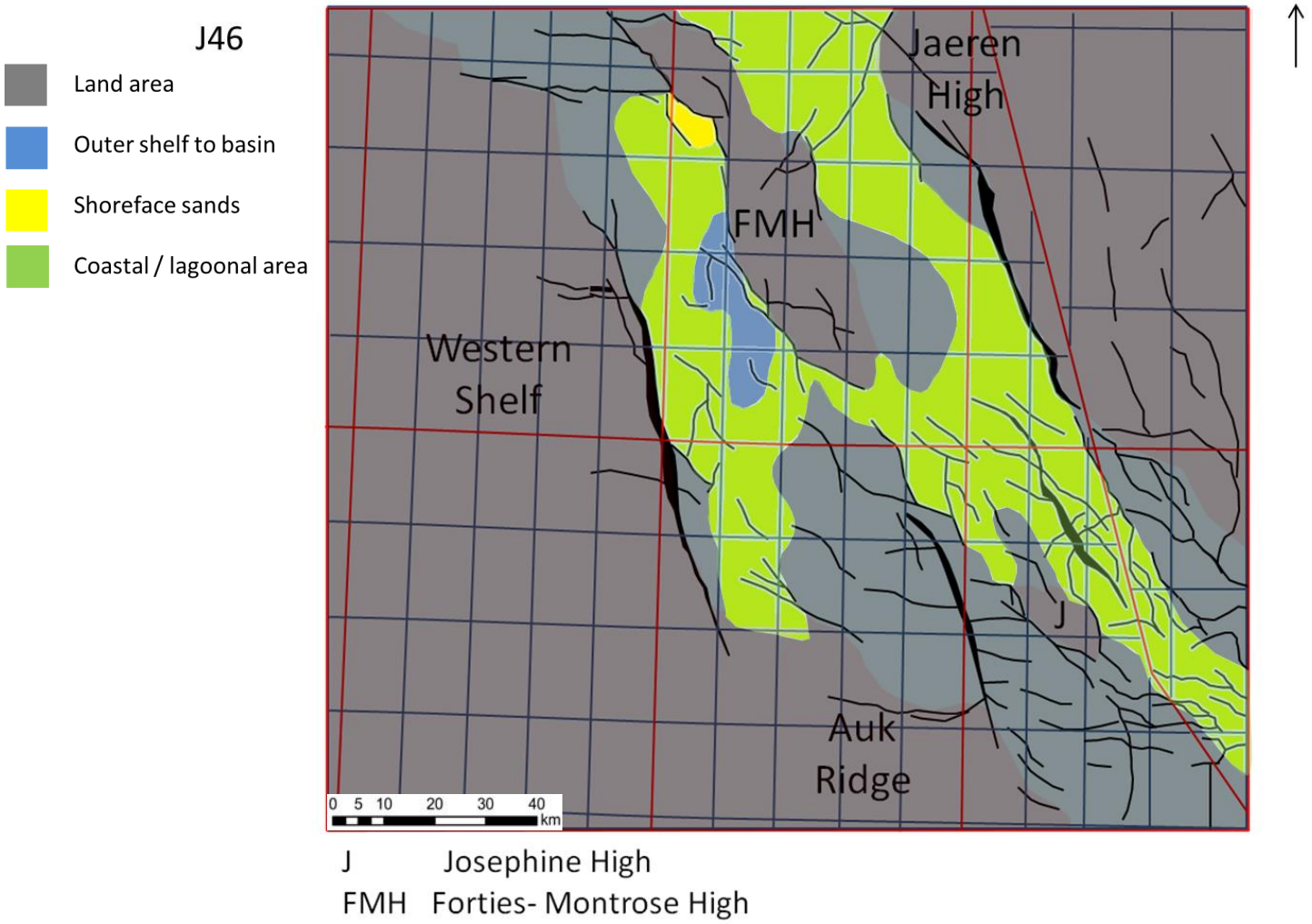

Figures 4.18 (pages 214-221): Facies maps of the Central North Sea through the Jurassic highlighting the control of the preserved relay ramp on the flooding geometries.

Environmental interpretation based on log and core analyses undertaken by Sansom 2010

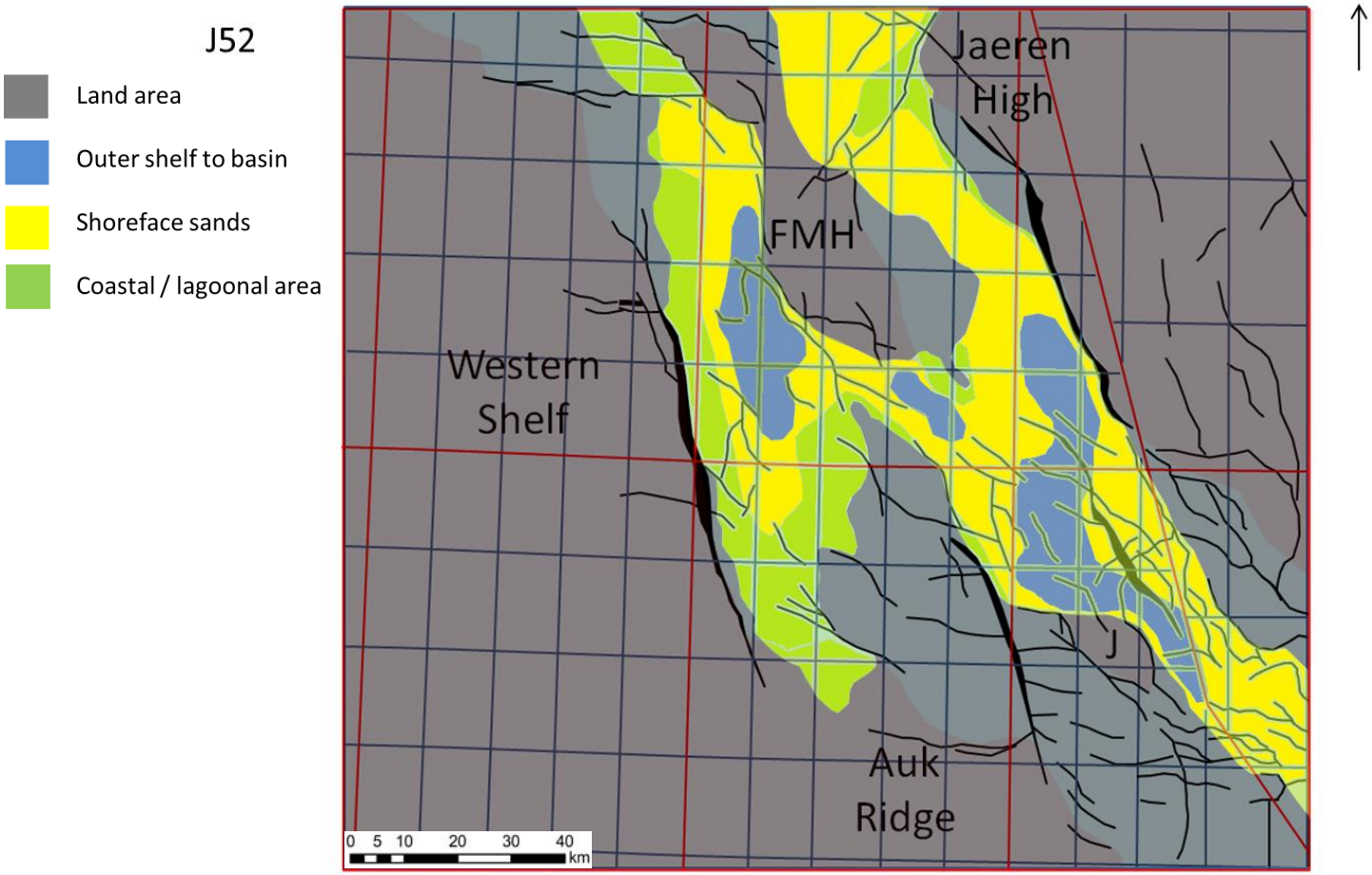

J Josephine High
FMH Forties- Montrose High

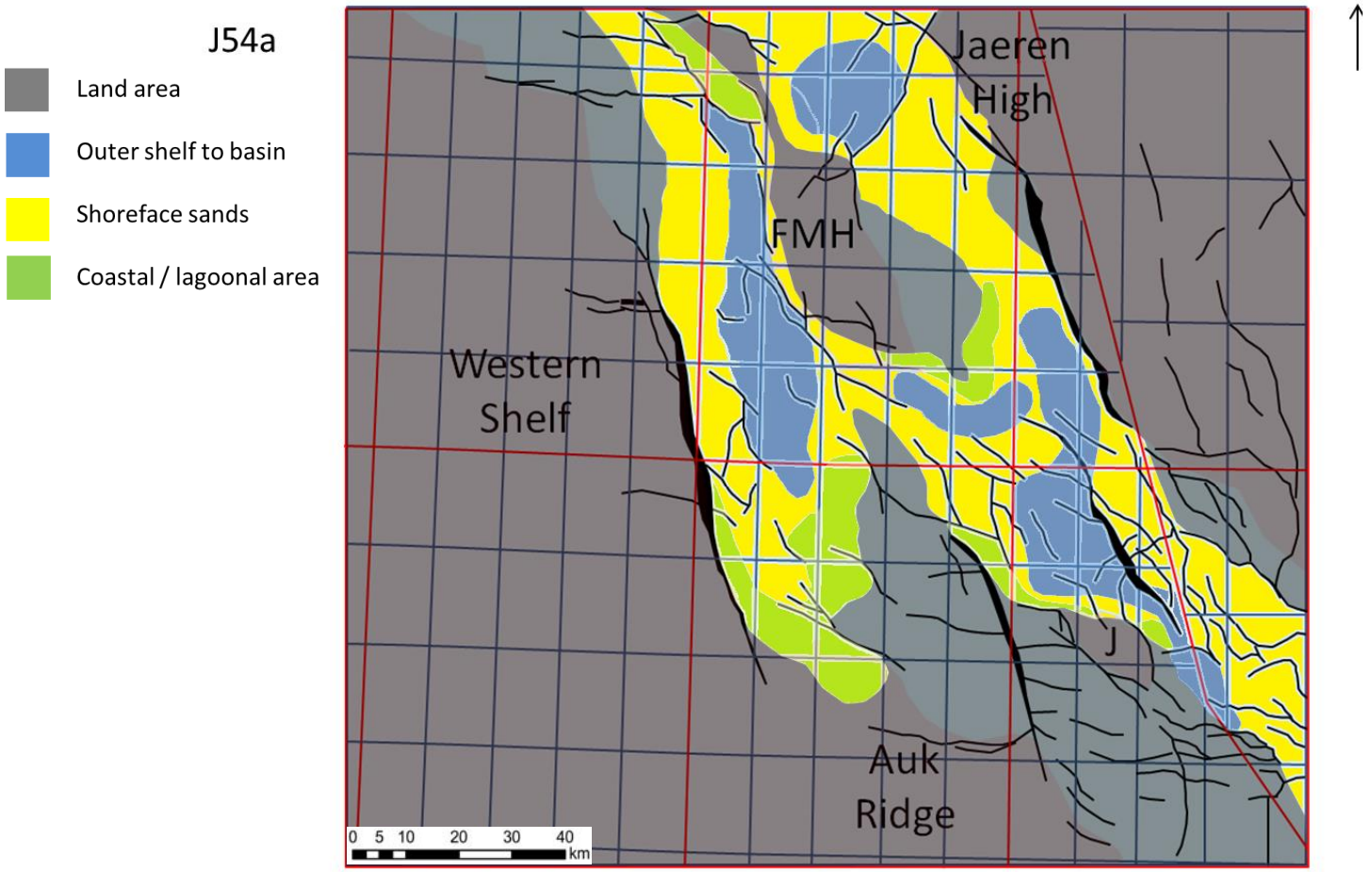

J Josephine High
FMH Forties- Montrose High

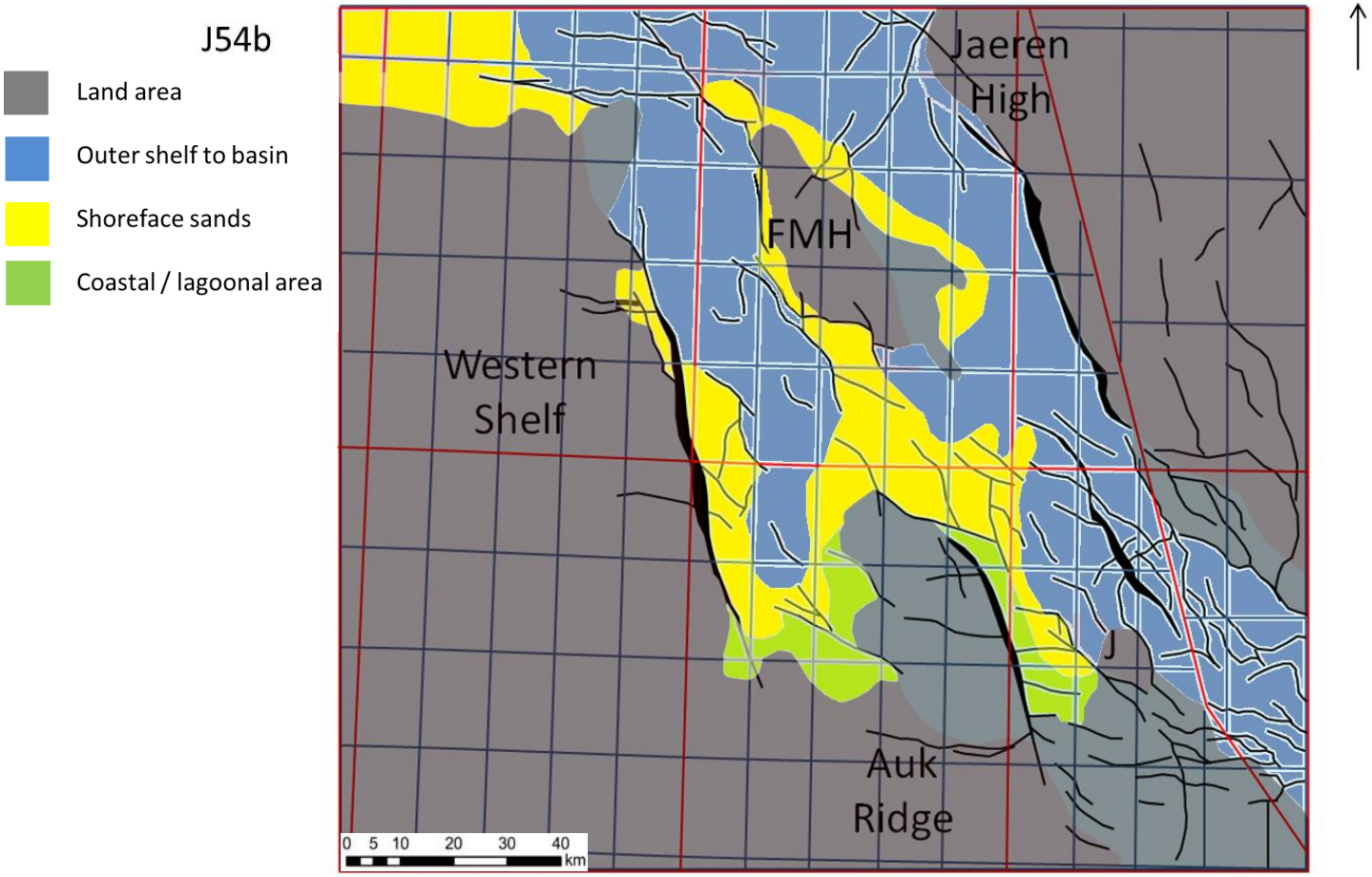

J Josephine High
FMH Forties- Montrose High

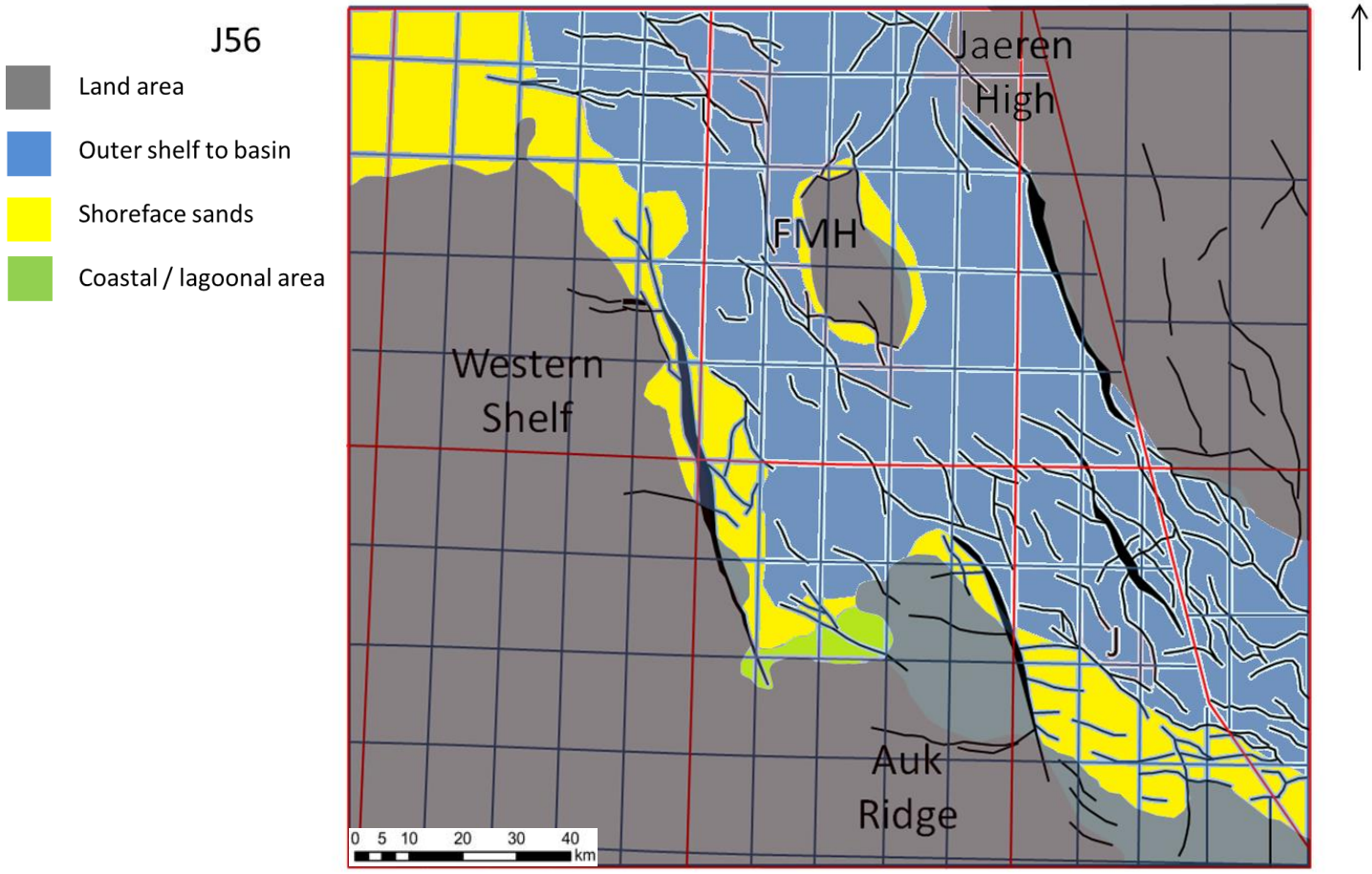
J56
Land area
Outer shelf to basin
Shoreface sands
Coastal / lagoonal area
Jaeren
High
FMH
Western
Shelf
J
Auk
Ridge
0 5 10 20 30 40
km
J Josephine High
FMH Forties- Montrose High

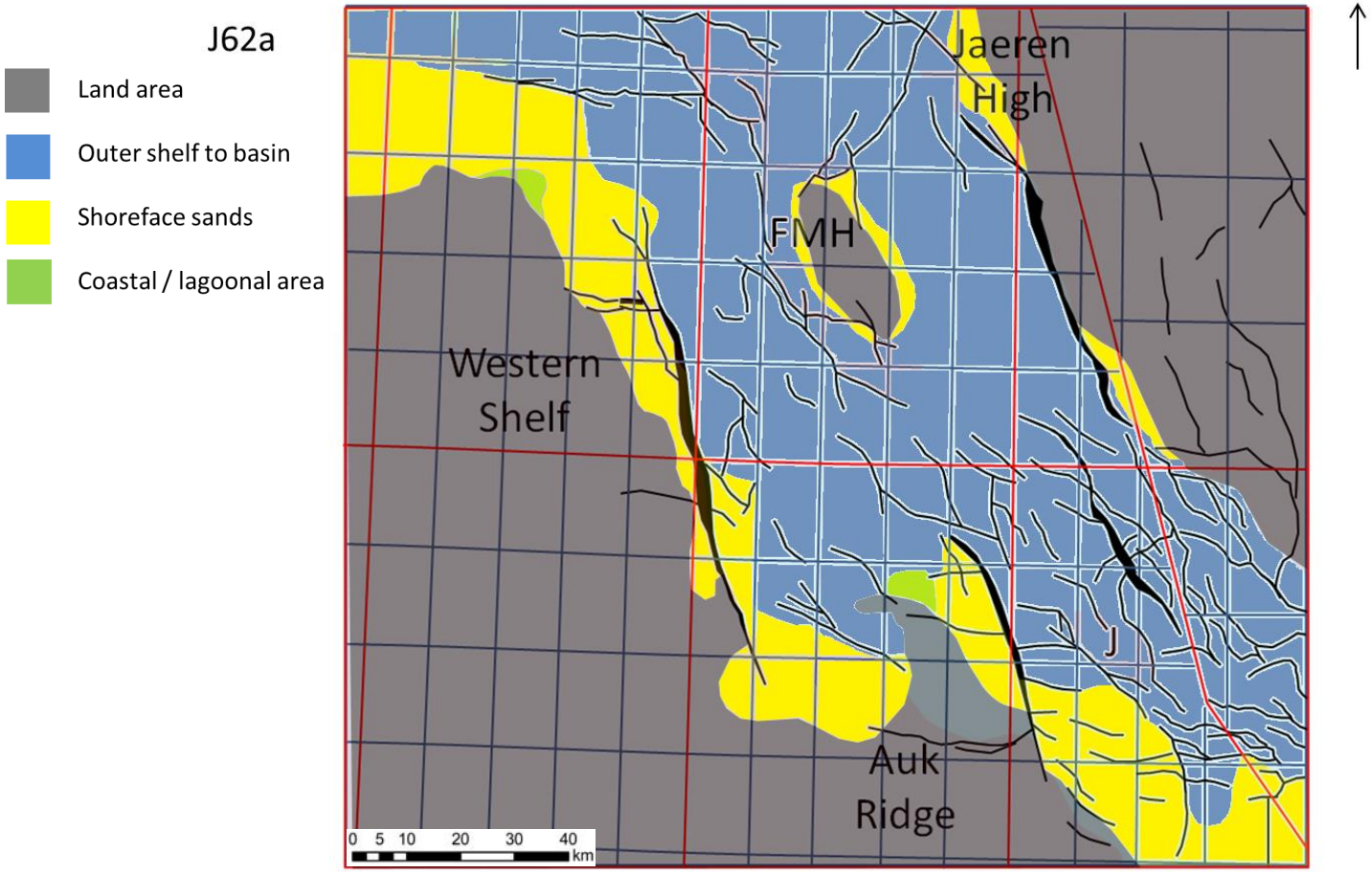

J Josephine High
FMH Forties- Montrose High

J62b

Land area

Outer shelf to basin

Shoreface sands

Coastal / lagoonal area

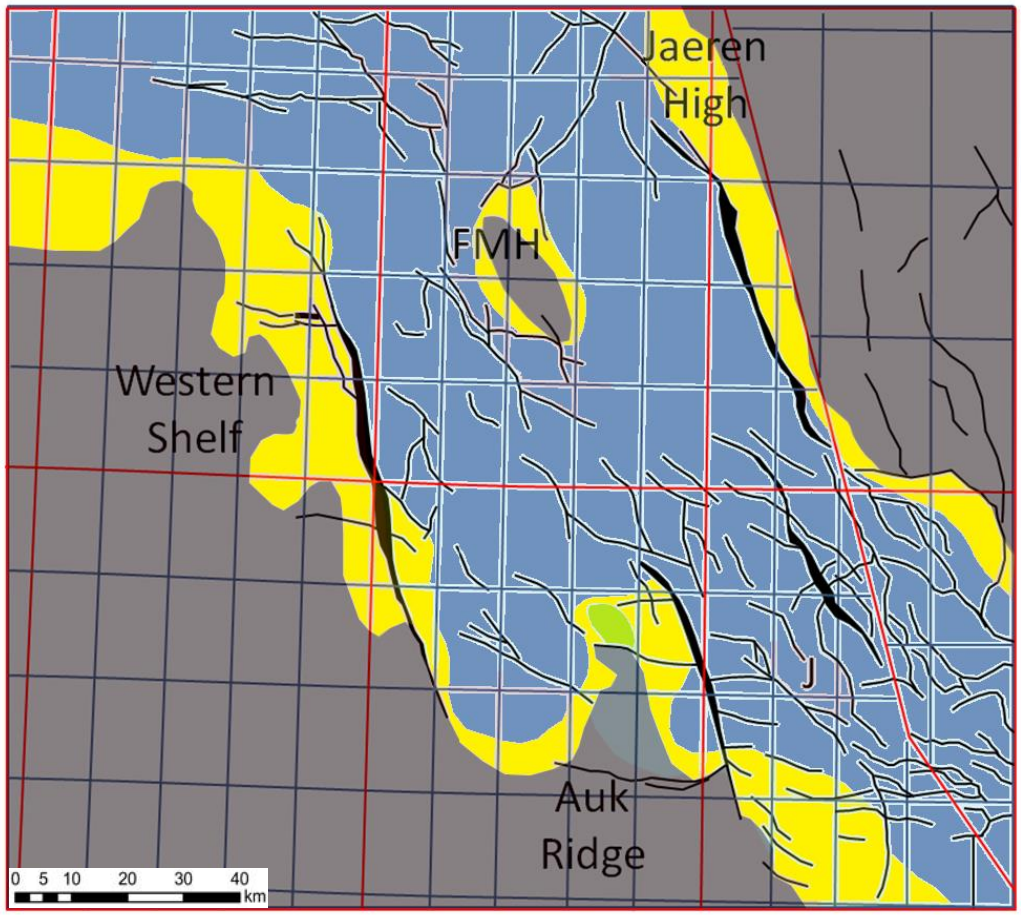

J Josephine High

FMH Forties- Montrose High

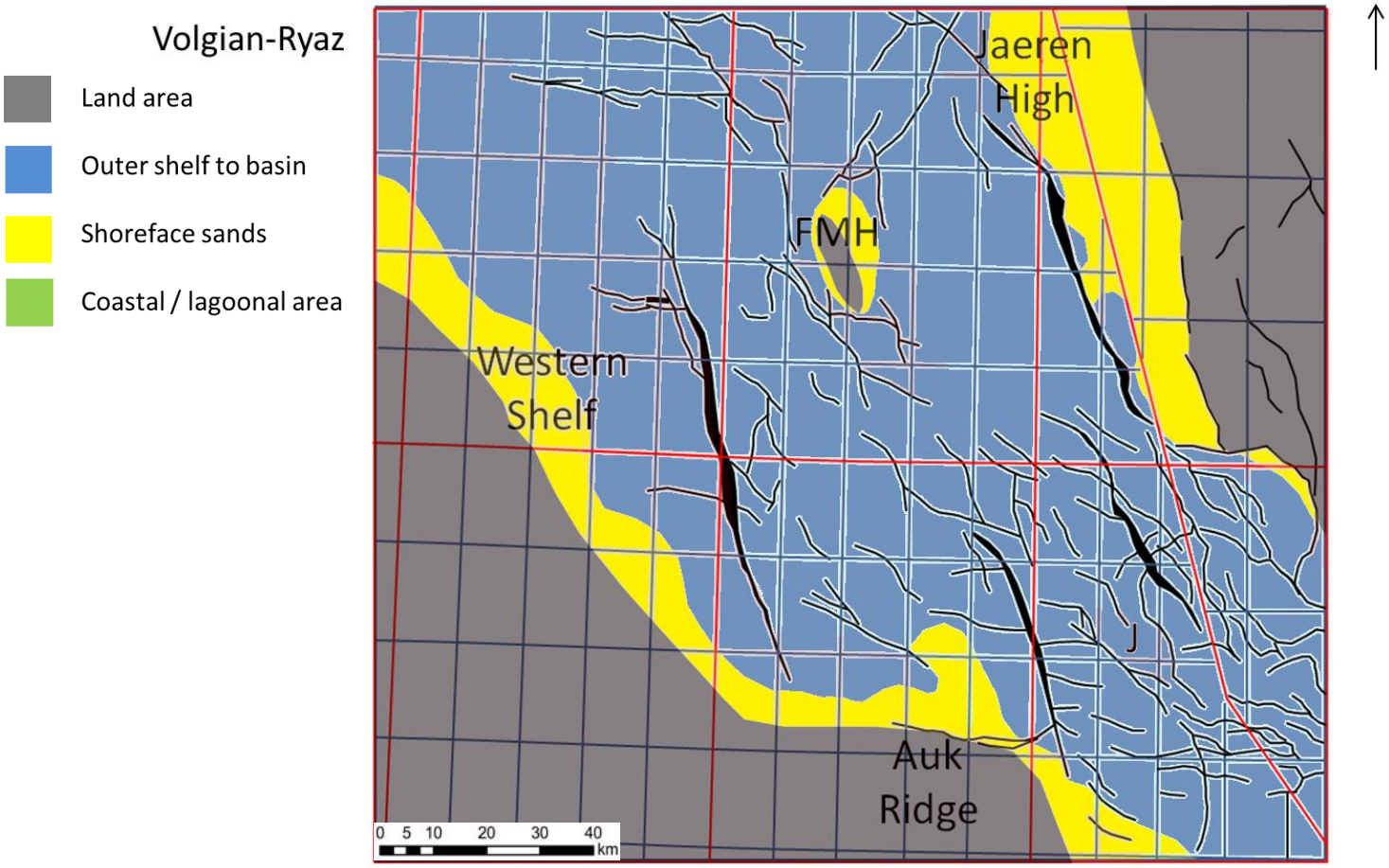
Volgian-Ryaz
Land area
Outer shelf to basin
Shoreface sands
Coastal / lagoonal area
Jaeren High
FMH
Western Shelf
J
Auk Ridge
0 5 10 20 30 40
km
J Josephine High
FMH Forties- Montrose High

4.1.3 CROSS-RIFTING IN OTHER AREAS

The data from the Central North Sea demonstrates that cross-cutting of underlying rifts by later ones can have effects on both the structural and stratigraphic evolution of an area. It is important to understand these effects since many rift zones around the world have been found to cross-cut older structures. An example of this occurs in the most visible of all current rift zones, the East African Rift.

The East African Rift System is expressed at the surface as a narrow (50-150kn) elongated system of normal faults stretching 3500km and consisting of two rift trends, the East and West branches (Morley 1999) (Figure 4.19). The eastern branch is made up of the volcanically active Kenya and Ethiopian rifts and the western branch is composed of a series of deep lakes.

The modern configuration of the rift is superimposed on earlier rift geometries formed during the Jurassic and Cretaceous-Paleogene. The Jurassic rift phase is poorly documented but Cretaceous-Palaeocene rift depocentres have been mapped to reconstruct a trilete rift system of this age consisting of the Muglad, Melut and Anza Grabens (Morley 1999) (Figure 4.20). This older rift is then transected by the later Miocene rift which is still active at present.

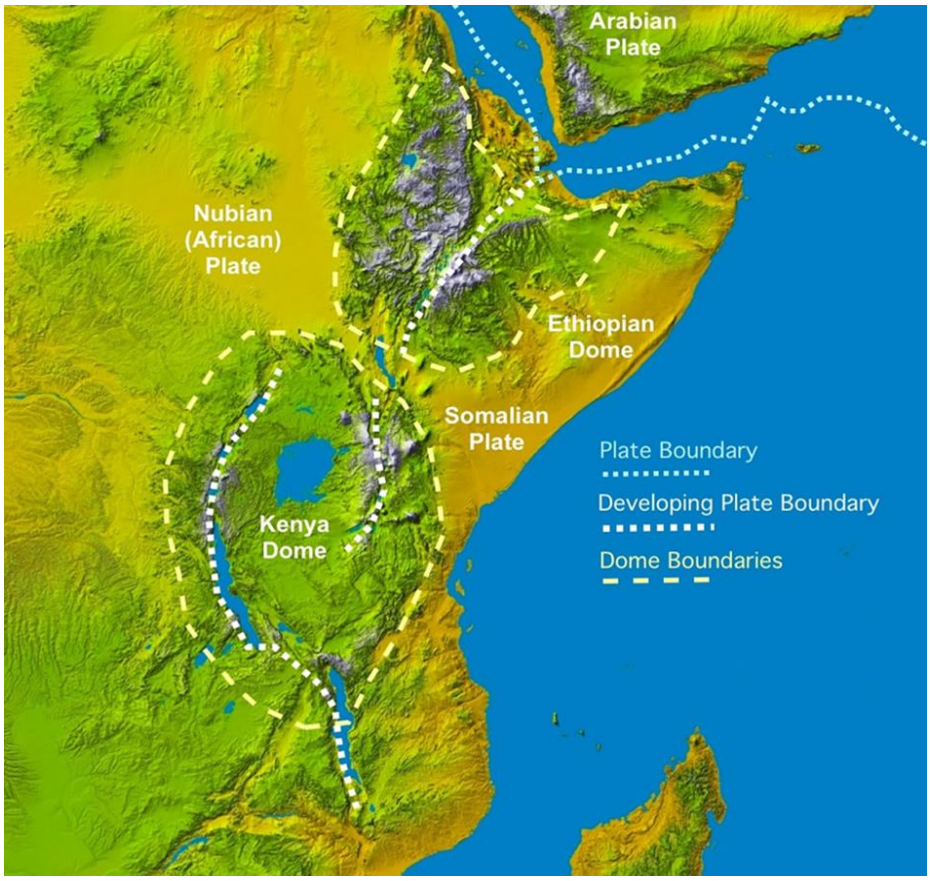

Figure 4.19: Space Shuttle radar topography image by NASA with the East African Rift System indicated
Image after (Wood et al. 2012)

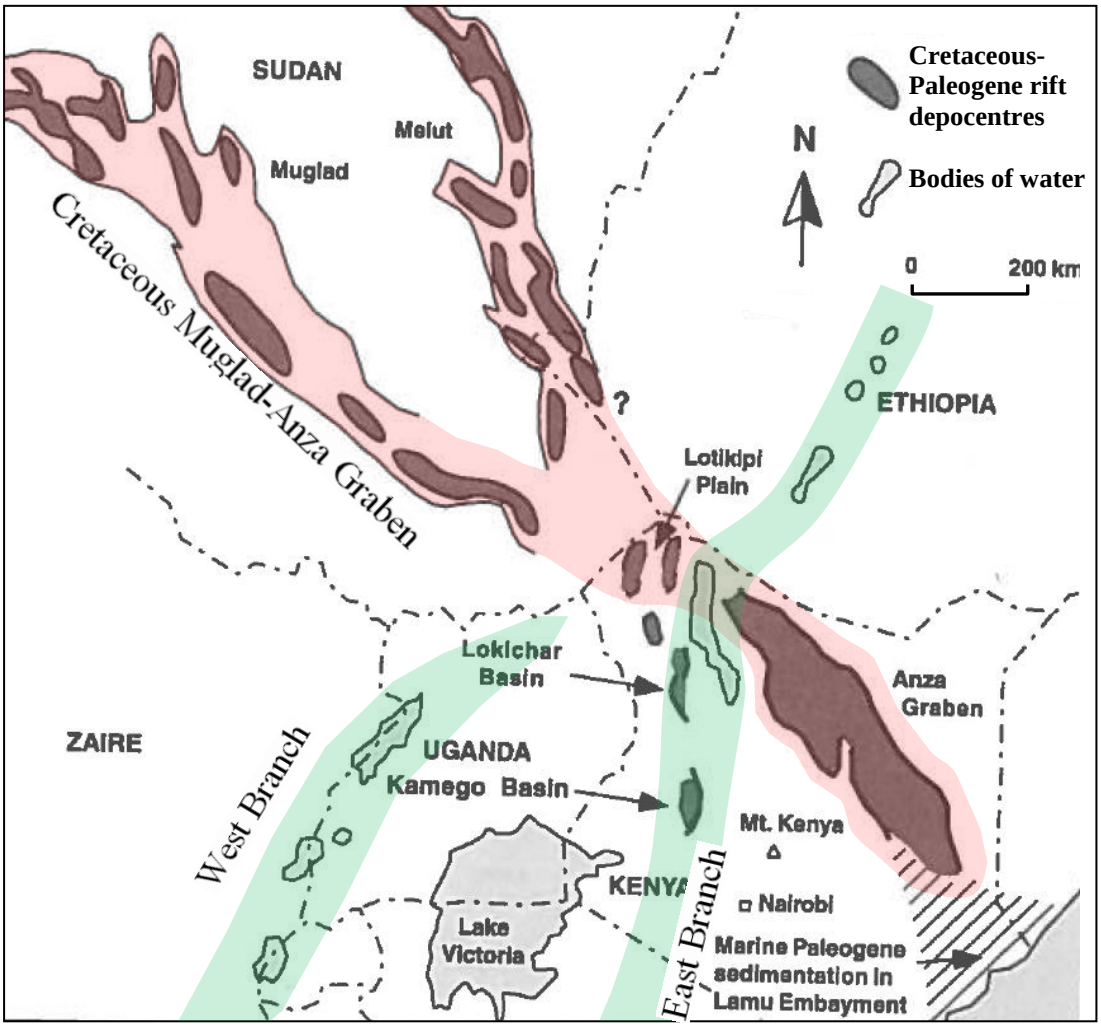

Figure 4.20: Precursor Cretaceous-Paleogene rift system which is cross-cut by the Neogene system seen today.
Image after (Morley 1999)

A transected rift is also described by seismic sequence stratigraphic mapping in the Labrador Sea (Hubbard et al. 1985) proving that the transection of old fault geometries by later ones is not a phenomenon limited to the North Sea. Analogues from the well-calibrated seismic data available in the Central North Sea may therefore be useful in deciphering sub-surface structures in other areas worldwide which do not have data of this quality.

4.5 TECTONO-STRATIGRAPHIC MEGASEQUENCE 2: SYN-RIFT EVOLUTION SUMMARY

In the Jurassic, the formation and collapse of a thermal dome developed over a transient mantle plume located beneath the Central North Sea, led to the formation of a trilete rift system which eventually failed to develop into a true mid-ocean ridge.

This rift cut across the previous lineaments developed during Caledonian, Permian and Triassic deformation and the new mapping demonstrates the importance of these underlying fault trends in the development of later ones. Three separate depocentres can be identified on an isochron of the Jurassic interval in the East Central Graben rift arm. This provides conclusive evidence that propagation of the Jurassic rift occurred by linkage of fault segments. The coincidence of mapped underlying Permo-Triassic faults between the depocentres suggests that these lineaments acted first as barriers to fault growth and then as soft linkage (relay) zones between separate strands of the Jurassic graben-bounding fault. These latest findings suggest a reimagining of the process of Jurassic rifting as it is now evident that the location and formation of the major Jurassic faults was influenced by the underlying Permo-Triassic trend.

In most cases, the relay zones between the Jurassic fault strands were breached as extension continued and the fault became hard-linked. However one of these relay ramps has been preserved, possibly due to the presence of a zone of solid igneous

material between the two Jurassic fault strands. Mapping of the evolution of the Late Jurassic shoreline and depositional environments demonstrates that the final flooding of the rift system was influenced by the presence of the preserved relay ramp. Flooding from the north filled the footwalls of the W-E striking Permo-~Triassic faults in the relay ramp before spilling over to the hanging walls and this discovery has implications for the areal extent and age of the prospective shoreface Fulmar Sands in the area.

The results of the new interpretation in the Central North Sea are important as cross-cutting of older fault trends has been demonstrated in other areas of the world indicating that it may be a common feature of many rift provinces. The Central North Sea may therefore be a good analogy for areas where data is sparser.

CHAPTER 5

TECTONO-STRATIGRAPHIC MEGASEQUENCE 2: POST-RIFT EVOLUTION

5.1 DRAPE AND PUNCTUATED SUBSIDENCE

The end of the Jurassic period is marked by a regional unconformity, the Mid-Cimmerian or Base Cretaceous Unconformity related to the final stages of the Jurassic rift event (Underhill et al. 1993; Underhill 2003). In many areas the event is marked by the Late Jurassic syn-rift Humber Group of which the easily seismically identifiable Heather and Kimmeridge Clay Formation (Figure 5.1) form a component part. In the North Sea the Cretaceous is split into the Lower Cretaceous Cromer Knoll Group and Upper Chalk Group and has typically been thought of as a period of passive post-rift thermal sag (Evans et al. 2003) with sequence stratigraphy controlled by successive eustatic sea-level fluctuations (Figure 5.2).

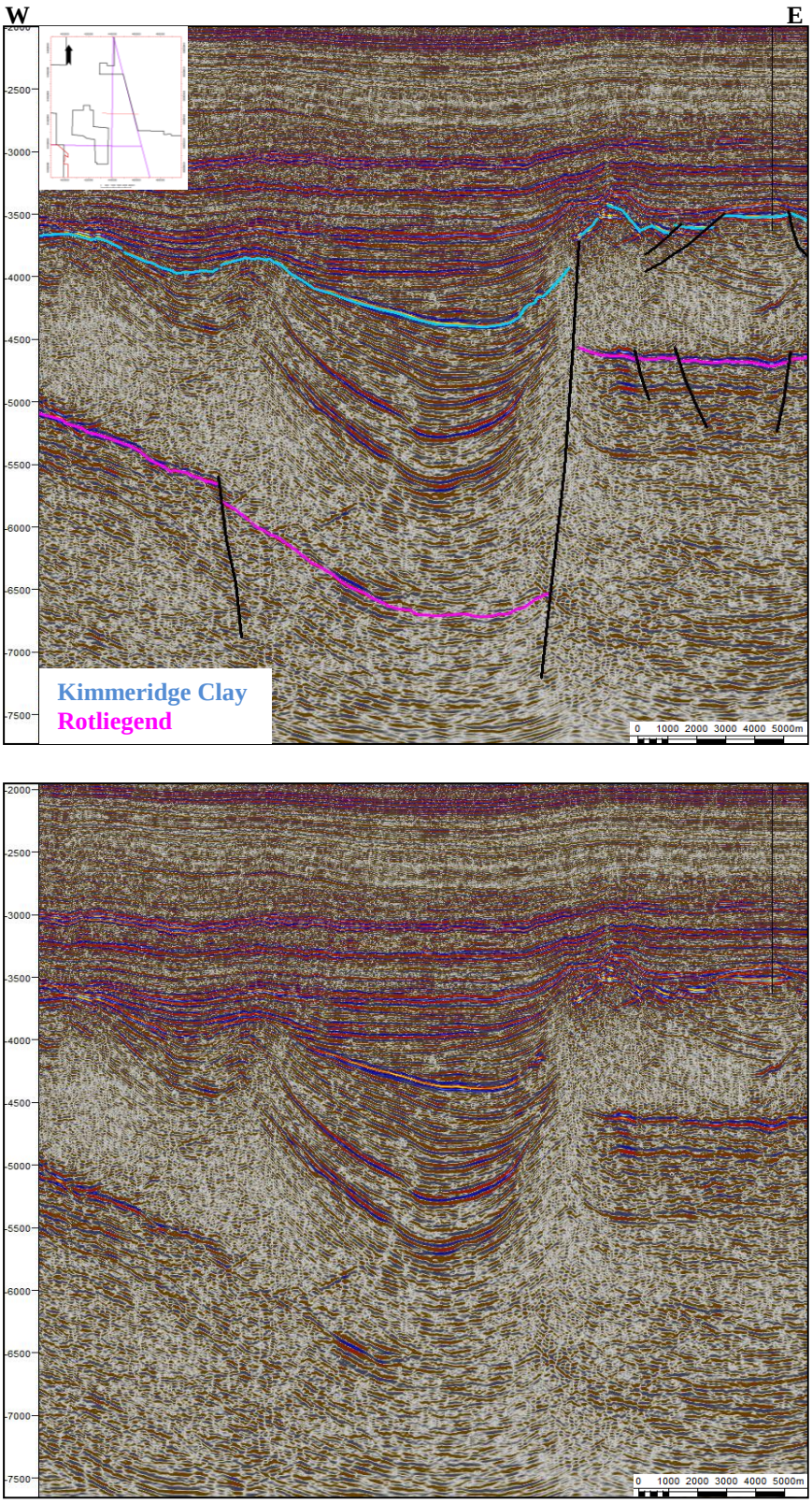

Figure 5.1: Seismic sections illustrating the high amplitude Kimmeridge Clay Formation.

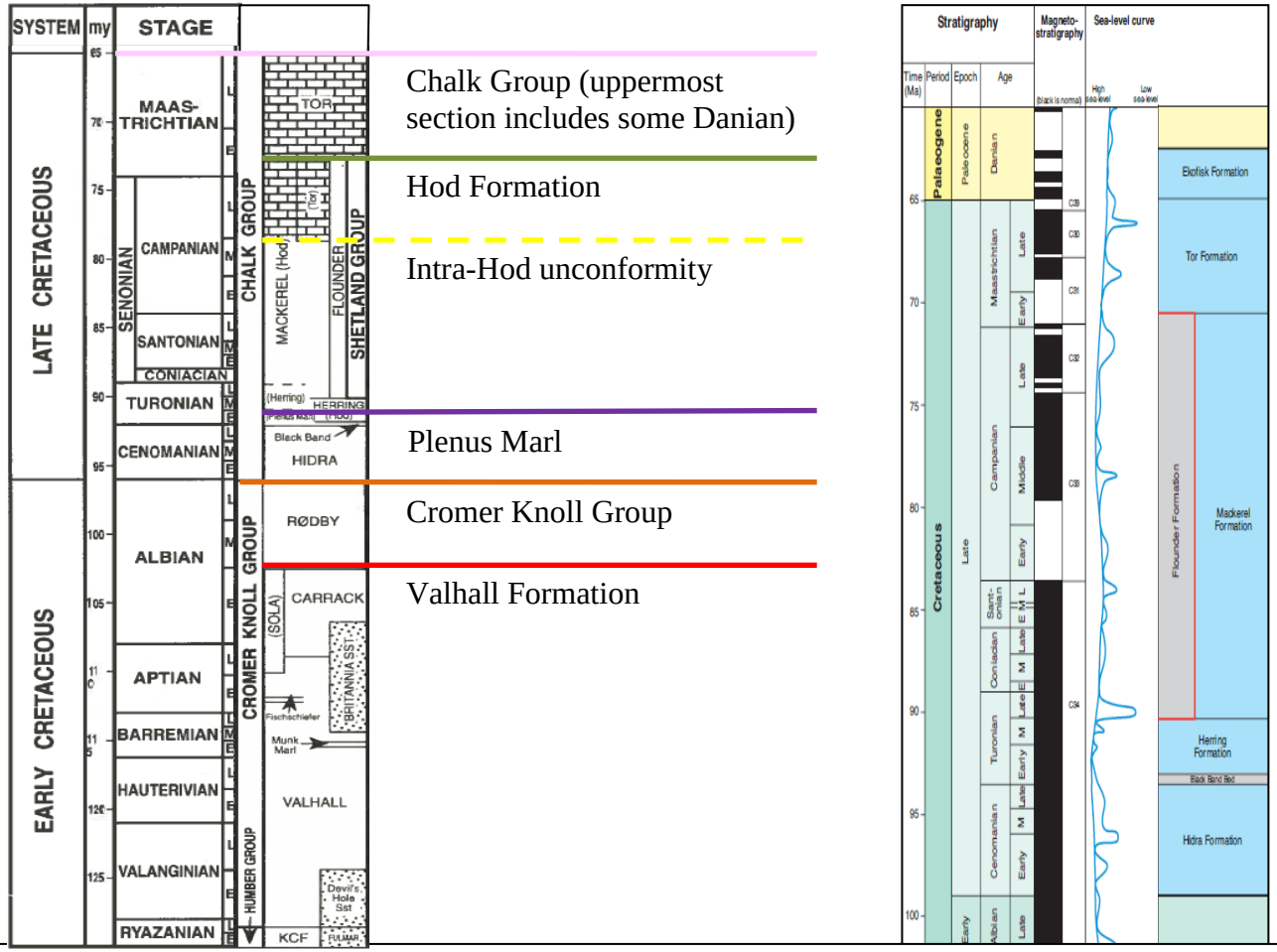

Figure 5.2: Stratigraphy of the Cretaceous sequence in the Central North Sea with horizon picks marked and comparison of the Upper Cretaceous Chalk Group with the global sea-levels.

Note that Ryazanian is a British Lower Cretaceous stage and is roughly equivalent to the Berrasian.

Figures after (Glennie 1998; Evans et al. 2003)

A TWTT structure map of the Base Cretaceous Unconformity and a dip angle map show the bathymetry which was then infilled by the Cretaceous Cromer Knoll Group and Chalk Group (Figures 5.3-5.5). However some anomalous features can be observed which do not fit with a model of drape over remnant structural features. Seismic lines across these features show complex structures formed by halokinetic movements post-dating Kimmerigian deposition (Figure 5.6).

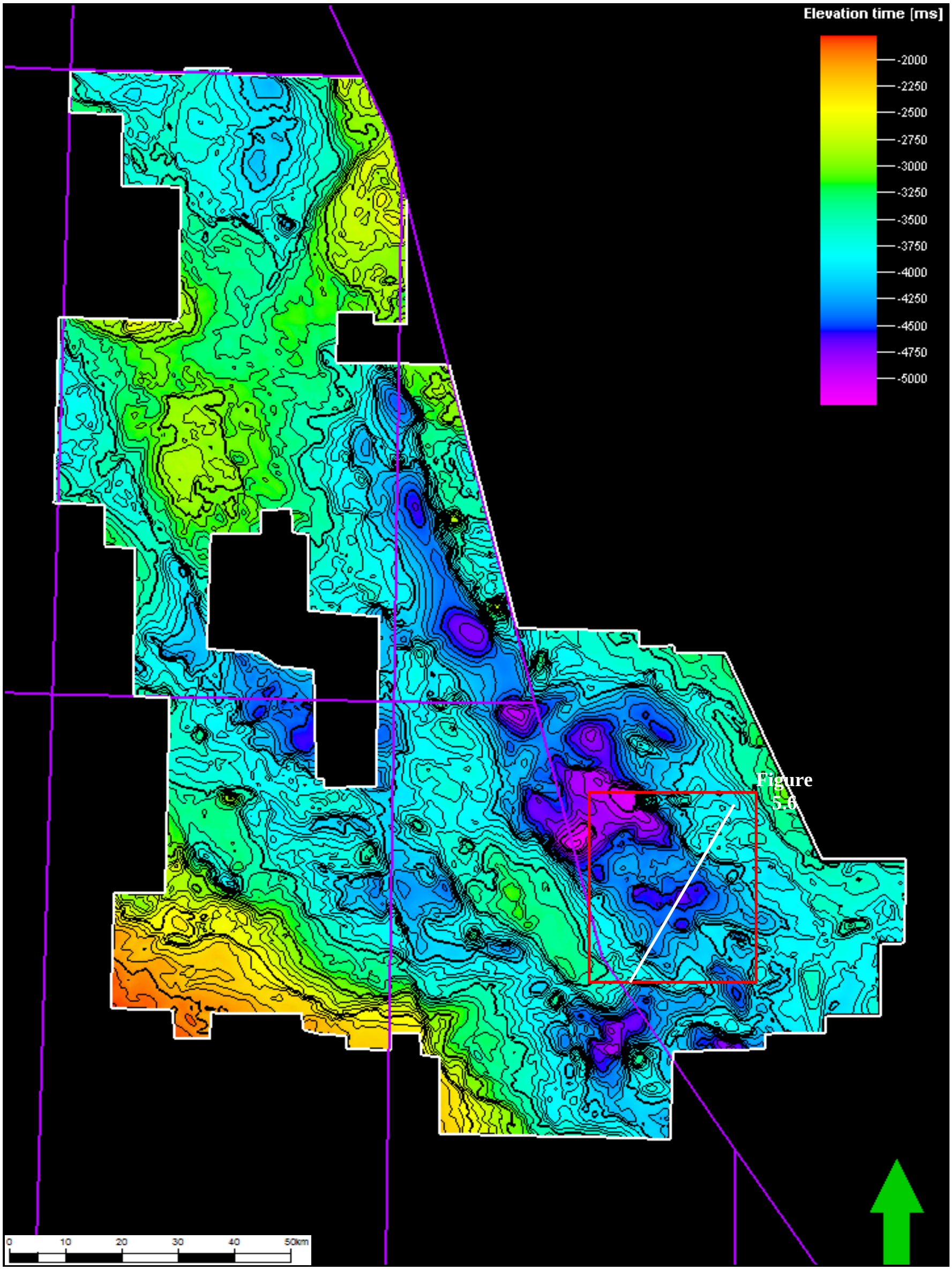

Figure 5.3: TWTT structure map of the Base Cretaceous pick.
Note the unusual features highlighted which are investigated in more detail in Figure 5.6.

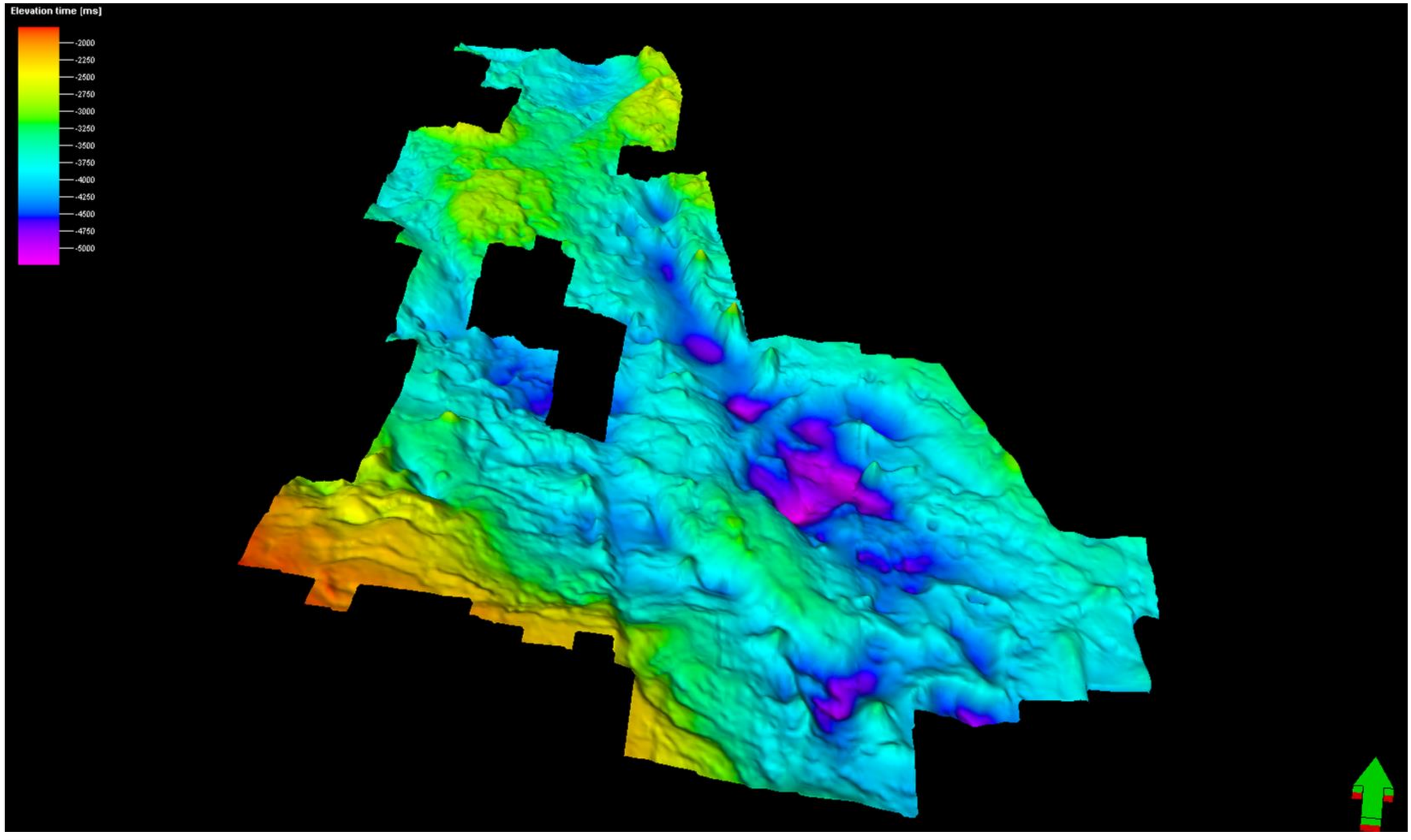

Figure 5.4: 3D view of the Base Cretaceous surface showing the diapirs which were formed by salt migration up the rift arms.

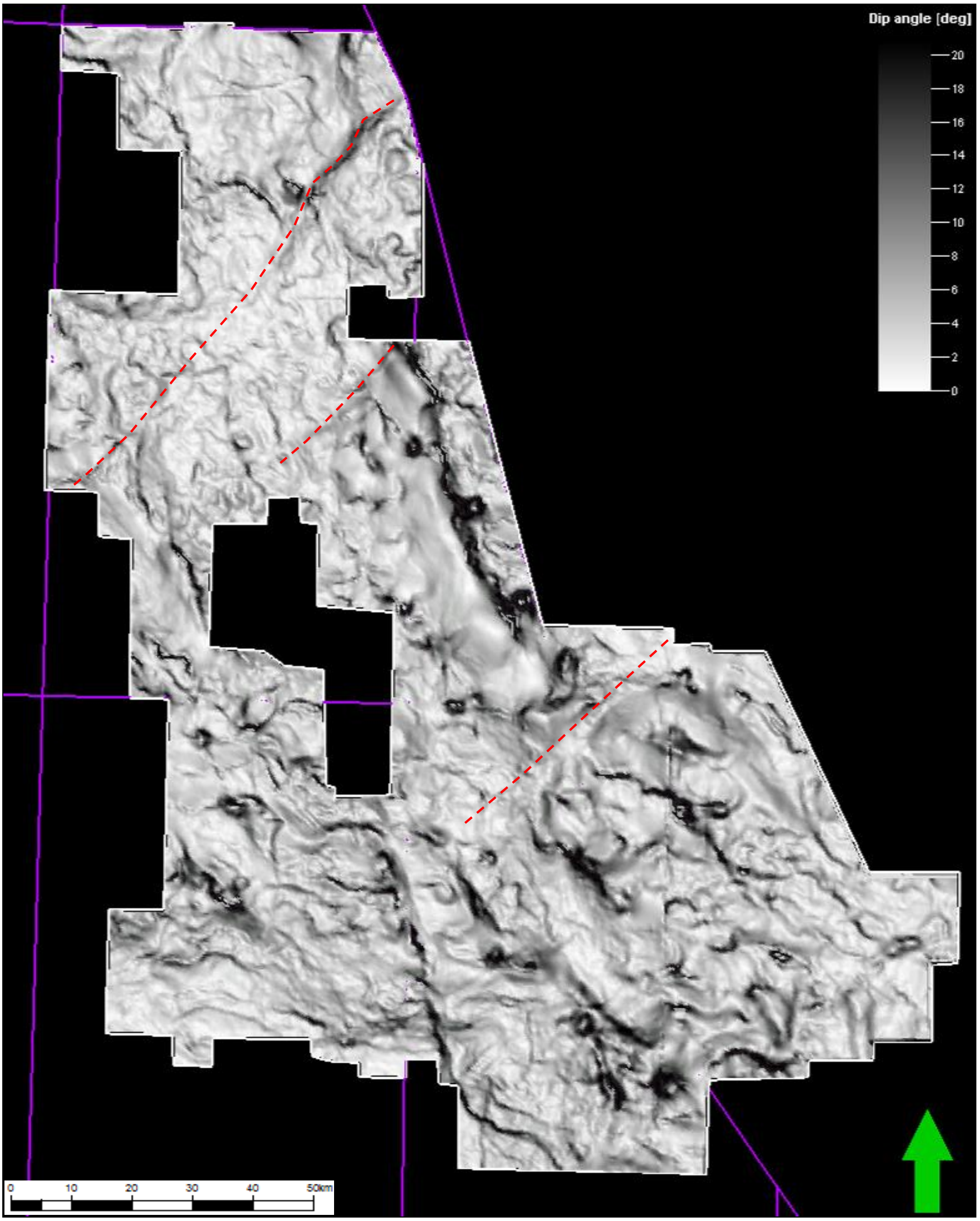

Figure 5.5: Dip angle map of the Base Cretaceous. Note the indications of further Caledonian trend faults which are not so easily observed on the Rotliegend dip angle map. This suggests some reactivation on these lineaments post-Permian.

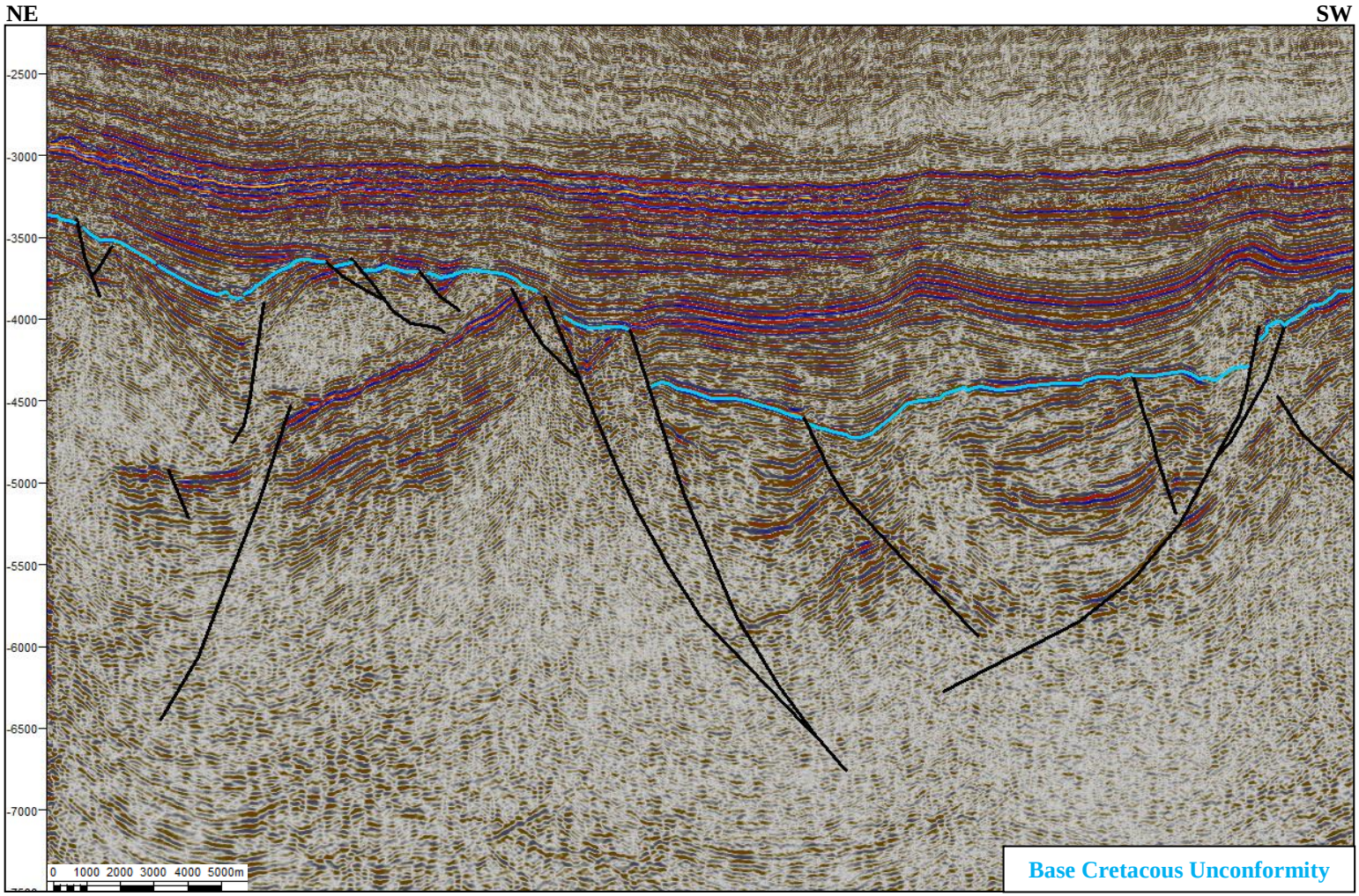

Figure 5.6: Seismic line showing the some of the structures seen on the Base Cretaceous structure map.

In order to investigate the configuration, timing and regional significance of these structural events, horizons were interpreted corresponding to the top of the Chalk Group, Hod Formation, Plenus Marl, Cromer Knoll Group and Valhall Formation. TWTT structure maps were then created (Figure 5.7-5.11)

These surfaces were then used to create isochrons. An isochron between the top Chalk Group and base Cretaceous shows the total Cretaceous infill (Figure 5.12).

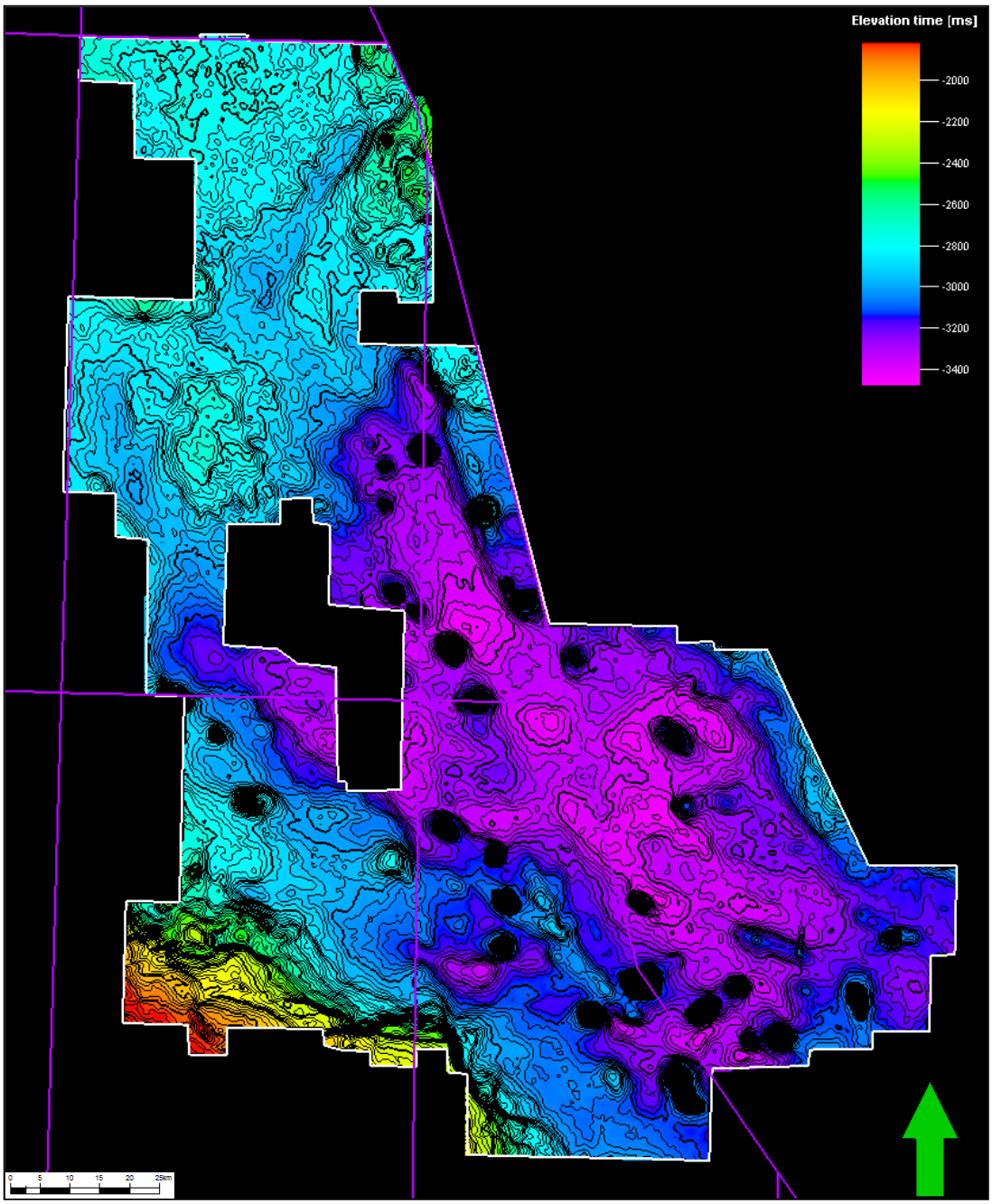

Figure 5.7: TWTT structure map of the top Chalk Group. Black circles indicate positions of diapirs.

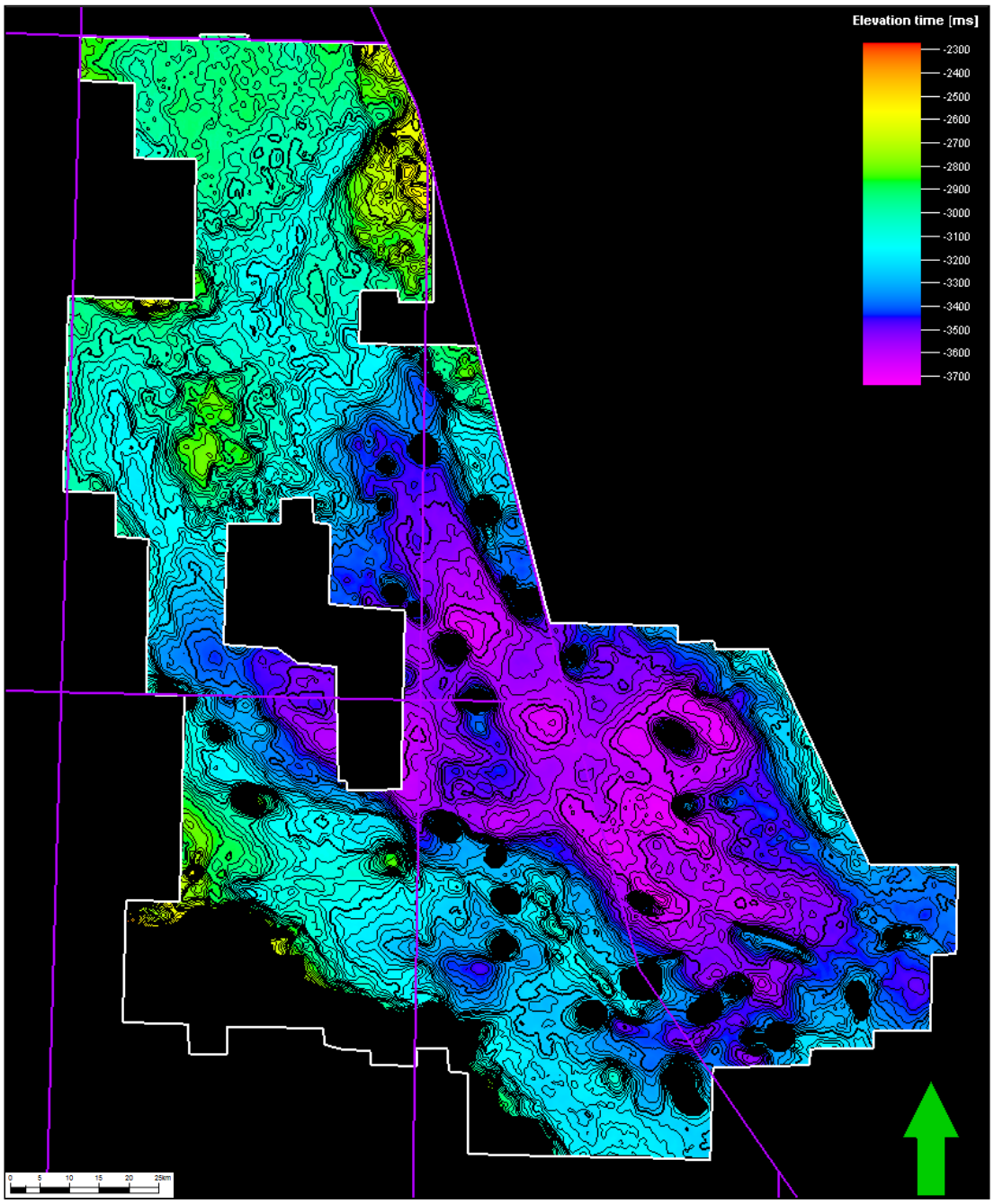

Figure 5.8: TWTT structure map of the Hod Formation.

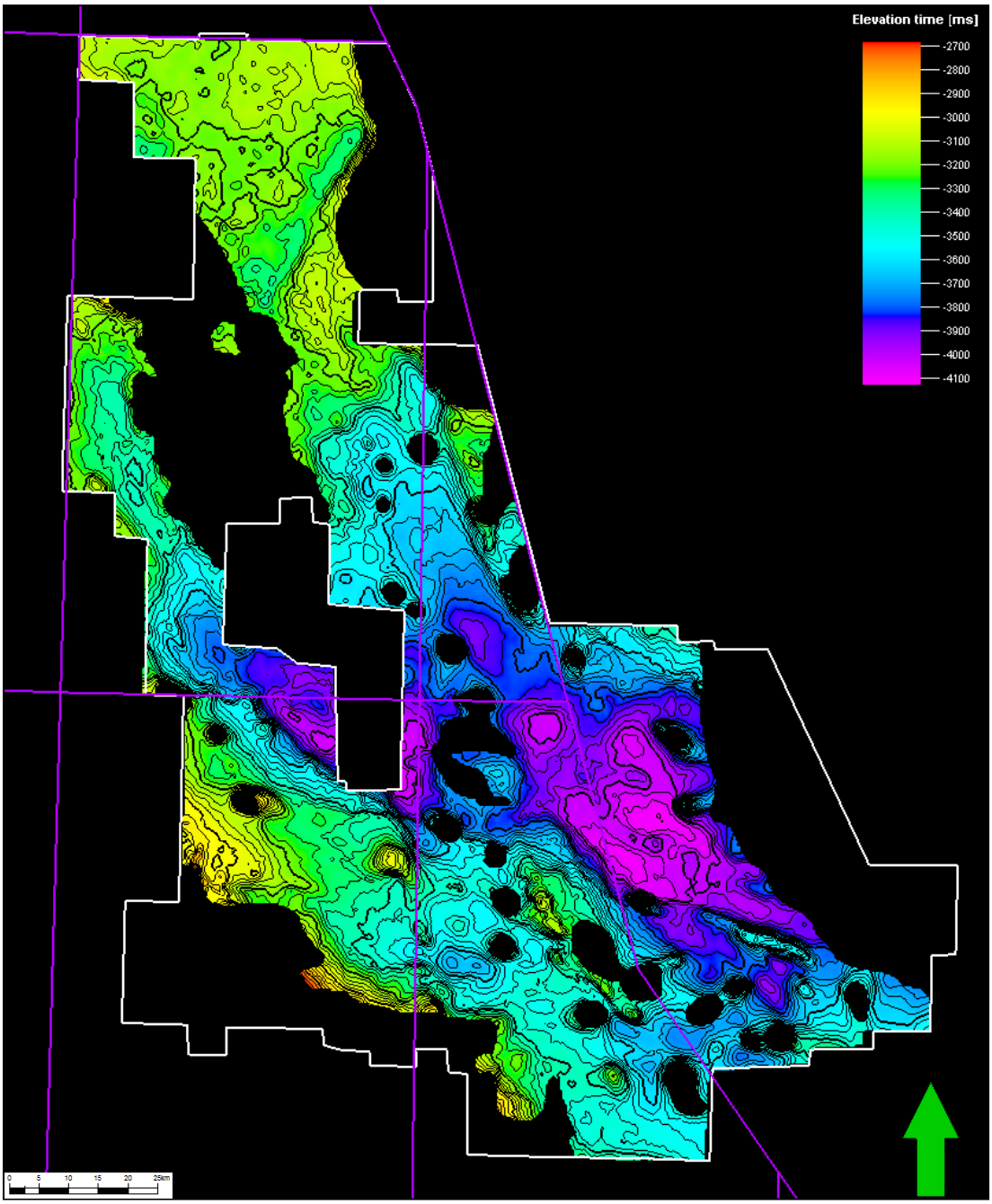

Figure 5.9: TWTT structure map of the Plenus Marl.

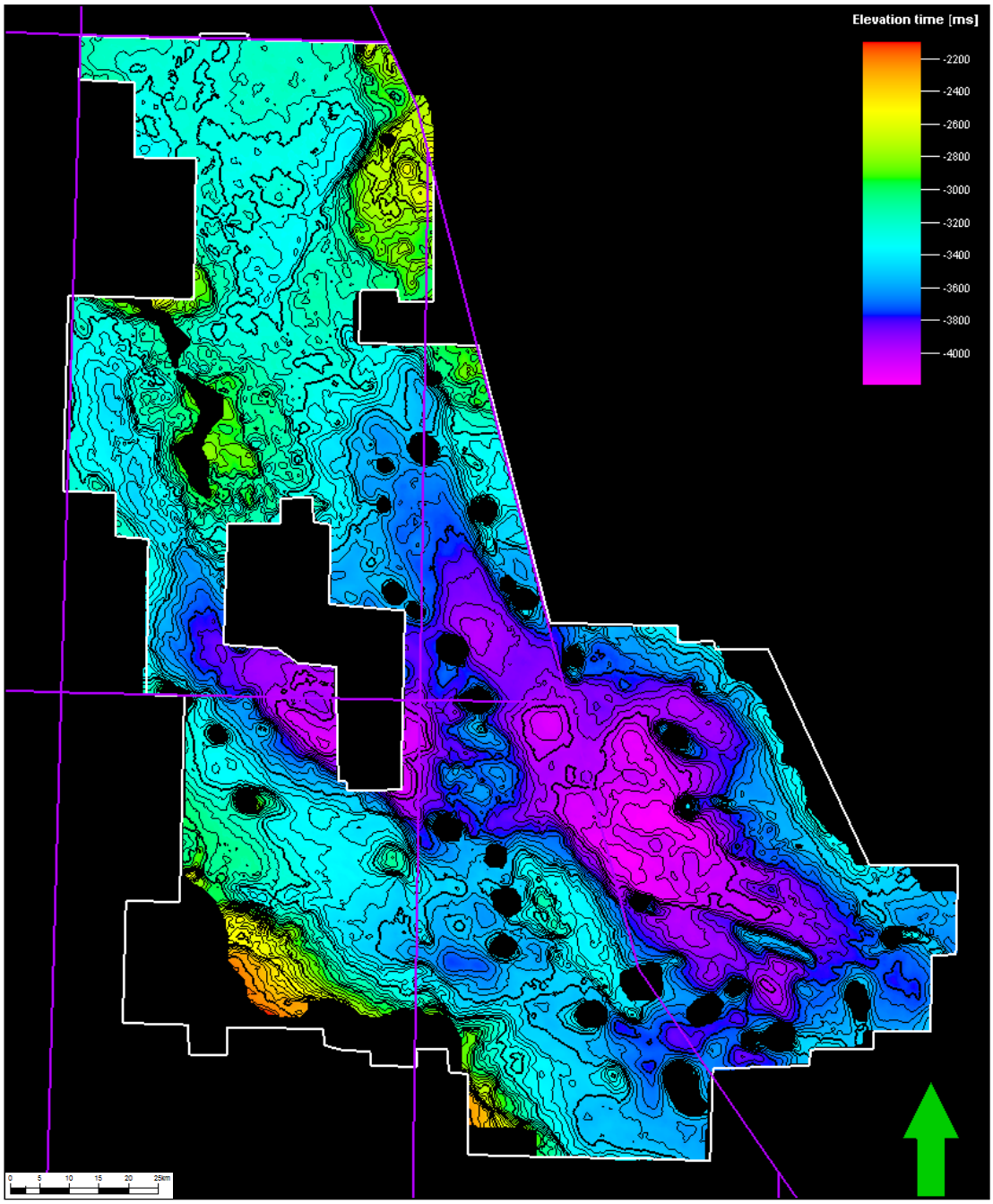

Figure 5.10: TWTT structure map of the Lower Cretaceous Cromer Knoll Group.

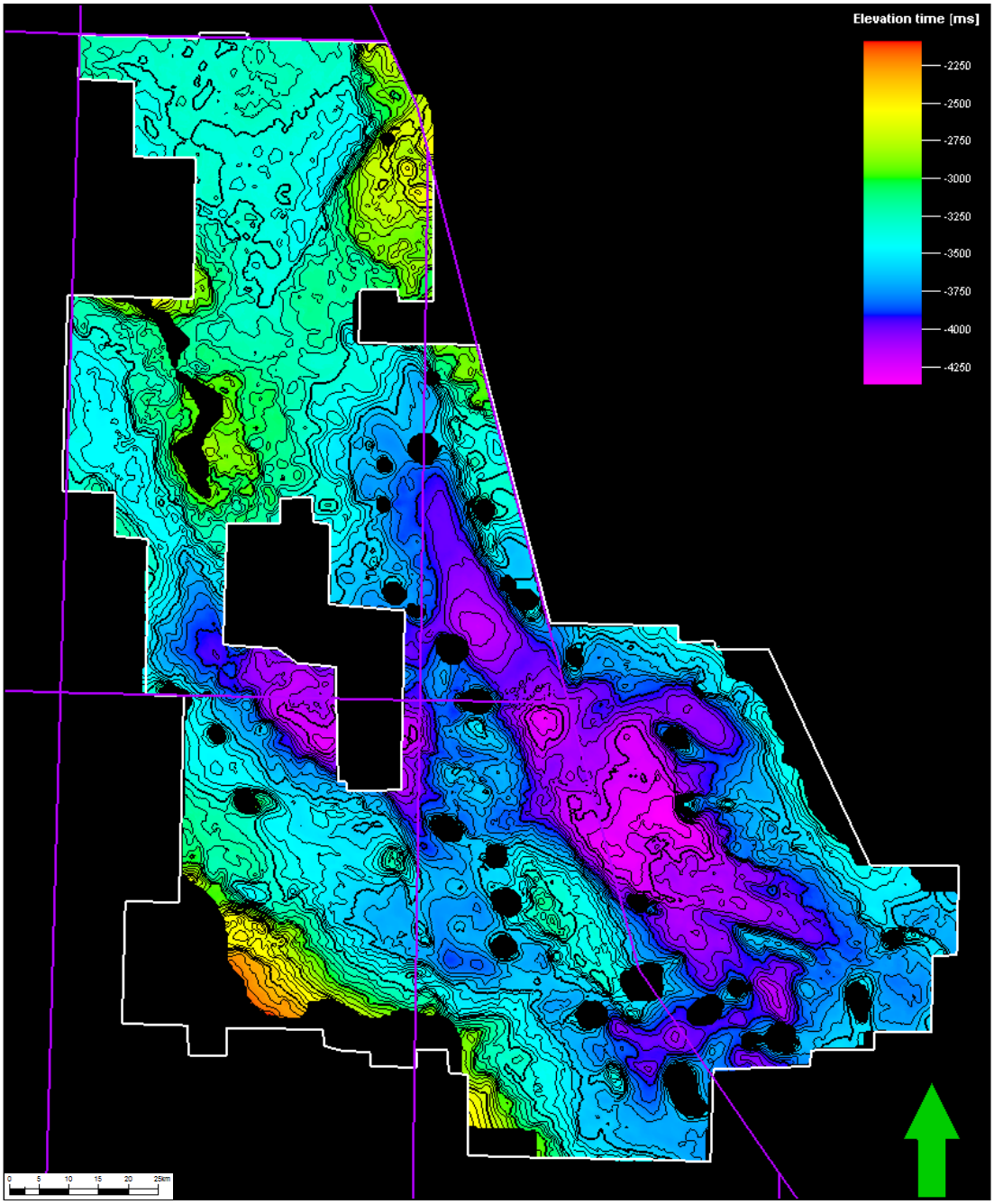

Figure 5.11: TWTT structure map of the Valhall Formation

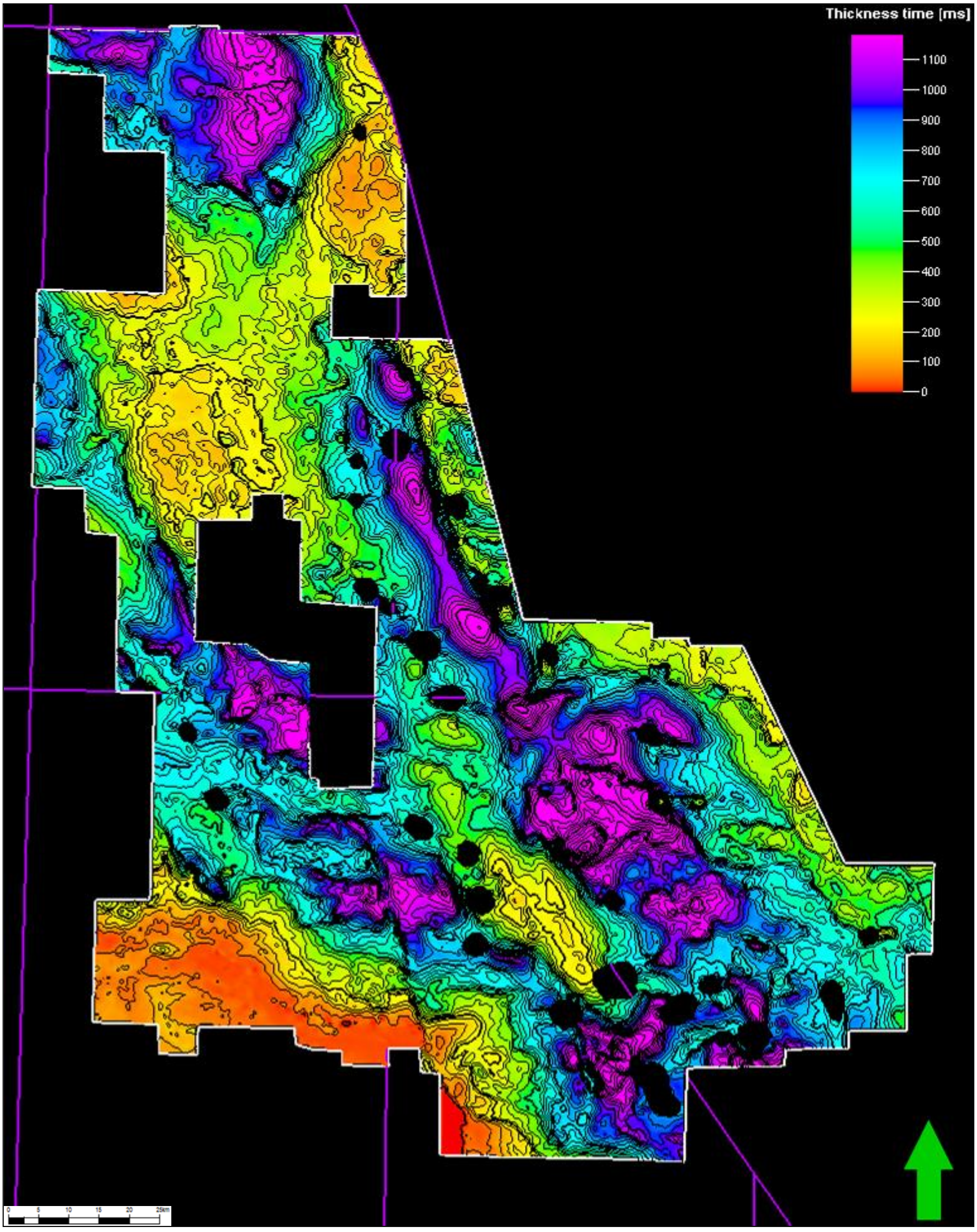

Figure 5.12: Isochron of the entire Cretaceous section. This can be subdivided in order to ascertain the timing of structural events.

The intra-Cretaceous reflectors picked stratigraphically on the basis of major facies changes can be used to create isochrons corresponding to periods of geological time (Figure 5.13-5.20) and can thus be used to tie structural events in the Central North Sea to global tectonic events.

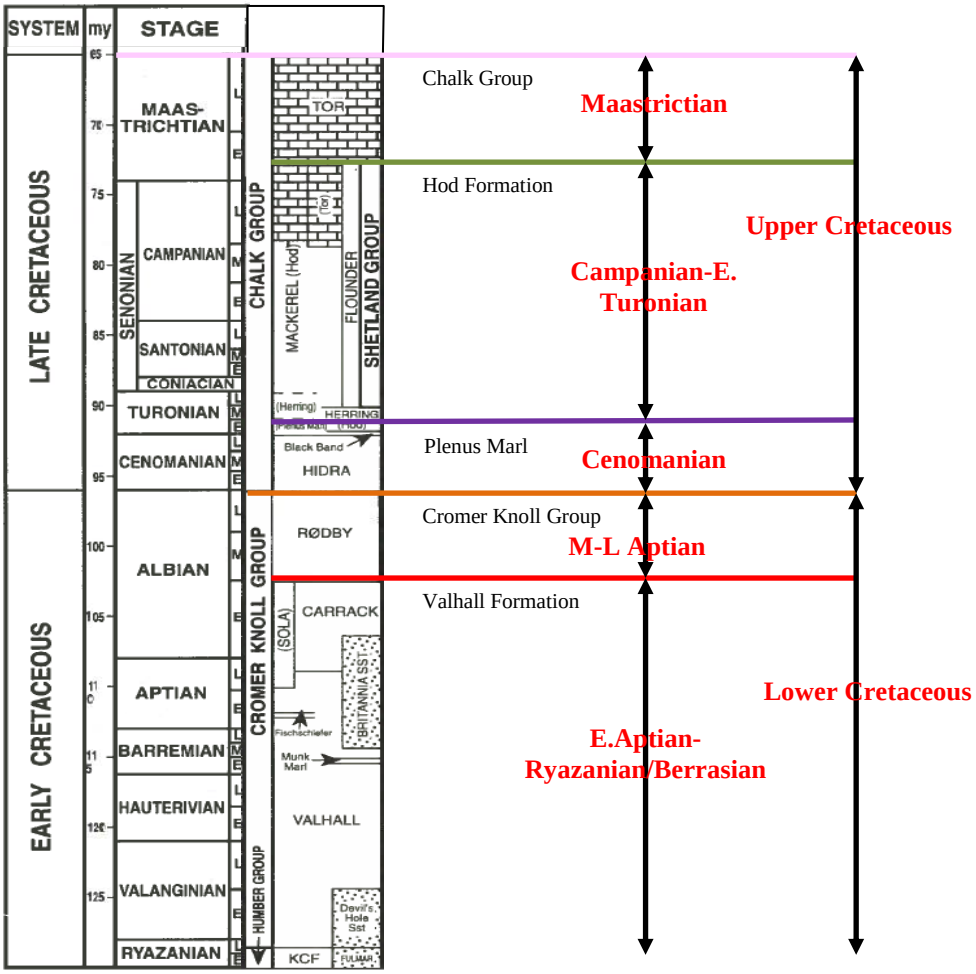

Figure 5.13: Isochrons created from horizon picks with corresponding chronostratigraphy.
Note that Ryazanian is a British Lower Cretaceous stage and is roughly equivalent to the Berrasian.

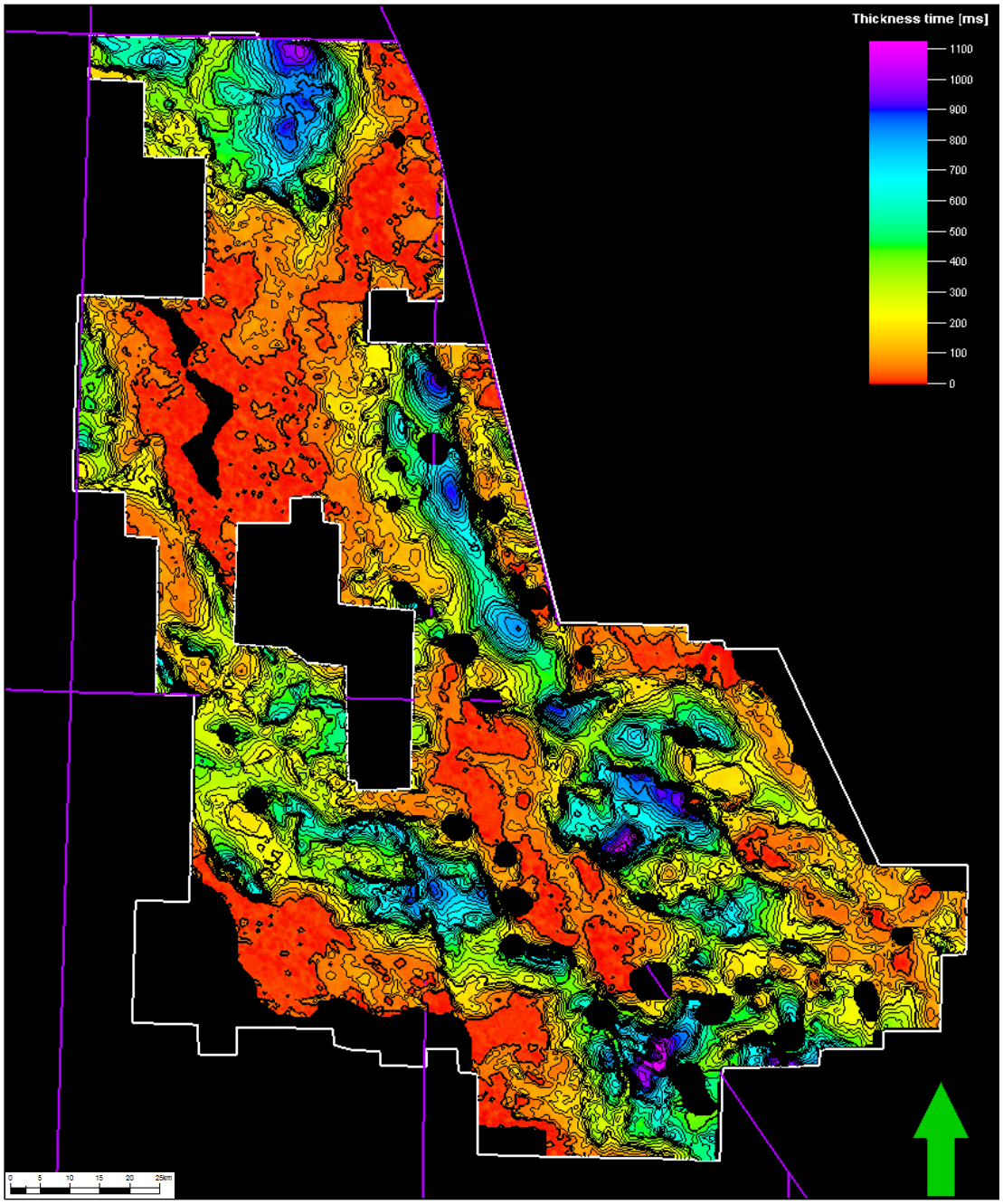

Figure 5.14: An isochron of the entire Lower Cretaceous section showing the major depocentres.

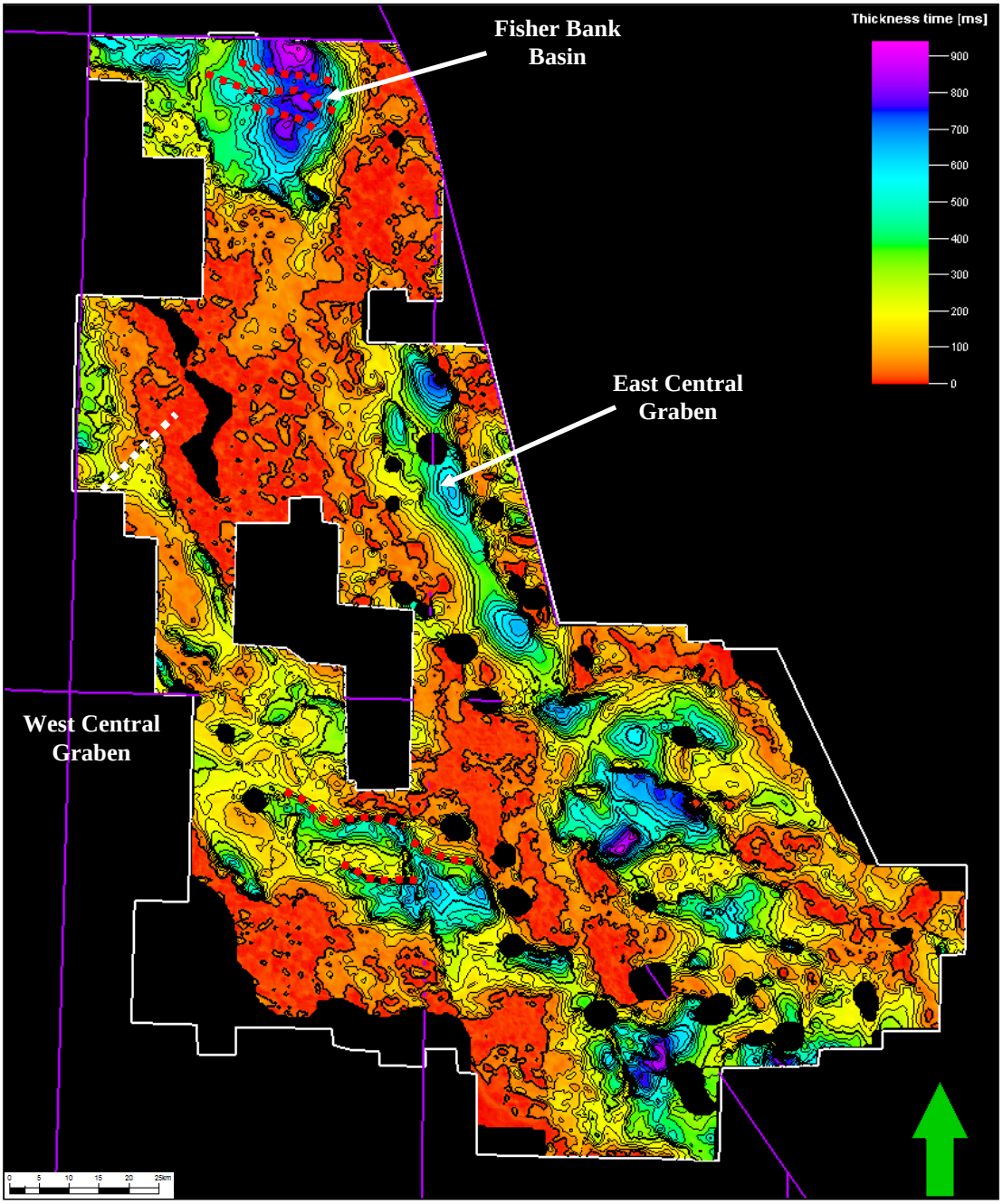

Figure 5.15: An isochron between the Valhall Formation and Base Cetaceous equivalent to Early Aptian-Berrasian.

The major depocentres during this time were the East and West Central Grabens and the Fisher Bank Basin. There are W-E lineaments (red) which appear to control the locations of the Early Cretaceous thickening packages while a NE-SW fault (white) is seen cutting the West Central Graben with Cretaceous thickening into its hanging-wall.

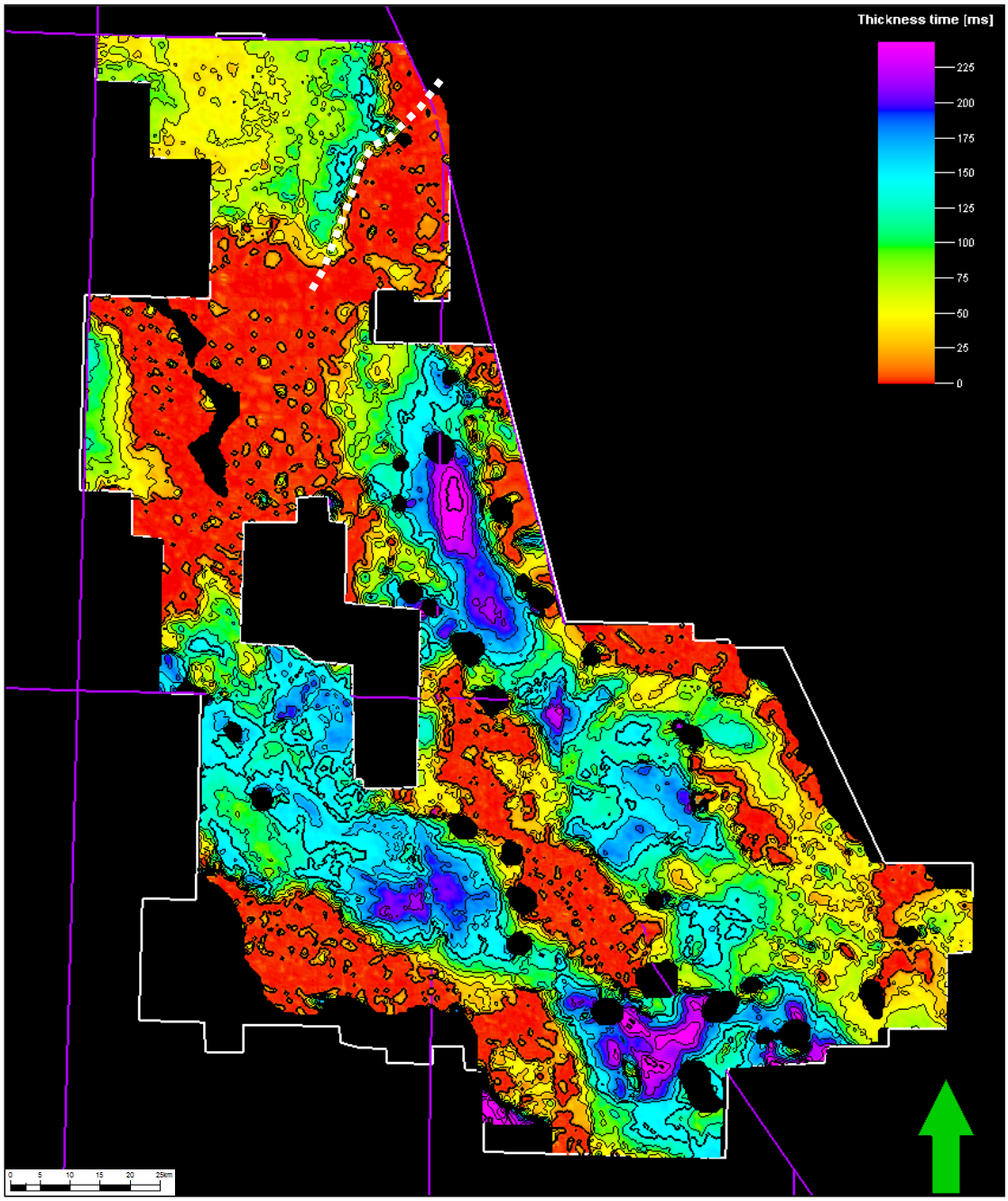

Figure 5.16: An isochron between the top of the Cromer Knoll Group and the Valhall Formation equivalent to the Mid-Late Aptian.

There is an obvious change in deposition between this and earlier Cretaceous times as there is no longer a major depocentre in the Fisher Bank Basin. There is however, thickening into the NE-SW Jaeren High Fault (white).

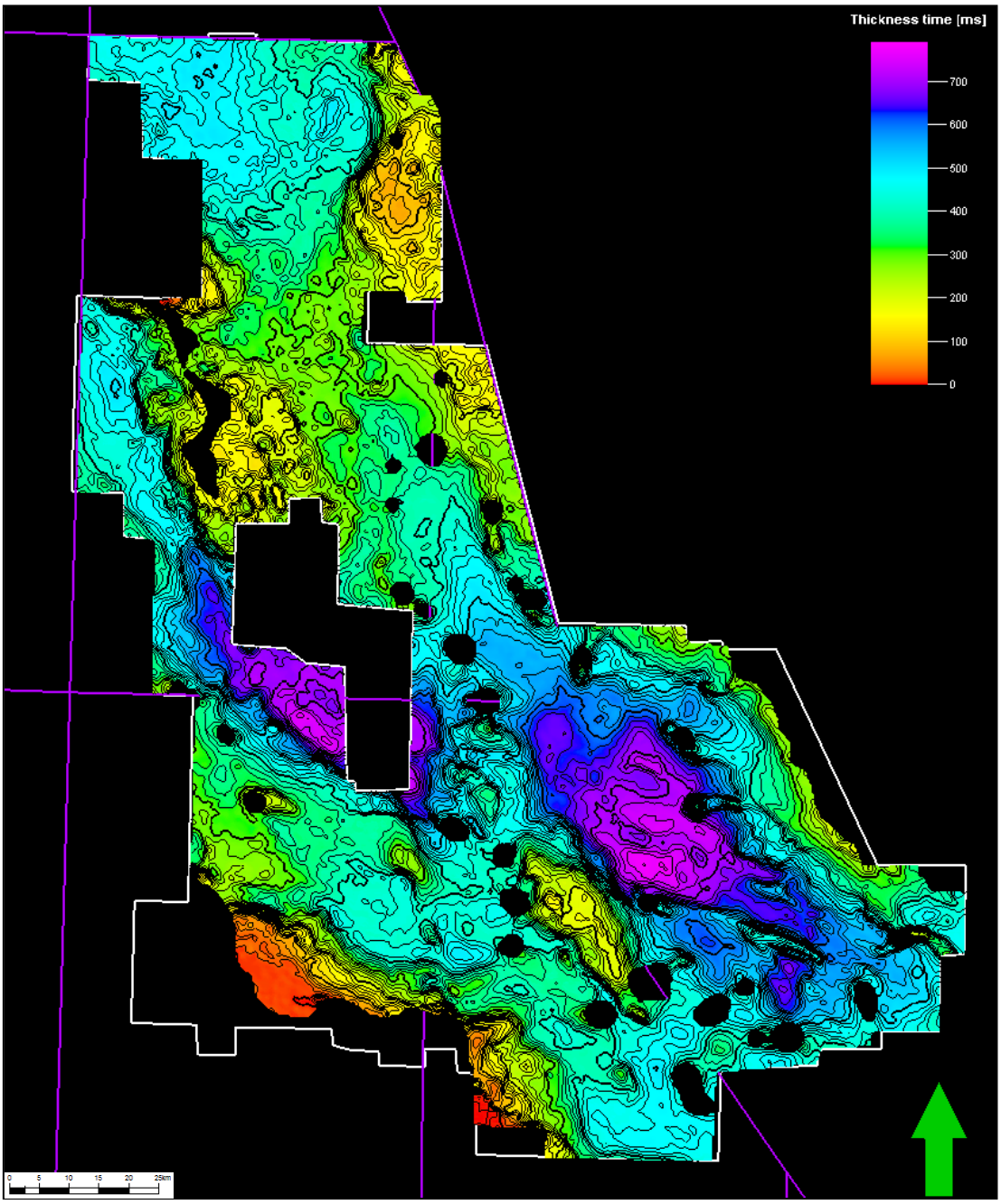

Figure 5.17: An isochron of the entire Upper Cretaceous Chalk Group section showing the main Late Cretaceous depocentres.

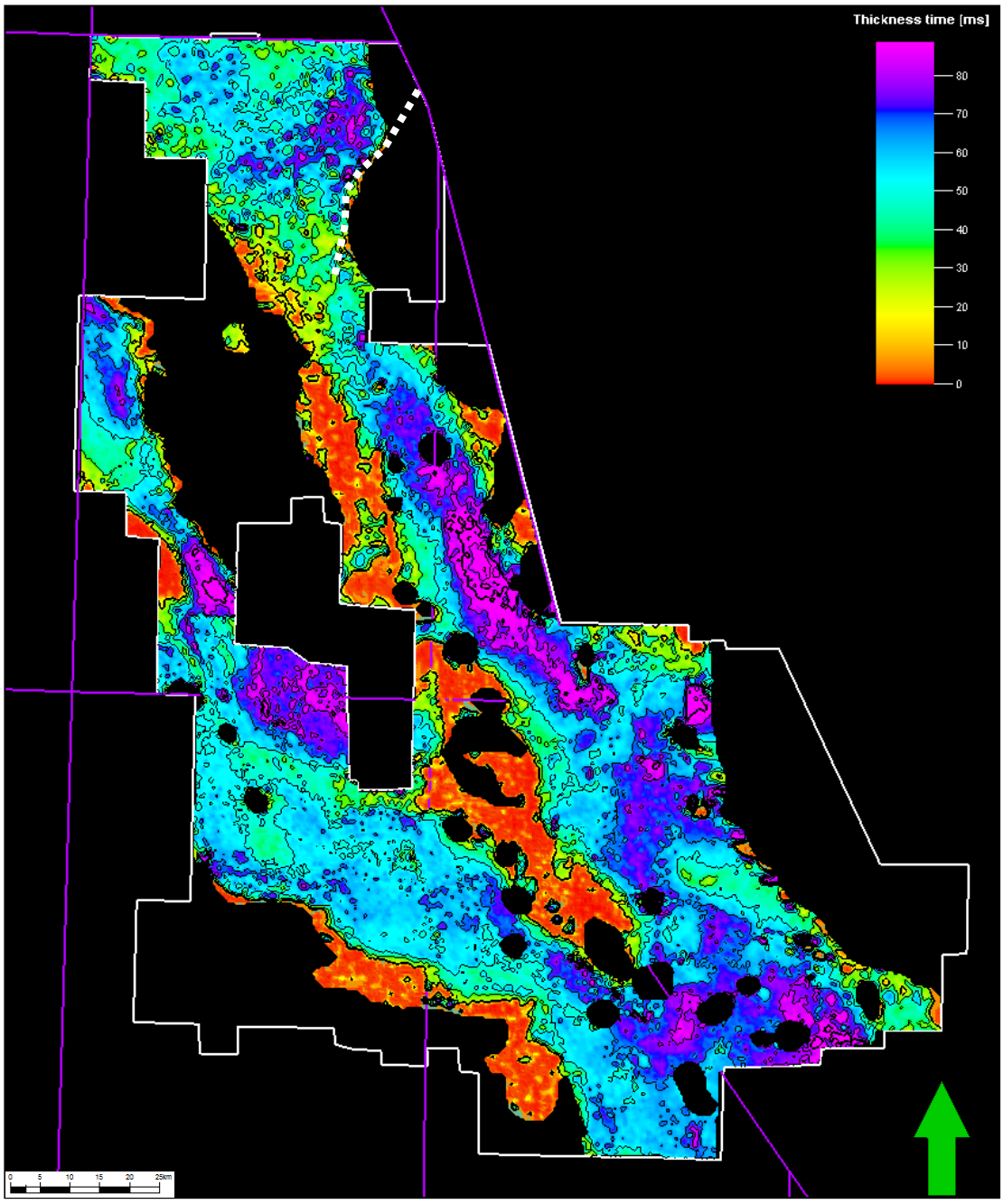

Figure 5.18: An isochron between the Plenus Marl (Lower-Middle Chalk Group) and Cromer Knoll Group equivalent to the Early Turonian and Cenomanian.

During this period thickening into the Jaeren Fault (white) continued.

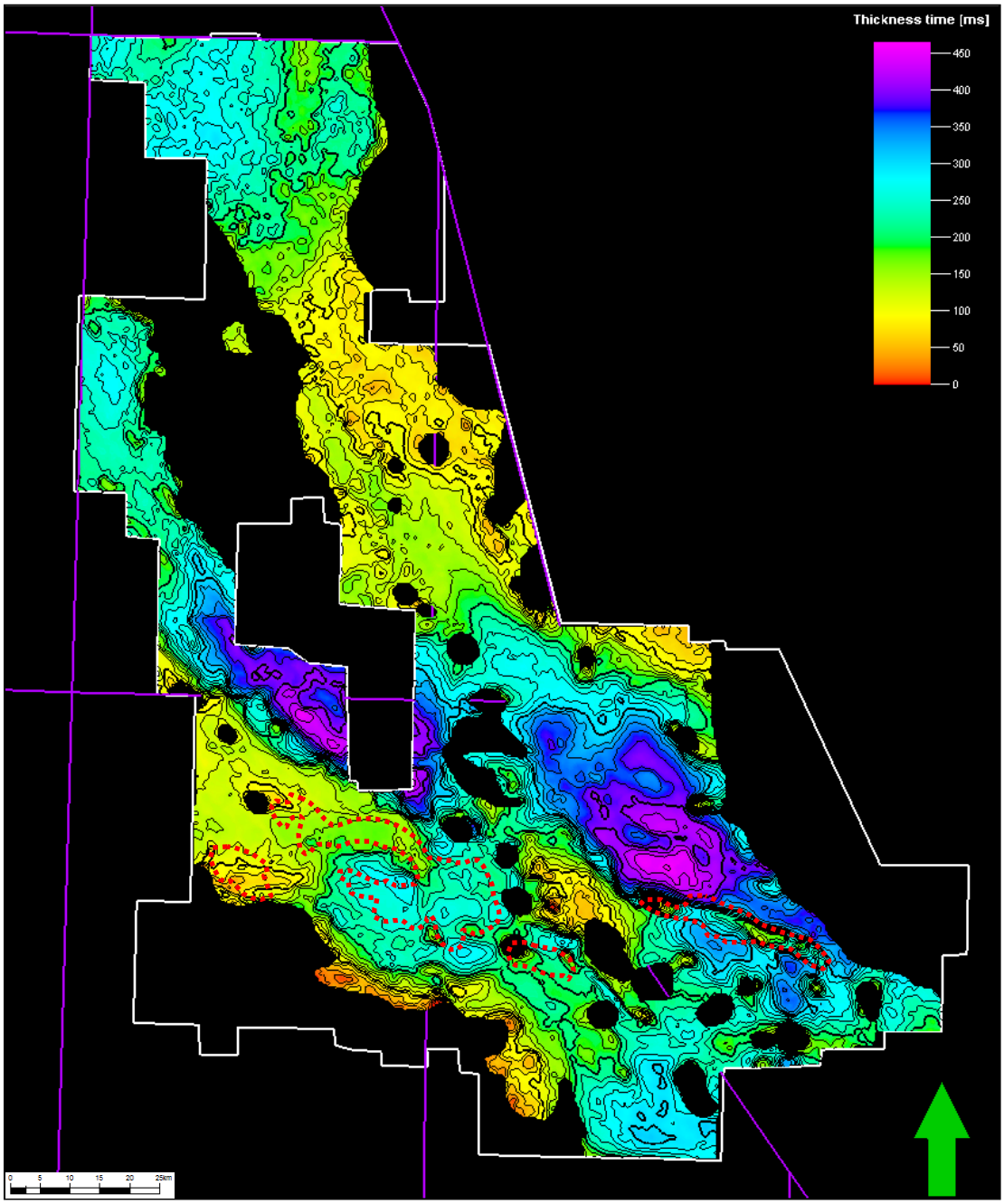

Figure 5.19: An isochron between the Hod Formation and Plenus Marl, equivalent to Campanian-Early Turonian.

Significant changes occurred during this period. Some areas which were Early Cretaceous depocentres (red boxes) have undergone uplift and have a thinner Mid-Late Cretaceous cover.

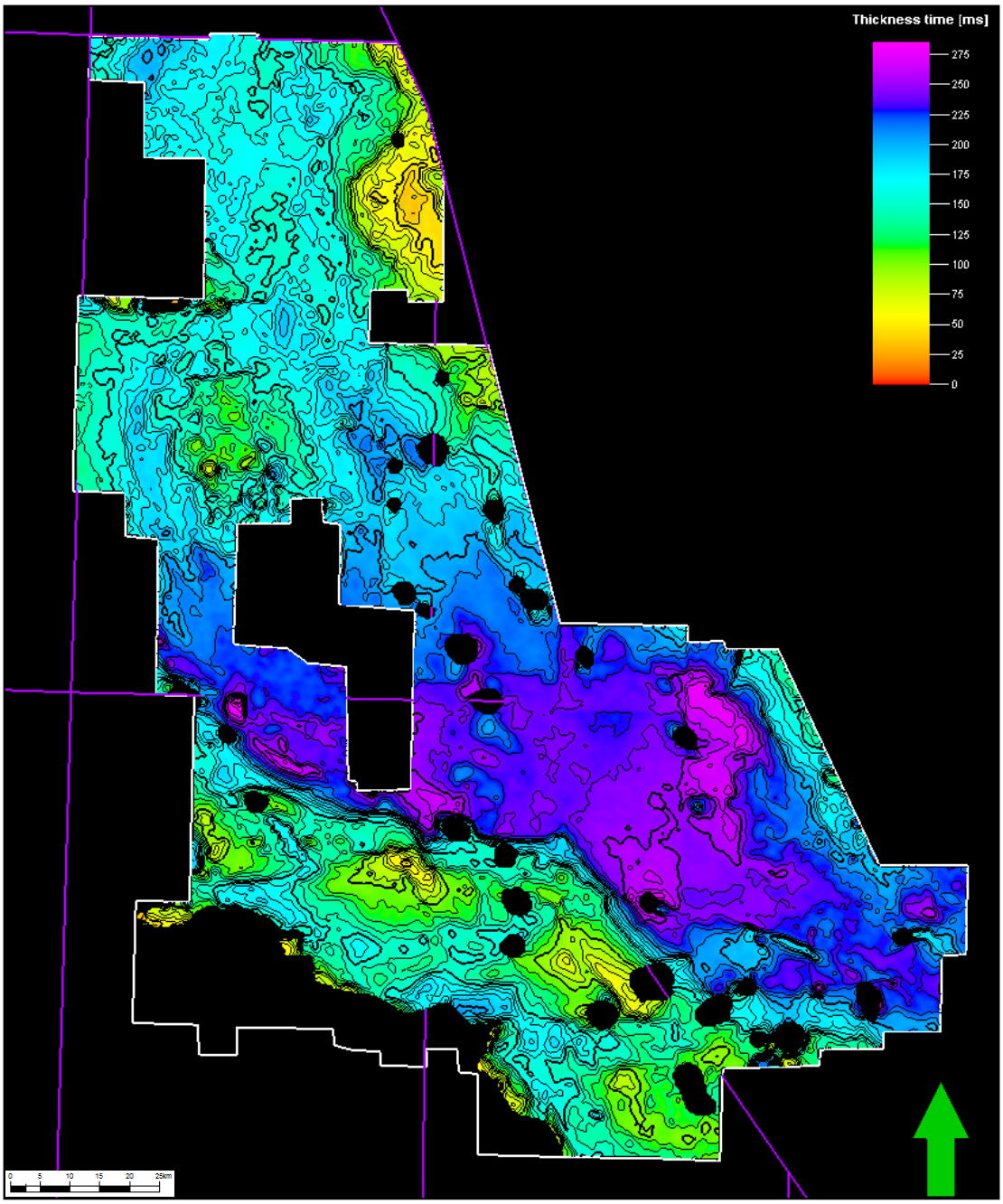

Figure 5.20: An isochron between the top Chalk Group and Hod Formation equivalent to the Maastrichtian.

The depocentres during this period are removed from the Early Cretaceous ones which have undergone uplift (essentially the majority of the southernmost West Central Graben).

In order to make sense of the structural events seen in the North Sea we must be able to relate them to large-scale tectonic processes. No tectonism occurred in the Central North Sea directly during the Cretaceous but far-field stresses from the opening of the Atlantic Ocean to the west and the Alpine orogeny to the south appear to have exerted a significant control on its structural evolution. Inversion tectonics in the Southern North Sea have traditionally been linked to Alpine orogenesis (Ziegler 1990) but mapping undertaken in this study notes evidence of Mid-Cretaceous age unconformities (seen in Figure 5.34) which correspond with those mapped in the Southern North Sea (Figure 5.40 and Appendix 4) and indicate a North-Atlantic component to the inversion.

Investigation of the relative influences of both these events must begin with an evaluation of the timing of events in each tectonic episode which can be compared with the ages of the reactivated faults and inversion structures seen in the Central and Southern North seas.

The history of the North Atlantic rift began with extension in the Triassic. Data from the Rockall trough, East Irish Sea, Newfoundland and the Labrador Sea all point to a Late Triassic initiation of rifting, linked to the divergence of Africa from the North American regions of Pangaea and Greenland from Canada (Chadwick et al. 1989; Knott et al. 1993; Musgrove et al. 1996; Roberts et al. 1999; Sinclair et al. 1999; Larsen et al. 2009). At this stage the north propagating Atlantic rift and south propagating Arctic rift were separate but during the Late Jurassic they joined through

the Bay of Biscay to become the Rockall Trough, Faroe - Shetland , Vøring and Møre Basins (Roberts et al. 1999).

Sea-floor spreading commenced in the Middle Jurassic in the Central Atlantic but was decoupled from the north along the Azores-Gibraltar Fracture Zone (Dore et al. 1999; Roberts et al. 1999). The locus of spreading instead moved east through the Gibraltar Transform to initiate separation of Iberia and North America and the opening of the western Tethys (Figure 5.21).

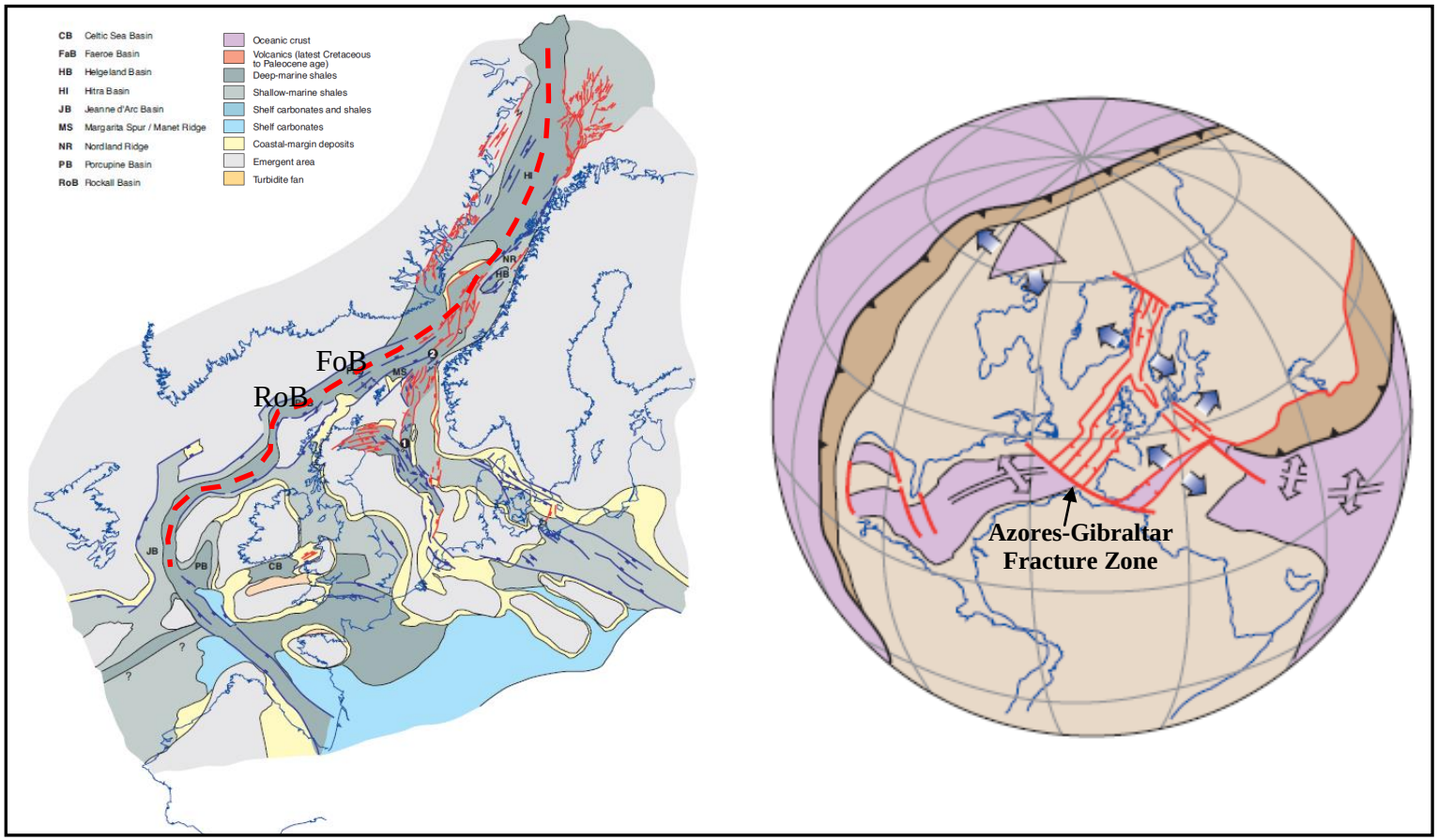

Figure 5.21: During the Late Jurassic the North Atlantic rift joined with the Arctic rift through the Rockall and Faroe-Shetland Basins but was separated from the mid-Atlantic rift by the Azores-Gibraltar Fracture Zone. The locus of extension instead moved east.
Images modified after (Evans et al. 2003)

In the Early Cretaceous, Tethyan spreading ceased and subduction began on its northern margin (Coward et al. 1989; Dore et al. 1999) (Figure 5.22). During the Berriasian to Valanginian, extension continued in the Labrador Sea along with emplacement of dike swarms (Larsen et al. 2009) and rifting also occurred in the Rockall Trough, Faroe -Shetland Basin and Lusitanian Basin (Knott et al. 1993; Roberts et al. 1999; Sinclair et al. 1999). Rotation of the stress direction from E-W to NW-SE in the Hauterivian may signify a change in rift direction which resulted in propagation of the North Atlantic Rift away from the Rockall, Faroe-Shetland region and towards the Labrador Sea, forming a triple junction (Dore et al. 1999; Roberts et al. 1999) (Figure 5.23). The emplacement of the mantle plume which was to cause uplift of the Scotland-Shetland Plateau in the Palaeocene was possibly the driving force for this change in plate motion.

The Aptian marked a major change in rift propagation towards the Labrador rift and the northern rift was effectively terminated by the end of the age. The Bay of Biscay also opened in the Late Cretaceous but movement had ceased by the Early Palaeocene. A major sea-level fall marked this tectonic pulse (Ziegler 1990). Oceanic crust was also established between the North Iberian margins and Grand Banks (Dore et al. 1999). Extension continued through the Late Cretaceous punctuated by pulses of activity, the most significant of which occurred in the Santonian to Early Maastrichtian (Chalmers 1991; Roberts et al. 1999).

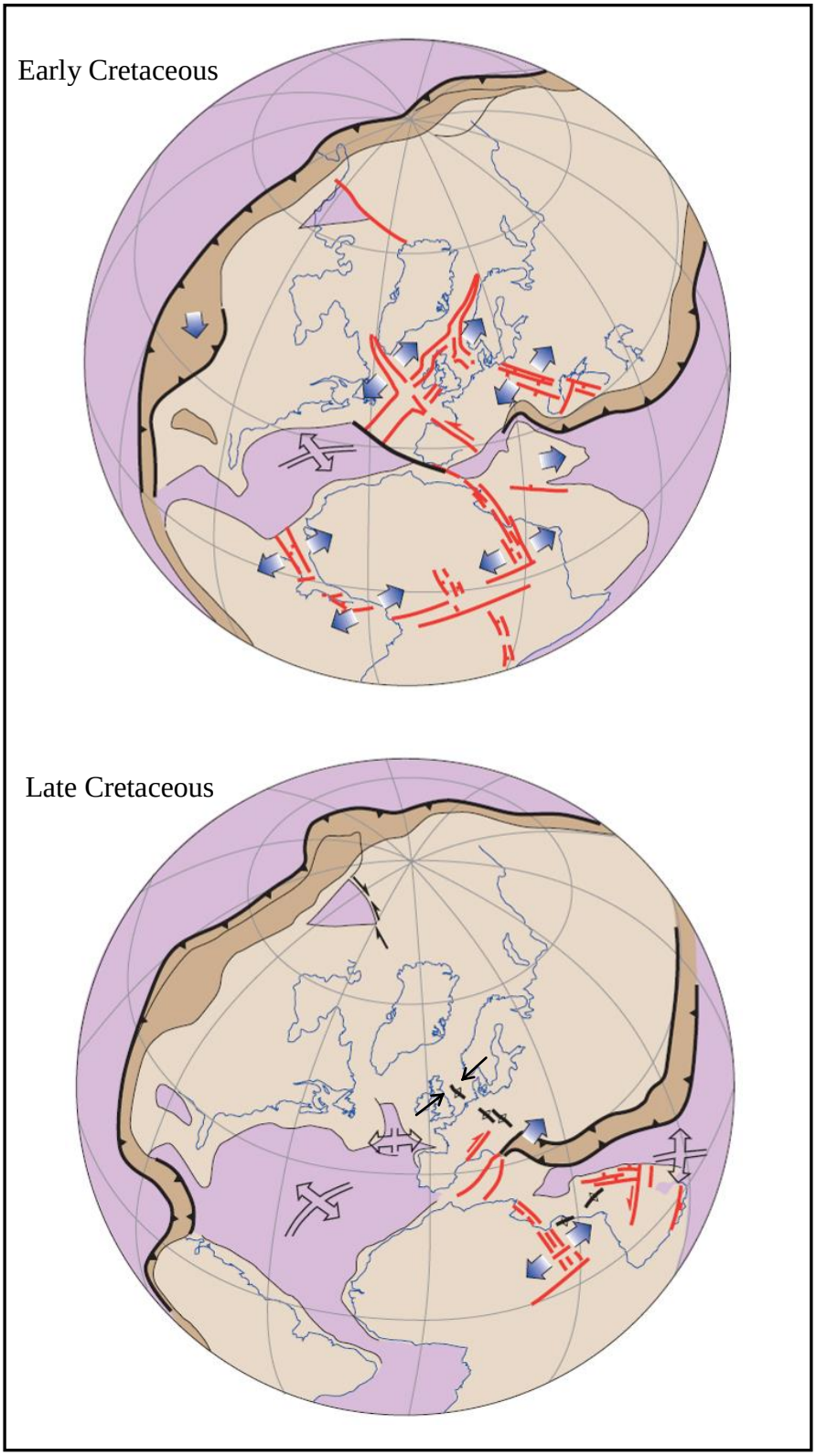

Figure 5.22: Global tectonics during the Early and Late Cretaceous showing the influence of the North Atlantic rift, Labrador Sea and Alpine orogeny.
Images modified after (Evans et al. 2003)

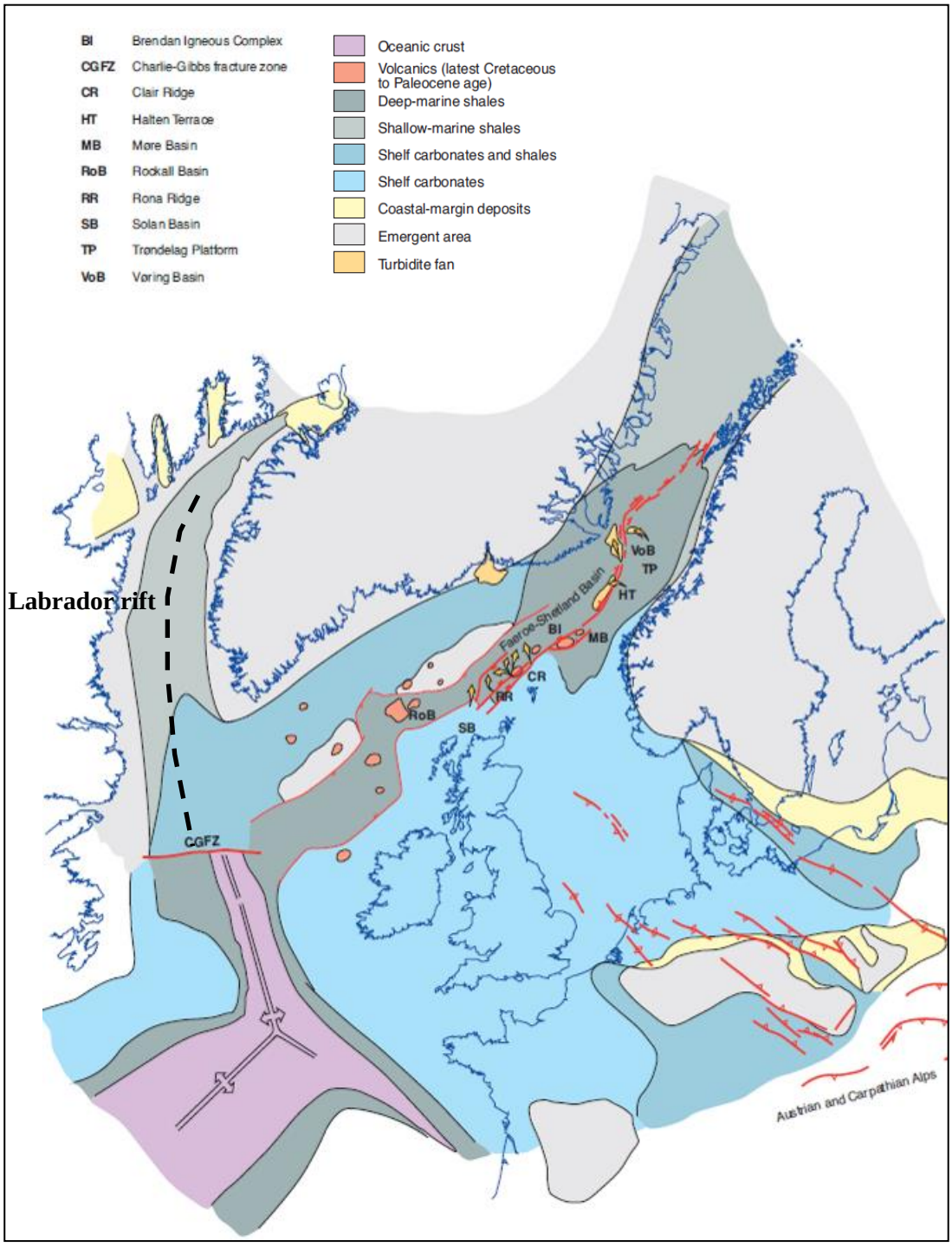

Figure 5.23: A change in rift direction occurred in the Mid-Cretaceous as the locus of extension shifted away from the Arctic rift to the Labrador Sea.
Image modified after (Evans et al. 2003)

Alpine tectonics (Figure 5.24) resulted from subduction of the Tethys Ocean and continental collision. Intense deformation and the emplacement of successive thrust slices have made the initial onset of deformation difficult to date. It is suggested that evidence of high pressure metamorphics of Jurassic and Cretaceous age indicate that convergence began very early in the eastern Tethys (Ziegler 1990). However, it is possible that Cretaceous ophiolite obduction occurred before continental collision or that the radiometric dates derived may be due to older rocks being caught up in younger tectonic events (Hunziker 1986; Coward et al. 1989). Mid Cretaceous compression is observed in the Central French Alps where gently dipping Upper Cretaceous rocks rest on tightly inclined Coniacian age folds (Coward et al. 1989) and further folding elsewhere in eastern areas is dated as Aptian-Albian. These compressional structures could be the result of collision between microcratons prior to true orogenesis or result from stress transmitted from the subduction front (Ziegler 1990). True convergence, beginning after subduction of the ocean floor was complete began in the Palaeocene (Doornebal 2010).

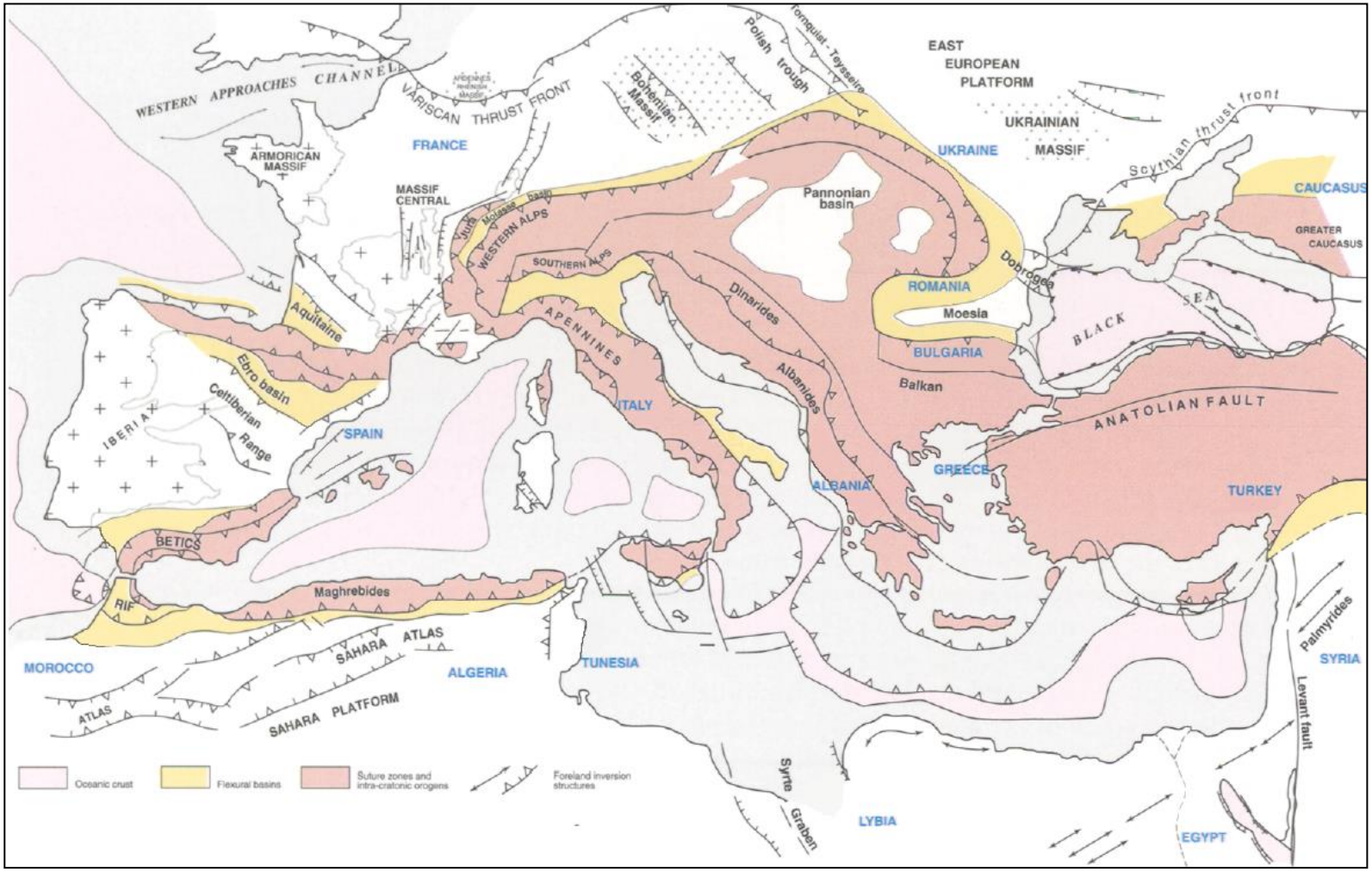

Figure 5.24: Tectonic framework of the Alpine area.
Image modified after (Ziegler et al. 1999)

The structures created in Northwest Europe by the intra-plate forces set up by and as a consequence of, North Atlantic or Alpine tectonic events range from locally inverted faults to large-scale inversion anticlines. The earliest compressive structures seen in the North Sea are of Barremian- Berrasian age and can be observed by comparing the Early Cretaceous and Jurassic isochron maps. Movement on E-W striking faults in the Fisher Bank Basin observed on Early Cretaceous isochrons are not seen on the Jurassic isochron and therefore represent reactivated Permo-Triassic lineaments (Figure 5.25). In other areas, early structural inversion was confined to narrow zones with reverse faulting (Vejbaek et al. 2002) but the influence of salt in the Central North Sea along with renewed movement on major faults led to large-scale structures. This can be observed in the shifting of depocentres through the Early Cretaceous due to doming of the entire Fisher Bank Basin (Figures 5.26 and 5.27). Localised inversion of a NE-SW striking Caledonian age fault is also noted (Figures 5.28 and 5.29).

Separate inversion pulses during this period such as those which are suggested to occur at the Valangian-Hautervian boundary can be distinguished in some areas but in the Central North Sea it is difficult to sub-divide the Valhall Formation and the earliest inversion pulses are grouped together.

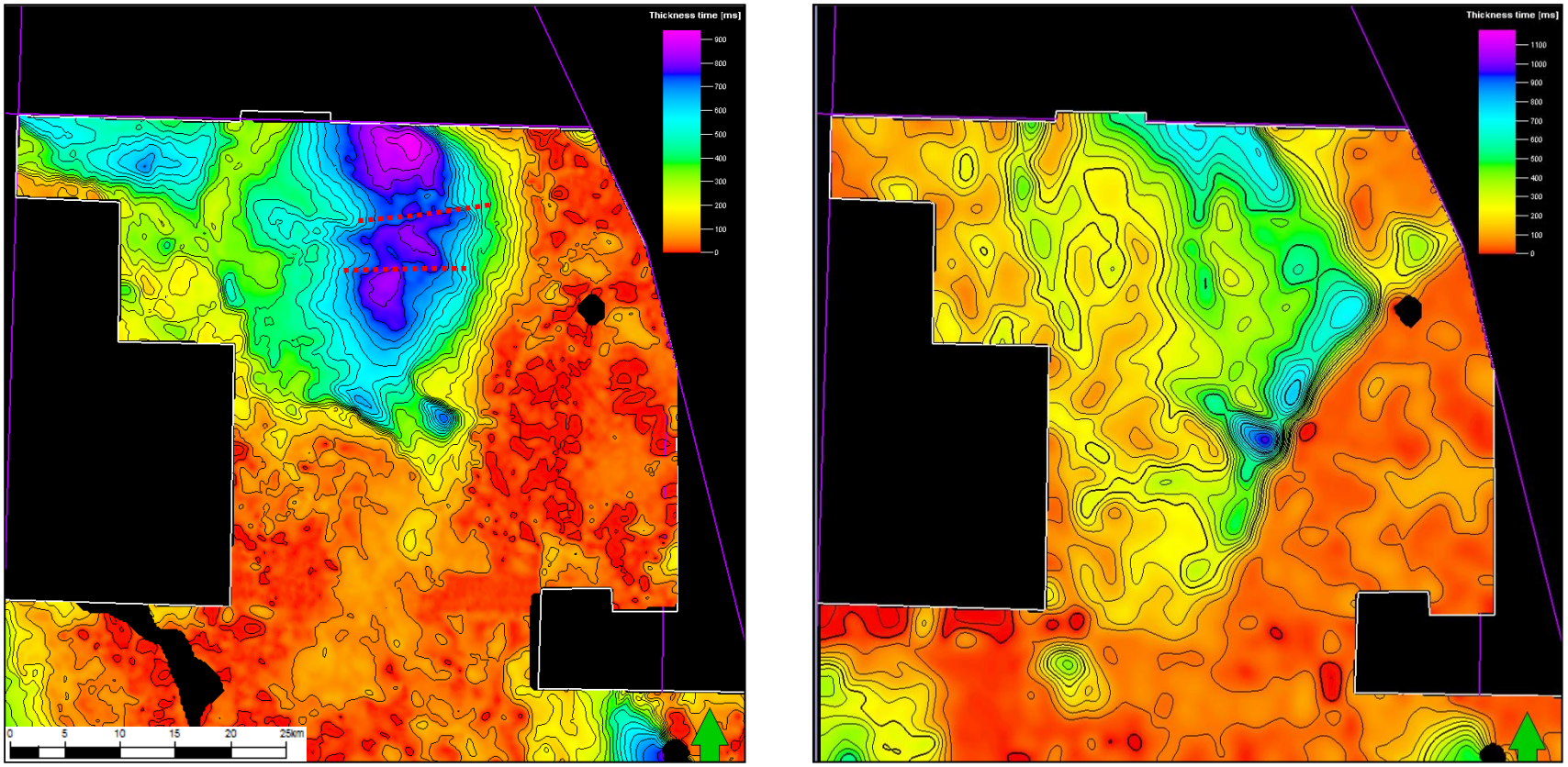

Figure 5.25: An isochron of the Early Aptian-Berrasian interval showing the W-E faults controlling the locations of the depocentres compared to a Jurassic isochron in which these faults are not seen.

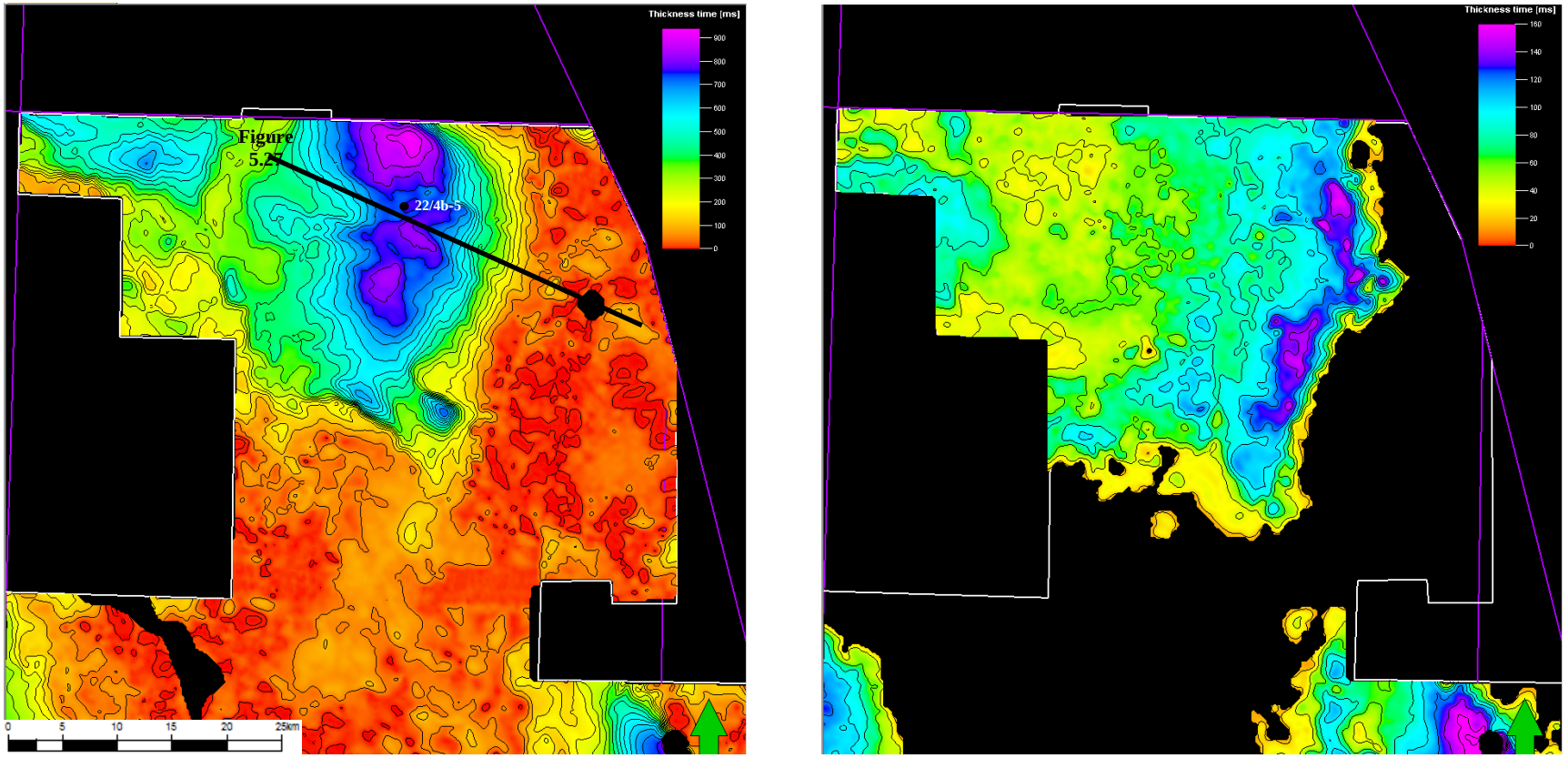

Figure 5.26: A comparison of the Early Aptian-Berrasian isochron with the Mid-Late Aptian isochron. Deposition in the Fisher Bank Basin does not occur later than the Early Aptian. After this period the depocentres move to the hanging-wall of the Jaeren Fault and areas to the west which appear to have been structurally higher during the earliest Cretaceous. This suggests that the basin may have been slightly inverted.

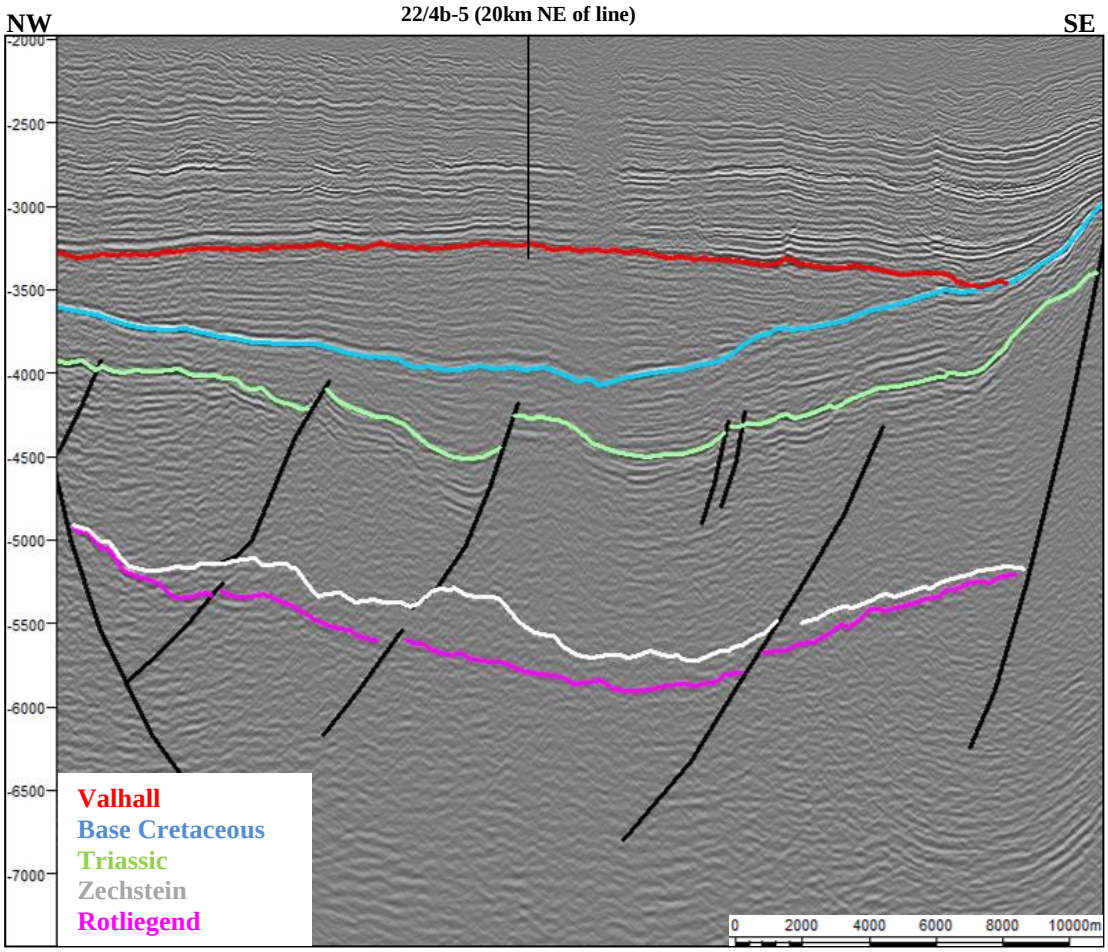

Figure 5.27: NW-SE seismic section across the Fisher Bank Basin showing the inverted Early Cretaceous infill and the influence of the Zechstein salt.
Location of section shown in Figure 5.26

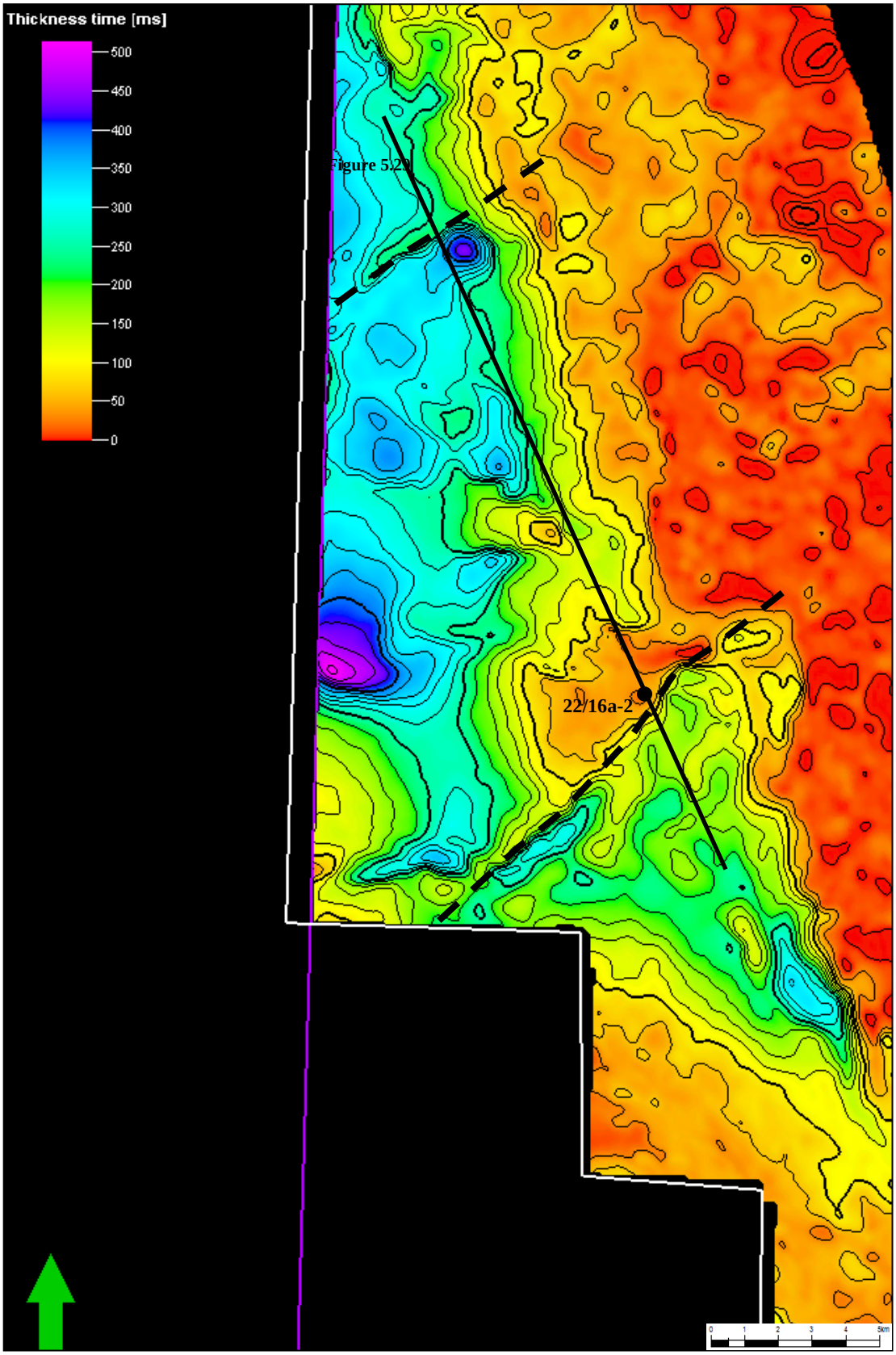

Figure 5.28: An Early Aptian-Berrasian isochron showing thickening into Caledonian NE-SW striking faults.
Location of Figure 5.29 noted.

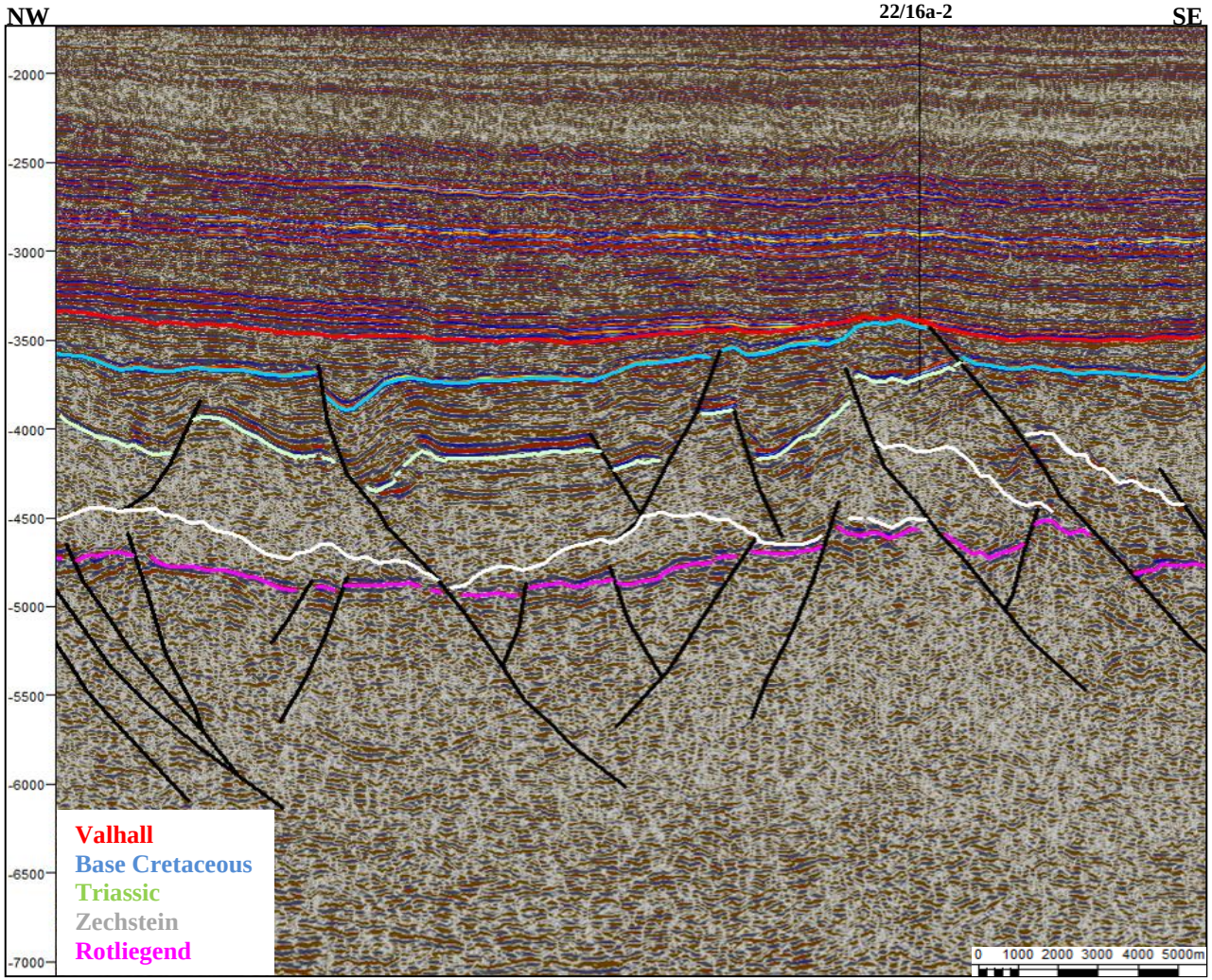

Figure 5.29: NW-SE seismic section showing the Caledonian trend faults with Early Cretaceous thickening into them.

In the Broad Fourteens Basin in the Dutch sector of the North Sea the first inversion structures are also noted as early as the Berrasian (Oakman et al. 1998).

Aptian inversion is also well documented in the Broad Fourteens Basin with this pulse being known as the Austrian Event (Ziegler 1990; Oakman et al. 1998). In the Central North Sea, reactivation of the major Caledonian-trend Jaeren Fault may be linked to this compressional pulse (Figures 5.30 and 5.31).

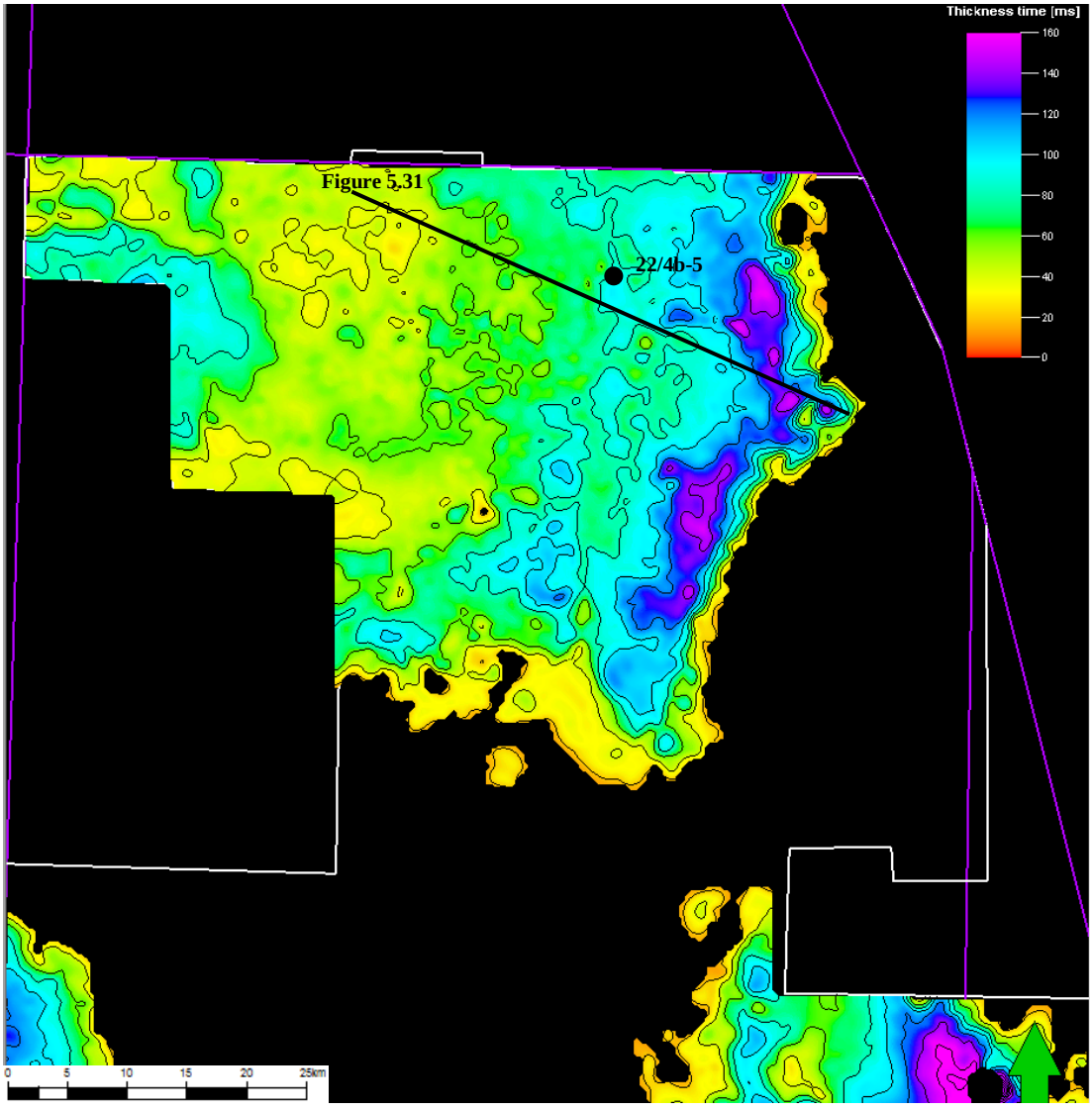

Figure 5.30: A Mid-Late Aptian isochron showing deposition into the hanging-wall of the Jaeren Fault.
Location of Figure 5.31 noted.

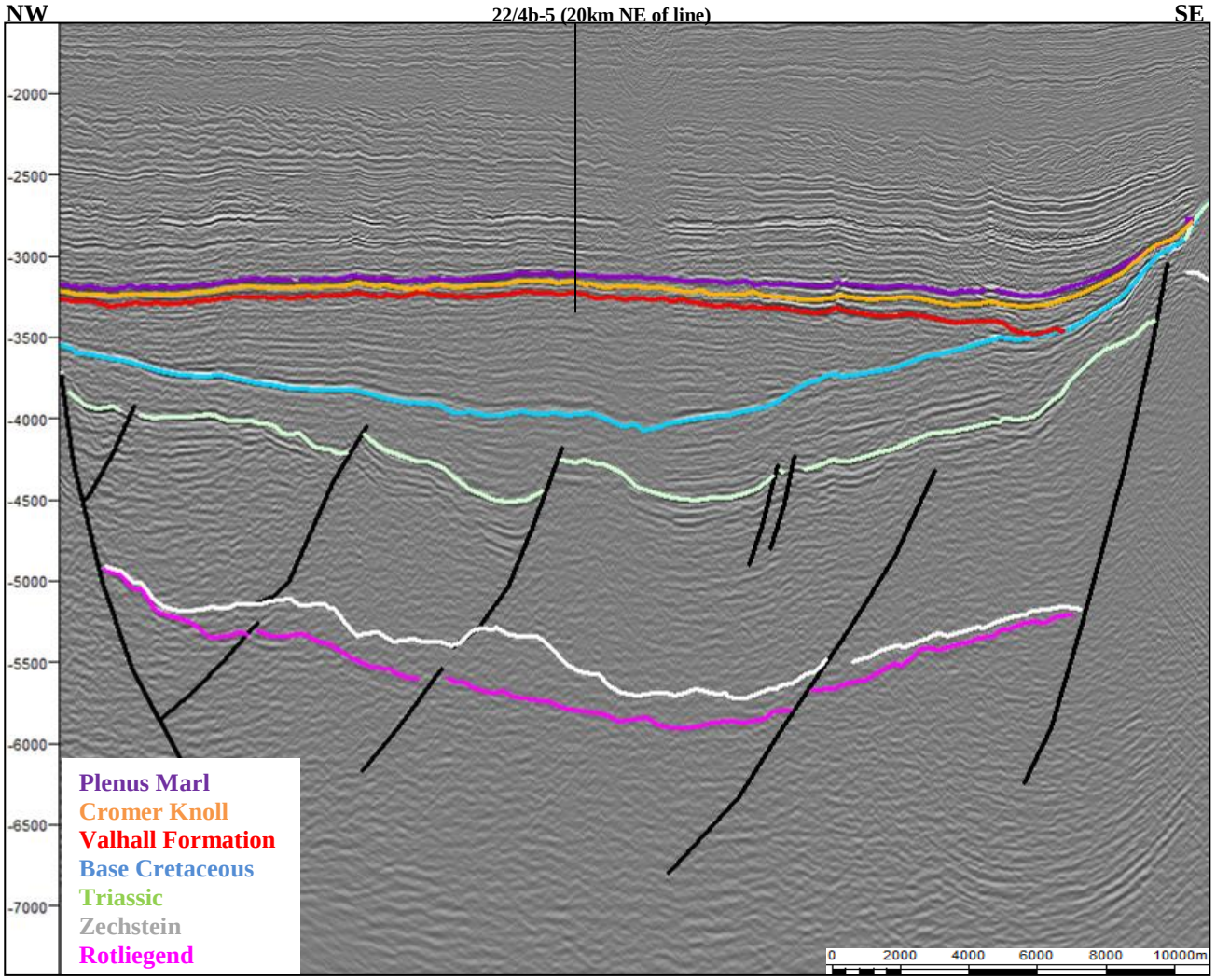

Figure 5.31: NW-SE seismic section demonstrating Aptian-age thickening into the Jaeren Fault

These early inversion features appear only on W-E or NE-SW striking faults which is consistent with both compression from the south Alpine region or the propagating Arctic rift. However, the proximity of the Arctic rift and the lack of evidence for early Alpine compression strongly suggests that the tectonic stresses which led to the geometries observed in the Central North Sea were transmitted from the North Atlantic and were not linked to Alpine deformation as is the current model.

In the Mid-Late Cretaceous, inversion pulses were much stronger and the resulting deformation can be imaged well on seismic. Strong inversion began in the Turonian and large scale ridges and anticlines in the Central North Sea began to form aided by Zechstein movements. Further south, the Dutch Vlieland and Terschelling Basins also underwent uplift (de Jager 2007). Tectonic stresses abated slightly during the Coniacian and then a further pulse occurred during the Santonian.

The compression associated with the Santonian pulse caused renewal of salt tectonics in the Central North Sea and uplift of Early Cretaceous depocentres. A case study from the East Central Graben (Figure 5.32) illustrates some of these structures.

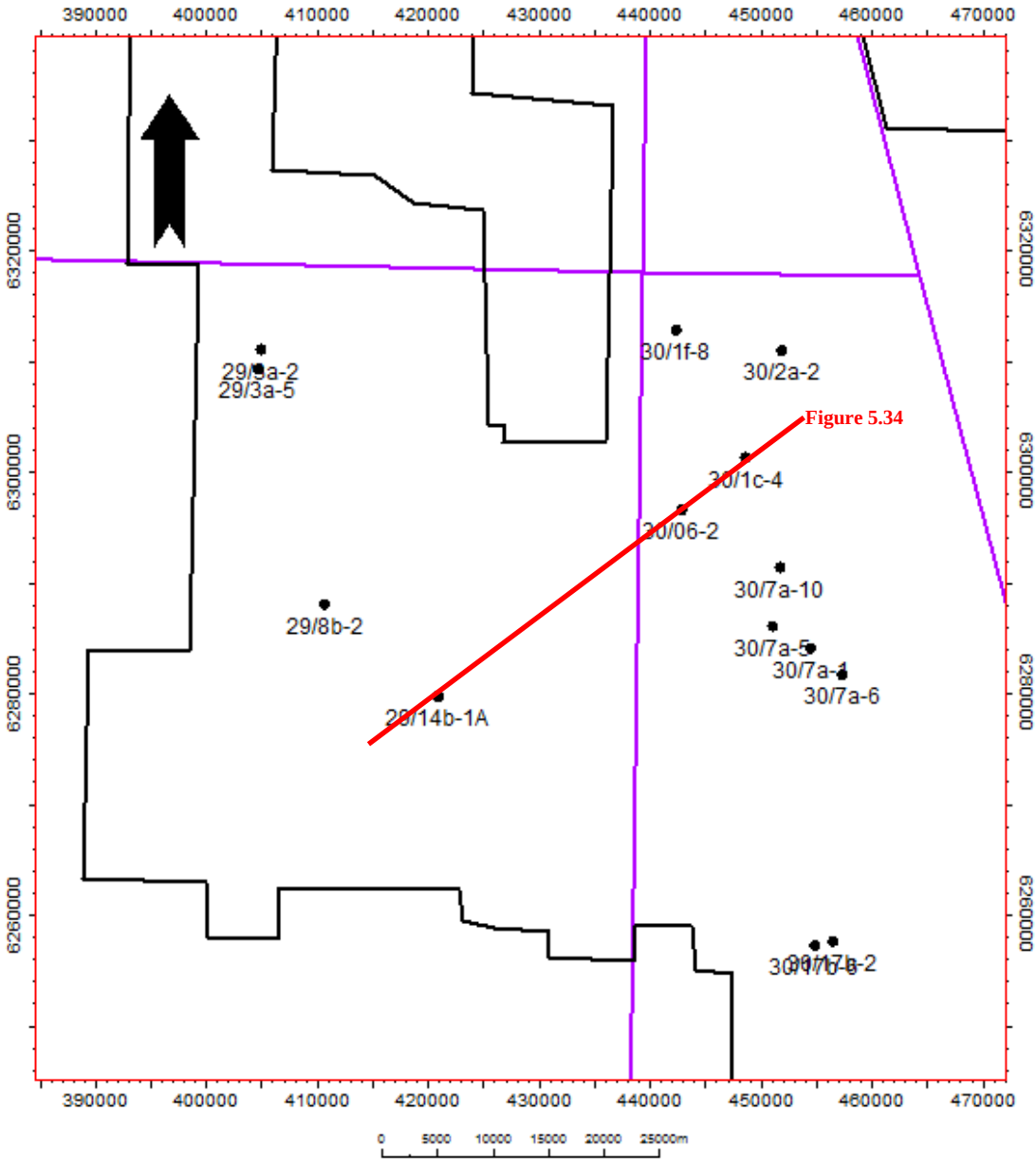

Figure 5.32: Location of the study area showing the wells used for seismic calibration and biostratigraphic dating.

In this area comparison of the pre-Turonian isochrons with the Campanian-Early Turonian one shows that the depocentres have shifted (Figure 5.33). Seismic interpretation of the area demonstrates that this is due to uplift of these Early Cretaceous depocentres by salt intrusion beneath them (Figure 5.34). There may also be a component of true structural inversion of underlying fault planes to create some of the anticlines but the sub-salt imaging precludes any positive statement either way about this.

The timing of the uplift can be constrained by the significant unconformity within the Upper Cretaceous Hod Formation seen on the seismic data which formed as erosion occurred on the uplifted anticlines (Figure 5.34). Where this is mapped to its correlative conformity biostratigraphic data from wells 29/3a-2, 29/3a-5, 29/8b-2, 30/1f-8, 30/2a-2, 30/7a-10, 30/7a-5, 30/7a-1, 30/7a-6, 30/17b-2, 30/17b-6 dates it as Santonian.

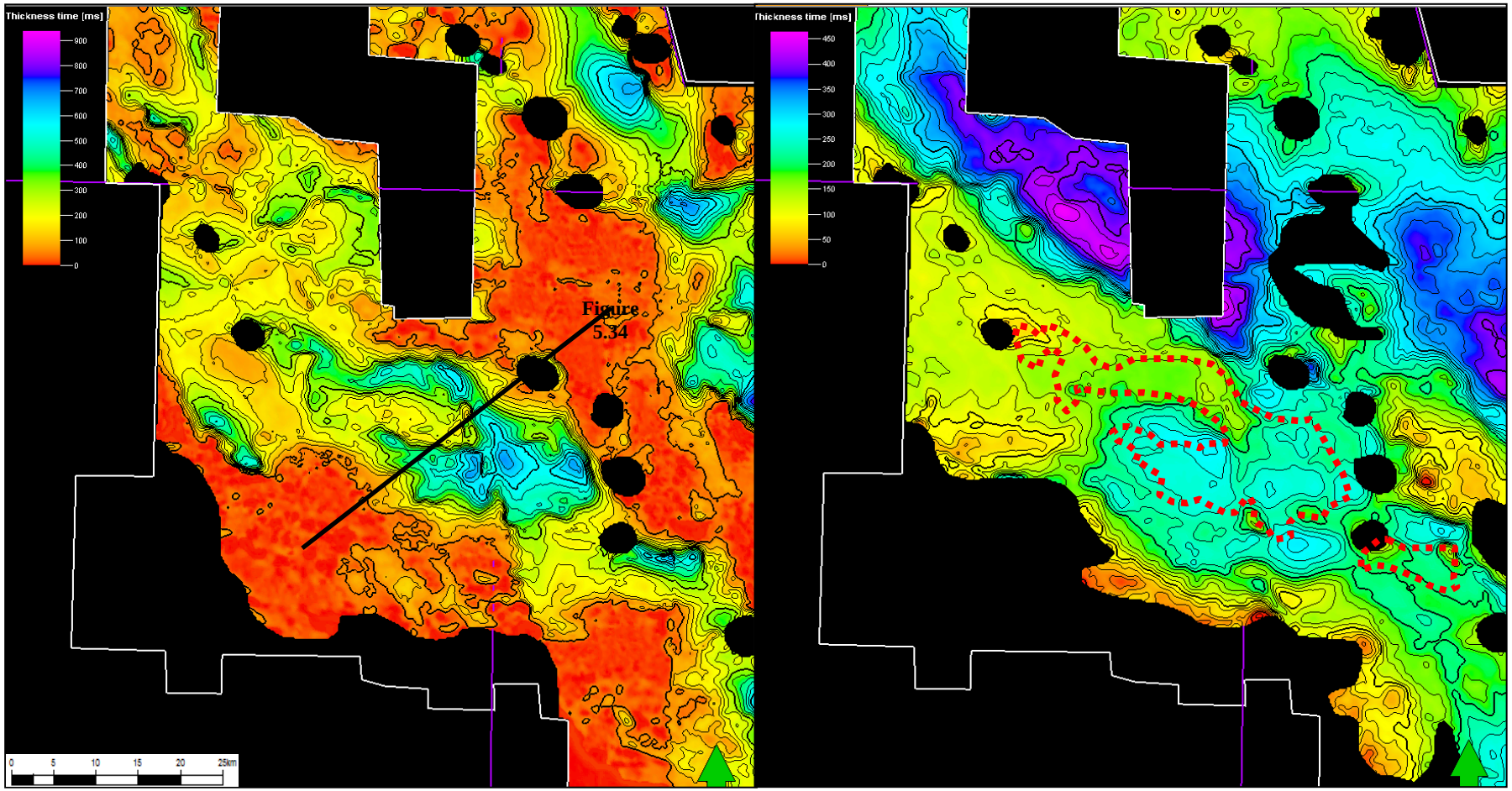

Figure 5.33: An isochron of the Early Aptian-Berrasian interval compared to one of the Campanian-Early Turonian showing shifting of the depocentres.

Line of section of Figure 5.34 is shown, well locations can be found in Figure 5.33.

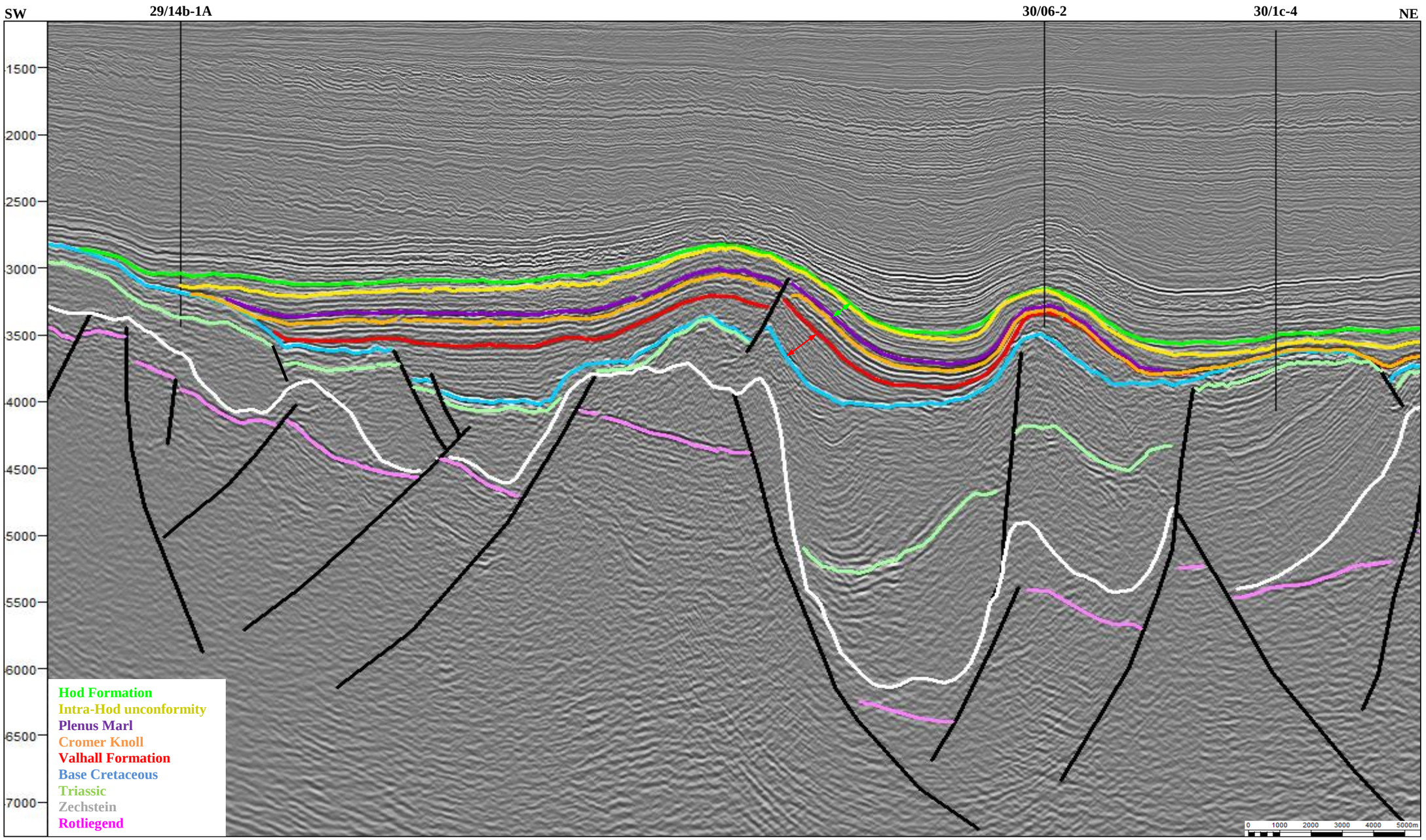

Figure 5.34: SW-NE seismic section across the uplifted Early Cretaceous depocentres showing the influence of renewed movements of the Zechstein salt and the creation of a significant Intra-Hod unconformity as the result of the doming.

Intervals shown by isochrons in Figure 5.33 are denoted by coloured arrows.

The unconformity, generated by fault reactivation and renewed salt movements, can be mapped over a significant area (Figure5.35). In some areas, it has been found to have extended through the Maastrichtian (Caillet et al. 1997; Bramwell et al. 1999; Farmer et al. 1999; Vejbaek et al. 2002). An isochron between the Hod Formation and the Santonian unconformity demonstrates the presence of many inversion and salt-induced ridges (Figure 5.36).

These structures are important in terms of prospectivity as many of the inversion anticlines are structural traps. Additionally, uplift of the Cretaceous Chalk Group led to intense fracturing creating permeability in a lithology which would not be considered a typical reservoir. Re-deposited chalk is also shed off the crests of the uplifted areas and this also has potential as a reservoir for hydrocarbons (Glennie 1998). This may be observed on the seismic data as a brightening of the reflectors on the flanks of the anticline (Figure 5.37)

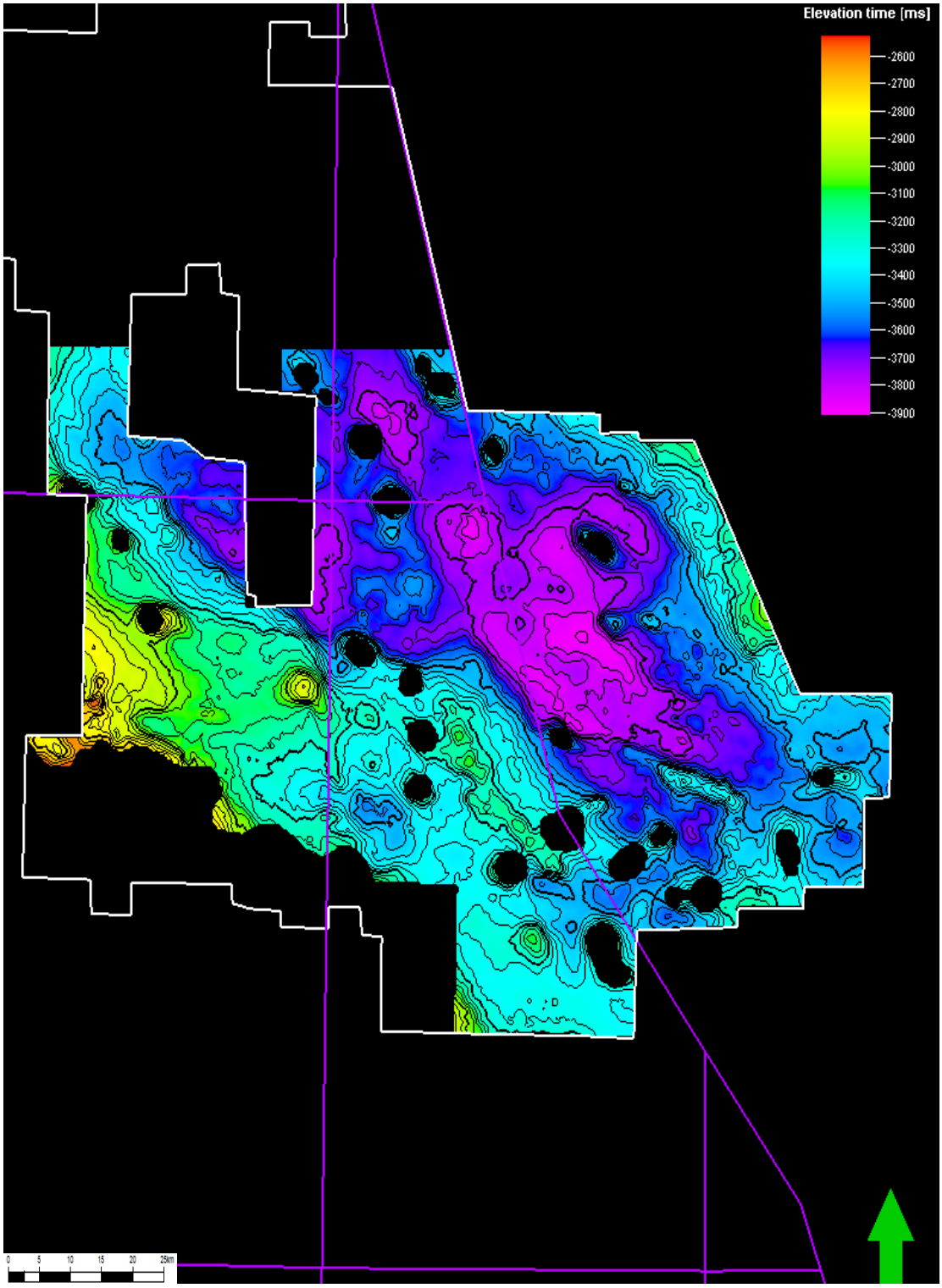

Figure 5.35: TWTT structure map of a prominent intra-Hod unconformity.

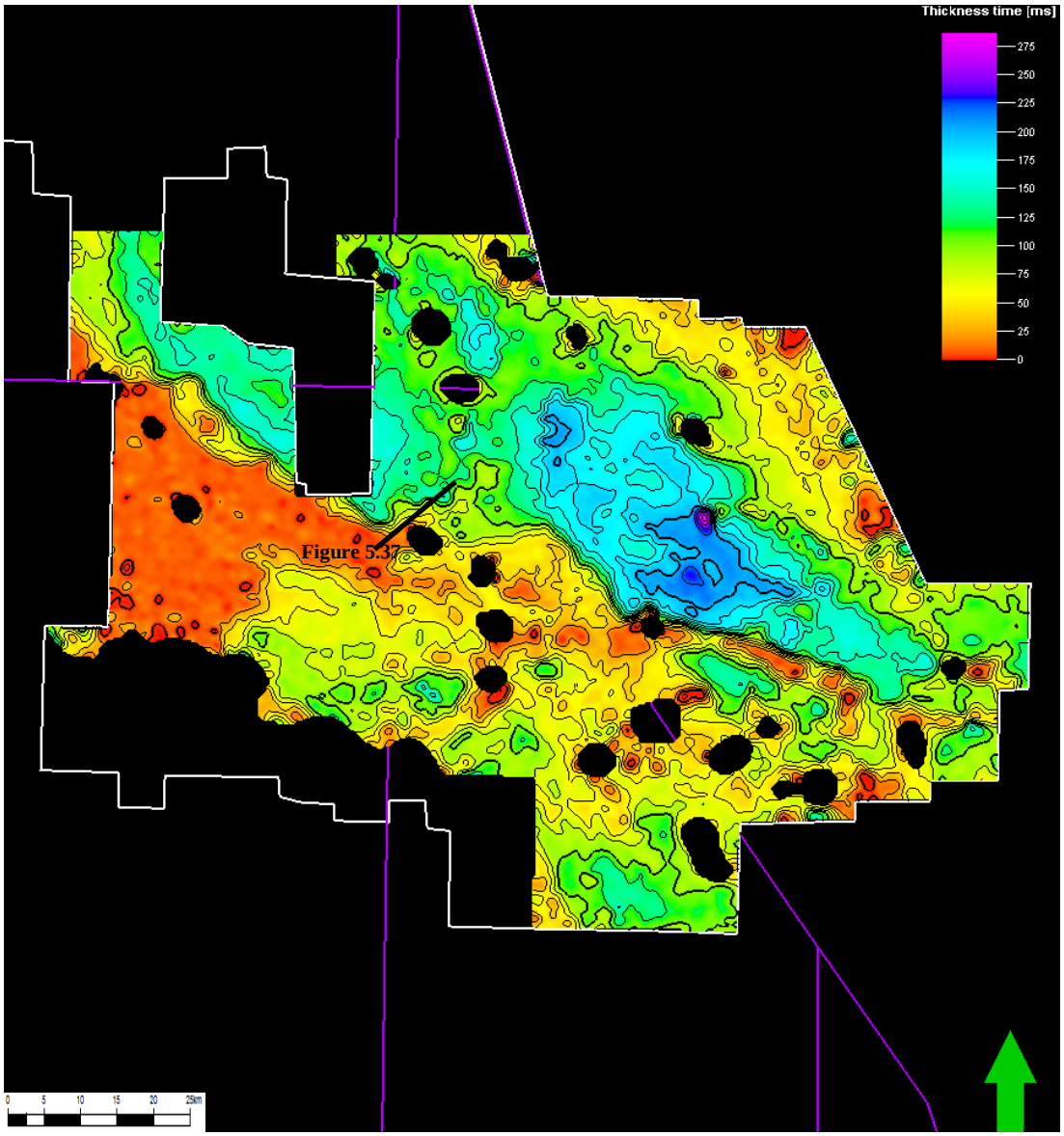

Figure 5.36: An isochron between the Hod Formation marker and the intra-Hod unconformity showing further ridges due to salt movements.
Location of Figure X noted.

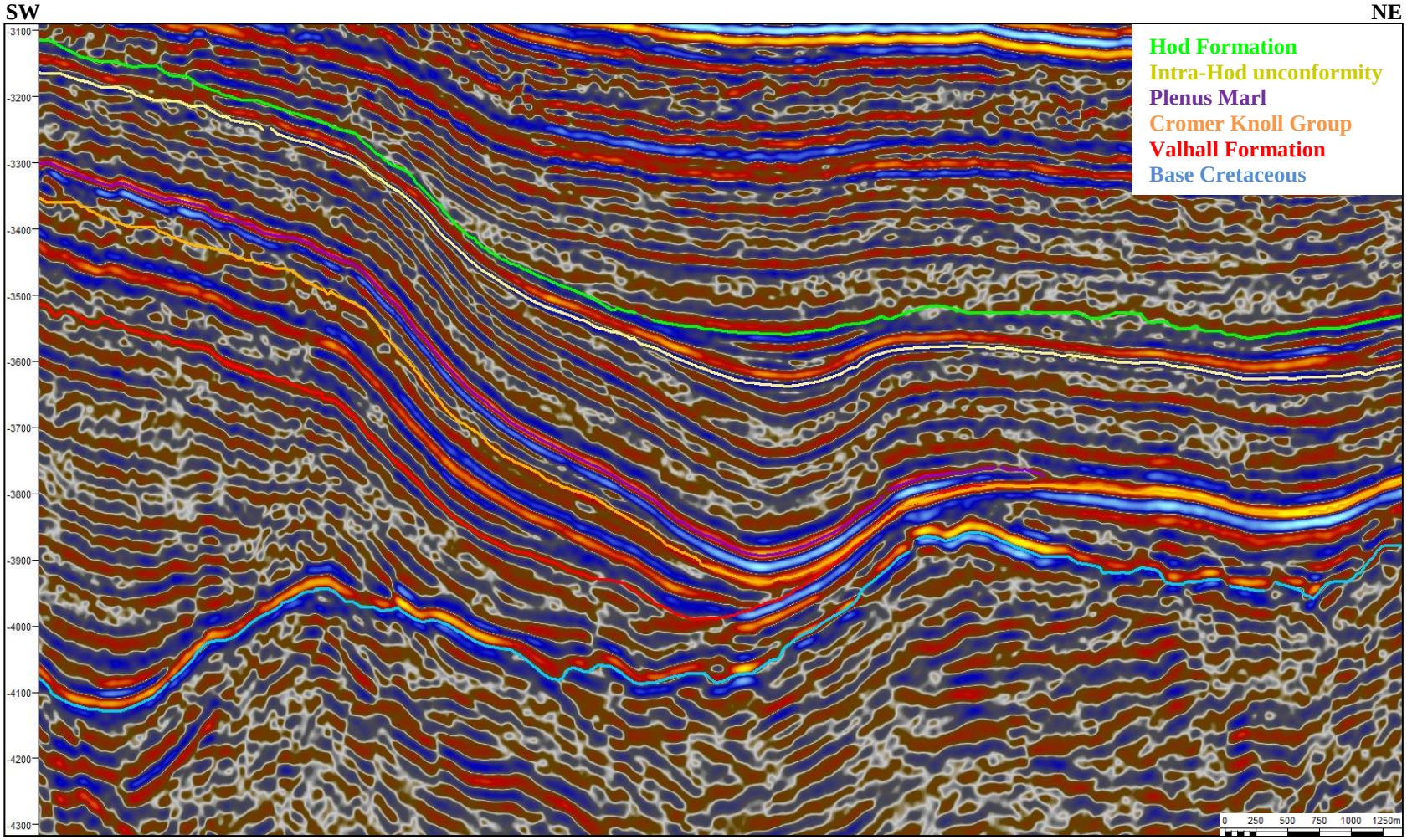

Figure 5.37: SW-NE section with brightening of the seismic reflector observed at the intra-Hod unconformity suggesting re-mobilised or fractured chalk which may be filled with hydrocarbons.

In the Norwegian North Sea many large hydrocarbon fields have a primary reservoir in fractured and re-deposited chalk (Figure 5.38). In the Danish Sector similar inversion structures are also observed and have been found to contain hydrocarbons (Figure 5.39).

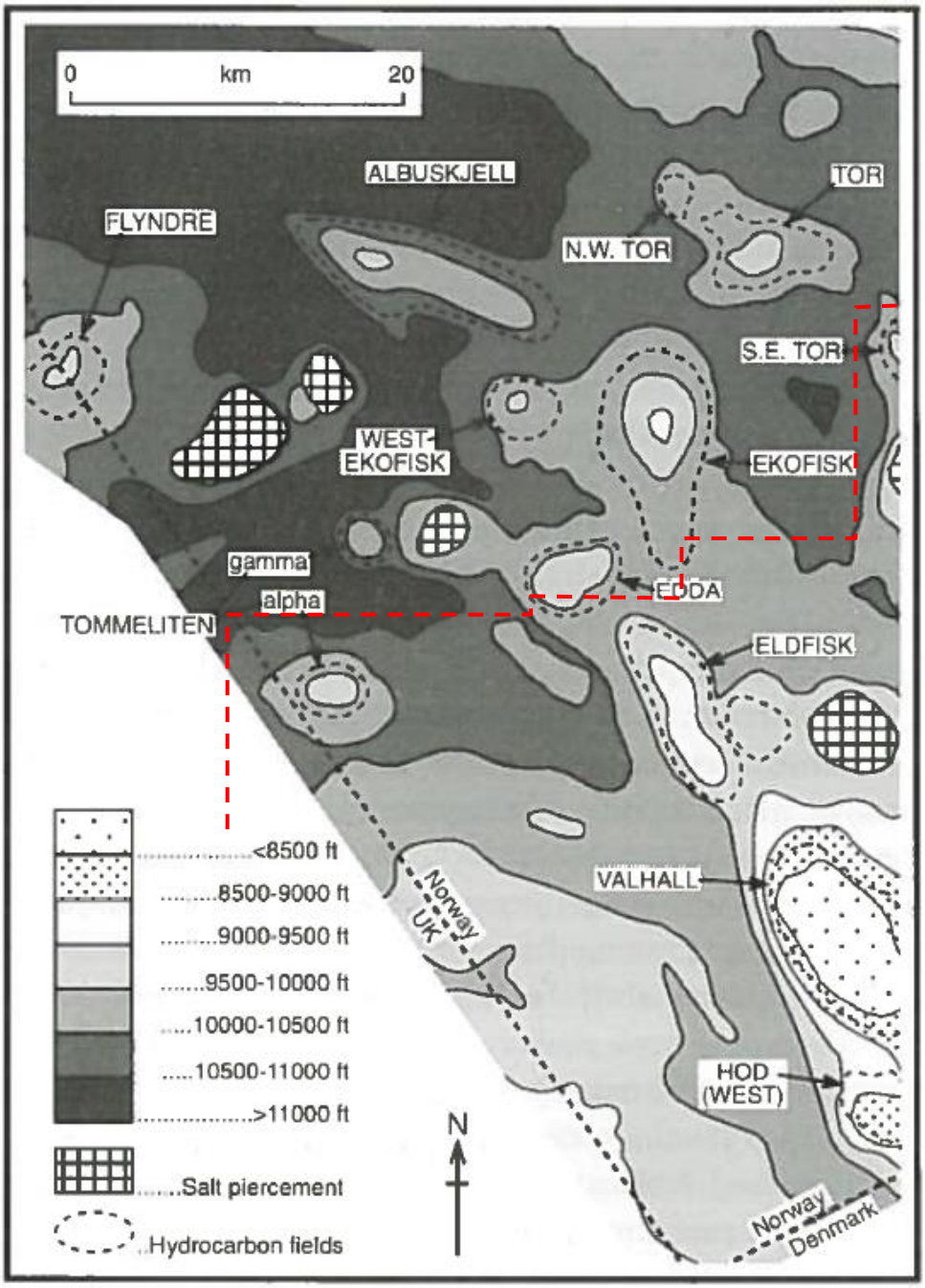

Figure 5.38: Locations of hydrocarbon fields with a Cretaceous chalk reservoir.
Boundary of dataset shown in red.
Image modified after (Glennie 1998)

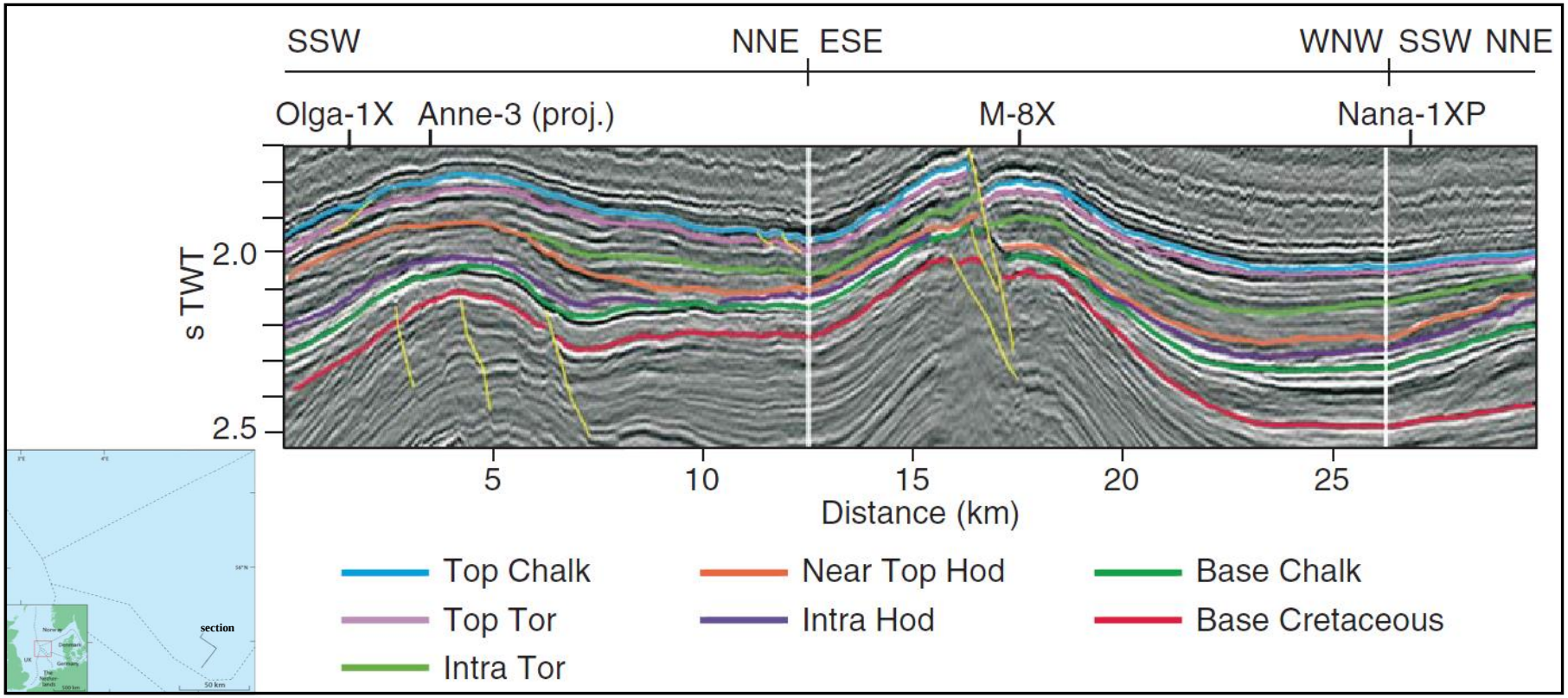

Figure 5.39: Seismic section across an uplifted chalk structure in the Danish Sector. Note the presence of a Santonian age Intra-Hod unconformity in this area too along with a later Near Top Hod unconformity of Campanian age.
Images and age dates from (Abramovitz et al. 2010)

Santonian inversion has also been recorded in the Sole Pit Basin (Ziegler 1990) and a prominent unconformity, dated biostratigraphically is also mapped in the Southern North Sea (Figure 5.40 and Appendix 4).

Another pulse of inversion, more regional and pronounced in its effects than the Santonian one occurred in the Mid Campanian through to the Early Maastrichtian and is recognised in both the Southern and Central North Sea (Stewart et al. 1996; Sikora et al. 1999; Vejbaek et al. 2002; Megson et al. 2005; Abramovitz et al. 2010). It is imaged better in the Southern North Sea as in the northern areas it is difficult to separate this event from the Santonian one (Figure 5.40)

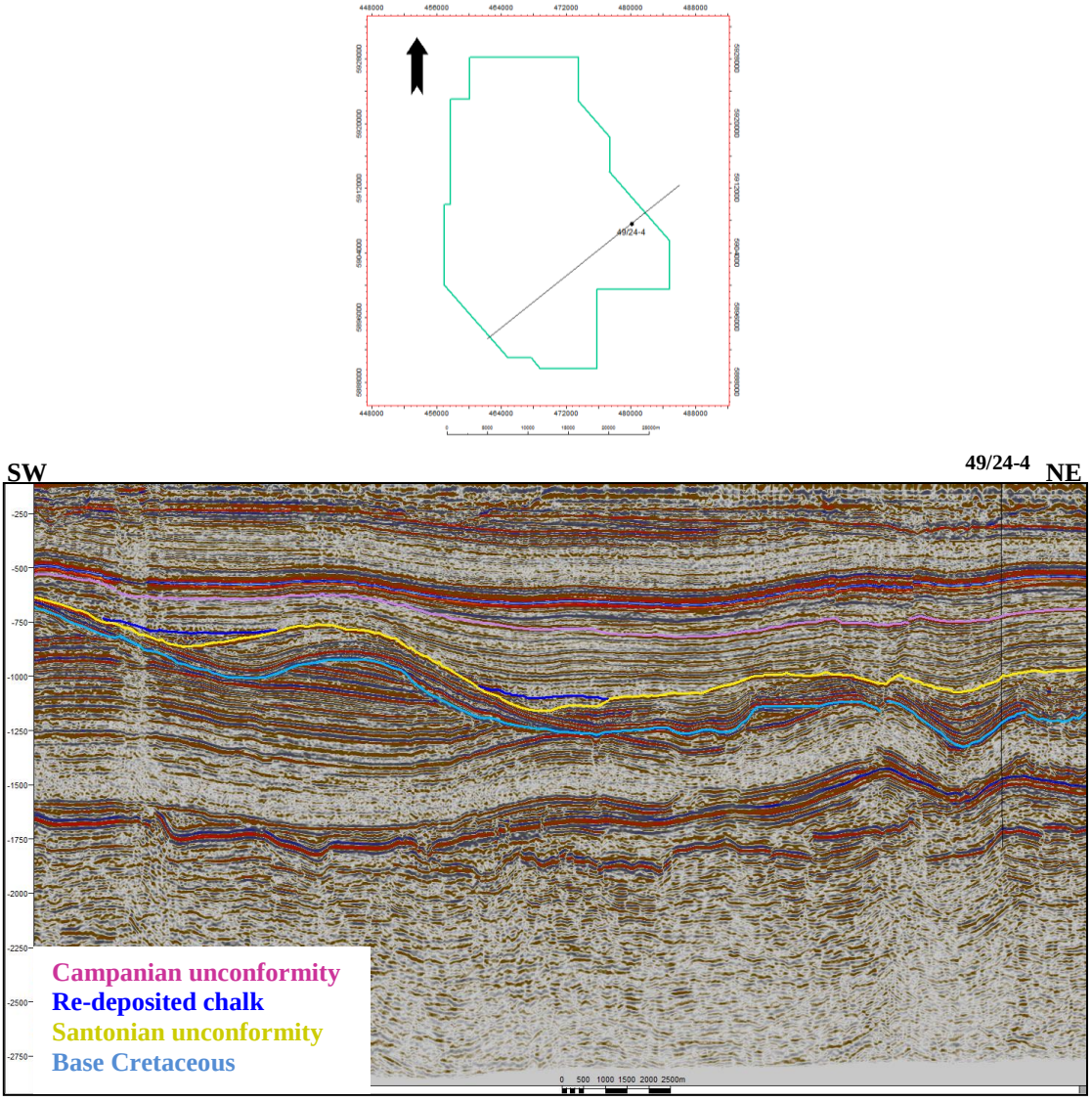

Figure 5.40: Two unconformities, one of Santonian and one of Campanian age are observed in the Southern North Sea and are related to inversion and halokinesis. Re-deposited and slumped chalk is seen.

Maastrichtian inversion also occurred and is reported from the Southern North Sea and Norwegian Central North Sea but is not observed in the study area. From the evidence it is apparent that events in the North Atlantic were the main driver for the inversion of the Central North Sea Basin from the Earliest Cretaceous until at least the Coniacian. However, the main periods of Cretaceous inversion are not seen until the Turonian, and Alpine thrusts of Coniacian age have been mapped in the Central French Alps suggesting that Tethyan subduction and possible collisions of the advancing continental edge with microcratons may have occurred at this time. The increase in intensity of the reactivation pulses could therefore be due to a combination of ridge-push from the west and compressive intra-plate stress transmitted from the Alpine area. However, although it is difficult to say how intense the stress transmitted from the Tethyan region was, it seems unlikely that it was enough to cause structural features as far north as the Central North Sea. Collision with microcontinents could have transmitted more intense pulses but these are speculative and probably fairly localised if they occurred.

The increase in the intensity of the inversion events in the Turonian is likely to have been linked to the fundamental re-orientation of the North Atlantic rift which occurred during the Aptian to Albian and led to the spreading centre shifting to the Labrador rift away from the Arctic rift which became inactive. It is suggested that true sea-floor spreading began in the Labrador Sea during the Coniacian (Evans et al. 2003).

Additionally, the eustatic sea-level curves for the Late Cretaceous show very high sea-levels from the Albian until the Maastrichtian with a distinctive fall during the Coniacian which corresponds with a quiescent period in the compressive regime in the Central North Sea (Figure 5.41). Eustatic sea-levels vary through geological time and are primarily controlled by the volume of water available or the volume of the ocean basins. Increase in water volume can occur by changes in the volume of land ice, by changes in water temperature due to thermal expansion of seawater or by desiccation of enclosed water bodies. Ocean basins can vary due to continental deformation or variations in sea-floor spreading rates (Underhill 2003). High spreading rates create areas of hot, new lithosphere which is buoyant, creating an uplifted area around the mid-ocean ridge and decreasing the amount of water which can be held in the basin.

High spreading rates, along with a greenhouse climate, are thus envisaged to drive the eustatic variations seen in the Late Cretaceous which correspond with the record of intense reactivation under compressive stress in the Central and Southern North Seas indicating that North Atlantic tectonic movements were the main influence on the development of compressive structures in these areas.

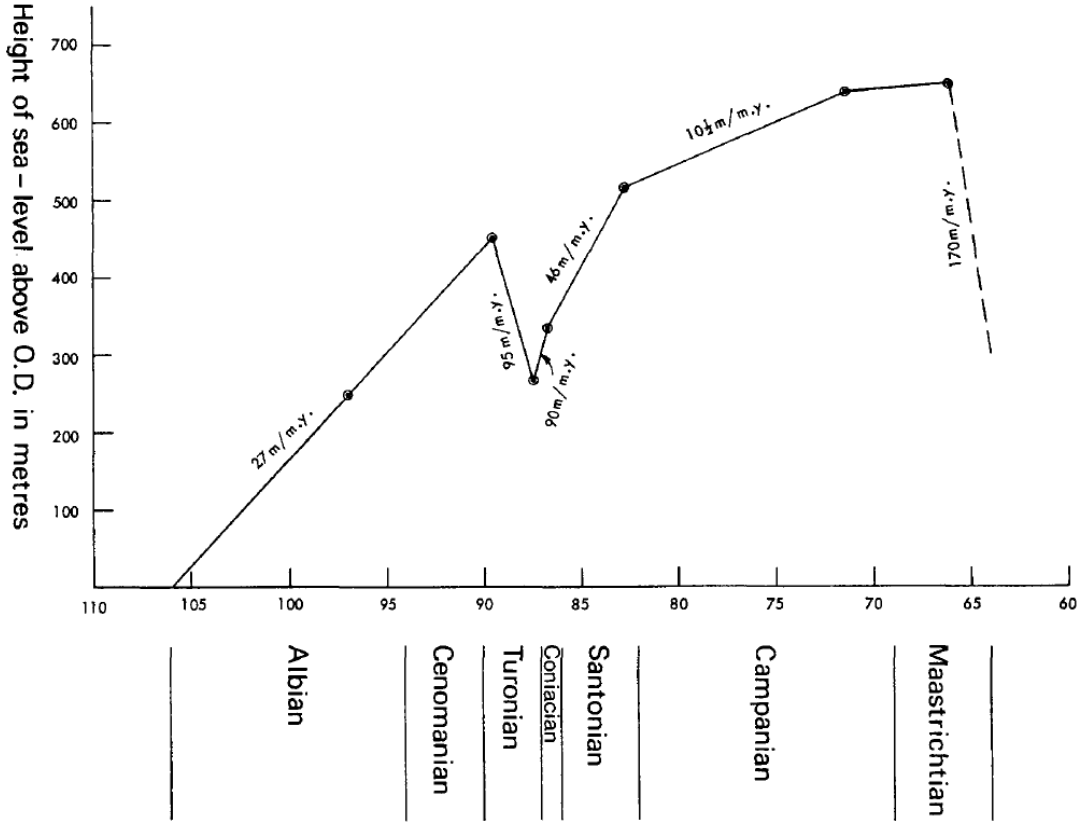

Figure 5.41: Eustatic sea-levels through the Mid-Late Cretaceous.
Image after (Hancock et al. 1979)

Later inversion structures and unconformities created in the Palaeocene through to the Oligocene are well imaged in the Southern North Sea but evidence for this period of compression is not obvious within the Central North Sea dataset suggesting that later reactivation was concentrated further south and may have a larger component of Alpine compression as its driver. A Palaeocene age for the start of true continental collision has been suggested (Doornebal 2010) which fits with this hypothesis.

5.1.1 DRAPE AND PUNCTUATED SUBSIDENCE SUMMARY

Following the Jurassic rifting, the Cretaceous in the Central North Sea has typically been considered as entering a post-rift thermal sag phase. However, the latest mapping shows that this post-rift subsidence has been punctuated by periods of reactivation. The lack of direct tectonic movements in the Central North Sea at this time indicates that these events were induced by far-field compressive stresses. During the Cretaceous the North Atlantic rift was slowly propagating, held back by pervasive Variscan and Caledonian lineaments. At the same time creation and subduction of the Tethys Ocean on the Alpine margin was occurring leading to eventual continental collision. Typically this Alpine collision event has been considered the driver for the inversion structures seen in the North Sea but the evidence for the relative contributions of both tectonic events has never fully been investigated.

Careful mapping of the new high-fidelity seismic data shows that in the Lower Cretaceous post-rift subsidence patterns have been punctuated by reactivation of buried Caledonian and Permo-Triassic faults while in the Mid-Upper Cretaceous, structures resulting from inversion of previous normal faults and reactivation of salt movements are found. The Lower Cretaceous structures are important as Alpine compression had not yet begun and these can therefore be attributed to compression resulting from events related to the propagating Atlantic rift system. Reactivation on Caledonian faults also demonstrates the longevity of these basement lineaments.

In the Upper Cretaceous, the discovery of a significant unconformity resulting from reactivation of underlying faults and halokinesis allowed the timing of this period of inversion to be constrained. Use of well logs and biostratigraphy to provide age dates and correlation with areas in the Southern North Sea demonstrates the regional extent of this pulse of compression which correlates with enhanced sea-floor spreading rates in the Turonian to Maastrichtian

The latest mapping results seem to point to a North Atlantic source for the majority of the tectonic stresses exerted on the Central North Sea up until the Late Cretaceous-Palaeocene. This contradicts the previously held view that compression transmitted from the Alpine continental collision was the driver for North Sea Cretaceous inversion.

5.2 PALEOGENE UPLIFT AND HINTERLAND REJUVENATION

The end of the Cretaceous heralded a period of great regional and global change. The Cretaceous-Paleogene (K-Pg) boundary event saw the extinction of an estimated 75% of all species on earth, the most-well known of which are the non-avian dinosaurs (Jablonski et al. 1994). The warm Cretaceous climate and high sea-levels abated, possibly due to less activity at mid-ocean ridges.

The Central North Sea at the start of the Palaeocene was still undergoing thermal subsidence following Late Jurassic rifting as predicted by standard rift-drift (syn- to post-rift subsidence) curves which show a pattern of rapid initial subsidence followed by a longer period of exponentially decreasing subsidence rates. Inversion is not evident in the Central North Sea, although it continued further south, and it is considered that the last inversion pulse to affect the study area occurred in the Latest Cretaceous (Caillet et al. 1996; Caillet et al. 1997), consistent with a lull in ocean ridge activity.

In the Mid Palaeocene however, tectonic events in the North Atlantic once again began to affect the North Sea. In the final stages of opening, compressive stress was transmitted either side of the developing mid-ocean ridge. On the European side, this compression was buttressed against the rigid European plate causing flexure. This, coupled with the emplacement of a mantle plume caused transient uplift which

punctuated the post-rift subsidence pattern and led to enhanced sedimentation rates as equilibrium was retained (Joy 1992; Joy 1993) (Figure 5.42)

This uplift is considered to have been linked to a plume of magma. The plume was initially emplaced under Greenland, possibly as early as the Mid Cretaceous and may previously have had a role in shifting the spreading centres away from the Arctic rift. After impacting stretched crust beneath Greenland during the Earliest Palaeocene, causing thermal doming, it breached the lithosphere producing volcanism and causing intrusives to be emplaced (Jolley et al. 2002) (Figure 5.43).

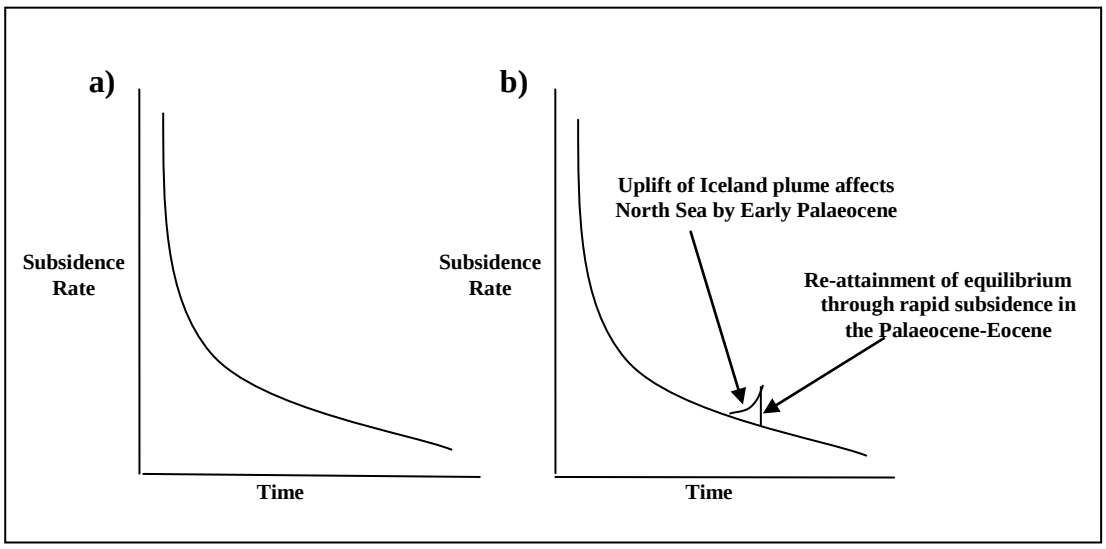

Figure 5.42 a) and b) Standard rift-drift curve and modified example from the North Sea.
Modified after (Joy 1993)

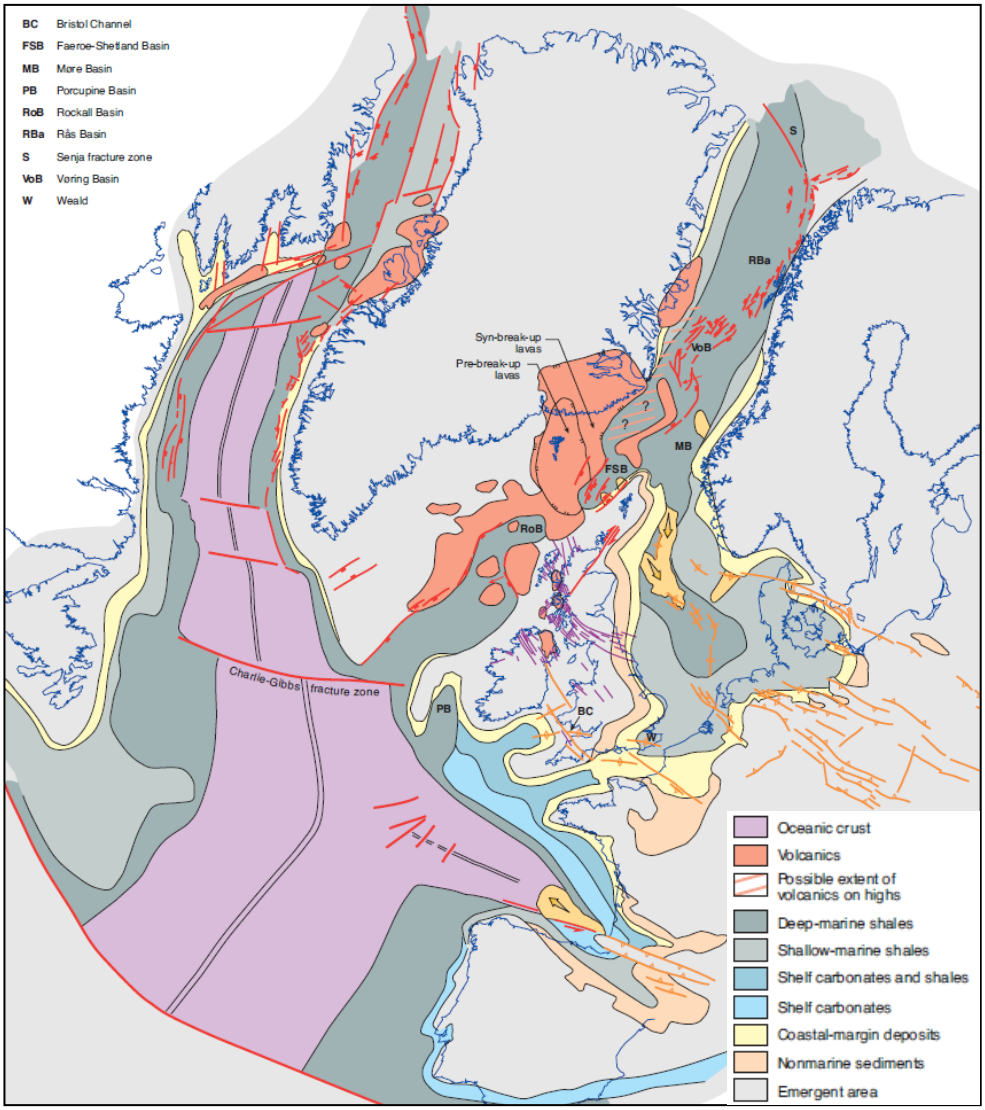

Figure 5.43: Tectonic elements of the Palaeocene showing the location of the Iceland Plume and subsequent volcanism.
Image after (Evans et al. 2003)

Evidence for this uplift is demonstrated by the shallower depth of Jurassic sediments and major sea-bed unconformity found in the Inner Moray Firth (IMF) rift arm (Underhill 1991; Hillis et al. 1994). Apatite Fission Track and seismic studies from the area also show that an extreme amount of exhumation occurred during the Tertiary (Argent et al. 2002) (Figure 5.44) linked to thermal uplift of the Scotland-Shetland Plateau under which the Iceland Plume was emplaced. At the height of uplift, Palaeocene age coals are present in the Moray/Ninian delta, indicating that basinal sediments rose above sea-level and were incised as base-level continued to fall (Milton et al. 1990).

The extreme amount of exhumation was due to the large size and extent of the plume, a hot, sub-vertical sheet of asthenosphere which welled up beneath an axis running from the Faeroes through the Irish Sea (Jones et al. 2002). The upwelling can be confirmed by use of gravity surveys showing that the free-air gravity field over the northern hemisphere is dominated by a long-wavelength high centred on Iceland, stretching from the Azores to Siberia and from Baffin Island to Denmark (Figure 5.45). Positive anomalies such as this are generally associated with mantle upwelling and dynamic uplift (McKenzie 1994).

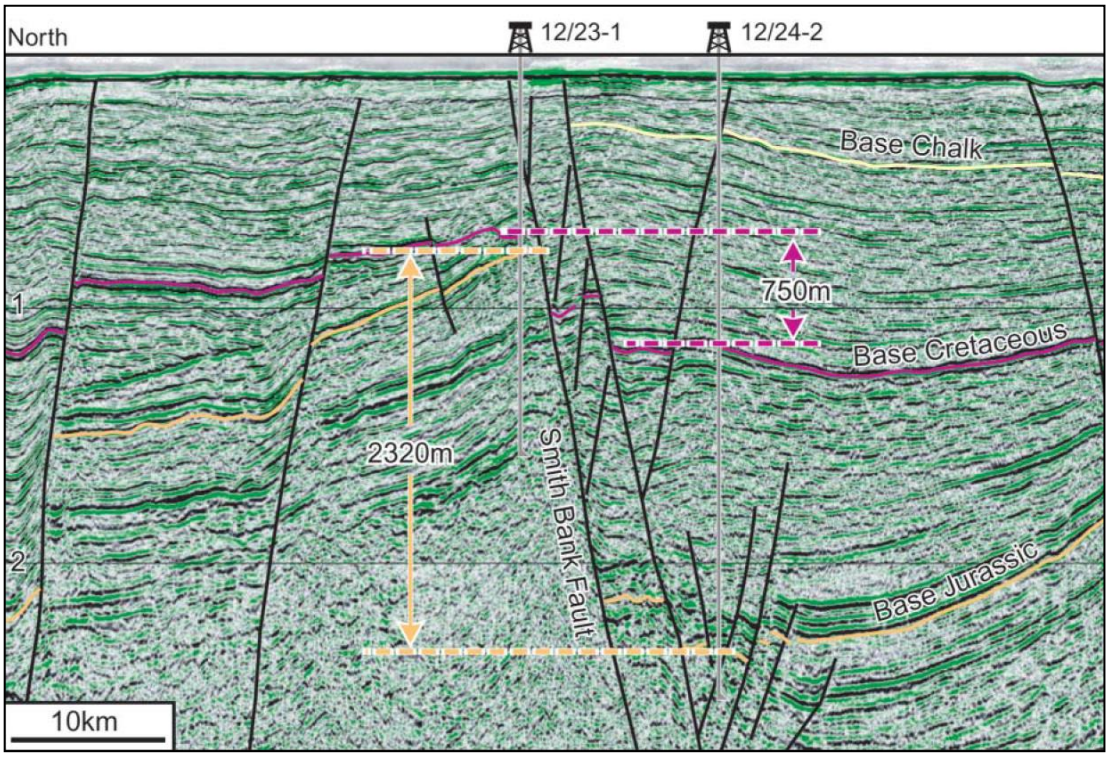

Figure 5.44: Seismic interpretation in the IMF demonstrates that 2320m of post-Triassic displacement has occurred, with 750m of this in the post-Jurassic section. As both extensional faulting and basin exhumation occurred in the Tertiary the actual amount of uplift may actually be underestimated.
Image after (Argent et al. 2002)

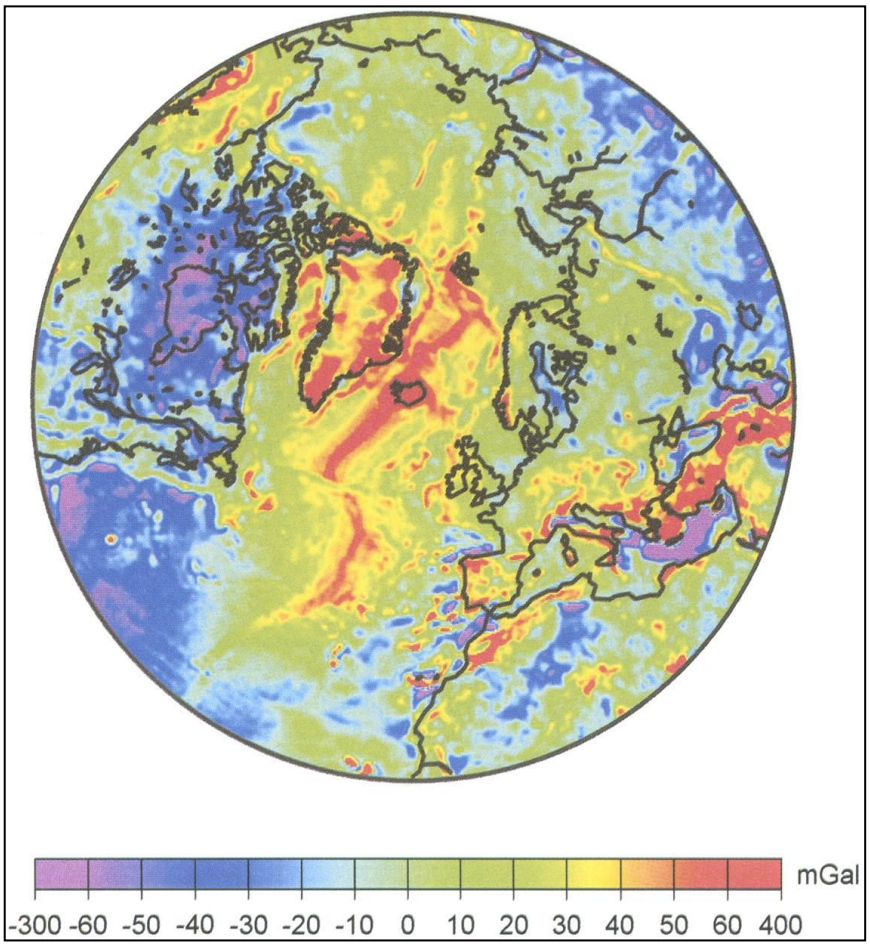

Figure 5.45: Free-air gravity anomaly over part of the northern hemisphere.
(Jones et al. 2002)

5.2.1 THE EFFECTS OF NORTH ATLANTIC TRANSMITTED STRESSES AND UPLIFT ON THE BASIN MARGINS

The tectonic stresses transmitted from the North Atlantic and thermal uplift of the Iceland Plume had an important effect on the geometry of the North Sea and surrounding areas. Seismic interpretation in the Faroe -Shetland Basin (Figure 5.46) identifies a WNW-ESE striking fault complex of Mid-Late Palaeocene age (59.4-57.5Ma) (Figure 5.47). A similar trend is noted in the dike complexes which are mapped across Scotland, Northern England and in the Southern North Sea where they are dated to approximately 58Ma (Wall et al. 2009) (Figure 5.48). It has been suggested previously that dike emplacement occurs within the plane perpendicular to the minimum principal stress (σ_3) (England 1988) and that these dikes are therefore linked to the evolving Atlantic margin. However, the dikes are thought to follow underlying basement lineaments with the orientation of these considered a more important control on dike occurrence than that of the regional stress field (England 1988). Examples of large fault complexes of this orientation have never been examined in detail and those recognised have never been fully explained despite these faults acting to compartmentalise major oil fields such as Schiehallion and Foinaven (Leach et al. 1999; Freeman et al. 2008; Rodriguez et al. 2010) (Figure 5.49).

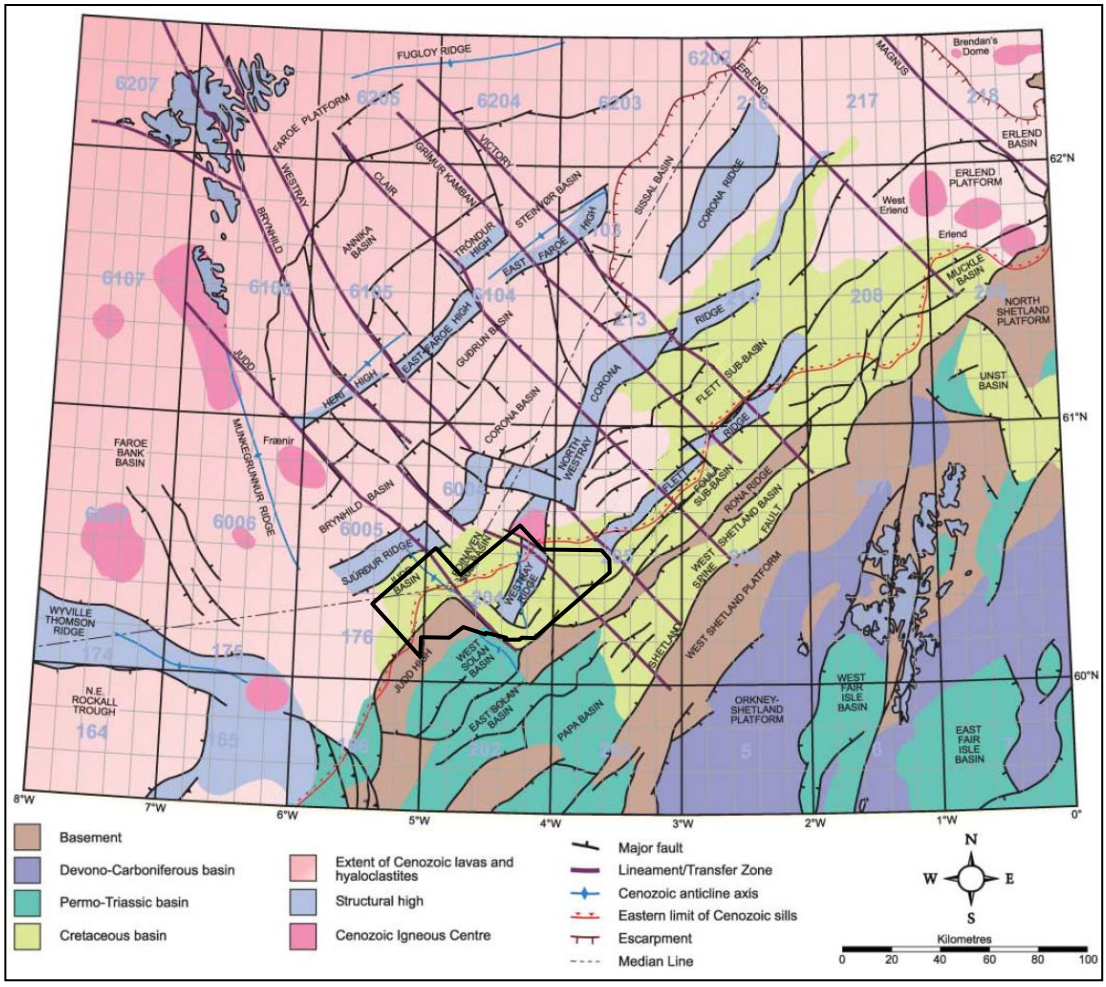

Figure 5.46: Structural elements of the Faroe-Shetland area with dataset outline superimposed.
The Faroe-Shetland Basin comprises a series of NE-SW trending sub-basins separated by horst blocks that formed during a sequence of Devono-Carboniferous, Permo-Triassic and Palaeocene rift events.
Image modified after (Ellis et al. 2009)

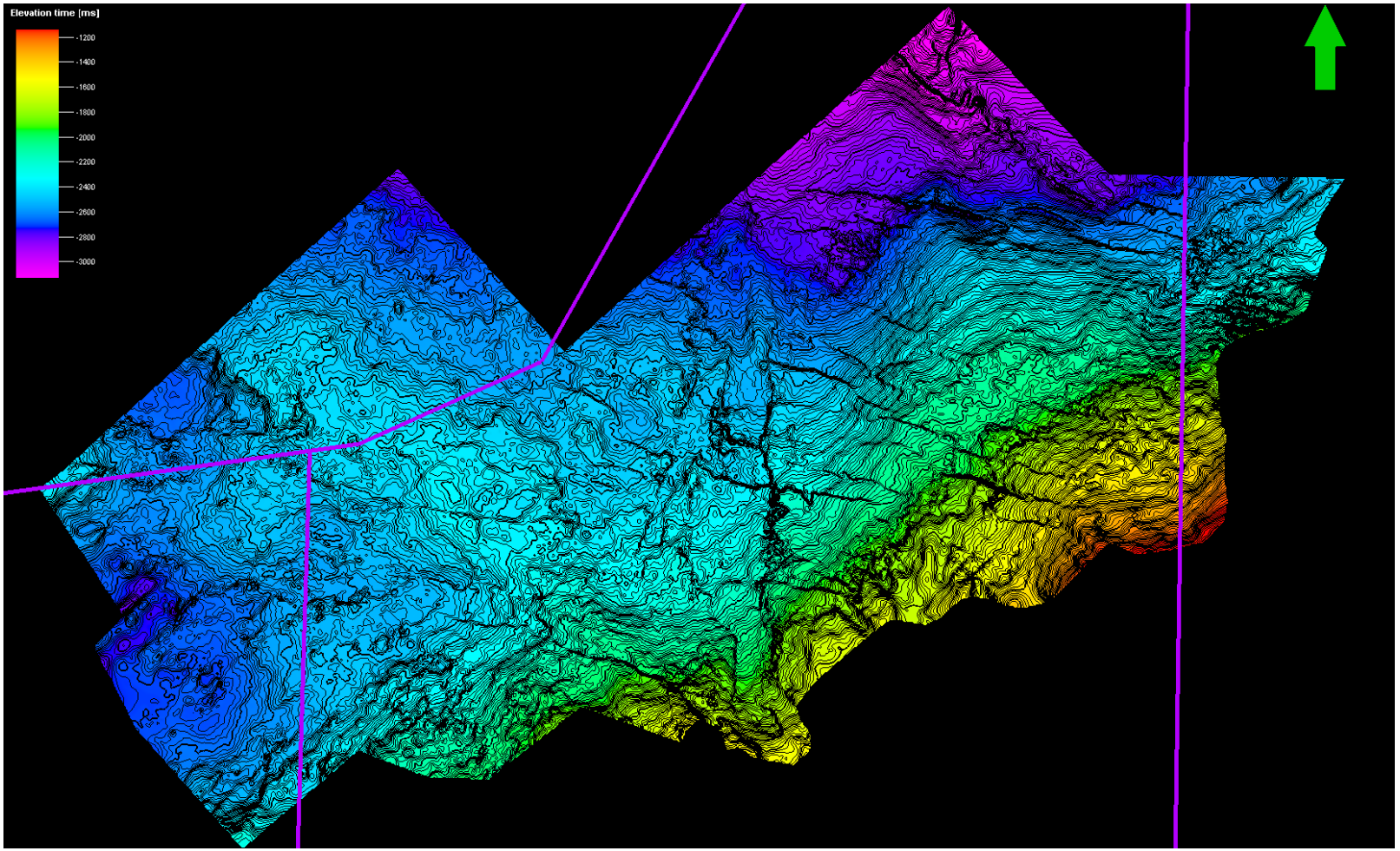

Figure 5.47: A TWTT structure map of the Palaeocene (T36) Kettla Tuff, a thick tuff deposit sourced from explosive volcanism in the North Atlantic Igneous Province showing extensional faults which occurred due to stresses generated by opening of the North Atlantic. In the Central North Sea corresponding volcanic deposits are present within the Mey Formation.

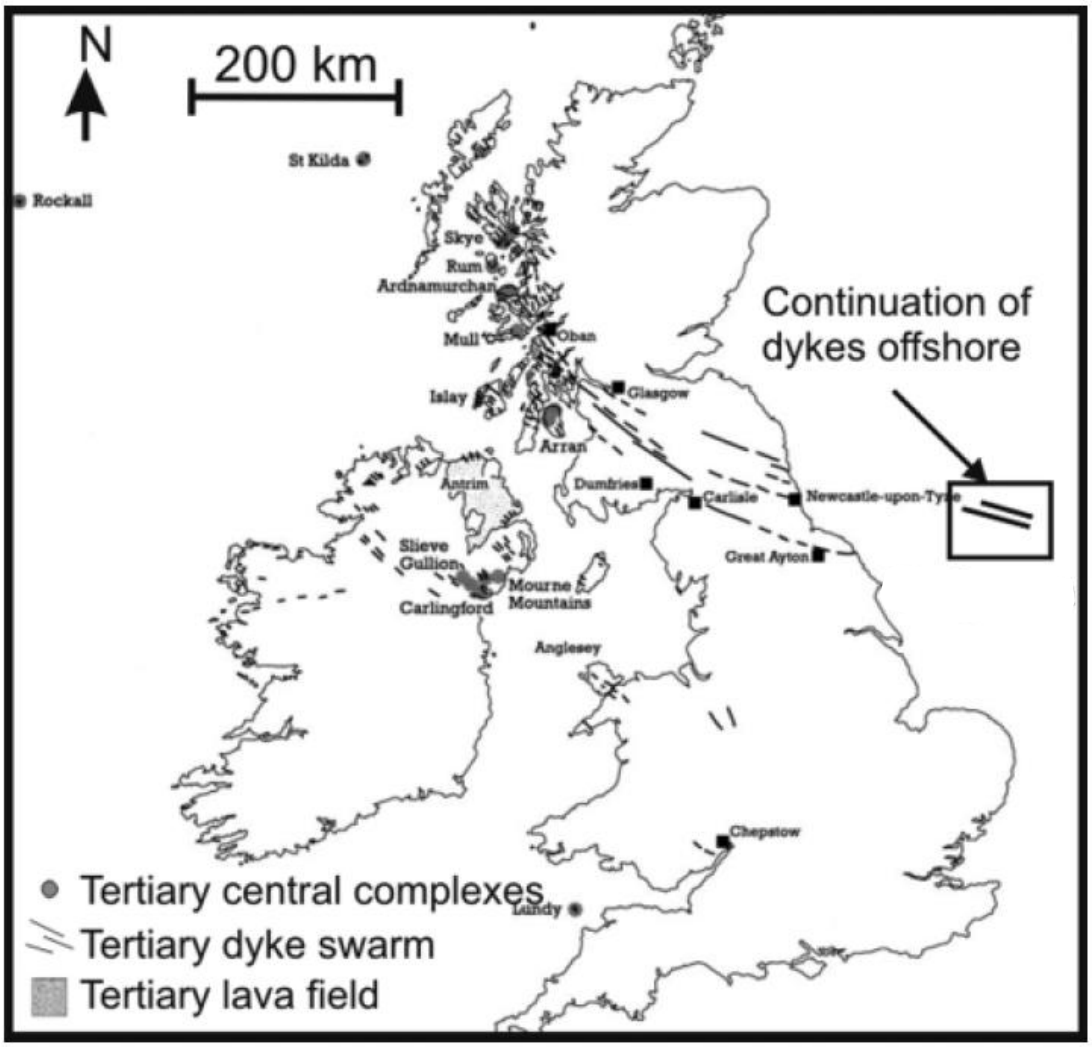

Figure 5.48: Location and strike directions of Tertiary dikes mapped onshore and offshore.
Image modified after (Wall et al. 2009)

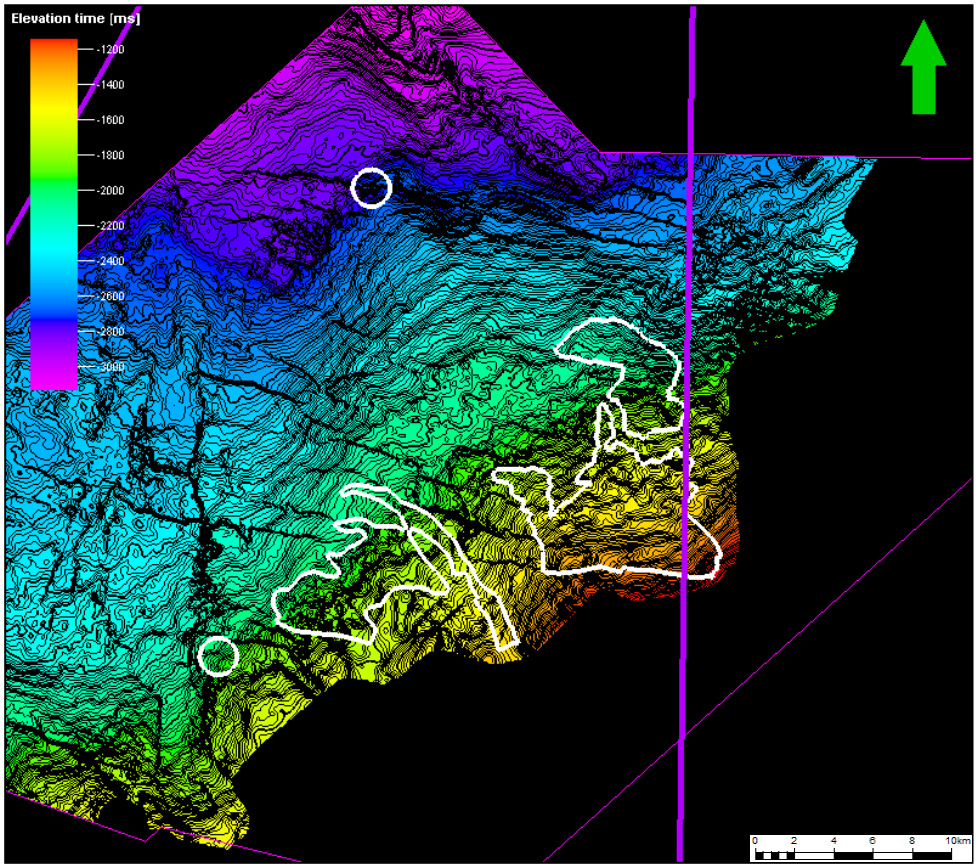

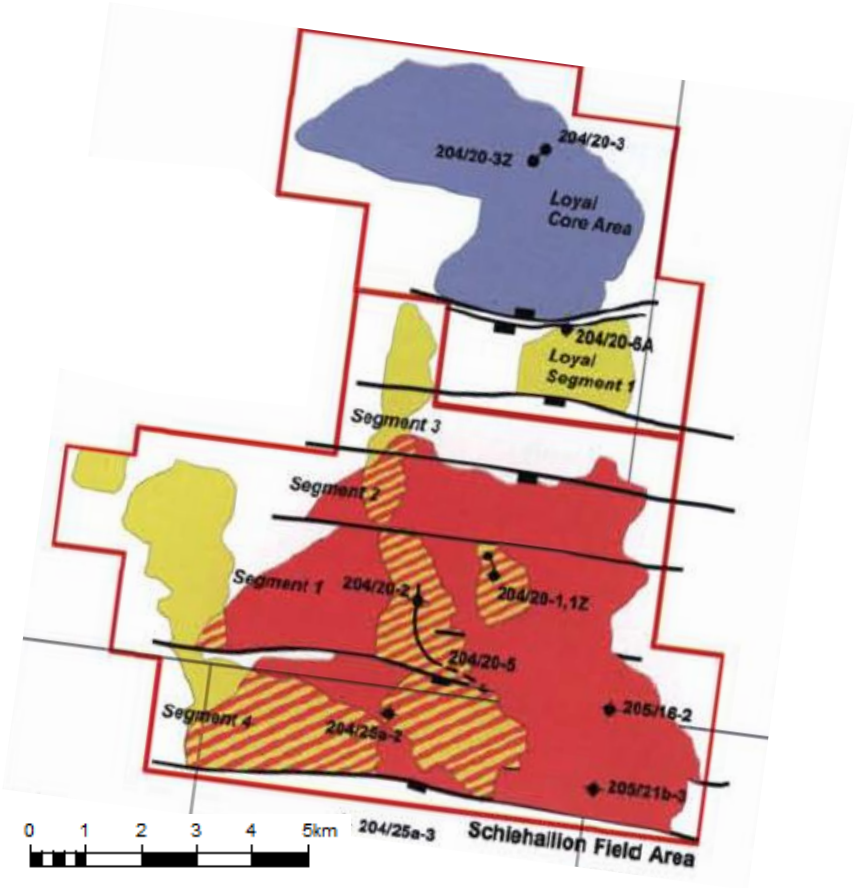

Figure 5.49: Schiehallion Field segments compared to a Kettla TWTT map demonstrating that it is these pervasive WNW-ESE faults which compartmentalise the field.
Right hand figure after (Leach et al. 1999)

Detailed mapping of the Palaeocene-age faults in the West of Shetland area shows that many of the faults do indeed follow a basement trend but that some were formed away from these lineaments under SW-NE directed stress (Figure 5.50). When plotted on a paleogeographic map showing the principal stress directions it can be demonstrated that the faults, along with the dikes, occur at an orientation perpendicular to the minimum principal stress (Figure 5.51 and 5.52). It is therefore suggested that these formed during the final stages prior to the Atlantic opening when SE-directed extension was impeded by the presence of the rigid European Plate and was taken up instead by intra-plate extensional and wrench faulting. Evidence of wrench motion on the Great Glen Fault in the Moray Firth Basin at this time supports this interpretation (Underhill et al. 1993). Later deposits are not affected by this faulting and it is possible that this cessation in activity marks the start of oceanic crust generation.

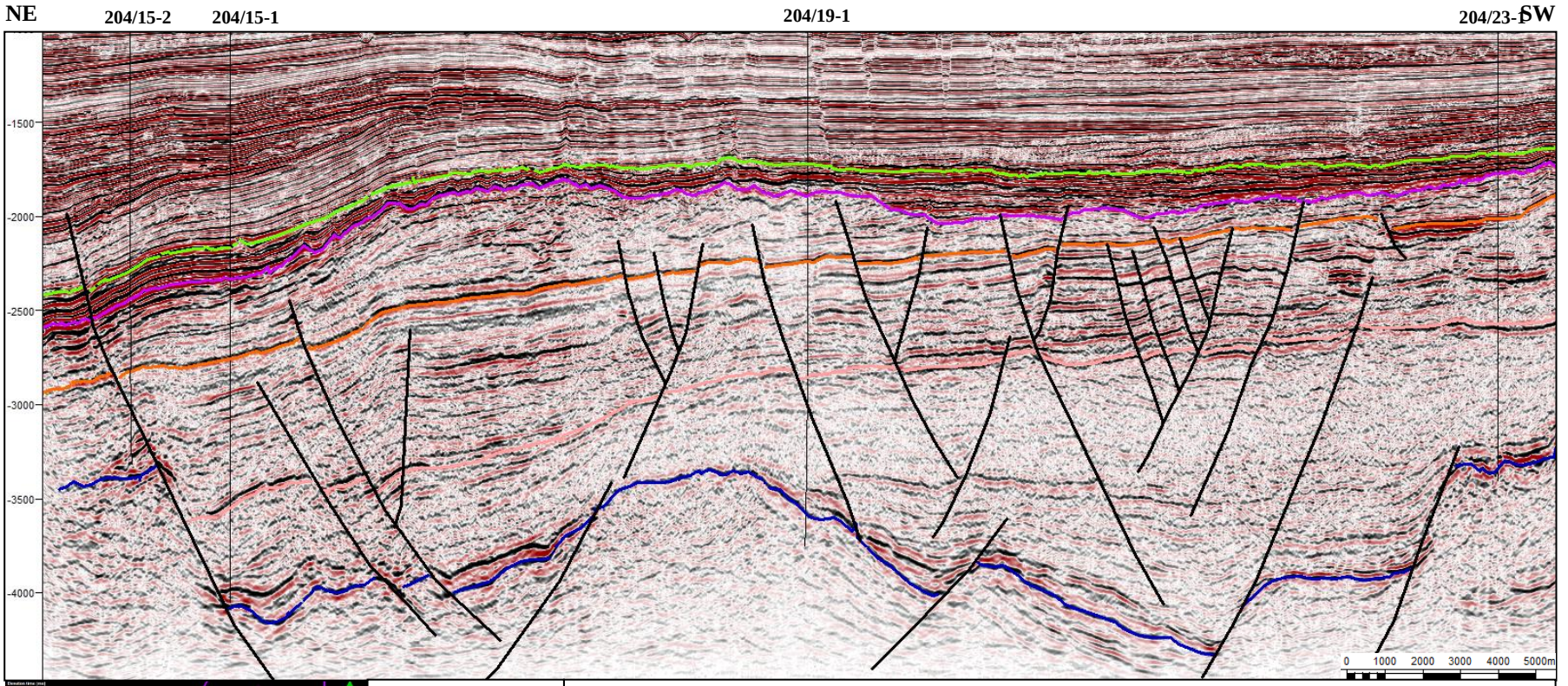

Figure 5.50: Faulting of Mid-Late Palaeocene age can be seen to follow the basement lineations in many cases and some new faults also developed under the stress regime caused by North Atlantic tectonics.

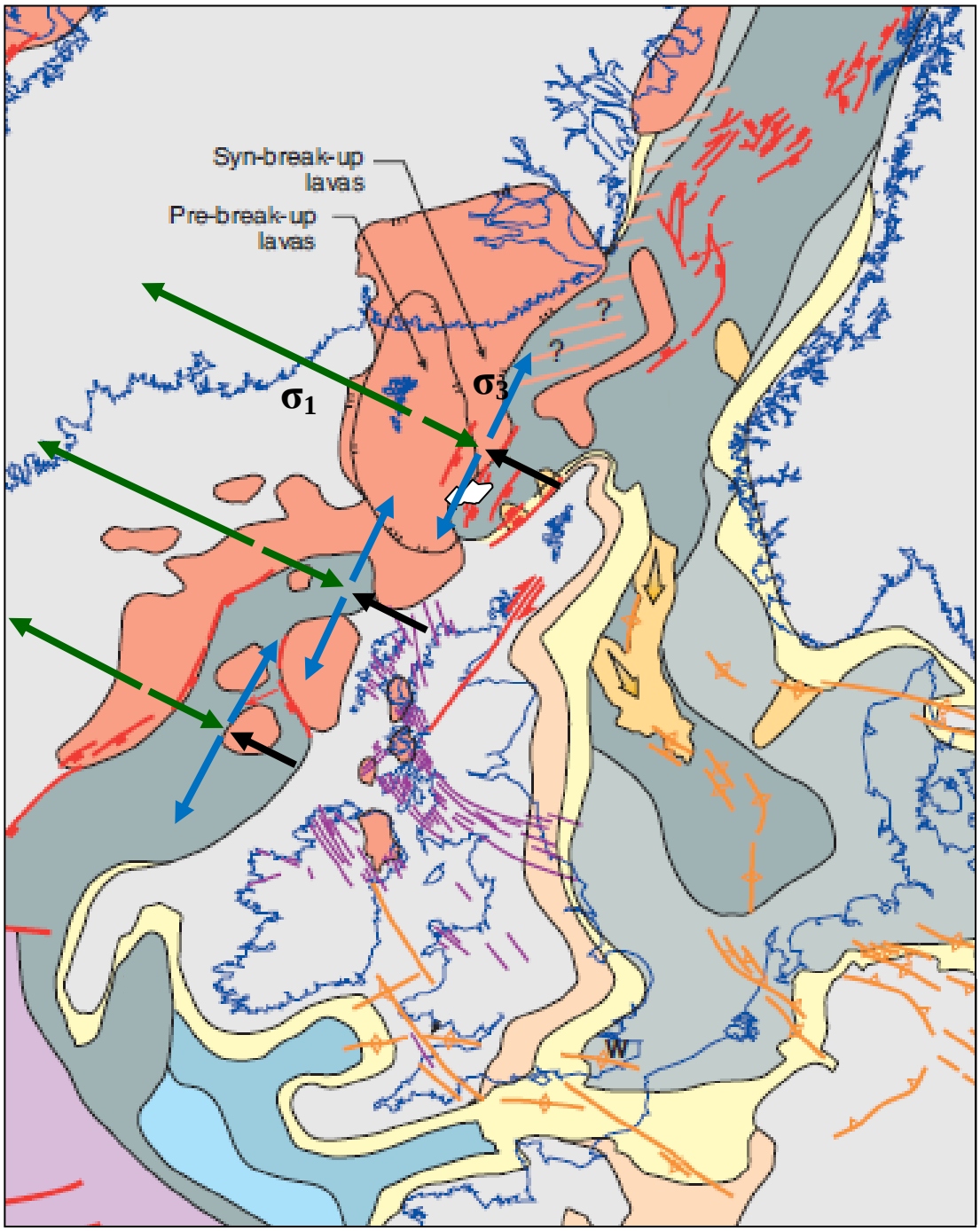

Figure 5.51: Tectonic elements of the Mid-Late Palaeocene showing the principal extensional and compressive stresses (σ_1). Compression can be seen to result from extension against a buttress formed by the rigid European Plate. The faults observed in the study area and the dike complexes are perpendicular to the direction of minimum stress (σ_3).
Green arrows denote the direction of extension, black arrows show the compression created due to the rigid plate behind. Blue arrows denote the orientation of minimum stress. Red arrows show renewed wrench movement on the Great Glen Fault.

Location of seismic volume shown in white and enlarged in Figure 5.52.
Image modified after (Evans et al. 2003)

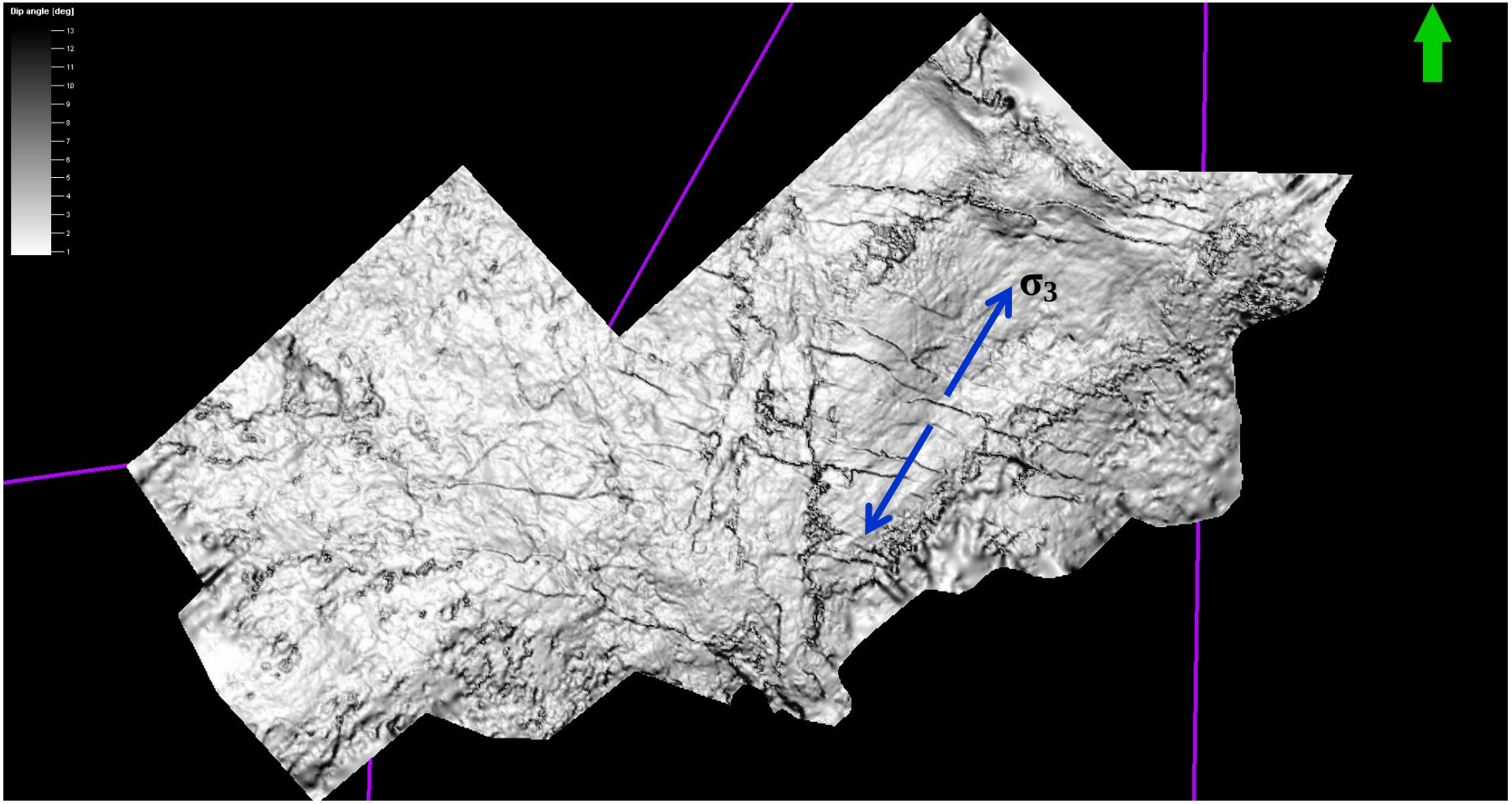

Figure 5.52: A dip angle map of the Kettla surface showing the faulting perpendicular to the σ_3 orientation.

Subsequently deposition in the Faroe -Shetland Basin predominantly consists of prograding complexes shed off the hinterland due to plume-driven uplift. These were then incised during a later period of uplift at 54.7Ma when the area became sub-aerial and large, complex drainage systems formed (Biskopsø 2004). Seismic interpretation in the West of Shetland area demonstrates this and mapping of a pronounced unconformity at the Palaeocene-Eocene boundary shows a highly intricate dendritic drainage system (Figures 5.53-5.56). In the areas of greatest incision the entire Late Palaeocene section has been removed amounting to as much as 400m of erosion (Biskopsø 2004) .

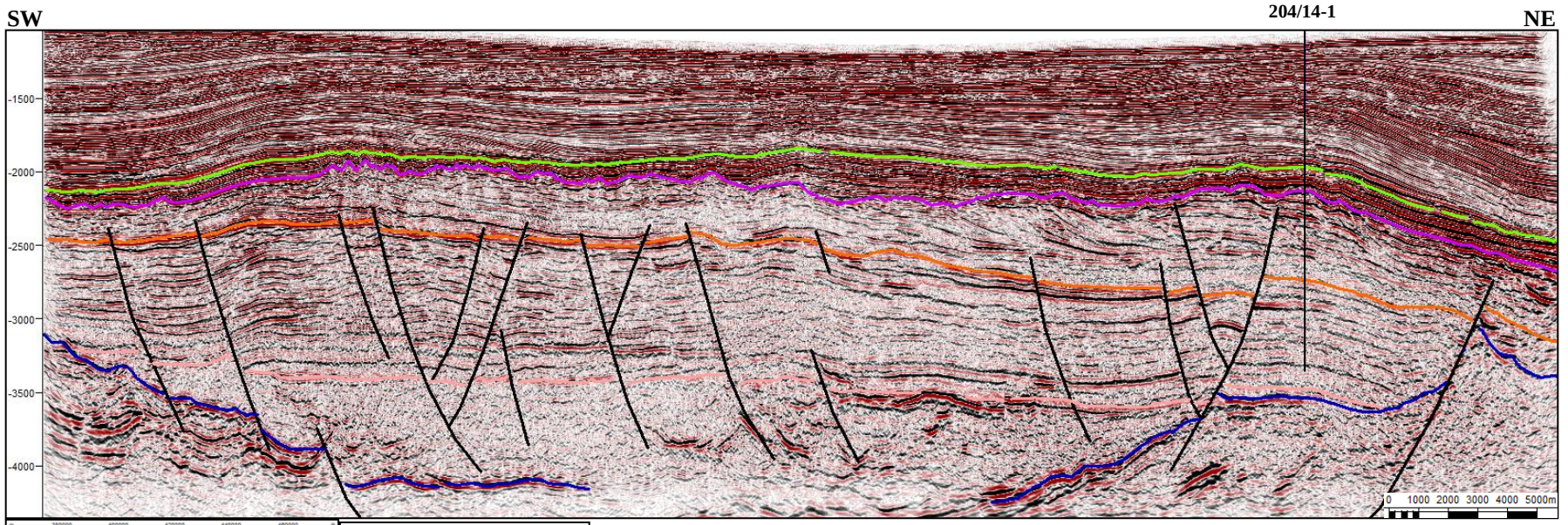

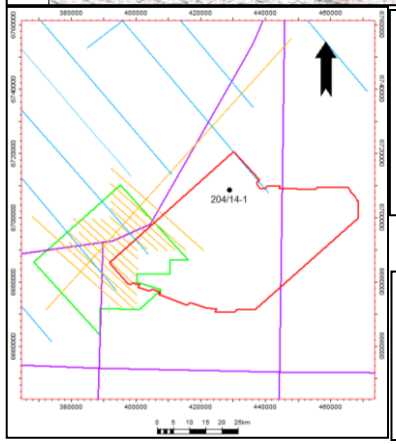

Early Eocene
(pseudo Balder Fmn)
Unconformity
Kettla Tuff
Shetland Group
Basement

Figure 5.53: SW-NE section showing the prograding wedges shed off the hinterland which are then incised by the formation of a large scale dendritic drainage system during the Early Eocene. The entire area was then inverted in the Eocene in response to compressive stress from the North Atlantic.

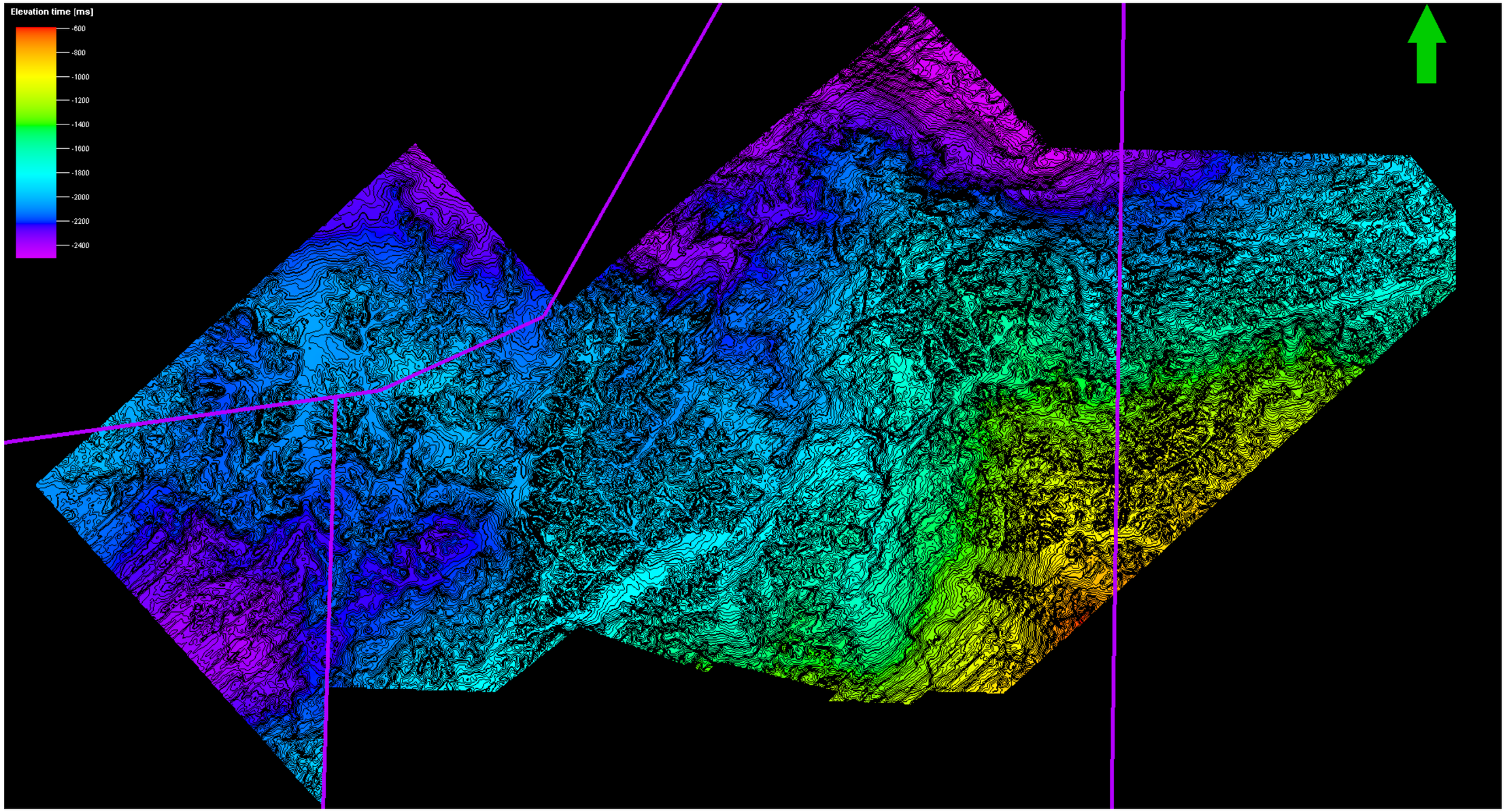

Figure 5.54: TWTT structure map of the T40/45 unconformity showing the dendritic drainage pattern.

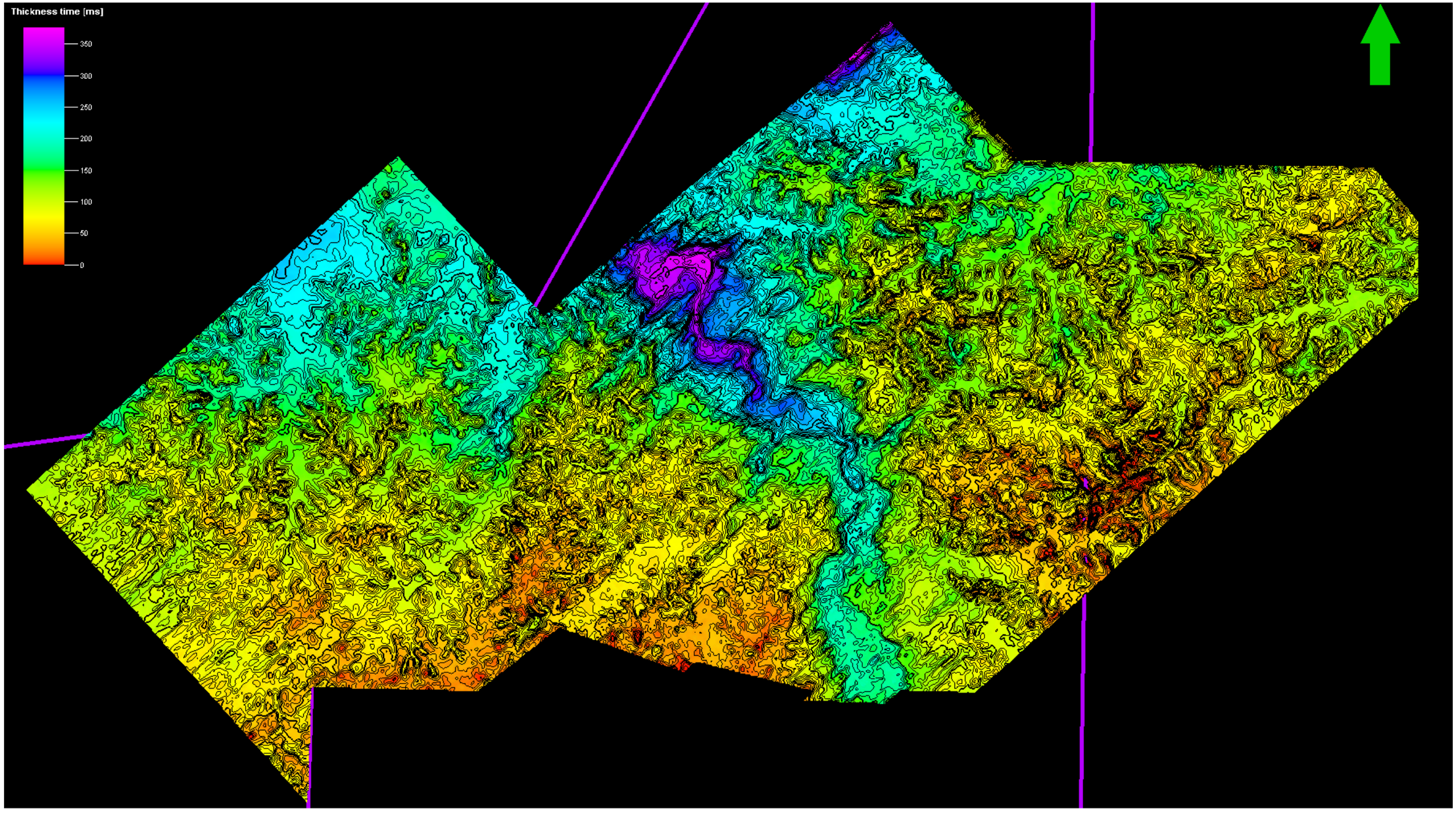

Figure 5.55: An isochron between the pseudo- Balder Formation (earliest Eocene) and the T40/45 unconformity showing the thick infill of the channels left by the incision of the dendritic drainage system.

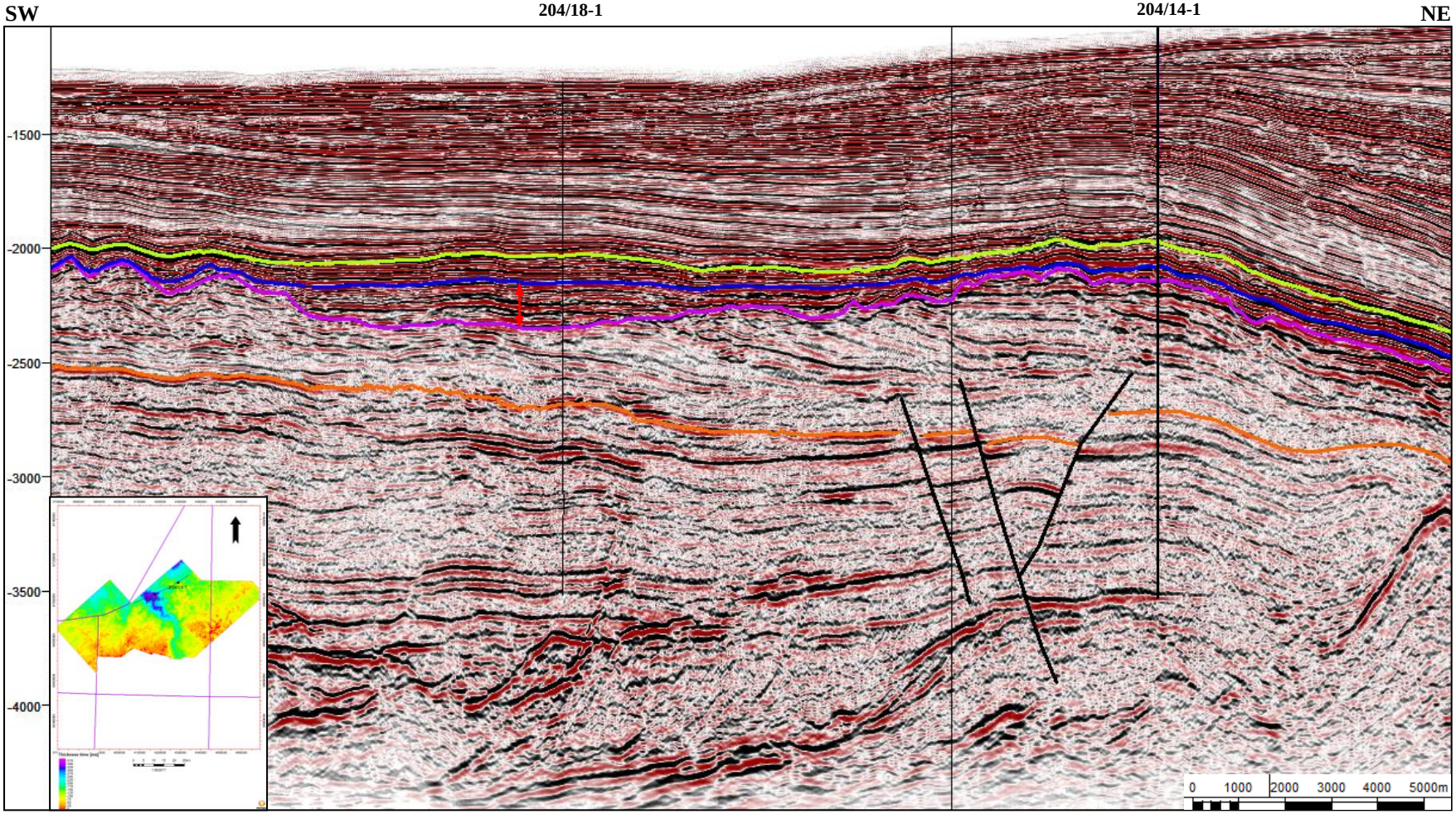

Figure 5.56: The exact amount of incision is difficult to quantify but the infill of the Sele (Flett) Formation (red arrow) is 169m in the deepest channelized area of the dataset but the figure is much larger to the north outwith the bounds of the seismic.

5.2.2 THE EFFECTS OF HINTERLAND UPLIFT ON THE BASIN CENTRE

Deposition of prograding delta complexes followed by high erosion rates and deposition of coal and lignite beds are evidence of thermal uplift in the areas flanking the Scotland-Shetland Plateau. However, in the Central North Sea the same event led to a different depositional geometry. Uplift of the hinterland, coupled with tilting led to enhanced subsidence and extremely thick volumes of sediment being shed into the basin throughout the Palaeocene. The source of these clastic pulses can be constrained by Sm-Nd isotopic analysis and the results fall within the compositional field of British river sediments (analytical report found in Appendix 3).

Clastic influx to the basin was pulsed with times of high input evidenced by thick basinal turbidite sand deposits which are inter-bedded with the shales and clays which signify more quiescent periods. These pulses have been suggested to be linked to changes in relative sea-level allowing a sequence stratigraphic framework to be applied (Stewart 1987; Milton et al. 1990).

Sequence stratigraphy is a method of stratigraphic and sedimentological analysis of sediments within a time-stratigraphic framework and puts great emphasis on eustatic or relative sea-level cyclicity. The most commonly cited sequence stratigraphic model is the Exxon model (Frazier 1974; Jervery 1988; Posamentier et al. 1988; Van Wagoner et al. 1988) in which the basic units are known as depositional sequences formed by one cycle of relative sea-level change. Subsequent amendments to this

model were then made in order to fit the model to more complex depositional sequences (Embry et al. 2007).

The top and basal boundaries of a depositional sequence are known as sequence boundaries and correspond with unconformities or their correlative conformities. A depositional sequence consists of four systems tracts, the Lowstand Systems Tract (LST), deposited during relative sea-level fall, Transgressive Systems Tract (TST) deposited during relative sea-level rise (transgression), Highstand Systems Tract (HST), deposited during highstand of sea-level and the Forced Regressive Systems Tract (also known as a Falling Stage Systems Tract) (FRST) (Figure 5.57). The LST unit encapsulates all of the strata deposited during base-level fall and is bounded by the sequence boundary below and Transgressive surface above. The TST, bounded by the Transgressive surface at the base and the Maximum Flooding Surface (MFS) above, forms during rapid relative sea-level rise where the rate of accommodation space development exceeds sediment supply. The HST is bounded by the MFS below and the sequence boundary above (although it may be overlain by the FRST downdip) and represents a decreasing rate of relative sea-level rise towards a highstand and a basinwards translating shoreline as sedimentation outstrips accommodation space development.

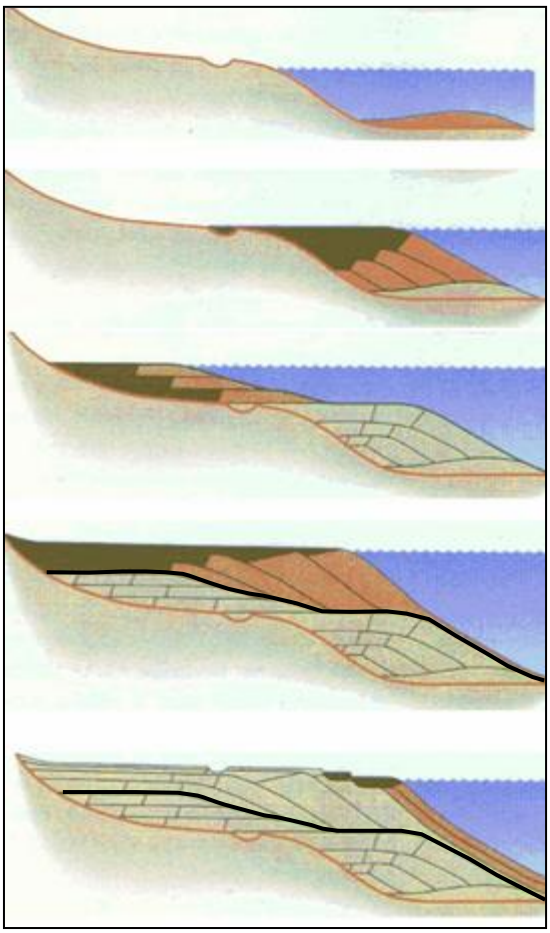

Lowstand systems tract
Falling sea-level.
Basin- floor fan

Lowstand systems tract.
Start of sea-level rise.
Lowstand wedge.

Transgressive systems tract
Rising sea-level.

Highstand systems tract.
Maximum sea-level.
Maximum flooding surface
separates it from the TST.

Falling stage systems tract
Falling sea-level.

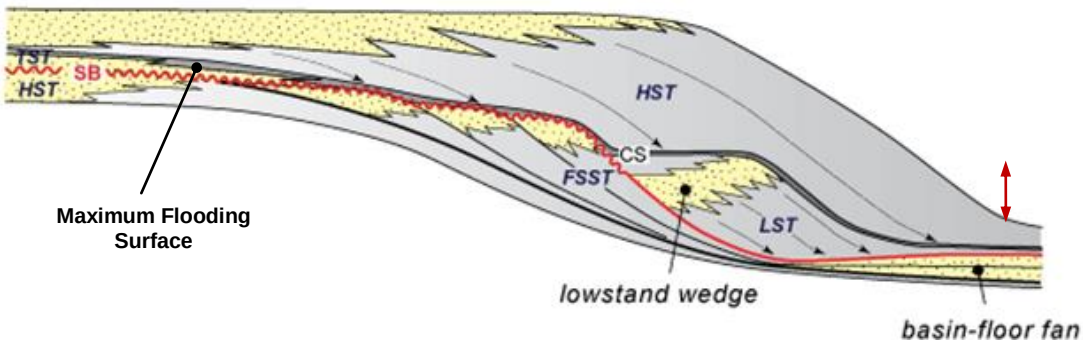

Figure 5.57: Illustrations of the creation of a complete depositional sequence and the resulting geometry. Red arrow denotes probable position of the Central North Sea sections with respect to this model.
Image after (Hunt et al. 1992; SEPM 2013)

It has been suggested that each of the relative sea-level changes and consequent discrete pulses of sedimentation corresponds with a period of thermal activity of the Iceland Plume (Maclennan et al. 2002). It has also been suggested that a Late Palaeocene hyperthermal climate led to increased humidity, run-off and clastic input to the basin (Kender et al. 2012). Thermal uplift coupled with volcanism along the already narrow seaway of the Northern North Sea led to this conduit becoming progressively narrower with the effect of isolating the North Sea basin from the rest of the world's oceans, giving rise to anoxic shale deposition and high concentrations of pyrite in areas not affected by turbidite deposition.

Due to the importance of the Palaeocene sands as hydrocarbon reservoirs, the pulses of clastic sedimentation corresponding to the basin floor fans of the LST have been carefully refined into a high resolution stratigraphic framework (Figure 5.58).

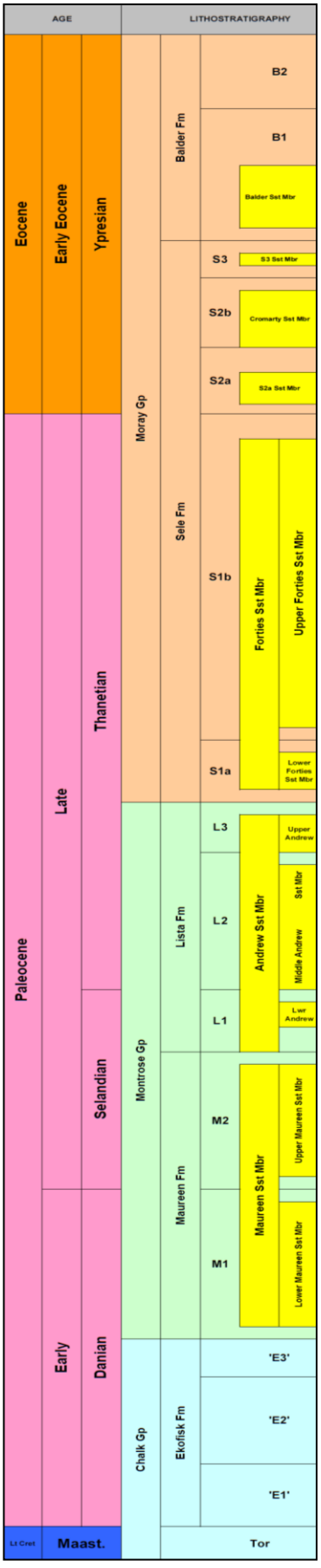

Figure 5.58: Palaeocene lithostratigraphy.

Seismic mapping of the Palaeocene sequence in the Central North Sea shows the direction of flow from the NW hinterland and an isochron demonstrates the great thicknesses which built up throughout the Palaeocene (Figures 5.59-5.61). Discrete channels can be observed which correspond to vast turbidite flows during periods of uplift.

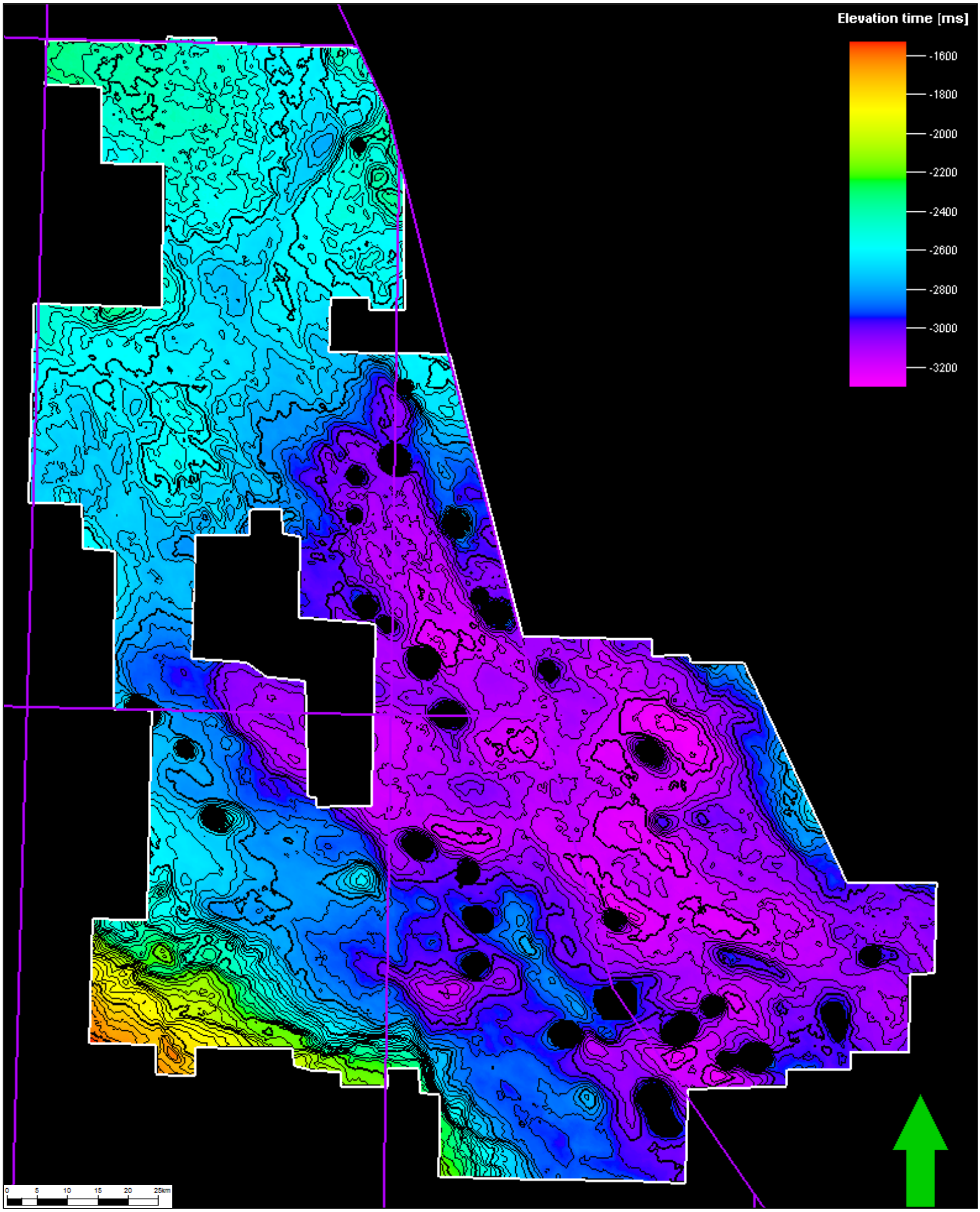

Figure 5.59: TWTT structure map of the top Palaeocene. It is possible to see some of the channel structures coming in from the northwest on this map due to the mounding of the sand channels and differential compaction giving them a bathymetric expression. An isochron between this surface and the base of the Palaeocene clastics can be created to image these more clearly.

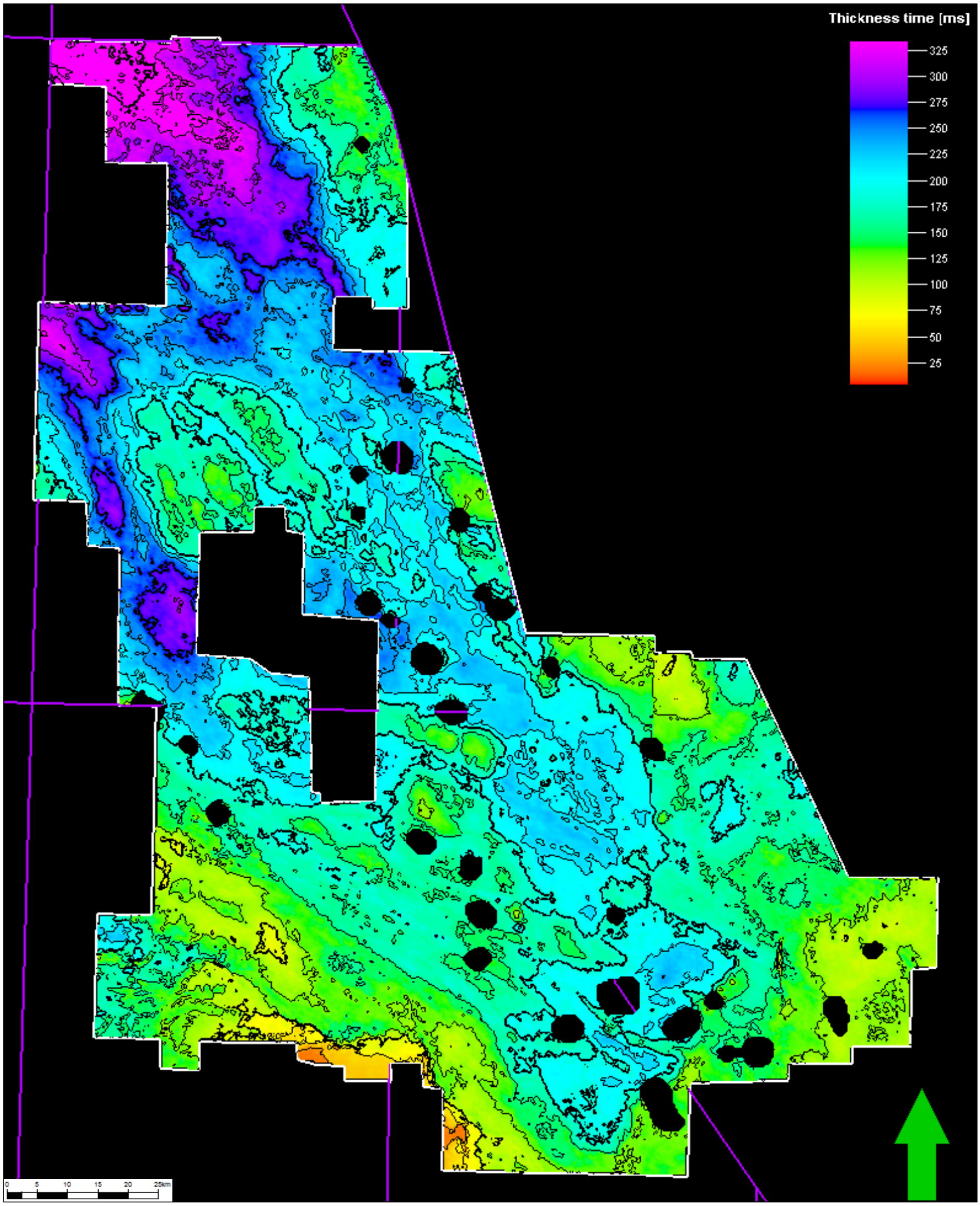

Figure 5.60: An isochron of the Palaeocene clastic interval showing NW-SE channel complexes shed into the basin from the uplifted hinterland. Well penetrations prove thicknesses which exceed 480m.

True thickness information based on well penetrations in thickest channelized areas

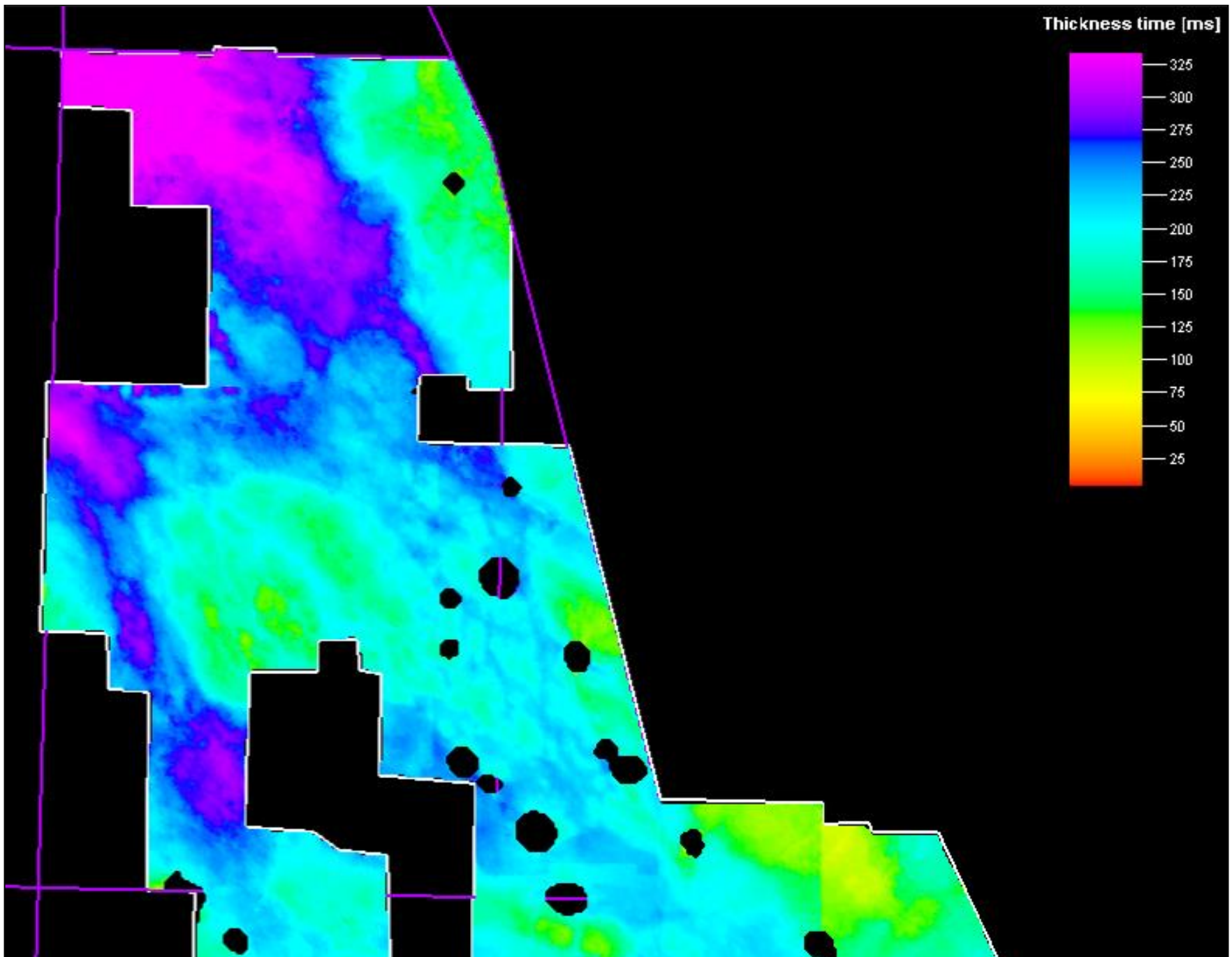

Figure 5.61: An uncontoured isochron which better images the detail of the individual channels as they lose energy and coarse material further south become smaller and more localised.

The initial channels lacked cohesive levees leading to erratic deposits of chalky debris, sand and shale. However, soon after the initiation of fan deposition in the North Sea, the total sediment flux reached a maximum and thereafter began to decline. Thus, later stages of sediment input created channels that were more stable and aggradation of massive sand bodies could occur (Jager et al. 1993).

The first clastic influx into the previously chalk-dominated shallow sea, occurred at the end of the Cretaceous and into the early Palaeocene, initiated by the uplift of the Scotland-Shetland Plateau. Deposits tended to consist of poorly organised slope apron slump and debris flows (Figure 5.62) derived from erosion of the plateau and reworking of basin margin chalks due to lack of an integrated drainage network. Sands deposited in this package are ascribed to the Maureen Formation, despite containing variable amounts of chalk and shale. An isochron of this clastic sequence shows the large volume of material and lateral extent of the early Palaeocene channels (Figure 5.63).

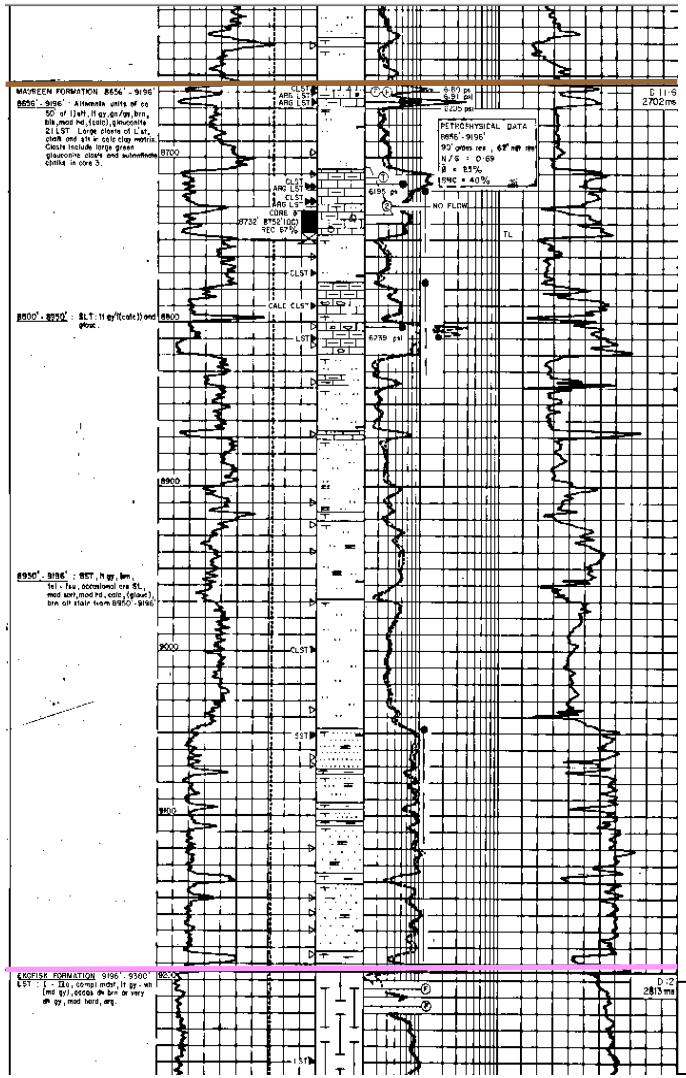

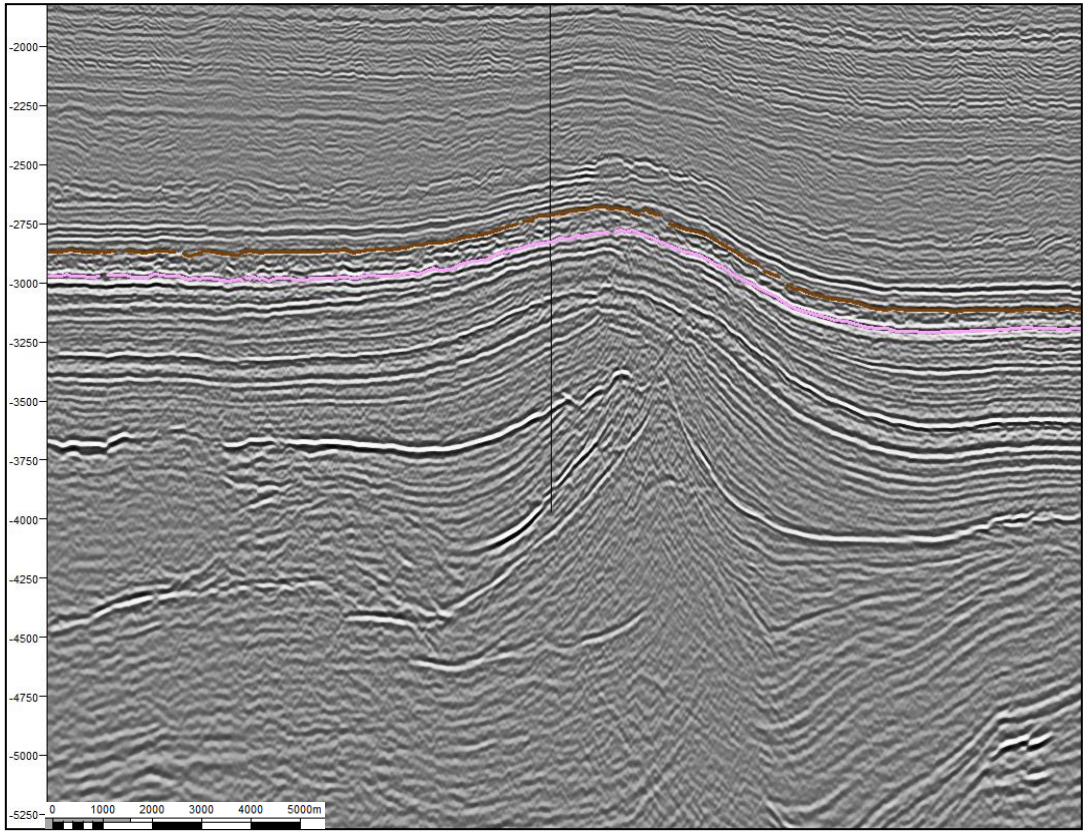

Figure 5.62: Palaeocene channel recognised from seismic data as a chaotic reflective package and tied back to well data.

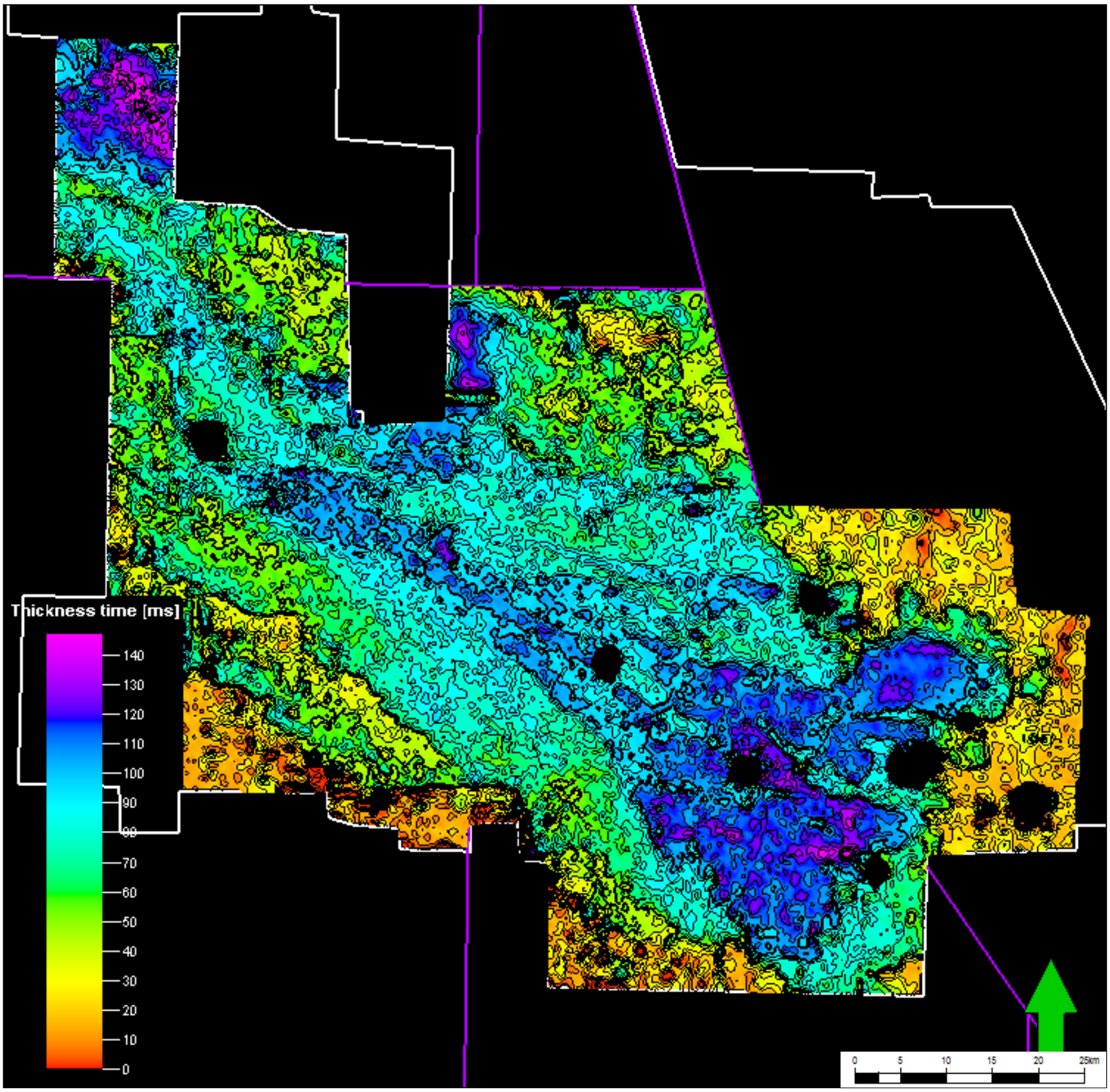

Figure 5.63: An isochron of an Early Palaeocene channel. It is composed of a mixture of chalky debris, limestone, sand and clay and is larger and higher energy than later channels as evidenced by its continuation into the far south of the dataset and the bulky nature of the debris within it which would have required a high velocity flow to carry it.

Note that this package contains variable amounts of Mid-Palaeocene Mey sands as it was not possible to separate these seismically. Biostratigraphic evidence provides a reason for this in the large amounts of reworked Maastrichtian and Early Palaeocene material.

By the early Thanetian (58Ma) the drainage systems of the source area had fully developed, covering an area of 45,000km^2 and focusing the bulk of the sediment into the northwest Moray Firth Basin. Deposition reached its maximum at this time and high sediment flux caused overriding of the shelfal margins and basin centre deposition of delta-fed submarine aprons and basin floor fans. The Lista sequence can be divided into time equivalent sand members developed within the Moray Firth Basin (Andrew/Mey and Balmoral), East Shetland Basin (Heimdal) and Viking Graben (Heimdal) and Central Graben (Andrew/Mey and Balmoral) (Knox et al. 1992). The Andrew/Mey Sand Member consists of thick submarine fan deposits and tuffs deposited in a prograding delta building south and east along the Moray Firth axis. As the pulse of clastic sediment waned during the Late Thanetian, the Lista shale was again deposited.

In the latest Thanetian, the last period of aggradation took place depositing the Forties Sandstone Member during the Palaeocene-Eocene Thermal Maximum (PETM) hyperthermal. Due to the global importance of the PETM, a chronostratigraphic subdivision is used in this document rather than the typical lithostratigraphic one. In lithostratigraphic terms, the sand-prone sequence deposited during this period is known as the Forties Sandstone Member and is assigned to the Sele Formation while in this document the term Forties Formation is used to represent the lower part of the Sele Formation regardless of sand content. Forties Formation sands are more proximal than those in the Lista (Vining et al. 1993) and have a thickness of over 250 m in the graben centres. They are constrained to the

west and east by rapid thinning on to the margins of the Forties-Montrose High and Jaeren High where mudstones are deposited instead (Figure 5.64).

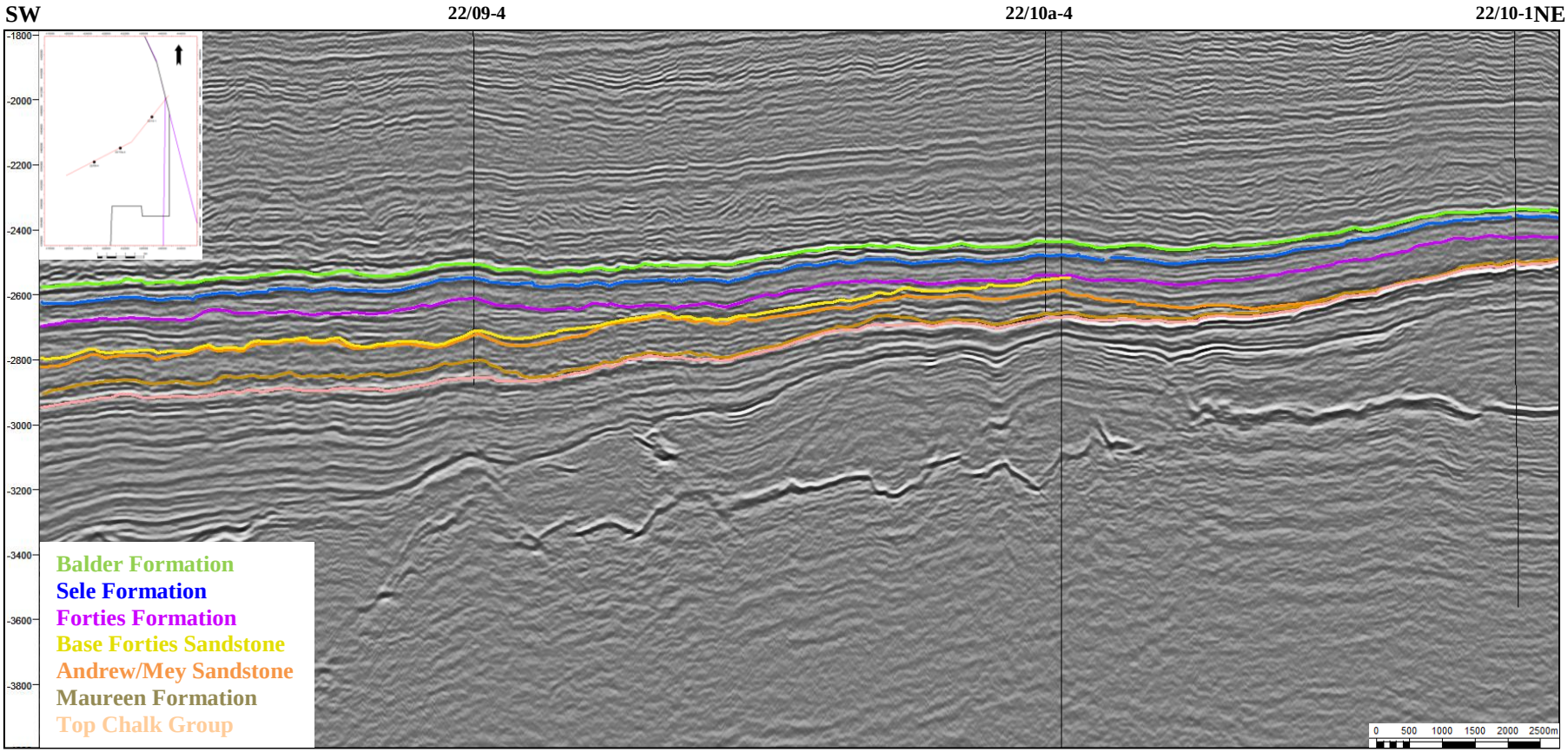

Figure 5.64: Seismic line over the Jaeren High showing the successive pinch-out of the Palaeocene clastic sequences.

The clastic sequences of the Forties Formation in the Central North Sea are distinctly channelized with sands deposited in discrete submarine fans separated by shale-prone inter-channel areas. A number of NNW-SSE striking sand-prone fairways can be located over the East Central Graben (Figure 5.65) which show similarity with 3.5 kHz echograms and seismic data from a number of present-day submarine fans including the Mississippi (Feeley et al. 1985) and Amazon (Damuth et al. 1988) submarine fan systems. Detailed biostratigraphic analysis (Chapter 6) suggests that changes in relative sea-level occurred throughout deposition of the Forties Formation and may have led to a series of clastic pulses recorded in these discrete fans.

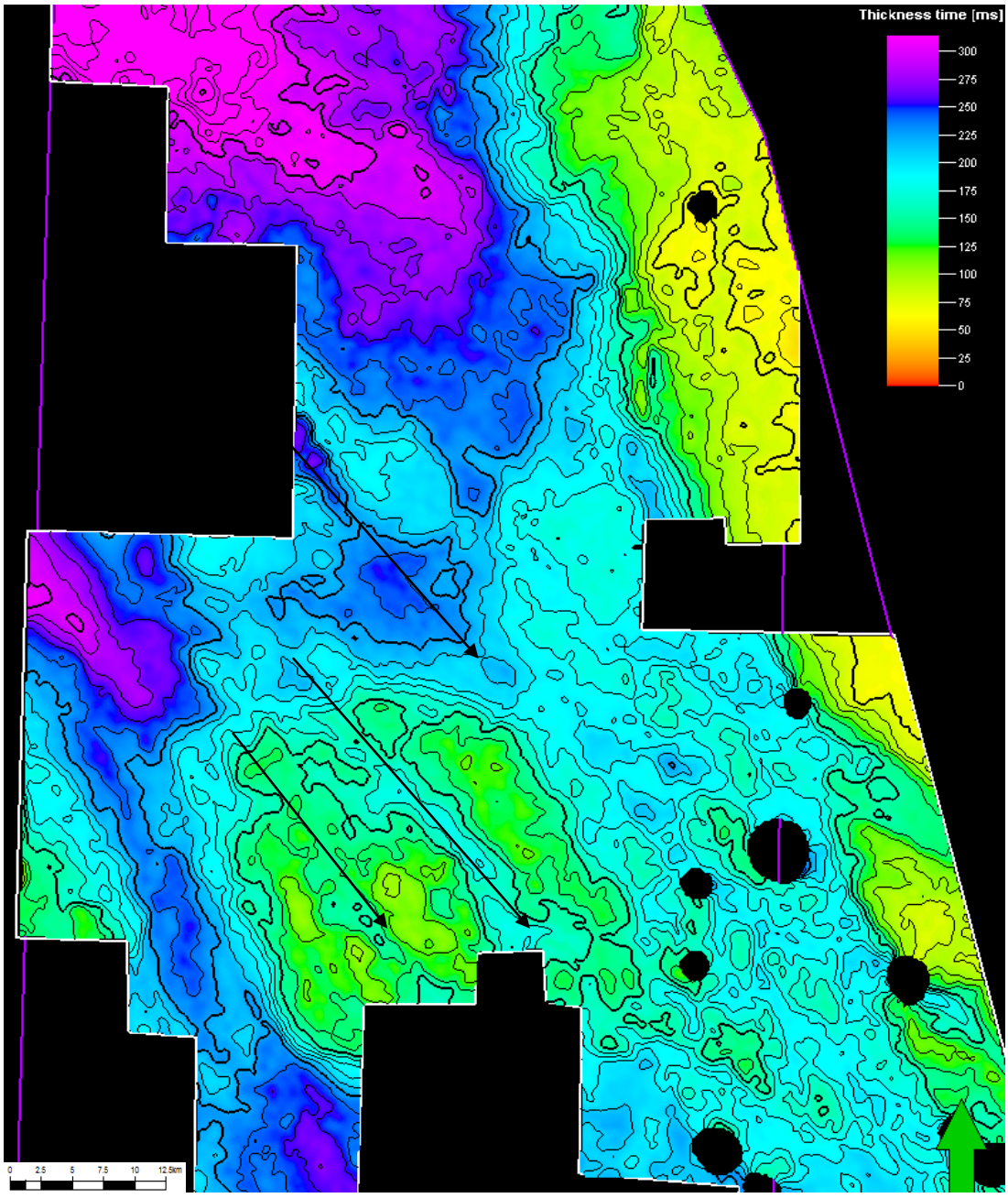

Figure 5.65: Discrete sediment transport pathways can be recognised in the Palaeocene sand unit similar to present day submarine fan systems.

Palaeocene channels appear to have been influenced by the underlying basin topography. Diapirism was reactivated in the Central North Sea by the regional tilt caused by uplift to the north and Palaeocene turbidites interacted with the bathymetry created by diapirs which reached the sea-floor. The relative distribution of Palaeocene clastic turbidite deposits around diapirs is dependent on a number of factors, foremostly the growth history and position of each individual diapir but also the composition and velocity of the turbidite flows. The interaction of these factors can be observed by placing the diapir locations on the Lower Palaeocene channel isochron (Figure 5.66). It is apparent that in some cases flows seem to terminate against diapirs, this occurs at the south-eastern extent of the turbidite flow and although it is possible that the flow had naturally reached the limit of its carrying capacity by this point, its termination by major diapirs seems to indicate that the bathymetric relief created by these features caused the clastic material held in suspension to drop out. This may be due to a simple loss of kinetic energy brought about by a slight change in slope gradient or a hydraulic jump whereby on encountering sharp breaks in basin topography, turbulence causes the water above a sediment flow to mix with it, reducing flow density and velocity and thus its ability to hold sediment in suspension (Hodgson et al. 1992). In other cases, turbidite flows appear to go straight over diapirs suggesting that these salt structures post-date the Palaeocene.

The final type of interaction noted involves the turbidites being deflected around the diapir leaving a shadow behind it. This suggests that bathymetric relief created by this salt structure was significant enough for the coarse, dense clastic material to be

deflected around it while only the mud-rich less dense material could pass over it. This has been postulated to lead to the deflected flow becoming overly dense and unstable leading to deposition around the flanks of the diapir (Piper et al. 1983; Hodgson et al. 1992) but this does not appear to be the case in the Central North Sea diapir observed on the isochron map. Possibly the low net/gross ratio of the Lower Palaeocene sequence in this example meant that the average flow density was not as affected by loss of finer material as later flows with higher net/gross ratios. Deposition of the late Palaeocene Forties Sand is reported to occur on the lee sides of diapirs (Hodgson et al. 1992).

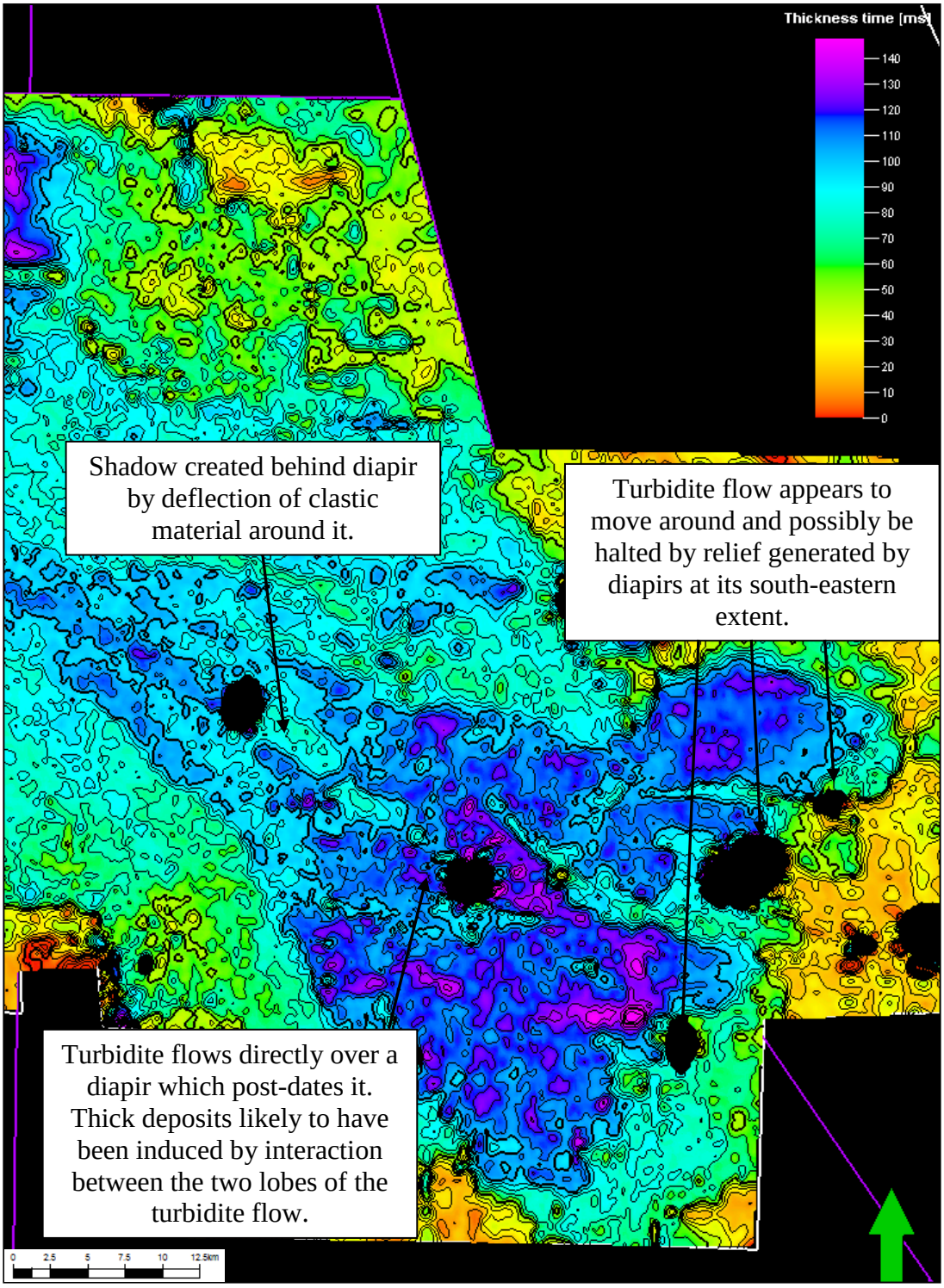

Figure 5.66: Isochron of the Lower Palaeocene sequence showing the different interactions which can occur between turbidites and diapirs.

5.2.3 PALEOGENE UPLIFT AND HINTERLAND REJUVENATION

SUMMARY

During the Palaeocene, post-rift thermal subsidence was interrupted by the effects of tectonic stresses in the North Atlantic and the subsequent emplacement of a mantle plume beneath Iceland which uplifted and tilted the Scotland-Shetland Plateau. Seismic interpretation in the Central North Sea and Faroe-Shetland Basin demonstrated the significant changes brought about by these tectonic events.

In the Faroe-Shetland Basin, faulting occurred during the Late Palaeocene and dikes of the same orientation were emplaced in both the onshore and offshore UK. These events were probably linked to stresses generated by regional compression within an extensional province due to the space problem posed by the rigid buttress of the Eurasian Plate. Plume-driven uplift caused prograding complexes to be shed off the hinterland into the Faroe -Shetland Basin. Further south, shelfal areas in the Inner Moray Firth were uplifted and exposed while in the Central North Sea large volumes of clastic sediments were shed into the basin in the form of lowstand fans. A major climatic event occurred during the Latest Palaeocene known as the Palaeocene-Eocene Thermal Maximum (PETM) at approximately 55Ma which may have influenced rainfall patterns and also contributed to the high erosion rates and volumes of clastics shed into the basin during this time. Mapping of these submarine turbidite flows shows that early channels were large and unconfined, composed of chalky debris, sand and shale while later flows were more channelized. The channel

systems appear to have been influenced by basin topography and pinch-out onto basement highs and are affected by bathymetric relief caused by diapirism.

A later period of uplift at 54.7Ma caused areas in the Faroe-Shetland Basin to become sub-aerial and incision occurred creating a highly intricate dendritic drainage system. This period of incision following uplift is represented in the Central North Sea as an unconformity or correlative conformity at the top of the Forties Formation.

4.3 RE-ESTABLISHMENT OF POST-RIFT SUBSIDENCE

4.3.1 NORTH ATLANTIC TECTONICS AND SEDIMENT SUPPLY

During the remainder of the Early Eocene, the plume moved away from the Highland area resulting in foundering of the plateau (Hall et al. 2002). Rapid decay of uplift in the Eocene is attributed to a temperature decrease of the plume, and loss of dynamic support as the Atlantic opened. This coincides with a decrease in volcanic activity within the British Tertiary and Greenland Igneous Provinces, and the initiation of true sea-floor spreading between Greenland and northwest Europe (Nadin et al. 1997). Inversion structures such as the Wyville-Thomson Ridge and Helland Hansen Arch are seen in the Vøring, Møre and Faroe Shetland Basins attributed to compressive stresses generated in the North Atlantic. There is also evidence that continental collision had truly begun in the Alpine region (Dal Piaz et al. 1972; Coward et al. 1989; Ford et al. 2004) although this is still debated by some authors.

It is likely that the effects of the Iceland Plume were predominantly thermal and therefore transient in nature but there may have been an element of magmatic underplating which would have led to permanent elevation (Maclennan et al. 2002) of the area. However, this alone was not sufficient to maintain the high sedimentation rates that characterised the Late Palaeocene and in the Central North Sea the amount of clastic influx to the basin centre dramatically reduced. Deposition during the Early Eocene was no longer initiated by uplift but the shifting of delta channels through

time. Progradation led to sediments building towards the shelf and deposition became more proximal to the source as sediments no longer bypassed the shelf edge easily. Eocene sediment flux was also steadily diminishing as the basin filled and uplift slowed leading to smaller more confined channels such as the Tay Sand channel mapped in the Central North Sea (Figures 5.67-5.69).

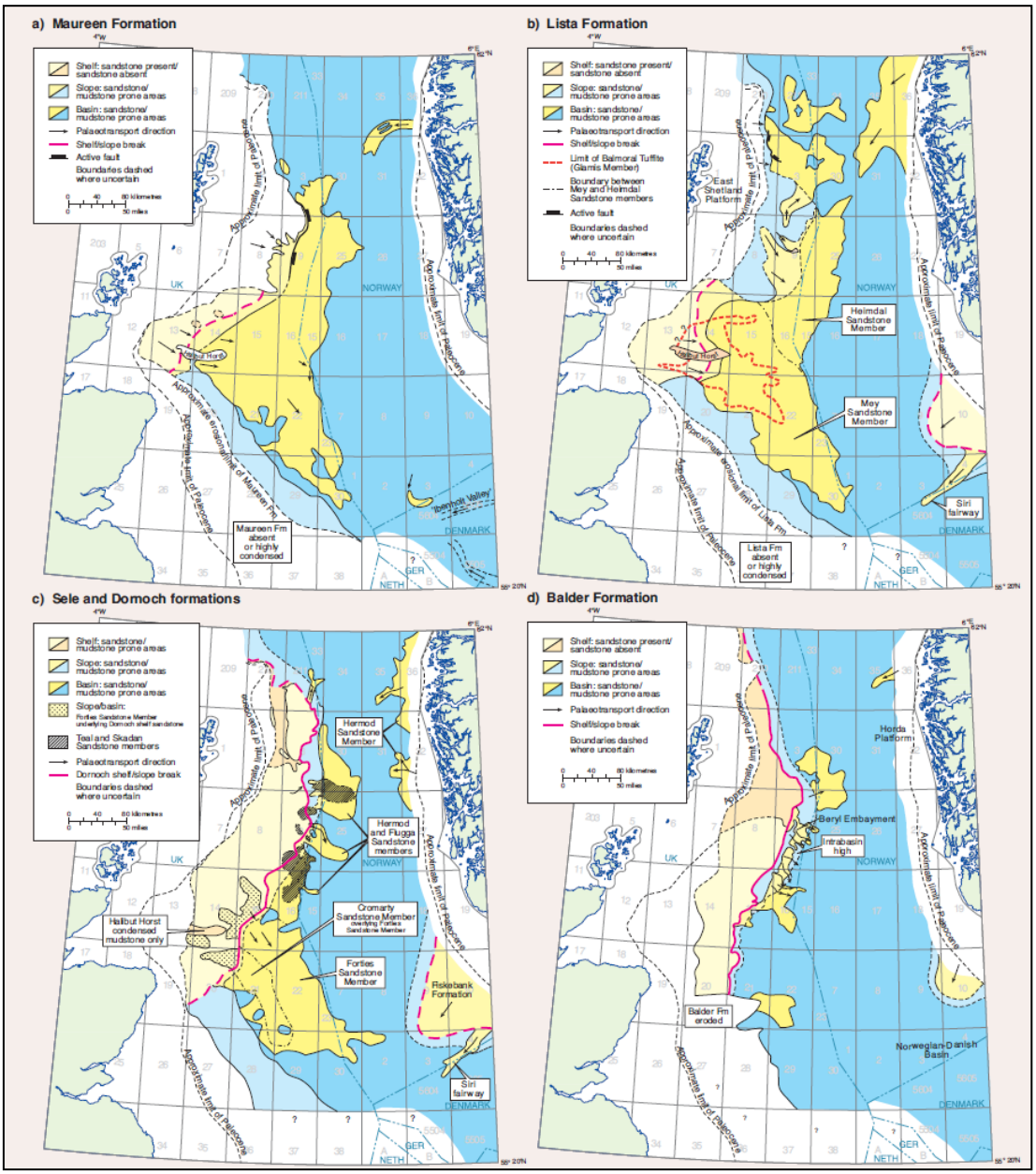

Figure 5.67: Paleogeographic maps of the Palaeocene showing the location of the shelf and basinal sandstones throughout the Epoch.
Image after (Evans et al. 2003)

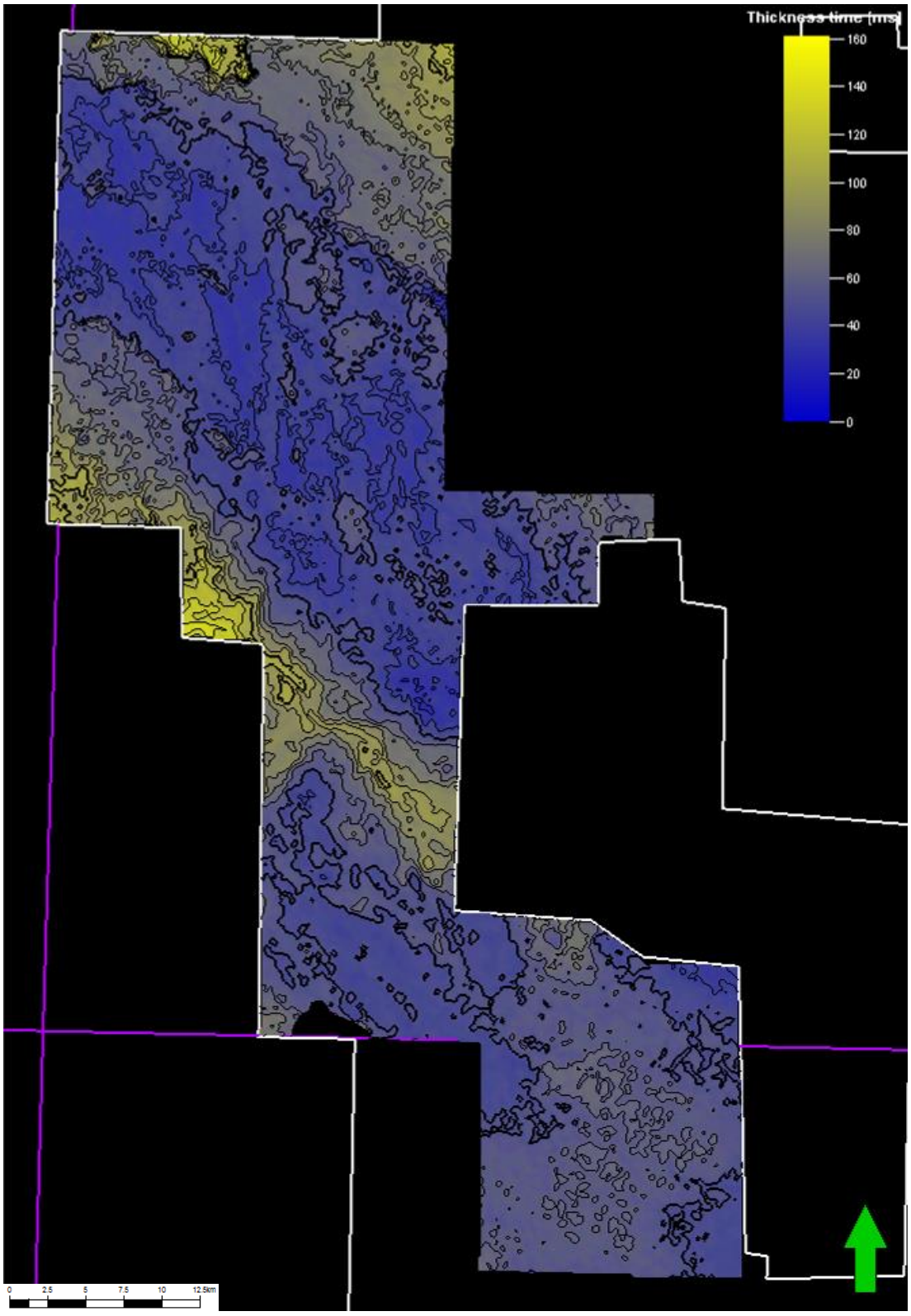

Figure 5.68: An isochron of the Eocene-age Tay fan demonstrating its smaller, more confined nature compared to the Palaeocene fans.

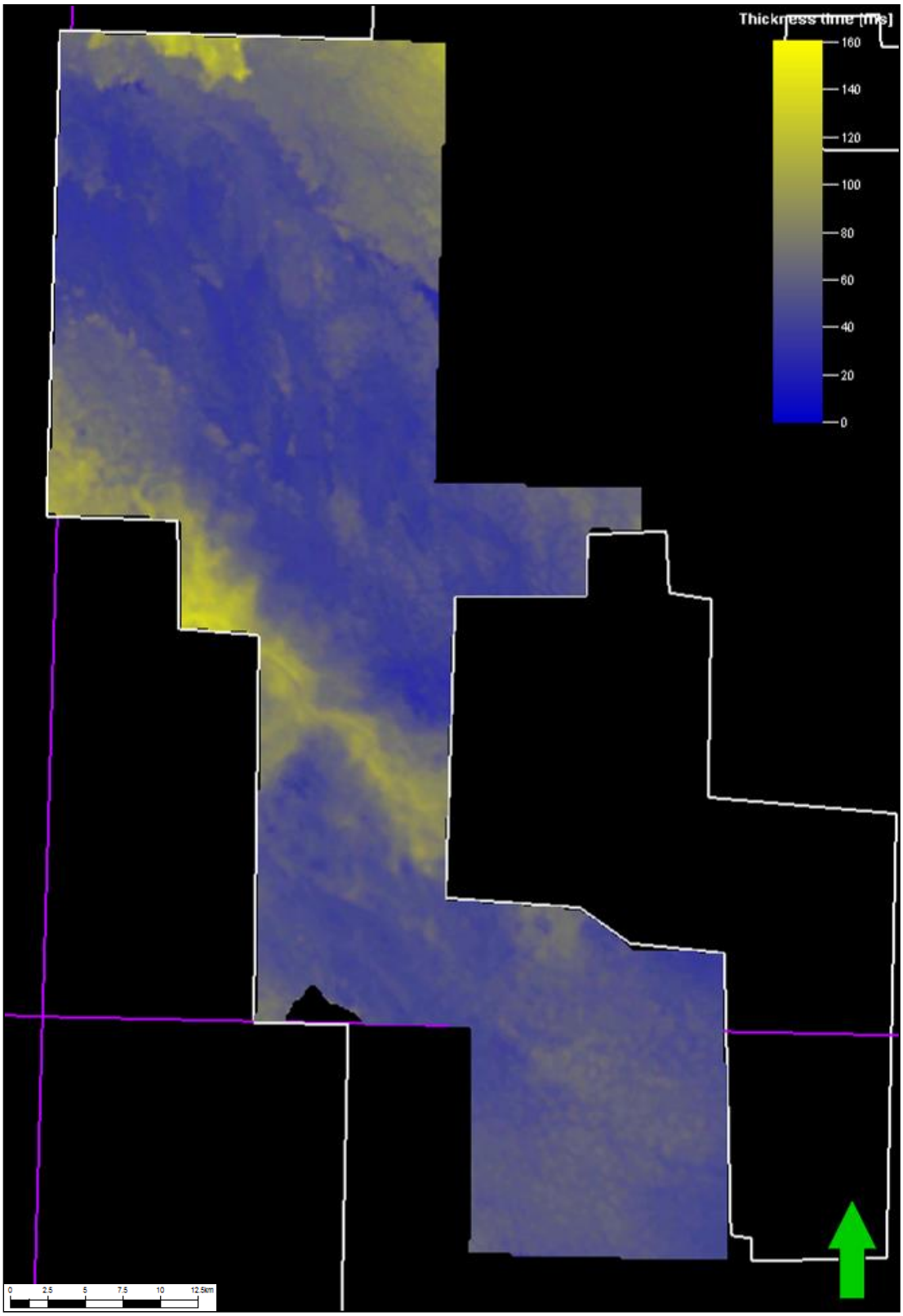

Figure 5.69: An uncontoured version of the Tay isochron which highlights the intricately braided channel system.

4.3.2 SEDIMENTARY FEATURES IN A SUBSIDING BASIN

Compressive stress due to North Atlantic rifting continued throughout the Eocene in northern areas leading to inversion in the Faroe -Shetland Basin. However, in the Central North Sea, extensional polygonal fault complexes are seen which are anomalous given this compressive stress field (Figure 5.70). It is therefore difficult to link this deformation to regional events but similar patterns are observed in other basins such as the Qiongdongnan Zhongijanan Basin in the South China Sea and Lake Hope in Southern Australia where there is also no regional tectonic activity which could have created them (Watterson et al. 2000; Chen et al. 2011).

Polygonal faults have been previously attributed to gravitational spreading/sliding (Cartwright 1994), gravitational instability due to density inversion (Cartwright et al. 1996) and fluid expulsion during early compaction (Lonergan et al. 1998). The normal faults in the study area have a restricted strike distribution, consistent dip direction and abrupt terminations and show similarities with desiccation cracks occurring in drying muds. It is thus envisaged that fluid expulsion from Eocene sediments led to contractional shrinkage and high pore fluid pressures which caused failure of the cohesive sediments.

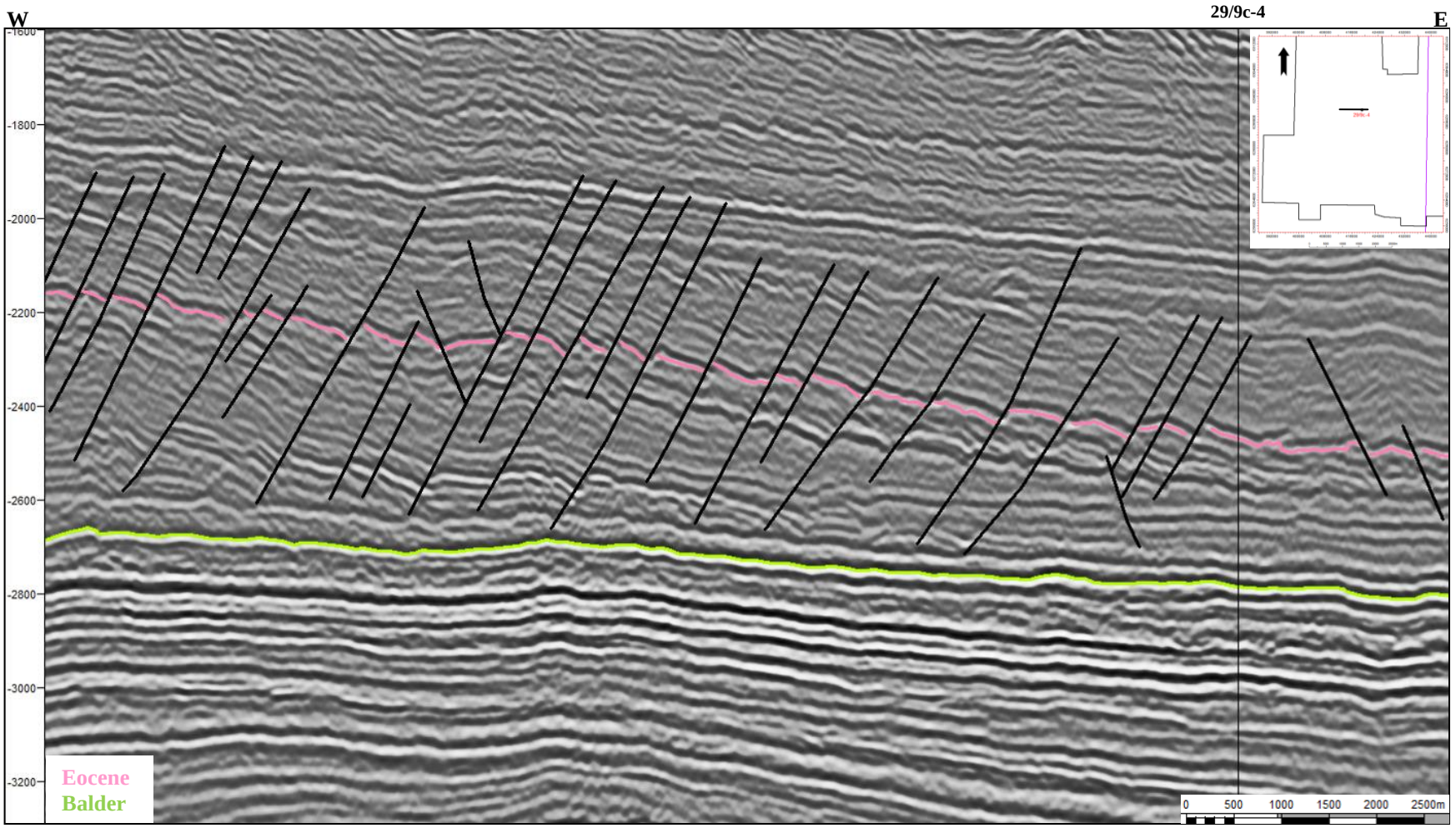

Figure 5.70: W-E section showing extensional polygonal faults in the Early Eocene- Oligocene section. Note that none of the faults offset the Earliest Eocene Balder Formation which acts as a seal for Palaeocene hydrocarbon reservoirs.

Also observed in the Eocene seismic section were amplitude anomalies which appeared to be distributed in clusters with no observable relationship with the underlying geology (Figure 5.71). Well penetrations and reports in the area show that these features are clean sandstones surrounded by a muddy matrix and biostratigraphy dates them as Palaeocene in age. There are several theories as to how sands are injected into younger layers, proposed mechanisms include, liquefaction by earthquakes or impacts, overpressure due to rapid burial or migration of hydrocarbons or groundwater, disequilibrium compaction and lateral transfer pressure (Huuse et al. 2005). In the Central North Sea high pore-fluid pressure is already suggested to have created the polygonal fault patterns therefore it seems likely that this also played a role in the formation of sand injectites. Over-pressuring may have occurred due to rapid burial with low permeability mudstones or migration of fluids into sealed sand bodies leading to rupturing of the top sea and fluidisation of the sand grains.

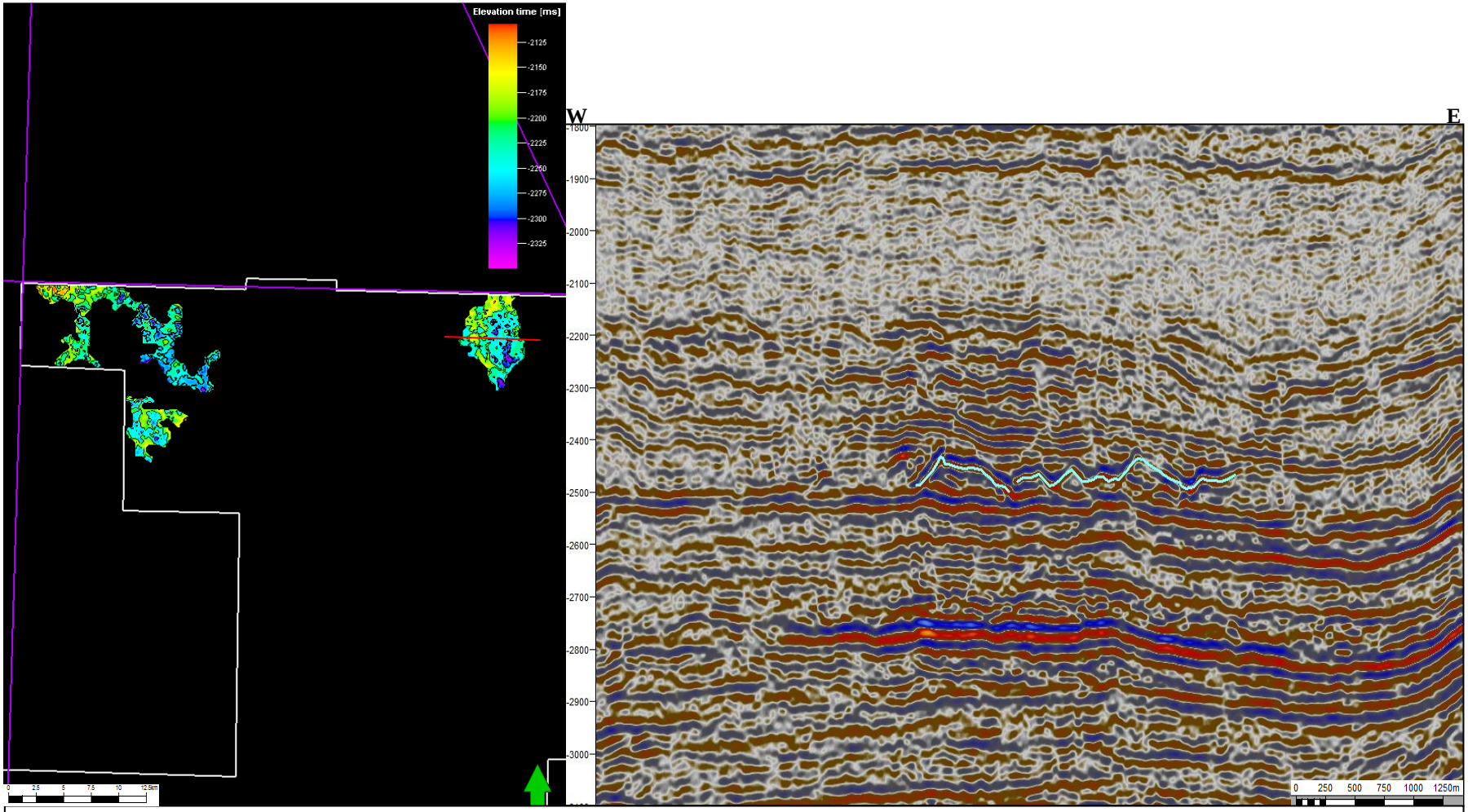

Figure 5.71: TWTT surface map and seismic section across injectite structures in the Central North Sea.

During the Oligocene to Miocene, the North Sea was affected by changes in water-mass movements due to the closure of the Tethys and the barrier between Greenland and Scotland (Iceland- Faroe Ridge) which eventually breached in the Mid Miocene (Evans et al. 2003). Compressional folds east of Greenland, and in the Porcupine Basin, areas decoupled from the Alpine foreland show that North Atlantic compression was still exerting a strong force on its margins (Dore et al. 1999). Continued inversion in the Sole Pit Basin of the Southern North Sea and other areas was coincident with a change in North Atlantic spreading direction (Dore et al. 1999; Evans et al. 2003) but also could have been aided by Alpine transmitted stresses as analysis of depocentres in the molasses basins dates peak collision to the Early Oligocene (Ford et al. 2004).

Compressive events during the Miocene led to inversion in the Central North Sea and reactivation of diapirs (Davison et al. 2000). Subsidence was also rapid leading to large volumes of sediment accumulating in the North Sea Basin. None of these events were mapped in the project however, although this is considered a possible area for further work.

Mapping of biostratigraphically dated Lower Pliocene units led to the discovery of unusual elongate mounds (Figure 5.72). Two separate families of these structures were mapped, separated by a period of uniform shale deposition. Surface structure maps and isochrons showed a distinctive NW-SE trend, with the lower family of structures seeming to curve around at the southern extent (Figures 5.73-5.75).

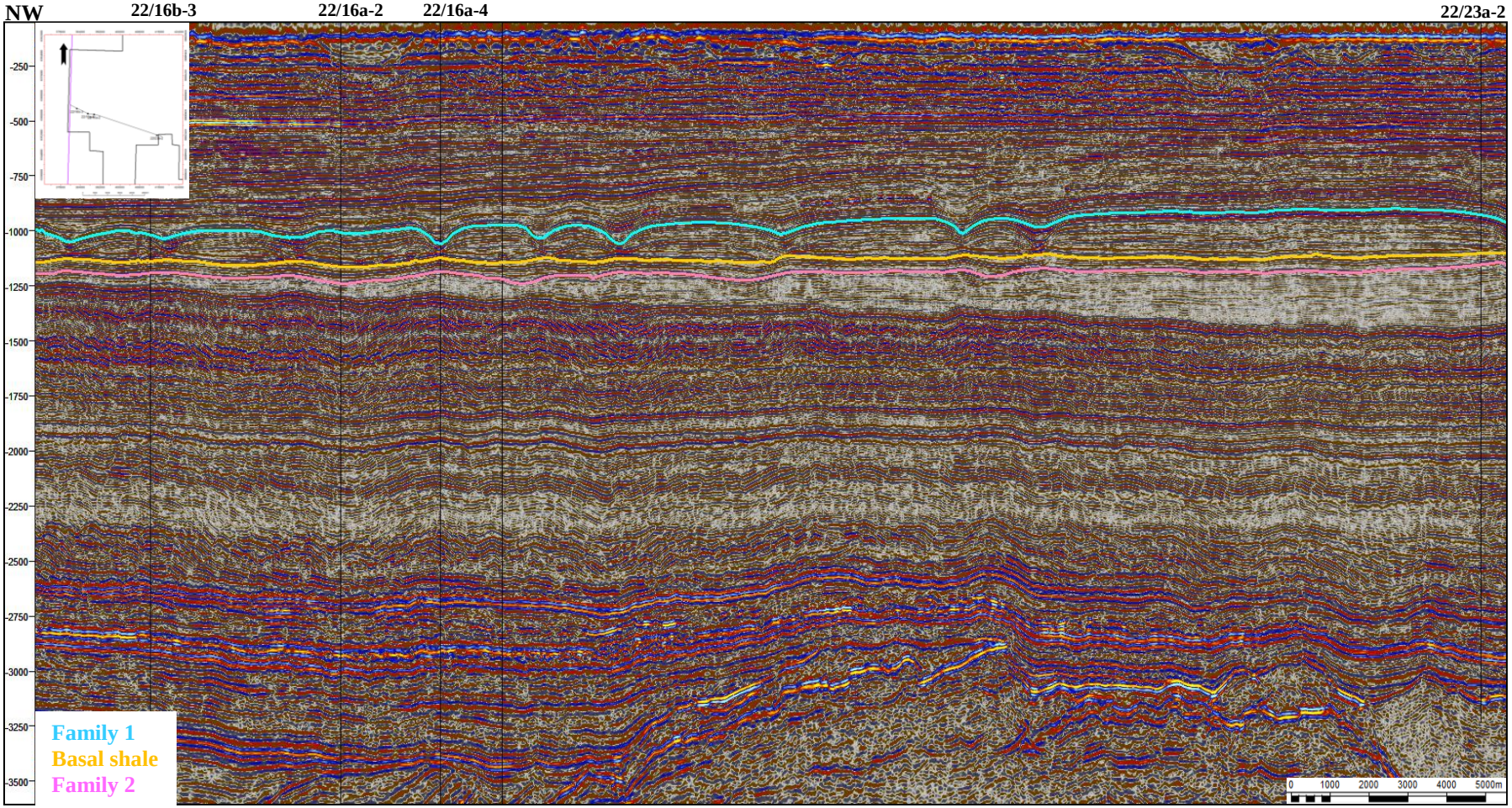

Figure 5.72: Composite seismic section showing the mounded structures in the Pliocene section.

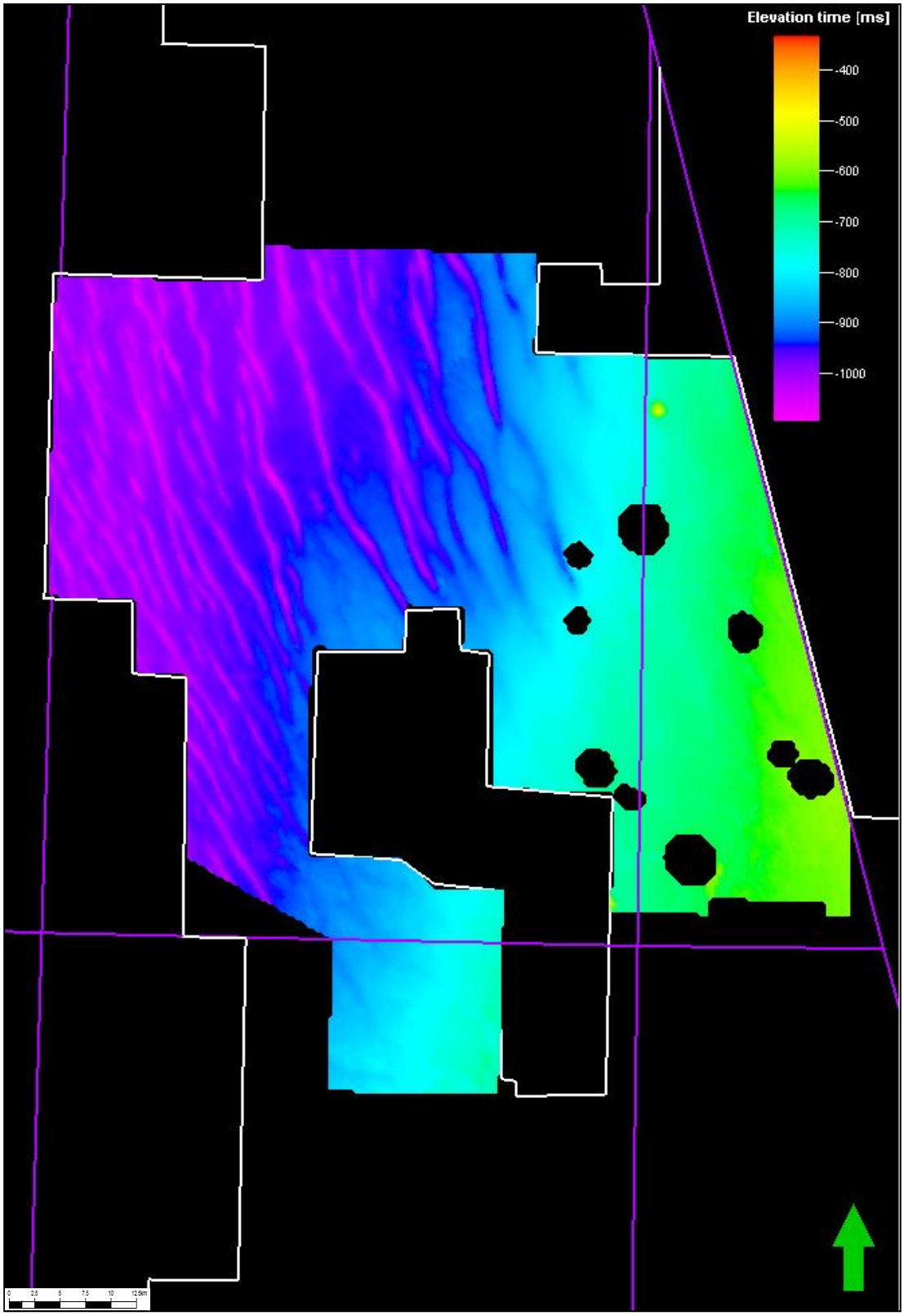

Figure 5.73: TWTT structure map of Family 1 of the mounded structures showing the NW-SE trend.

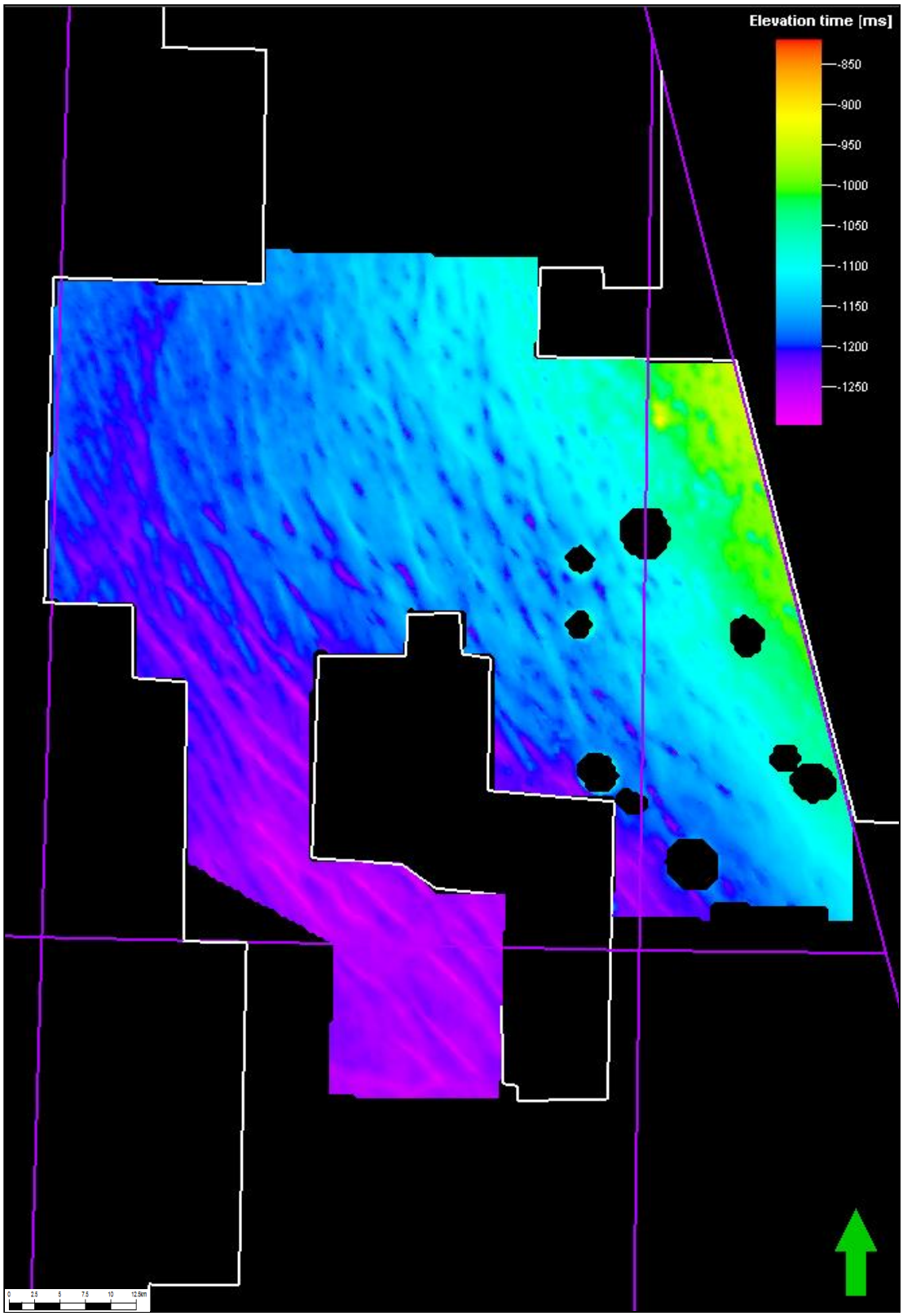

Figure 5.74: TWTT map of Family 2 showing the curvature of the structures.

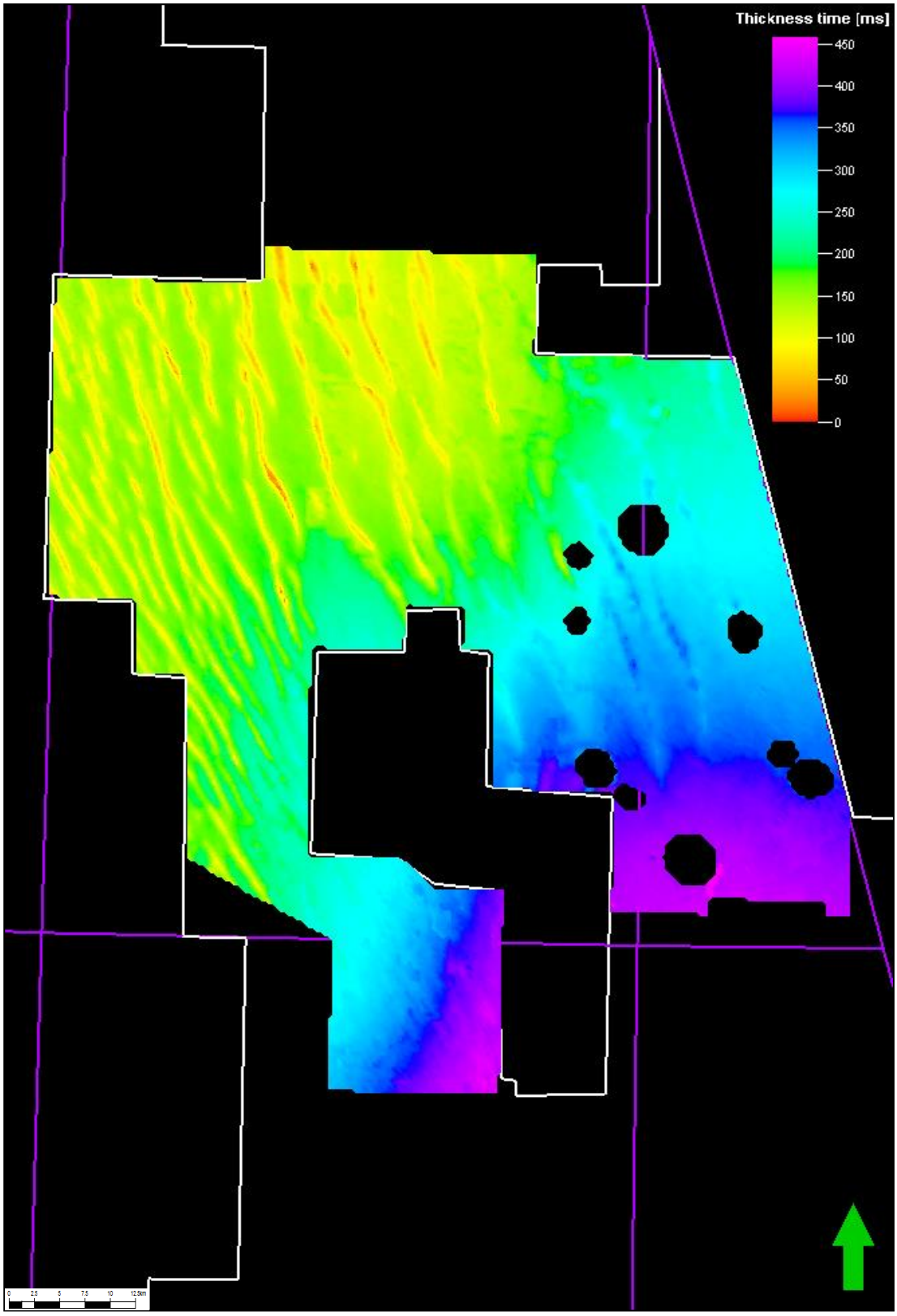

Figure 5.75: An isochron between Family 1 and the basal shale sequence clearly demonstrating thinning between the mounds.

These structures have previously been considered to be contourites, sedimentary deposits produced by deepwater bottom currents which usually occur due to oceanic thermohaline circulation but have also been recorded in the Faroe -Shetland Basin (Knutz 2010). The structures also superficially resemble channelized deposits from an up-dip source but there appears to be no regional inclination for gravity transport. They also resemble glacial features known as valley cambers which have been mapped from outcrop (Figure 5.76) (Parks 1991) but these require freeze-thaw to be in action and evidence from borehole biostratigraphy and sedimentology proves the basin was deep in the Pliocene and freezing of the sea-bed is highly unlikely.

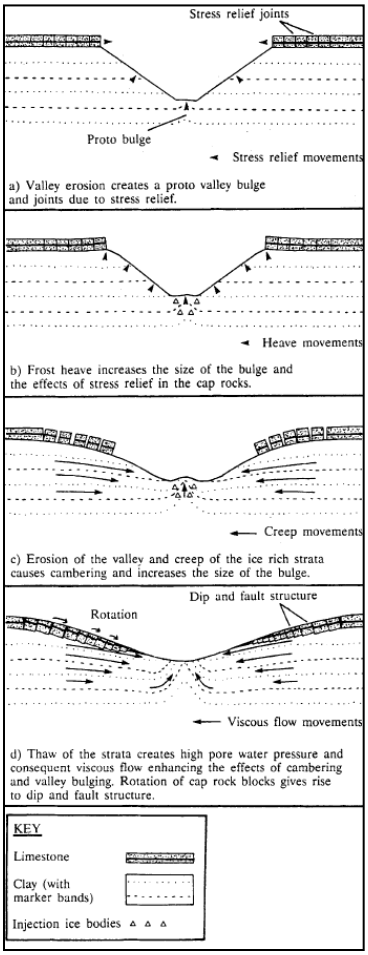

Figure 5.76: A proposed mechanism for valley cambering.
Image after (Parks 1991)

Contour currents seem to fit well with the data, although they have previously been mapped mainly in oceanic settings. The semi-parallel pattern of the North Sea structures resembles contour ridges developed by geostrophic bottom currents such as those observed in the Faroe -Shetland Basin (Knutz 2010). Amplitude anomalies occur over the structures (Figure 5.77) which could be evidence of shallow gas accumulations, and drilling reports suggest overpressure which can indicate shallow gas. Mapping of these bright anomalies shows they are concentrated near the terminations of the features (Figures 5.78 and 5.79). As yet there is no explanation for this observation.

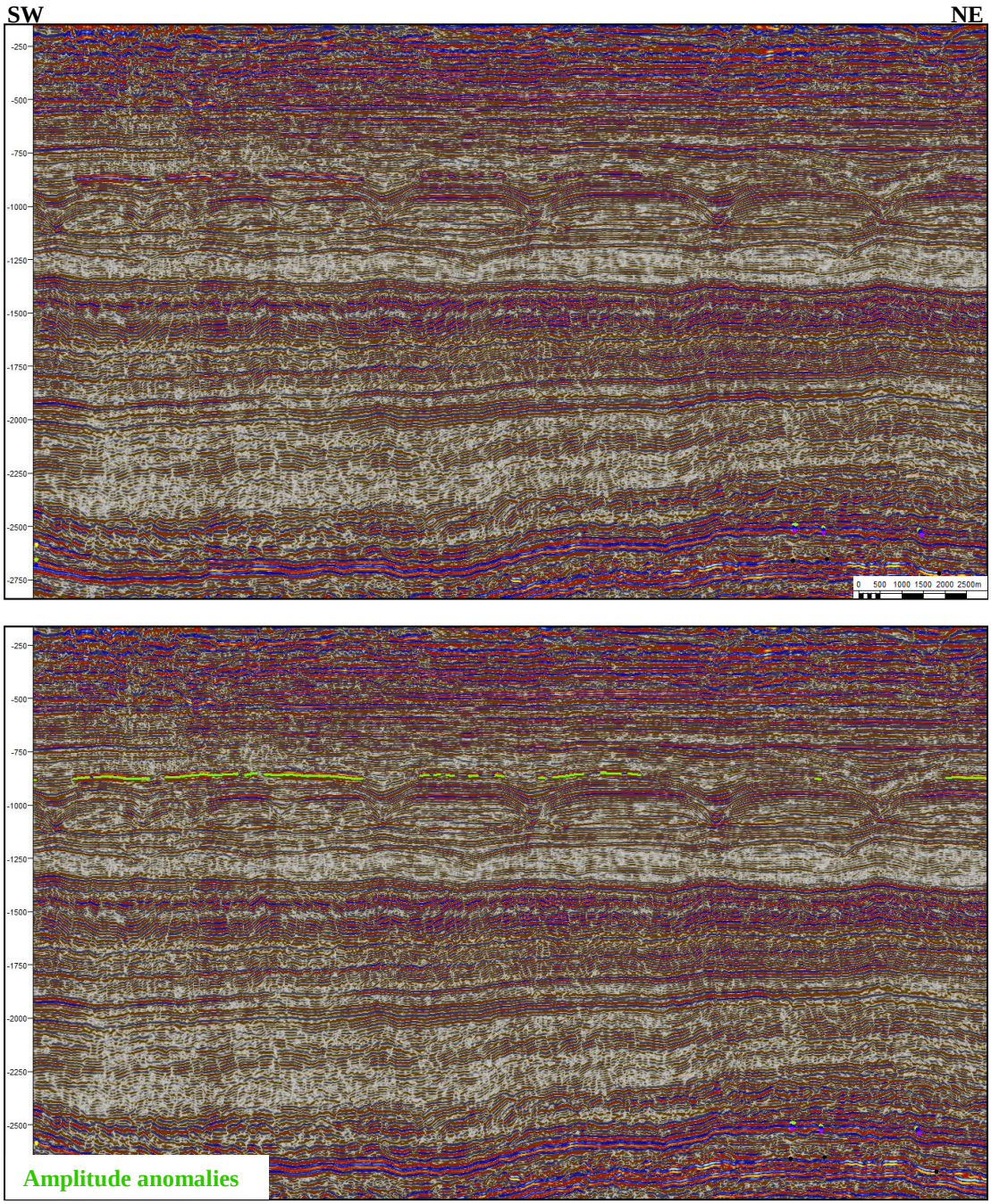

Figure 5.77: Amplitude anomalies above Pliocene mounded structures.
Location of section shown in Figure 5.78

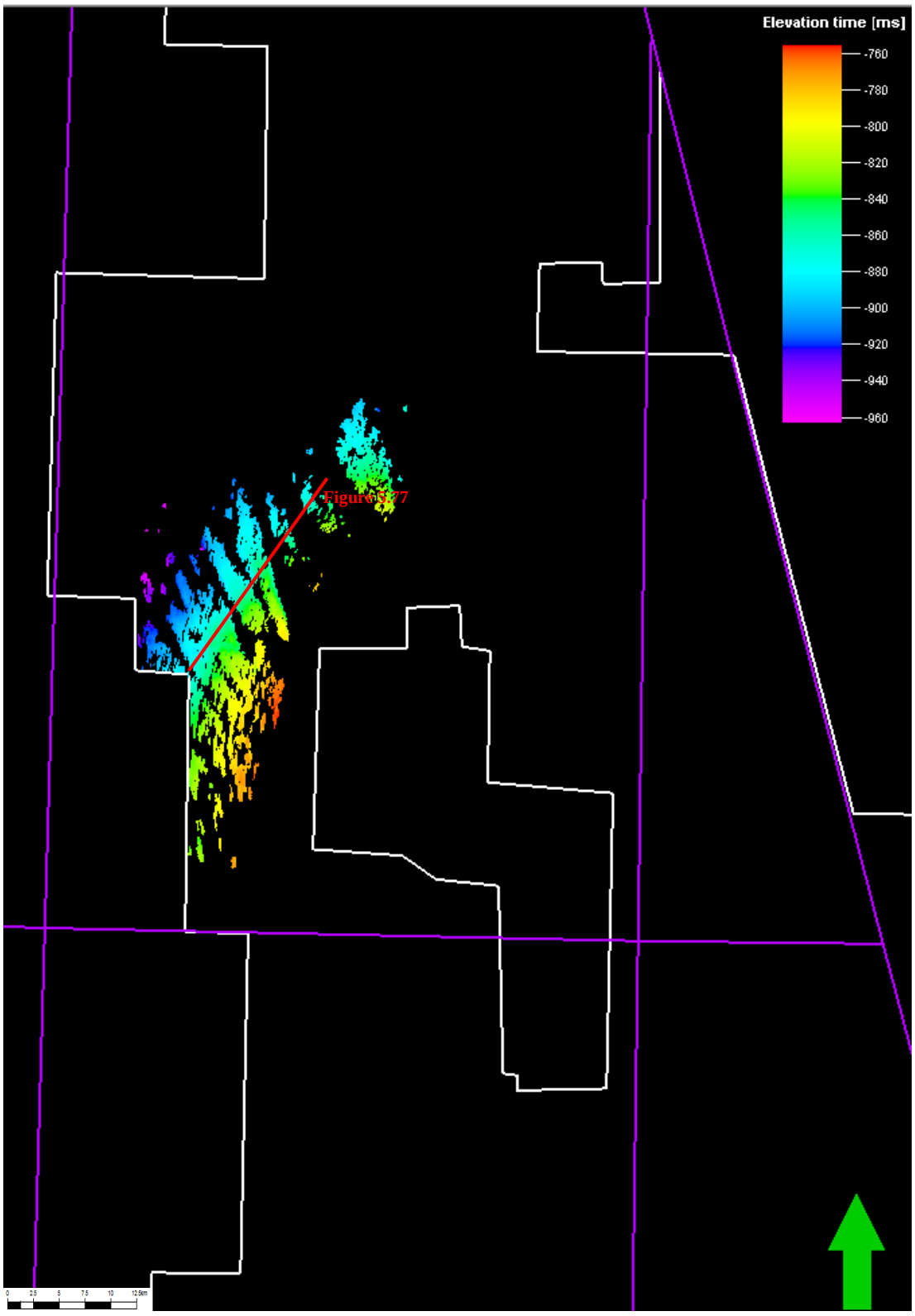

Figure 5.78: Amplitude picks showing their occurrence at the southern extent of the mounded structures.

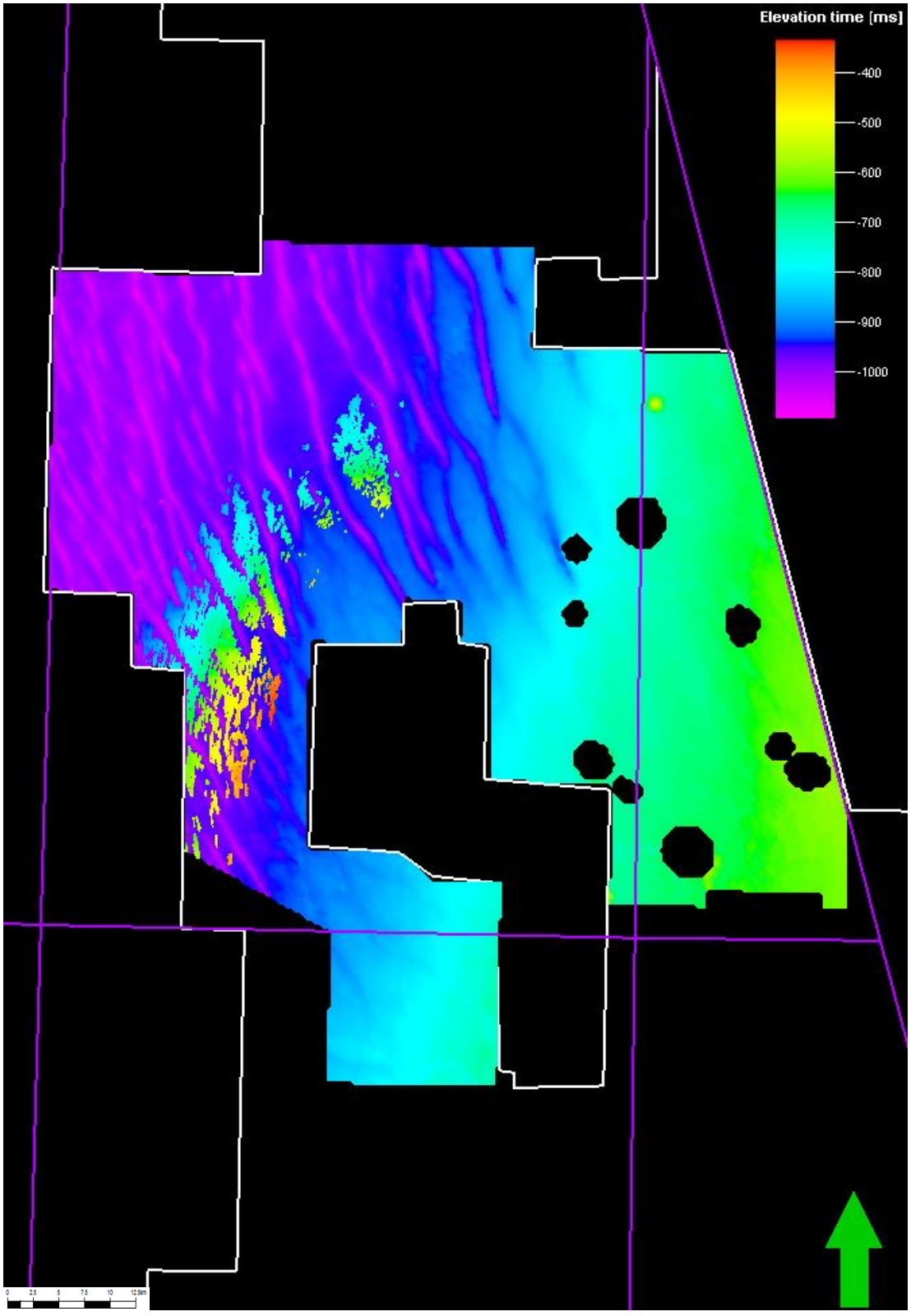

Figure 5.79: Amplitude picks superimposed on the structure map of Family 1 demonstrating the occurrence of high amplitude events over the top of the mounds and not between them. This suggests possible shallow gas in sands within the mounds.

Glaciation had begun by the Pleistocene and large glacial scour channels can be recognised and mapped in the Central and Southern North Sea Basins (Figure 5.80 and Appendix 4). These can be important for seismic processing and depth estimation as they are filled with glacial outwash with a different interval velocity to the surrounding rocks.

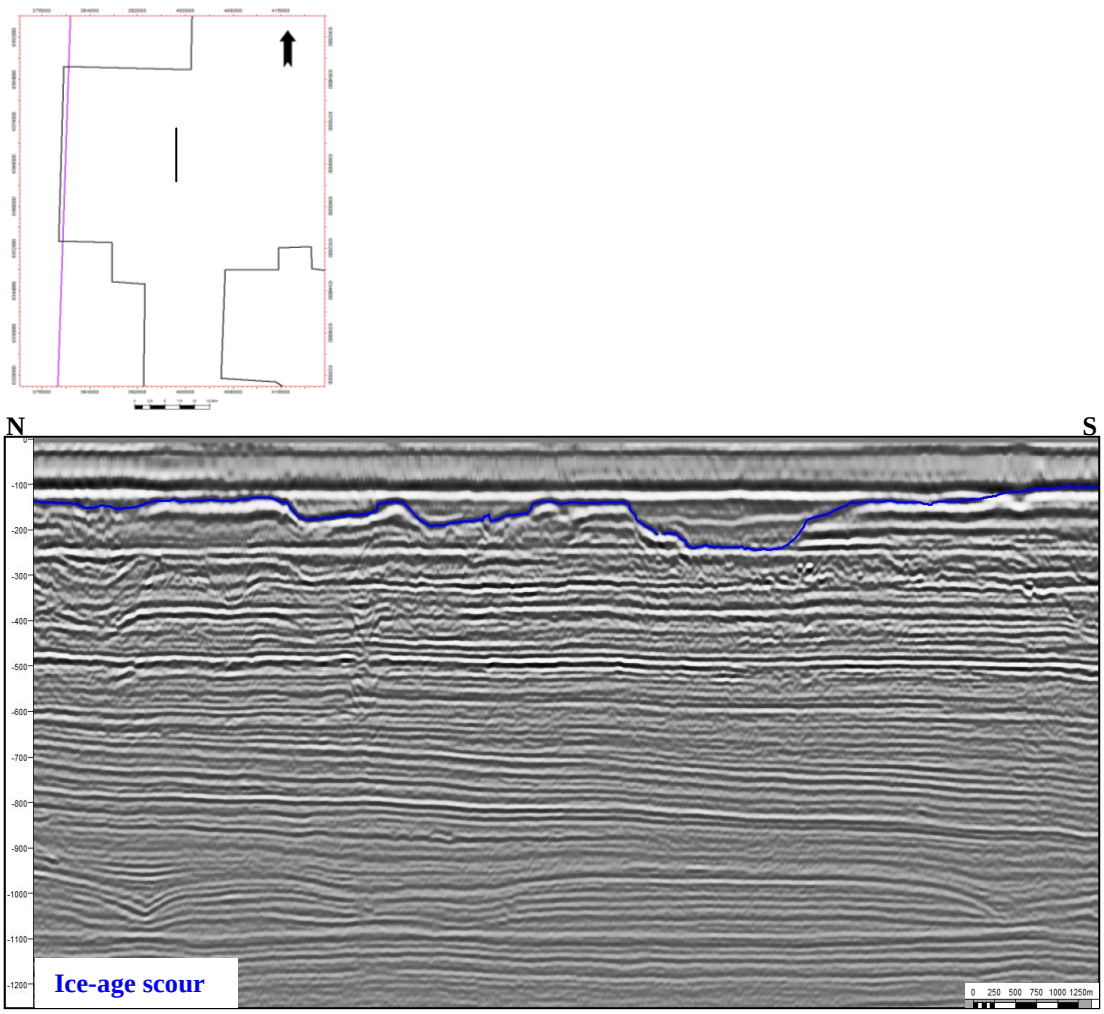

Figure 5.80: Examples of ice-age scour channels in the Central North Sea.

4.3.3 RE-ESTABLISHMENT OF POST-RIFT SUBSIDENCE SUMMARY

By the Early Eocene the Iceland plume was deflating and true sea-floor spreading in the North Atlantic had begun causing widespread inversion in northern areas. Transmitted stresses from the North Atlantic and possibly Alpine collision continued to cause inversion of pre-existing faults until the Mid Miocene. Pliocene to Pleistocene sedimentation was influenced by uplift of the basin margins, oceanic circulation changes and climate changes.

The results of seismic interpretation demonstrated that clastic sediment flux to the basin declined significantly in the Early Eocene and channels reaching the basin centre such as the Tay channel mapped were smaller and more confined than earlier Palaeocene ones. Relatively little mapping of sequences younger than Eocene age was undertaken in the Central North Sea datasets but anomalous structures of Pliocene age were mapped over much of the dataset. These structures have been considered to represent contourites and this conclusion is upheld by the current study despite superficial resemblances to other structures.

Mapping in the Pleistocene section found evidence of incised glacial channels which have implications for geophysical studies.

CHAPTER 6

THE PALAEOCENE-EOCENE THERMAL MAXIMUM

The previous chapter demonstrates that within the post-rift evolution of the Central North Sea the subsidence phase of the standard rift-drift curve was punctuated by the effects of far-field stresses from the North Atlantic region which culminated in the emplacement of a large plume beneath the Scotland Shetland Plateau. This major event had wide ranging effects and exerted a strong control on depositional geometries in the Central North Sea. High volumes of clastic sediment were shed off the uplifting basin margins and their cyclical nature has been linked to uplift-driven relative sea-level changes. However, during deposition of the most extensive of these clastic pulses the climate became extremely warm in what is known as the Palaeocene-Eocene Thermal Maximum (PETM) hyperthermal. Warming has been suggested to lead to enhanced humidity (Nicolo et al. 2007; Kender et al. 2012) and it is therefore possible that the clastic influx previously linked to tectonic events, could have in fact been climatically induced.

Climate has been recognised as having an important influence on the evolution of a basin and the North Sea basin is no exception. An arid continental climate during the Permian gave rise to the Rotliegend dune sands while movement into a more humid climate belt during the Triassic led to deposition of the Smith Bank mudstones and Skagerrak sandstones. After flooding of the basin in the Jurassic, a greenhouse

climate during the Cretaceous allowed microplankton to flourish and a thick chalk sequence to be laid down. During the Palaeocene the climate was warming again from a cooler period at the Cretaceous-Tertiary boundary and superimposed on this was a sudden intense period of warming, the PETM.

Since climate is so important in basin evolution it is vital to explore the ways in which it affects the geochemical, sedimentological, oceanographic and environmental conditions in greater detail. Concerns about present-day global warming are also very much at the forefront of public and scientific consciousness and thus studies of previous periods of climate change may provide useful analogies for present and future climate models.

Absorption of seismic energy with depth means that shallow events are imaged at higher resolution on seismic data and nearly all of the wells drilled in the Central North Sea penetrate at least as far down as the Palaeocene-age Sele Formation giving a higher degree of confidence to interpretation of stratigraphically young events. Biostratigraphic correlation and environmental interpretation is also more accurate in younger sequences as many of the species encountered will have living relatives and thus the limits of their ecological tolerance will be well known. Due to these factors it was considered that the most recent climate event, the PETM hyperthermal should be investigated in greater detail as it could provide analogies for the effects of past and future climate on basin evolution. Additionally the coincidence of this event with volcanism in the Faroe -Shetland Basin may provide important information on the possible link between hyperthermal climates and igneous activity.

The main objective in the study of the PETM hyperthermal is to investigate the way in which the event affected the depositional systems outlined in the previous chapter and use this as an analogue for past climatic influences on basin evolution. However, due to its importance as a hydrocarbon reservoir, the Palaeocene interval, especially in the Central North Sea where this study is centred, is peppered with boreholes (Figure 6.1), providing a unique opportunity to calibrate the hyperthermal event at a variety of scales. It is therefore possible to investigate in more detail the possible causal mechanisms and environmental effects of the PETM which may be a useful analogue for use in predicting the effects of future climate change.

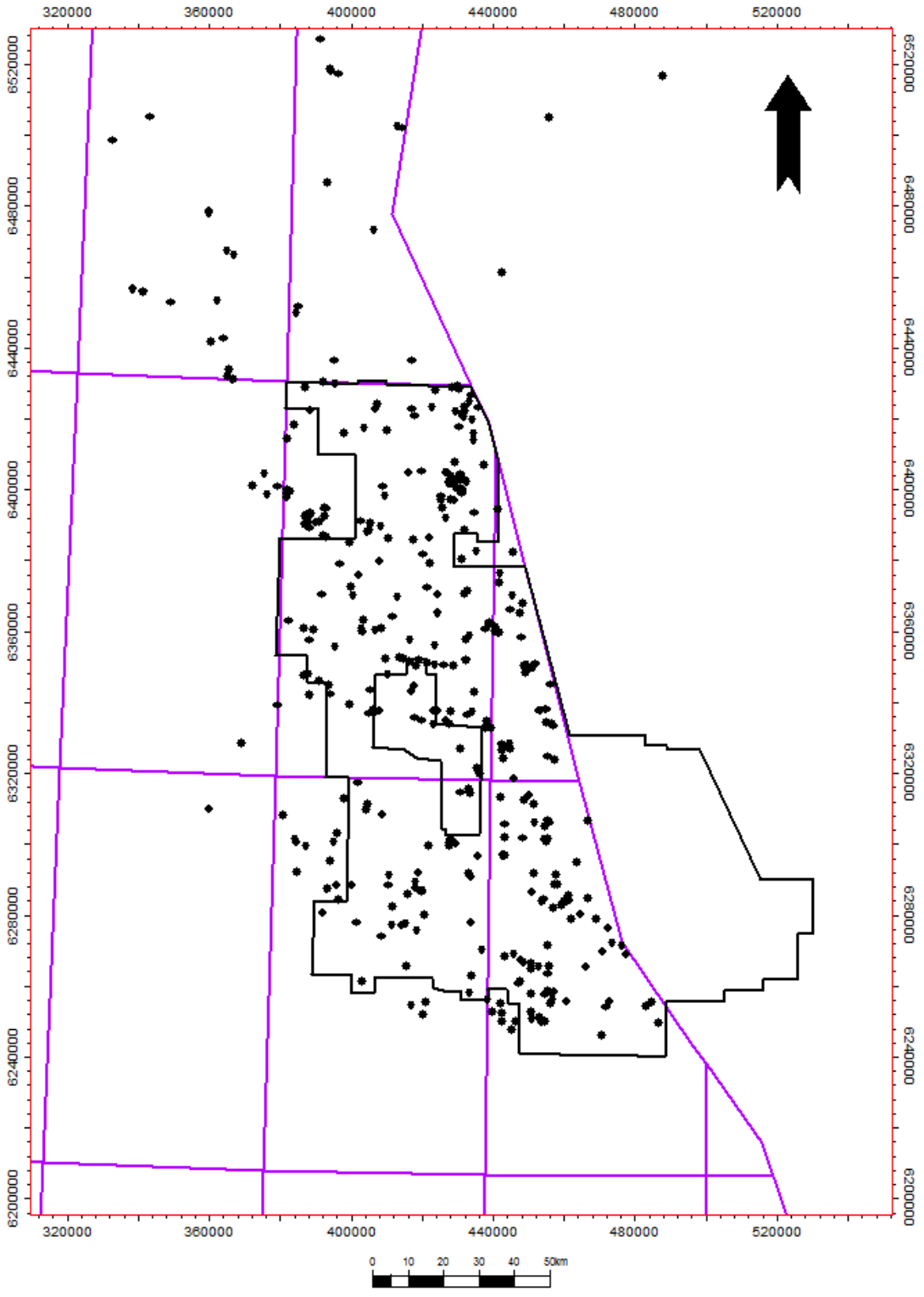

Figure 6.1: Well penetrations in the Central North Sea dataset demonstrating the large number of calibration points for interpretation of the Palaeocene section.

6.1 INTRODUCTION TO THE PALAEOCENE-EOCENE THERMAL MAXIMUM (PETM)

In order to successfully investigate the event in the North Sea and decide upon the most important areas to research it is important to be aware of the results of previous research and the current understanding of the PETM.

During the Late Palaeocene (59-55Ma)**,** a long term global warming trend began which cumulated in the Early Eocene in a period known as the Early Eocene Climatic Optimum (EEOC) (Zachos et al. 2001) (Figure 6.2). Superimposed on this warming trend was a sharp excursion known as the PETM characterised by a sudden strong negative δC^{13} excursion and extreme global warming, particularly of polar regions, linked to high concentrations of atmospheric CO_2. Since the initial discovery of this event in the Southern Ocean (Kennett et al. 1991) evidence of this warming has been identified worldwide in the oxygen and carbon isotope ratios of marine and terrestrial deposits with effects indicative of a massive perturbation of the global carbon cycle. It is also inferred to have been a causal factor in the widespread extinctions and migrations of both terrestrial and marine flora and fauna. The exact degree of CO_2 release and temperature rise during the PETM has proved difficult to quantify due to the complexity of climatic feedback mechanisms but the event is thought to have led to an increase in atmospheric CO_2 of 700ppm and warming of 5°C (Kennett et al. 1991; Zachos et al. 2003; Tripati et al. 2005; Zeebe et al. 2009). Comparison with current estimates of atmospheric CO_2 change which according to

the Intergovernmental Panel on Climate Change rose from 280ppm to 367ppm over the period 1750-1999 and more worryingly from 367 to 379ppm over the period 1999-2005 (IPCC 2007) demonstrates that the rapid increase in CO_2 and global temperatures over the PETM are in line with or even surpassed by anthropogenic warming. It is therefore vital to study these episodes of past hyperthermal climate not only to identify the effect these may have on basin evolution but also to inform on the possible future effects of continued CO_2 increase and climate warming.

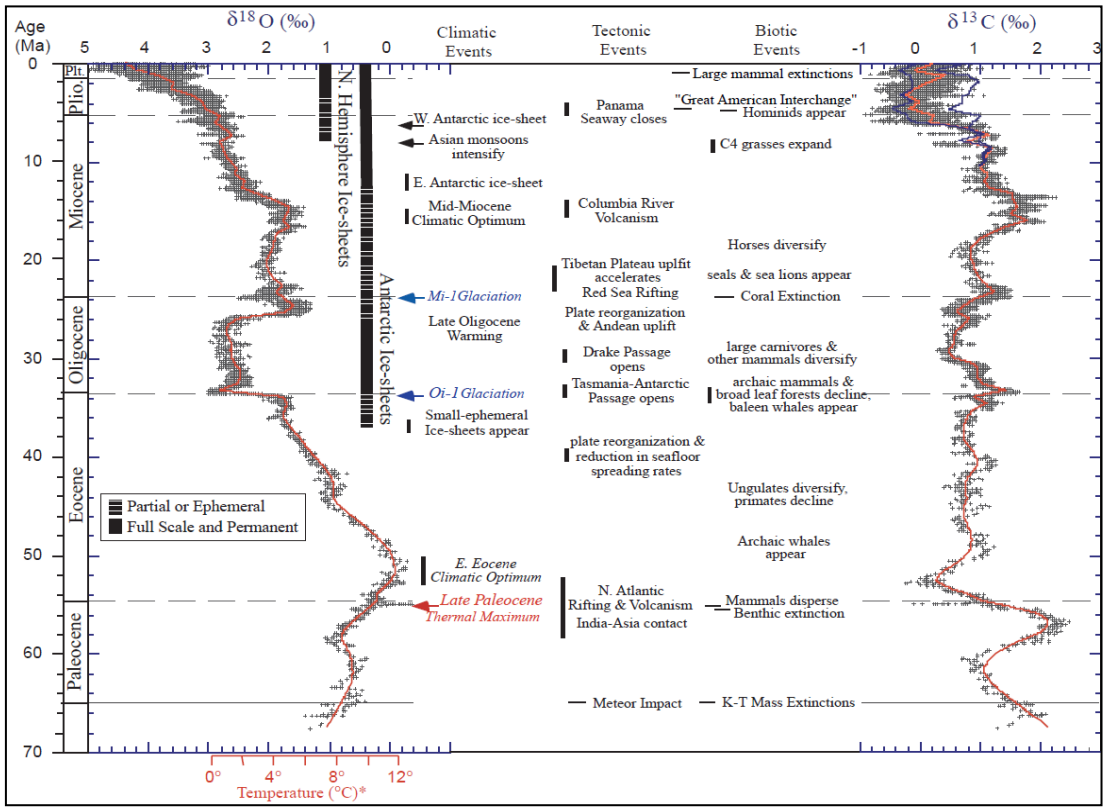

Figure 6.2: Global deep-sea oxygen and carbon isotope records from deep marine boreholes showing the general warming trend of the Palaeocene and the PETM event superimposed.
(Zachos et al. 2001)

The duration of the PETM is believed to be only in the order of 170kyr (Farley et al. 2003; Rohl et al. 2007) with a period of increasing global temperatures and atmospheric CO_2 followed by a gradual recovery to pre- excursion carbon values, temperatures and ecosystems, in effect an abrupt climatic spike in the geo-record. The exact timing of the recovery and the duration of the PETM itself have proved difficult to quantify due to the scarcity of worldwide zone fossils and other correlation datum. This is partially due to the provincial geography of the Palaeocene continental configuration and partially an effect of deep sea carbonate dissolution in response to the initial δC^{13} decrease. Recent research has focused on locating sections away from deep ocean sites which could provide more expanded sections and allow identification of background orbital cycles which may constrain the duration and timing of the event (Zachos et al. 2010; Charles et al. 2011). The exact cause of the global warming excursion at the end of the Palaeocene is as yet unknown although several hypotheses have been proposed.

Sites in which the expression of the PETM can be observed have been located and studied around the world yet the North Sea is an area which has been neglected due to the lack of complete sections in neighbouring land outcrops and the difficulties in locating areas outwith the oil and gas infrastructure in which to drill Ocean Drilling Project (ODP) cores. However, a recent discovery of a large negative carbon isotope excursion in the Late Palaeocene (Kender et al. 2012) of the Central North Sea may prove to be one of the most interesting discoveries yet as the high sedimentation rates in the Central North Sea mean that it may contain an unattenuated sedimentary record.

6.1.1 GLOBAL HISTORY OF THE PETM AND ITS EFFECTS

In 1990, analysis of marine sediments from Ocean Drilling Project (ODP) site 690 cored from the flank of the Maud Rise, Weddell Sea, Antarctica showed distinctive perturbations between 56 and 57Ma (Kennett et al. 1991). Micropalaeontological examination of the core showed a large extinction event of 35-50% of all species benthic foraminifera; this is now considered to be a worldwide event and a characteristic feature of the PETM and is known as the Benthic Foraminifera Extinction Event (BFEE). Isotopic analysis also showed considerable excursions in the δC^{13} and δO^{18} records of biologically-precipitated carbonates (Figure 6.3), indicating that average water temperatures during this time were in the region of 18-21°C. This rise in temperature corresponds with an influx of subtropical microfossils and a peak in the clay mineral kaolinite which indicates that the inferred source of the clay-rich sediment, Antarctica, was experiencing warm, humid conditions. Kennett and Stott concluded that the changes were due to an injection of isotopically light carbon into the ocean-atmosphere system, possibly by reorganisation of global oceanic circulation systems and subsequently published their findings in the journal Nature the following year (Kennett et al. 1991).

Once published, the scientific community spent the next few years investigating other oceanic sites around the world and it became apparent that the isotope excursion, and warming indicated by it, observed in Antarctica was a global signature. As more evidence has emerged other potential explanations for the

dramatic and rapid environmental changes were put forward in addition to the oceanic circulation model including dissocation of methane hydrates (Dickens et al. 1995; Bains et al. 1999), high rates of volcanic out gassing (Bralower et al. 1997) and tectonic activity (Kerrick et al. 1993).

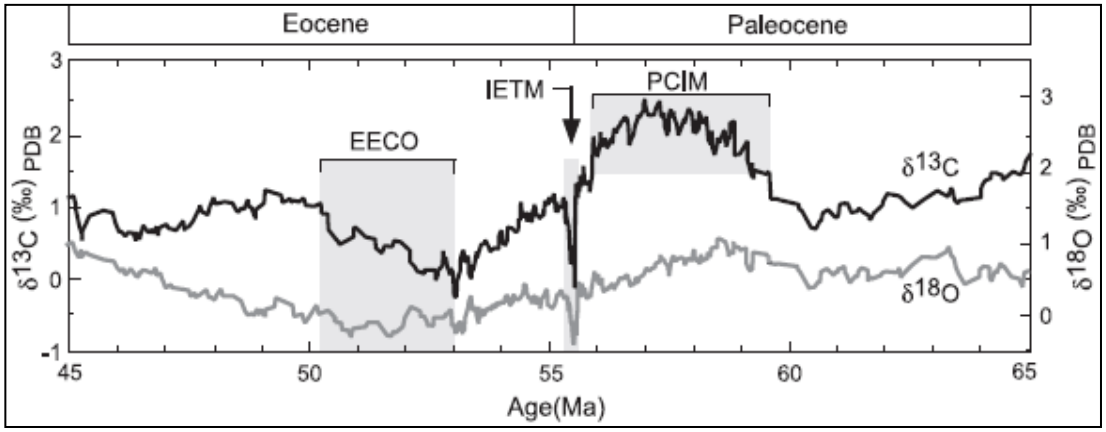

Figure 6.3: Global deep-sea oxygen (y18O) and carbon (y13C) isotope records of benthic foraminifera from early Palaeocene to middle Eocene (65–45 Ma)
Plotted values are five-point running averages for data from over 40 DSDP and ODP sites
Late Palaeocene carbon isotope maximum = PCIM
Initial Eocene thermal maximum = IETM (PETM)
Early Eocene climatic optimum = EECO
(Hollis et al. 2005)

6.1.2 CARBON ISOTOPE EXCURSIONS

The most consistent geochemical signature recorded in deposits from the Palaeocene-Eocene boundary is the negative carbon isotope excursion that characterises it (the CIE) (Kennett et al. 1991). This excursion is typically marked by a sharp, transient 2-2.6 ‰ negative carbon excursion followed by a phase of low values and a subsequent recovery of substantially longer duration than the initial drop to a value slightly lower than that which typified the preceding Palaeocene (Figure 6.4). It has been suggested that the initial fall in values can be separated into two or even three separate pulses which have been attributed to multiple injections of isotopically light carbon (by methane dissocation or carbon dioxide degassing) into the global pool. More recent evidence (Lu et al. 1996; Zeebe et al. 2009), finds that the initial fall in isotope values may have occurred over a longer time period than previously suggested and the deep marine sections which have been used to characterise the PETM may be truncated and thus, incomplete.

In terrestrial sequences, a ~2 ‰ negative signature can be observed in land plants which incorporate and preserve the isotopic signature of atmospheric CO_2 fixed by photosynthesis (Beerling et al. 1998). Soil carbonate nodules also preserve disturbances in the carbon cycle as evidenced by a 5-6 ‰ negative step in δC^{13} at the onset of the PETM in the Bighorn Basin, Wyoming (Koch et al. 1995).

Although the carbon isotope shift is essentially a worldwide phenomenon there are still discrepancies between the records of different areas and even those from the same sample depending on the source of carbonate utilised (Sluijs et al. 2011) (for example calcareous nannoplankton show shifts which are generally lower than those of planktonic foraminifera, both of which are, in turn, lower than those of land plants). These differences can be attributed to the changing digenetic and environmental parameters in widely spaced regions such as variations in water pH and differences in the idiosyncratic methods of isotopic fractionation used by organisms respectively (Koch et al. 1992; Harding et al. 2011).

The injection of large amounts of isotopically light carbon into the ocean-atmosphere system should promote dissolution of deep sea carbonates as the system re-establishes isotopic equilibrium through oxidation and absorption of this carbon into the oceans. Absorption increases the pH of oceanic waters triggering rapid shoaling of the carbonate compensation depth (CCD) - the depth at which carbonates are dissolved- until the system has returned to a steady state. Indications from the South Atlantic (Lourens et al. 2005; Zachos et al. 2005) are that the CCD shoaled rapidly in this area, evidence further substantiated by dissolution of carbonate tests in the Tethyan region (Canudo et al. 1995; Alegret et al. 2005; Agnini et al. 2006; Agnini et al. 2007), Caribbean (Bralower et al. 1997), Central Atlantic (Mutterlose et al. 2007) and New Zealand (Nicolo et al. 2007). However, some areas of the ocean do not appear to have suffered the same shoaling as dissolution is not found in the seas surrounding the Antarctic continent nor in the shelfal seas on America's east coast (Bains et al. 1999), and although northern Pacific sites do show moderate decreases

in carbonate content, it is not intense and could be ascribed to differences in sedimentation rate. This suggests that other variables affect the carbonate signatures of oceanic carbonates and serves to highlight the problems encountered in correlating widely spaced areas with differing oceanic characteristics. Some of the latest research from IODP site 1172 suggests that the magnitude of CCD shoaling may have been overestimated due to differences between the current CCD and that of the Palaeocene (Sluijs et al. 2011).

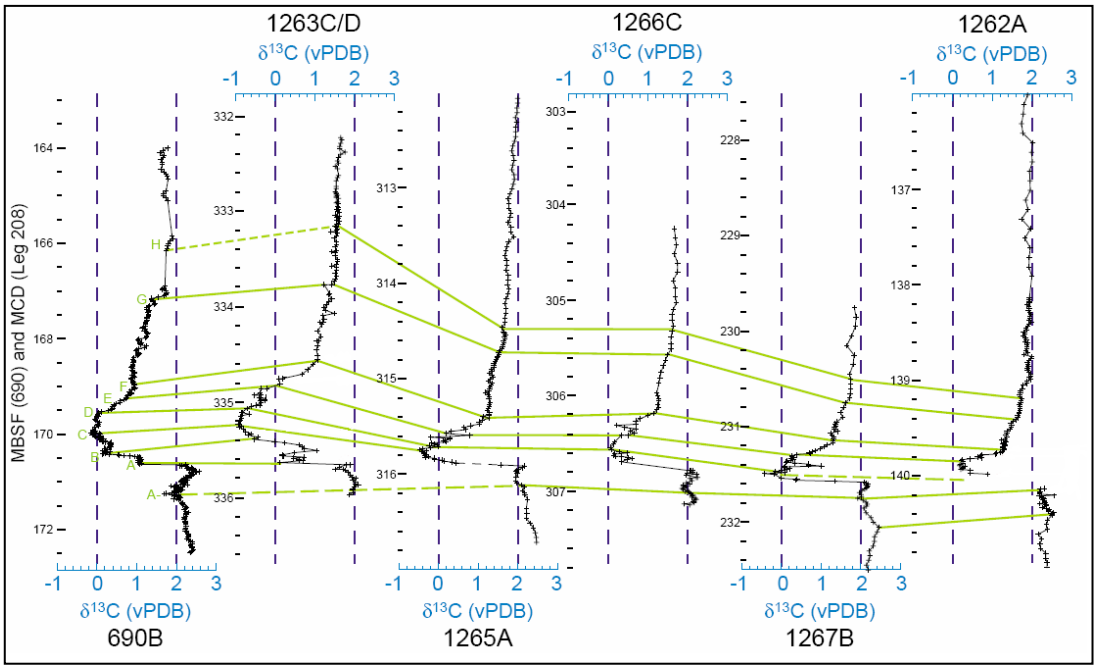

Figure 6.4: Example of the characteristic isotope curve from deep ocean sites around the Walvis Ridge, SE Atlantic
Far left curve comes from Antarctic ODP site 690
Image modified after (Zachos et al. 2005)

6.1.3 SEA SURFACE TEMPERATURES, CIRCULATION PATTERNS AND EUSTACY

Warming associated with the PETM has been indicated in sites around the globe by both marine and terrestrial proxy records. Temperatures can be estimated from oxygen isotopes in organic and inorganically precipitated carbonates using the empirical relationship first proposed by Shackleton (Shackleton et al. 1981). Carbon and oxygen are common chemical elements that are essential for life. Carbon is found in two stable isotopic forms of differing atomic weights, common ^{12}C (w98.9% of all carbon) and rare ^{13}C (1.1%). The radioactive form ^{14}C is even rarer. Oxygen is found in three stable forms of differing atomic weights, common ^{16}O (99.8% of all oxygen), rare ^{18}O (0.2%), and very rare ^{17}O. Isotopic compositions are fractionated by various metabolic and physicochemical processes, which affect the relative proportions of ^{12}C and ^{13}C, or of ^{16}O and ^{18}O.

The Use of ^{12}C and ^{13}C Ratios

$\delta^{13}C$ is a measure of the ratio of stable isotopes ^{13}C:^{12}C, reported in parts per thousand (per mil, ‰).The definition is $\delta^{13}C$ (in per mil) = $10^3[(R_{sample}/R_{standard})-1]$, where $Rx = (^{13}C)/(^{12}C)$ is the ratio of isotopic composition of a sample compared to that of the established standard for marine carbonates Vienna Pee Dee Belemnite (VPDB). $\delta^{13}C$ varies as a function of productivity, organic carbon burial and vegetation type. Organisms preferentially take in light ^{12}C and have a $\delta^{13}C$ signature

of about −2.5‰, depending on their metabolic pathway, due to the lower energies required to break down the chemical bonds in the atomically lighter isotope. An increase in primary productivity causes a corresponding rise in $\delta^{13}C$ values as more ^{12}C is locked up in plants and during organic carbon burial in sediments. The Palaeocene–Eocene Carbon Isotope Excursion (CIE) is an important clue to the cause of the PETM because it involved a negative shift of $\delta^{13}C$ in the oceans and atmosphere on the order of 2.5‰. Mass balance calculations show that the only practical way to decrease d13C by this amount is to add some 1500 gigatonnes of -60‰ light carbon to the oceans and atmosphere. Methane has a very light $\delta^{13}C$ signature: biogenic methane of −60‰ thermogenic methane −40‰ so the release of large amounts of clathrate is proposed to have caused the CIE (Heritier et al. 1981; Dickens et al. 1995).

The Use of ^{16}O and ^{18}O Ratios

$\delta^{18}O$ is a measure of the ratio of stable isotopes ^{18}O:^{16}O. The definition is reported in parts per thousand as carbon above relative to a standard. It is commonly used as a measure of mean temperature, precipitation, as a measure of groundwater/mineral interactions, as an indicator of processes that show isotopic fractionation, like methanogenesis. The main use of the ^{18}O:^{16}O ratio in paleoclimatology is as a proxy for temperature.

Carbonates (organic or otherwise) ($X+CO_3$), having oxygen in them can be used to derive estimates of the mean temperature of the medium in which they were

originally precipitated providing they represent primary sedimentation and have not undergone digenetic alteration.. The ratio of ^{18}O to ^{16}O in water derived carbonates varies slightly depending on the temperature of the surroundings, as well as other factors such as the water salinity, the initial isotope ratio of the waters from which they are precipitated which depend on local evaporation and freshwater inputs. If these other factors can be ignored or accounted for with initial calibrations, the signal can be attributed to temperature change with a $\delta^{18}O$ increase of 0.22‰ equivalent to a 1 °C cooling. Temperature can also be calculated using the equation:

$$T\ (°C) = 16.9 - 4.0(\delta^{18}O_{calcite} - \delta^{18}O_{seawater})$$

Output from this calculation is expressed relative to a standard in the form of a delta notation (δ). The standard for oxygen isotopes is Standard Mean Ocean Water (SMOW). When the world's oceans are ice-free, as they potentially were during the latest Palaeocene and early Eocene, an increase in d18O of 1‰ corresponds to warming of 4. 8°C thus the observed increase of 1–2‰ at the beginning of the PETM is the basis for thinking that the deep oceans warmed by 5–7°C at that time.

Temperature increase can also be inferred from shifts in faunal and floral composition with warm-adapted species able to extend their ranges further north. The magnitude of temperature increase varies latitudinally and with depth, perhaps as a result of the configuration of the oceanic circulation patterns which transport heat across latitudinal boundaries. Stable-isotope investigations on deep-water benthic foraminifera document a rapid increase in deep-sea temperature by 5 to 6 °C

in less than 6 ka (Thomas 2003). Sea-surface temperatures obtained from planktonic foraminiferal isotope records also show an 8 °C increase at high latitudes, while tropical sea-surface temperatures increased by about 5 °C. This magnitude of warming is confirmed by increased Mg/Ca ratios in planktonic (Zachos et al. 2003) and benthic (Tripati et al. 2005) foraminifera. Estimates from the terrestrial realm (e.g. Bighorn Basin in the United States), based on oxygen isotope composition of carbonate soil nodules (Koch et al. 1995) and fossil plants (Wing et al. 2005), are also in the range of 5 °C. Lack of preserved fossils in some areas, due to dissolution, diagenetic processes, extinction or non-deposition has previously hindered the quantification of temperature increases but new organic geochemistry methods utilising lipid membranes (Sluijs et al. 2006) and n-alkenones are now being applied which show a linear correlation with temperature in the modern day environment and appear independent of changes in salinity or nutrient availability.

Current climate models simulating the early Palaeocene underestimate recorded Arctic temperatures by 15 °C for the PETM and 10 °C for the surrounding late Palaeocene and early Eocene (Sluijs et al. 2006). Such warm high latitude temperatures as is evident from proxy records would predict a pole-pole gradient of 30 °C which then significantly overestimates tropical sea surface temperatures. This suggests that high greenhouse gas concentrations at this time must have been coupled with another mechanism to reduce the latitudinal temperature gradient and prevent tropical areas from warming excessively. Ocean heat transport alone could not reduce the gradient by the required amount unless it was increased threefold (Huber

et al. 2003) and investigation into the validity of the temperature estimates along with possible mechanisms for gradient reduction are on-going (Zeebe et al. 2009).

The warming trend initiated in the late Palaeocene and the associated reduction in pole-pole temperature gradient is likely to have had profound effects on oceanic circulation patterns since these are driven by the density and salinity differences between cold polar and warm equatorial waters. The expected effect of a reduced thermal gradient would be to slow the rate of oceanic overturning leading to a more stratified and possibly anoxic ocean (Muttoni et al. 2007). Evidence of anoxic conditions are inferred from faunal changes in Kazakhstan and the Tethyan region (Bolle et al. 2000), the Caribbean (Bralower et al. 1997), North Pacific (Kaiho et al. 2006), North Atlantic (Tremolada et al. 2004) and the North Sea (Mitlehner 1996). This interpretation however, cannot explain the evidence for a more intense hydrological cycle seen in New Zealand (Nicolo et al. 2007). Anoxic conditions can be the result of increased surface productivity brought about by increased levels of nutrient cycling from continental margins into the oceans thus both lines of evidence could be supported by more intense weather systems. Complex changes in circulation patterns to accommodate both the temperature and hydrological cycle increases have been suggested by Tripati (Tripati et al. 2005), but this mismatch has not yet been clearly unified by a single theory.

Sea levels were also affected by the warm temperatures in the late Palaeocene and are thought to have been substantially higher than today due to the absence of large polar ice caps. Ice may have been present at the poles during the mid-Palaeocene and

its melting could have in part contributed to the worldwide transgression linked to the PETM (Sluijs 2006) as could thermal expansion of seawater during the thermal maximum. Transgressive trends, whether thermally driven or otherwise, have effects on marine life and could have in part contributed to the faunal extinctions and migrations seen at the Palaeocene-Eocene boundary. However, global sea level trends may be locally overprinted by tectonic events as appears to be the case in the North Sea area.

6.1.4 EFFECTS ON ECOLOGICAL SYSTEMS

The PETM's effects on marine biota had been known for many years prior to the discovery of the isotope excursion and quantification of the temperature increase. Studies showed a significant turnover in the composition of the benthic community in worldwide locations (Miller et al. 1987) and this has been dubbed the Benthic Foraminiferal Extinction Event (BFEE) (Thomas 1998). The extinction event of the Palaeocene/Eocene boundary is the largest amongst benthic foraminiferal taxa of the last 90 million years. Benthic events of this magnitude are rare in the geological record and species turnover usually takes place gradually over millions of years. The BFEE at the PETM was relatively abrupt, occurring over a few tens of thousands of years or less (Kennett et al. 1991; Thomas 1992; Ortiz 1995). The event is marked by extinction of 30-50% of intermediate and deep-water benthic foraminiferal species as well as some shallow dwelling species (Kaiho et al. 2006).

The Tethyan region contains some of the most expanded records of the PETM anywhere in the world and it is here that high resolution paleontological work has been carried out to constrain the timing and duration of the BFEE (Ortiz 1995; Schmitz et al. 1997; Ouda 2003; Alegret et al. 2005) This work has resulted in the assignment of the Global Stratotype Section and Point (GSSP) for the Palaeocene-Eocene boundary to Dababiya Quarry in the Nile Valley, Egypt. The Palaeocene-Eocene boundary is defined on the basis of a strong negative δC^{13} excursion, the mass extinction of abyssal and bathyal benthic foraminifera, the transient occurrence

of excursion taxa among the planktonic foraminifera and an acme of the peridinoid dinoflagellate *Apectodinium* complex (Berggren et al. 1998). The Palaeocene/Eocene GSSP is approximately 0.8 m.y. older than the base of the standard Eocene Series as defined by the base of the Ypresian Stage in epicontinental northwestern Europe. The events at Dababiya also show that the benthic foraminiferal extinctions began slightly before the largest carbon isotope spike (Figure 6.5). This has been attributed to anoxic or euxinic conditions (Alegret et al. 2005). The benthic fauna recovers slowly and the early Eocene consists of an impoverished group of survivors.

Discussions on the causes of the extinctions have concentrated on food availability, temperature, oxygen depletion and acidification. In terms of food supply benthic foraminiferal assemblages point to an increased supply in the central and southern Pacific Oceans (Thomas 2003), which intuitively should mean a greater proliferation of fauna but is negated by the increased food requirements of forams in warming waters due to increasing metabolic rates. Increased food availability may also be linked to low oxygen conditions as organic matter is not decomposed, an anoxic environment may also have been one of the main causes of the BFEE. Acidification of the ocean may have resulted in benthic foraminifera taxa being unable to form their calcium carbonate tests due to energy barriers although such a scenario seems unlikely due to the extinction of deep marine agglutinated foraminifera which do not use calcite to construct their tests.

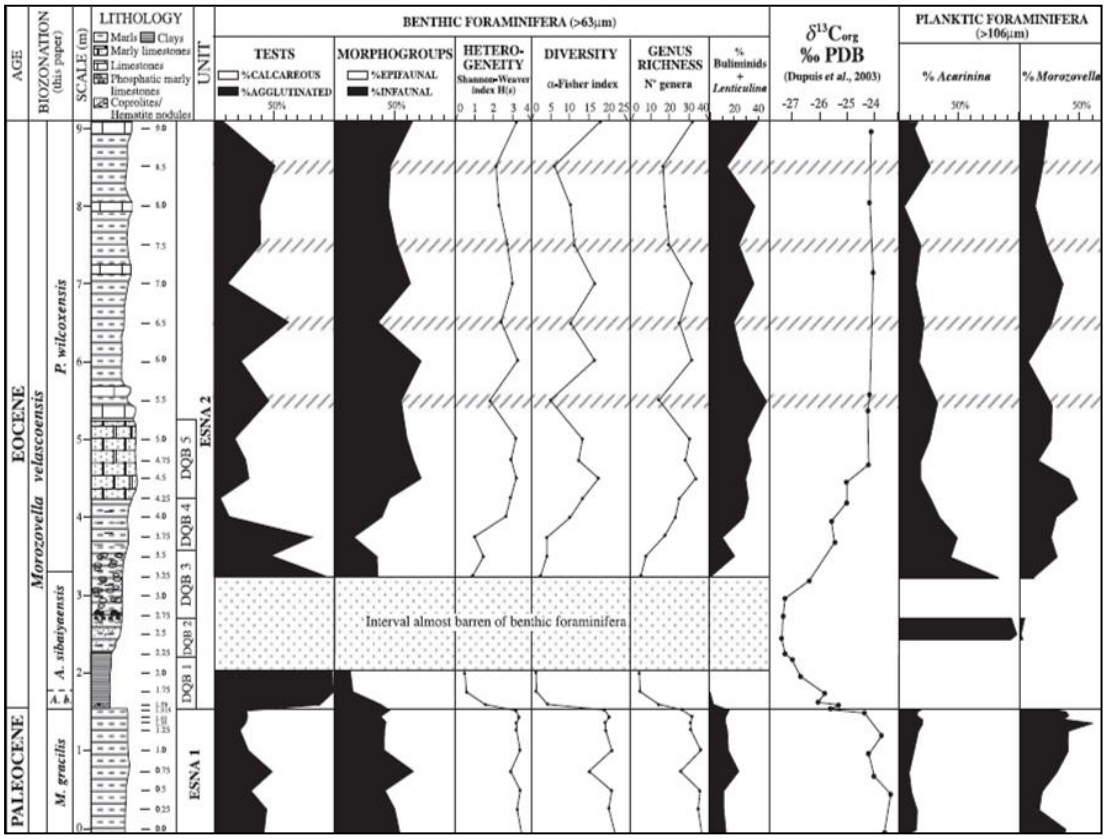

Figure 6.5: The BFEE as recorded at the Egyptian Dababiya section (GSSP). Various benthic foraminiferal indices are plotted with bulk carbon isotopes Benthic extinctions which occur prior to the lowest carbon isotope values are suggested to have responded to anoxic conditions linked to warming and stratification during the PETM.
Note the sudden change in facies at the PETM which could indicate an unconformity and missing section in the area
Modified from (Alegret et al. 2005)

In most studied sections, planktonic microfossils do not show an extinction event at the PETM boundary but do undergo a minor radiation pole-wards. In the tropics, thermocline dwellers such as the foraminiferal species *Subbotina* disappear while *Morozovella* diversify with the appearance of exotic taxa (Kelly et al. 1998). In mid-latitudes, the event triggered a migration of tropical–subtropical planktonic foraminiferal assemblages toward the poles which caused a sudden increase in lower-latitude warm-water dwellers (*Morozovella*, and compressed *Acarinina*) in mid and high latitudes (Arenillas et al. 1999). The acarininid peak seems to be a global feature since it has been reported in different sections worldwide, such as at Alamedilla, Caravaca and Zumaya in Spain (Canudo et al. 1995; Schmitz et al. 1997), Ocean Drilling Project (ODP) Site 738 in the Antarctic and Sites 865 and 577 in the Pacific (Kelly et al. 1998). Since this faunal turnover generally resulted in the replacement of one fauna by another, there was no net loss in species diversity and conversely, no mass extinction. Increases in the size of planktonic foraminiferal tests has also been reported (Kaiho et al. 2006). Abundance and size of planktonic foraminifera are influenced by several factors including nutrient fluxes and productivity. In the modern environment, nutrient supply seems to be inversely correlated with test size suggesting that calcification is inhibited by high nutrient availability thus large test size could be a response to low nutrient availability. Conversely, an increase in test size could indicate an increase in the occurrence of forams bearing symbionts in response to high nutrient levels as these aid calcification.

Calcareous nannofossils show a faunal turnover at the PETM boundary with assemblages indicative of high nutrient concentrations (Agnini et al. 2007) and stressed environments (Raffi et al. 2005). Jiang and Wise (2006) report that in the Central Atlantic dominance of relative abundance switched from K-mode specialists, such as *Discoaster*, *Fasciculithus*, and *Toweius*, to excursion taxa and R-mode opportunistic species, such as *C. pelagicus, H. arca*, and *Chiasmolithus* perhaps in response to the original taxa finding conditions too harsh (Jiang et al. 2006) . However an opposite dominance shift was observed in the Southern Ocean in response to the requirement for species with oligotrophic and stratification tolerances, which further serves to highlight the different ways in which faunas can adapt to the same environmental event (Sluijs 2006).

Organic-walled dinoflagellate cysts (dinocysts) record perhaps the most dramatic signature of the planktonic realm at the Palaeocene-Eocene. Dinoflagellates are very sensitive to the physiochemical characteristics of the surface waters (Barbosa 2009). The taxon *Apectodinium*, which originated close to the Danian-Selandian boundary undergoes an explosive radiation at the PETM (Figure 6.6) and is present in almost every studied section of this age which bears dinocysts (Sluijs et al. 2005). The globally synchronous acme of *Apectodinium* is one of the key characteristics which identifies the PETM interval. *Apectodinium* is heterotrophic and the diversification of this species is indicative of high nutrient availability possibly associated with an intensified hydrological cycle and associated higher rates of sediment input from rivers (Bujak et al. 1998). *Apectodinium* acmes are indicative of environmental conditions markedly different to 'normal background settings' of the late Palaeocene-

early Eocene. *Apectodinium* 'blooms' are intricately linked to enhanced runoff and increased nutrients in surface waters, possibly as a result of intensification of the weathering cycle and other possible specific oceanic conditions (Crouch et al. 2001).

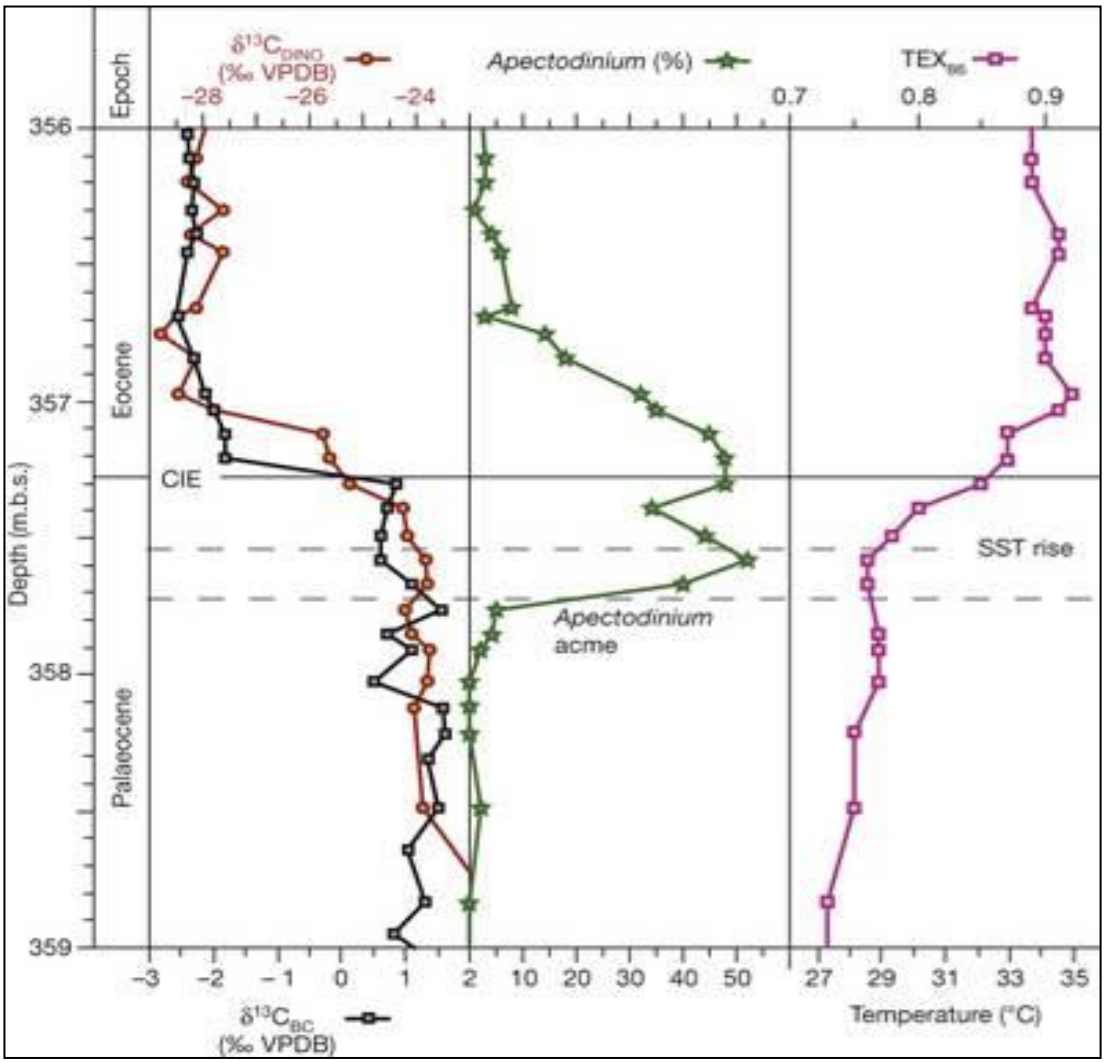

Figure 6.6: PETM record of *Apectodinium* acme from a section at Bass River, New Jersey plotted with other bulk carbonate ^{13}C and the temperature proxy TEX_{86}.
Note that the Apectodinium acme pre-dates the isotope excursion indicating that warming may have preceded the PETM.

Image after (Sluijs et al. 2007)

6.1.5 SEDIMENTATION RATES AND COMPOSITION

The high nutrient concentrations suggested by faunal variations may be linked to more intense climate systems and rates of continental erosion during the PETM due to a more active hydrological cycle (Crouch et al. 2003; Harding et al. 2011). This link must however be substantiated through the discovery of coeval increases in proxies for terrestrial runoff such as clay minerals. In the north-western Tethys, abundance of siliceous plankton indicates high nutrient levels in oceanic surface waters of the basal Eocene. A coeval increase in both sedimentation rates and the amounts of terrestrially derived quartz and feldspar suggests that this high primary productivity was the result of enhanced continental run-off (Egger et al. 2005) (Figure 6.7). It is assumed that the establishment of a pronounced monsoonal climate caused this increase in continental erosion (Egger et al. 2005). Chert formation reached a peak in the early Eocene indicating that increased terrestrial runoff caused silica to build up in the oceans which could not be removed organically due to lower productivity and was instead precipitated as inorganic chert (Muttoni et al. 2007). Inorganic chert formation is associated with other periods of extreme greenhouse conditions such as the Cretaceous but is not observed to occur naturally today thus suggesting that this mode of silica removal acts only under extreme greenhouse conditions when ocean circulation becomes upwelling-deficient and incapable of sustaining a siliceous biomass adequate to level off, upon burial, the input of silica to the ocean. In the terrestrial realm, increases of the clay mineral kaolinite were found to correlate directly with the shift in dominant taxa assemblages at the PETM

providing a link between floral ecosystems, climate and sedimentation (Harrington et al. 2004)

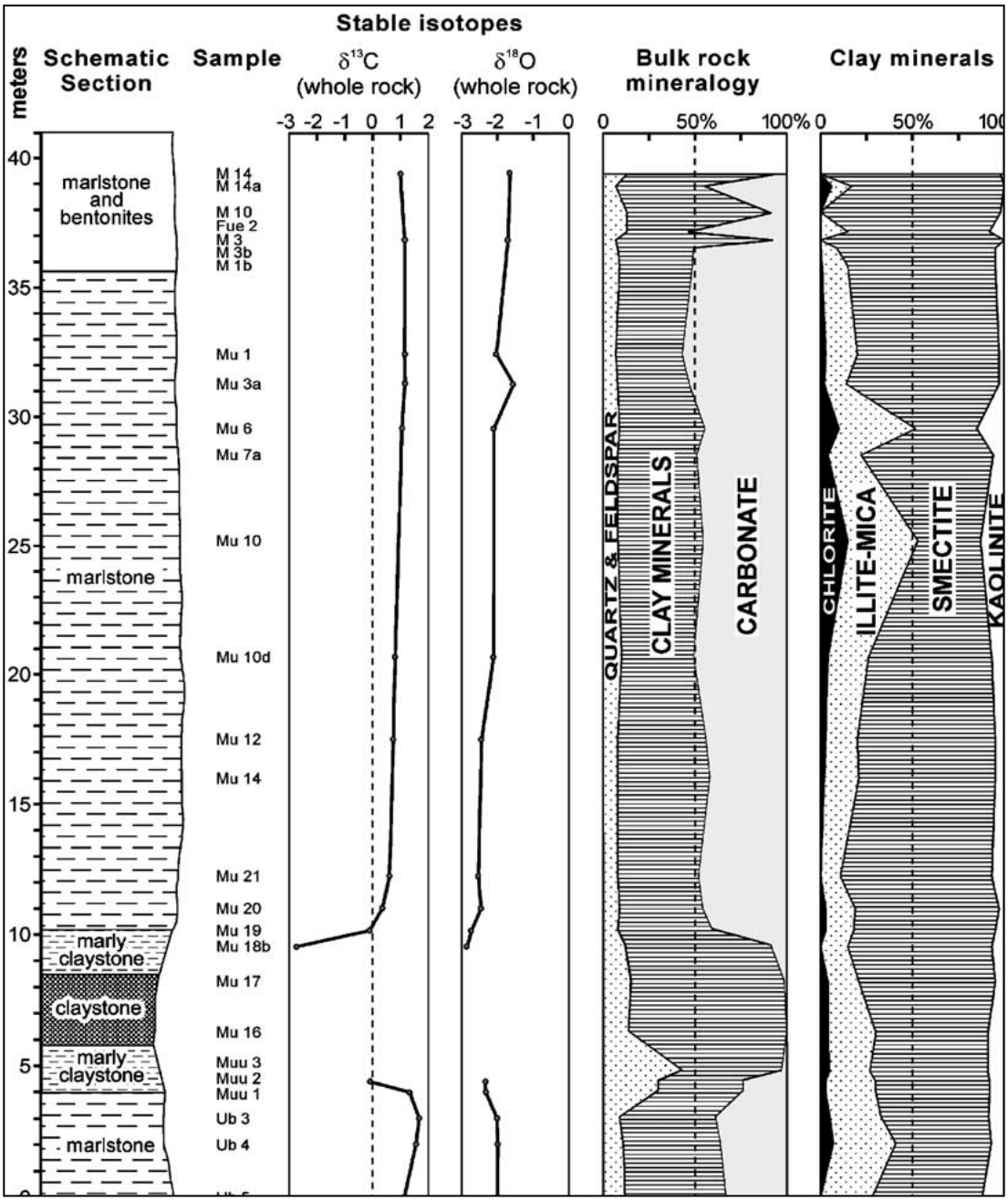

Figure 6.7: Carbon isotope values, bulk rock mineralogy and composition of clay mineral assemblages across the Palaeocene–Eocene boundary in Northwest Europe. Key observations include the predominance of quartz/feldspar and clay minerals at the expense of carbonates coincident with the negative carbon and oxygen isotope shifts.
Image after (Egger et al. 2005).

6.2 POSSIBLE CAUSES OF THE PETM HYPERTHERMAL

6.2.1 VOLCANISM AND TECTONIC OUTGASSING

The coincidence of the PETM hyperthermal with igneous activity in the North Atlantic Igneous Province (NAIP) may indicate a causal link. Volcanism is a plausible theory to explain the warming at the PETM since the time period was characterised by increased CO_2 levels which acted as a greenhouse gas causing climate warming. It is suggested that high levels of volcanic activity in the NAIP (Figure 6.8) and along Indian Ocean spreading zones may have produced this CO_2. The biostratigraphical and geochemical correspondence of the North Sea Balder and Sele Formation ash and tuff layers and ash layers found in Denmark and Norway, suggests that these pyroclastic deposits originated from the same area. This indicates that the source volcanoes lay on the proto-Greenland-Scotland Ridge, with the tephras showing several features that ally them to the early Palaeogene Faroe - Greenland igneous province (Knox et al. 1979; Knox et al. 1988; Morton et al. 1990; Knox 1996). The distance the tephras in the North-Western Tethyan sections were dispersed from their proposed magmatic source in the North Atlantic igneous province (ca. 4000 km) indicates that the eruptions were extremely powerful and emitted large volumes of ash and gases into the lower stratosphere (Egger et al. 2005). It is postulated that this volcanism in the North Atlantic warmed high latitude climate and led to the switching of the dominant source of deep waters to low latitudes as in the circulation models. However the timing of the NAIP explosive

volcanism has been revised and appears to post-date the PETM (Passey et al. 2008). Additionally, the lower degree of tropical warming at the PETM (Zachos et al. 2003) is at odds with the theory of volcanic CO_2 -induced warming which would not have preferentially warmed high latitudes. Additional volcanism in the Caribbean could have slowed the rate of warming in the tropics and reduced the difference between high and low-latitude sea surface temperatures thus allowing circulation reorganization (Bralower et al. 1997) but it is unlikely that the magnitude of the carbon emitted would be sufficient to match the volumes calculated from studying the isotope excursion. It has also been suggested that NAIP volcanism may actually have acted to cool the climate due to the reflective properties of (Jolley et al. 2005) SO_2 .

In addition to outgassing from volcanoes, metamorphism can also release carbon dioxide during mountain building, episodes of which were common in the late Palaeocene. Widespread pluton-induced hydrothermal flow occurred during the Eocene in the Himalaya–Karakoram mountain belt and the Cordilleran belt of western North America. Syn-metamorphic intrusions, which are common in metamorphic belts, may cause significant regional fluid flow. A representative CO_2 flux from such environments was computed from petrologic and geochemical studies of the Palaeozoic plutonic–metamorphic belt in New England. For the Eocene metamorphism in the North American Cordillera, the CO_2 fluxes derived from the New England metamorphic belt yield an area-integrated flux of $3x10^{18}$ mol/Ma. If a significant fraction of this CO_2 entered the atmosphere, this degassing flux would alone account for Eocene greenhouse global warming. Compared to other Eocene

metamorphic belts, the widespread hydrothermal activity in the North American Cordillera may have been the largest, and most climatically significant, source of metamorphic CO_2 to the Eocene atmosphere since CO_2 degassing by active metamorphism is most significant in extensional regimes of high heat flow. In addition during subduction zone metamorphism, ophicarbonate rocks undergo decarbonation and thus release some CO_2 but it is yet unclear whether this is released at shallow depths and is thus fluxed into the overlying mantle or whether degassing occurs at depth and provides CO_2 for arc magmatism (Kerrick et al. 1993; Kerrick et al. 1998). Although a plausible mechanism for carbon dioxide release over long time scales, metamorphism does not explain the preferential heating of high latitudes, although the resultant heating effect of CO_2 could then trigger oceanic circulation adjustments. In addition degassing due to metamorphism would tend to be released over long time scales leading to a prolonged build-up of carbon dioxide rather than the instantaneous input indicated by the sharp carbon isotope excursion. The calculations of the volumes of gas released make many assumptions as to the chemical composition of the rocks underlying ancient orogens and the ability of reaction products to escape into the atmosphere.

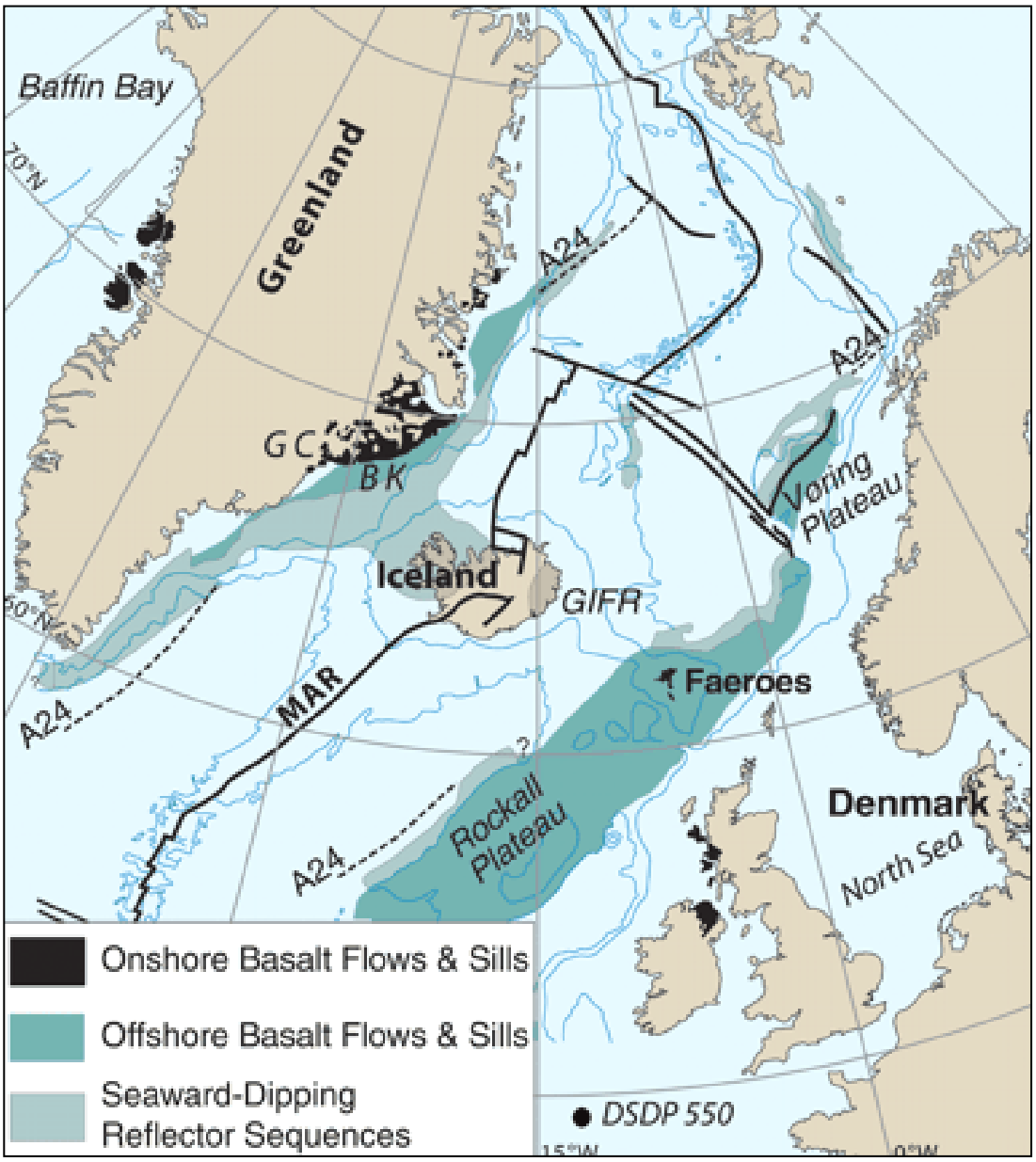

Figure 6.8: Map of the North Atlantic region showing the distribution of igneous rocks related to the North Atlantic Igneous Province (NAIP).

DSDP = site 550, where Danish Ash-17 closely overlies the PETM.
A24 = sea-floor magnetic anomaly 24r which shows extent of sea-floor spreading since the early Eocene
MAR, Mid-Atlantic Ridge.

Image after (Storey et al. 2007)

6.2.2 METHANE RELEASE

The release of methane into the atmosphere through destabilization of methane clathrates is perhaps the most well-known hypothesis to explain the warming at the PETM. First proposed in 1995, it was suggested that as latitudinal geothermal gradients reached a minimum at the end of a steady Late Palaeocene warming trend, sinking warm waters pushed submarine methane hydrates beyond their dissociation threshold (Dickens et al. 1995). Critically, this theory fully explains the magnitude of the carbon isotope excursion which other theories struggle to due to the vast quantities of CO_2 required. The minimum change in $\delta^{13}C$ is estimated at 2.5‰, which requires the addition and mixing of a significant amount of ^{12}C -rich carbon (i.e. carbon that is depleted more than usual in ^{13}C) in the ocean and atmosphere. In the present day situation, carbon reservoirs capable of rapidly injecting the required amount to generate the CIE are scarce. Methane is produced by anoxic bacterial decomposition or thermogenic breakdown of organic matter and is stored as methane hydrate (clathrate or ice) in shallowly buried sediments on the continental slopes of ocean margins. Biogenic methane is extraordinarily light, with a $\delta^{13}C$ value of approximately -60‰. Even so, mass balance calculations show that almost 1500 gigatonnes of light carbon must have been added to the oceans and atmosphere to alter the whole reservoir by 2.5‰ (Gingerich 2006). Warming methane hydrate by a few degrees makes it volatile, enabling it to migrate from shallowly buried sediments to the sediment–water interface and then to mix in the oceans and atmosphere. Oxidation of Methane produces CO_2 and it is a potent greenhouse gas. Methane

hydrate accumulations are geographically diverse and they can occur across a broad range of depths (between 920- 4000 m for the Late Palaeocene) consequently it seems unlikely that their dissociation would take place simultaneously (Bains et al. 1999). Detailed analysis of the structure of the PETM reveals the possibility of several 'pulses' of isotopically negative carbon injection and related climatic change which further strengthen the argument that the source of the carbon lies here.

However, the proposed duration of the PETM onset (Sluijs et al. 2007) and the re-calculated magnitude of CCD shoaling (Sluijs et al. 2011) create a large discrepancy between the temperature rise conceivably produced by continuous methane injection and that which has been proven by proxies.

6.2.3 OCEANIC CIRCULATION RECONFIGURATION

Initially the PETM was considered to be an oceanic phenomenon caused by circulation changes in the Atlantic and Pacific Oceans. This theory attributes the BFEE to a rapid temperature increase of deep waters and associated reduction of oxygen concentration which resulted from an almost total dominance in the oceans of warm saline deep waters produced at mid-latitudes. At present, ocean currents are controlled by sinking dense cold waters at the ice-capped poles which slowly move southwards to be replaced by warmer currents (Figure 6.9). A different global geography in the Palaeocene and warmer climate altered the density distributions in the oceans and led to a significant reorganization of ocean circulation (Kennett et al. 1991). A refinement on the circulation related model (Tripati et al. 2005) proposes that the PETM was associated with a unique mode of ocean circulation, consisting of a warm, saline North Pacific deep-water mass that was younger and denser than South Atlantic and Southern Ocean waters, consistent with convection in the North Pacific and decreased deep-water formation in the Southern Ocean. Data also indicate a switch from mostly thermally stratified to a salinity-stratified, isothermal deep ocean. However, both models require a mechanism for initiating the warming and only serve to explain how this warmth could be amplified and transported by oceanic circulation systems. They fail to explain the isotopic evidence of high carbon dioxide levels in the late Palaeocene- early Eocene and the associated shoaling of the CCD.

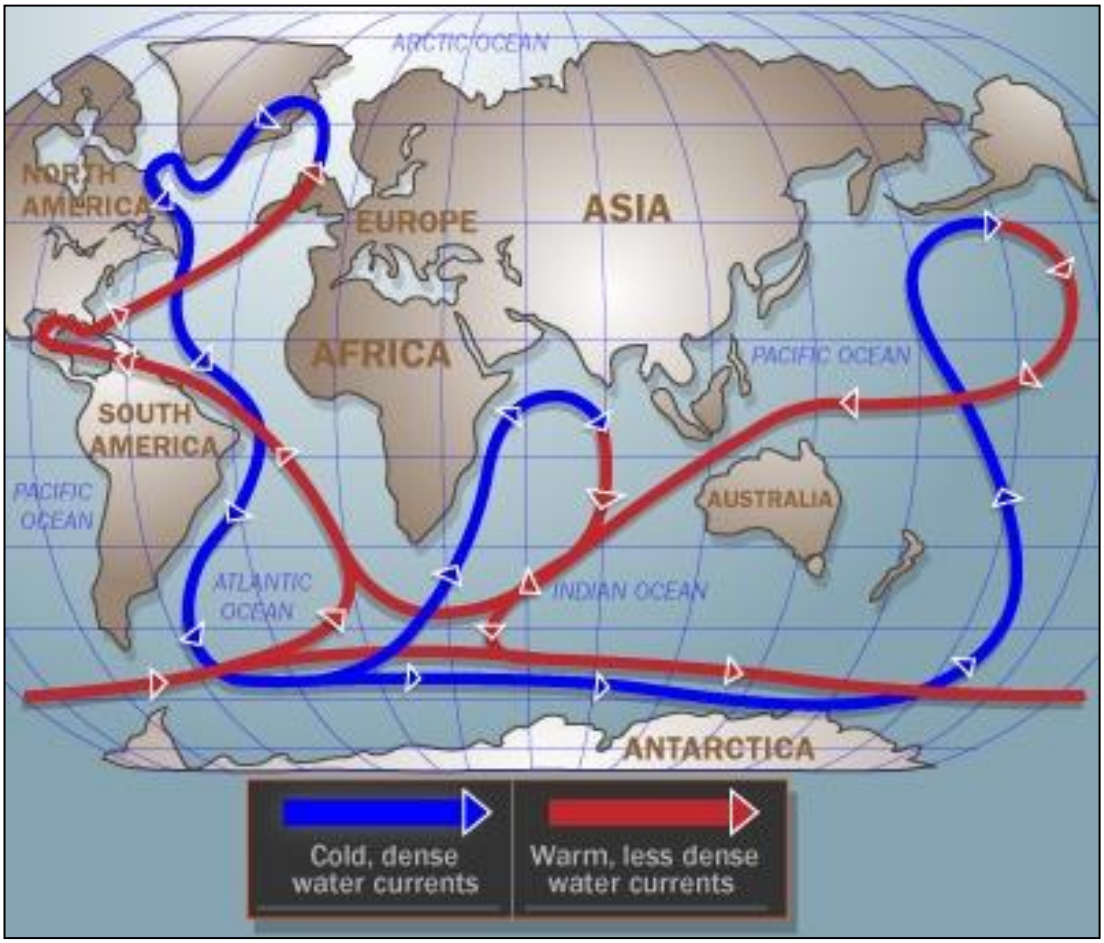

Figure 6.9: Oceanic circulation on present-day Earth with deep ocean currents driven by temperature and density variations. During the PETM such currents may have been driven by salinity giving rise to a different global geometry.

6.3 THE PETM IN THE CENTRAL NORTH SEA.

6.3.1INITIAL STUDY AND STRATIGRAPHY

It is important to take into account all of the proposed models and to build on the research already undertaken on the PETM when investigating its expression in the Central North Sea. Previous and on-going studies in the basin by the British Geological Survey have led to the discovery of an expanded expression of the PETM in well 22/10a-4 (Figure 6.10) contained within the Forties Formation. The results of isotope and biostratigraphic analysis carried out in the initial study show a 2.5‰ negative carbon excursion within a laminated clay interval of the Forties Formation accompanied by coeval shifts in the palynological assemblages (Figure 6.11).

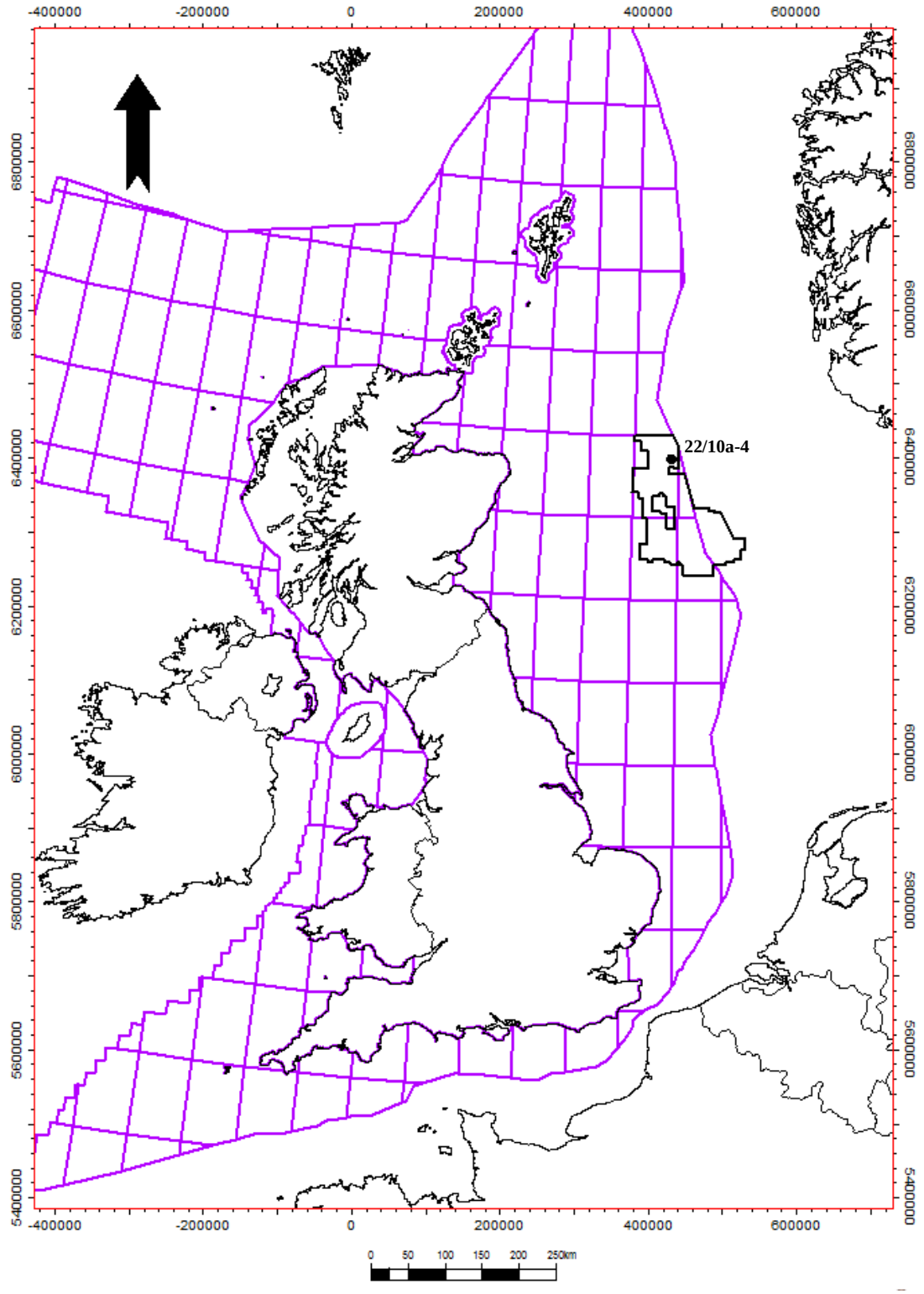

Figure 6.10: Location map of North Sea and well 22/10a-4.
UK North Sea quadrants are marked in purple.

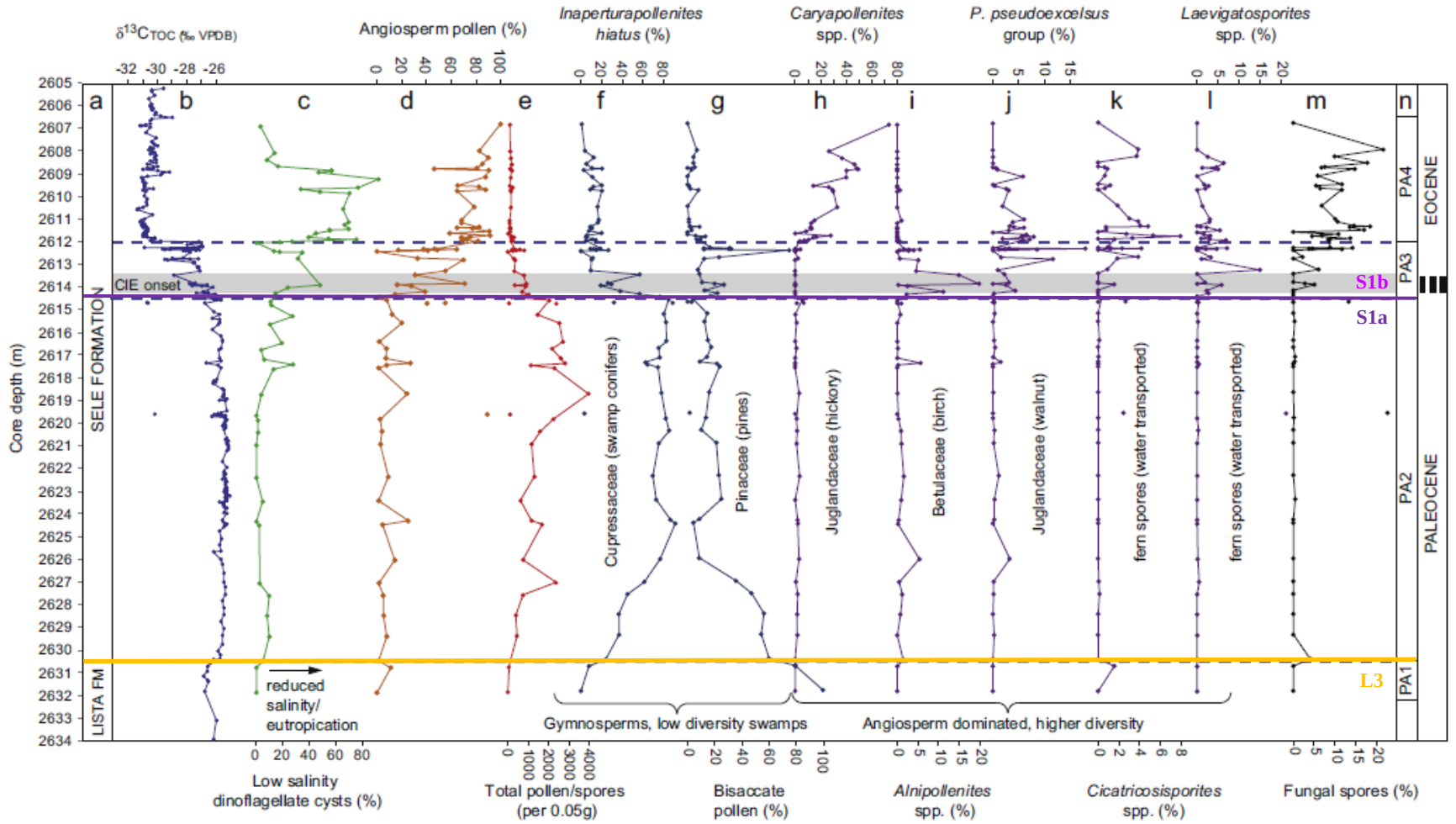

Figure 6.11: Carbon isotope excursion from 22/10a-4 with coeval shifts in palynological assemblages indicating environmental changes.

Note that S and L units of Knox et al 1992 are noted for correlation with later sections

Image after (Kender et al. 2012)

The section from 22/10a-4 showed evidence of a long onset period of gradually falling isotope values while many other PETM sections throughout the world have isotope excursions which occur very suddenly (Bralower et al. 1997; Giusberti et al. 2007; Rohl et al. 2007). The high resolution study of 22/10a-4 also found large spikes in $\delta^{13}C_{org}$ (Figure 6.12), which have been interpreted as representing shifts in the relative proportions of terrestrial and marine organic material present within the sampled bulk organic matter. Such proportional variations can also be observed in the amount of woody material in the samples and is proposed to be the result of highly variable and extreme rainfall during the PETM (Kender et al. 2012). However, it cannot be ruled out that these fluctuations could represent separate events within the overall PETM expression and may provide important information on the likely cause of the hyperthermal. Alternatively, they could indicate basin-wide events such as re-uptake of isotopically light carbon during periodic turnovers of the stratified basin (Saelen et al. 1998; Schouten et al. 2000) which would indicate that greater care may need to be taken when interpreting climatic changes from carbon isotope data. However, with only a single section it could not be ruled out that these fluctuations were due to reworking of older sediments into the core material or misplacement of pieces of core, despite the laminated nature of the section making this seem unlikely.

These results suggest that the PETM had a more highly variable and protracted onset than has previously been recorded in other sections. However, it is important that another site is identified and tested to corroborate the results and place them in a regional context which was the purpose of this study.

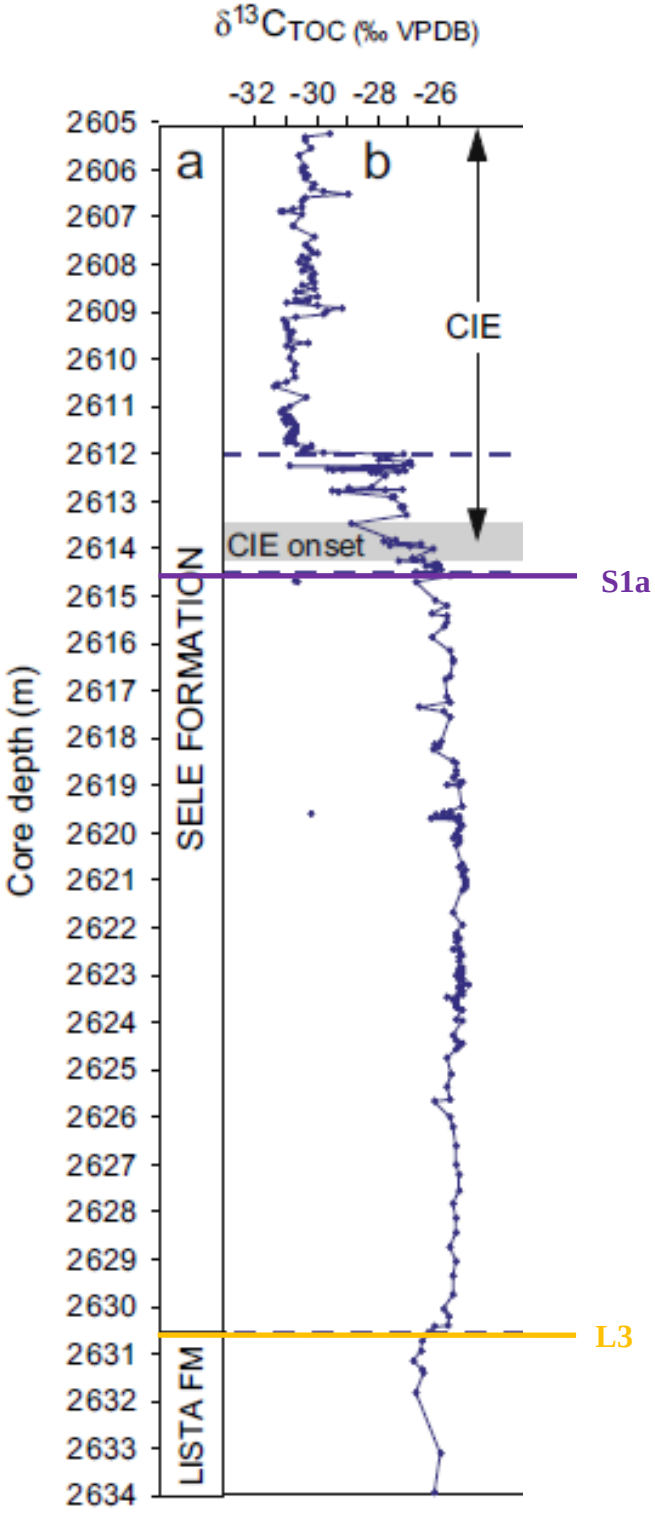

Figure 6.12: Carbon isotope excursion from well 22/10a-4 showing prolonged onset phase and increased isotope variability at the PETM.
Image after Kender et al 2012

The PETM was found to occur within the lower Forties shale unit beneath the Forties Sandstone Member and above the Lista Formation shale. In order to place this in a stratigraphic context the M,L,S and B units of Knox and Holloway 1992 (Figure 6.13) were identified. These units are known to be regionally correlatable and are separated by maximum flooding surfaces. Maximum flooding surfaces as discussed previously occur within a period of extensive condensation, that is, the preservation of relatively long geologic timespans in a relatively thin layer of sediment, and can be recognised in wire-line logs and cores by their high gamma signal. In expanded sections it is difficult to pick the start of the CIE and the isotope record from 22/10a-4 exemplifies this as it has a prolonged period of falling isotope values and no sudden shift. In this volume the CIE is picked at the onset of falling isotope values although this may not be in line with other researchers. The start of the CIE found in 22/10a-4 corresponded with the S1a/S1b stratigraphic boundary (Kender et al. 2012) however the environmental changes which exemplify the PETM start within unit S1a prior to the isotopic excursion. As before, the term Forties Formation corresponds with units S1a and S1b regardless of sand content.

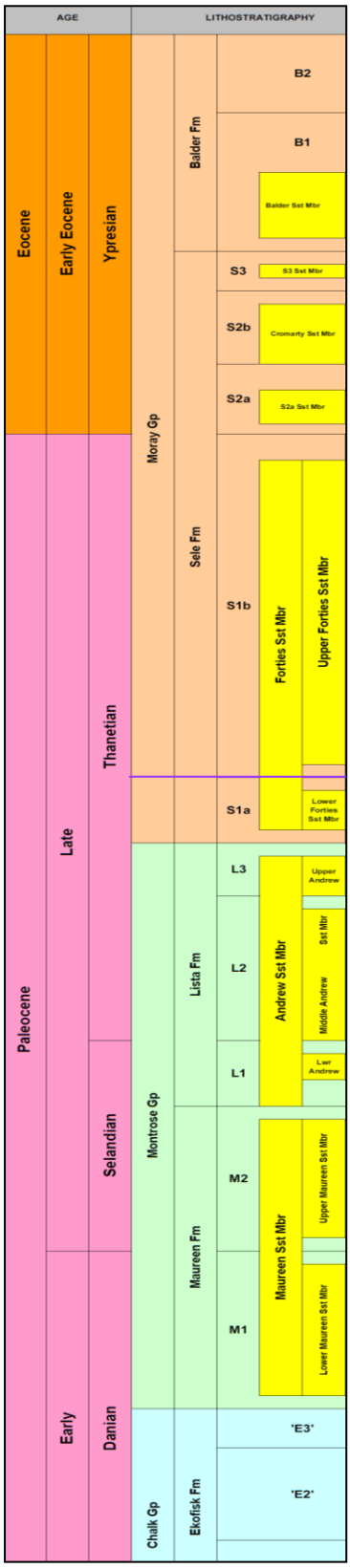

Figure 6.13: High resolution Palaeocene stratigraphic chart with the B,S,L and M units of Knox and Holloway 1992.

6.3.2 ISOTOPIC ANALYSIS

From consideration of the previous work undertaken on the PETM both globally and in the North Sea, it was considered that three main areas should be investigated. The first of these, aims to characterise the effect of a hyperthermal climate on depositional systems using seismic interpretation, mineralogical and elemental analysis. Biostratigraphic data from 66 Central North Sea sections provides the raw data used to investigate the environmental effects of the PETM while analysis of the isotopic signature allows inferences to be made as to possible causal mechanisms.

However, these investigations require that the expression of the hyperthermal be identified regionally throughout the North Sea basin. The carbon isotope excursion is the most recognisable and globally correlatable effect of the PETM and as such this was considered the best method of identification. Using seismic and wire-line log correlation, two sections, 22/10a-T6 and 22/09-3, were selected for isotopic analysis close to the initial discovery section to try to closely tie the isotopic signal seen in the 22/10a-4 section with others in the area (Figures 6.14 and 6.15). Another section, 22/06-1, was located some distance from the initial section and is more sand-prone than the others and may thus be expected to contain a more expanded expression. Sand-prone sections can be a barrier to biostratigraphic and isotopic analyses which require sufficient organic matter for testing but this section still had substantial shale-prone intervals.

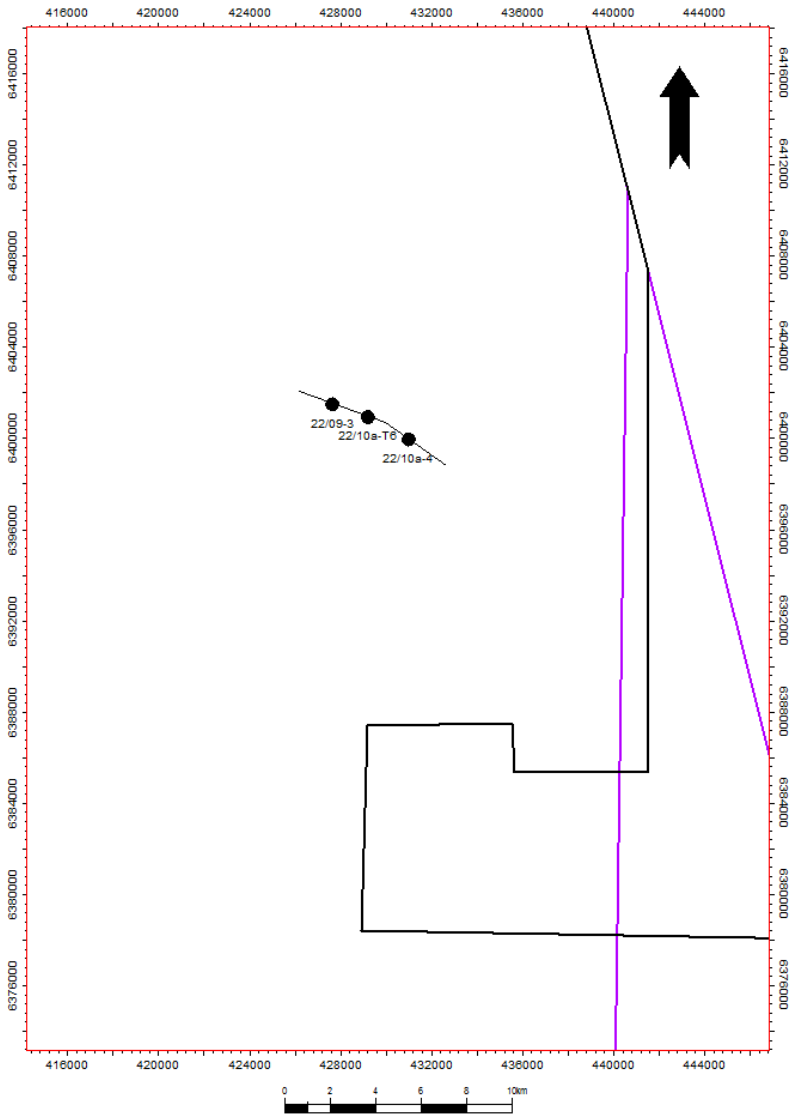

Figure 6.14: Location of wells 22/09-3 and 22/10a-T6 with respect to the type well 22/10a-4 and the seismic database.
Location of seismic line in Figure 6.15 shown.

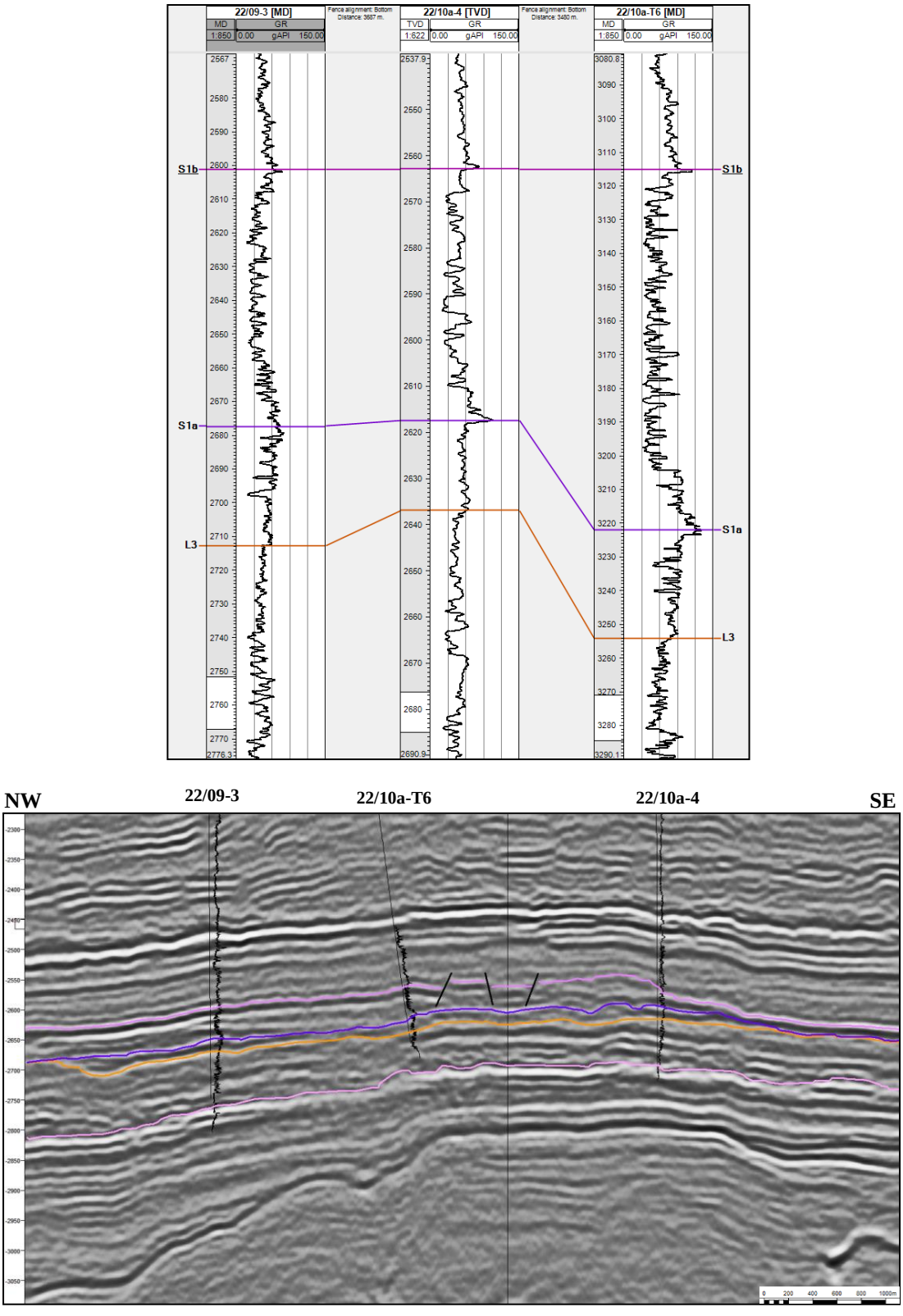

Figure 6.15: Wire-line log and seismic ties between wells 22/09-3, 22/10a-4 and 22/10a-T6 demonstrating the close correlation of the sections. Note the thinning of the S1a section both to the NW and SE which has implications for the preservation of the important onset period.

Well 22/10a-T6 is located 3.47km from 22/10a-4 and is the closest cored section to it. The well is inclined with the maximum dip occurring over the Forties interval and therefore the core contains 138m of Forties Formation rather than the true vertical thickness of 103.9m. Potential problems were identified prior to sampling and analysis of this section. Firstly, the inclined nature of the core meant that it would be difficult to make any inferences about sedimentation rate and absolute timing of events based on samples taken and there would also be uncertainties introduced due to the possibility of lateral variations. Secondly, the difficulties in extracting the core from an inclined path led to the loss of small pieces at the base of the two core segments where ideally sampling should be continuous all through the interval. However, 22/10a-T6 represents an extremely expanded section and its similarity in character to the type section meant that it was considered that the possible benefits of testing this core outweighed the potential difficulties.

Wire-line log and seismic correlation located the S1a/S1b boundary where the PETM CIE was discovered in 22/10a-4 and the isotopic analysis confirms this stratigraphic position. Unfortunately, the core of 22/10a-T6 proved much more broken up and out of sequence than anticipated and even with careful sampling; there were still many erroneous points (Figure 6.16). Despite the problems with the core, the shape of the CIE can still be seen; however tying the isotope curve with 22/10a-4 is not possible. Interestingly this section appears to be missing the protracted onset period seen in the 22/10a-4 section but this is hard to state definitively due to the potential for erroneous depth measurements in the broken up core.

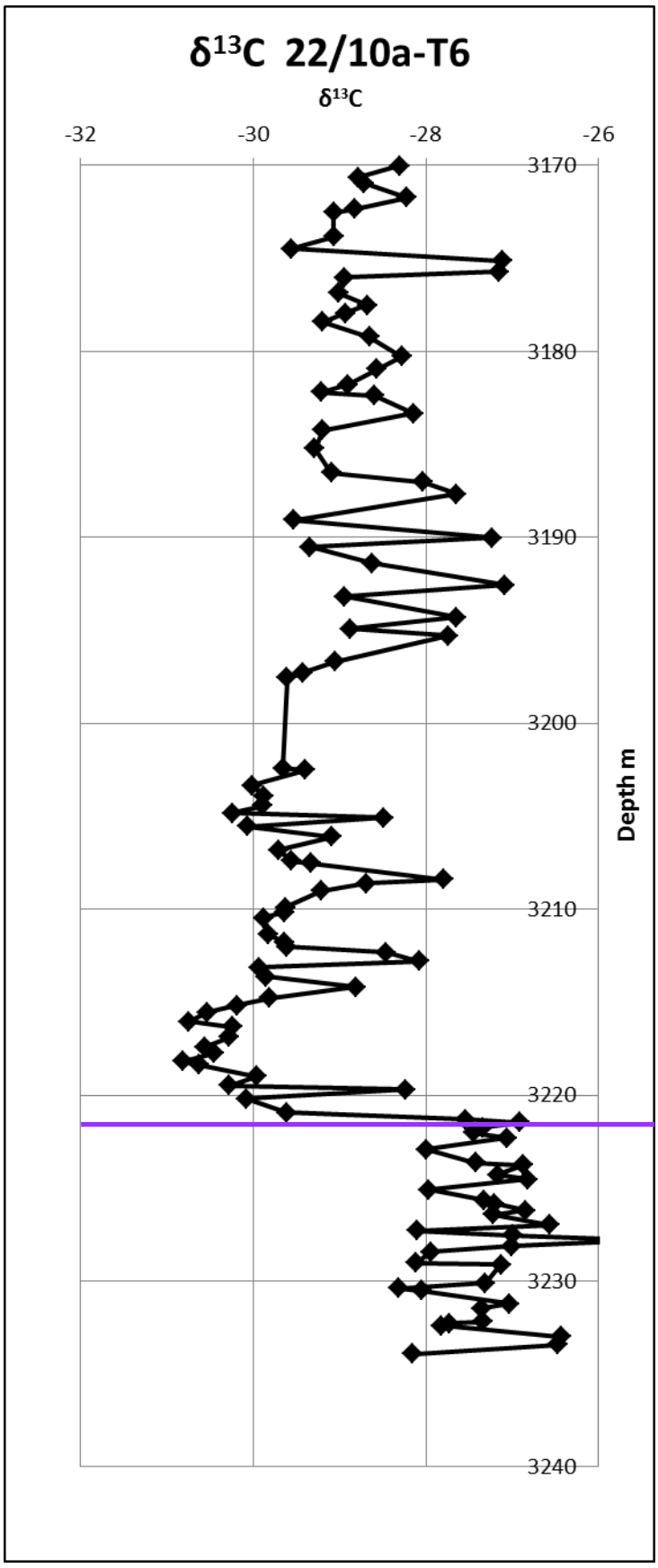

Figure 6.16: Carbon isotope $\delta^{13}C$ results from well 22/10a-T6 showing erroneous points caused by sampling and core problems.

Well 22/09-3 also lies close to the type section but the isotopic signature obtained (Figure 6.17) is necessarily of lower resolution, due again to problems with core sampling. In many places the core was broken up and it was not possible to be certain of the exact stratigraphic positions of material so samples had to be collected only where their position could be verified leading to a lower sample resolution than would have been ideal. Despite the low sample count there are still recognisable variations in the initial move towards low $\delta^{13}C$ values and a prolonged onset period, features which are also seen in 22/10a-4. There appear to be several steps where $\delta^{13}C$ values decrease and then increase again before the final move to continuously low values but the variations cannot be correlated to those in 22/10a-4. The isotope values reach a minimum value of -31 and remain around an average of -30 for the remainder of the section analysed so the decay of the CIE is unfortunately not captured within the core. Despite being truncated, the isotope excursion in this well occurs over approximately 46m, which is far more expanded than any previous section.

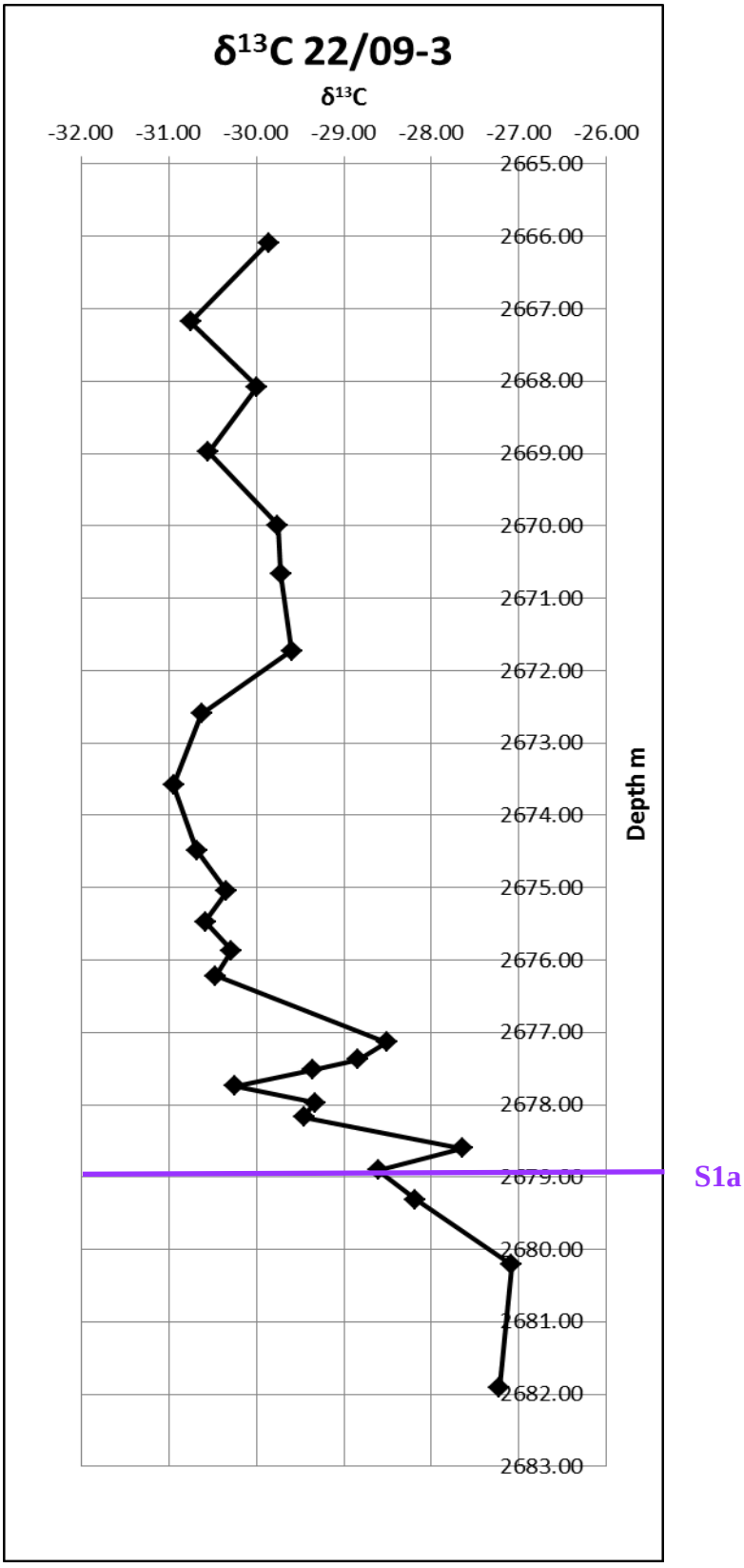

Figure 6.17: Carbon isotope data over the PETM onset from well 22/09-3

Well 22/06-1 is situated about 50km west of 22/10a-4 (Figure 6.18) and is located in the centre of a sand channel. As such this section may provide evidence of the effect of the PETM on depositional systems or conversely, the effect of depositional systems on the PETM signal. Terrestrial and marine $\delta^{13}C$ ratios are known to be different; with terrestrial organic matter having a distinctly higher $\delta^{13}C$ ratio than marine sediments (Pagani et al. 2006; Handley et al. 2008) so sections with significant terrestrial sedimentation may produce a different isotopic record to those with primarily marine deposition.

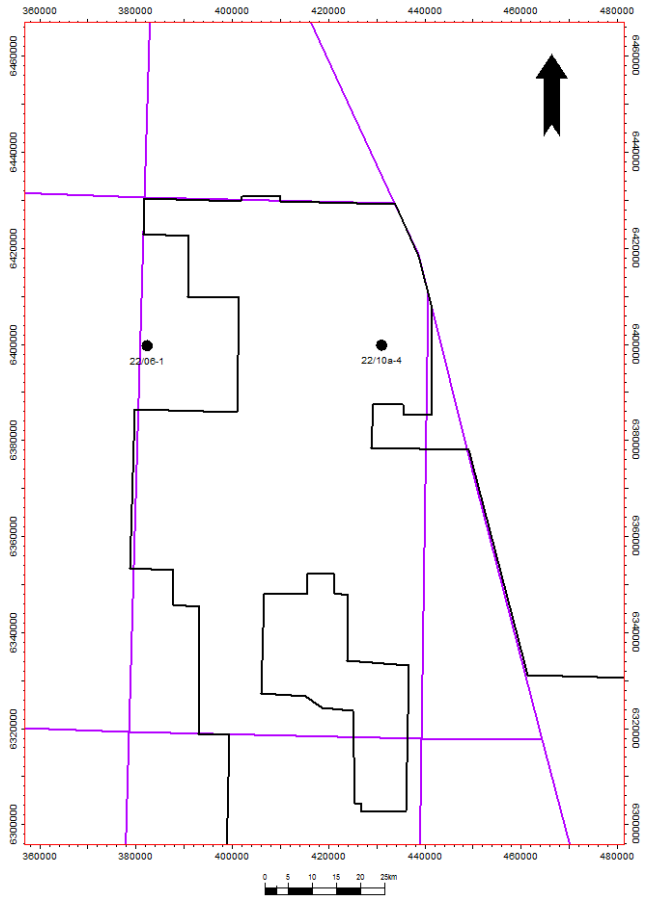

Figure 6.18: Location of section 22/06-1 relative to 22/10a-4.

The isotopes from well 22/06-1 (Figure 6.19) show the onset phase of the PETM over 26m (85ft) and the section is so expanded that the core does not capture the lowest isotope values. The variations in the isotope data are clearly seen, as they are in 22/09-3 and 22/10a-4. These spikes are therefore considered to be a regional signal at the PETM within the North Sea.

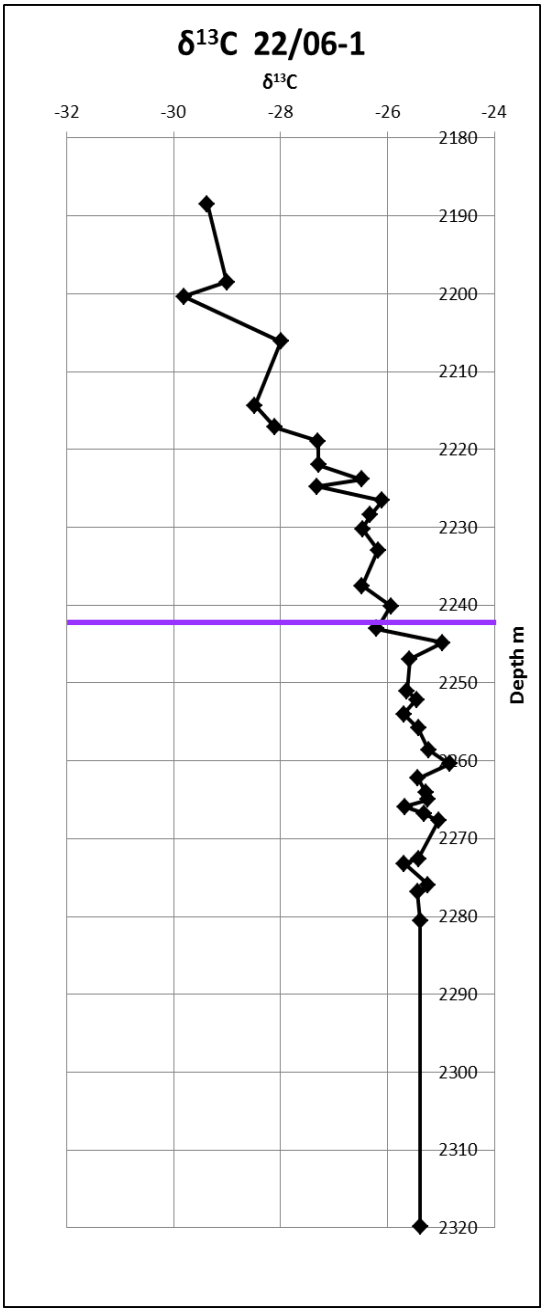

Figure 6.19: $\delta^{13}C$ isotope results from well 22/06-1 showing the spikes characteristic of North Sea sections.

In order to investigate the regional extent of the PETM in the Central North Sea, well 30/14-1 in the extreme south of the dataset was examined (Figure 6.20). This well had previously been studied at low resolution and the CIE identified on the basis of bulk carbon isotopes and the position of the *Apectodinium* acme (Figure 6.21).

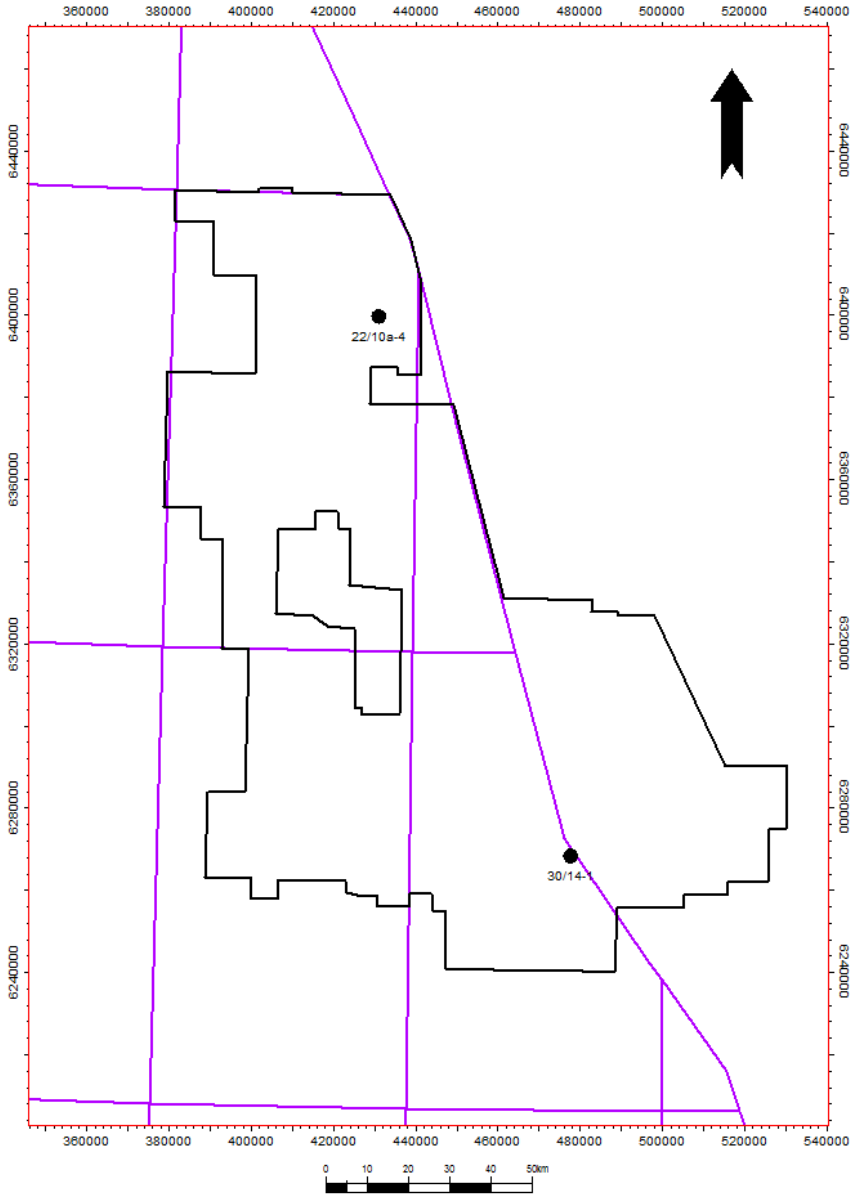

Figure 6.20: Location of well 30/14-1 with respect to 22/10a-4.

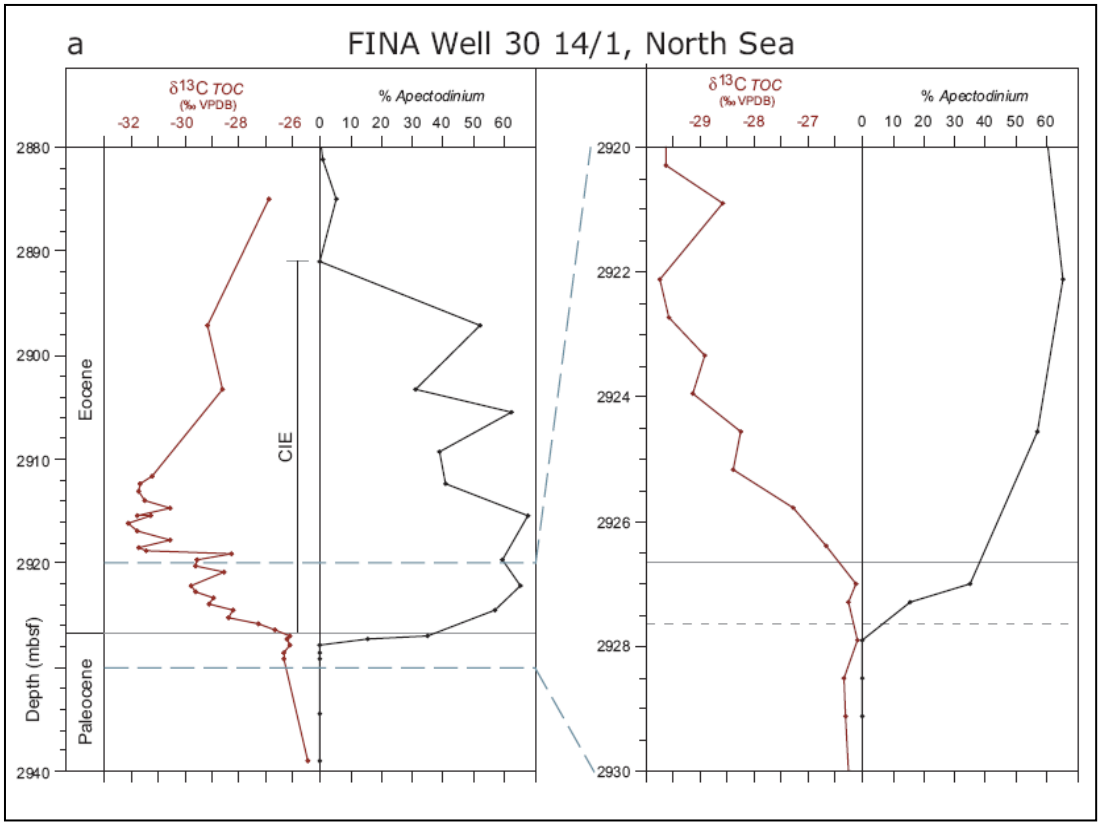

Figure 6.21: Analysis of well 30/14-1. Right hand image shows a scaled up version of the data.

DINO = dinocysts, TOC = Total Organic Carbon, VPDB = Vienna Pee Dee Belemnite, mbs = meters below surface, mbsf = meters below sea floor

Image after (Sluijs et al. 2007)

The new high resolution data gathered in this study from well 30/14-1 shows both the onset and decay of the PETM isotope excursion (Figure 6.22 and 6.23). The onset period is very condensed which could indicate that some section is missing or more likely that sedimentation rates varied widely throughout the basin and were significantly lower during deposition of the S1a section in 30/14-1 than in other areas of the basin. The return to normal isotope values occurs at the S1b/S2a boundary and was not recorded in the initial study of 22/10a-4. This data is therefore unique in that it provides a complete, high resolution record of the PETM isotope curve in the Central North Sea and can therefore provide information on the effects of declining temperatures on depositional and environmental systems as well as increasing ones. The core also continues into the Early Eocene and appears to show a later excursion which could also correspond with environmental perturbations which have not previously been recorded in the Central North Sea. The comparison between later excursions and the PETM is important as they may have the same underlying mechanism or represent a single recurring earth system process.

This isotopic data, along with complementary data from wire-line logs, biostratigraphy, sedimentology, geochemistry and mineralogy can be used to provide information on the sedimentological effects of the PETM hyperthermal in the North Sea. It can also be utilised to hypothesise about the possible casual mechanisms and environmental effects of the PETM.

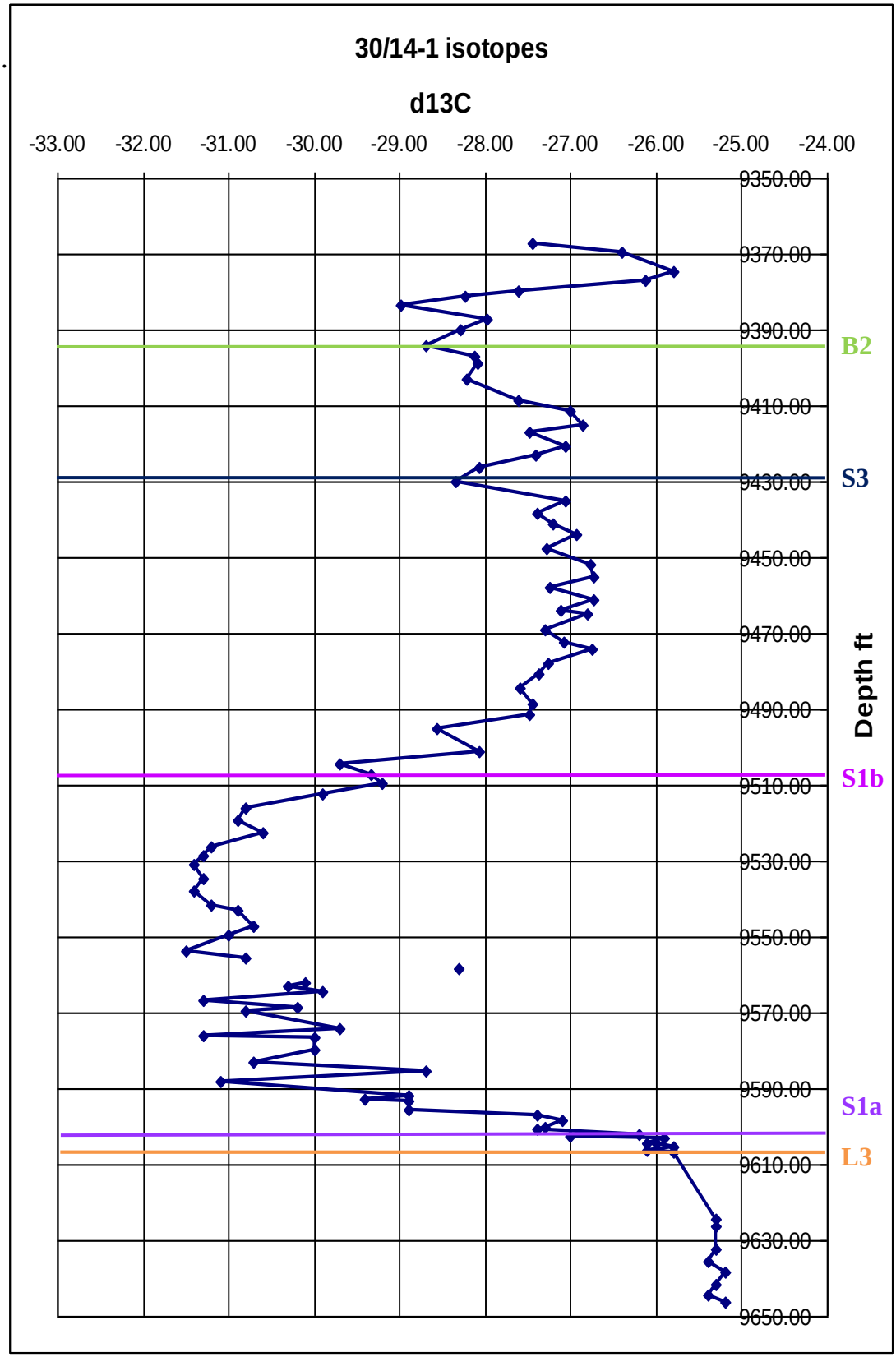

Figure 6.22: $\delta^{13}C$ isotope results from well 30/14-1 showing the onset, body and decay of the PETM isotope curve.
Note that the S1a/S1b boundary picked in this study as representing the start of the onset phase of the PETM differs from that picked in the previous study of this core highlighting the difficulties in picking a 'start' for this gradual event.

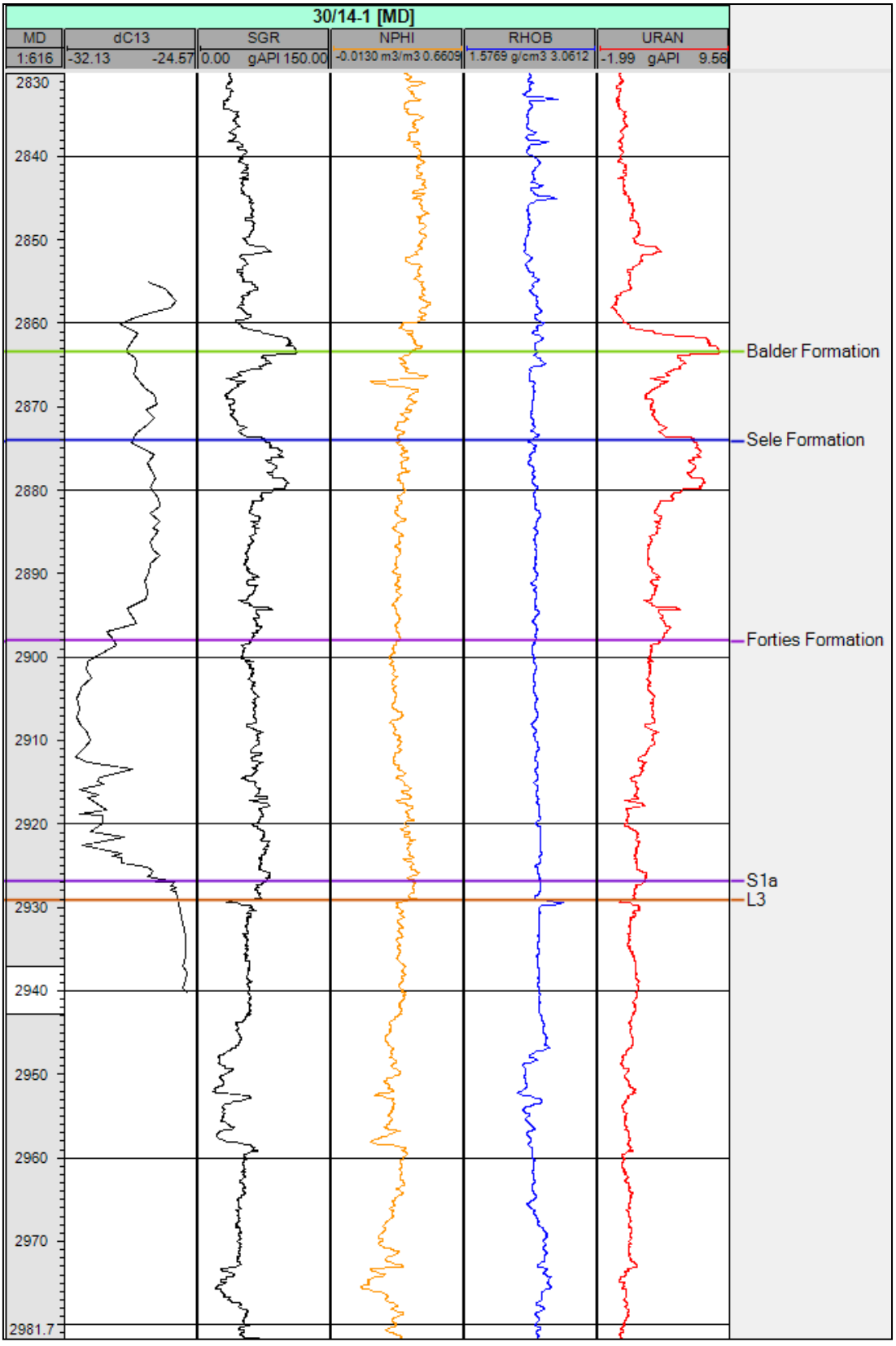

Figure 6.23: Suite of available wireline logs for well 30/14-1 (spectral gamma ray, neutron density, density and uranium) displayed against carbon isotopes showing where lithological sub-divisions have been made.
Balder Formation = B2, Sele Formation = S3, Forties Formation = S1b
Note that sonic logs were not available for this well.

6.4 DEPOSITIONAL AND SEDIMENTOLOGICAL EFFECTS OF THE PETM

In the 22/10A-4 well the PETM CIE was found to occur at the S1a/S1b boundary and this was corroborated by isotopic evidence from wells 22/09-3, 22/10-T6, 22/06-1 and 30/14-1. The wells lie within the 3D seismic dataset previously used to characterise structural and depositional styles in the basin and therefore seismic mapping of the PETM interval may allow the internal geometries of the Latest Palaeocene sequences to be studied in detail.

In 22/10a-4 the S1a/S1b boundary was marked by a distinctive gamma spike in the wire line well log (Figure 6.24) and this was also found to be the case in the other sections (Figure 6.25). Close inspection of the natural gamma spectral logs (which separate the overall gamma into elements, specifically uranium, thorium and potassium) correlates the spike with an excess of uranium (O'Connor et al. 1993; Knox 1996) which is possibly the result of condensation at the maximum flooding surface (MFS) at the S1a/S1b boundary. Since regional correlation of this high gamma MFS is possible using wire-line logs, seismic mapping of this unit may therefore allow the lateral extent and thickness of the PETM section to be recognised throughout the Central North Sea basin. Such a large-scale analysis has never been undertaken before as almost all of the PETM studies have been restricted to single sections. Mapping of the thickness of the section therefore has potential to lead to

inferences about sedimentation rates during the event which some authors have found to be enhanced by higher rainfall during the hyperthermal.

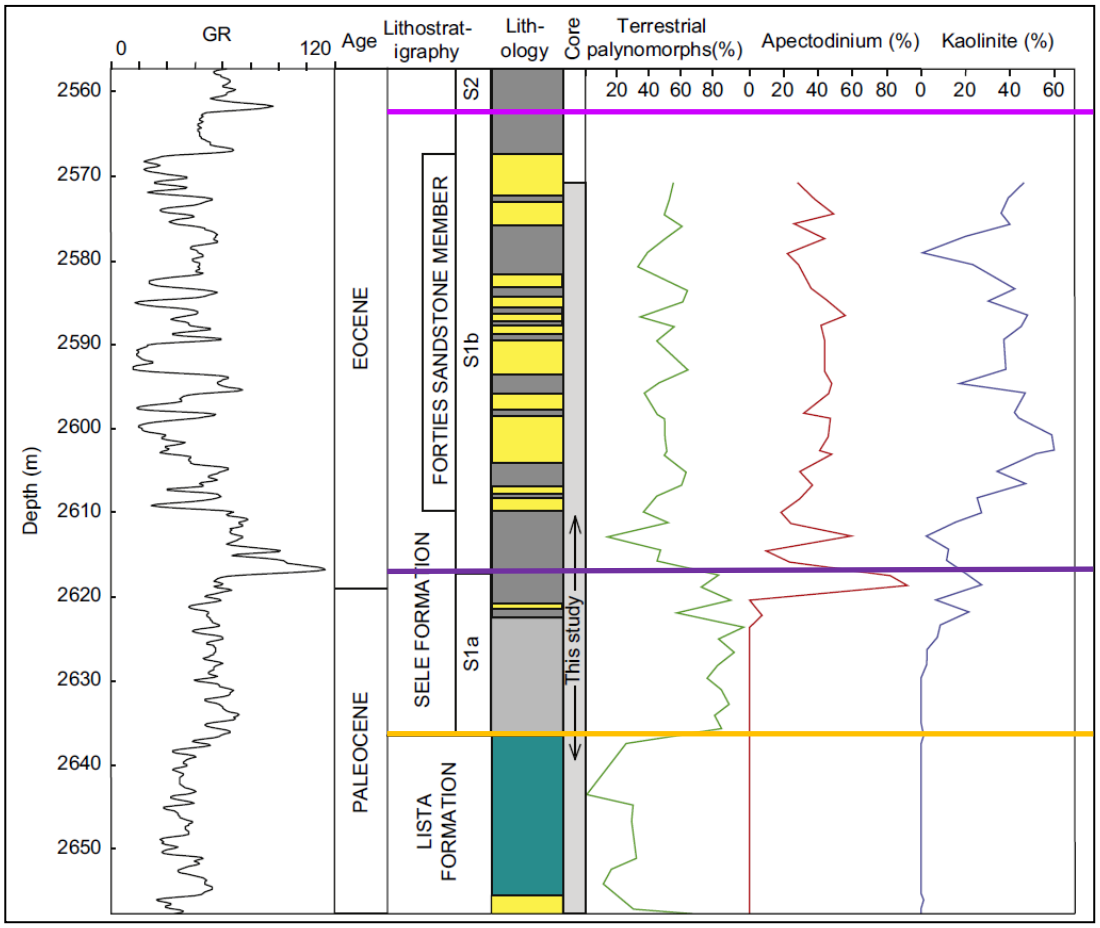

Figure 6.24: Correlation of S1a/S1b boundary in well 22/10a-4 with a spike in the gamma log.

Note the slight difference in 'depth' and 'core depth' between this and the previous diagram. This is due to differences between 'drillers depth' and 'loggers depth' which occur during drilling. Cores from a certain drillers depth are matched to the wireline log and the difference is estimated as a 'core shift'

Image after (Kender et al. 2012)

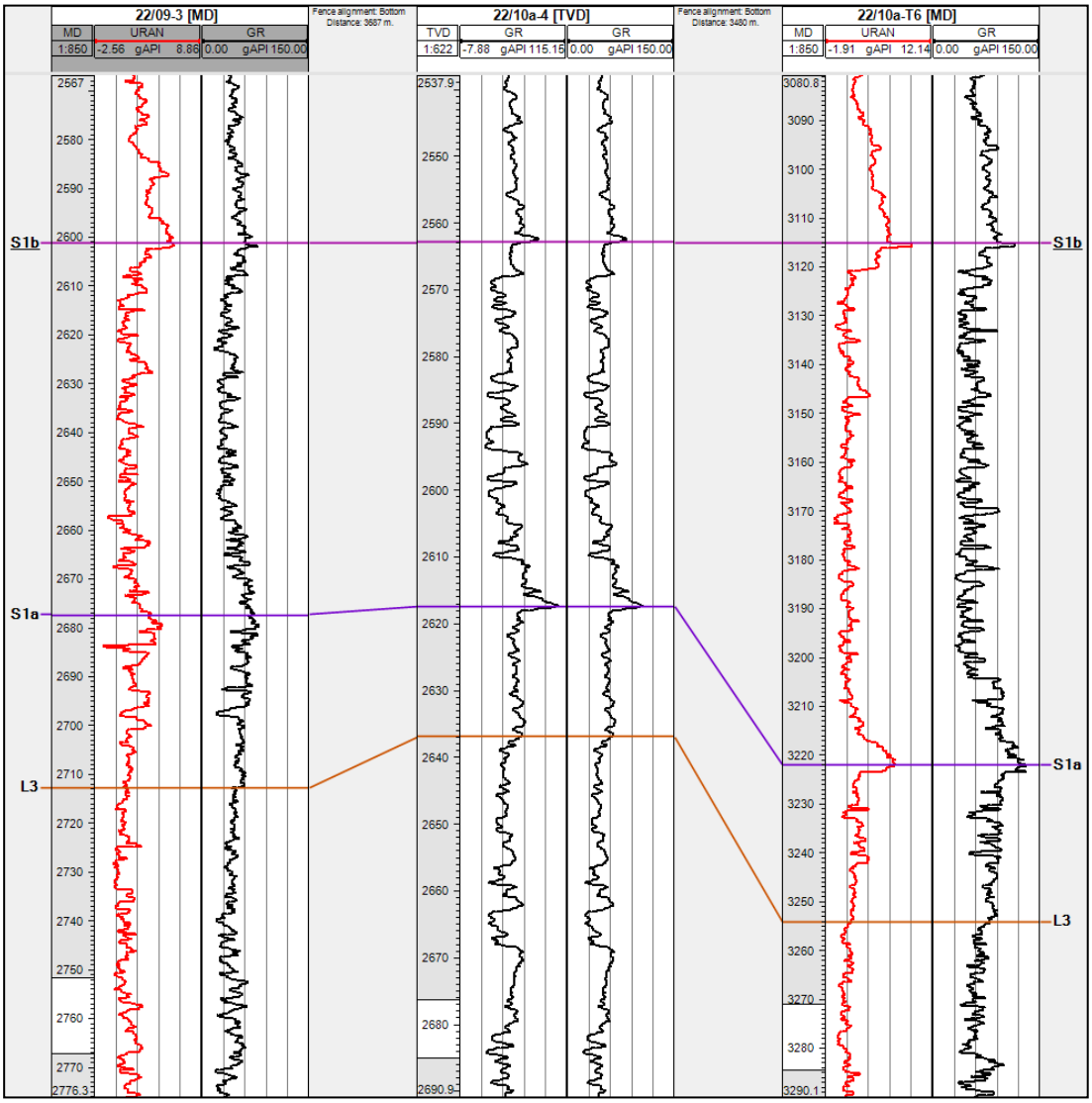

Figure 6.25: Seismic tie between wells 22/09-3, 22/10a-4 and 22/10a-T6 showing the high gamma peak at the S1a/S1b boundary caused by an increase in the element uranium.

However, gamma ray fluctuations do not necessarily always have corresponding expressions seismically and unfortunately the uranium spike did not correspond to a consistent expression due to it having an effect on the gamma response only, while successful imaging requires a corresponding change in the sonic, density or resistive response passing into the horizon (Figure 6.26). It is also possible that the uranium-rich layer was not thick enough to be imaged on seismic due to resolution limits.

Although direct mapping of the PETM onset proved impossible, because of the lack of acoustic impedance contrast, it was possible to get an indirect picture of the extent and thickness of the interval by identifying the end of the PETM or its top down-hole expression which corresponds to the top of the Forties Formation. The top Forties Formation is a basin-wide marker due to a regional condensation surface (MFS). This surface is marked by a peak in uranium but also by a change from clastic sedimentation to the organic rich clays of the Sele Formation giving it a strong acoustic impedance contrast and thus an identifiable expression on seismic (Figure 6.27). The base of the Palaeocene sands was also mapped regionally and the resulting isochron between these surfaces creates a useful proxy for the thickness of the interval of interest (Figure 6.28).

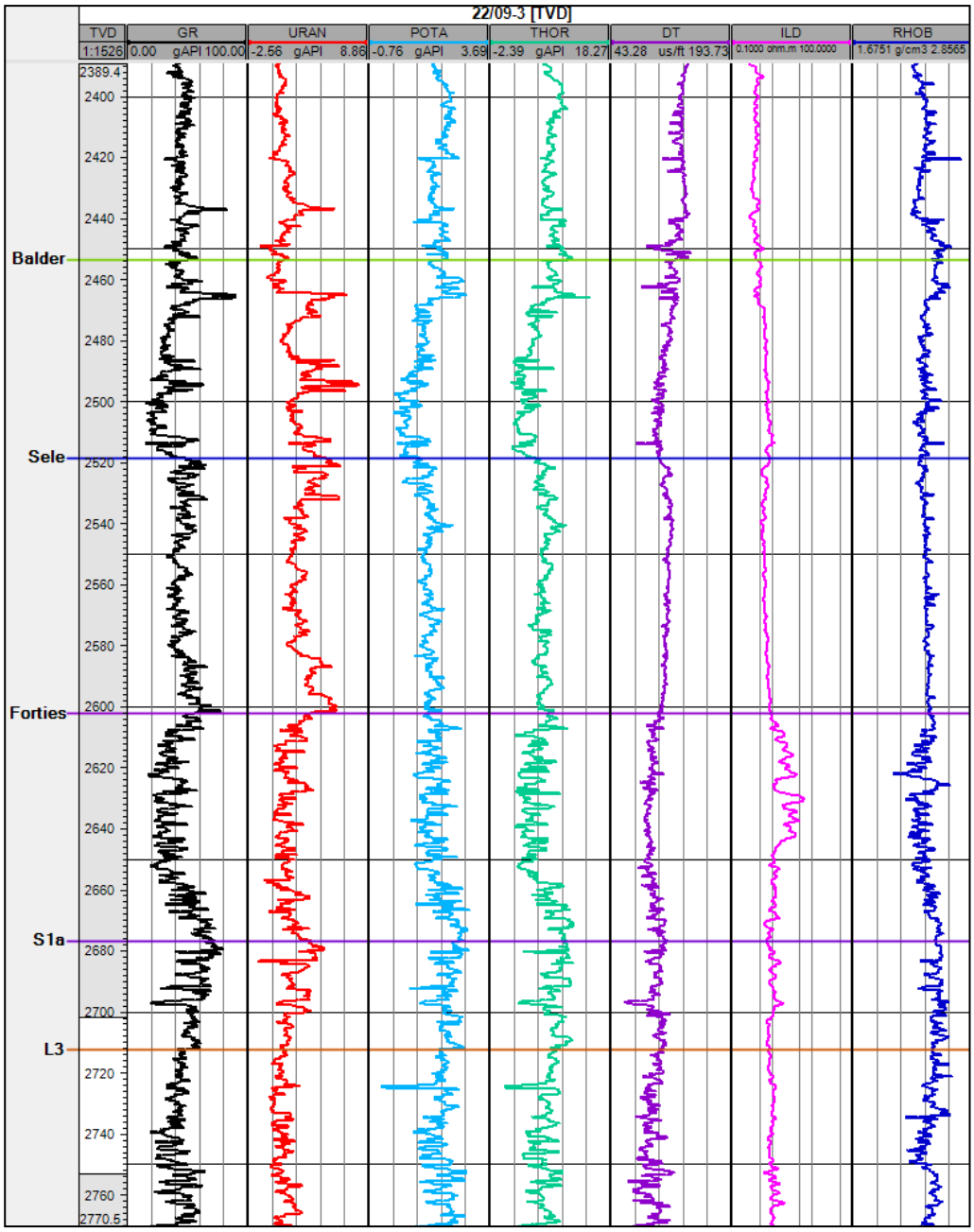

Figure 6.26: Wire-line log suite over the Palaeocene section in 22/09-3 showing the total gamma-ray, spectral gamma-ray (uranium, potassium and thorium), sonic, resistivity and density logs. Where there is an identifiable change in the sonic, density and resistivity response such as occurs the top of the Forties Formation, they will have a corresponding expression on seismic. This response is very small at the S1a/S1b boundary and is thus not identifiable throughout the basin.

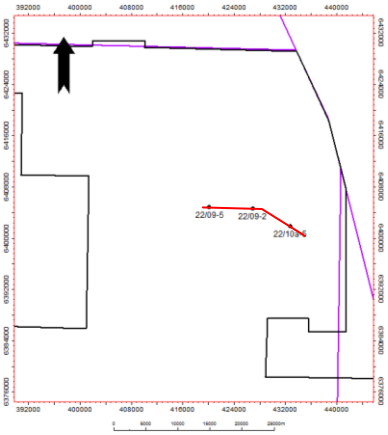

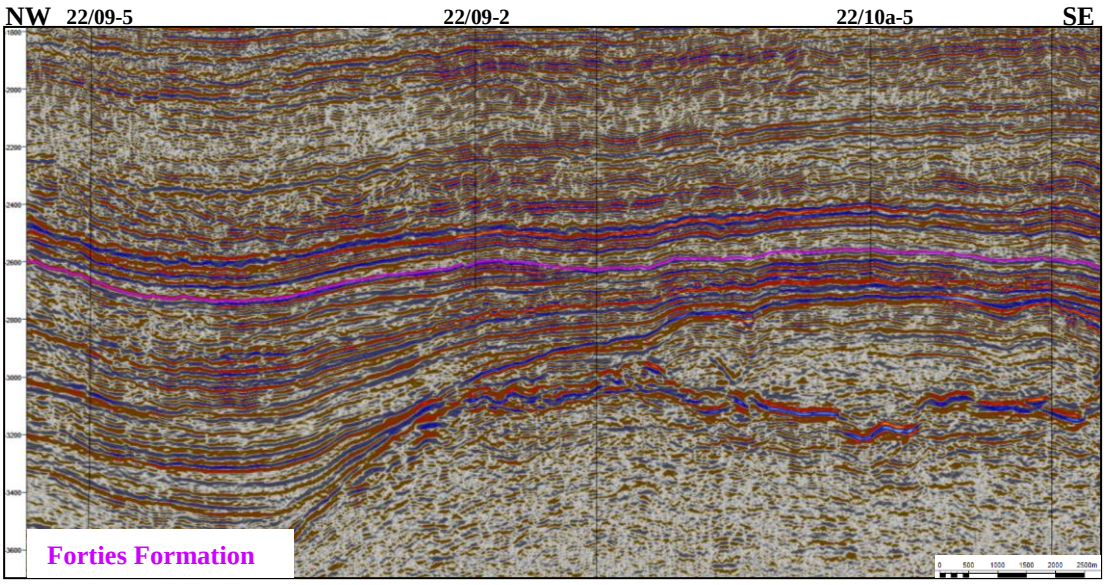

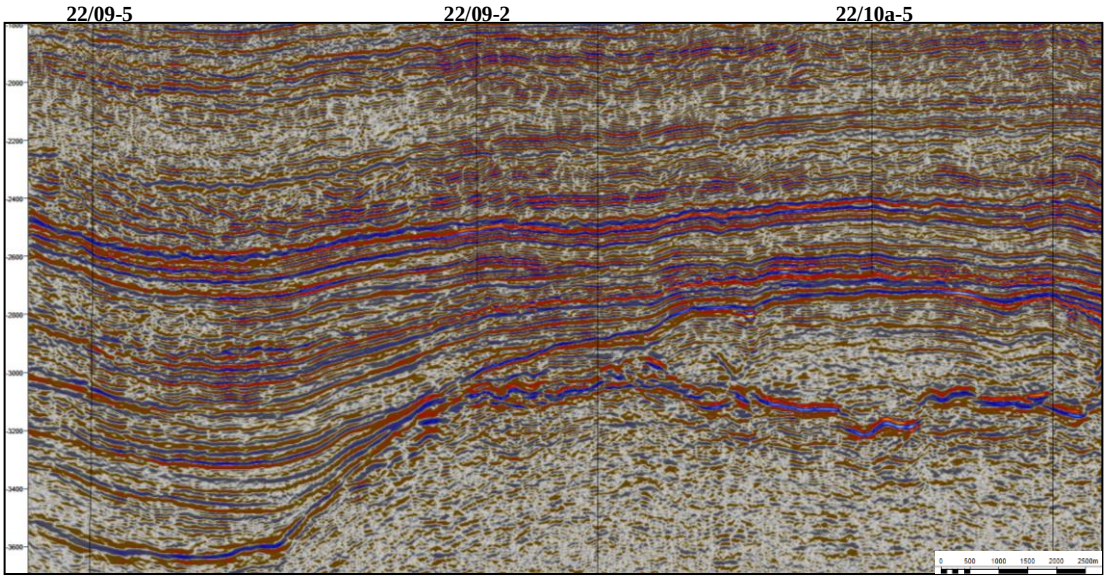

Figure 6.27: Seismic section showing the high amplitude expression of the top of the Forties Formation on seismic.

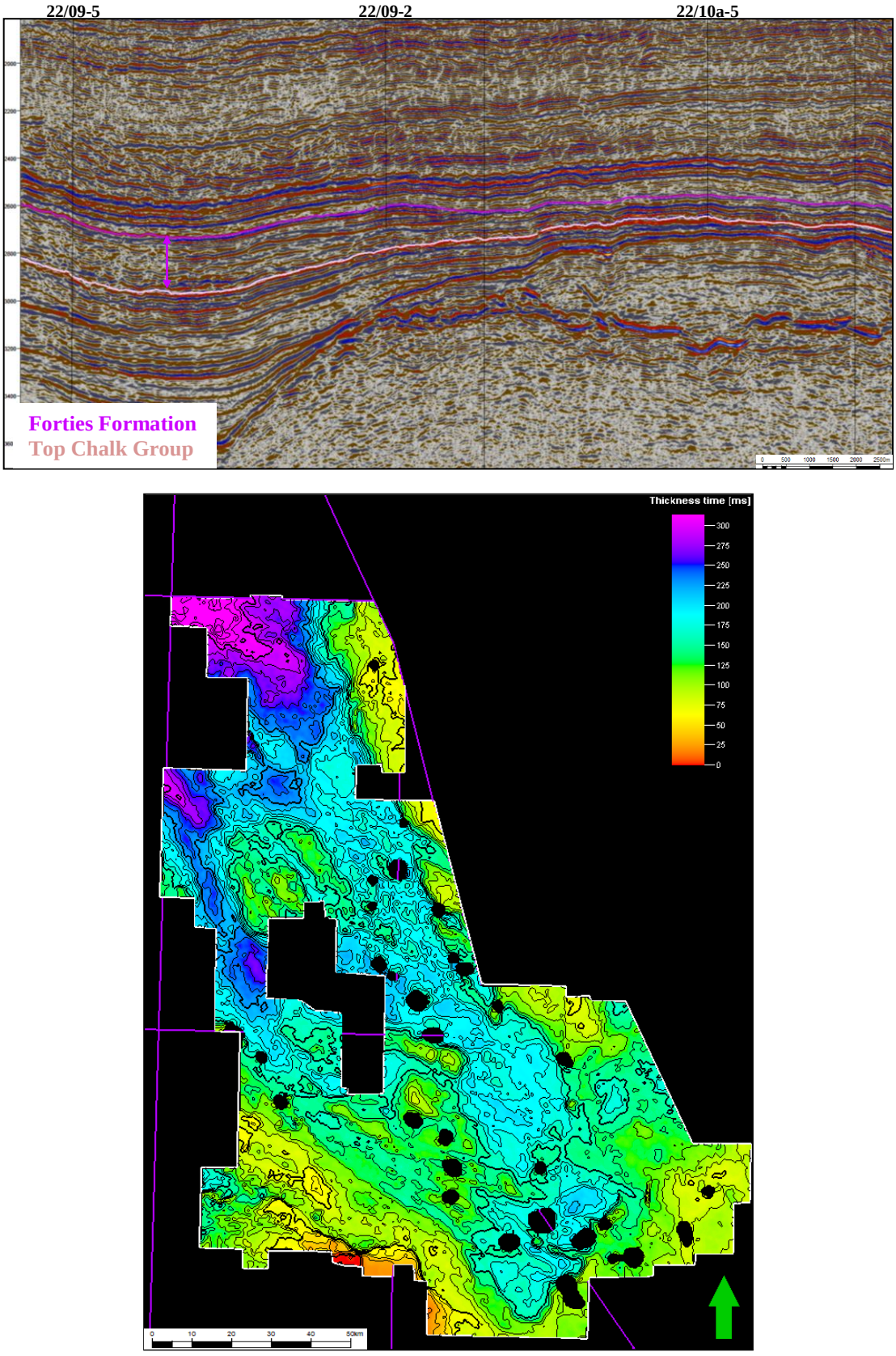

Figure 6.28: Seismic mapping of the Forties Formation and base Palaeocene clastics creates an isochron which is a useful proxy for the thickness of the section of interest. Basin floor turbidite channels can be clearly observed.

The isochron demonstrates that sedimentation rates during the Palaeocene were extremely high and the Forties Sandstone, which was deposited during the PETM is particularly extensive. It is therefore suggested that increased humidity with consequent erosion and run-off was the reason for its great thickness. However, seismic mapping of the stratigraphically older Maureen clastic influx in the previous chapter shows that channel complexes were deposited throughout the Palaeocene and it is hard to differentiate between earlier uplift-generated influxes and later ones which may have been influenced by increased temperatures. Reworking of earlier channel systems by later ones and the difficulties in defining sand on sand contacts on seismic means that an estimation of the total volumes of each depositional system in the Late Palaeocene is was not possible. The effect of uplift in causing a land-wards shift in source areas coupled with the channelized nature of the Palaeocene sands also makes it difficult to hypothesise about the relative energy of the fan systems and thus their link to a more intense hydrological cycle. It could be argued that the Maureen clastic pulse appears to be more extensive and to have reached further into the centre of the basin than the Forties. However, seismic mapping shows that each successive sequence infills the areas left by the previous sequence (Figure 6.29) and therefore the bathymetric relief created by the Maureen fan may have been sufficient that later sediment pulses could not be deposited over the top of them.

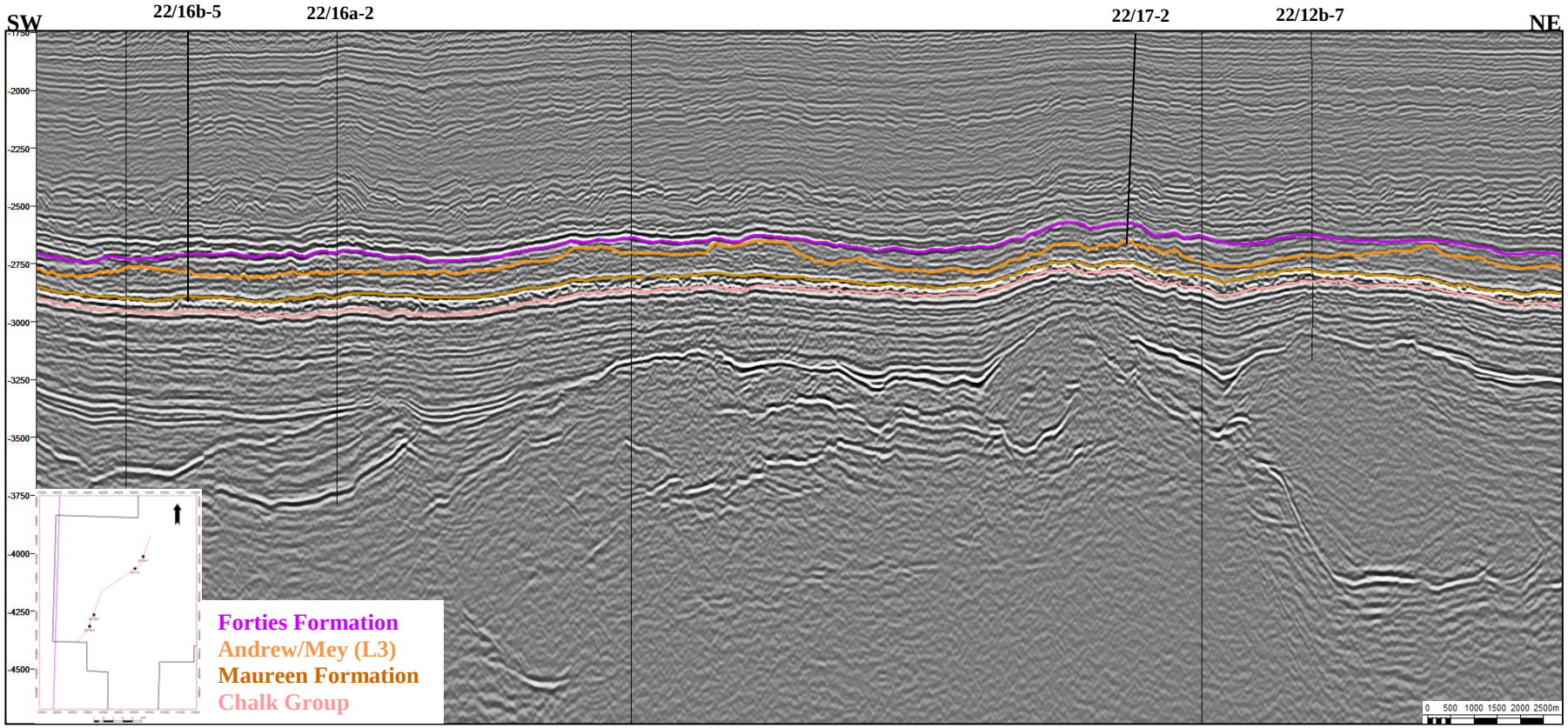

Figure 6.29: A SW-NE seismic section demonstrating the opposing thickening trends of successive Palaeocene fans as they infill the accommodation space left by previous influxes.

These factors mean that seismic data does not provide any information which would allow the effect of climate on deposition of the Forties Formation to be distinguished from the effect of basin margin uplift. However the identification of basin floor turbidite channels has direct implications, not for the effect of the PETM on depositional systems but for the effect of these systems on the PETM record.

Theoretically an extremely expanded section ought to allow higher resolution analysis of the PETM. However, since the majority of this thickness is due to basin floor turbidites which occur during the Lowstand Systems Tract, with the Transgressive Systems Tract and Highstand Systems Tract present only as condensed sections, the PETM carbon isotope curve may not be representative since parts may be very much expanded in relation to others. This can be seen in the comparison of the onset period in the isotope curves from 22/06-1, which has a very sand-prone section and 30/14-1, which is shale-prone (Figure 6.30). In 22/06-1 the onset period seems to represent a longer period of time than that seen in 30/14-1 despite being equal. This may not be a problem if it is properly taken into account that sandy sections will be expanded, but the distinctly channelized nature of the turbidites which make up the Late Palaeocene section in the Central North Sea mean that in different sections different parts of the isotope curve will be expanded as channelized sands move over time and may in some cases be incomplete. Seismic interpretation shows the large variations in thickness of the Forties interval and close analysis of the un-contoured Palaeocene isochron shows complex braided channels which probably switched direction over time with variations in sand influx and the bathymetric relief created by earlier deposits (Figure 6.31). This is a common

problem in all sections barring deep marine boreholes as sedimentation rates are rarely constant but is not usually highlighted. The Central North Sea therefore provides an important case study as there are a number of analyses in the same area and a highly fluctuating sedimentation rate which is very rarely the case in other areas of the world.

Very shale-prone sections representing background marine sedimentation may provide a more complete picture but muddy turbidites also form at the distal edge of the lowstand fan and the majority of areas in the UK CNS are likely to be affected.

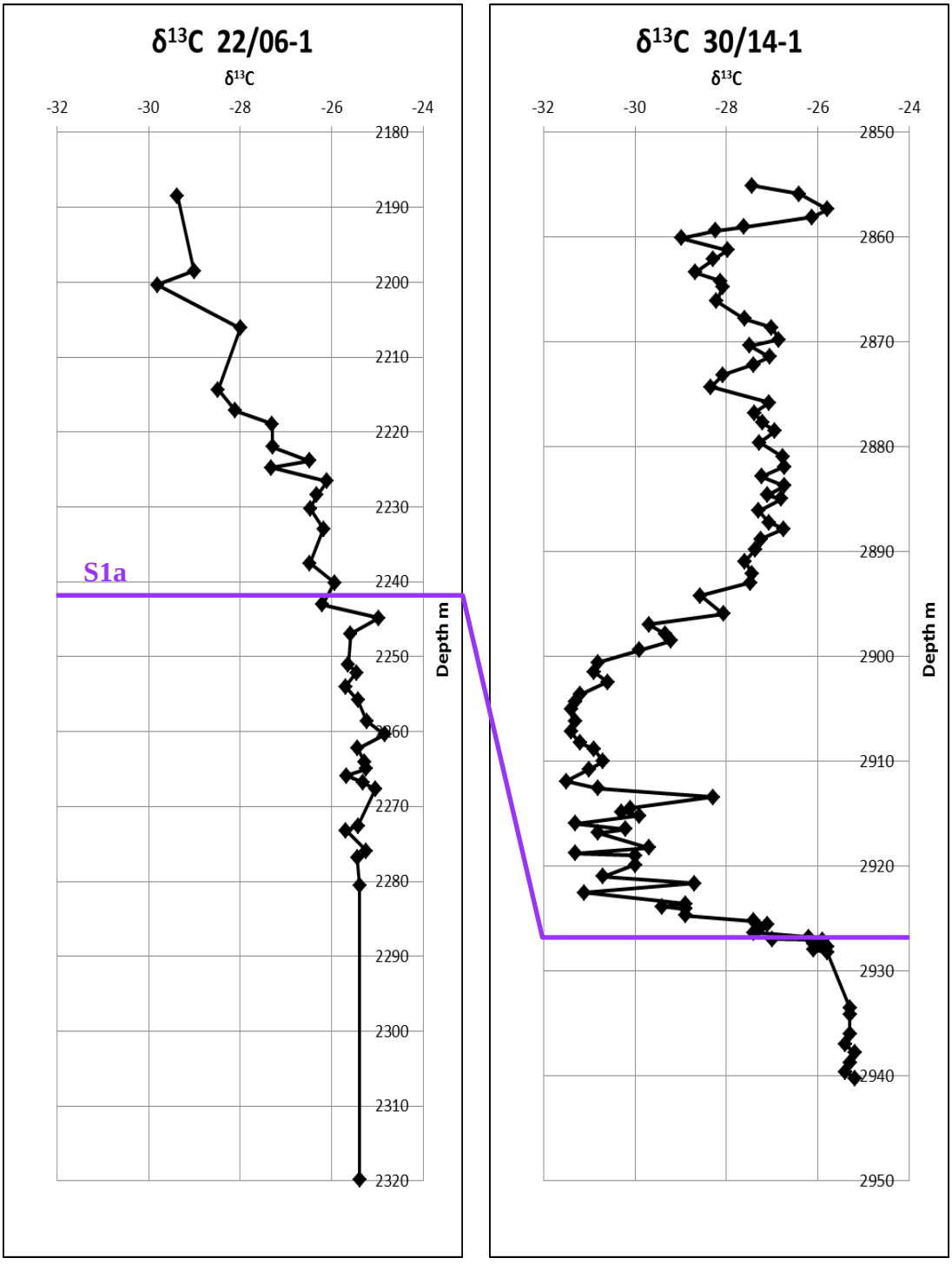

Figure 6.30: Comparison of the $\delta^{13}C$ isotope results from wells 22/06-1 and 30/14-1 demonstrating the effect on the shape of the isotope excursion with increased sedimentation rates.
The 'CIE' as picked in this volume is at the S1a/S1b boundary as described previously

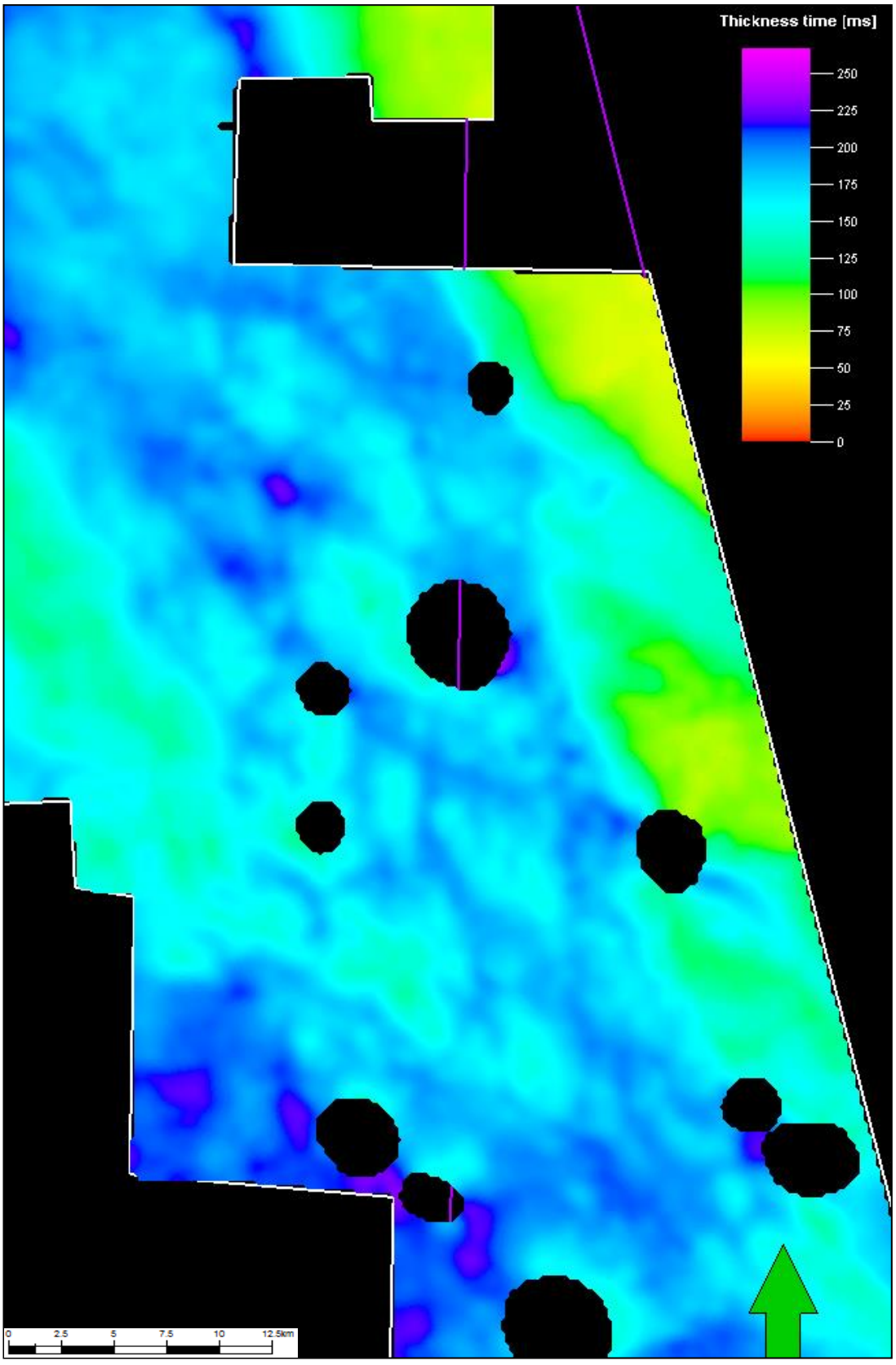

Figure 6.31: A Palaeocene isochron showing braided channel systems.

In order to circumvent the problem of variable sedimentation rates leading to disproportionately expanded sections, it is necessary to have an absolute age model with which to correlate them. Previous studies of the PETM have utilised elemental analyses in order to determine variations in the sedimentary sequences which correlate with orbitally induced changes in insolation (Rohl et al. 2000; Rohl et al. 2007). Orbital cycles (Milankovitch cycles) describe the effects of changes in the Earth's movement on its climate. X-Ray Fluorescence (XRF) analysis was undertaken on samples from 30/14-1 to investigate the possibility of cyclicity in the data corresponding to Milankovitch orbital cycles. There are 3 different orbital cycles each of a different duration with different effects on climate. Eccentricity is the change in the shape of the Earth's orbit around the sun from almost circular to elliptical over a 95,000 year cycle. Obliquity is the change in the angle of the earth's axial tilt with respect to the plane of revolution around the sun which varies from 22.1° to 24.5° over a 42,000 year cycle and the 26,000 year Precession cycle is due to the gyroscopic motion of the Earth's axis. In deep marine boreholes, iron (Fe) and calcium (Ca) show cyclicity over the PETM period (Figure 6.32) which can be linked to precessional cycles.

The elements aluminium (Al), iron (Fe), magnesium (Mg), calcium (Ca), sodium (Na), potassium (K), titanium (Ti), manganese (Mn), phosphorus (P) and silica (Si) were analysed and the resulting percentages graphed (Figure 6.33).

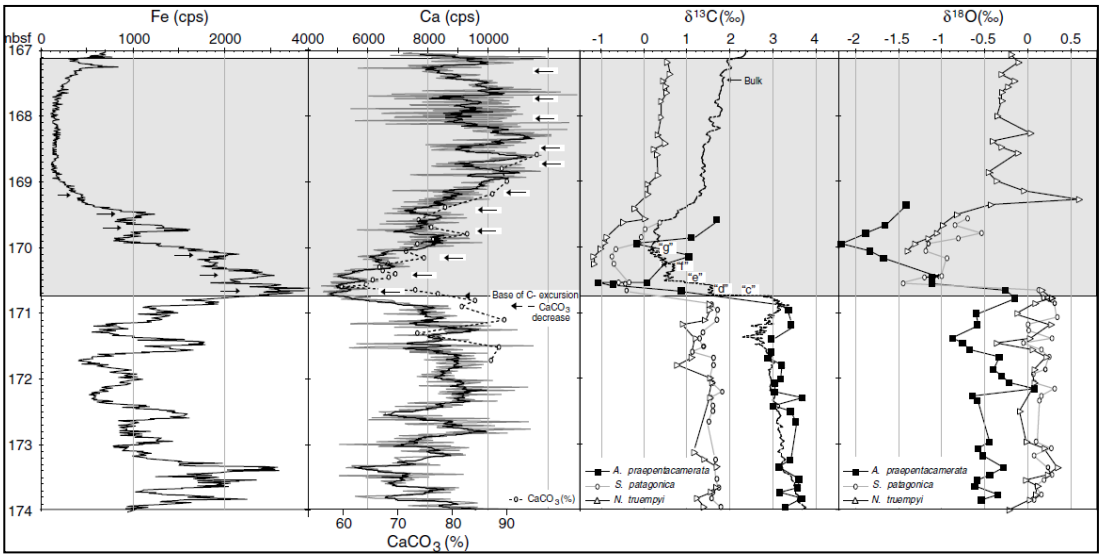

Figure 6.32: Distinct perturbation and cyclicity seen within the Fe and Ca intensity curves derived from XRF analysis of deep sea IODP core 690.
Image after (Rohl et al. 2000)

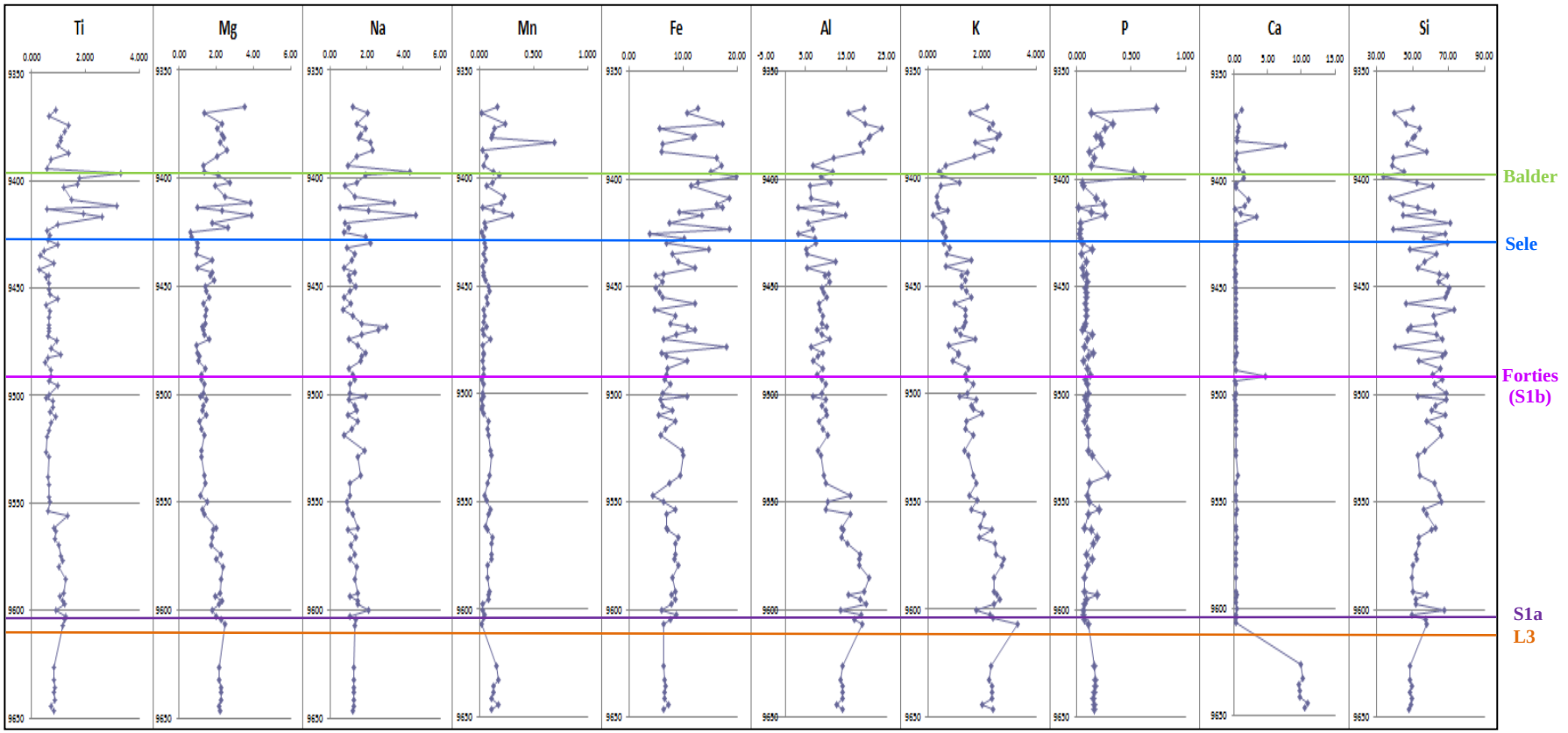

Figure 6.33: Results of XRF analysis of samples from well 30/14-1.

Neither iron (Fe) nor calcium (Ca) showed any evidence of the cyclicity demonstrated in marine cores although since the Ca content of deep marine cores comes from calcium carbonate ($CaCO_3$) which was not present in the clastic dominated North Sea sections, this was not unexpected. Some Ca is also derived from weathering of carbonates but the source area for the clastic input to the North Sea was the uplifted Scotland-Shetland Plateau where carbonates were not the parent rock type.

Although the XRF data does not appear to show any evidence of cyclicity there are some features which could be linked to the effects of the PETM on the chemical composition of the sediments deposited during it. The Ca data shows a distinct decline to zero at the start of the PETM period and could be an indication of carbonate dissolution which occurs in deep marine boreholes due to lowering of the CCD. This would have implications for estimates of the duration of the PETM. However, the North Sea was unlikely to have been deep enough for this to have occurred and furthermore the reduced Ca lasts until well into the Early Eocene after isotope values have fallen to background levels. It is therefore likely that reduced Ca was due to a decrease in the percentage of reworked carbonates of the Early Palaeocene as clastic influx increased.

The distinctive variable onset period observed in the isotope data (Figure 6.34) is also seen in the chemical data. This may indicate that there was instability in the ocean chemistry during the onset of the PETM but it is more likely that this reflects sedimentation rates (R.O'B.Knox pers comm). The lower part of the Forties

Formation may have been deposited more slowly than the upper giving rise to higher variability in elemental concentrations.

The ash-rich Balder Formation showed peaks in the percentages of titanium (Ti), magnesium (Mg), sodium (Na). The percentages of manganese (Mn), phosphorus (P) and calcium (Ca) also rose but there were still low values of some of these elements in the lower Balder suggesting a fundamental difference between the lower and upper parts of the formation possibly due to changes in the composition or frequency of the ash-layers. Further analysis of these changes may link them to changes in the volcanic eruptive types or source areas in the NAIP.

The fact that no cyclicity could be discerned within any of the elements seems to indicate that, at least in the North Sea, elemental concentrations are not controlled by orbital variations and it was thus considered not possible to produce an age model with which to correlate the different sections. A more mathematical approach, for example Fourier analysis, may be useful to see if any long wavelength cycles are obscured by noise in the data but this was outwith the scope of the project (see suggestions for further work).

.

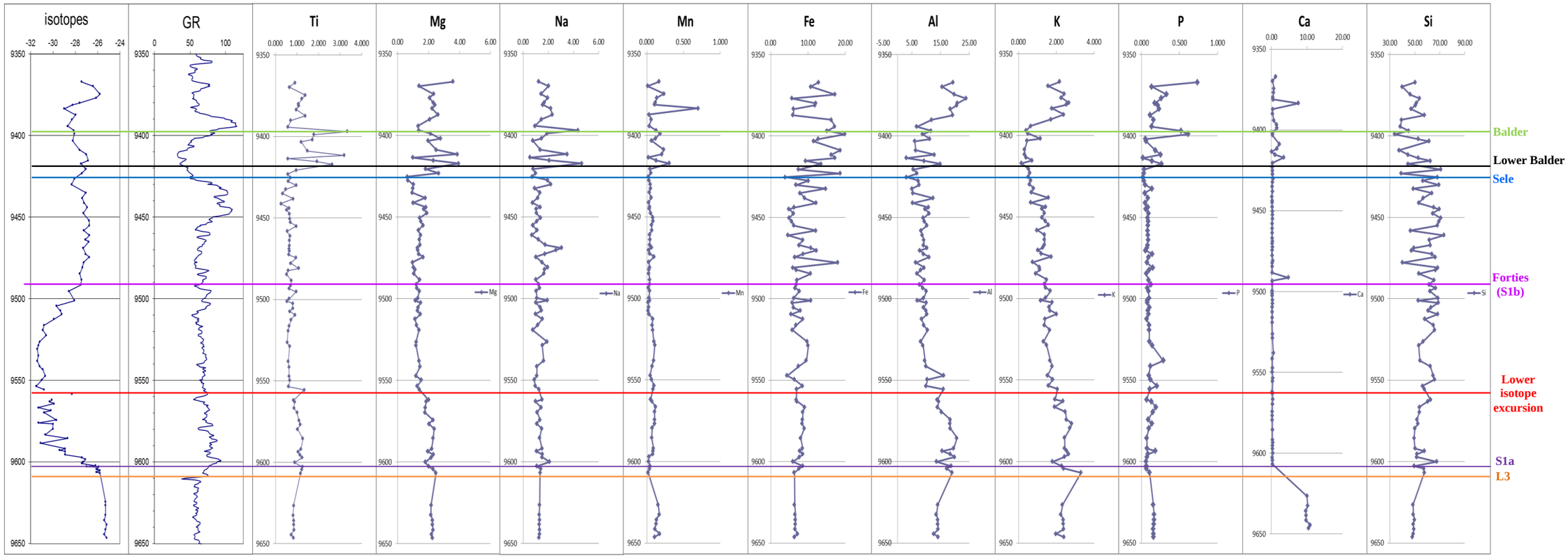

Figure 6.34: XRF data shown beside the isotope and gamma ray curves from 30/14-1.
Note the decline in Ca over the Late Palaeocene- Early Eocene. Also there is a lower Balder unit which appears to significantly differ from the upper section.

Although the relative influences of tectonics and climate on large scale depositional processes could not be determined, the PETM may also have had more subtle effects on deposition in the North Sea by altering the chemical composition of the surface waters and sediments. The start of the PETM is marked by a distinctive gamma spike which correlates with an excess of uranium and has previously been considered to represent a Maximum Flooding Surface (MFS). High levels of marine organic matter within condensed sequences are often associated with high levels of exotic elements such as phosphates and uranium which have an identifiable effect on the gamma-ray log (Rider 1996). However, the spike at the S1a/S1b boundary is a particularly strong signal to be associated with a MFS which is generally assumed to have been fairly short-lived, and its correlation with the CIE invites further investigation.

Uranium is usually found in acid igneous rocks and passes into water bodies in the form of a soluble salt uranyle, U^{6} which is stable in oxidising conditions. Its uranous form U^{4+} is more stable in reducing conditions. Most uranium is transported in river water attached to clay particles (Durrance 1986) and its prevalence at the PETM could indicate a higher river flux. However, uranium passes into sediments in very specific ways- either through chemical precipitation, adsorption by organic matter or through chemical reactions in phosphates.

Natural chemical precipitation of Ur is very unusual but does occur in very acidic, reducing conditions (a PH of 2.5-4.0 is required). This criterion could be fulfilled in stagnant, anoxic waters with slow sedimentation rates and high uranium contents are one of the characteristics of Black Shales. These conditions could have occurred

during the PETM since an anoxic, reducing environment is likely given the evidence from increased pyrite concentrations and the complete disappearance of Agglutinating Foraminifera. High levels of released methane at the PETM would have been rapidly oxidized and subsequent oceanic dissolution of this CO_2 would alter ocean carbon chemistry, principally by lowering the pH and carbonate ion content [CO_3^{2-}] of seawater (Zachos et al. 2005; Robinson 2011). The uranium spike also seems to be present only at the onset of the CIE which may indicate that this unusual environment occurred for only a short period of time, at the maximum input of carbon to the ocean-atmosphere system. However, a PH as low as 2.5-4.0, does not fit with the suggested magnitude of acidification (Zachos et al. 2008; Ridgwell et al. 2010). Due to its enclosed nature, the North Sea would not have had the same buffering capacity as the open ocean so this may have made acidification more acute here but it is not in line with current models.

Uranium is also linked with organic matter and in a stagnant, anoxic ocean there would be less degradation of organic material, allowing it to accumulate. The link between organic matter and uranium is hard to establish though, as the exact mechanism by which uranium is enriched is poorly defined and in some cases, high levels of organic matter do not equate to high levels of uranium (Rider 1996).

Uranium can indicate a stratigraphic hiatus as it builds up over long time periods and is thus present at higher concentrations where a lot of time is represented by a thin bed of rock. The presence of a maximum flooding surface at the S1a/S1b boundary

seems to corroborate this interpretation and condensation could have occurred over a longer time period than previously considered.

It is suggested that the high rates of freshwater run-off and clastic influx in unit S1a shown from seismic mapping and biostratigraphy, could have brought more uranium into the basin. Restriction of the basin and high temperatures may have led to anoxia and acidification allowing increased organic matter production and preservation and possibly direct precipitation of uranium. A hiatus at the S1a/S1b boundary would then have led to concentration of this excess uranium in a condensed section giving rise to a gamma spike on wire-line logs.

It has been suggested that the PETM hyperthermal climate caused an increase in humidity and although this cannot be proved using seismic interpretation, increased levels of terrestrial run-off and high temperatures may have had an effect on the major element composition and clay mineral assemblages of the Forties Formation. The concentrations of dissolved elements such as potassium (K), phosphorus (P), silica (Si) and magnesium (Mg) may be expected to increase with a greater degree of continental weathering and run-off as these are mobile elements with K and Si particularly associated with silicate weathering and increased river discharge (Emiliane 2005) (Figure 6.35).

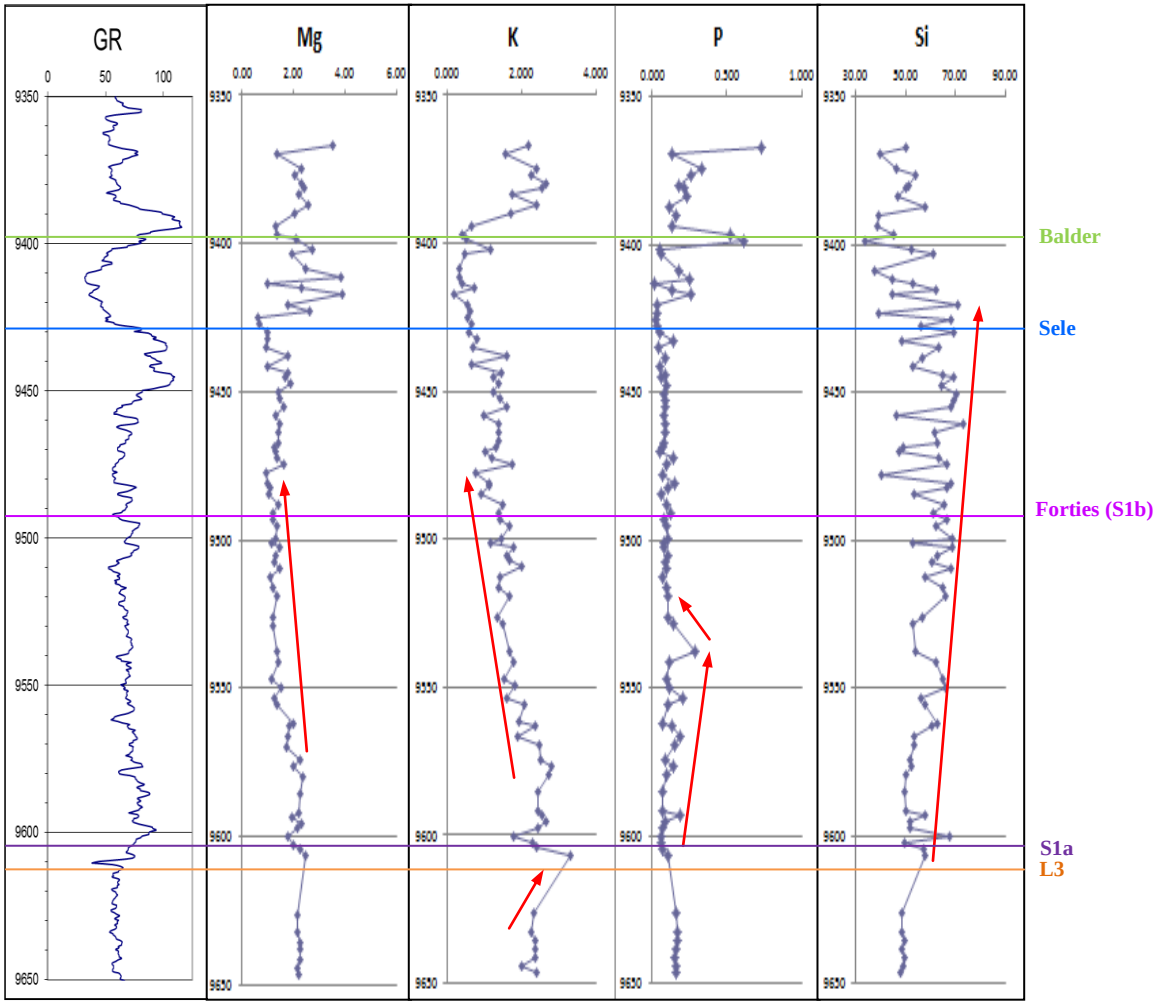

Figure 6.35: Selected elemental percentages from well 30/14-1 showing variations which could be linked to increased weathering and run-off at the PETM.

Silica content increases until the Lower Balder which is consistent with the periods of sand influx to the Central North Sea which occur throughout the Palaeocene before being cut off by the flooding of the delta in the Early Eocene. However, the highly variable silica concentrations seem to be independent of the gamma-ray curve which represents facies. This may indicate that the silica content is derived not only from sand deposition but also from authogenic silica but this is difficult to test without further chemical analysis and therefore does not permit any link between this and increased silicate weathering.

Levels of K and P may show variations which could be linked with the PETM as K increases at the L3/S1a boundary and then gradually decreases up to the top of the Forties Formation while P appears to display a slight increase over the lower part of the Forties Formation. Mg shows no change from the L3 unit into the Lower Forties but begins to decline in the Upper Forties perhaps suggesting that high run-off rates began to fall at this point. Increased levels of P could indicate higher input from rivers and, as this is one of the macro-nutrients vital for all living organisms, this hypothesis could be tested by comparing the P values to the numbers of heterotrophic phytoplankton which are discussed in Section 6.5.

The increase in K from the L3 unit may indicate increased discharge and this could be further tested by looking at spectral gamma logs from wells within the North Sea to investigate any potential increases in potassium over the PETM (Figure 6.36).

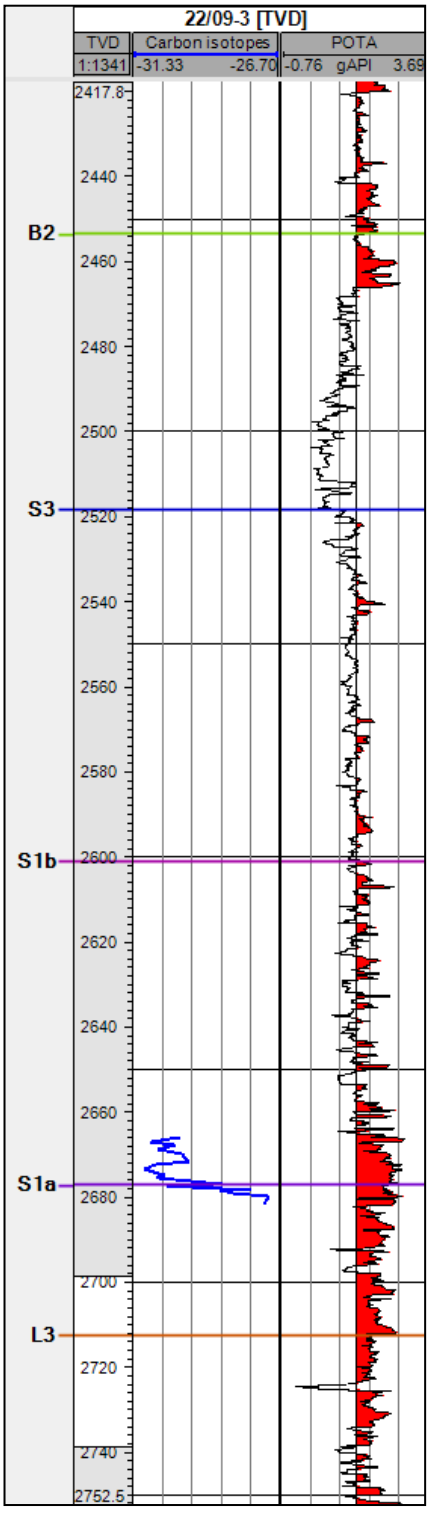

Figure 6.36: Spectral gamma log for well 22/09-3 with high potassium sections highlighted shown with carbon isotope values. Increased levels of potassium in the S1a unit preceding the main isotope excursion and PETM are observed indicating that this element is not linked to increased levels of run-off.

Potassium levels are highest in the L3 and S1a units preceding the PETM which the isotopes demonstrate begins at the S1a/S1b boundary. This seems to indicate that either run-off did not increase, which is unlikely to be the case given the sedimentological evidence, or this element is not linked to terrestrial influx. Changes in clay mineral assemblages could account for this as illites are particularly rich in potassium whereas smectite and kaolinite contain little (Rider 1996).In other PETM sections, an increase in the clay mineral kaolinite is considered indicative of increased runoff under a warm, humid climate (Bolle et al. 2000; Bolle et al. 2001) but within the North Sea, clay minerals assemblages are influenced by the mineralogy of and proximity to the clastic source areas and by late Palaeocene volcanism (Thyberg et al. 2000) with climatic influences difficult to unravel.

In order to understand the link between clay mineralogy and climate it is necessary to understand the principal mechanisms by which clay minerals form (Reeves et al. 2006). Clay mineral assemblages within the North Sea are dominated by inter-layered smectite and illite with lower percentages of kaolinite and chlorite.

The type of clay mineral found in sediment is a function of provenance, transport, climate (weathering), and the diagenetic history of the sequence. The provenance of the sediments is unlikely to have altered in this instance, although the source rock may have changed over a long time scale from upper sediments to crystalline basement as erosion progressed. Transport plays a part in explaining the differences in the percentages of clay minerals in different basinal areas as those fractions with a smaller grain-size area (such as illite and smectite) are transported further and this

may mean that more distal areas of the basin do not show an equivalent increase in kaolinite (Figure 6.37).

Abundant smectite within the clays of the Upper Palaeocene is primarily a product of the alteration of volcanic ashes which are present stratigraphically from the Andrew/Mey Formation (or lateral equivalent) into the basal Horda Formation (Knox et al. 1988). Illitization of this mineral on diagenesis accounts for the intercalated illite and smectite and illite was probably also derived from weathering of pre-existing muscovite or the transformation of kaolinite. Shales of the Sele Formation are distinguished from those of the Forties by their higher smectite contents owing to the higher quantities of volcanic ashes within them and the lower amounts of burial diagenesis undergone.

Kaolinite shows an increase in well 22/10a-4 (Kender et al. 2012) which could be interpreted as due to increased chemical weathering under a humid- tropical climate with alternate wet and dry seasons. Alternatively it can be interpreted as resulting from stronger water currents under an intensified hydrological cycle which moved the larger kaolinite particles further out into the basin. The increase in kaolinite is difficult to investigate regionally since much of the data readily obtainable does not include clay mineral analysis in a usable form and the rise in kaolinite percentage is small in comparison with that of other clay minerals. Additionally, in several of the reports considered it is shown from thin section and scanning electron microscope analysis that the majority of the kaolinite in Forties Formation shales and sandstones is replicative or of a secondary pore-filling nature (Figure 6.38) and whole-rock X-

ray diffraction (XRD) is unlikely to reflect the true abundance of kaolinite (additional details in Appendix 3).

It therefore seems likely that the seemingly anomalous decrease in potassium over the PETM was due to a change in the clay mineral assemblage to one with increased levels of smectite from alteration of volcanic ash and kaolinite possibly derived from warming but also of a replacitive nature due to diagenesis.

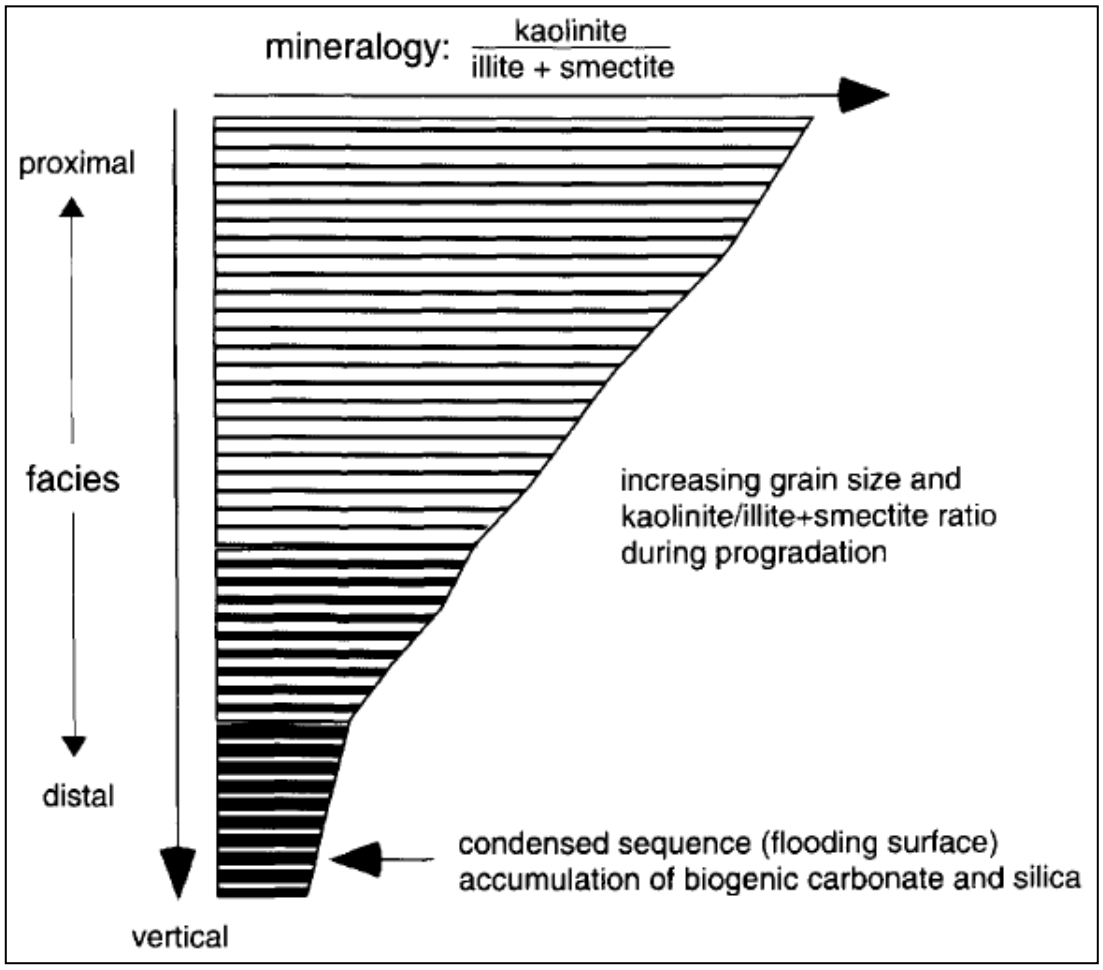

Figure 6.37: Conceptual model for lateral variation in clay mineralogy
(Thyberg et al. 2000)

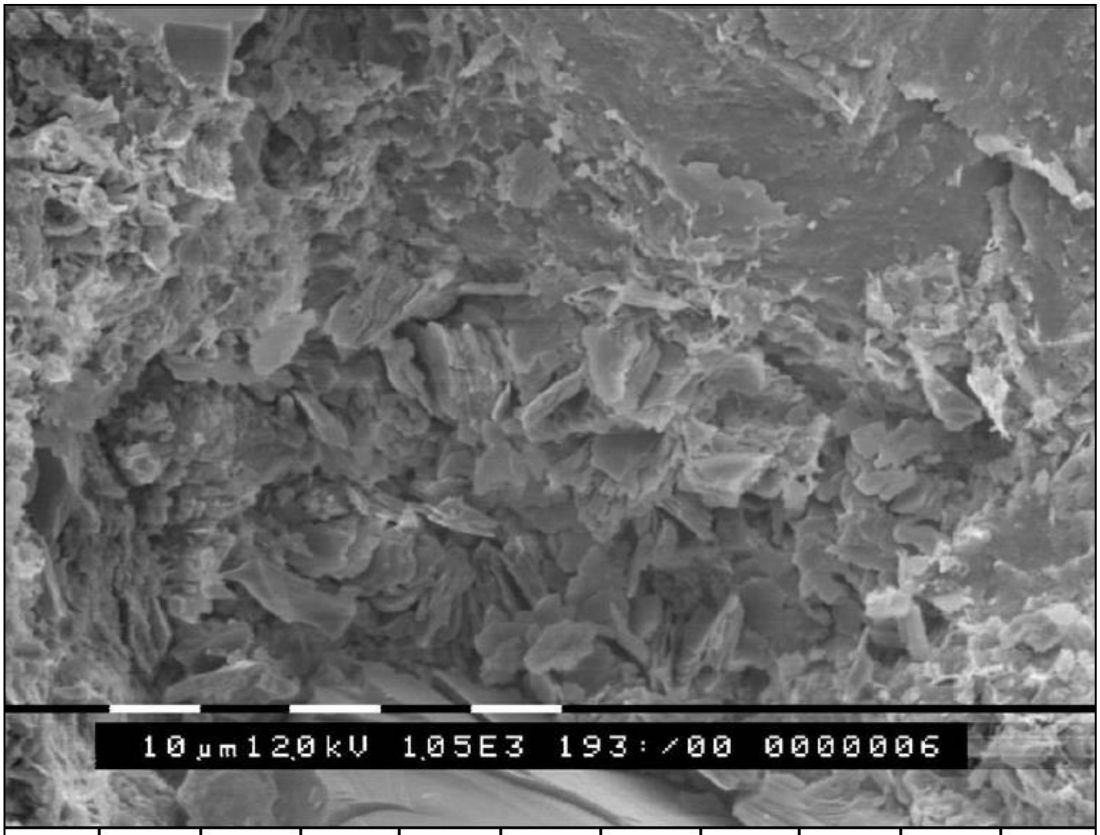

1	2	3	4	5	6	7	8	9	10	11

Figure 6.38: In this SEM image from well 30/2a-5 kaolinite is seen forming poorly-defined booklets and may be replicative of detrital grains or muds. The $\delta^{13}C$ of this sample was measured and found to be -28.445 and so corresponds with the PETM interval.

Image from Ichron Ltd report for Maersk Oil. Further sedimentological information from well 30/2a-5 in Appendix 3

6.5 ENVIRONMENTAL EFFECTS OF THE PETM

6.5.1 NORTH SEA BIOSTRATIGRAPHIC FRAMEWORK

The second aim of the PETM study was to investigate the environmental effects of the PETM using biostratigraphic data. Such data may also aid in unravelling the relative contributions of tectonic uplift and possible humidity increase at the PETM to deposition of the Forties Formation.

A wealth of biostratigraphic information exists for the North Sea area due to its importance as a hydrocarbon province and the first attempts at constructing a Palaeocene/Eocene biostratigraphic framework for the North Sea were in the 1970s after the discovery of the large Forties Field which produced oil from Palaeocene sandstones. Much of this work, however, focussed on foraminifera as these were the standard microfauna used in biostratigraphic analysis and the loss of these species during the late Palaeocene had yet to become common knowledge. Additionally, there was so much oil and gas to be found untapped in the North Sea that only large, structurally simple fields were considered economically viable and a fairly low resolution biostratigraphic framework could be used. There were attempts made to subdivide the Palaeocene more finely (Ioakim 1978; King 1983; Powell 1988), but it was only once more complex stratigraphic traps such as Everest were discovered and became economic in the late 1980s and early 1990s that higher resolution frameworks were required and published (Gradstein et al. 1992; Powell 1992).

The latest biostratigraphy is even more refined in the wake of the declining hydrocarbon industry in the North Sea as the search for more subtle traps and more effective ways to target specific horizons continues (Figure 6.39).

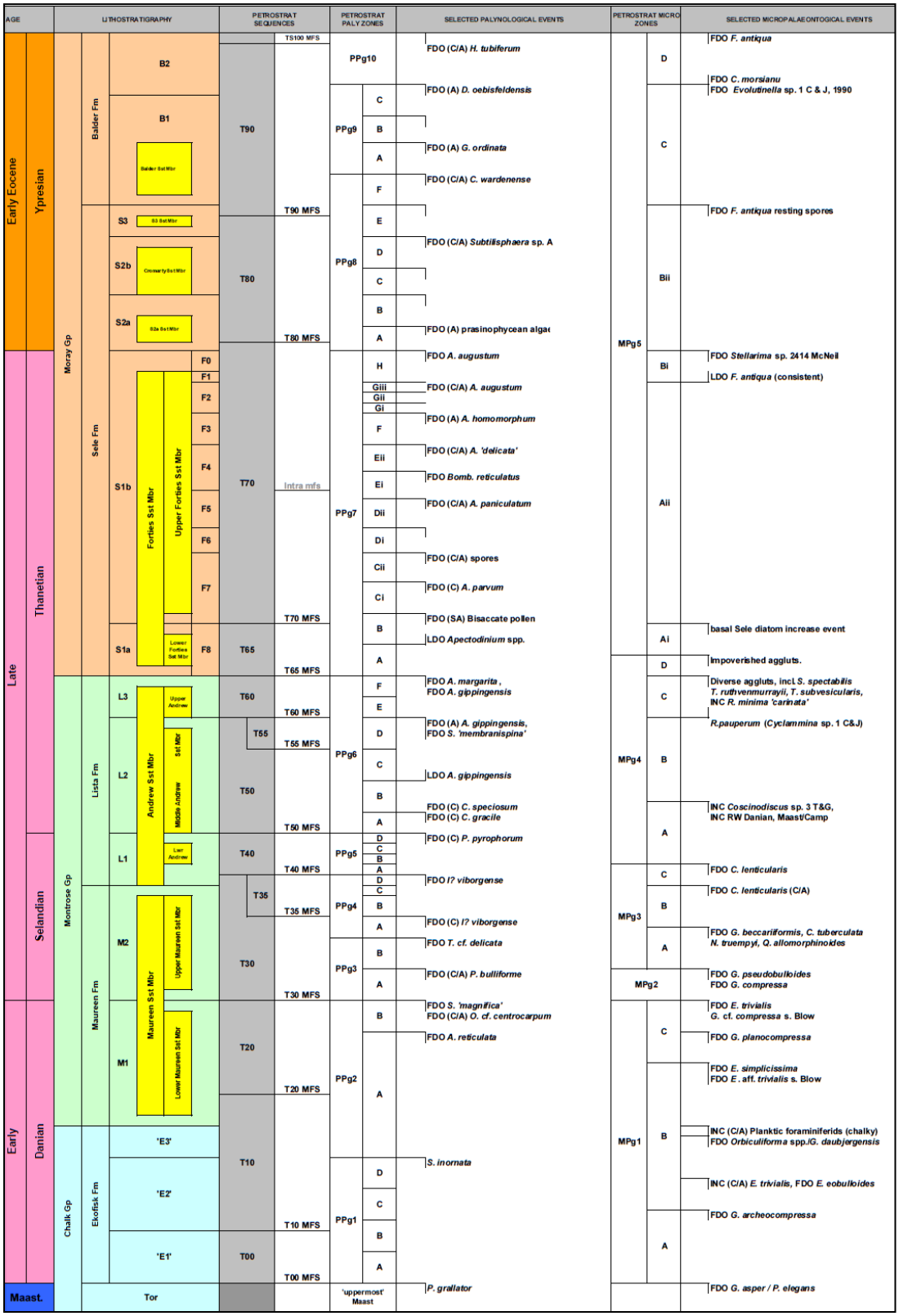

Figure 6.39: Petrostrat's biostratigraphical framework for the Central North Sea with respect to the B, S, L and M lithostratigraphic units of Knox and Holloway. 1992. Note that the Forties Formation as defined in this volume contains units S1a and S1b

Image after Petrostrat Ltd

6.5.2 ECOLOGICAL CHANGES IN THE NORTH SEA AT THE PETM

It is possible to use this large volume of biostratigraphical analysis to interpret changes in the envirionmental conditions in the marine and terrestrial realms over the PETM. To this end, a database consisting of biostratigraphical reports, publically released and distributed through the Schlumberger-operated CDA datastore (CDA 2009) over the Palaeocene and Early Eocene from 140 wells in the North Sea was created (Appendix 2). It can be observed from the description of the data provided in Appendix 2 that there are distinct variations in the number of samples analysed and in the age and type of analyses. This introduces some variability into the database as sample resolution differs from section to section and older analyses may rely on different index fossils as they may pre-date construction of the biostratigraphuic framework. Different companies may also use different processing techniques leading to variations in the type of fossils preserved and details such as sieve size and slide preparation techniques were not availiable. Despite these caveats it was considered that the large number of studies over a geographically small area was such that the main variations in faunal composition would be evident regardless of the uncertainties inherant in a database with such mixed source material.

From previous studies worldwide there may be expected to be evidence of dinoflagellate migrations and changes in assemblage, faunal extinctions or higher numbers of thermophillic species. Assemblage changes may also provide

information about possible changes in salinity due to higher freshwater run-off under a warm, humid climate and indications of anoxia or euxinia.

Within the database, the first noticeable incursion around the PETM is the dinoflagellate cyst *Apectodinium*. The *Apectodinium* acme is considered a globally synchronous characteristic of the PETM (Crouch et al. 2001; Sluijs et al. 2005) This acme is present in every well within the studied area and correlates with the Forties Formation. Its sudden increase in numbers at this time is considered to have been opportunistic, taking advantage of the decline of other flora and fauna although it's tolerance for warmth and stressed conditions also played a part.

In the North Sea 22/10a-4 section, the base of common occurrence of *Apectodinium* corresponds with the CIE. However, the dinoflagellate cyst has been suggested to occur stratigraphically below the PETM, within the Early Palaeocene age Maureen Formation (Thomas 1996) (Figure 6.40). An explanation for this earlier appearance of *Apectodinium* was proposed as a short-lived migration in response to a pulse of early Palaeocene climate warming (Bujak et al. 1998). *Apectodinium* at this stratigraphic level is observed in a few of the wells within the database but this analysis is based on cuttings rather than core data therefore these occurrences may be caved during drilling and not in-situ.

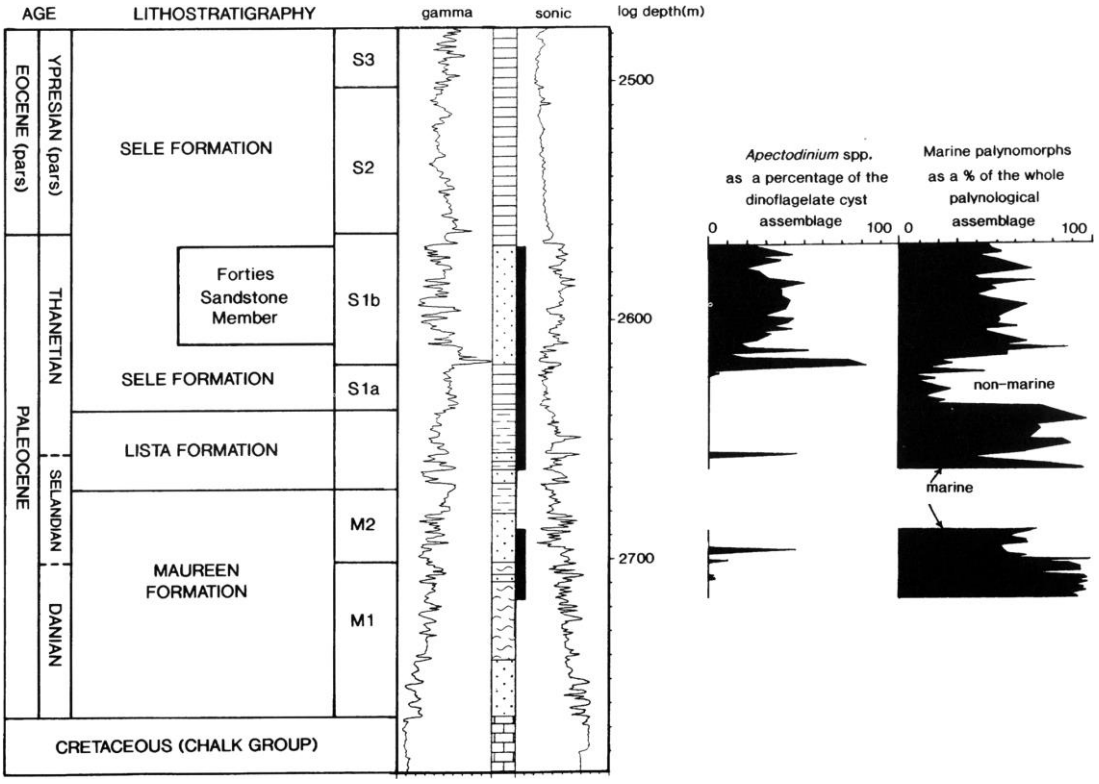

Figure 6.40: Previous analysis of the 22/10a-4 well found earlier influxes of *Apectodinium* at the M1/M2 boundary.
Image after (Thomas 1996)

It was noted in the 22/10a-4 section and the majority of the sections within the database, that the first influx of *Apectodinium* within the Late Palaeocene occurs prior to the CIE, in the S1a unit (Figure 6.41). Isotope analysis shows this unit to correspond with the 'onset phase' of decreasing $\delta^{13}C$ values before the largest divergence which is considered the main CIE. This indicates that warming may have preceded the release of light carbon into the ocean- atmosphere system or that this release was somehow buffered for a while and may have occurred over a longer time period than previously considered. *Apectodinium* then steadily increase in numbers before gradually falling or being truncated by the condensed section at the top of the Forties Formation (S1b) which can be correlated in well 30/14-1 to the return to normal isotope values and thus the end of the hyperthermal (Figure 6.42).

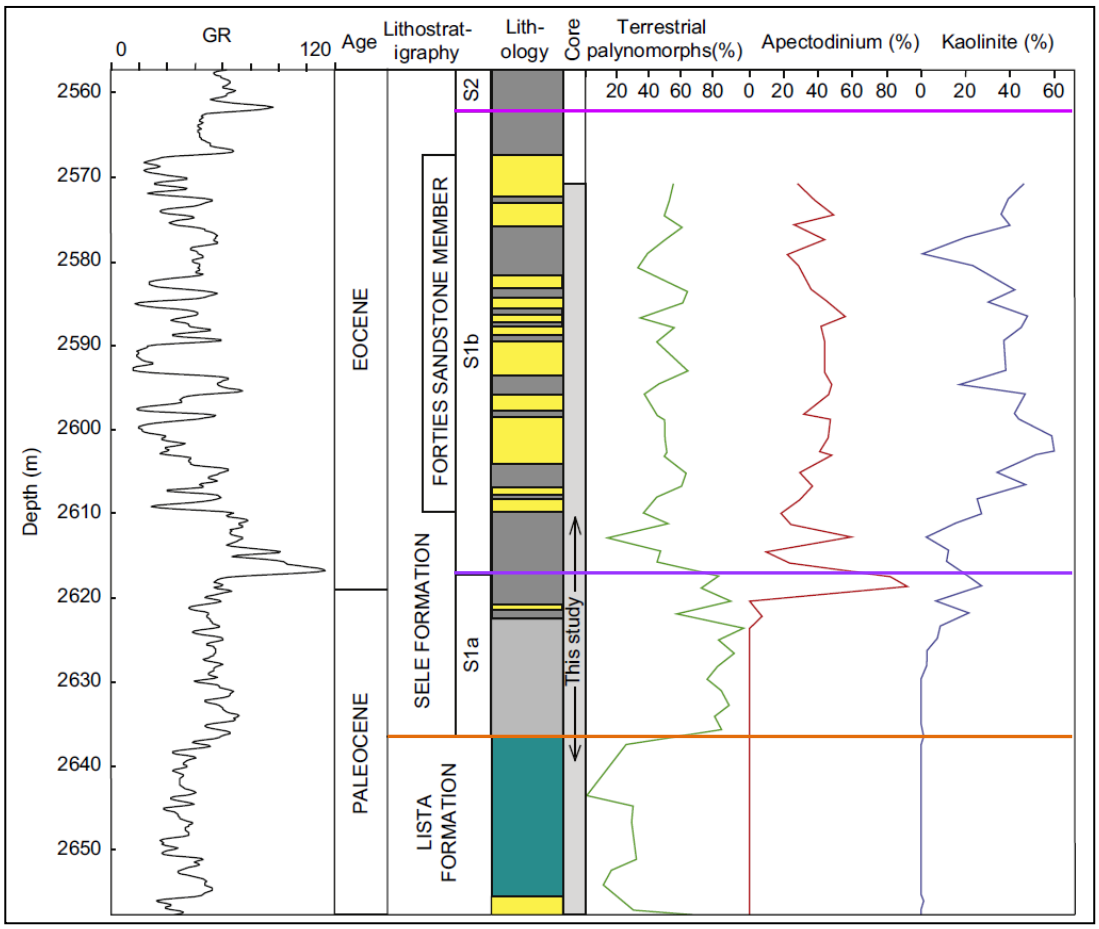

Figure 6.41: Correlation of the *Apectodinium* acme with the S1a/S1b boundary in well 22/10a-4.
Image after (Kender et al. 2012)

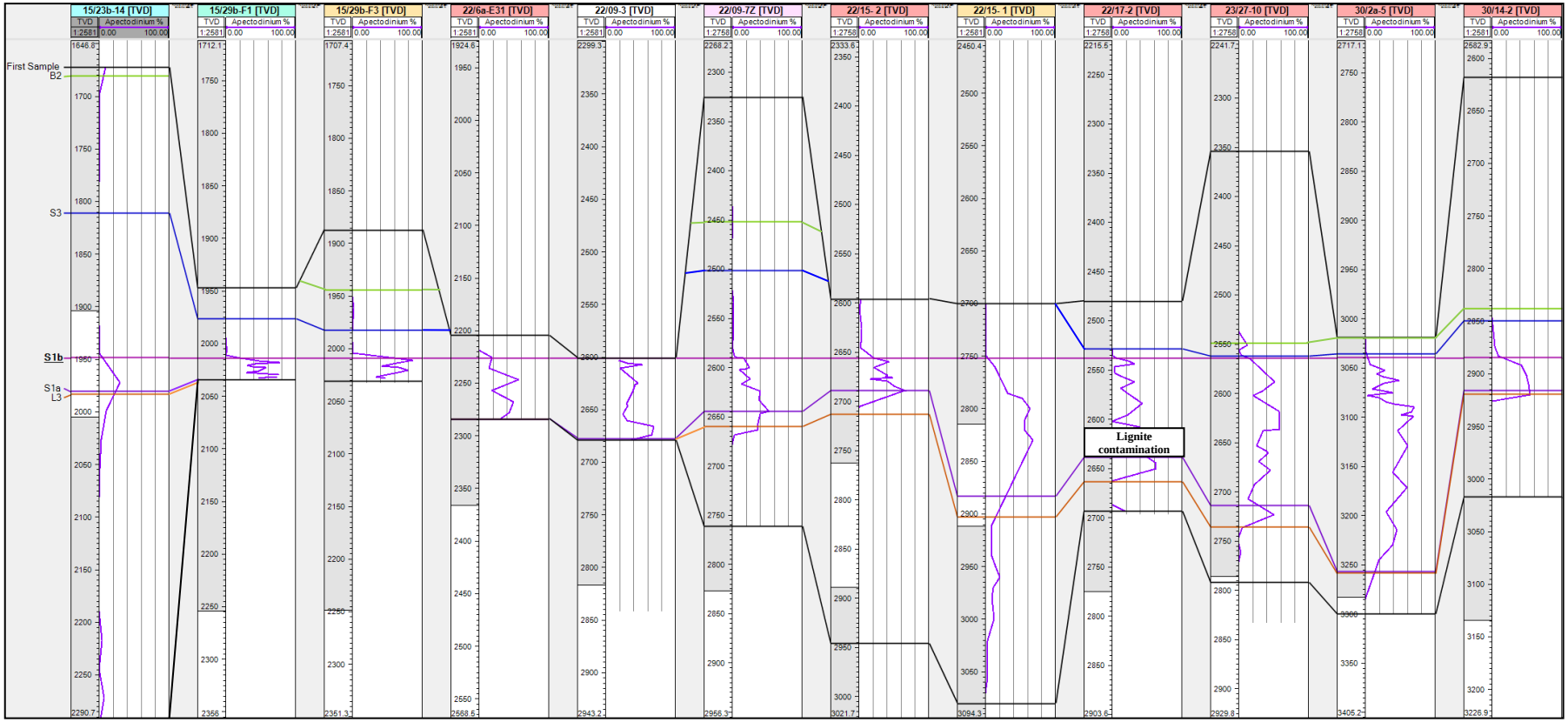

Figure 6.42: N-S well section showing regional extent of the *Apectodinium* acme. The species is initially seen in the S1a unit prior to the PETM and rises to its acme within it.

It has been noted that *Apectodinium* locally became outnumbered by low-salinity tolerant dinocysts during the PETM indicating that very low salinities were not optimal for the species (Sluijs et al. 2006). Within the biostratigraphic results from the closely sampled 22/10a-4, there was an identifiable trend towards lower salinity forms (Kender et al. 2012) and this was also seen in the reports from the database. A loss of dinoflagellates associated with oceanic influence such as *Areoligera gippingensis* (Powell et al. 1996) and lowered numbers of *Impletosphaeridium* and the *Spiniferites* group at the top of the Lista Formation also indicates lowered salinity (Wall et al. 1977; Brinkhuis 1994; Devillers et al. 2000; Sluijs et al. 2005) (Figure 6.43).

However, (Zacke et al. 2009) reported that the North Sea had become extremely fresh throughout the PETM due to the enclosed nature of the basin and increased run-off. *Apectodinium* should have therefore found this environment very challenging but in contrast appear to thrive. This may indicate that *Apectodinium* are less affected by salinity than previously thought and the occurrence of the species in the London Bain in back barrier environments seems to corroborate this (Knox 1996).

Apectodinium are Peridinoids (details on dinoflagellate taxonomy in Chapter1) and are considered by most to be heterotrophic organisms. This means they cannot fix carbon by using energy from sunlight and must use organic carbon for growth and metabolic processes. They therefore thrive in areas where there is high nutrient availability such as upwelling zones and close to shore-lines which support the algae,

diatoms and other primary producers on which they feed. Autotrophic dinoflagellates, which harbour symbionts capable of fixing carbon from sunlight, mainly belong to the order Gonyaulacales and can live anywhere there is sufficient light for photosynthesis (within the bounds of their ecological tolerance). The Peridinoid/Gonyaulacoid ratio (P: G) is therefore used as a measure of productivity and nutrient availability (Bujak et al. 1998; Reichart et al. 2003; Roncaglia 2004; Sprangers et al. 2004; Sluijs et al. 2005).

Over the PETM in the North Sea there is a marked transient rise in the number of Peridinoids relative to Gonyaulacoids (P/G ratio) which signifies that there was an increase in productivity at this time. There is also a noticeable rise in heterotrophic organisms at the Maureen/Lista Formation boundary. This link between heterotrophic organisms and increased nutrients could be tested by comparing the phosphorus values derived from elemental analysis with the P/G ratio (Figure 6.44).

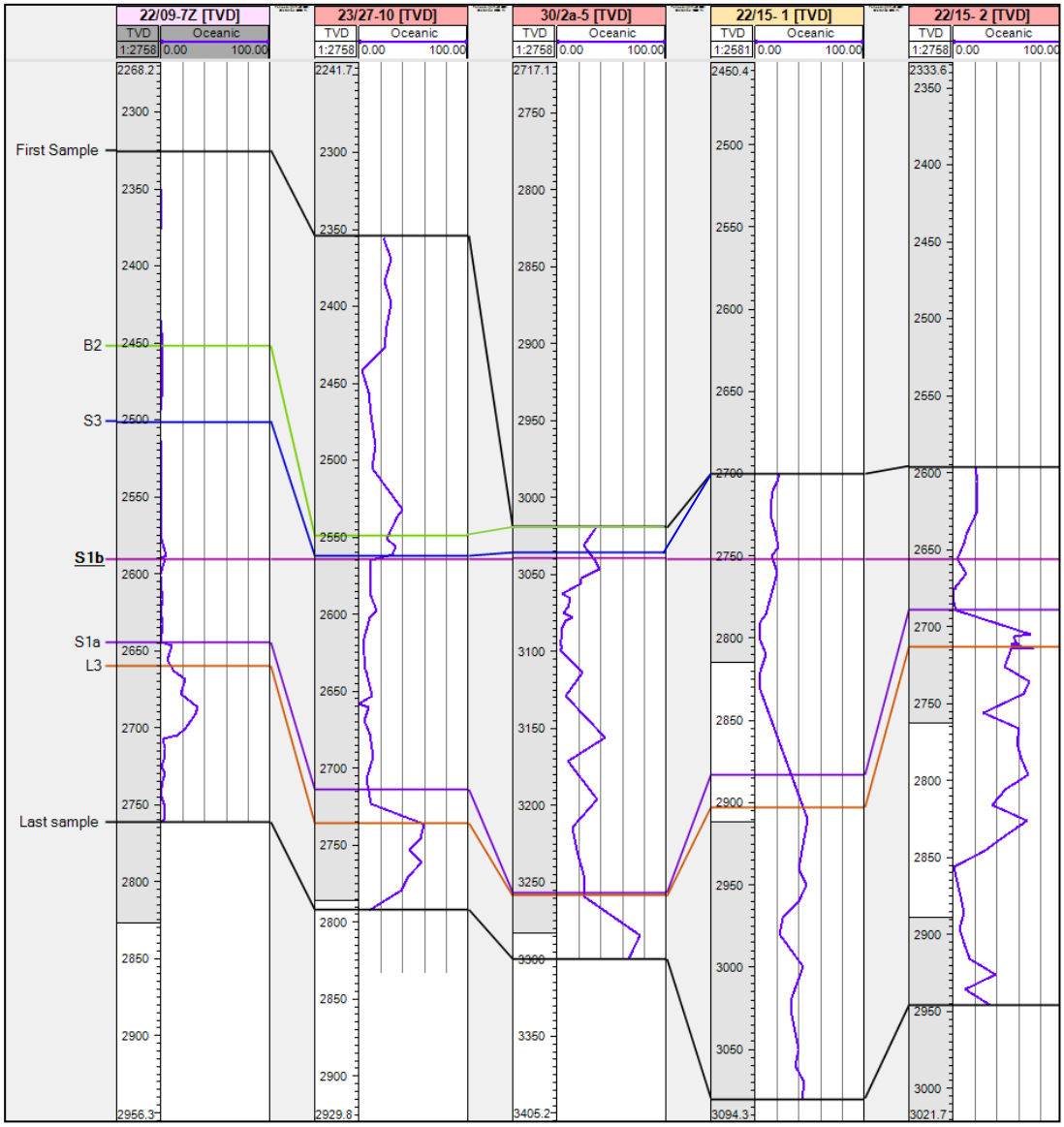

Figure 6.43: Well section from the Central North Sea showing a distinct fall in the percentage of dinoflagellates associated with oceanic influences at the L3/S1a boundary.

Details of dinoflagellate species contained in this group in section 5.5.3

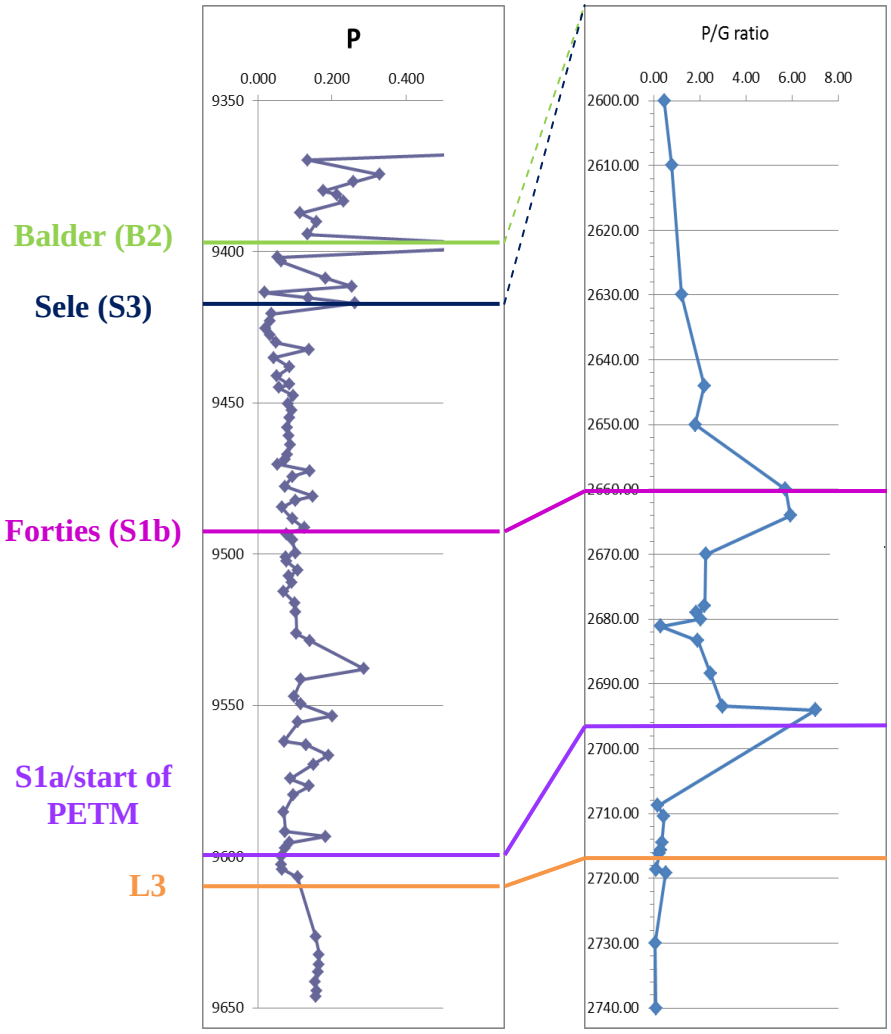

Figure 6.44: Comparison of the P values derived from section 30/14-1 and the P/G ratio from one of the sections within the wider North Sea dataset showing correlation of the increased levels of this element with numbers of heterotrophic organisms.

Although it is usually better to graph P against another element oxide to reduce the influence of varying clastic input this simplistic comparison does convincingly show increased P values corresponding with the increased numbers of peridinoid dinoflagellates. This indicates that nutrient availability was the driver for the increase in the P/G ratio observed over the PETM. This could also point to increased humidity due to warming leading to greater amounts of run-off.

There are no apparent extinctions within the dinoflagellate assemblage but there are amongst the Foraminifera. Lista Formation sediments contain diverse assemblage of agglutinating Foraminifera which disappear before the Forties Formation PETM. There is a distinctive change at the Lista/Forties Formation boundary (L3/S1a) as foraminiferal assemblages become sparse, consisting mainly of *Rhizammina* and *Haplophragmoides* (Figure 6.45). These then seem to disappear at the onset of the PETM in some sections, but carry on into the lower part of S1b in others so it is difficult to say for certain whether one or the other is the case. Palaeocene foraminiferal assemblages contain a number of agglutinating Foraminifera that outside the North Sea, range up to the Recent, and which therefore have known bathymetric distributions. Many of these taxa have upper depth limits of between 200 and 1000m which confirm a deep-water environment but also one which is importantly far shallower than the carbonate compensation depth (CCD). This proves that there was no carbonate dissolution in this area associated with the PETM as was suggested by the XRF Ca data, and thus the decline of calcitic foraminiferal species is not a preservational feature. Instead this indicates that at this time, the physics or chemistry of the benthonic environment deteriorated to the point where it was

uninhabitable by even opportunistic epifaunal foraminifera, perhaps an expression of the Benthic Foraminiferal Extinction Event (BFEE) although there are no true extinctions as the species return to the basin in the Early Eocene.

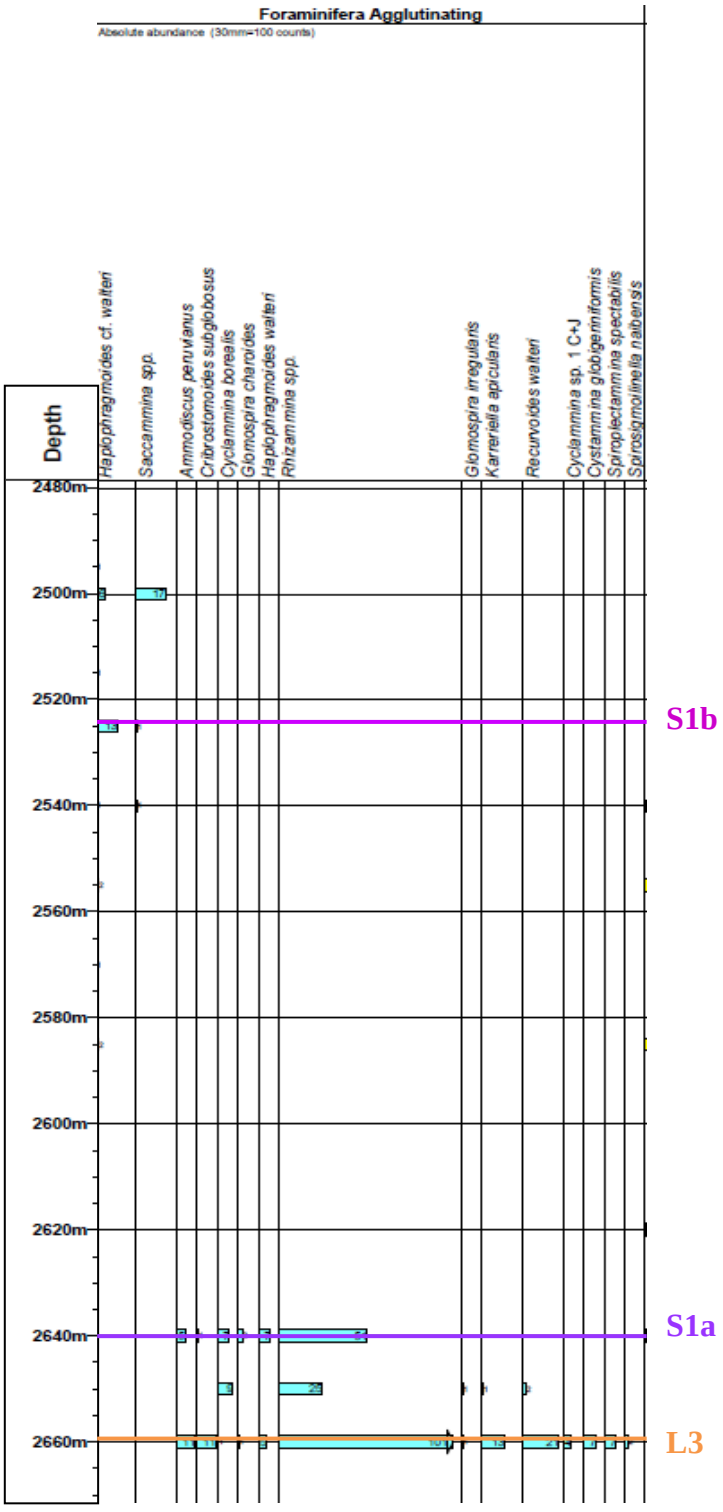

Figure 6.45: Biostratigraphic analysis from well 22/06a-31 showing a reduction in Foraminiferal numbers in unit S1a and an apparent extinction at the S1a/S1b boundary which corresponds with the CIE.

Biostratigraphic analysis originally undertaken by R.Dyer, Geostrat Ltd

As well as an influx of *Apectodinium* and peridinoid dinoflagellates, there is also a marked increase in angiosperm pollen seen in North Sea cores at the onset of the PETM warming. Like the *Apectodinium* influx, the increasing trend begins earlier than the PETM and also seems to continue after the S1b boundary which corresponds with the return to normal isotope values and thus the end of the hyperthermal (Figure 6.46). There had been a world-wide trend towards increased angiosperms since they originated in the Early Cretaceous, but during the latest Cretaceous they rapidly diversified, a trend which continued into the Palaeocene. It is therefore unusual that there is little evidence of these angiosperms in North Sea cores until the Mid-Late Palaeocene. It has been suggested that angiosperms are better suited to wetter climates than gymnosperms and, due to their higher growth rates, proliferate in disturbed or aquatic sites (Berendse et al. 2009). Their increase in abundance over the PETM may therefore indicate increased humidity. However taphonomic and experimental conditions may also have a role to play in determining the proportions of angiosperm pollen that are observed within the North Sea sections. Transport to the basin is important and low salinity surface waters during the PETM may have increased transport efficiency. Palynological preparation methods also favour dinoflagellates and larger pollen grains as sieve sizes vary and can sometimes have mesh sizes too large to trap minute pollen grains.

Thermal uplift of the areas fringing the North Sea due to emplacement of the Iceland Plume may also have created newly emerged land areas which would have provided exposed substrate on which a lowland angiosperm-dominated community could flourish. Angiosperms may then have been present onshore for some time before the

PETM but have been under-recorded in North Sea cores due to a combination of absence of these coastal communities, high sea-levels and low terrestrial influx into the basin.

Within the angiosperms there is also an identifiable trend towards increased diversity over the PETM interval which may indicate that high CO_2 concentrations allowed the group to diversify rapidly. Among the angiosperms there is also a distinctive rise in the amount of pollen from swamp and mire vegetation indicating that there was a well-developed wetland coastal community. Increased freshwater run-off and higher rainfall over the area can be hypothesised. However, these trends continue into the Early Eocene indicating that humid conditions lasted well after the PETM and there may be other factors controlling their presence (Figure 6.45).

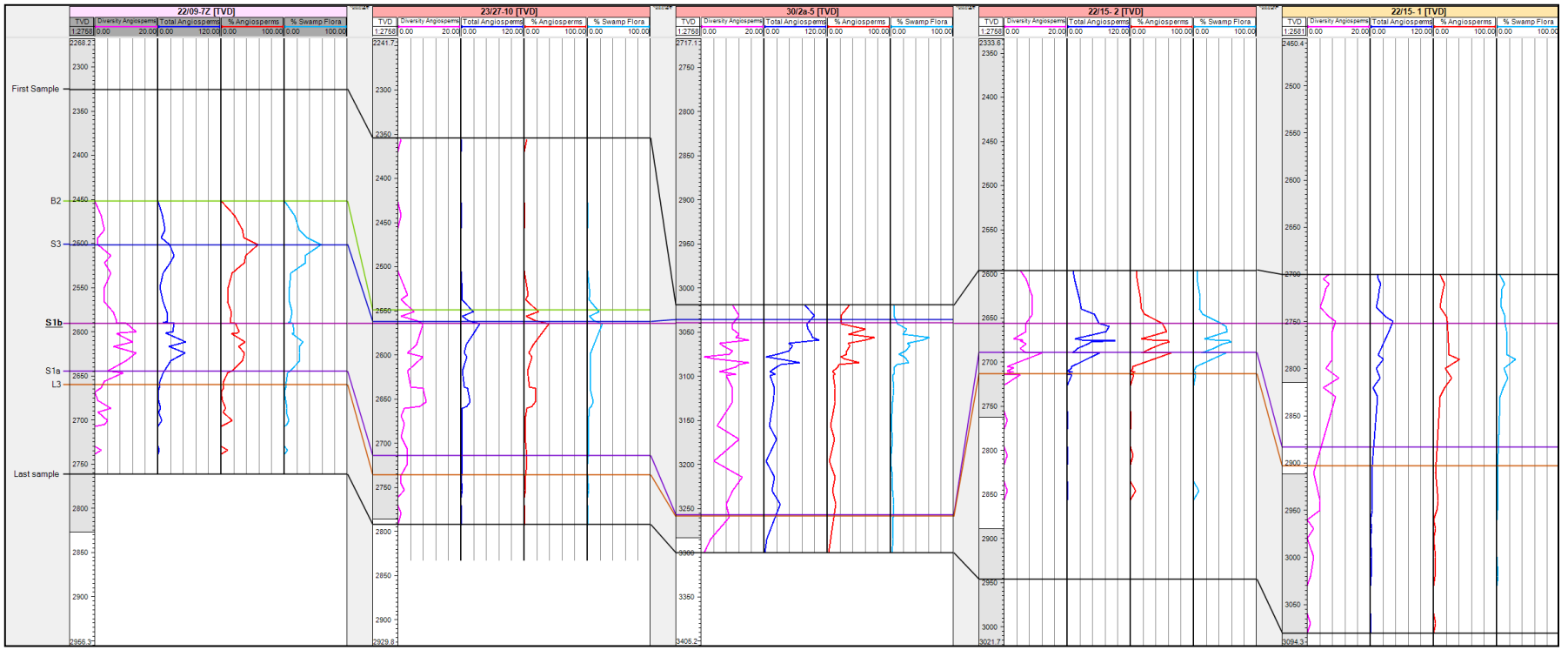

Figure 6.46: An increase in the number and diversity of Angiosperms is seen over the PETM period. Within the Angiosperms swamp and mire vegetation also rises. However, angiosperms remain at high levels into the Eocene.

6.5.3 BIOSTRATIGRAPHY DISCUSSION

The biostratigraphic observations appear to show evidence for distinctive changes in environment around the PETM. However, it has been noted that uplift and tectonic events exerted a strong influence on the North Sea and much of northwest Europe during the latest Palaeocene. It is therefore important to understand the effects both of these processes would have on the environment and compare these to the evidence from the biostratigraphic data.

As outlined previously, the PETM temperature increase has readily identifiable effects in other worldwide sections. These include increased humidity and correspondingly run-off, sea-level rise due to expansion of seawater, more humic acid and chemical weathering due to plants fixing more CO_2 and breaking down faster, an increase in diversity and numbers of thermophillic plants and phytoplankton, an increase in low salinity forms (with humidity rise), extinctions of foraminifera and acidification of oceanic waters.

Regional thermal uplift would be expected to lead to increased orographic rainfall, run-off and freshwater. This fresh water input, coupled with restriction of the North Sea basin by the uplifted northern landmass, may be expected to lead to decreased salinity in the North Sea and correspondingly an increase in low-salinity tolerant phytoplankton. Restriction may lead to a slowing of intra-basinal water currents leading to potential anoxic bottom waters which would be exacerbated by freshening

of the surface waters and less overturning. Higher sedimentation rates would also result, increasing the influx of nutrients to the basin. The area of the coastline would increase as deltas build out, allowing plants to colonise these newly exposed land areas and increase in abundance and diversity.

It is evident that these different processes can have similar effects which must be picked apart to gather information on the impact of the PETM on the North Sea area. In order to investigate this, qualitative and quantitative biostratigraphic data from the 66 wells in the Central North Sea was analysed with particular attention paid to those wells which had quantitative data (Appendix 2). The differences in resolution between all of the separate datasets meant that there was a higher degree of variability than would have been preferable but the volume of data allowed the true patterns to emerge.

Two of these wells were selected to represent the findings, 22/15-2 and 30/2a-5, as they have biostratigraphic samples derived from core data and 30/5a-2 has sedimentological data provided courtesy of Maersk Oil (Appendix 3). Samples from side-wall cores and cuttings often suffer from down-hole contamination so core data is preferable for biostratigraphy as samples are more likely to represent in-situ assemblages. Isotopic analysis was also carried out on well 30/2a-5 to identify the PETM definitively (Figure 6.47). The wells were each divided stratigraphically on the basis of wireline log information into the M (Maureen), L (Lista) and S (Sele) units of Knox and Holloway 1992 which are known to be regionally correlatable and separated by maximum flooding surfaces. Intra-S1b maximum flooding surfaces

(MFS 1 and 2) were also identified from wire-line logs and core data and used to split the unit into 3 sections. Further divisions were recognised in the expanded section 30/2a-5 but biostratigraphic resolution was poor and these could not be correlated with other less expanded wells to aid in their interpretation (Figures 6.48 and 6.49).

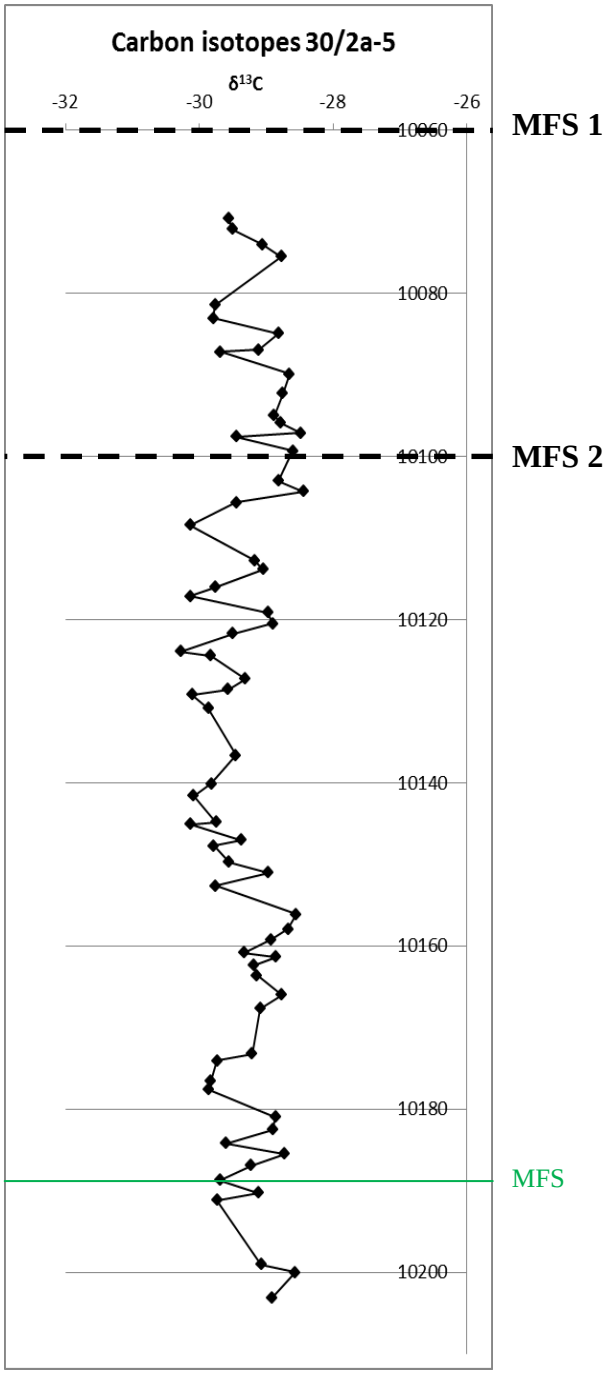

Figure 6.47: Carbon isotopes ($\delta^{13}C_{org}$) from 30/2a-5 showing that the PETM is very expanded and the entirety of the cored section was deposited during it. MFS 1 and 2 used to divide the S1b unit are noted along with another MFS recognised from log and core data.

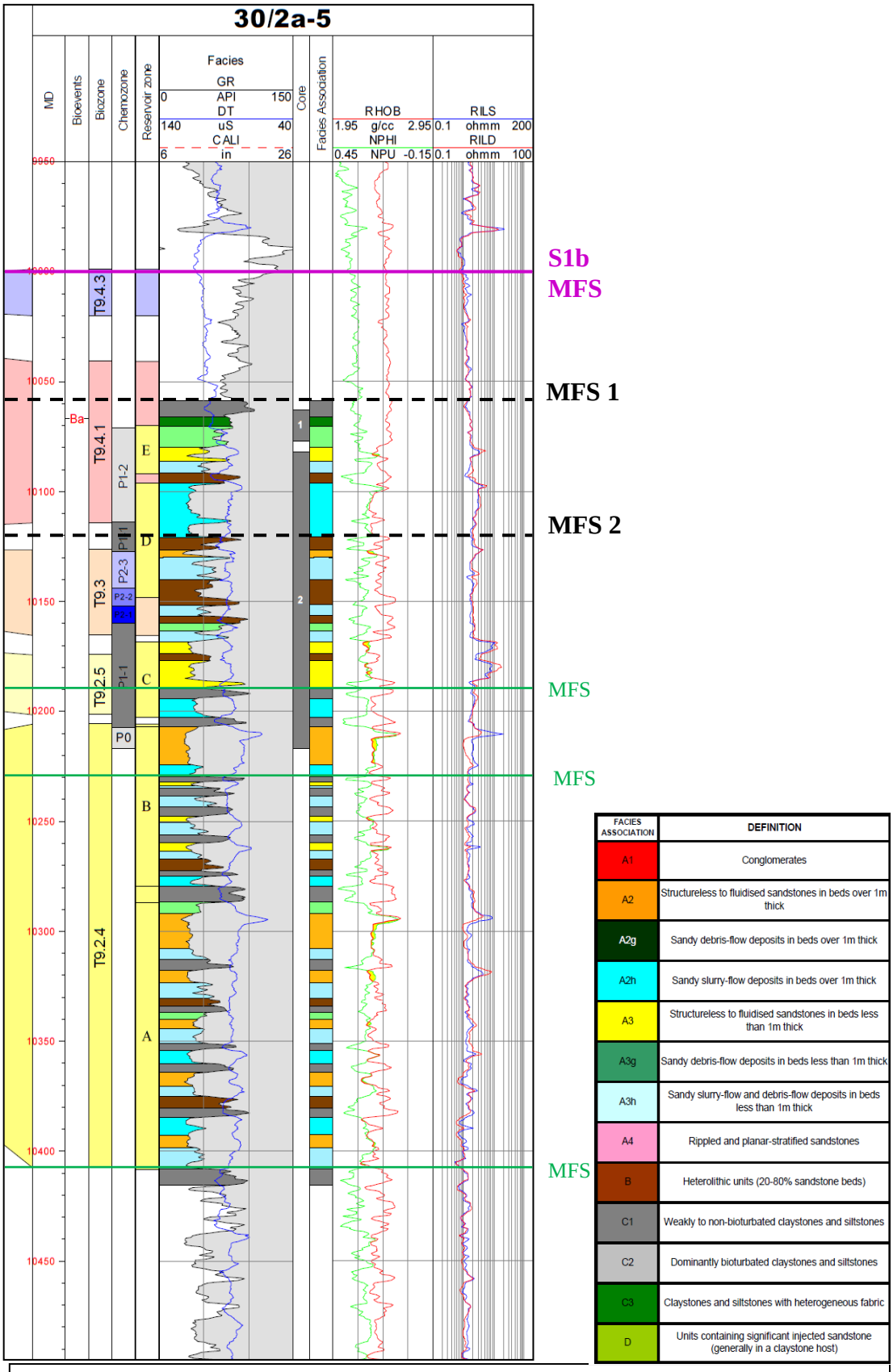

FACIES ASSOCIATION	DEFINITION
A1	Conglomerates
A2	Structureless to fluidised sandstones in beds over 1m thick
A2g	Sandy debris-flow deposits in beds over 1m thick
A2h	Sandy slurry-flow deposits in beds over 1m thick
A3	Structureless to fluidised sandstones in beds less than 1m thick
A3g	Sandy debris-flow deposits in beds less than 1m thick
A3h	Sandy slurry-flow and debris-flow deposits in beds less than 1m thick
A4	Rippled and planar-stratified sandstones
B	Heterolithic units (20-80% sandstone beds)
C1	Weakly to non-bioturbated claystones and siltstones
C2	Dominantly bioturbated claystones and siltstones
C3	Claystones and siltstones with heterogeneous fabric
D	Units containing significant injected sandstone (generally in a claystone host)

Figure 6.48: Sedimentological and biostratigraphical analysis of 30/2a-5 with the two MFS used to split the S1a unit noted.
Other such surfaces were noted below these but the lower resolution of the data over this part of the section coupled with the more condensed nature of the majority of the other sections observed precluded characterisation of these.
Data courtesy of Maersk Oil. Analysis by Ichron Ltd.

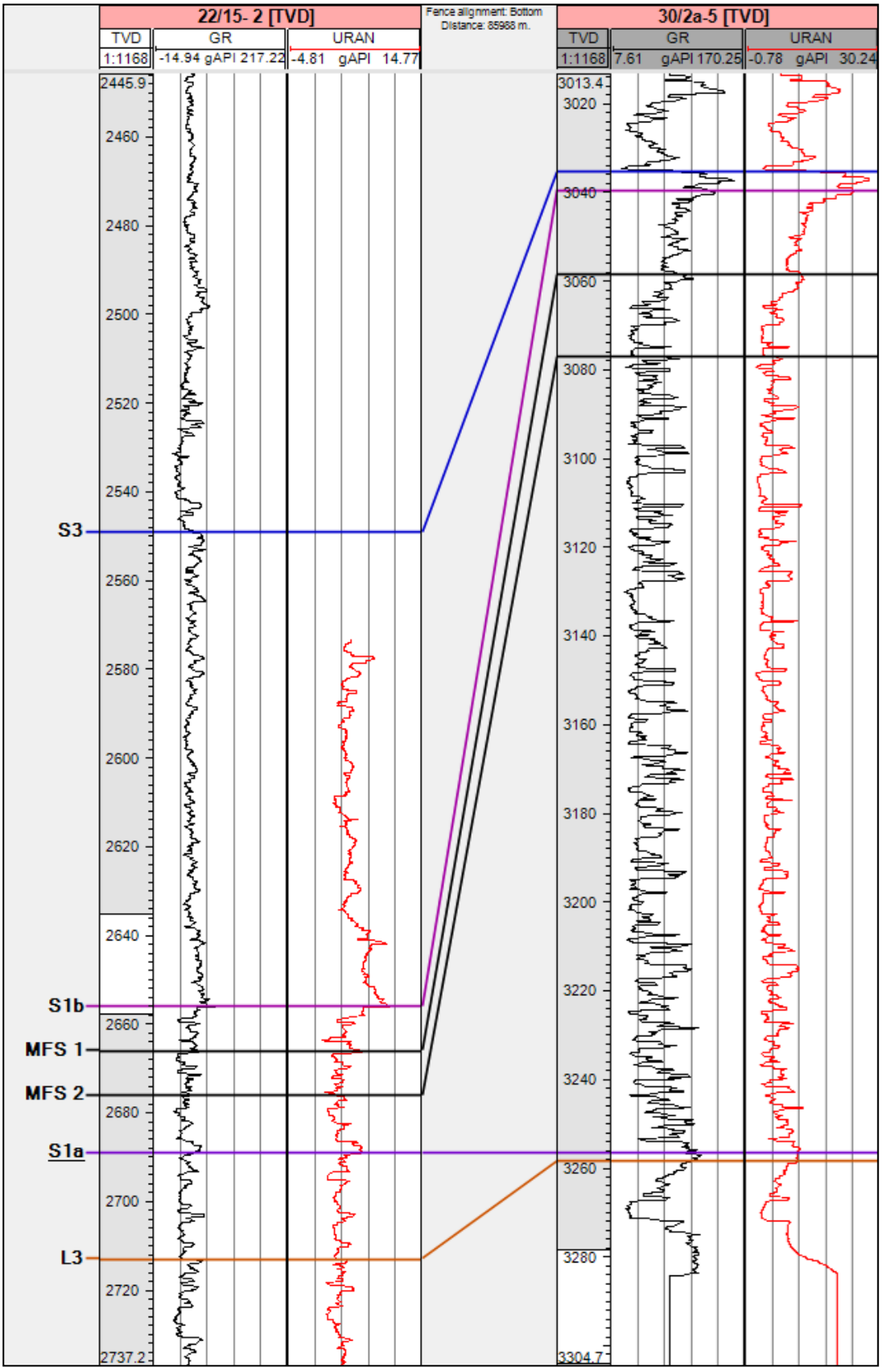

Figure 6.49: Correlation of the two wells used to represent the biostratigraphic findings of analysis of the data from the regional study.
Well section flattened on S1a

The floral and faunal assemblages in the analysis were grouped according to their environmental affiliations in order to investigate changes in the terrestrial and marine environment over the Mid-Late Palaeocene and Early Eocene.

The marine dinoflagellates were divided into;

Apectodinium: A warming proxy and a possible indicator of salinity changes.

Gonyaulacoids and **Peridinoids**: Indicators of changes in nutrient availability.

High salinity/Oceanic Species: *Areoligera gippingensis* is included in this environmental group as it is associated with oceanic influence (Powell et al. 1996). The *Spiniferites* group and *Impletosphaeridium* were also included as they are also thought to indicate high salinity although these interpretations are difficult to be confident of (Wall et al. 1977; Brinkhuis 1994; Devillers et al. 2000; Sluijs et al. 2005). Note that these oceanic indicators are only applicable in units L3 to S3.

Terrestrial miospores were grouped into;

Angiosperms and Gymnosperms

Undifferentiated Bisaccates: Belonging to the Pinaceae family of conifers these represent upland forests which have a widespread distribution but tend to be restricted to higher altitudes and drier substrates.

Cupressaceae Forest: Made up mainly of *Inaperturopollenites* of the Taxodiaceae sub-family. *Inaperturopollenites* is the pollen of a flood-tolerant subtropical-temperate Cypress.

Swamp and Mire Vegetation: This early-mid successional group consists mainly of *Caryapollenites, Momipites Platycaryapollenites* and the Normapolles, *Interpollis*, , *Nudopolis*, *Oculapollis*, *Trudopollis*, *Plicapollis* and *Labrapollis*. *Caryapollenites*, *Momipites* and *Platycaryapollenites* belong to the Juglandaceae family. *Caryapollenites* (hickory) is particularly associated with mire vegetation.

Myricaceae: Includes *Triatriopollenites* and *Triporopollenites*, trees with a cosmopolitan distribution which possibly represent coastal swamps.

Freshwater: This group consists of a group of species which flourish in coastal and wetland environments. It includes *Alnipollenites* (Betulaceae) and *Platycaryapollenites* (Juglandaceae) which are associated with abandoned channels and alluvial fans and *Sparganiaceaepollenites* (Sparganiaceae) an aquatic species whose extant relative is the common bulrush. *Azolla* is an aquatic fern of the Salviniaceae family while *Pediastrum, Botrycoccus* are freshwater green algae which are included despite not being higher plants as these groups represent those species which occupy environmental niches regardless of taxonomic distinction.

Freshwater angiosperms: A sub-set of the Freshwater group containing only *Alnipollenites* and *Sparganiaceaepollenites*.

Pteridophyte Spores: This group contains almost all of the terrestrial spores, both trilete and monolete observed in the data. Ferns within this group are particularly associated with initial colonisation of newly exposed substrate. The most common species include *Deltoidospora* and *Cicatricosisporites*, both of the family Schizaceae. *Laevigatosporites*, *Rouseisporites* and Pteris-type spores also dominate.

In the study, the 22/15-2 and 30/2a-5 wells are used to show the results derived from the wider database. Biostratigraphic data is graphed and expressed both as a numerical total and a percentage of total dinoflagellate and pollen and spore counts (Figures 6.50-6.55).

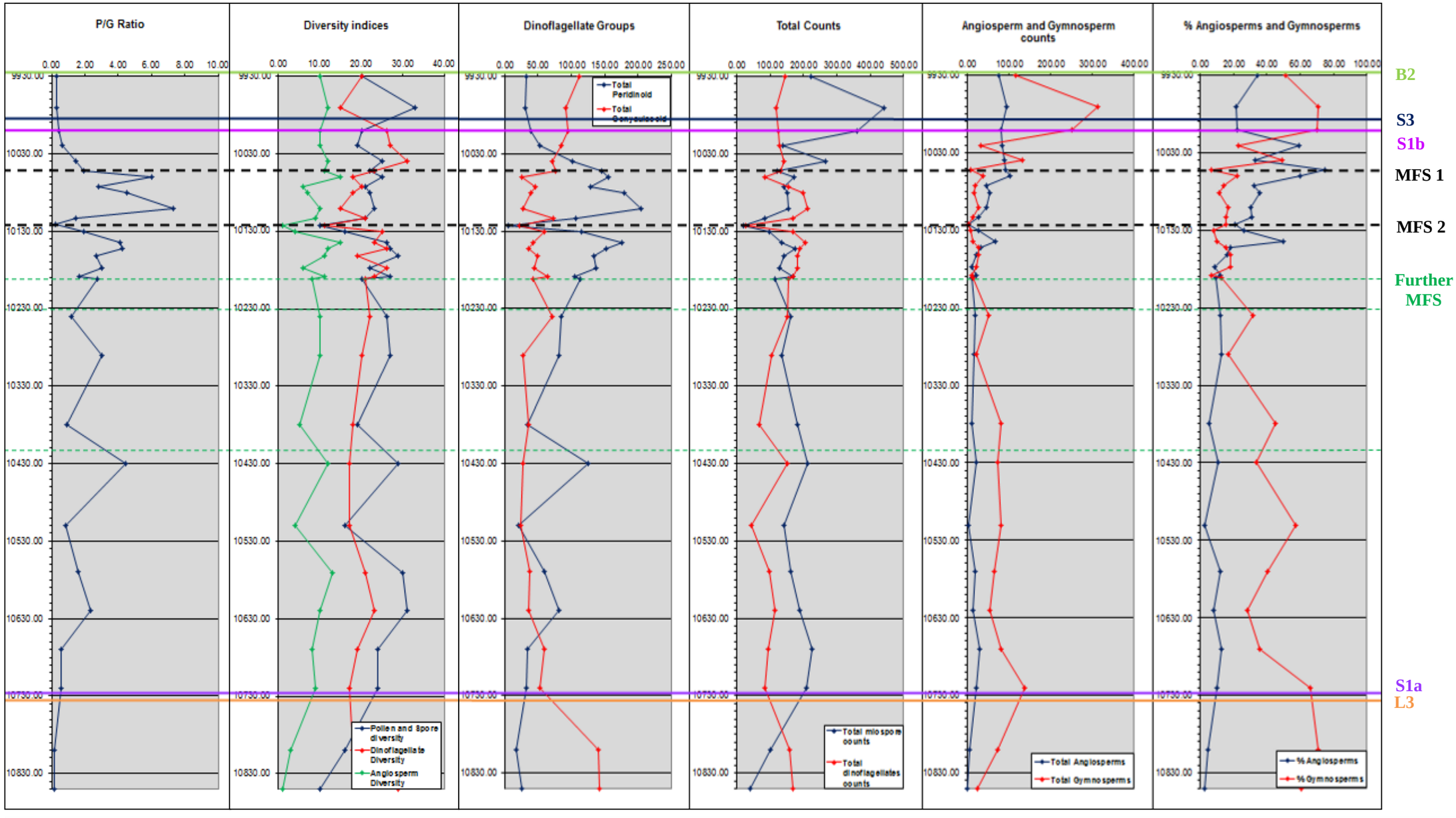

Figure 6.50: Biostratigraphic data from well 30/2a-5.
Original analyses by Ichron Ltd.

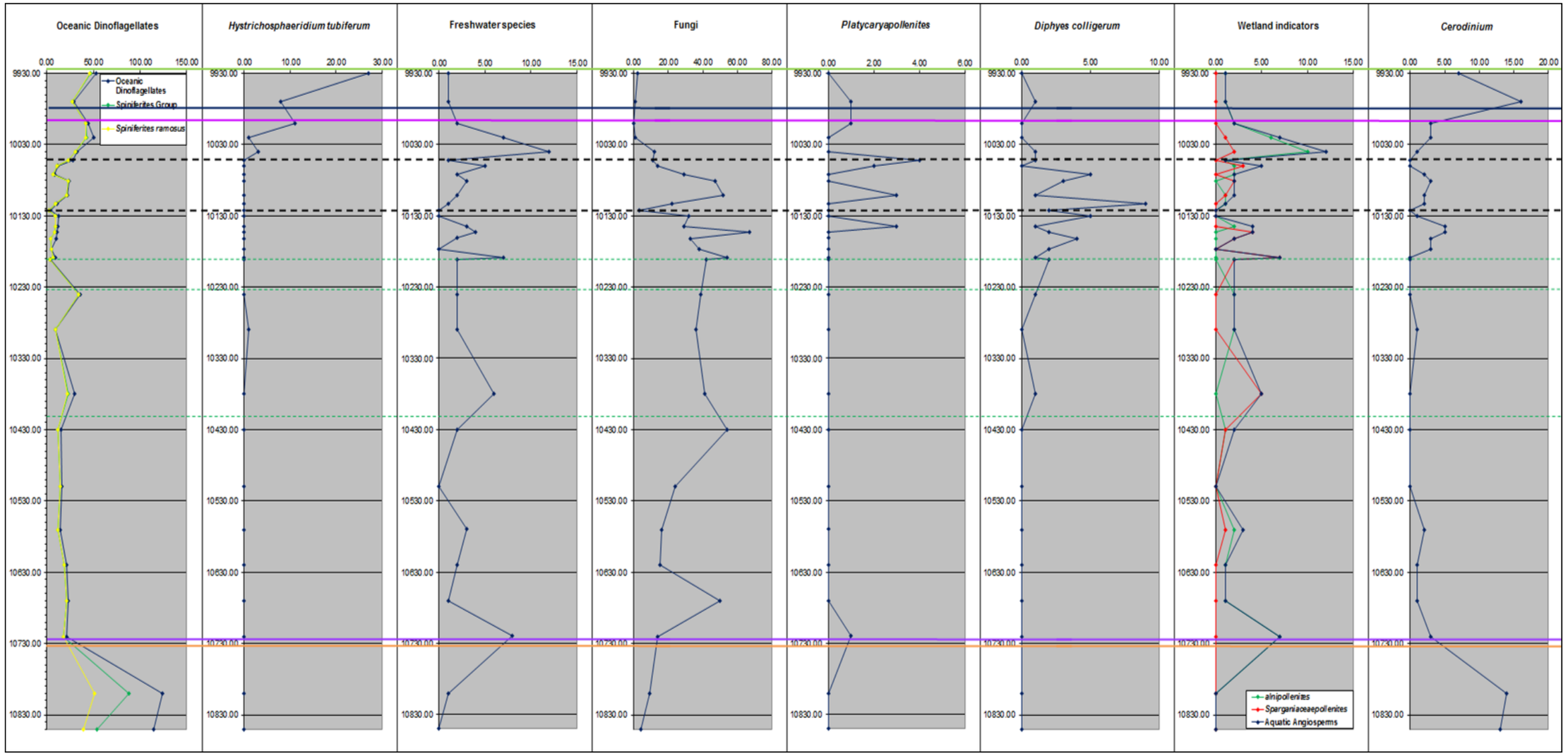

Figure 6.51 (pages 468-470): Biostratigraphic counts of selected species and groups from well 30/2a-5

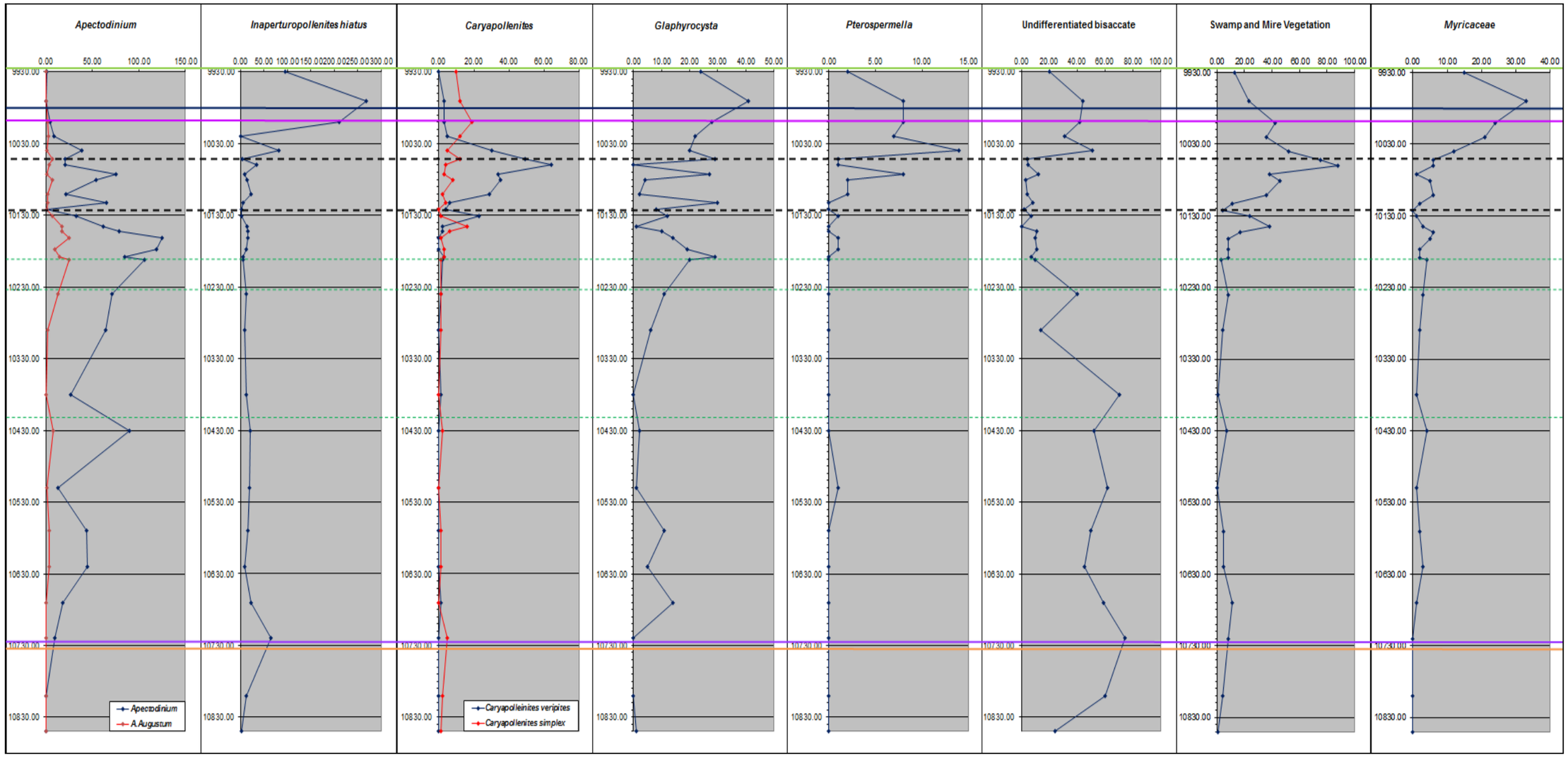
Apectodinium
Inaperturopollenites hiatus
Caryapollenites
Glaphyrocysta
Pterospermella
Undifferentiated bisaccate
Swamp and Mire Vegetation
Myricaceae
Apectodinium
A.Augustum
Caryapollenites veripites
Caryapollenites simplex

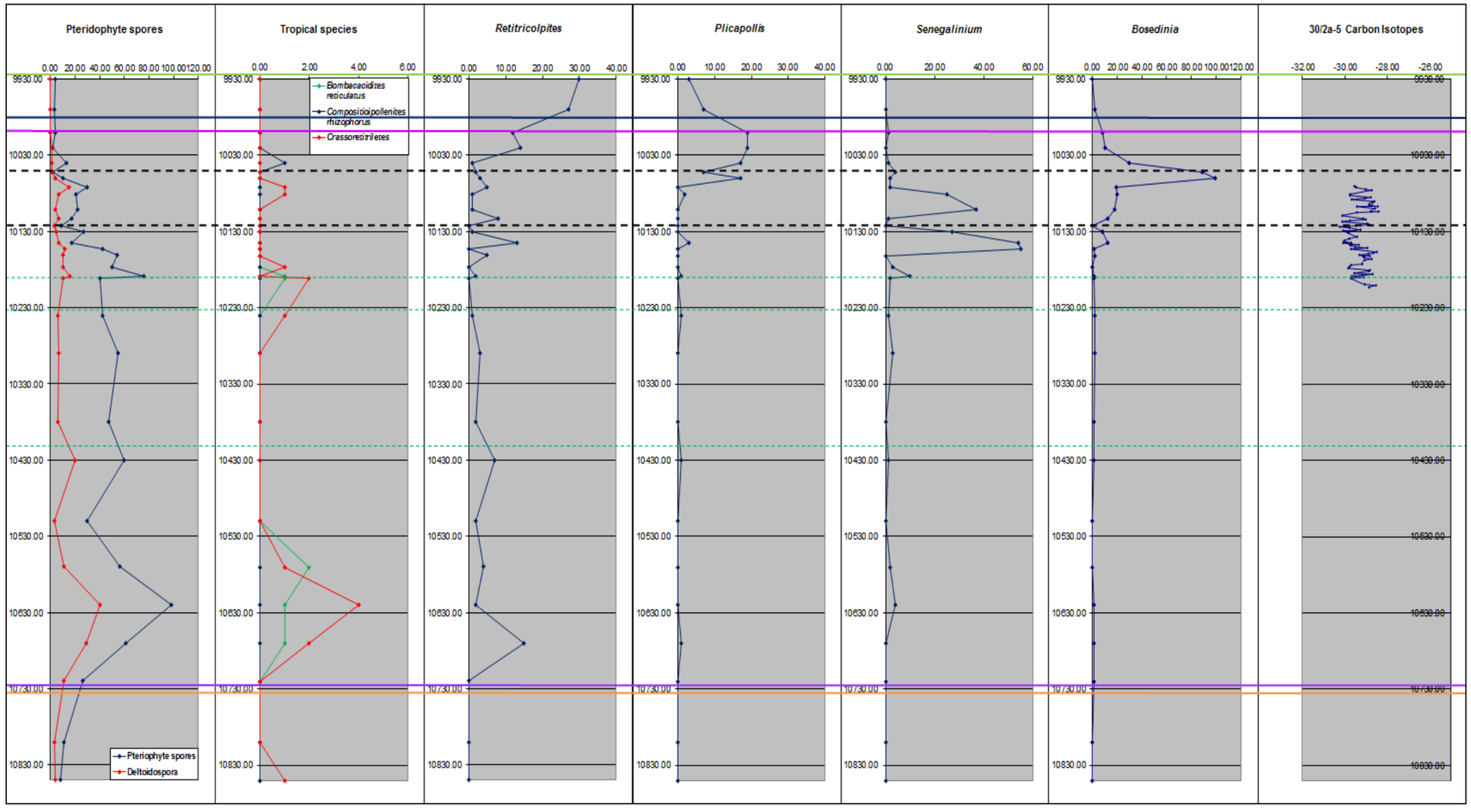
Pteridophyte spores
0.00 20.00 40.00 60.00 80.00 100.00 120.00
Tropical species
0.00 2.00 4.00 6.00
Bombacacidites reticulatus
Compositicolpollenites rhizophorus
Crassoretitriletes
Retitricolpites
0.00 10.00 20.00 30.00 40.00
Plicapollis
0.00 10.00 20.00 30.00 40.00
Senegalinium
0.00 20.00 40.00 60.00
Bosedinia
0.00 20.00 40.00 60.00 80.00 100.00 120.00
30/2a-5 Carbon Isotopes
-32.00 -30.00 -28.00 -26.00
9830.00
10030.00
10130.00
10230.00
10330.00
10430.00
10530.00
10630.00
10730.00
10830.00
Pteriophyte spores
Deltoidospora

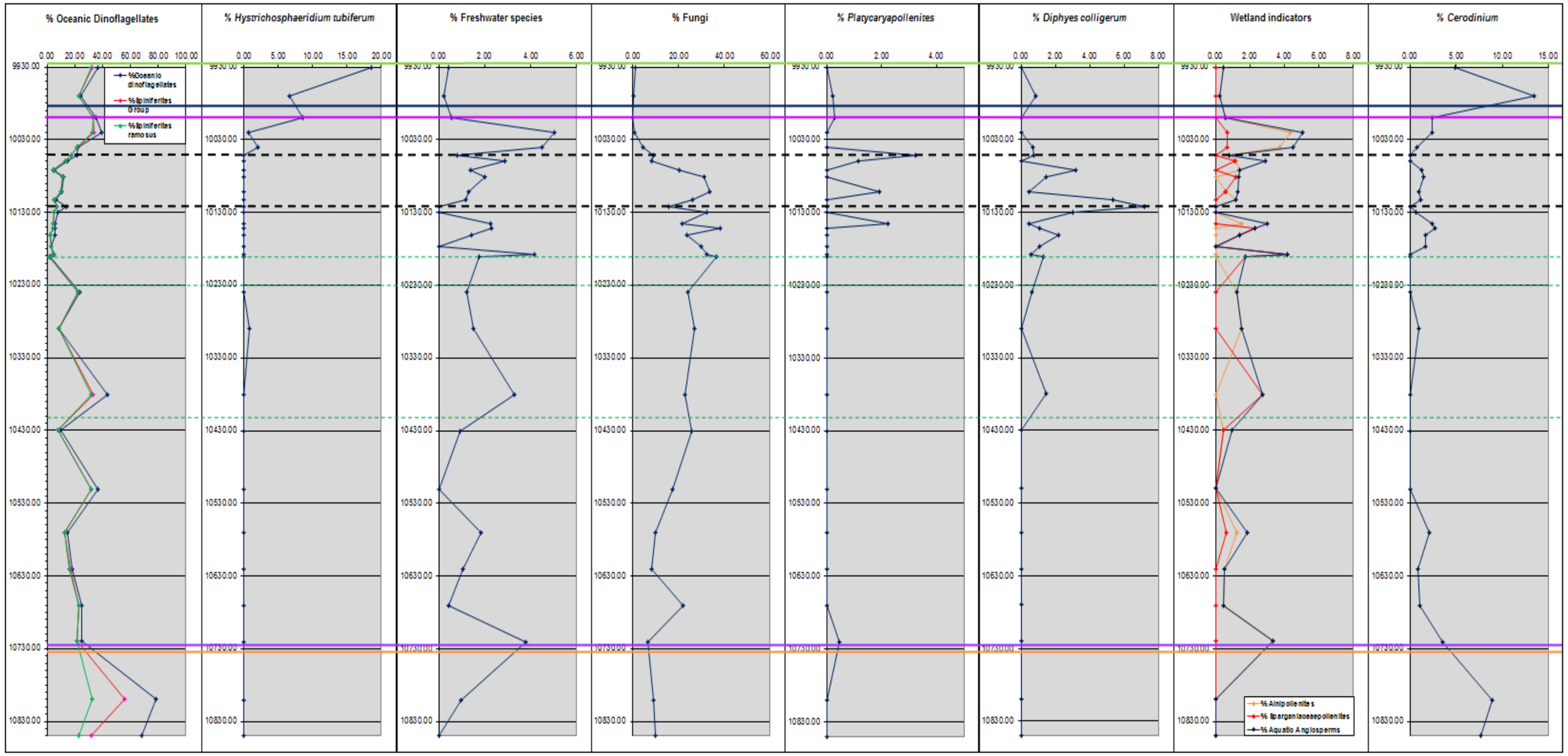

Figure 6.52 (pages 471-473): Biostratigraphic data from 30/2a-5 as percentages.
Dinoflagellate figures are expressed as percentage of total dinoflagellate counts and spores and pollen as a percentage of the total counts of this group.

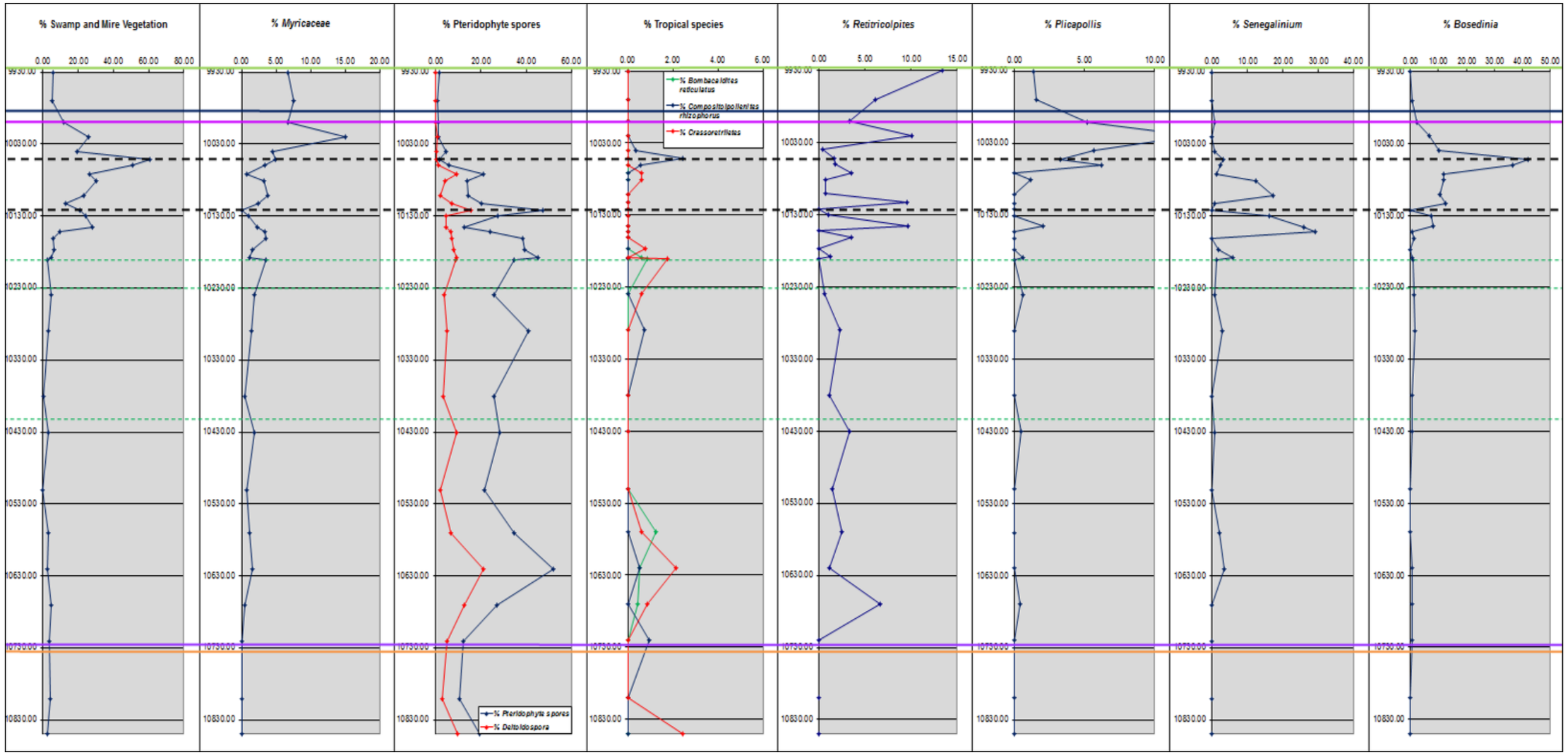
% Swamp and Mire Vegetation
% Myricaceae
% Pteridophyte spores
% Tropical species
% Retitricolpites
% Plicapollis
% Senegalinium
% Bosedinia
% Bombacaditres reticulatus
% Compositopollenites rhizophorus
% Crassoretrilletes
% Pteridophyte spores
% Deltoidospora

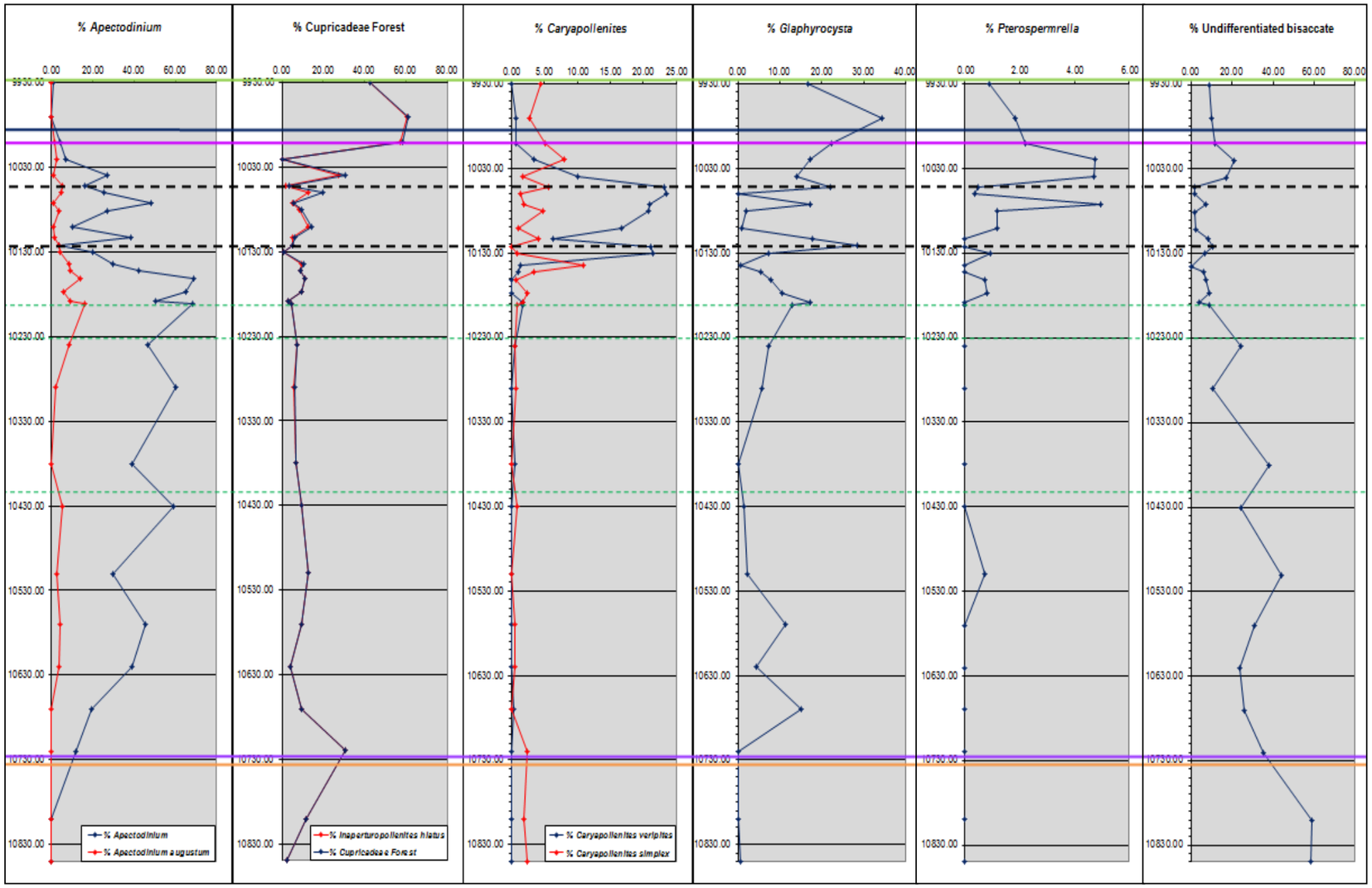
% Apectodinium
% Cupricadeae Forest
% Caryapollenites
% Glaphyrocysta
% Pterospermrella
% Undifferentiated bisaccate
0.00 20.00 40.00 60.00 80.00
0.00 5.00 10.00 15.00 20.00 25.00
0.00 10.00 20.00 30.00 40.00
0.00 2.00 4.00 6.00
9930.00
10030.00
10130.00
10230.00
10330.00
10430.00
10530.00
10630.00
10730.00
10830.00
% Apectodinium
% Apectodinium augustum
% Inaperturopollenites hiatus
% Cupricadeae Forest
% Caryapollenites veriplites
% Caryapollenites simplex

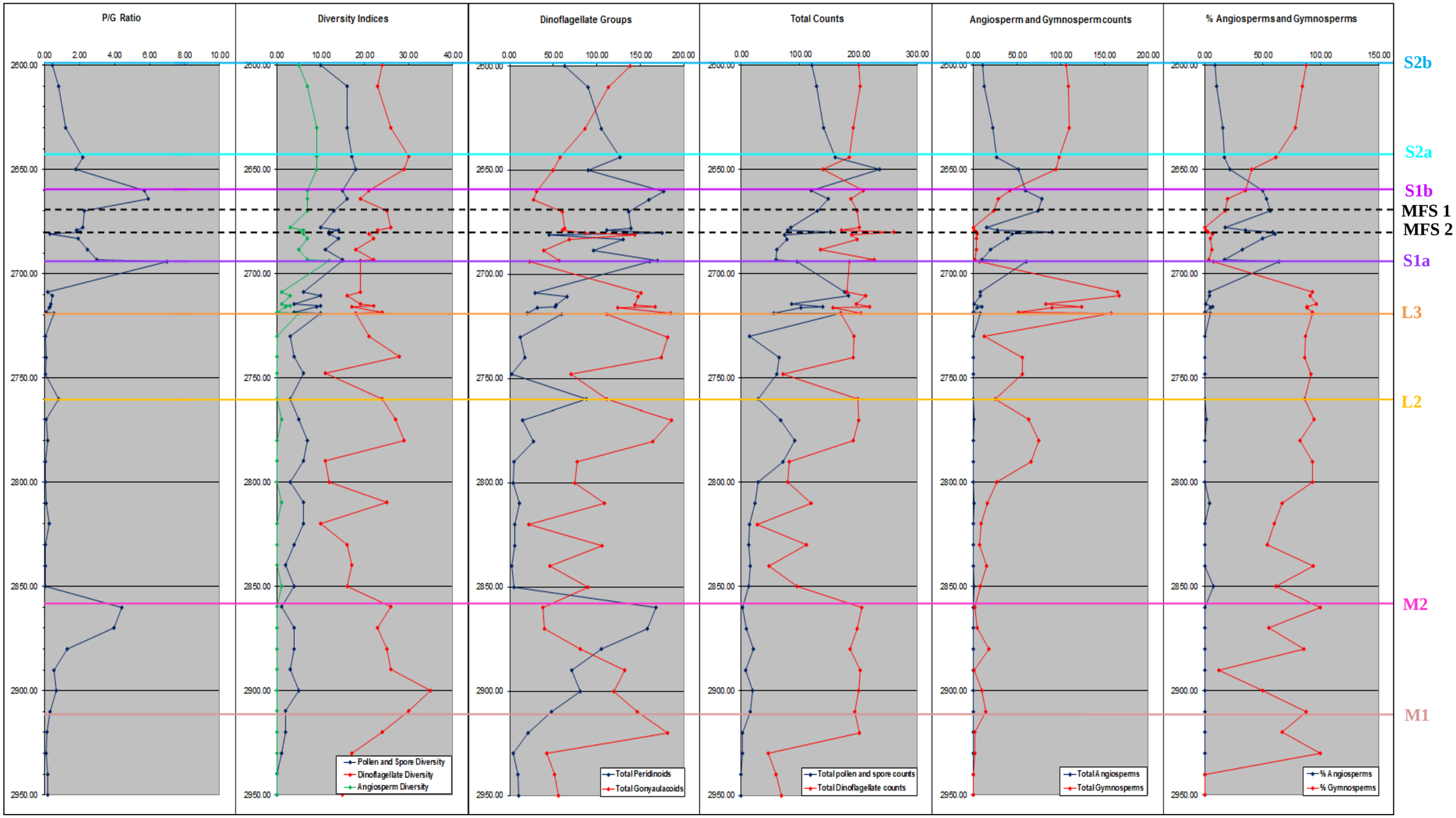

Figure 6.53: Biostratigraphic data from well 22/15-2
Original analysis by Geostrat Ltd

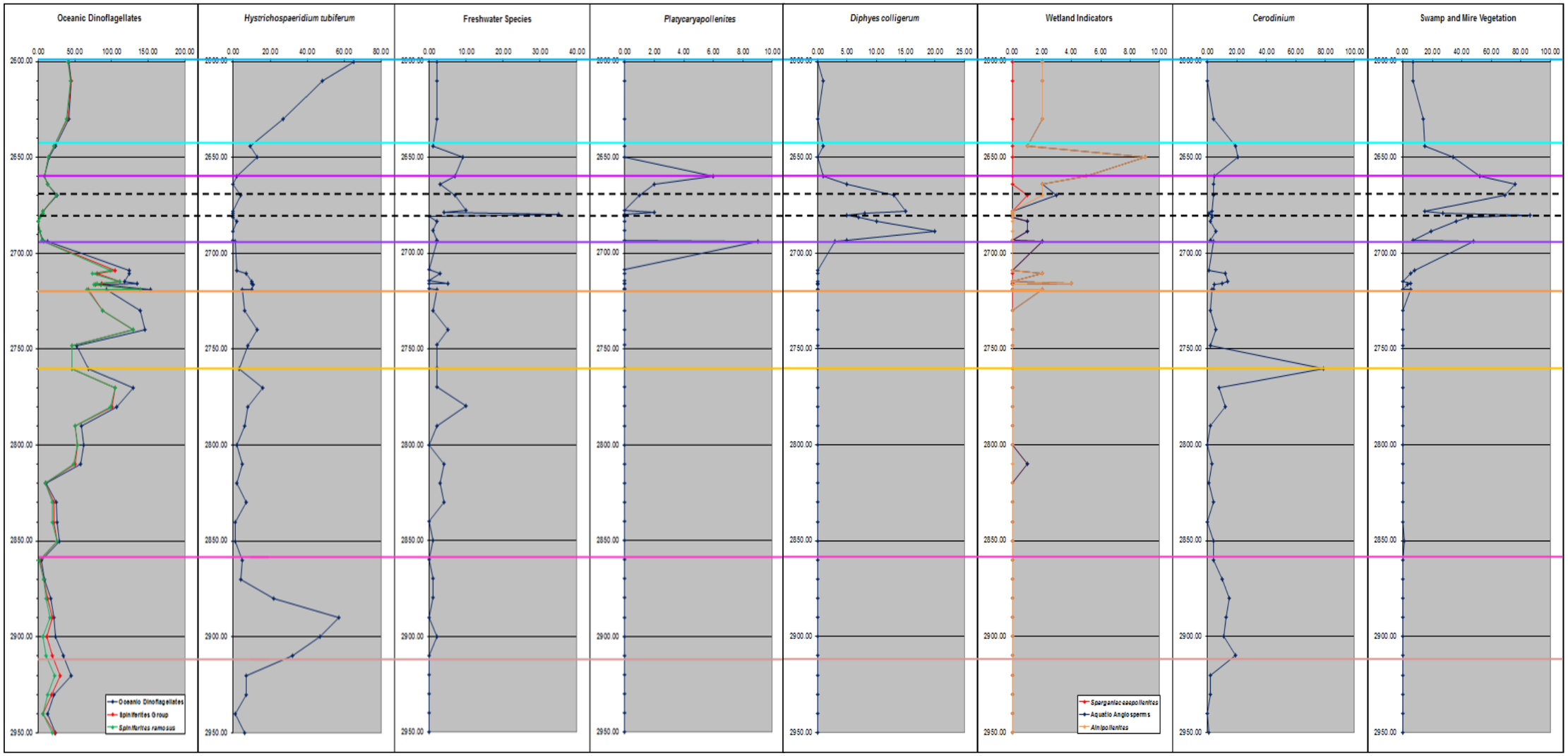

Figure 6.54 (pages 475-477): Biostratigraphic counts of selected species and groups from well 22/15-2.
Original analysis by Geostrat Ltd

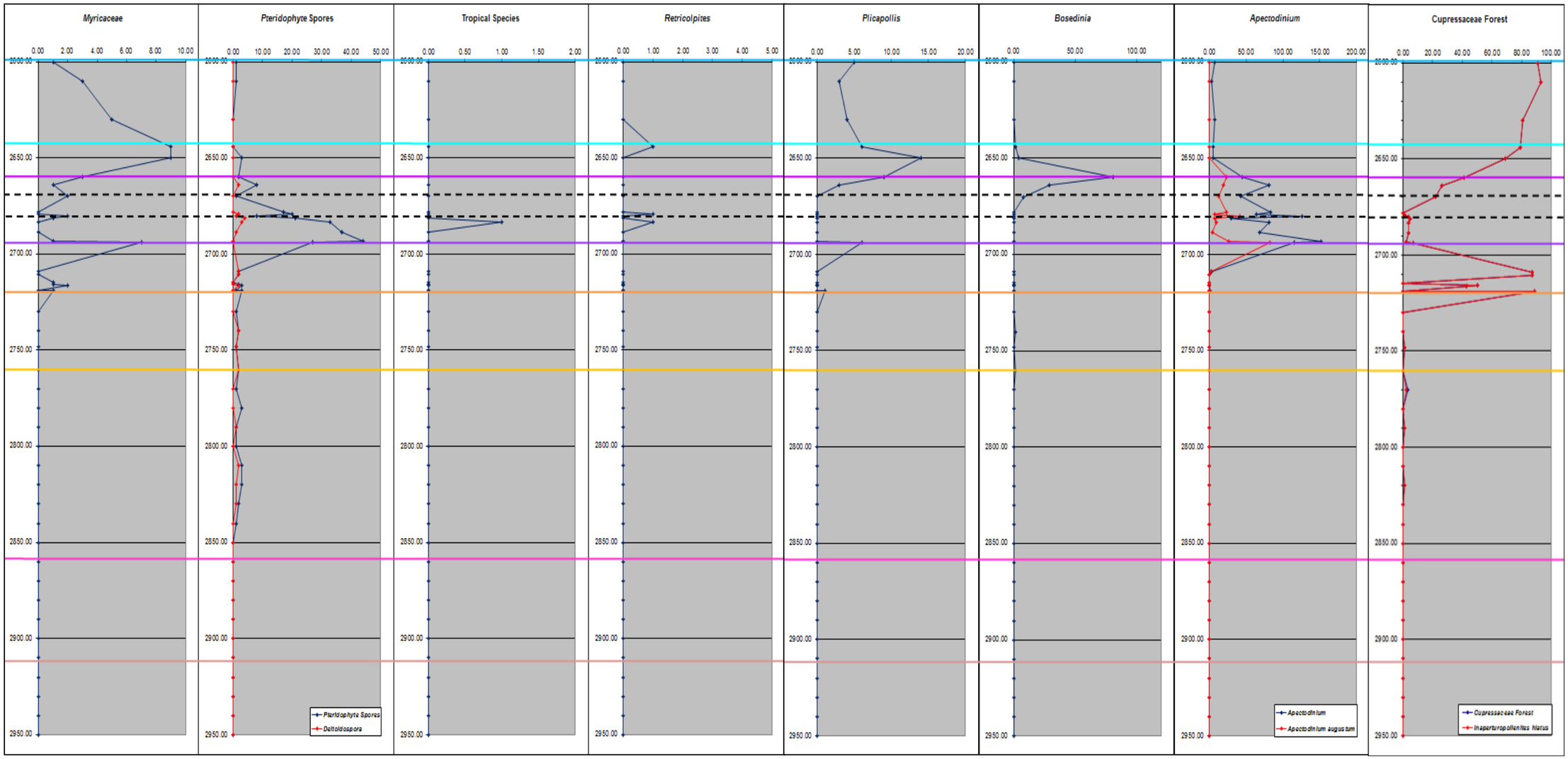
Myricaceae
Pteridophyte Spores
Tropical Species
Retricolpites
Plicapollis
Bosedinia
Apectodinium
Cupressaceae Forest
2650.00
2700.00
2750.00
2800.00
2850.00
2900.00
2950.00
Pteridophyte Spores
Deltoidospora
Apectodinium
Apectodinium augustum
Cupressaceae Forest
Inaperturopollenites hiatus

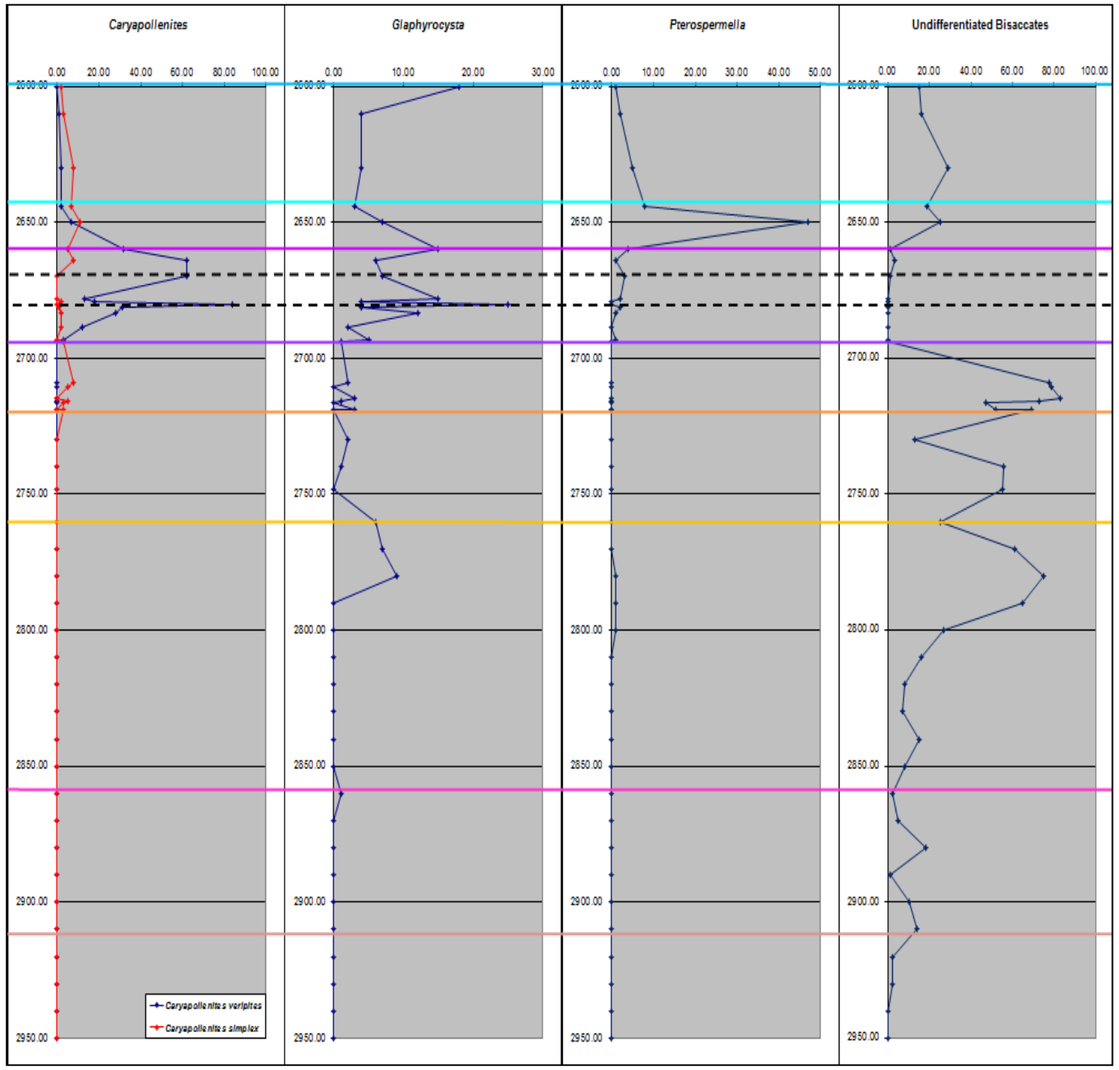
Caryapollenites
Glaphyrocysta
Pterospermella
Undifferentiated Bisaccates
0.00
20.00
40.00
60.00
80.00
100.00
10.00
30.00
50.00
2600.00
2650.00
2700.00
2750.00
2800.00
2850.00
2900.00
2950.00
Caryapollenites veripites
Caryapollenites simplex

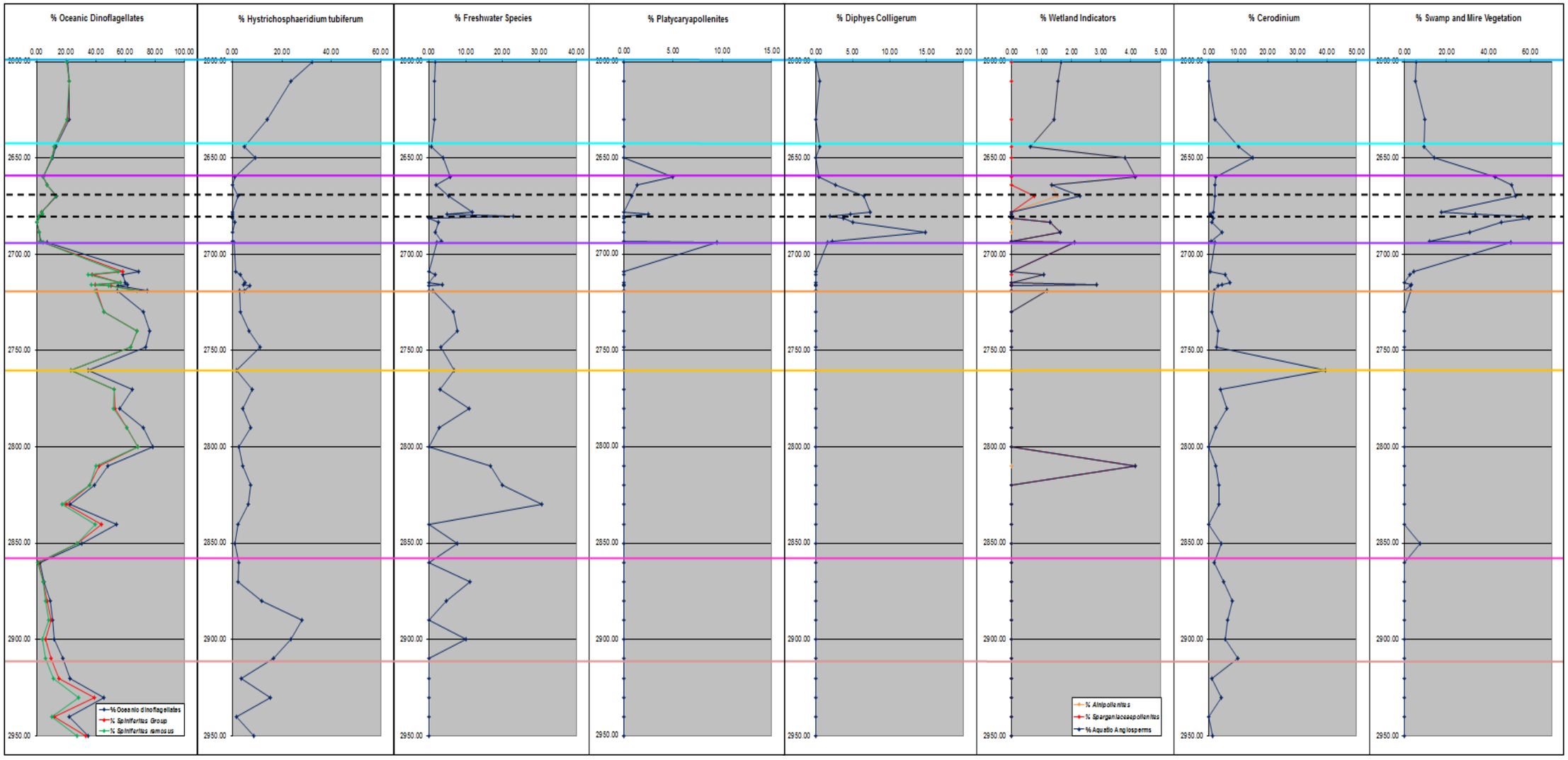

Figure 6.55 (pages 478-480): Biostratigraphic analyses from well 22/15-2 as percentages of total dinoflagellate and spore and pollen counts.

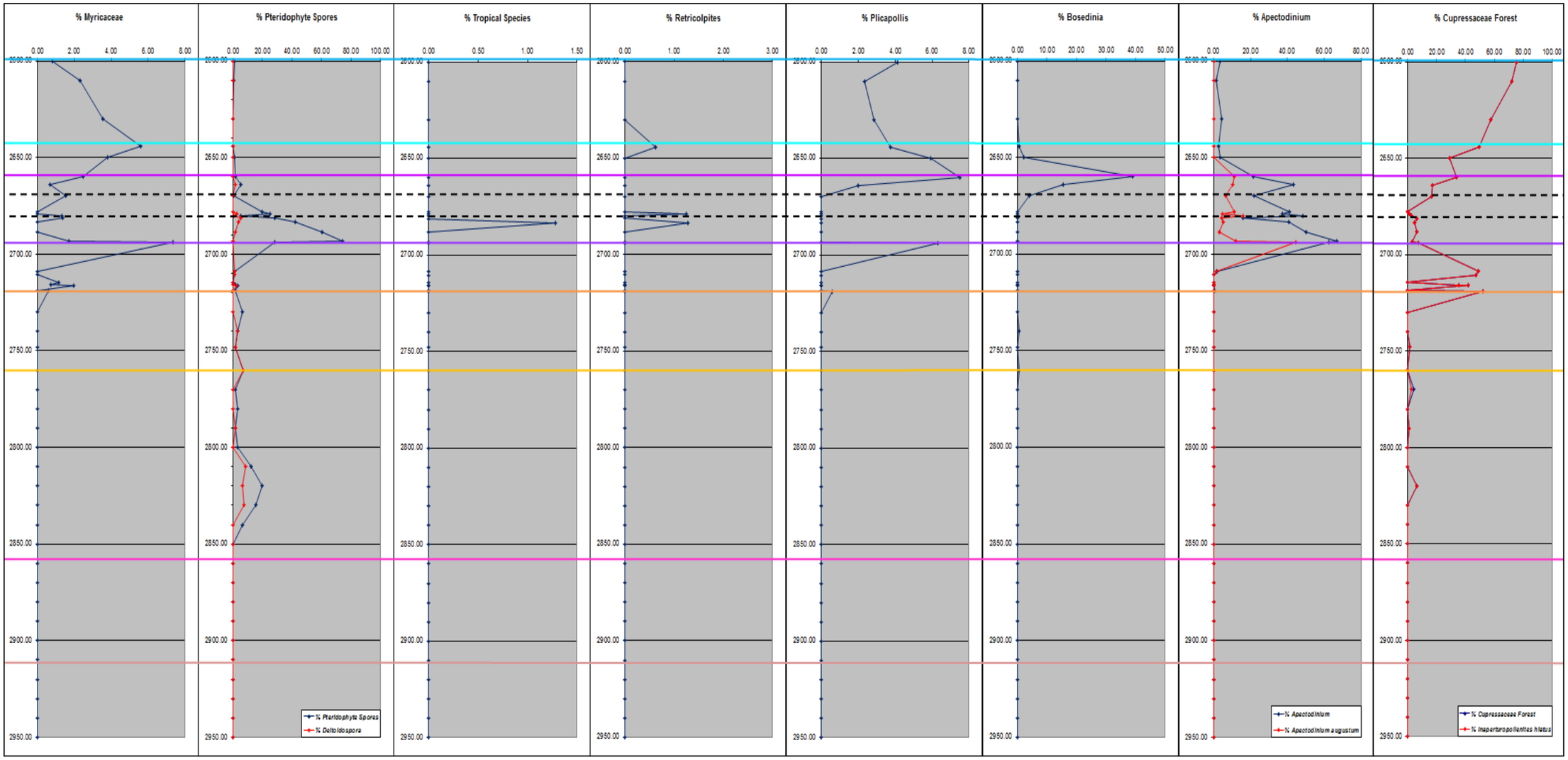
% Myricaceae
% Pteridophyte Spores
% Tropical Species
% Retricolpites
% Plicapollis
% Bosedinia
% Apectodinium
% Cupressaceae Forest
2650.00
2700.00
2750.00
2800.00
2850.00
2900.00
2950.00
% Pteridophyte Spores
% Deltoidospora
% Apectodinium
% Apectodinium augustum
% Cupressaceae Forest
% Inaperturopollenites hiatus

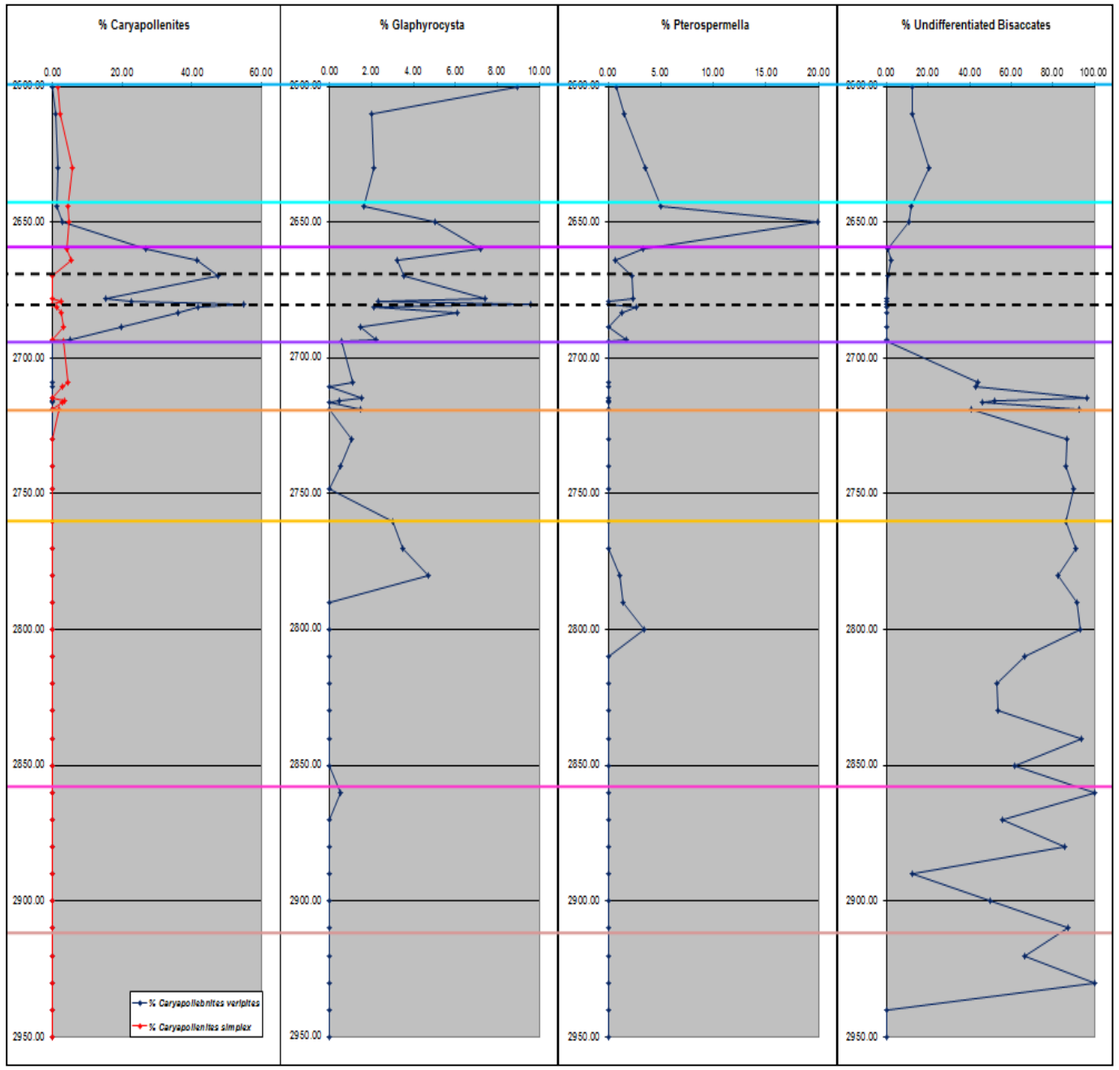
% Caryapollenites
% Glaphyrocysta
% Pterospermella
% Undifferentiated Bisaccates
0.00
20.00
40.00
60.00
0.00
2.00
4.00
6.00
8.00
10.00
0.00
5.00
10.00
15.00
20.00
0.00
20.00
40.00
60.00
80.00
100.00
2600.00
2650.00
2700.00
2750.00
2800.00
2850.00
2900.00
2950.00
% Caryapollenites verrpites
% Caryapollenites simplex

Those analyses corresponding with unit M1 show dinoflagellates as the dominant component of the assemblage. The dinoflagellates are diverse with high numbers of gonyaulacoid species such as the *Spiniferites* group, which is associated with oceanic influences (Wall et al. 1977; Brinkhuis 1994; Devillers et al. 2000; Sluijs et al. 2005) and *Hystrichosphaeridium tubiferum* which has a wide range of salinity tolerance (Powell et al. 1996; Crouch et al. 2005). High numbers of the *Cerodinium* group are also observed which had been suggested to be an indicator of low salinity (Kender et al. 2012) but in this study is found to be the opposite. Foraminifera are also abundant.

The predominance of oceanic dinoflagellates along with the presence of Foraminifera indicates a deep-water environment with good connection to oceanic waters. Gonyaulacoid dinoflagellates are numerous while peridinoids are sparse indicating little nutrient influx into the basin from terrestrial run-off. That terrestrial spores and pollen constitute a very low percentage of the total count and consist almost solely of bisaccates, known overproducers of pollen, also suggests high sea-levels and absence of a lowland community.(Versteegh 1994; Santarelli et al. 1998; Prauss 2001). It has also been shown that there are onshore records of facies that contain good diverse pollen assemblages in the pre-PETM (Jolley 1992; Knox 1996)so it is likely that the lack of these found in deposits from the deep basin reflects transport efficiency and the lack of fringing lowland communities rather than being a true reflection of plant diversity. Although bounded by maximum flooding surfaces, unit M1 represents background marine sedimentation with little in the way of clastic influence.

In unit M2, dinoflagellates still vastly outnumber miospores and are highly diverse. The *Spiniferites* group and *Hystrichosphaeridium tubiferum* remain present in high numbers with the addition of *Glaphyrocysta* and increased numbers of peridinoids. The spore and pollen assemblage represents a slightly larger proportion of the overall palynomorph counts and is dominated by bisaccate pollen from upland/boreal forests along with an influx of pteridophyte spores.

The presence of Foraminifera and dinoflagellates with a normal range of salinity tolerance indicates that the North Sea was still in good communication with the rest of the global ocean. There is however, evidence of variations in terrestrial influx as a rise in peridinoids relative to gonyaulacoids indicates higher nutrient influx into the basin. *Glaphyrocysta* is also present which, due to the correspondence of this group with *Apectodinium* in later units, may also indicate higher nutrient influx. This corresponds with the presence of turbiditic units containing reworked chalk and clastics and the terrestrial pollen and spore assemblage, although still dominated by bisaccates, it contains variable numbers of Pteridophyte spores suggesting transport from an area of exposed coastline. Since clastic systems are primarily controlled by changes in base-level, this suggests a period of relative sea-level fall (Embry et al. 2007) which is not in line with eustatic models.

There is little climatic information which can be garnered from data from either of the M units as the dinoflagellate assemblage is mainly a cosmopolitan one and terrestrial spores and pollen are sparse and dominated by undifferentiated bisaccates.

Apectodinium has not been found to be present within the Lower Palaeocene units although some authors suggest an influx within unit M2 (Thomas 1996).

Due to the condensed nature of unit L1 and corresponding low sample resolution in the majority of sections it was not considered possible to characterise this unit. In unit L2 there is a distinctive change in the palynomorphs assemblage as pollen and spores become more numerous and diverse. At the start of the unit the dinoflagellate numbers fall drastically with most of this reduction within the peridinoids. *Hystrichosphaeridium tubiferum*, *Cerodinium* and the *Spiniferites* group decline also. Bisaccates still dominate the sparse pollen and spore assemblage.

Through the rest of the unit the bisaccate proportion increases and freshwater species, pteridophyte spores and representatives of the Cupressaceae Forest become part of the terrestrially-derived assemblage. Peridinoid dinoflagellates recover slightly and *Glaphyrocysta* again makes an appearance. Towards the top of the unit and the L2/L3 boundary and maximum flooding surface, the number of terrestrial spores and pollen decreases relative to the dinoflagellates with the loss of the freshwater component and Cupressaceae. *Spiniferites*, *Cerodinium* and *Hystrichosphaeridium tubiferum* also increase to the top of the unit.

The changes in dinoflagellate assemblage in the lower part of the unit may be related to decreased salinity in the basin as the species representative of normal salinities fall in numbers. The fall in peridinoids is more difficult to explain but could also relate to a decrease in species with a low tolerance for decreased salinity. Alternatively the

high numbers in unit M2 could have been in response to something other than increased terrestrial and nutrient influx such as increases in the diatom population on which the dinoflagellates feed. A diatom study was not included in this project so this cannot be proven. This lowered salinity seems likely to have been brought about by a fall in base-level and increased transport to the basin centre as by the middle of the unit there is an larger and diversified pollen and spore assemblage with freshwater elements which includes pteridophyte spores along with small amounts of *Inaperturopollenites hiatus* (the main component of the Cupressaceae Forest group). *Inaperturopollenites hiatus* is the pollen of a cypress found in fringing mangrove swamps (Farley 1989; Ellis et al. 2002) and this, along with the presence of *Sparganiaceaepollenites* (bulrush pollen) indicates an environment in which areas of flooded lowland, probably the floodplains of major rivers, existed (Schröder 1992; Harrington et al. 2004). Increased transport from these areas to the basin centre.in the form of basinal turbidites of the lowstand systems tract also signifies a possible fall in relative sea-level as all of the L units correspond with the Mey Sandstone Member. Seismic mapping has shown these clastic flows to be more confined than earlier ones due to an increased area of delta-top and more structured drainage systems. There is no record of eustatic sea-level changes at this time and the North Sea was therefore decoupled from the global ocean and relative sea-level changes were probably linked to thermal uplift of the hinterland.

The final L unit, L3 features a general rise in terrestrial elements and decline in dinoflagellates throughout the unit. A diverse agglutinating Foraminifera assemblage is also present which in some sections appears to become less diverse towards the top

of the unit. Angiosperms rise in numbers and include freshwater species and members of the Juglandaceae and Cupressaceae families. Pteridophyte spores also increase particularly at the start of the unit where *Spiniferites ramosus* and *Cerodinium* fall.

The environment suggested by this assemblage is one in which oxygenation of the basin may have begun to decline, evidenced by the slight reduction in Foraminifera diversity. Increasing terrestrial influx, including primary vegetation and also some Cupressaceae and Juglandaceae suggests enough exposed coastline for limited swamps to form. These elements are present particularly at the start to middle of the unit indicating a relative sea-level fall to expose the area and bring the pollen into the basin followed by a gradual drowning again towards the maximum flooding surface at the top of the unit.

The boundary between unit L3 and S1a corresponds with a distinctive change in marine and terrestrial ecosystems. The diverse Foraminiferal assemblage of the L3 unit is replaced by an impoverished one which then disappears in the second half of the unit. Upland vegetation, dominantly undifferentiated bisaccates, along with representatives of the Cupressaceae Forest which was established at the end of L3, increases in abundance with limited numbers of aquatic angiosperms. One of these angiosperms is *Alnipollenites* (Betulaceae) which is associated with abandoned channels and alluvial fans. Oceanic indicators remain high at the start of the unit with increased numbers of *Hystrichosphaeridium tubiferum* and *Spiniferites* especially *Spiriferites ramosus.*

This suggests a period of relative sea-level fall and corresponding restriction of the basin after the highstand of the S1a/L3 boundary. Bottom-water anoxia is considered the reason for the Foraminiferal decline and is hypothesized to have resulted from the North Sea being cut off from the global ocean due to the combination of uplift and sea-level fall. The core samples of Sele Formation clays contain pyrite and glauconite nodules both of which indicate reducing conditions. Additionally an increase in sapropelic organic matter, an indicator of an increasingly anaerobic environment has been recorded (Schröder 1992). This sea level variation may have been eustatic in origin as it is recorded in other Northern Hemisphere sections (Steurbaut et al. 2003; Sluijs et al. 2008; Egger et al. 2009; Harding et al. 2011). Increased areas of coastal lowland may have led to the build-up of extensive Cupressaceae-dominated swamps with *Alnipollenites*, freshwater species and limited pteridophyte spores colonising the delta edge.

Apectodinium makes its first appearance in this unit, prior to the PETM. Its presence along with increased numbers of angiosperms and aquatic species may signify increased humidity and that warming had already begun. However, it is difficult to say whether the increase in pollen from the angiosperms occurred due to environmental change preceding the PETM as several authors have proposed (Sluijs et al. 2007) or whether the previously high sea-level prevented these species from colonizing and their pollen from reaching the basinal sections.

The PETM CIE occurs at the S1b/S1a boundary and MFS coincident with a period of extreme change in the marine and terrestrial environments. Unit S1b is divided into 3

sub-units, separated by clay intervals which are interpreted as intra-Forties maximum flooding surfaces. Additional events which could represent further periods of flooding are noted in the wire-line log and lithological data from well 30/2a-5 but low resolution sampling does not permit interpretation of these. In the 30/2a-5 well isotopic analysis was undertaken to conclusively prove that the environmental changes described by the palynomorph assemblages occurred over the PETM period (Figure 6.46).

In the first of the S1b sub-units, S1b (i), bisaccate numbers fall dramatically along with falling *Inaperturopollenites hiatus*, the main component of the Cupressaceae-dominated swamps which built-up throughout unit S1a. The numbers and diversity of the pollen and spore assemblage rises due to the inclusion of increased numbers of angiosperms particularly early successional species such as *Alnipollenites*, *Sparganiaceaepollenites* and *Platycaryapollenites*. Most of the increase however is due to a huge rise in the numbers of pteridophyte and fungal spores. Towards the end of the sub-unit there is an increase in mid-successional species such as *Plicapollis* and *Caryapollenites* which rise to an acme. *Apectodinium* numbers also rise as do other indicators of tropical climates such as *Diphyes colligerum* which (Bujak et al. 1994) suggested may be thermophillic. In the terrestrial realm the tropical tree *Bombacacidites reticulatus*, *Compositoipollenites rhizophorus*, and *Crassoretitriletes,* also appear which indicate warming (Schröder 1992; Harrington et al. 2004).*Apectodinium* temporarily decline at the top of the sub-unit and is replaced by *Senegalinium*. Gonyaulacoid dinoflagellates fall in numbers while peridinoids increase although much of this is due to the appearance of several sub-

species of *Apectodinium*. Oceanic species reduce and dinoflagellate diversity falls to a minimum.

These environmental changes are proposed to be due to the combined influence of uplift and warming. It is proposed that a regional relative sea-level fall due to uplift superimposed on the background eustatic mean would account for the severity of the changes at the S1a/S1b. The lowstand period of this relative sea-level fall, when most of the clastic influx to the basin occurs, is suggested to have left extensive areas of the coastline exposed. The amount of Cupressaceae and bisaccate pollen falls drastically indicating that the shoreline has been shifted a substantial distance basin-ward leaving the upland areas and cypress swamps far from the delta-edge. These elements are replaced with Pteridophyte spores from ferns and club moss spores such as *Deltoidospora*, *Cicatricosisporites*, *Lycopodiumsporites*, and pioneer species such as *Laevigatosporites* and *Crassreotriletes* which are the first species to colonize newly exposed land (Jolley 1992; Jolley et al. 2009). This increase in fern spores has been compared to the 'fern spike' at the Cretaceous/Tertiary boundary (Orth et al. 1981; Nichols et al. 1986) which was considered to represent the first colonizers of the barren land brought about by ecosystem collapse (Adams 2009). This comparison is possible but considered unlikely due to the evidence for regression and high numbers of fern spores prior to the PETM.

After primary species have colonized an area there is an increase in secondary vegetation as the community builds up and this is seen with the first occurrences of species representative of swamp or mire vegetation such as *Caryapollenites* and wetland angiosperm species such as *Alnipollenites*, which grow in abandoned

channels and alluvial fans (Jolley et al. 2009) along with the mid-late successional dry-soil *Myricaceae* which occupied the better drained areas of the alluvial fans. These are interpreted as mid-successional colonizers of lowland and wet substrates (Wing et al. 1984; Ellis et al. 2002). *Apectodinium* continues to increase in abundance and the thermophillic *Apectodinium augustum* makes its first appearance. At the top of the sub-unit the maximum extent of this community occurs with the acme of *Caryapollenites veripites* and the large amount of fresh-water run-off is shown by the replacement of *Apectodinium* and *Glaphyrocysta* by *Senegalinium* which has been proposed to be more tolerant of lowered salinities (Harding et al. 2011). Additionally, the isotopic analysis shows that minimum $\delta^{13}C$ (-31‰) values which have been demonstrated by correlation with the temperature proxy $\delta^{18}O$ in other worldwide sites to indicate warming (Thomas et al. 1999), are seen throughout the upper part of S1b(i) and all of S1b(ii). It is therefore likely that the decline in *Apectodinium* is not an indicator of cooling. The appearance of the prasinophyte *Pterospermella* also suggests large amounts of freshwater run-off as it is linked to low-salinity environments (Bujak et al. 1994; Powell et al. 1996; Ellis et al. 2002).

At the boundary between the S1b(i) and (ii) there is a reversal of the trends seen in the lower sub-unit with increased bisaccate and reduction in angiosperms and pteridophytes. In the marine realm oceanic elements also rise, all of which signifies a rise in relative sea-level and drowning of the lowland community.

After this event in S1b (ii) the miospore assemblage recovers to its previous diversity. Peridinoid dinoflagellates including *Apectodinium* rise in numbers with the addition of *Bosedinia* and *Senegalinium*.

Another short relative drop in sea-level is envisaged to have allowed the fringing vegetation to re-colonize which it did more rapidly due to the continued existence of these elements inland. A warm climate is indicated by the presence of *Apectodinium*, *Crassoretitriletes*, *Compositoipollenites rhizophorus* and *Diphyes colligerum* but the tropical tree *Bombacacidites reticulatus* does not recover. Increasing freshwater run-off is indicated by the presence of the low salinity dinoflagellates *Bosedinia* and *Senegalinium* which outnumber *Apectodinium*. Increased humidity due to warming seems unlikely for this increase since the main PETM period was already fully underway and there is no reason that such an increase would have begun at this point. It is therefore suggested that this marks the maximum extent of the coastal lowlands as species typical of swamp and mire vegetation such as *Caryapollenites veripites*, increase to an acme at the end of this sub-unit.

The boundary between this sub-unit and the overlying one is similar to the S1b(i)/S1b(ii) one in that angiosperms, particularly swamp taxa, freshwater elements and pteridophyte spores all decline and there is a rise in bisaccates and oceanic dinoflagellates of the *Spiniferites* group. However, after this there is less of a full recovery in the lowland community. Freshwater species including aquatic angiosperms rise as do the Myricaceae but swamp and mire vegetation continues to decline with *Caryapollenites veripites* particularly affected although it is partially replaced by *Caryapollenites simplex*. Similarly pteridophyte spores do not recover

and the tropical species *Crassoretitriletes* and *Bombacacidites reticulatus* do not occur.

This suggests a period of relative sea-level fall but one which was less significant than the previous ones. There does not appear to have been a large amount of fresh substrate uncovered and the lowlands were being slowly submerged.

Throughout the rest of this final sub-unit of S1b there is a general decline in angiosperms and increase in bisaccates and Cupressaceae. Aquatic angiosperms decline and pteridophyte spores are no longer a major part of the assemblage. In the marine realm, dinoflagellate diversity increases and normal salinity indicators such as *Spiniferites* and *Hystrichosphaeridium tubiferum* rise significantly. *Bosedinia* and *Senegalinium* do not continue past the top of this sub-unit and *Apectodinium* also declines to be replaced by *Glaphyrocysta*.

The final submergence of the coastal lowlands and Juglandaceae swamp occurs within this sub-unit as *Caryapollenites veripites* and *Caryapollenites simplex* decline along with freshwater elements, aquatic angiosperms and pteridophyte spores. Oceanic dinoflagellates such as *Spiniferites ramosus* and *Hystrichosphaeridium tubiferum* increase indicating that this transgression may have led to a greater connection with the Norwegian Sea to the north and may therefore be linked to a period of thermal subsidence of the hinterland. The decline of *Apectodinium* at the top of this sub-unit corresponds with the end of the PETM hyperthermal and the loss of *Diphyes colligerum* and the fully tropical vegetative elements *Bombacacidites reticulatus*, *Crassoretitriletes* and *Compositoipollenites rhizophorus* may also

indicate cooling. Climate cooling may also be represented by the decline of *Caryapollenites veripites* with respect to *Caryapollenites simplex* which is considered to have a more temperate distribution.

The MFS at the top of the Forties Formation represents a hiatus in sedimentation seen in northern areas which becomes less obvious and grades to a correlative conformity in the Central Graben. Sand influx after this event becomes more proximal and the basin-floor fans reaching the basin centre are smaller in scale suggesting that this was a significant transgression and the delta had moved a great distance landwards. Wire-line logs which show a large spike of uranium, an element associated with condensation (Rider 1996) at this point providing further evidence of this major event.

The return of the PETM isotope curve to background values and a significant reduction in *Apectodinium* both occur at the S1a/S2a boundary. However, it is unclear what length of time the condensation surface here represents and the decline in both these indicators may have been much more gradual than the data seems to suggest. In the West of Shetland area there is evidence that this hiatus represented a significant length of time as large dendritic drainage complexes formed (Chapter 4) and it is therefore difficult to define the end of the PETM from North Sea evidence.

In S2a an impoverished Foraminiferal assemblage is once again recognised. Dinoflagellate diversity rises as do indicators of normal salinity such as *Spiniferites* and *Hystrichosphaeridium tubiferum*. *Apectodinium* numbers fall while representatives of the *Deflandrea* group rise. Bisaccates rise in numbers, as do

representatives of the Cupressaceae Forest. The Juglandaceae are present again along with Myricaceae, freshwater species, *Alnipollenites*, *Plicapollis* and *Platycaryapollenites*. Prasinophyte algae are abundant. At the top of the unit the angiosperm component decreases along with concurrent decreases in the bisaccates and Cupressaceae.

Increasing numbers of oceanic dinoflagellates indicate that greater connection with the global ocean had been established. This is hypothesised to have been a product of gradual deflation of the thermal dome underpinning the hinterland leading to the punctuated transgression seen throughout the S1b (ii) and (iii) sub-units. *Apectodinium* fall in numbers and diversity and is replaced by other peridinoids such as *Deflandrea* (primarily *Deflandrea oebisfeldensis*), a heterotrophic species which probably grazed on the algae or diatoms attracted by them (Powell 1992; Powell et al. 1996; Sluijs et al. 2005). Since this species occupies much the same environmental niche as *Apectodinium* it is suggested that its decline may have been due to decreasing global temperatures. *Deflandrea oebisfeldensis* is also suggested to indicate cooling (Bujak et al. 1998). Cooling is also indicated by the increase in more temperate elements such as *Retitricolpites* and *Plicapollis* at the expense of *Caryapollenites veripites*, *Sparganiaceaepollenites* and *Trudopollis*. Aquatic and freshwater elements such as *Sparganiaceaepollenites* along with pteridophyte spores are significantly reduced in this unit. This may suggest that freshwater run-off was lower due to decreased humidity but this is difficult to discern due to the similar effects of the transgression in drowning the areas of coastline which would have supported these communities. The Juglandaceae swamp community recovers

somewhat and pollen from the Cupressaceae, represented mainly by the swamp cypress *Inaperturopollenites hiatus*, increases significantly indicating that a basin-wards translation of the shoreline occurred following the transgression at the top of S1b allowing the swamp community to become re-established. The change from a Juglandaceae dominated swamp to one dominated by cypress is hypothesised to be due to the situation of the Juglandaceae swamp seaward of the cypress-dominated one, leading to this being most affected by relative sea-level rise. prasinophyte algae may have thrived in the areas of drowned vegetation. At the top of the unit a flooding event is observed which is consistent with the sedimentary record of continued clastic pulses during lowstands although the volume and extent of these fans is severely reduced relative to earlier pulses. The lowland angiosperms are affected as are the cypress.

In unit S2b there is a further decline in the angiosperm component of the terrestrial assemblage and terrestrial diversity falls. Bisaccates rise at the start of the unit but fall towards the end while a trend of continually increasing *Inaperturopollenites hiatus* is seen although some expanded sections show a decline at the very end of the unit also. Myricaceae, *Caryapollenites simplex, Plicapollis* and freshwater elements present at the start of the unit decline towards the top. Peridinoid dinoflagellates fall relative to gonyaulacoids and numbers of *Spiniferites* and *Hystrichosphaeridium tubiferum* rise dramatically. Within the dinoflagellate assemblage *Deflandrea* numbers are also high.

The increasing representatives of the Cupressaceae swamp and additional angiosperms indicate that a relative sea-level fall after the MFS may have increased the area for colonisation but that the majority of the Juglandaceae swamp and wetlands remained submerged. Alternatively the vegetation community may have changed little and the lowstand fans may be providing the pulses of sediment with a higher terrestrial component. The presence of *Deflandrea* still suggests that terrestrial influx and correspondingly nutrient influx was high and the *Spiniferites* group along with *Hystrichosphaeridium tubiferum* attest to the decreasing restriction of the basin.

Unit S3 is not recorded by the two cored wells but sections from the database suggest that it is very similar to the underlying unit with no aquatic elements or spores and an overwhelmingly dominant swamp community consisting of minor Juglandaceae and Cupressaceae. This again suggests that the coastal lowland environment had been transgressed leaving the fringing mangrove swamps. A slight declining trend in *Inaperturopollenites hiatus* from unit S2b appears to reverse towards the top of the unit possibly representing a relative sea-level fall and increase in coastal and mire vegetation. The number of dinoflagellates relative to miospores continues to increase although the assemblage still reflects high terrigenous input with heterotrophic peridinoids, mainly *Deflandrea* outnumbering autotrophic gonyaulacoids. *Inaperturopollenites hiatus* and *Caryapollenites simplex* are considered indicators of temperate climates demonstrating a possible cooling trend.

The top of the S3 unit is a major flooding surface evidenced from the high gamma shales seen in cores and on wire-line logs. A sharp decline in swamp taxa occurs at

the boundary as the coastal swamps moved landwards and high numbers of Prasinophytes are again noted corresponding with this period of flooding. Balder Formation units B1 and B2 represent the final back-stepping of the coastline probably linked to deflation of the thermal dome. The Balder Formation itself is a thick tuffite unit deposited during a period of sub-aerial volcanism. Palynological assemblages are representative of the high-nutrient input from ashfall and high numbers of diatoms and algae are found.

The biostratigraphic evidence demonstrates clearly that the PETM was superimposed on a period of major tectonic activity. Prior to the PETM, relative sea-level variations can be observed controlling sediment dispersal and the amount of terrestrial influx to the basin through changes in the extent of the coastal plain. Increased diversity in the vegetative community began before the hyperthermal in response to periods of relative sea-level fall and the distinctive cyclical changes in the biostratigraphic assemblages brought about by these can be seen throughout the Palaeocene. There is little evidence of global sea-level fluctuations during this period being as rapid or frequent as most sites record a general rise in sea-level through the Late Palaeocene-Early Eocene (Sluijs et al. 2006; John et al. 2008). The cycles observed in the North Sea are therefore likely to be related to thermal uplift of the hinterland and it appears that this uplift may not have been a continuous process but one with several jumps followed by periods of subsidence. This is entirely consistent with the presence of a thermal dome as it inflates during periods of high heat-flow and magma emplacement with thermal sag occurring during periods of lowered heat flow.

A sea-level fall at the beginning of unit S1a may have been eustatic in origin and led to distinctive changes in the marine and terrestrial assemblages due to increased restriction and colonization of exposed substrates. Warming may also have coincided with this as the dinoflagellate *Apectodinium* is seen. At the S1a/S1b boundary there is a very distinctive change in vegetation which, when compared with the patterns observed in earlier units and the dominance of primary vegetation, appears to indicate an extreme fall in relative sea-level. This could have been due to the superimposition of tectonically driven and eustatically driven sea-level fall but it cannot be discounted that this was the most extreme period of thermal uplift and signified intensification of events in the North Atlantic Igneous Province (NAIP). An increase in fern spores at the start of the PETM could be due to devastation of the vegetation due to increased temperatures but could also represent the first colonization of the vast exposed coastline. A large swamp community then built up on the hinterland. Clastic influx to the basin was high and the extensive Forties fan was deposited. High run-off rates could be due to increasing temperature gradients and a more intense hydrological cycle or could be a consequence of uplift-generated orographic rainfall.

Foraminifera reduced significantly during the PETM, possibly as an expression of the BFEE although it is not possible to determine whether affected taxa were completely extinct as there are a few representatives through the interval in many of the studied wells and the speed with which they recolonized at the end of the PETM suggests they may have been present throughout. Alternatively uplift and increased run-off may have rendered the basin so restricted and anoxic that the Foraminifera

could not survive. The relative sea-level rise at the top of the Forties may then have been enough to ameliorate the environment so they could once more colonize. Increased run-off into a restricted basin is also hypothesized to be the reason for the North Sea having become extremely fresh over the PETM. Low salinities appear to have increased to a maximum level where even the opportunistic *Apectodinium* could not tolerate them. However, there is an observable cyclicity within the periods of freshening and increased lowland vegetative elements which seems to suggest that these were controlled by changes in relative sea-level. It is possible that these changes were caused by distinct climatic cycles, possibly orbitally induced, but the evidence for increasing and decreasing restriction in the marine dinoflagellate assemblages suggests that a tectonic explanation is more likely. Additionally the units following the end of the PETM also show evidence of similar cyclicity superimposed on a generally rising relative sea-level.

The abundance and diversity of plants, particularly angiosperms, increases during the PETM which may be due to warming and increased carbon-dioxide but may also be due to an increased area of coastal exposure. Abundance and diversity of miospores is continually high throughout the Latest Palaeocene and Earliest Eocene and could be due to increased basin-wards transport by low salinity water currents. There is evidence of increasing temperatures with the presence in low numbers of thermophillic species during the PETM although much of the vegetation has a temperate to tropical distribution so it is difficult to observe a significant difference.

From consideration of the evidence from the regional biostratigraphic interpretation it is proposed that both warming during the PETM hyperthermal and tectonic/relative sea-level variations played a role in all of the environmental changes observed throughout the Late Palaeocene-Early Eocene in the North Sea. However, the effects on ecosystems that high CO_2 levels, increased temperatures and humidity might have and those changes generated by uplift-generated orographic rainfall, increased coastline exposure and basin restriction are so similar that how large their relative contributions are, is impossible to ascertain. Although there are a limited number of tropical elements in the PETM assemblages, the extreme change in the vegetative community seen in other areas over the PETM is not observed due to its remaining within a single biozone while the largest changes are observed where a pre-PETM community exists on the edge of a temperate biozone and moves into a tropical one (Harrington 2003; Harrington et al. 2004). The correlation between the time of greatest relative sea-level variation and the PETM may have important implications if these changes are considered to represent periods of thermal uplift and sag of the Iceland plume as it could indicate that the onset of the PETM was linked to changes in the Atlantic Igneous Province.

6.6 CAUSAL MECHANISMS OF THE PETM HYPERTHERMAL

Previous theories have attributed the PETM to volcanism, changes in oceanic circulation patterns and dissocation of methane clathrates. The highly expanded section in the Central North Sea may provide evidence for one or other of these hypotheses.

The analyses of four PETM sections in the Central North Sea all demonstrate a period of gradually decreasing isotope values and no sudden CIE ‘event’ such as is seen in condensed marine sections where it is suggested that dissolution and condensation has removed much of this onset phase (Bralower et al. 1997) (Figure 6.56).

If such a protracted onset phase was truly the case, it would challenge the previously held notion that the PETM was an instantaneous event. Recently, other sections have been located with a more gradual onset and recovery period such as the New Jersey (Sluijs et al. 2007) and Spitsbergen records (Harding et al. 2011) (Figure 6.57) suggesting that this may be the true shape of the PETM isotope curve in complete sections.

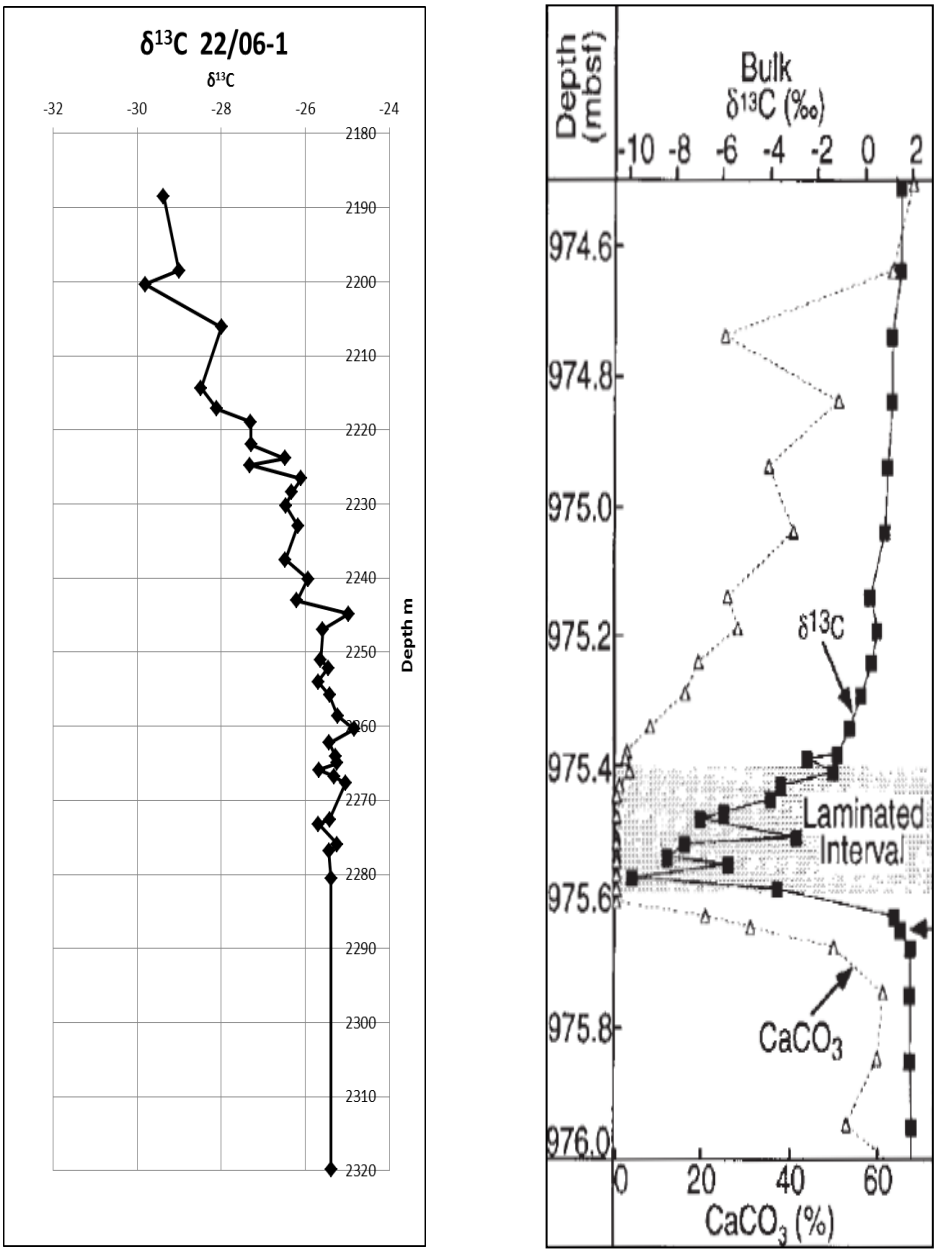

Figure 6.56: Comparison of the prolonged onset phase seen in section 22/06-1 with a PETM site in the Caribbean with a rapid onset which has been interpreted to be due to dissolution of carbonates during CCD shoaling.
Right image after (Bralower et al. 1997)

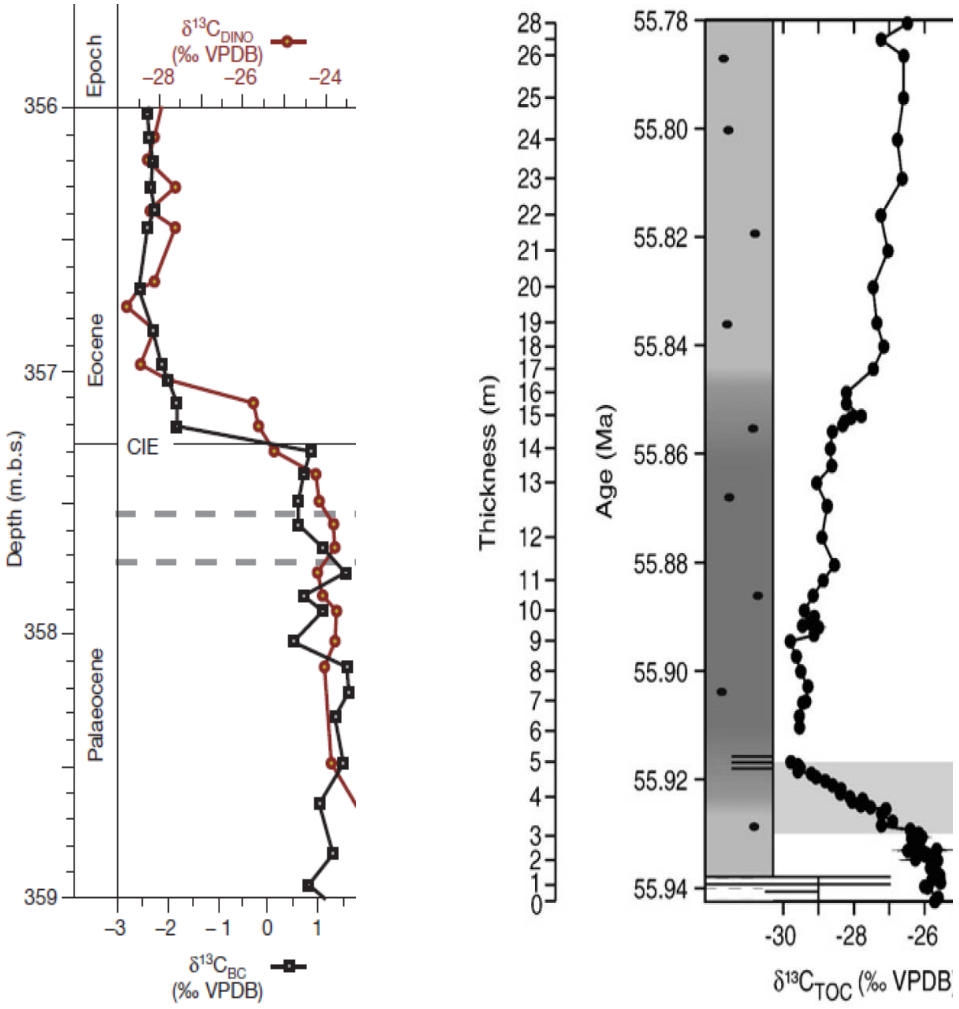

Figure 6.57: Expanded sections from Bass River, New Jersey and Spitsbergen.
Images after (Sluijs et al. 2007; Harding et al. 2011)

It has been suggested in other sites, that distinct steps occur during the onset phase of lowering isotope values and that these may represent short-duration fluctuations or discrete periods of CO_2 release into the ocean-atmosphere system. The high resolution isotope studies in the Central North Sea showed unusually variability with many short-duration fluctuations in isotope values. This could be due to the more expanded nature of the North Sea sites but it is important to first explore other possibilities for the variations before assuming them to be a world-wide phenomenon.

Wells 22/10a-4 first showed the highly variable isotope values in the PETM onset phase, and a possible mechanism for generating such fluctuations was hypothesised (Kender et al. 2012). It was thought to be due to the effect of differing amounts of terrestrial and marine sediments making up the total organic carbon (TOC) tested. Although all species fractionate carbon isotopes slightly differently, in general terrestrial organic matter has a lower $\delta^{13}C$ than marine organic matter (Pagani et al. 2006; Handley et al. 2008), assuming that the majority of the flora in the area uses C_3 carbon fixation (the most common of three metabolic pathways for carbon fixation in photosynthesis) (Kump et al. 1999). Additionally there is a difference in the $\delta^{13}C$ values of angiosperms, gymnosperms and spores which may also contribute different amounts of organic carbon. Variations in the ratio of these constituents in the bulk organic carbon analysed may therefore produce variations in $\delta^{13}C$ between samples.

It is difficult to test the relative input from each of the types of organic carbon without compound specific analysis which was outwith the scope of the study. It was

considered however, that this could be indirectly tested by comparing samples from sandier facies which may have a more terrestrial influence with shale-prone samples which may contain more organic matter of a marine origin. Samples from 30/14-1 were analysed for grain-size with the assumption that a higher grain-size would correlate with sandy sediments, sourced from the hinterland whereas finer clay fragments would represent background pelagic sedimentation. Grain size was then graphed against $\delta^{13}C$ value (Figure 6.58).

Samples were chosen depending on their $\delta^{13}C$ result in order to test the samples with the highest derivation from the mean.

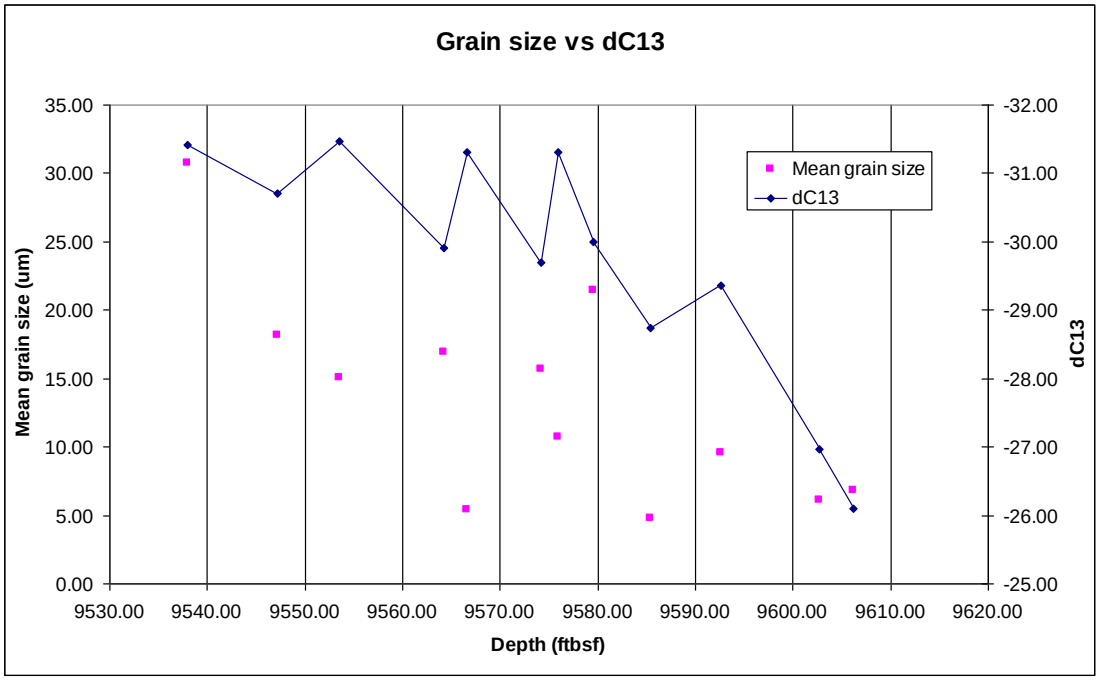

Figure 6.58: Mean grain size vs isotope values of selected samples from 30/14-1

From the results (Figure 6.57), it appears that grain size does not have a significant effect on $\delta^{13}C$ values in 30/14-1 and variations in the terrestrial and marine contributions to the total organic matter analysed may not be the cause of the fluctuating isotope results. An alternative explanation is that there was very little difference in the size of grains in the 30/14-1 samples as they were mainly within the silt-clay fraction and the assumption that sandier sections would have a greater amount of terrestrial material was flawed since minute, light terrestrial palynomorphs may be swept in by sand-rich influxes but tend to float in the water column and settle on top along with the oceanic palynomorphs.

.

It was therefore considered that if the isotope variations are not due to variations in marine and terrestrial organic matter then there must be another driver for them. The North Sea is also a hydrocarbon province with the Palaeocene section particularly prolific. Hydrocarbons can affect isotope values in spite of efforts to remove them. One of the noticeable characteristics of the North Sea PETM sections are the extremely low $\delta^{13}C$ values of -30 to -31‰. Although such extreme variations are common in Carboniferous and Permian sections (Payne et al. 2004) , Palaeocene organic carbon analyses from around the world show higher values of $\delta^{13}C$. At Dababiya in Egypt minimum values only reach -27.5 whilst Lleida, in the South Central Pyrenees of Spain records values of -27.6 and -26.7 (Bolle et al. 2000; Dupuis et al. 2003; Ouda 2003; Sluijs et al. 2007; Domingo et al. 2009). The seemingly anomalously low values in the North Sea could be considered a product of possible hydrocarbon contamination as residual hydrocarbons can dramatically affect the outcome of isotopic analysis (Stephenson et al. 2005).

To test this, half of the material from all of the samples from 30/14-1 were de-oiled and analysed for $\delta^{13}C$ (details supplied in Chapter 1). The remaining half of a few selected samples (Figure 6.59) were then analysed without de-oiling and the results graphed.

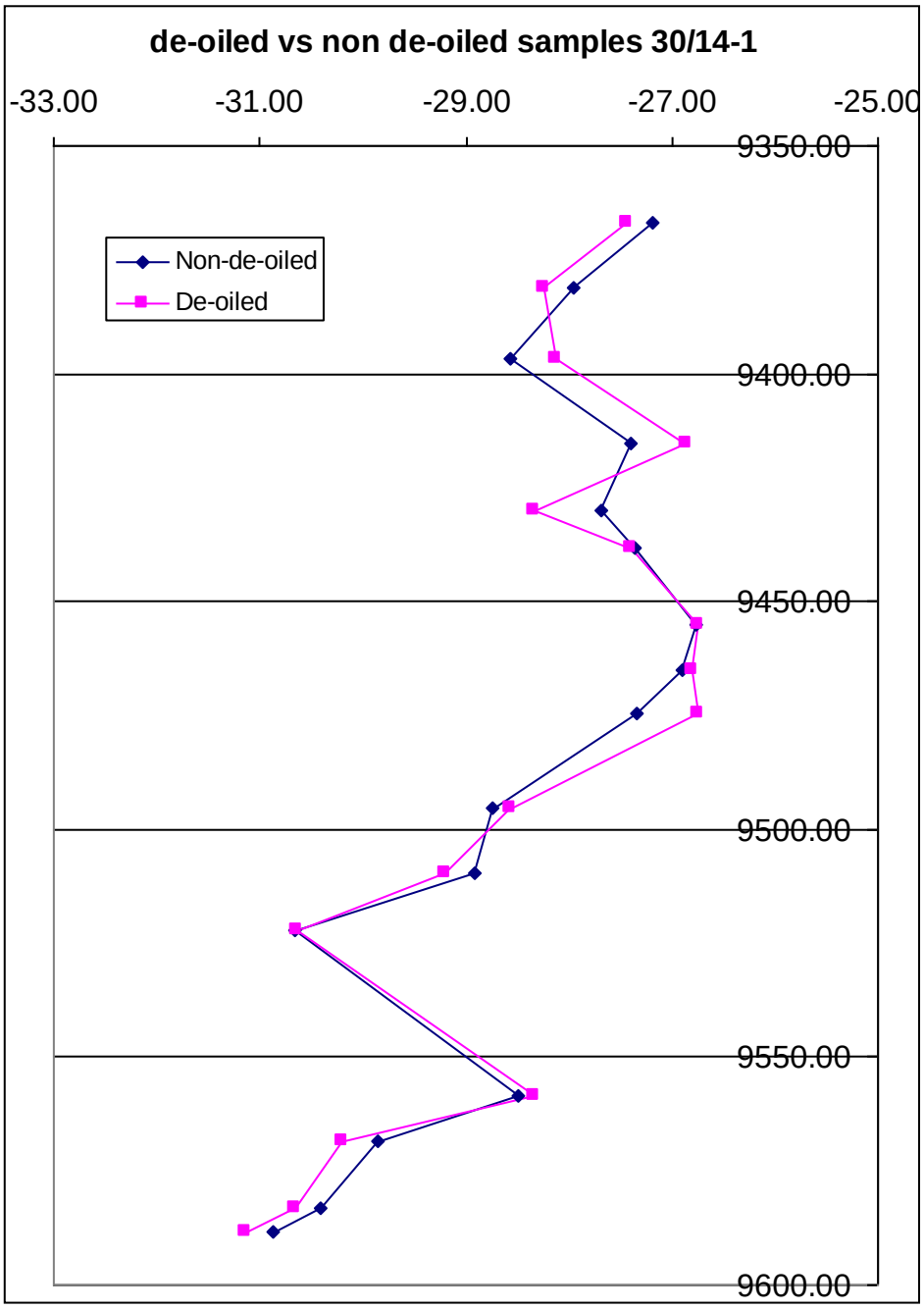

Figure 6.59: Original de-oiled d13C samples from 30/14-1 graphed with the non-de-oiled data.

There seems to be little difference between the de-oiled samples and the normally processed ones. This may be due to the shale-prone nature of the sediments in question but since most studies involving isotopes are undertaken on shales due to their organic carbon content, this may not be unique to this section. The lack of correlation may be due to the $\delta^{13}C$ value of the interstitial hydrocarbons being similar to the mean bulk isotopic signal and therefore having a muted effect. Testing of sections 22/09-3, 30/14-1 and 22/06-1 demonstrates that the isotopic value of the hydrocarbons within the 3 wells is -30.1, -28 and -27.6 respectively so this interpretation is possible. However, if the interstitial hydrocarbons were affecting the isotopic values they would be expected to do so in a single direction i.e. increase or decrease the isotope ratios of the bulk carbon. The de-oiled and non-de-oiled values seen in the graph, when they differ at all, seem to do so at random indicating that residual hydrocarbons do not dramatically affect bulk carbon isotope values in North Sea sections.

Hydrocarbon contamination is also unlikely due to other high latitude sites such as the Arctic PETM section located on the Lomosov Ridge, having a minimum $\delta^{13}C$ of -31‰. Other evidence seems to corroborate this; at a Spitsbergen section -30‰ is recorded and Tawanui in Southern New-Zealand has minimum PETM carbon isotope values of -29.5‰ (Sluijs et al. 2007; Sluijs et al. 2008; Harding et al. 2011) suggesting a latitudinal trend (Figure 6.60).

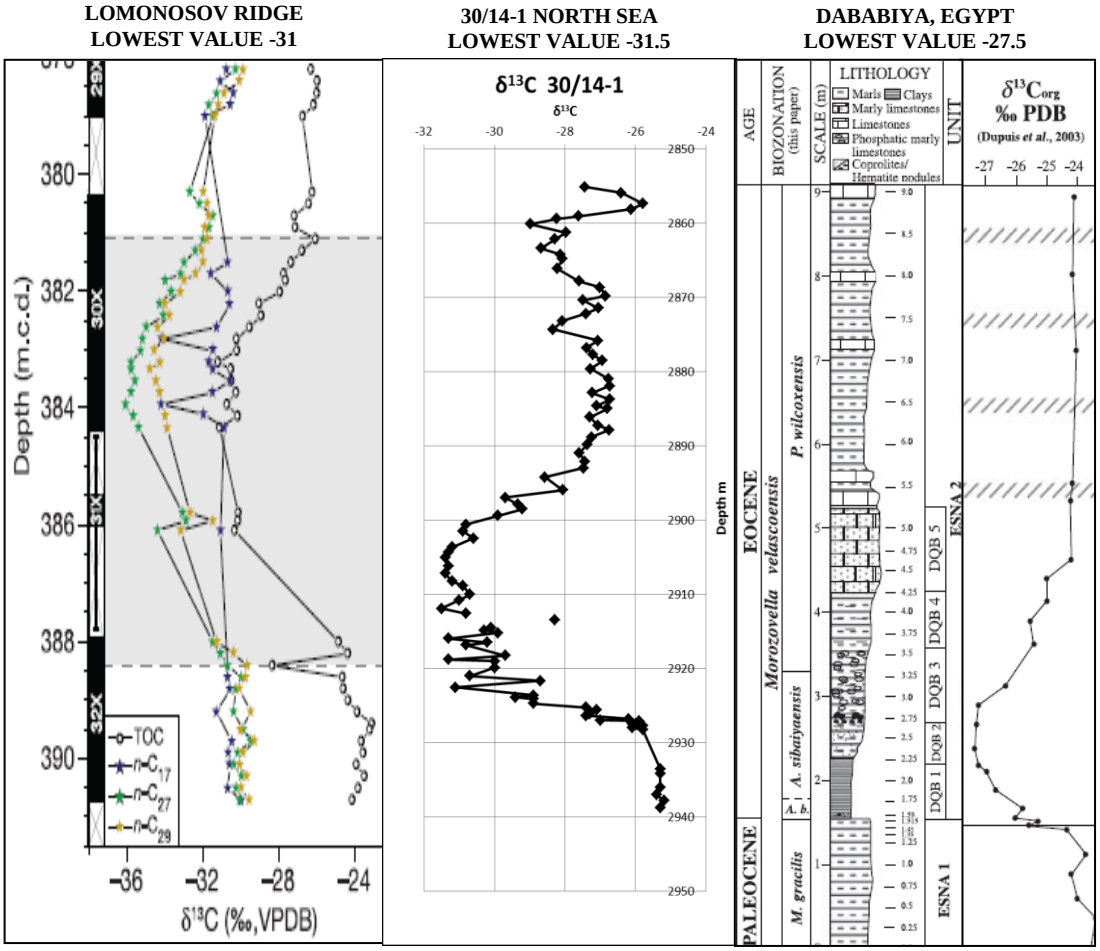

Figure 6.60: Differences in the absolute values of isotope shifts from different areas around the world. The minimum isotope value at the two high latitude sites is significantly lower than the lower latitude site

(Analyses all using bulk Organic Carbon)

L and R Images after (Ouda 2003; Sluijs et al. 2008)

Terrestrial organic matter has a lower $\delta^{13}C$ value than marine but a reduced input of terrestrial material at lower latitudes is inconsistent with evidence from many low latitude sites which suggest an increase in humidity and correspondingly, run-off, at the PETM therefore there must be another reason for the low $\delta^{13}C$ values at the poles.

It is possible that the terrestrial component at high latitudes has a lower $\delta^{13}C$ value than at lower latitudes. It has been ascertained experimentally that low intensity, long duration light levels such as occur during the Arctic summer, act to lower $\delta^{13}C$ values in plants (Yang et al. 2009). Additionally, Angiosperm $\delta^{13}C$ values are typically more negative by a magnitude of 1-3‰ than gymnosperms and these undergo a distinct radiation at the PETM in North Sea sections.

$\delta^{13}C$ values have also been found to increase with decreased precipitation (Kohn 2010) thus it is possible that humidity increased to a greater extent at higher latitudes than lower ones although there is conflicting evidence for this.

The stagnation of the North Sea may have led to lower isotope values as, during a period of stagnation, bottom water CO_2 derived by bacterial decomposition, may rise in concentration due to the lack of incoming inorganic carbon (Kuspert 1982; Schouten et al. 2000). At the same time, due to the lack of transport and consumption of O_2 in bacterial processes, oxygen concentrations may be diminished. Since the bacterially-derived CO_2 will be out of sync with atmospheric CO_2 and will be isotopically lighter then, if some of this is utilised by phytoplankton and re-fixed, the

result will be a negative shift in the isotopic composition of the organic matter and carbonate. Increasingly more stagnant bottom waters should lead to a higher build-up of isotopically light CO_2 and more negative isotope values.

This model assumes periodic overturning but is plausible as evidence from the North Sea (Zacke et al. 2009), Spitsbergen (Harding et al. 2011), Lomosov Ridge (Sluijs et al. 2008) and Southern New Zealand (Crouch et al. 2003; Sluijs et al. 2011)all confirm that freshening and associated stratification occurred in these areas at the PETM due to increased terrestrial run-off.

The results of analysis of the PETM isotope signatures found in the North Sea sections are inconclusive. There is evidence of a protracted onset phase as seen in other expanded sections but unlike the data from other areas, the North Sea sections show extreme variability in the isotope values in this period. Variations in the ratio of marine and terrestrial organic matter could create such a pattern but this can only be proven with compound-specific analysis to separate the marine and terrestrial organic matter. The study does suggest that the type of terrestrial organic matter can affect the isotope signature which is an important consideration when interpreting environmental changes using this data.

Taken on its own the data from the PETM in the North Sea does not seem to permit many inferences about causal mechanisms of the PETM. The extended onset period does provide evidence against the interpretation of a sudden catastrophic event and a mechanism must therefore be able to continually produce greenhouse gases on a long time-scale but the fluctuating and anomalously low isotope values are difficult to fit

to a model. However, this study was undertaken to look at the structural, stratigraphic and climatic history of the Central North Sea over geological time and use of analogies from other parts of the UK aided interpretation. It is therefore prudent to take the same approach when investigating the PETM climate excursion and to this end other climate excursions were investigated both pre and post-dating the PETM in order to look for similarities which may signify a common causal mechanism.

An isotope excursion has been documented from a Toarcian (Lower Jurassic) section from the North Yorkshire coast (Cohen et al. 2007) which bears a striking resemblance to the complete section in 30/14-1 and also has similar variations in isotope values (Figure 6.61). This suggests a common mechanism or a common response in this area, to climatic variations through time and investigation of the similarities and differences between the two periods may provide further clues as to what this is.

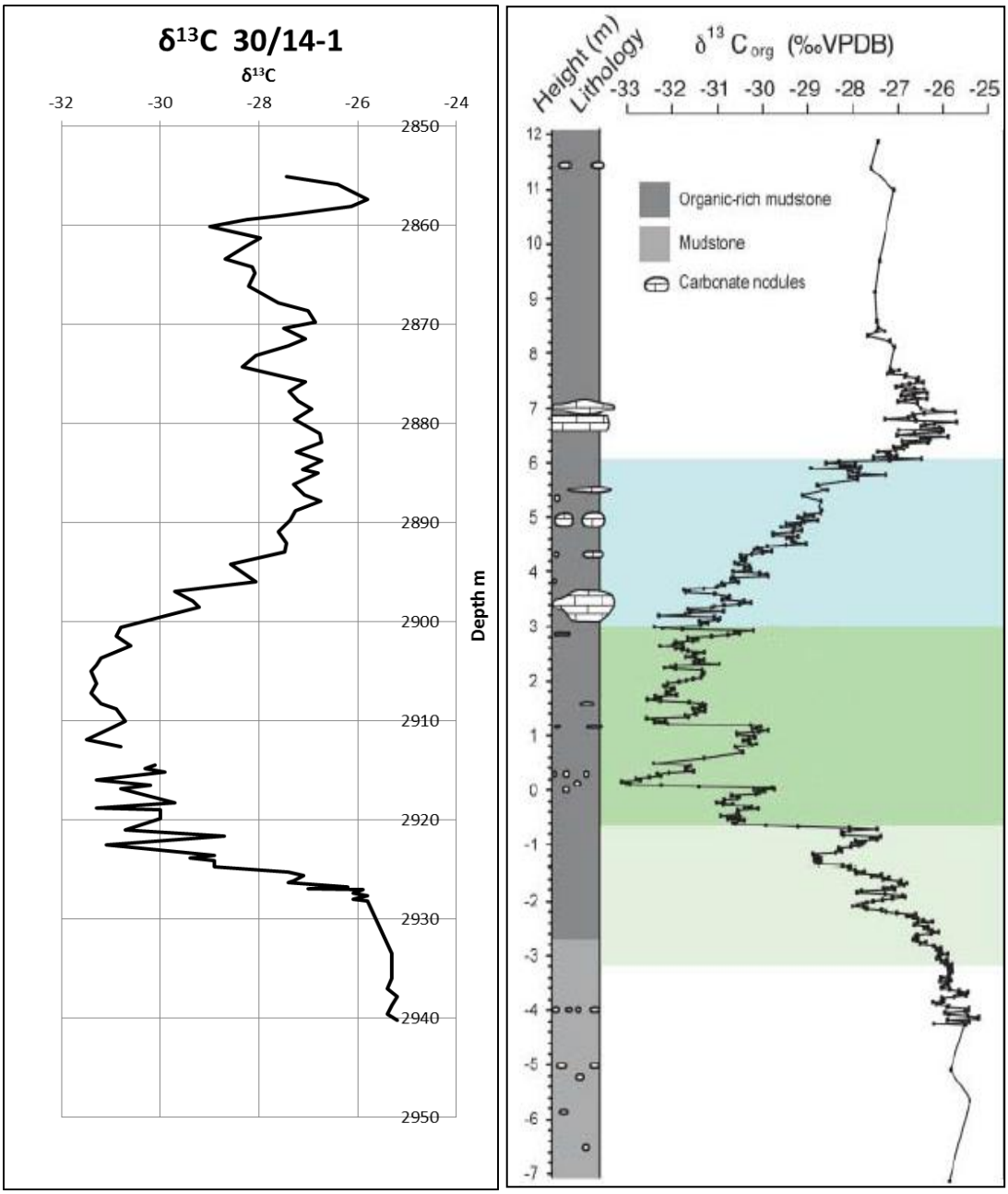

Figure 6.61: Comparison of the PETM isotope curve from the Central North Sea well 30/14-1 (L) and the Toarcian curve (R) showing the similarity in magnitude and shape of the excursions.

Toarcian data after (Cohen et al. 2007)

The isotope curve from 30/14-1 extends into the Early Eocene and seems to contain a later excursion above the PETM (Figure 6.62). The second isotope excursion seems unusual as, although other hyperthermal events have been identified in the Eocene, none are as old as the one identified by carbon isotopes in 30/14-1.

This excursion event was compared with those discovered in other areas of the world. The most consistent Early Eocene hyperthermal has been dubbed the 'Elmo' horizon and occurred some 2 million years after the PETM (Lourens et al. 2005; Sluijs 2006). At site 1263 Walvis Ridge 'Elmo' isotope values of $\delta^{13}C$ show a bulk negative shift of 1.4–1.6‰ which is similar in shape to the excursion at the PETM although much shorter lived (Figure 6.63) Other such events have been tentatively identified from Ocean Drilling Project cores (Nicolo et al. 2007; Westerhold et al. 2011) and an Arctic section (Sluijs et al. 2008) (Figure 6.64).

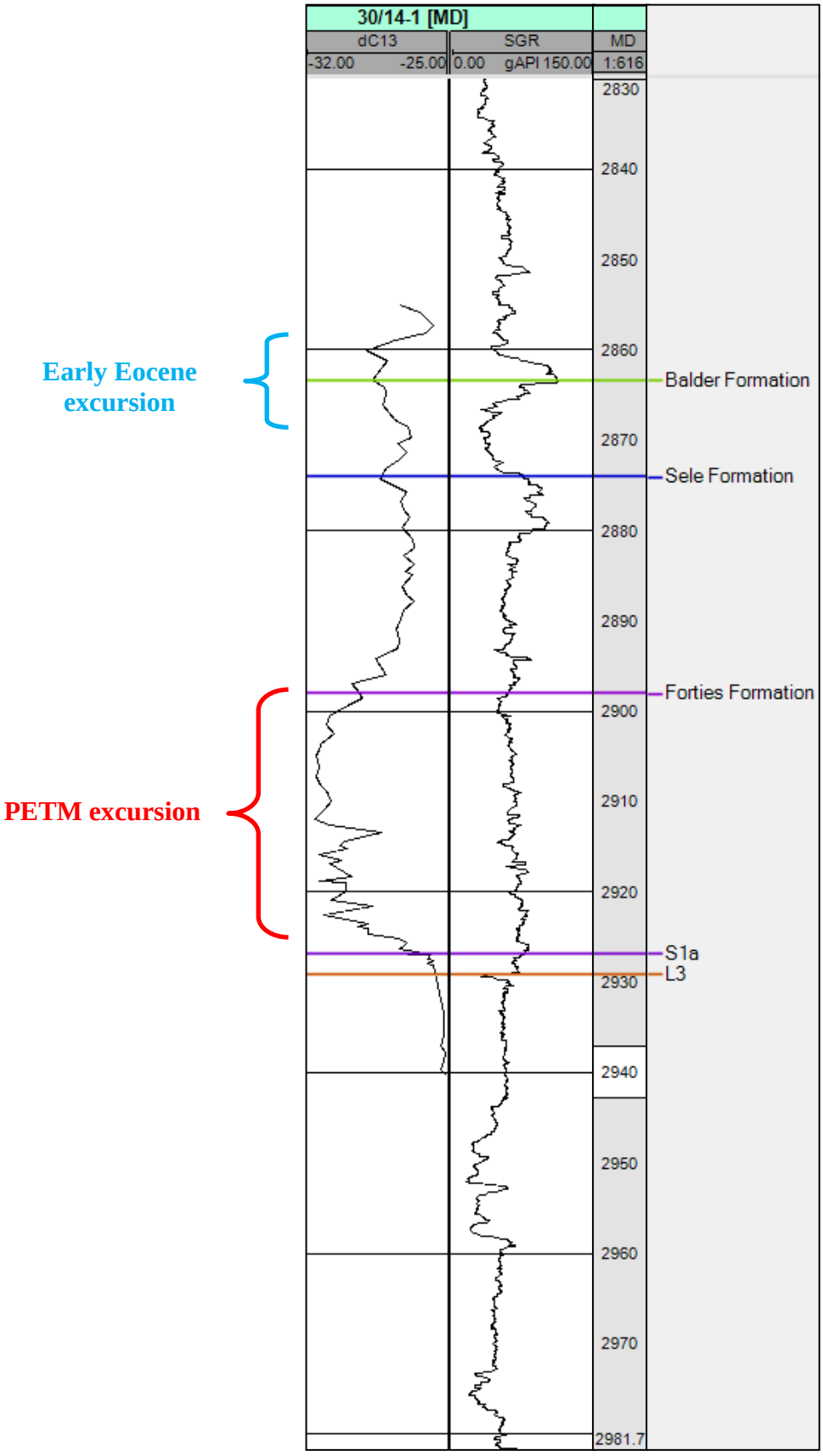

Figure 6.62: The isotope curve from 30/14-1 appears to show a later excursion within the upper Sele and Lower Balder Formations which may correspond with the Early Eocene hyperthermals which have been discovered in deep ocean cores.

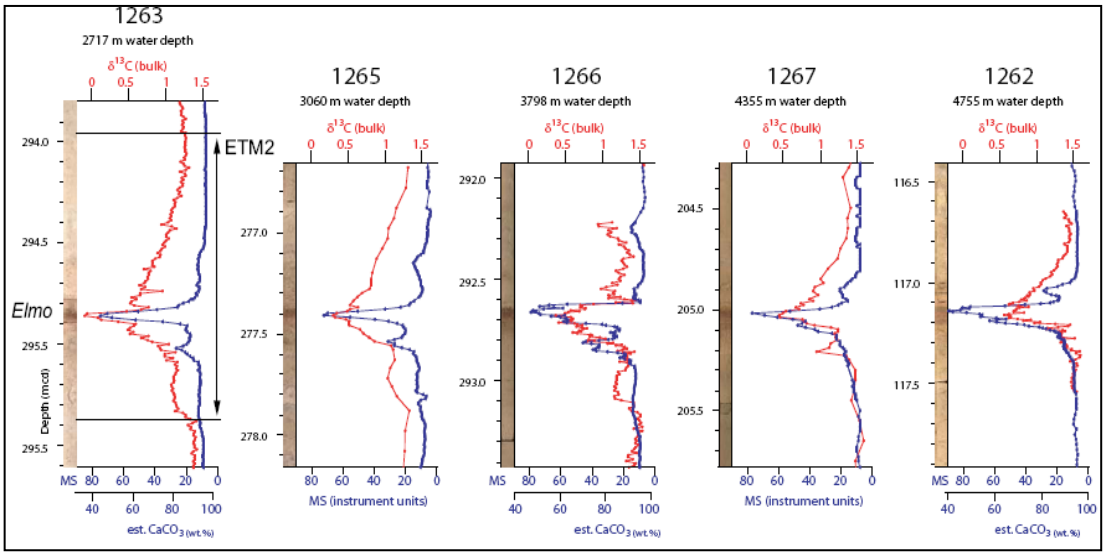

Figure 6.63: Bulk carbonate δ13C and magnetic susceptibility records across the Elmo horizon at five ODP Leg 208 sites.
Lithological images are placed at the left of the charts.
Image after (Lourens et al. 2005)

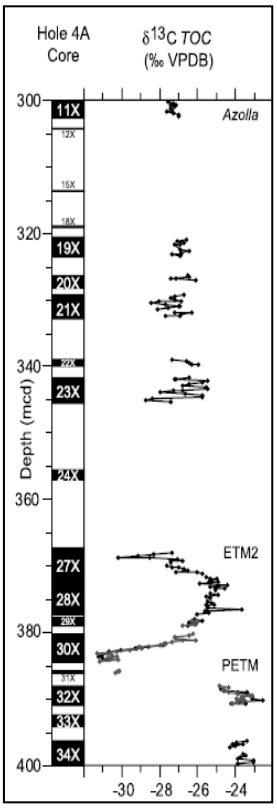

Figure 6.64: The Eocene isotope excursion discovered in boreholes at Lomosov Ridge in the Arctic.
Image after (Sluijs et al. 2008)

The magnitude of the 30/14-1 second excursion above the PETM seems to fit with the Arctic excursion. However, it is anomalous as it lies just above the Balder Formation, dated by tephra-chronology and isotope dating to the Lower Eocene 54.2Ma (Passey et al. 2008). This is at least 1Ma earlier than the date suggested by orbital stratigraphy for the Arctic ETM2 and may thus represent the first recognition of another short-lived hyperthermal. Analysis of the Arctic section was hampered by poor recovery so it cannot be ruled out that they are the same event due to uncertainty in the Arctic stratigraphic correlations.

6.6.1 CAUSAL MECHANISMS DISCUSSION

The similarity between the Toarcian and PETM isotope curves suggests a common causal mechanism. Uplift and erosion in the Middle Jurassic removed the Toarcian-age sequence from the Central North Sea but investigation of the global tectonic events during the period shows that eruption of the Karoo-Ferarr flood basalts covering much of South Africa and Antarctica are dated to this period (Palfy et al. 2000). Work carried out on the stratigraphy of Palaeocene-age sediments and basalts in the West of Shetland region of the North Atlantic Igneous Province (NAIP) and Indian Ocean suggests that the PETM was also synchronous with igneous activity (Jolley et al. 2002) and this may indicate that carbon isotope excursions are linked to flood basalts. A negative $\delta^{13}C$ spike has also been documented coinciding with eruption of Wrangellia flood basalts in the late Triassic (Hesselbo et al. 2002; Dal Corso et al. 2012) which further strengthens this argument. Warming linked to volcanic CO_2 release may also have been sufficient to destabilise methane hydrates on the continental shelves intensifying warming.

Any causal mechanism predicted for the PETM may therefore be expected to have also produced the second Early Eocene hyperthermal evidenced by the isotope data from 30/14-1. Volcanism was still occurring in the NAIP during the Early Eocene. The vast quantities of dust ejected are preserved as the Balder Tuff and core logging in 30/14-1 shows that volcanic ash layers are present until 3010ft so the isotope spike occurred completely during a period of volcanic activity. However, explosive

volcanism may be expected to have a cooling effect on the climate (Jolley et al. 2005). Volcanic gases such as sulphur dioxide condense in the stratosphere to form sulphate aerosols which reflect radiation from the sun back into space causing cooling of the atmosphere or troposphere. Since isotope signatures are linked to increased levels of isotopically light carbon in the form of methane or CO_2, the occurrence of one during a period typically regarded as having a cooling climate. (Jolley et al. 2005) is therefore difficult to explain.

It has also been suggested that Eocene hyperthermals show variation on Milankovitch timescales and could be linked to orbital variations (Westerhold et al. 2011). The PETM may therefore represent mantle out-gassing coupled with one of these cyclical variations amplifying its effects. It is also possible however, that the isotope excursion in 30/14-1 may be due to insoluble carbonates affecting the isotope values. Another section which extended into the Eocene section would be required to test whether this is a real phenomenon.

6.7 THE PALAEOCENE-EOCENE THERMAL MAXIMUM SUMMARY

During the Late Palaeocene a period of extreme climate warming known as the PETM hyperthermal occurred. This event had an influence on depositional systems within the Central North Sea basin and was also investigated due to its similarity in terms of CO_2 increase to present day global warming.

Identification of the PETM by isotopic analysis confirmed its presence in the Central North Sea and its stratigraphic position in S1a and S1b units. It was considered that increased humidity at the PETM such as that evidenced in other high latitude sites could have led to the deposition of the extensive Forties Sandstone Member and that seismic mapping of this may provide information about possible effects on sedimentary geometries. However, the evidence of tectonic uplift and the effect of underlying basin floor fans on the distribution of the Forties Formation meant that this link could not be proven. The evidence for earlier fans of equal or greater extent also suggests that the PETM had little influence on the deposition of Palaeocene basin-floor fans in the Central North Sea. This is important for basin studies as it implies that basin evolution is almost entirely controlled by tectonics and that climate has only a secondary role to play on geological timescales.

More subtle effects of the PETM on sedimentation were found in the identification of increased levels of the element uranium at the PETM onset which could be due to a

combination of restriction and high temperatures leading to anoxia and acidification coupled with increased uranium input from run-off. A maximum flooding surface at the S1a/S1b boundary could have acted to concentrate the increased levels of the element. Evidence of restriction, anoxia and acidification in other PETM sites has been considered to provide evidence for a decreased thermal gradient leading to a more stratified and anoxic ocean and shoaling of the CCD. However in the North Sea, tectonic uplift led to narrowing of the northern seaway causing the basin to become isolated and this, coupled with increased terrestrial influx would also be expected to have similar effects on oceanographic conditions. The evidence from cores shows that the shales of the Sele formation are full of pyrite and glauconite which signify that reducing conditions continued after the end of the PETM but biostratigraphy shows that Foraminifera disappear only over the PETM period suggesting that warming may have led to a greater degree of restriction. A low percentage of the element calcium may indicate acidification and shoaling of the CCD but is more likely to be due to anoxia and a reduction in the amount of reworked chalk debris in later Palaeocene basin floor fans. The bathymetric distributions of the Foraminifera present prior to the PETM also proves that the North Sea was far shallower than the CCD.

Increased humidity at the PETM may also have been expected to have affected the soluble elements silica, potassium, magnesium and phosphorus since high rates of silicate weathering and run-off may cause concentrations of these elements to increase. However, no such patterns were observed in the North Sea data. Silica percentages increase which could indicate increased silicate weathering but the

values vary widely and their lack of correspondence with the gamma ray log which represents facies, suggests that some of this is biogenetic in origin. Potassium percentages appear to decrease over the PETM which may indicate that rates of weathering and run-off fell which is unlikely to be the case due to the evidence for high levels of clastic influx to the basin. These elements therefore appear to be influenced primarily by clay mineral proportions and diagenesis. The clay mineral kaolinite is an indicator of warm climates but kaolinite found in shales of the Forties Formation was shown in thin section to be due to replacement of other minerals during diagenesis. A rise in phosphorus over the start of the PETM may indicate increased nutrients and therefore terrestrial run-off.

This link was tested by looking at the ratio of heterotrophic peridinoid dinoflagellates to autotrophic gonyaulacoid dinoflagellates. This ratio has been suggested to indicate increased nutrient availability in other PETM sites as has the presence of the peridinoid *Apectodinium*. A rise in the P/G ratio over the PETM is found in North Sea sections but the number of peridinoids remains high into the Early Eocene indicating that increased run-off may have lasted for a time after temperatures had fallen again. The transient rise in *Apectodinium* found in other PETM sections is also noted in all of the wells studied in the Central North Sea and may also be linked to enhanced nutrient availability and terrestrial input. Angiosperms also undergo an apparent radiation at the PETM but this is likely to be due to transport efficiency and increased lowland environment and they continue to be abundant and diverse in the post-PETM section. The evidence from initial biostratigraphic analysis showed that the PETM may have had effects on the environment but that the hyperthermal was

superimposed on a background of tectonic changes which could have produced similar results.

Biostratigraphic analysis was therefore undertaken on 66 wells with quantitative and qualitative biostratigraphic data of varying quality in order to determine the relative importance of these events but the results were inconclusive. Prior to the PETM, relative sea-level variation controlled the composition of the assemblages found in the basin and during the PETM these variations increased in magnitude and speed. The evidence for increased humidity during the hyperthermal such as increased numbers of freshwater species and swamp taxa was indistinguishable from that which would result from tectonic uplift and increased areas of delta top. Incoming species with a tropical distribution show that the climate was warm but these never diversify and the bulk of the terrestrial elements remain within a single biozone. The evidence for increased eustatic sea-level over the PETM seen in other sites is also not observed in the North Sea due to overprinting by tectonic events.

Isotopic analyses over the PETM section show the characteristic $\delta^{13}C$ decrease but it is noted that this decrease occurs gradually rather than the sharp decrease seen in other deep-sea sections. This indicates that such sites may be incomplete or extremely condensed. A hypothesised causal mechanism for the PETM must therefore continually produce greenhouse gases as a gradually falling isotope ratio cannot result from a single injection of methane.

Other PETM sections show evidence for several steps of lowering in the isotope data and North Sea sections also show fluctuations in the isotopic record which may represent discrete injections of methane into the ocean-atmosphere system. However, they could also represent variations in the ration of terrestrial and marine organic matter in the samples or be the result of hydrocarbon contamination. Grain size analysis to look at whether terrestrially derived samples had different $\delta^{13}C$ values proved inconclusive and compound-specific isotope analysis would be required to separate the types of organic matter. Hydrocarbons were not found to affect the $\delta^{13}C$ values of the samples but the particularly low $\delta^{13}C$ values of high latitude samples suggests that the type of terrestrial organic matter can affect the isotope values which is an important consideration when comparing data from different sites and when using the isotope curve to investigate temperature and environmental variations.

Comparison of the North Sea PETM isotope curve with one from the Toarcian from samples in England showed them to be very similar in shape and absolute values which could suggest they have the same casual mechanism or regional response to it. Flood basalts have been recorded in sites during the Toarcian while the PETM corresponds with a period of igneous activity in the North Atlantic Igneous Province (NAIP) and Indian Ocean. A second isotope excursion was also recorded in the North Sea, present within the Early Eocene Balder Formation and Hordaland Group which could be the oldest example of an Eocene hyperthermal. However, its occurrence during a period typically regarded as having a cool climate is anomalous and further investigation is required to ensure the isotopes were not affected by insoluble carbonates.

The evidence from the Central North Sea therefore suggests that tectonic influences were a more important driver of depositional and ecological changes during the Late Palaeocene than the PETM hyperthermal. This is important as it underlines the overriding importance of large-scale tectonic processes in shaping past and present landscapes. This study also shows that the effects of climate change can be very subtle and their interpretation is affected by many different processes. Analysis of the Central North Sea sections has demonstrated the importance of the type of organic carbon analysed in isotopic studies. It also highlighted the importance of understanding sedimentation rates, transport and diagenesis before making inferences on climate using proxies such as clay mineralogy, elemental analyses and pollen analysis. The highly intricate links between regional tectonic uplift, sedimentology, ecological change and climate change found in this study demonstrate that a clear understanding of the geological history of an area is vital when interpreting climatic events as many of the proxies which can be linked to temperature and humidity changes can also be linked to other events.

CHAPTER 7

CONCLUSIONS AND RECOMMENDATIONS FOR FURTHER RESEARCH

7.1 CONCLUSIONS

The Central North Sea has a long history of tectonic and climatic events which have created the structural configuration seen today. Whilst many of the oldest structural episodes have been overprinted by more recent events, careful analysis of well calibrated regional (> 17,000 sq. km) 3D seismic volumes has provided a new-found basis by which to understand the tectonic and stratigraphic evolution of the highly prospective Central Graben, the NW-SE striking rift arm of the North Sea trilete (failed) Upper Jurassic rift system. The results have permitted new insights into the basin's development aided by the definition and mapping of two complete tectono-stratigraphic megasequences of Triassic and Jurassic age are now confidently identified where previously only the later deformational episode had been described in detail. Further integration with well data, in the form of electrical well log correlations, cores, side wall samples and cuttings allowed investigation of the regional geology and environment to be undertaken at an unprecedented level of detail beyond the resolution of the seismic data.

Within the pre-rift sequence of tectono-stratigraphic megasequence 1, which includes all rocks deposited prior to the Triassic, older deformational fabrics can be identified. The oldest tectonic events which affected the Central North Sea occurred during the Caledonian and Variscan plate cycles which took place from the Cambrian to Devonian (Caledonian) and Devonian to Carboniferous (Variscan). Although well-

penetrations of Lower Paleozoic rocks in the Central North Sea are sparse, onshore analogues helped to constrain interpretation of these events. Where pre-Devonian well penetrations occur, they demonstrate the presence of highly metamorphosed Ordovician rocks which lie on the Auk Ridge. The seismic character of this area and onshore analogues suggests that this may be a granite-cored basement block dating back to the Caledonian orogeny.

Mapping of Devonian sequences demonstrates that faulting mapped onshore related to Caledonian deformation also extends offshore. Syn-rift thickening is observed into these NE-SW striking faults but no large basins were recorded in the area mapped. Carboniferous rocks are not penetrated in the study area and Devonian sequences lie directly underneath the Permian Rotliegendes Group. This may indicate that they were never deposited or have been subsequently completely eroded but this seems unlikely due to the evidence of thick sequences onshore. These onshore analogues suggest that either Carboniferous rocks are present in now deeply buried half-grabens or in the centre of large-scale synclines such as those observed in the Midland Valley of Scotland. Seismic interpretation south of the Jaeren High, itself bounded by a Caledonian age fault, shows evidence for possible Carboniferous sequences thickening into a graben or syncline but it cannot be determined which structure is shown with the limited area imaged. NE-SW striking faults of a Caledonian trend are pervasive in the Central North Sea, bounding several major highs and are seen to reactivate under later stress-regimes demonstrating the importance of understanding basement trends.

Following Variscan inversion, which probably results in the lack of preserved Carboniferous rocks, a long period of erosion occurred. This created the widespread unconformity mapped in the Central North Sea and identified all over north-west Europe known as the Base Permian Unconformity (BPU). Mapping of the BPU and the top of the Lower Permian Rotliegendes Group shows that the Permian sequence is cut by WSW-ESE striking faults linked to the formation of two large intra-continental basins during the Early Permian, the North and South Permian Basins. Evidence for this rift episode is found on the two Late Jurassic (Western Platform and Utsira High) margins and along the median Forties-Montrose High, where the Permian sequences have remained relatively elevated and their internal structural and stratigraphic architecture can be imaged and resolved. The structure of the Forties-Montrose High in particular is reconsidered in light of mapping of Permian and pre-Permian sequences. It can now be shown that the NW-SE striking Forties Montrose High was formed by transection of a WSW-ENE Permian high by later Jurassic faults. The W-E trend is observed throughout the Central North Sea and, as with the Caledonian lineations, these faults are reactivated under later stress regimes. During the Late Permian, thick Zechstein Supergroup evaporites were deposited in the basin which had a profound effect on the subsequent evolution of the basin.

The Triassic saw the start of the deformational episode which formed tectono-stratigraphic megasequence 1. The evidence for Triassic rifting in the Central North Sea has been debated due to the evidence for Permian movement on the majority of the faults mapped and the lack of well-defined syn and post-rift packages. However, seismic interpretation in the Northern North Sea demonstrates the presence of Triassic-age extensional structures which have been later transected by Jurassic-age

faults. It is therefore likely that far-field extensional stresses saw Permian age faults reactivated in the Central North Sea due to their favourable orientation with respect to the stress field but this relatively simple episode of extensional movement was complicated by early mobility of the salt-bearing parts of the underlying Zechstein succession.

Investigation of three separate case studies within the dataset demonstrates that although the typical pre-, syn- and post-rift geometries are not apparent, extensional tectonics did occur during this period. Extension and differential loading created a depositional geometry of thick Triassic Smith Bank pods separated by Zechstein salt walls. Later deposition of the fluvially derived Skagerrak Formation occurred in a post-rift environment but continued and often diachronous halokinesis means that the relationship between the Skagerrak and Smith Bank Formations does not resemble a typical post-rift geometry. The Skagerrak Formation could be considered to have been deposited in a post-rift, syn-halokinetic environment where accommodation space was created by continued evaporite movement and salt-wall collapse, possibly linked to dissolution under a more humid climatic regime.

Rifting in the Upper Jurassic heralded the start of tectono-stratigraphic megasequence 2 and was generated by a period of doming accompanied by regional erosion that removed the Lower Jurassic from the area and resulted in the formation of the Mid Cimmerian Unconformity. Well results in the Puffin area demonstrate that the unconformity was associated with igneous intrusion and volcanic extrusive activity supporting the notion that the uplift was driven by thermal doming.

Rifting initially led to non-marine deposition as base-level rose in a tectonic setting in which extensional faults began to nucleate in response to thermal collapse of the domed area. The faults that define the component parts of the extensional rift arm governed the position of two prominent depocentres termed the Western and Eastern Troughs (that are separated by the Forties-Montrose High). Their fault arrays appear to have grown by segment linkage which also utilised (in part) reactivated buried Permo-Triassic precursors. Nowhere is this better illustrated than in Quadrants 29 and 30, where a major breached relay ramp consists of the WSW-ESE striking structures. The latter focused sediment dispersal, controlled the limits of rift-related transgression and governed the position of (backstepping) shoreface reservoir play fairways in the Fulmar Formation. Diapir position is also shown to be dependent on the juxtaposition of the two rifts as salt piercements overlie areas where W-E striking Permo-Triassic faults are cross-cut by NW-SE striking Jurassic ones.

Cross-cutting of older fault trends has been demonstrated in other areas of the world and the evidence from this study suggests that underlying rifts can often have important effects on later fault patterns.

Subsequent Cretaceous, Paleogene and younger sequences largely conform to the model of the post-rift phase of tectono- stratigraphic megasequence 2 with gentle thermal subsidence leading to the creation of an elongated canoe-shaped basin. However, the development of unconformities within the Cretaceous section attests to structural complexity driven by salt mobility and structural inversion. The timing of deformation within the Cretaceous section provides clues as to the tectonic events responsible for their creation. Cretaceous inversion had previously been ascribed to

transmitted compressive stresses from continental collision in the Alpine region but the new mapping suggests that the timing of the most intense phase of deformation corresponds with events in the North Atlantic and that this is likely to have been the driver for the structures observed.

During the Palaeocene, the post-rift subsidence was again interrupted by events centred west of Britain with the initial development of the Iceland Plume. In the Faroe -Shetland basin faulting occurred during the Late Palaeocene and dikes of the same orientation were emplaced in both the onshore and offshore UK. These events were probably linked to regional compression within an extensional province due to extension on the SE margin of the North Atlantic rift being buttressed against the rigid Eurasian plate. Thermal uplift on the basin margins caused prograding complexes to be shed into the Faroe -Shetland basin which were then incised when the area became sub-aerial and complex drainage systems began to form.

Further south, coals and lignites were deposited on uplifted and exposed shelfal areas of the Inner Moray Firth. In the basin, the rejuvenated hinterland areas caused slope instability and collapse resulting in deep-water clastic deposition. Synchronous with this period of high clastic influx was a hyperthermal climate event, the Palaeocene-Eocene Thermal Maximum (PETM) which could also have contributed to increased sediment flux to the basin centre. Seismic mapping shows that early channels were large and unconfined while later flows were more channelized. The channel systems are shown to have been influenced by basin-floor topography and pinch-out onto basement highs.

Deflation of the Iceland Plume and opening of the North Atlantic in the Early Eocene led to waning clastic input to the Central North Sea and seismic mapping of Eocene channels reaching the basin centre shows them to be smaller and more confined than earlier Palaeocene ones. Transmitted stress from the North Atlantic triggered basin inversion throughout continental Europe, a process that continued until the mid-Miocene. In contrast, the Eocene-Pleistocene sedimentation in the Central North Sea was mainly influenced by compaction, oceanic circulation and climate.

The high resolution seismic data over the post-rift section of the Jurassic tectono-stratigraphic megasequence 2 allows sedimentological features to be mapped in detail. Extensional faulting and injected sands mapped in the Eocene section are linked to compaction and fluid expulsion. A family of unusual structures mapped in the Pliocene section may provide evidence for contourite currents which have previously been mapped mainly in deep oceanic settings. Bright spots directly above mounds created by these currents may point to accumulations of shallow gas which may represent drilling hazards or even potential reservoirs. Identification of channels scoured by ice-age glaciers is also an important outcome of this study as such features can affect depth conversion of seismic as they are filled with material of a different sonic velocity to that surrounding them.

Investigation of the possible influence of climate on depositional systems was also made possible by the high quality seismic data over the post-rift 2 section and the highly prospective nature of the Palaeocene clastic sequences (in particular the sand of the Forties Formation) which have been heavily sampled for the purposes of

hydrocarbon exploration. Seismic data, biostratigraphic, isotopic and elemental analyses provided the unique opportunity to study the hyperthermal on a regional scale and make inferences about its effects on sedimentation rates, composition, environmental effects and possible causal mechanisms.

The results of the investigation showed that it was not possible to separate the effects of uplift-driven and climatically controlled deposition seismically but that more subtle effects of the PETM on sediment composition and mineralogy could be observed. Increased levels of phosphorus may indicate increased nutrient flux and thus run-off over the PETM period perhaps due to increased humidity and biostratigraphic evidence supports this interpretation. Changes in clay minerals also occur over the PETM but appear to be more affected by the inclusion and alteration of volcanic ash layers. The clay mineral kaolinite which is linked to warm climates was shown in one North Sea section to increase over the PETM but examination of Palaeocene samples from other sections shows that at least some of this is due to alteration of other minerals during diagenesis and is not representative of the original composition.

Biostratigraphic analysis carried out on many wells within the North Sea found evidence for distinctive assemblage changes in the Latest Palaeocene. Several tropical species were introduced over the PETM period showing that temperatures in the region did increase but the majority of the vegetation remained within a single biozone. Cyclical changes in vegetation and dinoflagellate assemblages seem to be linked to relative sea-level changes of which there are several throughout the Latest

Palaeocene probably linked to periods of thermal uplift and deflation of the Iceland Plume. It was therefore considered not possible to separate the effects of uplift and increased orogenic rainfall from the effects of higher temperatures and increased humidity over the PETM.

The isotopic signature of the PETM was analysed from several North Sea sites and found to have a much expanded onset phase which would have to be taken into account when hypothesising about possible causal mechanisms for the hyperthermal. The isotope curves derived from all of the sections were also extremely variable which could represent the step-wise onset of the PETM seen in other sites. However, other possible explanations for these variations are fluctuating ratios of terrestrial and marine organic matter and hydrocarbon contamination, neither of which could be definitively disproved.

Comparison of the PETM isotope curve with one from the Toarcian showed them to be very similar in size and shape. This indicates that they may have the same causal mechanism or response to it. The rapid variations are also seen in the Jurassic isotope curve leading to the possibility that both curves represent discrete changes in the composition of the ocean-atmosphere system or a particular regional response to hyperthermal events in the North Sea and UK region. An Early Eocene isotope curve was also derived from the data from Central North Sea well 30/14-1 which could represent the latest example of an Eocene hyperthermal event. Flood basalts have been linked with hyperthermals and the Toarcian, PETM and Early Eocene hyperthermals all coincide with periods of volcanism.

7.1.1 FINAL SUMMARY

This study details the findings from regional seismic interpretation of datasets from the Central North Sea, Faroe-Shetland Basin and onshore UK. An additional case study of the Late Palaeocene PETM hyperthermal event was undertaken to explore the ways that extreme climate events may influence the development of a basin and to investigate the changes which occurred during a time of $CO_2$and temperature increase analogous to the present-day anthropogenic changes. The results add new elements to the current understanding of the structural and climatic history and configuration of the Central North Sea and are as follows.

1. A basement block, possibly granite-cored and emplaced during Caledonian tectonics exists underneath the Auk High in UKCS Quadrant 30 in the Central North Sea.

2. A NE-SW Iapetus trend is pervasive throughout the Central North Sea and Devonian-age syn-sedimentary faults or half-grabens can be observed for the first time.

3. A possible Variscan-age syncline may exist to the south of the Jaeren High analogous to those seen in the Midland Valley of Scotland.

4. The Base Permian Unconformity can now be mapped on the high-resolution seismic over a significant area.

5. A Permian-age ridge extending WSW-ENE from the current Forties-Montrose High to the south of the Jaeren High can be recognised for the first time. Cross-cutting by later faulting had previously obscured the true structure and led to its erroneous classification as a NW-SE striking structure.

6. Triassic sequences in the Central north Sea can now be placed in their tectono-stratigraphic context with the Smithbank Formation forming the syn-rift package and the Skagerrak Formation forming a post-rift, syn-halokinetic package.

7. It can now be shown that Jurassic rift-bounding faults grew by fault linkage and utilised older Permo-Triassic faults as soft-linkage zones.

8. The presence of a preserved relay zone can be demonstrated in Quadrant 30 with implications for deposition and preservation of Late Jurassic shoreface sands.

9. Far-field stresses in the Cretaceous can be shown to have reactivated buried Caledonian-age faults and to have led to doming of entire basins.

10. Inversion in the Lower Cretaceous is significant as it demonstrates that far-field stresses from the North Atlantic were responsible for movement during this period rather than from the Alpine region as previously thought.

11. A significant unconformity in the Late Cretaceous Hod Formation can be mapped and correlated with areas in the Southern North Sea and Dutch Central Graben. This can again be linked to events in the North Atlantic.

12. A pervasive fault system has been mapped in the Faroe-Shetland basin and can be linked to the emplacement of Tertiary-age dikes of the same orientation. This may be the result of stress release as compression from early North Atlantic extension was buttressed against the rigid Eurasian plate. These faults compartmentalise several hydrocarbon fields and have never previously been explained.

13. Thermal uplift caused Palaeocene basin-floor fans to be shed into the basin and their deposition was affected by bathymetry.

14. Uplift during at the end of the Palaeocene caused sub-aerial exposure and the formation of a highly intricate dendritic drainage system in the Faroe-Shetland Basin.

15. Clastic input to the Central North Sea basin declined significantly into the Eocene leading to deposition of more confined channels.

16. Pliocene deposition was affected by bottom-water currents.

17. Pleistocene glacial scour channels are common and may have implications for depth conversion models.

18. The PETM hyperthermal event can be recognised throughout the basin by its carbon isotope signature. Such a large number of sites within one basin have never previously been tested giving a regional view of the effects of the event rather than focusing on one section.

19. The deposition of the Forties depositional system was probably not climate induced. Older uplift-driven basin-floor fans are equal or larger in both volume and extent.

20. More subtle effects on depositional systems may have resulted from climate warming. Increased levels of uranium in PETM-age sediments may be linked to high temperatures but are also due to tectonically-controlled basin restriction and it is unclear how much of an effect temperature had.

21. Apparent extinctions within the Foraminifera may be linked to increased water temperatures but are most likely due to basin restriction and anoxia.

22. Elemental analyses show that increased humidity is not reflected in the sediment composition which is more influenced by diagenesis.

23. Ecological changes seem to reflect increased nutrient supply to the basin rather than increased temperature. The ratio of heterotrophic to autotrophic species and bloom of the heterotrophic species Apectodinium support this.

24. The apparent increase in angiosperms at the PETM is more likely reflective of increased transport efficiency.

25. Increased humidity occurred at the PETM allowing low-salinity surface waters to transport palynomorphs more efficiently and leading to changes in the dinoflagellate assemblages. However increased humidity can occur with climate change or with uplift.

26. There are no significant changes in floral or faunal assemblages over the PETM. Most of the species have wide tolerance ranges and continue through the hyperthermal. It is likely that the Central North Sea remained within a single biozone throughout.

27. Gradually declining isotope values at the start of the PETM provide clues as to the possible causal mechanism and show that many sections contain unrecognised unconformities.

28. Fluctuations in the isotope values from the North Sea sites and the increasingly more negative values of $\delta^{13}C$ with latitude suggest that the ratio of different types of organic carbon is important.

29. Comparison with other isotope excursions, particularly from the Toarcian may demonstrate a link between volcanism and isotope excursions and show that events such as the PETM have occurred regularly throughout geological time.

30. The discovery of a younger isotope excursion in the 30/14-1 core may represent one of a series of Early Eocene hyperthermal events which have been discovered and linked to orbital cyclicity.

7.2 RECOMMENDATIONS FOR FURTHER RESEARCH

Time considerations constrained this study and some suggestions for further work include;

- Full mapping of the Jurassic sequences over the entire study area.
- Further seismic interpretation of discrete Palaeocene channels.
- Mapping of the shelfal areas to the west (Western Shelf) and east of the Central Graben to investigate in more detail the pre-Permian section. Further datasets would be required in order to undertake this study.
- More detailed mapping of the post-Eocene section in order to discern the effects of possible Miocene inversion.
- Further investigation of the XRF data possibly using mathematical techniques such as Fourier analysis to look for cyclicity obscured by noisy data.
- Compound specific isotope analysis to determine whether the isotopic fluctuations seen in the PETM isotope curves are due to variations in the ratio of terrestrial and marine organic matter.
- Isotopic analysis of another Eocene section in order to look for evidence of the Eocene excursion seen in 30/14-1
- High resolution biostratigraphic analysis of samples from well 30/14-1 to investigate the environmental changes which occurred over the PETM. This would complement the XRF and isotopic analysis undertaken on the same samples from this well. Over 100 biostratigraphic slides were prepared for the

purposes of this study by the method outlined in Chapter 1, but at the time of submission the slides were not yet analysed.

ACKNOWLEDGEMENTS

Thanks are extended to the BGS and Edinburgh University for their support of this PhD through the BUFI award. Also greatly appreciated were the contributions of Professor John Underhill, Professor Michael Stephenson, Dr David Jolley and Dr Sev Kender by way of helpful comments and suggestions regarding this manuscript and the project as a whole. I am also very grateful to Dr James Riding for his invaluable help with providing highly detailed palynological analysis of core samples and the British Geological Survey for their work in preparing these samples. Thanks are also extended to BP and Maersk Oil and their joint venture partners for their kind donation of 3D seismic data for use within the project. Maersk Oil also kindly provided funds for isotope analysis and special mention must be given to Dr Nick Richardson for his part in arranging access to the data and his help with obtaining core samples. I am grateful to Dr Malcolm Butler for allowing data from the UK Onshore Geophysical Library (UKOGL) run by Lynx Information Systems to be shown in this thesis. I am also grateful to Schlumberger for providing the academic licence to use their interpretation software package, Petrel and to SMT for providing access to the Kingdom software. Additional thanks to Dr Melanie Leng for her aid in the isotope preparation and for running the samples at the NERC facility in Keyworth. Dr Chris Vane at the same facility provided invaluable support for the preparation of de-oiled isotope samples. Also greatly appreciated is the support and expertise of Chris Place and Magnus Hagdorn for their part in the configuration of the software utilized. Colleagues who have graciously helped with the usage of the

interpretation software include Ryan Williams, Nikolaos Lykakis and Jaume Hernandez Casado.

I would also like to make a special dedication to the late Dr Robert Knox. His willingness to help students coupled with his enthusiasm for geology and unparalleled knowledge meant that he often provided key observations and support without which this manuscript would have been much reduced.

REFERENCES

Abramovitz, T., et al. (2010). "3D seismic mapping and porosity variation of intra-chalk units in the southern Danish North Sea." Geological Society, London, Petroleum Geology Conference series 7: 537-548.

Adams, J. (2009). Species Richness: patterns in the diversity of life, Springer- Praxis Publishing Ltd.

Adams, J. A., et al. (1958). "Thorium - uranium ratios as indicators of sedimentary processes: example of concept of geochemical facies." Bulletin of the American Asscociation of Petroleum Geology 42(2): 387-430.

Agnini, C., et al. (2007). "Responses of calcareous nannofossil assemblages, mineralogy and geochemistry to the environmental perturbations across the Paleocene/Eocene boundary in the Venetian Pre-Alps." Marine Micropaleontology 63(1-2): 19-38.

Agnini, C., et al. (2006). "Eocene biostratigraphy and magnetic stratigraphy from Possagno, Italy: The calcareous nannofossil response to climate variability." Earth and Planetary Science Letters 241(3-4): 815-830.

Alegret, L., et al. (2005). "Palaeoenvironmental turnover across the Palaeocene/Eocene boundary at the stratotype section in Dababiya (Egypt) based on benthic foraminifera." Terra Nova 17(6): 526-536.

Alroy, J. (2000). "Successive approximations of diversity curves: Ten more years in the library." Geology 28(11): 1023-1026.

Arenillas, I., et al. (1999). "Planktic foraminiferal and partial derivative C-13 isotopic changes across the Paleocene/Eocene boundary at Possagno (Italy)." International Journal of Earth Sciences 88(2): 352-364.

Argent, J. D., et al. (2002). "Heterogeneous exhumation in the Inner Moray Firth, UK North Sea: constraints from new AFTA and seismic data." Journal of the Geological Society 159: 715-729.

Badley, M. E. (1985). Practical seismic interpretation. Boston, [Mass.], International Human Resources Development Corporation.

Bains, S., et al. (1999). "Mechanisms of Climate Warming at the End of the Paleocene." Science 285(5428): 724-727.

Banbury, N. J. (2006). The role of salt mobility in the development of supra-salt sedimentary depocentres and structural styles. School of Geosciences. Edinburgh, University of Edinburgh. PhD.

Barbosa, A., B, (2009). Dynamics of living phytoplankton: implications for paleoenvironmental reconstructions. IOP Conference Series: Earth and Environmental Science, IOP Publishing. 5.

Beerling, D. J., et al. (1998). "Fossil plants record an atmospheric 12CO2 and temperature spike across the Palaeocene-Eocene transition in NW Europe." Journal of the Geological Society 155(4): 591-594.

Berendse, F., et al. (2009). "The angiosperm radiation revisited, an ecological explanation for Darwin's 'abominable mystery'." Ecology Letters 12(9): 865-872.

Berggren, W. A., et al. (1998). Chapter 2: The Paleocene/Eocene Epoch/Series Boundary: Chronostratigraphic Framework and Estimated Geochronology Late Paleocene-Early Eocene Climatic and Biotic Events in the Marine and Terrestrial Records W. A. Berggren, Lucas, S. and Aubry, M-P. , Columbia University Press

BGS (2011). The Unconventional Hydrocarbon Resources of Britain's Onshore Basins- Shale Gas. Department of Energy and Climate Change, Promote UK, British Geological Survey.

Bishop, D. J. (1996). "Regional distribution and geometry of salt diapirs and supra-Zechstein Group faults in the western and central North Sea." Marine and Petroleum Geology 13(4): 355-364.

Biskopsø, F. (2004). Cenozoic Structural and Stratigraphic Development of the Faroe-Shetland Basin and Faroe Graben. Geosciences. Edinburgh, University of Edinburgh. PhD: 292.

Bolle, M. P., et al. (2001). "Palaeocene-early Eocene climatic evolution in the Tethyan realm: clay mineral evidence." Clay Minerals 36(2): 249-261.

Bolle, M. P., et al. (2000). "Climatic evolution on the southeastern margin of the Tethys (Negev, Israel) from the Palaeocene to the early Eocene: focus on the late Palaeocene thermal maximum." Journal of the Geological Society 157(5): 929-941.

Bolle, M. P., et al. (2000). "Climatic and environmental changes documented in the upper Paleocene to lower Eocene of Egypt." Eclogae Geologicae Helvetiae 93(1): 33-51.

Bralower, T. J., et al. (1997). "High-resolution records of the late Paleocene thermal maximum and circum-Caribbean volcanism: Is there a causal link?" Geology 25(11): 963-966.

Bramwell, N. P., et al. (1999). "Chalk exploration, the search for a subtle trap." Geological Society, London, Petroleum Geology Conference series 5: 911-937.

Brenchley, P. J., et al., Eds. (2006). The Geology of England and Wales. The Geological Society publication.

Brinkhuis, H. (1994). "Late Eocene to Early Oligocene dinoflagellate cysts from the Priabonian type-area (Northeast Italy): biostratigraphy and paleoenvironmental interpretation." Palaeogeography, Palaeoclimatology, Palaeoecology 107(1-2): 121-163.

Brinkhuis, H., et al. (2003). The end of the Early Eocene Climatic Optimum: Evidence for Concomitant Cooling of the Southern Ocean Surface Waters and Global Deep Waters From Dinoflagellate Endemism. AGU Fall Conference, Abstract volume. San Francisco: F887.

Brodie, C. R., et al. (2011). "Evidence for bias in C and N concentrations and Î´13C composition of terrestrial and aquatic organic materials due to pre-analysis acid preparation methods." Chemical Geology 282(3-4): 67-83.

Bujak, J., et al. (1994). "A high-resolution North Sea Eocene dinocyst zonation." Journal of the Geological Society 151(3): 449-462.

Bujak, J. P., et al. (1998). Chapter 14: Global Warming and Dinocyst Changes Across the Paleocene/Eocene Epoch Boundary Late Paleocene-Early Eocene Climatic and Biotic Events in the Marine and Terrestrial Records W. A. Berggren, Lucas,S. and Aubry, M-P., Columbia University Press

Caillet, G., et al. (1996). Structural history of the chalk fields in the Norwegian Central Graben. Fifth North Sea Chalk symposium, Joint Chalk Research. Reims France

Caillet, G., et al. (1997). "Overpressure and hydrocarbon trapping in the chalk of the Norwegian Central Graben." Petroleum Geoscience 3(1): 33-42.

Canudo, J., et al. (1995). "Planktic foraminiferal turnover and [delta]13C isotopes across the Paleocene-Eocene transition at Caravaca and Zumaya, Spain." Palaeogeography, Palaeoclimatology, Palaeoecology 114(1): 75-100.

Cartwright, J. A. (1994). "Episodic basin-wide hydrofracturing of overpressured Early Cenozoic mudrock sequences in the North Sea Basin." Marine and Petroleum Geology 11(5): 587-607.

Cartwright, J. A., et al. (1996). "Volumetric contraction during the compaction of mudrocks: a mechanism for the development of regional-scale polygonal fault systems." Basin Research 8(2): 183-193.

Cartwright, J. A., et al. (1995). "Fault growth by segment linkage: an explanation for scatter in maximum displacement and trace length data from the Canyonlands Grabens of SE Utah." Journal of Structural Geology 17(9): 1319-1326.

CDA (2009). Common Data Access Limited
Schlumberger

Chadwick, R. A., et al. (1995). The timing and direction of Permo-Triassic extension in southern Britain. Permain and Triassic Rifting in Northwest Europe. S. A. R. Boldy. London. Geological Society Special Publication 91: 161-192.

Chadwick, R. A., et al. (1991). "Deep crustal structure and Carboniferous basin development within the Iapetus convergence zone, northern England." Journal of the Geological Society 148(1): 41-53.

Chadwick, R. A., et al. (1995). The Structure and evolution of the Northumberland-Solway Basin and adjacent areas.

Chadwick, R. A., et al. (1989). Continental extension in Southern Britain and surrounding areas and its relationship to the opening of the North Atlantic Ocean. Extensional tectonics and stratigraphy of the North Atlantic Margins. A. J. Tankard, Balkwill, H.R. American Association of Petroleum Geologists Memoirs 46: 411-424.

Chalmers, J. A. (1991). "New evidence on the structure of the Labrador Sea/Greenland continental margin." Journal of the Geological Society 148(5): 899-908.

Charles, A. J., et al. (2011). "Constraints on the numerical age of the Paleocene-Eocene boundary." Geochem. Geophys. Geosyst. 12: Q0AA17.

Chen, D., et al. (2011). "Seismic Expression of Polygonal Faults and Its Impact on Fluid Flow Migration for Gas Hydrates Formation in Deep Water of the South China Sea." Journal of Geological Research 2011.

Cohen, A. S., et al. (2007). "The Late Palaeocene Early Eocene and Toarcian (Early Jurassic) carbon isotope excursions: a comparison of their time scales, associated environmental changes, causes and consequences." Journal of the Geological Society 164(6): 1093-1108.

Corfield, S. M., et al. (1996). "Inversion tectonics of the Variscan foreland of the British Isles." Journal of the Geological Society 153(1): 17-32.

Coward, M., et al. (1989). "Alpine tectonics — an overview." Geological Society, London, Special Publications 45(1): 1-29.

Coward, M. P., et al. (1989). "Devonian basins of Northern Scotland: extension and inversion related to Late Caledonian — Variscan tectonics." Geological Society, London, Special Publications 44(1): 275-308.

Crouch, E. M., et al. (2005). "Environmental change across the Paleocene-Eocene transition from eastern New Zealand: A marine palynological approach." Marine Micropaleontology 56: 138-160.

Crouch, E. M., et al. (2003). "The Apectodinium acme and terrestrial discharge during the Paleocene-Eocene thermal maximum: new palynological, geochemical and calcareous nannoplankton observations at Tawanui, New Zealand." Palaeogeography, Palaeoclimatology, Palaeoecology 194(4): 387-403.

Crouch, E. M., et al. (2001). "Global dinoflagellate event associated with the late Paleocene thermal maximum." Geology 29(4): 315-318.

Dal Corso, J., et al. (2012). "Discovery of a major negative Î´13C spike in the Carnian (Late Triassic) linked to the eruption of Wrangellia flood basalts." Geology 40(1): 79-82.

Dal Piaz, G. V., et al. (1972). "La zona Sesia-Lanzo e l'evoluzione tettonico-metamorphica delle Alpi nordocci-dentali interne." Memoire della Societa Geologica Italiana 11: 433-466.

Dale, B. (1996). Dinoflagellate cyst ecology: Modeling and geological applications. Palynology: Principles and Applications. J. Jansonius, McGregor, D.C. Dallas, American Association of Stratigraphic Palynologists Foundation: 1249-1276.

Dale, B., et al. (1994). Dinoflagellate cysts as palaeoproductivity indicators: state of the art, potential and limits. Carbon Cycling in the Glacial Ocean: Constraints on the Ocean's Role in Global Change. R. Zahn, NATO ASI Series 1. 17: 521-537.

Damuth, J. E., et al. (1988). "Anatomy and Growth Pattern of Amazon Deep-Sea Fan as Revealed by Long-Range Side Scan Sonar (Gloria) and High-Resolution Seismic Studies. ." AAPG Bulletin 92 885- 911.

Davison, I., et al. (2000). "Overburden deformation patterns and mechanisms of salt diapir penetration in the Central Graben, North Sea." Marine and Petroleum Geology 17(5): 601-618.

de Jager, J. (2007). "Geology of the Netherlands." Royal Netherlands Academy of Arts and Sciences.

Devillers, R., et al. (2000). "Distribution of dinocysts in surface sediments of the northern North Atlantic in relation with nutrients and productivity in surface waters." Marine Geology 166: 103-124.

Dickens, G. R., et al. (1995). " Dissociation of Oceanic Methane Hydrate as a Cause of the Carbon Isotope Excursion at the End of the Paleocene." Paleoceanography 10(6): 965-971.

Domingo, L., et al. (2009). "The Paleocene-Eocene Thermal Maximum record in the organic matter of the Claret and Tendruy continental sections (South-central Pyrenees, Lleida, Spain)." Earth and Planetary Science Letters 281(3-4): 226-237.

Doornebal, H., Stevenson, A. , Ed. (2010). Petroleum Geological Atlas of the Southern Permian Basin Area. , EAGE Publications.

.

Dore, A. G., et al. (1999). "Principal tectonic events in the evolution of the northwest European Atlantic margin." Geological Society, London, Petroleum Geology Conference series 5: 41-61.

Dupuis, C., et al. (2003). "The Dababiya Quarry section: Lithostratigraphy, clay mineralogy, geochemistry and paleontology." Micropaleontology 49: 41-59.

Durrance, E. M. (1986). Radioactivity in Geology. Principles and Applications. Chichester, Ellis Horwood.

Egger, H., et al. (2009). "From shelf to abyss: Record of the Paleocene/Eocene-boundary in the Eastern Alps (Austria)." Geologica Acta 7(1-2): 215-227.

Egger, H., et al. (2005). "Early Eocene climatic, volcanic, and biotic events in the northwestern Tethyan Untersberg section, Austria." Palaeogeography, Palaeoclimatology, Palaeoecology 217(3-4): 243-264.

Ellis, D., et al. (2002). "The stratigraphy, environment of eruption and age of the Faroes Lava Group, NE Atlantic Ocean." Geological Society of London, Special Publications 197: 253-269.

Ellis, D., et al. (2009). Transfer zones: the application of new geological information from the Faroe Islands applied to the offshore exploration of intra basalt and sub-basalt strata. Faroe Islands Exploration Conference: Proceedings of the 2nd Conference.

Embry, A., et al. (2007). Sequence Stratigraphy as a "Concrete" Stratigraphic Discipline. Report of the ISSC Task Group on Sequence Stratigrapy.

Emery, D., et al. (1996). Sequence Stratigraphy, Blackwell Science Ltd

Emiliane, C. (2005). The Oceanic Lithosphere, Howard University Press.

England, R. W. (1988). "The Early Tertiary stress regime in NW Britain: evidence from the patterns of volcanic activity." Geological Society Special Publications 39: 381-389.

Erratt, D. (1993). "Relationships between Basement Faulting, Salt Withdrawal and Late Jurassic Rifting, Uk Central North-Sea." Petroleum Geology of Northwest Europe: Proceedings of the 4th Conference: 1211-1219.

Evans, D., et al., Eds. (2003). The Millenium Atlas: Petroleum geology of the central and northern North Sea, The Geological Society London.

Farley, K. A., et al. (2003). "An alternative age model for the Paleocene-Eocene thermal maximum using extraterrestrial 3He." Earth and Planetary Science Letters 208(3-4): 135-148.

Farley, M. B. (1989). "Palynological Facies Fossils in Nonmarine Environments in the Paleogene of the Bighorn Basin." PALAIOS 4(6): 565-573.

Farmer, C. L., et al. (1999). "Influence of syn-depositional faulting on thickness variations in chalk reservoirs – Valhall and Hod fields." Geological Society, London, Petroleum Geology Conference series 5: 949-957.

Feeley, M. H., et al. (1985). Depositional Units and Growth
Pattern of the Mississippi Fan. . Submarine Fans and Related Turbidite Systems. . A. H. Bouma, Normak, W. R. & Barnes, N. E. New York, Springer: 253-258.

Fitton, J. G., et al. (1998). "Volcanic rocks from the Southeast Greenland margin at 63^{o}N: Composition, petrogenesis and mantle sources." Proceedings of the Ocean Drilling Program, Scientific Results 152: 331-350.

Ford, M., et al. (2004). "Foreland basin evolution around the western Alpine Arc." Geological Society, London, Special Publications 221(1): 39-63.

Fraser, A. J., et al. (1990). "Tectono-stratigraphic development and hydrocarbon habitat of the Carboniferous in northern England." Geological Society, London, Special Publications 55(1): 49-86.

Frazier, D. (1974). "Depositional episodes: their relationship to the Quaternary stratigraphic framework in the northwestern portion of the Gulf Basin." Bureau of Economic Geology, University of Texas, Geological Circular 74-1: 26.

Freeman, P., et al. (2008). "The Schiehallion Field: lessons learned modelling a complex deepwater turbidite." Geological Society, London, Special Publications 309(1): 205-219.

Geluk, M. C. (2007). Permian. Geology of the Netherlands. T. E. Wong, Batjes, D.A.J, de Jager, J., Royal Netherlands Academy of Arts and Sciences: 63-83.

Gingerich, P. D. (2006). "Environment and evolution through the Paleocene-Eocene thermal maximum." Trends in Ecology & Evolution 21(5): 246-253.

Giusberti, L., et al. (2007). "Mode and tempo of the Paleocene-Eocene thermal maximum in an expanded section from the Venetian pre-Alps." Geol Soc Am Bull 119(3-4): 391-412.

Glennie, K. W. (1998). Petroleum Geology of the North Sea: Basic Concepts and Recent Advances Blackwell Science.

Gochioco, L. M. (1991). "Tuning effect and interference reflections from thin beds and coal seams." Geophysics 56(8): 1288-1295.

Gradstein, F. M., et al. (1992). "Cenozoic Foraminiferal and Dinoflagellate Cyst Biostratigraphy of the Central North-Sea." Micropaleontology 38(2): 101-137.

Hall, A., et al. (2002). "Scotland's denudational history: an integrated view of erosion and sedimentation at an uplifted passive margin." Geological Society, London, Special Publications 196(1): 271-290.

Hancock, J. M., et al. (1979). "The great transgressions of the Late Cretaceous." Journal of the Geological Society 136(2): 175-186.

Handley, L., et al. (2008). "Large terrestrial and marine carbon and hydrogen isotope excursions in a new Paleocene/Eocene boundary section from Tanzania." Earth and Planetary Science Letters 275(1-2): 17-25.

Haq, B. U., et al. (1987). "Chronology of Fluctuating Sea Levels Since the Triassic." Science 235(4793): 1156-1167.

Harding, I. C., et al. (2011). "Sea-level and salinity fluctuations during the Paleocene-Eocene thermal maximum in Arctic Spitsbergen." Earth and Planetary Science Letters 303(1-2): 97-107.

Harrington, G., et al. (2004). "Palaeocene-Eocene paratropical floral change in North America: responses to climate change and plant immigration." Journal of the Geological Society 161(2): 173-184.

Harrington, G. J. (2003). Geographical patterns in the floral response to Paleocene-Eocene warming. Causes and consequences of globally warm climates in the early Paleogene. S. Wing, Gingerich, P., Schmitz, B., Thomas, E., The Geological Society of America. Special Paper 369

Heriot-Watt University, I. o. P. E. (2007). Reservoir evaluation and management. Introduction to the seismic method, Heriot-Watt University.

Heritier, F. E., et al., Eds. (1981). The Frigg Gas Field. Petroleum Geology of the Continental Shelf of North-West Europe. London, Heyden and Son.

Hesselbo, S. P., et al. (2002). "Terrestrial and marine extinction at the Triassic-Jurassic boundary synchronized with major carbon-cycle perturbation: A link to initiation of massive volcanism?" Geology 30(3): 251-254.

Heward, A. P. (1990). "Salt removal and sedimentation in Southern Oman." Geological Society, London, Special Publications 49(1): 637-651.

Hillis, R. R., et al. (1994). "Quantification of Tertiary erosion in the Inner Moray Firth using sonic velocity data from the chalk and Kimmeridge Clay." Marine and Petroleum Geology 11: 283-293.

Hodgson, N. A., et al. (1992). "Salt-related tectonics, sedimentation and hydrocarbon plays in the Central Graben, North Sea, UKCS." Geological Society, London, Special Publications 67(1): 31-63.

Hollis, C. J., et al. (2005). "The Paleocene-Eocene transition at Mead Stream, New Zealand: a southern Pacific record of early Cenozoic global change." Palaeogeography, Palaeoclimatology, Palaeoecology 215(3-4): 313-343.

Hubbard, R. J., et al. (1985). Depositional Sequence Mapping as a Technique to Establish Tectonic and Stratigraphic Framework and Evaluate Hydrocarbon Potential on a Passive Continental Margin. Seismic Stratigraphy 2: An Integrated Approach to Hydrocarbon Exploration. O. R. Berg, Woolverton, D.G. Tulsa, Oklahoma, The American Association of Petroleum Geologists. AAPG Memoir 39.

Hubbard, R. J., et al. (1985). Depositional Sequence Mapping to Illustrate the Evolution of a Passive Continental Margin. Seismic Stratigraphy 2: An Integrated Approach to Hydrocarbon Exploration. O. R. Berg, Woolverton, D.G. Tulsa, Oklahoma, The American Association of Petroleum Geologists. AAPG Memoir 39.

Huber, M., et al. (2003). Early Paleogene oceans and climate: A fully coupled modeling approach using the NCAR CCSM. Colorado, Boulder.

Hunt, D., et al. (1992). "Stranded parasequences and the forced regressive wedge systems tract: deposition during base level fall." Sedimentary Geology 81: 1-9.

Hunziker, J. C. (1986). "The Alps: a case of multiple collision." Geological Society, London, Special Publications 19(1): 221-227.

Huuse, M., et al. (2005). "Kilometre-scale sandstone intrusions in the Eocene of the Outer Moray Firth (UK North Sea): migration paths, reservoirs and potential drilling hazards." Geological Society, London, Petroleum Geology Conference series 6: 1577-1594.

Ioakim, C. (1978). Étude comparative des dinoflagellés du Tertiaire inférieur de la Mer du Labrador et de la Mer du Nord. . Paris, Université Pierre et Marie Curie (Paris VI). PhD: 205 pp.

IPCC (2007). IPCC Fourth Assement Report: Climate Change 2007. I. P. o. C. Change. Geneva.

Jablonski, D., et al. (1994). "Extinctions in the Fossil Record [and Discussion]." Philosophical Transactions of the Royal Society of London. Series B: Biological Sciences 344(1307): 11-17.

Jackson, M. P. A., et al. (1986). "External shapes, strain rates, and dynamics of salt structures." Geological Society of America Bulletin 97(3): 305-323.

Jackson, M. P. A., et al. (1994). "Regional extension as a geologic trigger for diapirism." Geological Society of America Bulletin 106(1): 57-73.

Jacobson, D. M., et al. (1986). "Thecate heterotrophic dinoflagellates: feeding behaviour and mechanisms." Journal of Phycology 22: 249-258.

Jager, D. D., et al. (1993). "Evolution of Paleogene Submarine Fans of the North-Sea in-Space and Time." Petroleum Geology of Northwest Europe: Proceedings of the 4th Conference: 59-71.

Jeremiah, J. M., et al. (1999). "Middle Oxfordian to Volgian sequence stratigraphy of the Greater Shearwater area." Geological Society, London, Petroleum Geology Conference series 5: 153-170.

Jervery, M. (1988). Quantitative geological modelling of sillicate rock sequences and their seismic expression. Sea level changes: an integrated approach: SEPM Special Publication. C. Wilgus, Hastings, B.S., Posamentier, H.W., Ross, C.A., Van Wagoner, J.C. 42.

Jiang, S., et al. (2006). "Surface-water chemistry and fertility variations in the tropical Atlantic across the Paleocene/Eocene Thermal Maximum as evidenced by calcareous nannoplankton from ODP Leg 207, Hole 1259B." Revue de Micropaléontologie 49(4): 227-244.

John, C. M., et al. (2008). "North American continental margin records of the Paleocene-Eocene thermal maximum: Implications for global carbon and hydrological cycling." Paleoceanography 23(2).

Jolley, D. W. (1992). "Palynofloral association sequence stratigraphy of the Palaeocene Thanet Beds and equivelant sediments in eastern England." Review of Palaeobotany and Palynology 74: 207-237.

Jolley, D. W. (1992). "Spore-dominated assemblages from the lowermost Reading Beds (Palaeocene) of North Essex." Proceedings of the Yorkshire Geological and Polytechnic Society 49(2): 149-153.

Jolley, D. W., et al. (2009). "Syn-eruption vegetation dynamics, paleosurfaces and structural controls on lava field vegetation: An example from the Palaeogene Staffa Formation, Mull Lava Field, Scotland." Review of Palaeobotany and Palynology 153(1-2): 19-33.

Jolley, D. W., et al. (2002). "Paleogene time scale miscalibration: Evidence from the dating of the North Atlantic igneous province." Geology 30(1): 7-10.

Jolley, D. W., et al. (2005). "Did Paleogene North Atlantic rift-related eruptions drive early Eocene climate cooling?" Lithos 79(3–4): 355-366.

Jones, S. M., et al. (2002). "Present and past influence of the Iceland Plume on sedimentation." Geological Society, London, Special Publications 196(1): 13-25.

Joy, A. M. (1992). "Estimation of Cenozoic water depths in the Western Central Graben, UK North Sea, by subsidence modelling." Geological Society, London, Special Publications 67(1): 107-125.

Joy, A. M. (1993). "Comments on the pattern of post-rift subsidence in the Central and Northern North Sea Basin." Geological Society, London, Special Publications 71(1): 123-140.

Kaiho, K., et al. (2006). "Anomalous shifts in tropical Pacific planktonic and benthic foraminiferal test size during the Paleocene-Eocene thermal maximum." Palaeogeography, Palaeoclimatology, Palaeoecology 237(2-4): 456-464.

Kelly, D. C., et al. (1998). "Evolutionary consequences of the latest Paleocene thermal maximum for tropical planktonic foraminifera." Palaeogeography, Palaeoclimatology, Palaeoecology 141(1-2): 139-161.

Kender, S., et al. (2012). "Marine and terrestrial environmental changes in NW Europe preceding carbon release at the Paleocene–Eocene transition." Earth and Planetary Science Letters 353–354(0): 108-120.

Kennett, J. P., et al. (1991). "Abrupt Deep-Sea Warming, Palaeoceanographic Changes and Benthic Extinctions at the End of the Paleocene." Nature 353(6341): 225-229.

Kerrick, D. M., et al. (1993). "Paleoatmospheric consequences of CO2 released during early Cenozoic regional metamorphism in the Tethyan orogen." Chemical Geology 108(1-4): 201-230.

Kerrick, D. M., et al. (1998). "Metamorphic CO2 degassing from orogenic belts." Chemical Geology 145(3-4): 213-232.

King, C. (1983). "Cainozoic micropalaeontological biostratigraphy of the North Sea." Report Institute Geological Sciences 82(6): 1-40.

Knott, S. D., et al. (1993). "Mesozoic to Cenozoic plate reconstructions of the North Atlantic and hydrocarbon plays of the Atlantic margins." Geological Society, London, Petroleum Geology Conference series 4: 953-974.

Knox, R. W. O. B. (1996). "Correlation of the early Paleogene in northwest Europe: an overview." Geological Society, London, Special Publications 101(1): 1-11.

Knox, R. W. O. B. (1996). "Tectonic controls on sequence development in the Palaeocene and earliest Eocene of southeast England: implications for North Sea stratigraphy." Geological Society, London, Special Publications 103(1): 209-230.

Knox, R. W. O. B., et al. (1979). "Stratigraphical relationships of the early Palaeogene ash-series of NW Europe." Journal of the Geological Society 136(4): 463-470.

Knox, R. W. O. B., et al., Eds. (1992). Paleogene of the Central and Northern North Sea. Lithostratigraphic nomenclature of the UK North Sea, British Geological Survey.

Knox, R. W. O. B., et al. (1988). "The record of early Tertiary N Atlantic volcanism in sediments of the North Sea Basin." Geological Society, London, Special Publications 39(1): 407-419.

Knutz, P. C. (2010). "Channel structures formed by contour currents and fluid expulsion: significance for Late Neogene development of the central North Sea basin." Geological Society, London, Petroleum Geology Conference series 7: 77-94.

Koch, P. L., et al. (1995). "Stable isotope stratigraphy and paleoclimatology of the Paleogene Bighorn Basin (Wyoming, USA)." Palaeogeography, Palaeoclimatology, Palaeoecology 115(1-4): 61-89.

Koch, P. L., et al. (1992). "Correlation between isotope records in marine and continental carbon reservoirs near the Paleocene/Eocene boundary." Nature 358: 319-322.

Kohn, M. J. (2010). "Carbon isotope compositions of terrestrial C3 plants as indicators of (paleo)ecology and (paleo)climate." Proceedings of the National Academy of Sciences 107(46): 19691-19695.

Kump, L. R., et al. (1999). "Interpreting carbon-isotope excursions: carbonates and organic matter." Chemical Geology 161(1-3): 181-198.

Kuspert, W. (1982). Environmental changes during oil shale deposition as deduced from stable isotope ratios. Cyclic and Event Stratification: . G. Einsele, and Seilacher, A.,. Heidelberg, Springer: 482-501.

Larsen, L. M., et al. (2009). "Tectonomagmatic events during stretching and basin formation in the Labrador Sea and the Davis Strait: evidence from age and composition of Mesozoic to Palaeogene dyke swarms in West Greenland." Journal of the Geological Society 166(6): 999-1012.

Larsen, P. H. (1988). "Relay structures in a Lower Permian basement-involved extension system, East Greenland." Journal of Structural Geology 10: 3-8.

Leach, H. M., et al. (1999). "The Schiehallion development." Geological Society, London, Petroleum Geology Conference series 5: 683-692.

Lonergan, L., et al. (1998). "Polygonal faulting in the Tertiary of the central North Sea: implications for reservoir geology." Geological Society, London, Special Publications 127(1): 191-207.

Lourens, L. J., et al. (2005). "Astronomical pacing of late Palaeocene to early Eocene global warming events." Nature 435(7045): 1083-1087.

Lu, G. Y., et al. (1996). "Long-term (10(5)) or short-term (10(3)) delta C-13 excursion near the Palaeocene-Eocene transition: Evidence from the Tethys." Terra Nova 8(4): 347-355.

Maclennan, J., et al. (2002). "Control of regional sea level by surface uplift and subsidence caused by magmatic underplating of Earth's crust." Geology 30(8): 675-678.

MacRae, R. A., et al. (1996). "Fossil dinoflagellate diversity, originations, and extinctions and their significance." Canadian Journal of Botany 74(11): 1687-1694.

Marret, F., et al. (2002). "Control of modern dinoflagellate cyst distribution in the Irish and Celtic seas by seasonal stratification dynamics." Marine Micropaleontology 47: 101-116.

Matthews, W. J., et al. (2007). "Controls on fluviolacustrine reservoir distribution and architecture in passive salt-diapir provinces: Insights from outcrop analogs." AAPG Bulletin 91(10): 1367-1403.

McKenzie, D. (1994). "The Relationship between Topography and Gravity on Earth and Venus." Icarus 112(1): 55-88.

Megson, J., et al. (2005). "The North Sea Chalk: an underexplored and underdeveloped play." Geological Society, London, Petroleum Geology Conference series 6: 159-168.

Miller, K. G., et al. (1987). "Abyssal Circulation and Benthic Foraminiferal Changes Near the Paleocene/Eocene Boundary." Paleoceanography 2(6): 741-761.

Milton-Worssell, R., et al. (2010). "The search for a Carboniferous petroleum system beneath the Central North Sea." Geological Society, London, Petroleum Geology Conference series 7: 57-75.

Milton, N. J., et al. (1990). "Early Palaeogene tectonics and sedimentation in the Central North Sea." Geological Society, London, Special Publications 55(1): 339-351.

Mitlehner, A. G. (1996). "Palaeoenvironments in the North Sea Basin around the Paleocene-Eocene boundary: evidence from diatoms and other siliceous microfossils." Geological Society, London, Special Publications 101(1): 255-273.

Morley, C. K., Ed. (1999). Geoscience of Rift Systems- Evolution of East Africa. AAPG Studies in Geology Tulsa, Oklahoma, The American Association of Petroleum Geologists.

Morton, A. C., et al. (1990). "Geochemistry of late Palaeocene and early Eocene tephras from the North Sea Basin." Journal of the Geological Society 147(3): 425-437.

Musgrove, F. W., et al. (1996). "Analysis of the pre-Tertiary rifting history of the Rockall Trough." Petroleum Geoscience 2(4): 353-360.

Mutterlose, J., et al. (2007). "Calcareous nannofossils from the Paleocene-Eocene Thermal Maximum of the equatorial Atlantic (ODP Site 1260B): Evidence for tropical warming." Marine Micropaleontology 65(1-2): 13-31.

Muttoni, G., et al. (2007). "Widespread formation of cherts during the early Eocene climate optimum." Palaeogeography, Palaeoclimatology, Palaeoecology 253(3-4): 348-362.

Nadin, P. A., et al. (1997). "Early Tertiary plume uplift of the North Sea and Faeroe-Shetland Basins." Earth and Planetary Science Letters 148(1-2): 109-127.

Nichols, D. J., et al. (1986). "Palynological and iridium anomalies at Cretaceous-Tertiary boundary, south-central Saskatchewan." Science 231: 714-717.

Nicolo, M. J., et al. (2007). "Multiple early Eocene hyperthermals: Their sedimentary expression on the New Zealand continental margin and in the deep sea." Geology 35(8): 699-702.

Norrish, K., et al. (1969). "An accurate X-ray spectrographic method for the analysis of a wide range of geological samples." Geochimica et cosmochimica acta 33: 431-451.

O'Connor, S. J., et al. (1993). "Paleocene Reservoirs of the Everest Trend." Petroleum Geology of Northwest Europe: Proceedings of the 4th Conference: 145-160.

Oakman, C. D., et al. (1998). Cretaceous. Petroleum Geology of the North Sea - Basic Concepts and Recent Advances. 4th edition. K. W. Glennie. Oxford, Blackwell: 294-349.

Olney, M. (2002). "Microfossil Image Recovery And Circulation for Learning and Education (MIRACLE)." Retrieved 25/10/11, 2011.

Orth, C. J., et al. (1981). "An iridium abundance anomaly at the palynological Cretaceous-Tertiary boundary in northern New Mexico." Science 214: 1341-1342.

Ortiz, N. (1995). "Differential patterns of benthic foraminiferal extinctions near the Paleocene/Eocene boundary in the North Atlantic and the western Tethys." Marine Micropaleontology 26(1-4): 341-359.

Ouda, K. (2003). "The Paleocene/Eocene boundary in Egypt: An overview." Micropaleontology 49: 15-40.

Pagani, M., et al. (2006). "Arctic hydrology during global warming at the Palaeocene/Eocene thermal maximum." Nature 442(7103): 671-675.

Palfy, J., et al. (2000). "Synchrony between Early Jurassic extinction, oceanic anoxic event, and the Karoo-Ferrar flood basalt volcanism." Geology 28(8): 747-750.

Parks, C. D. (1991). "A review of the mechanisms of cambering and valley bulging." Geological Society, London, Engineering Geology Special Publications 7(1): 373-380.

Passey, S. R., et al. (2008). "A revised lithostratigraphic nomenclature for the Palaeogene Faroe Islands Basalt Group, NE Atlantic Ocean." Earth and Environmental Science Transactions of the Royal Society of Edinburgh 99(3-4): 127-158.

Payne, J. L., et al. (2004). "Large Perturbations of the Carbon Cycle During Recovery from the End-Permian Extinction." Science 305(5683): 506-509.

Pharoah, T. C., et al. (2011). Structure and evolution of the East Midlands region of the Pennine Basin. . Keyworth, Nottingham.

Piper, D. J. W., et al. (1983). "Turbidite depositional patterns and flow characteristics, Navy submarine fan, California Borderland." Sedimentology 30: 681-694.

Posamentier, H., et al. (1988). Eustatic controls on clastic deposition, a conceptual framework. Sea level changes: an integrated approach. SEPM Special Publication. C. Wilgus, Hastings, B.S., Posamentier, H.W., Ross, C.A., Van Wagoner, J.C. 42.

Powell, A. J. (1988). "A modified dinoflagellate biozonation for the latest Palaeocene and earliest Eocene sediments from the central North Sea. ." Review of Palaeobotany and Palynology 56: 327-344. .

Powell, A. J. (1992). Dinoflagellate cysts of the Tertiary System. . A Stratigraphic Index of Dinoflagellate Cysts. A. J. Powell. London, Chapman and Hall 155-251. .

Powell, A. J., et al. (1996). "Upper Paleocene-Lower Eocene dinoflagellate cyst sequence biostratigraphy of southeast England." Geological Society, London, Special Publications 101(1): 145-183.

Prauss, M. (2001). "Sea-level changes and organic-walled phytoplankton response in a Late Albian epicontinental setting, Lower Saxony basin, NW Germany." Palaeogeography, Palaeoclimatology, Palaeoecology 174(1-3): 221-249.

Raffi, I., et al. (2005). "Changes in calcareous nannofossil assemblages across the Paleocene/Eocene transition from the paleo-equatorial Pacific Ocean." Palaeogeography, Palaeoclimatology, Palaeoecology 226(1-2): 93-126.

Rattey, R. P., et al., Eds. (1993). Sequence stratigraphy of a failed rift system: the Middle Jurassic to Early Cretaceous basin evolution of the Central and

Northern North Sea. Petroleum Geology of North West Europe: Proceedings of the 4th Conference. London, The Geological Society of London.

Reeves, G. M., et al. (2006). Clay materials used in construction, The Geological Society.

Reichart, G.-J., et al. (2003). "Late Quaternary Protoperidinium cysts as indicators of paleoproductivity in the northern Arabian Sea." Marine Micropaleontology 49(4): 303-315.

Richards, P. C., et al. (1993). Jurassic of the Central and Northern North Sea. Nottingham, British Geological Survey.

Richardson, N. J., et al. (2005). "The role of evaporite mobility in modifying subsidence patterns during normal fault growth and linkage, Halten Terrace, Mid-Norway." Basin Research 17(2): 203-223.

Rider, M. H. (1996). The geological interpretation of well logs. Caithness, Whittles Pub.

Ridgwell, A., et al. (2010). "Past constraints on the vulnerability of marine calcifiers to massive carbon dioxide release." Nature Geoscience 3(3): 196-200.

Roberts, D. G., et al. (1999). "Palaeozoic to Tertiary rift and basin dynamics: mid-Norway to the Bay of Biscay – a new context for hydrocarbon prospectivity in the deep water frontier." Geological Society, London, Petroleum Geology Conference series 5: 7-40.

Robinson, S. A. (2011). "Shallow-water carbonate record of the Paleocene-Eocene Thermal Maximum from a Pacific Ocean guyot." Geology 39(1): 51-54.

Rochon, A., et al. (1999). "Distribution of recent dinoflagellate cysts in surface sediments from the North Atlantic Ocean and adjacent seas in relation to sea-surface parameters." American association of Stratigraphic Palynologists Foundation, Contributions Series 35.

Rochon, A., et al. (2008). "Dinocysts as tracers of hydrographical conditions and productivity along the ocean margins: Introduction." Marine Micropaleontology 68(1-2): 1-5.

Rodriguez, J. M., et al. (2010). "Prospectivity of the T38 sequence in the Northern Judd Basin." Geological Society, London, Petroleum Geology Conference series 7: 245-259.

Rohl, U., et al. (2000). "New chronology for the late Paleocene thermal maximum and its environmental implications." Geology 28(10): 927-930.

Rohl, U., et al. (2007). "On the duration of the Paleocene-Eocene thermal maximum (PETM)." Geochemistry Geophysics Geosystems 8.

Roncaglia, L. (2004). "Palynofacies analysis and organic-walled dinoflagellate cysts as indicators of palaeo-hydrographic changes: an example from Holocene sediments in Skálafjord, Faroe Islands." Marine Micropaleontology 50(1-2): 21-42.

Saelen, G., et al. (1998). "Evidence of recycling of isotopically light CO2 (aq) in stratified black shale basins: Contrasts between the Whitby Mudstone and Kimmeridge Clay formations, United Kingdom." Geology 26(8): 747-750.

Sangiogi, F., et al. (2003). "Holocene seasonal sea surface temperature variations in the South Adriatic Sea inferred from a multi-proxy approach." Journal of Quaternary Science 18(8): 723-732.

Sansom, P. J. (2010). "Reappraisal of the sequence stratigraphy of the Humber Group of the UK Central Graben." Geological Society, London, Petroleum Geology Conference Series 7: 177-211.

Santarelli, A., et al. (1998). "Orbital signatures in a late Miocene dinoflagellate record from Crete (Greece)." Marine Micropaleontology 33(3-4): 273-297.

Schmitz, B., et al. (1997). "High-resolution iridium, [delta]13C, [delta]18O, foraminifera and nannofossil profiles across the latest Paleocene benthic extinction event at Zumaya, Spain." Palaeogeography, Palaeoclimatology, Palaeoecology 133(1-2): 49-68.

Schouten, S., et al. (2000). "Effects of an oceanic anoxic event on the stable carbon isotopic composition of early Toarcian carbon." Am J Sci 300(1): 1-22.

Schröder, T. (1992). "A palynological zonation for the Paleocene of the North Sea Basin. ." Journal of Micropalaeontology 11: 113-126. .

SEPM. (2013). "SEPM STRATA." Retrieved 01/03/13, 2013.

Shackleton, N., et al. (1981). "The climate of the Eocene ocean." Journal of the Geological Society 138(2): 153-157.

Sheriff, R. E., et al. (1995). Exploration Seismology, Cambridge University Press.

Sikora, P. J., et al. (1999). "Chalk palaeoenvironments and depositional model, Valhall-Hod fields, southern Norwegian North Sea." Geological Society, London, Special Publications 152(1): 113-137.

Sinclair, I. K., et al. (1999). "The Hibernia Oilfield – effects of episodic tectonism on structural character and reservoir compartmentalization." Geological Society, London, Petroleum Geology Conference series 5: 517-528.

Sluijs, A. (2006). Global change during the Paleocene – Eocene thermal maximum. Environmental Biology, Utrecht University. PhD: 228.

Sluijs, A., et al. (2011). "Southern ocean warming, sea level and hydrological change during the Paleocene-Eocene thermal maximum." Clim. Past 7(1): 47-61.

Sluijs, A., et al. (2008). "Eustatic variations during the Paleocene-Eocene greenhouse world." Paleoceanography 23(4).

Sluijs, A., et al. (2007). "Environmental precursors to rapid light carbon injection at the Palaeocene/Eocene boundary." Nature 450(7173): 1218-1221.

Sluijs, A., et al. (2005). "From greenhouse to icehouse; organic-walled dinoflagellate cysts as paleoenvironmental indicators in the Paleogene." Earth-Science Reviews 68(3-4): 281-315.

Sluijs, A., et al. (2008). "Arctic late Paleocene-early Eocene paleoenvironments with special emphasis on the Paleocene-Eocene thermal maximum (Lomonosov Ridge, Integrated Ocean Drilling Program Expedition 302)." Paleoceanography 23(1).

Sluijs, A., et al. (2006). "Subtropical arctic ocean temperatures during the Palaeocene/Eocene thermal maximum." Nature 441(7093): 610-613.

Smith, A. B. (2007). "Marine diversity through the Phanerozoic: problems and prospects." Journal of the Geological Society 164(4): 731-745.

Smith, K., et al. (1993). "Jurassic volcanic centres in the Central North Sea." Geological Society, London, Petroleum Geology Conference Series 4: 519-531.

Smith, N. J. P., et al. (2005). Structure and evolution of the south-west Pennine Basin and adjacent area. . Keyworth, Nottingham.

Sprangers, M., et al. (2004). "Modern organic-walled dinoflagellate cyst distribution offshore NW Iberia; tracing the upwelling system." Review of Palaeobotany and Palynology 128(1-2): 97-106.

Stephenson, M. H., et al. (2005). "Investigating the record of Permian climate change from argillaceous sedimentary rocks, Oman." Journal of the Geological Society 162(4): 641-651.

Steurbaut, E., et al., Eds. (2003). Palynology, paleoenvironments and organic carbon isotope evolution in lagoonal Paleocene-Eocene boundary settings in North Belgium. Causes and Consequences of Globally Warm Climates in the Early Paleogene, Geological Society of America. Special Paper 369.

Stewart, I. J. (1987). A revised stratigraphic interpretation of the Early Palaeogene of the central North Sea. . Petroleum Geology of North West Europe. . J. G. Brooks, K. . London, Graham & Trotman: 557-576.

Stewart, S. A., et al. (1996). "The Flamborough Tertiary outlier, UK southern North Sea." Journal of the Geological Society 153: 163-173.

Stewart, S. A., et al. (1999). Impact of salt on the structure of the Central North Sea hydrocarbon fairways, Geological Society London.

Storey, M., et al. (2007). "Paleocene-Eocene thermal maximum and the opening of the northeast Atlantic." Science 316(5824): 587-589.

Thomas, D. J., et al. (1999). "New evidence for subtropical warming during the late Paleocene thermal maximum: Stable isotopes from Deep Sea Drilling Project Site 527, Walvis Ridge." Paleoceanography 14(5): 561-570.

Thomas, E. (1998). Chapter 12: Biogeography of the Late Paleocene Benthic Foraminiferal Extinction Late Paleocene-Early Eocene Climatic and Biotic Events in the Marine and Terrestrial Records W. A. Berggren, Lucas,S. and Aubry, M-P., Columbia University Press

Thomas, J. E. (1992). Cenozoic deep-sea circulation: Evidence from deep-sea benthic foraminifera, in the Antarctic Paleoenvironment. Washington D.C, AGU.

Thomas, J. E. (1996). "The occurrence of the dinoflagellate cyst Apectodinium (Costa & Downie 1976) Lentin & Williams 1977 in the Moray and Montrose Groups (Danian to Thanetian) of the UK central North Sea." Geological Society, London, Special Publications 101(1): 115-120.

Thomas, J. E. (2003). Extinction and food at the sea floor: a high resoution benthic foraminiferal record across the Initial Eocene Thermal Maximum, Southern Ocean Site 690, Geological Society of America Special Papers.

Thyberg, B. I., et al. (2000). "Relationships between sequence stratigraphy, mineralogy and geochemistry in Cenozoic sediments of the northern North Sea." Geological Society, London, Special Publications 167(1): 245-272.

Tremolada, F., et al. (2004). "Nannofossil assemblage fluctuations during the Paleocene-Eocene Thermal Maximum at Sites 213 (Indian Ocean) and 401 (North Atlantic Ocean): palaeoceanographic implications." Marine Micropaleontology 52(1-4): 107-116.

Tripati, A., et al. (2005). "Deep-sea temperature and circulation changes at the Paleocene-Eocene thermal maximum." Science 308(5730): 1894-1898.

Trudgill, B., et al. (1994). "Relay-ramp forms and normal-fault linkages, Canyonlands National Park, Utah." Geological Society of America Bulletin 106(9): 1143-1157.

Underhill, J. R. (1991). "Implications of Mesozoic-Recent basin development in the Inner Moray Firth, UK." Marine and Petroleum Geology 8: 359-369.

Underhill, J. R. (2003). "The tectonic and stratigraphic framework of the United Kingdom's oil and gas fields." Geological Society, London, Memoirs 20(1): 17-59.

Underhill, J. R., et al. (1993). "Structural geology of Easter Ross, Scotland: implications for movement on the Great Glen fault zone." Journal of the Geological Society 150(3): 515-527.

Underhill, J. R., et al. (2008). "Controls on structural styles, basin development and petroleum prospectivity in the Midland Valley of Scotland." Marine and Petroleum Geology 25(10): 1000-1022.

Underhill, J. R., et al. (1993). "Jurassic thermal doming and deflation in the North Sea: implications of the sequence stratigraphic evidence." Geological Society, London, Petroleum Geology Conference Series 4: 337-345.

Underhill, J. R., et al. (2003). Structural Evolution and Basin-Fill Architecture of the Permo-Triassic Basins Northern North Sea.

Van Wagoner, J. C., et al. (1988). An overview of the fundamentals of sequence statigraphy and key definitions. Sea level changes: an integrated approach: SEPM Special Publication. C. Wilgus, Hastings, B.S., Posamentier, H.W., Ross, C.A., Van Wagoner, J.C. 42.

Vejbaek, O. V., et al. (2002). "Post mid-Cretaceous inversion tectonics in the Danish Central Graben- regionally synchronous teconic events?" Bulletin of the Geological Society of Denmark 49: 139-144.

Verardo, D. J., et al. (1990). "Determination of organic carbon and nitrogen in marine sediments using the Carbo Erba NA-1500 Analyser." Deep Sea Research 37(1): 157-165.

Versteegh, G. J. M. (1994). "Recognition of cyclic and non-cyclic environmental changes in the Mediterranean Pliocene; a palynological approach." Marine Micropaleontology 23: 147-171.

Vining, B. A., et al. (1993). "Stratigraphic Relationships of Some Tertiary Lowstand Depositional Systems in the Central North-Sea." Petroleum Geology of Northwest Europe: Proceedings of the 4th Conference: 17-29.

Wall, D., et al. (1977). "The environmental and climatic distribution of dinoflagellate cysts in modern marine sediments from regions in the North and South Atlantic Oceans and adjacent seas." Marine Micropaleontology 2: 121-200.

Wall, M., et al. (2009). "3D seismic imaging of a Tertiary Dyke Swarm in the Southern North Sea." Basin Research.

Waters, C. N., et al. (2007). Lithostratigraphic Framework for Carboniferous Successions of Great Britain (Onshore). British Geological Survey Research Report RR/07/01. Keyworth, British Geological Survey.

Watterson, J., et al. (2000). "Geometry and origin of a polygonal fault system." Journal of the Geological Society 157: 151-162.

Westerhold, T., et al. (2011). "A complete high-resolution Paleocene benthic stable isotope record for the central Pacific (ODP Site 1209)." Paleoceanography 26(2): PA2216.

Westerhold, T., et al. (2008). "Astronomical calibration of the Paleocene time." Palaeogeography, Palaeoclimatology, Palaeoecology 257(4): 377-403.

Wills, L. J. (1956). Concealed coalfields., Glasgow and London Blackie and Sons Ltd.

Wing, S. L., et al. (2005). "Transient floral change and rapid global warming at the Paleocene–Eocene boundary." Science 310: 993-996.

Wing, S. L., et al. (1984). "The Platycarya Perplex and the Evolution of the Juglandaceae." American Journal of Botany 71(3): 388-411.

Wood, J., et al. (2012). "East Africa's Great Rift Valley: A Complex Rift System." Retrieved 08/10/12, 2012.

Wood, S. E., et al. (1996). "An integrated palynological-palynofacies approach to the zonation of the Paleogene in the Forties-Montrose Ridge area, central North Sea." Geological Society, London, Special Publications 101(1): 121-128.

Yang, H., et al. (2009). "Carbon and hydrogen isotope fractionation under continuous light: implications for paleoenvironmental interpretations of the High Arctic during Paleogene warming." Oecologia 160 461-470.

Zachos, J., et al. (2001). "Trends, rhythms, and aberrations in global climate 65 Ma to present." Science 292(5517): 686-693.

Zachos, J. C., et al. (2008). "An early Cenozoic perspective on greenhouse warming and carbon-cycle dynamics." Nature 451(7176): 279-283.

Zachos, J. C., et al. (2010). "Tempo and scale of late Paleocene and early Eocene carbon isotope cycles: Implications for the origin of hyperthermals." Earth and Planetary Science Letters 299(1–2): 242-249.

Zachos, J. C., et al. (2005). "Rapid acidification of the ocean during the Paleocene-Eocene thermal maximum." Science 308(5728): 1611-1615.

Zachos, J. C., et al. (2003). "A transient rise in tropical sea surface temperature during the Paleocene–Eocene Thermal Maximum." Science 302: 1551-1554.

Zacke, A., et al. (2009). "Surface-water freshening and high-latitude river discharge in the Eocene North Sea." Journal of the Geological Society 166(5): 969-980.

Zeebe, R. E., et al. (2009). "Carbon dioxide forcing alone insufficient to explain Palaeocene-Eocene Thermal Maximum warming." Nature Geosci 2(8): 576-580.

Ziegler, P. A. (1982). Geological Atlas of Western and Central Europe. Amsterdam, Shell International Petroleum

Ziegler, P. A. (1990). Geological Atlas of Western and Central Europe (second edition), Geological Society for Shell International Petroleum.

Ziegler, P. A., et al. (1999). "Petroleum systems of Alpine-Mediterranean foldbelts and basins." Geological Society, London, Special Publications 156(1): 517-540.